frontiers

RESEARCH TOPICS

THE MICROBIAL SULFUR CYCLE

Hosted by
Martin G. Klotz, Donald A. Bryant
and Thomas A. Hanson

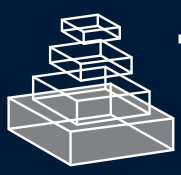

frontiers in
MICROBIOLOGY

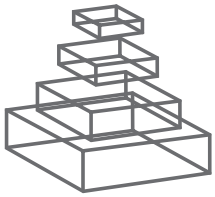

frontiers

Cover image provided by Ibbl sarl, Lausanne CH

ISSN 1664-8714
ISBN 978-2-88919-009-6
DOI 10.3389/978-2-88919-009-6

ABOUT FRONTIERS

Frontiers is more than just an open-access publisher of scholarly articles: it is a pioneering approach to the world of academia, radically improving the way scholarly research is managed. The grand vision of Frontiers is a world where all people have an equal opportunity to seek, share and generate knowledge. Frontiers provides immediate and permanent online open access to all its publications, but this alone is not enough to realize our grand goals.

FRONTIERS JOURNAL SERIES

The Frontiers Journal Series is a multi-tier and interdisciplinary set of open-access, online journals, promising a paradigm shift from the current review, selection and dissemination processes in academic publishing.
All Frontiers journals are driven by researchers for researchers; therefore, they constitute a service to the scholarly community. At the same time, the Frontiers Journal Series operates on a revolutionary invention, the tiered publishing system, initially addressing specific communities of scholars, and gradually climbing up to broader public understanding, thus serving the interests of the lay society, too.

DEDICATION TO QUALITY

Each Frontiers article is a landmark of the highest quality, thanks to genuinely collaborative interactions between authors and review editors, who include some of the world's best academicians. Research must be certified by peers before entering a stream of knowledge that may eventually reach the public - and shape society; therefore, Frontiers only applies the most rigorous and unbiased reviews.
Frontiers revolutionizes research publishing by freely delivering the most outstanding research, evaluated with no bias from both the academic and social point of view.
By applying the most advanced information technologies, Frontiers is catapulting scholarly publishing into a new generation.

WHAT ARE FRONTIERS RESEARCH TOPICS?

Frontiers Research Topics are very popular trademarks of the Frontiers Journals Series: they are collections of at least ten articles, all centered on a particular subject. With their unique mix of varied contributions from Original Research to Review Articles, Frontiers Research Topics unify the most influential researchers, the latest key findings and historical advances in a hot research area!
Find out more on how to host your own Frontiers Research Topic or contribute to one as an author by contacting the Frontiers Editorial Office: researchtopics@frontiersin.org

THE MICROBIAL SULFUR CYCLE

Hosted By
Martin G. Klotz, University of North Carolina at Charlotte, USA
Donald A. Bryant, The Pennsylvania State University, USA
Thomas E. Hanson, University of Delaware, USA

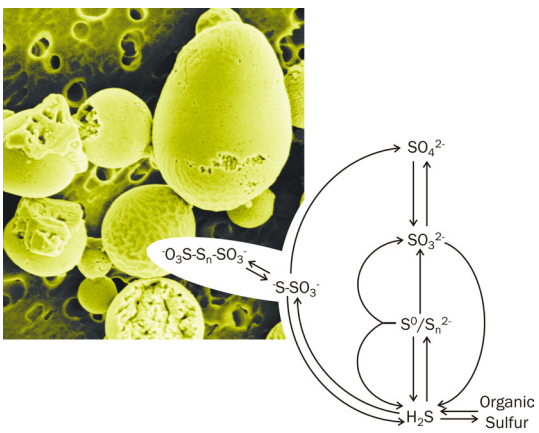

Sulfur is the tenth most abundant element in the universe and the sixth most abundant element in microbial biomass. By virtue of its chemical properties, particularly the wide range of stable redox states, sulfur plays a critical role in central biochemistry as a structural element, redox center, and carbon carrier. In addition, redox reactions involving reduced and oxidized inorganic sulfur compounds can be utilized by microbes for the generation and conservation of biochemical energy. Microbial transformation of both inorganic and organic sulfur compounds has had a profound effect on the properties of the biosphere and continues to affect geochemistry today. For these reasons, we present here a collection of articles from the leading edge of the field of sulfur microbiology, focusing on reactions and compounds of geochemical significance.

Table of Contents

frontiers in
MICROBIOLOGY

EDITORIAL
published: 02 December 2011
doi: 10.3389/fmicb.2011.00241

The microbial sulfur cycle

Martin G. Klotz[1]*, Donald A. Bryant[2] and Thomas E. Hanson[3]

[1] *Department of Biology, University of North Carolina at Charlotte, Charlotte, NC, USA*
[2] *Biochemistry and Molecular Biology, Eberly College of Science, The Pennsylvania State University, University Park, PA, USA*
[3] *College of Earth, Ocean, and Environment, University of Delaware, Newark, DE, USA*
**Correspondence: martin.klotz@frontiersin.org*

Sulfur is one example of an element whose transformation and fate in the environment are critically dependent upon microbial activities. Sulfur is the 10th most abundant element in the universe and the sixth most abundant element in microbial biomass. By virtue of its chemical properties, particularly the wide range of stable redox states, sulfur plays important roles in central biochemistry as a structural element, redox center, and carbon carrier. In addition, redox reactions involving reduced and oxidized inorganic sulfur compounds can be utilized by microbes for the generation and conservation of biochemical energy. Microbial transformation of both inorganic and organic sulfur compounds has had a profound effect on the properties of the biosphere and continues to affect geochemistry today.

While sulfur microbiology has a rich history, the last decade has changed our views on many aspects of microbially driven biogeochemical cycles, including the global sulfur cycle, in that tremendous advances in methods, techniques, and approaches have enabled the discovery of novel processes and characterization of the organisms and molecular mechanisms that facilitate them. This progress is documented in a collection of 20 articles at the leading edge of sulfur microbiology, focusing on microbes, reactions, and compounds of geochemical significance. Whether students or peer researchers in the field, it is the intent of this Research Topic issue to reach a wide audience whose interests and expertise spans from the molecular biochemistry of single enzymes and their reactions through pure culture physiology and genetic analysis to community level metagenomics and metatranscriptomics. This collection is especially timely given the recent publication describing one of the oldest microfossils to date that likely lived a sulfur-dependent chemolithoautotrophic lifestyle (Wacey et al., 2011). Microbial sulfur cycling may have had a hand in starting it all.

This collection of papers can be viewed as falling roughly into four clusters that deal with enzymes/activities, organisms/pathways/comparative approaches, symbiosis, and environments:

- At the level of enzymes and activities, new data are reported on a variety of systems. Structural analyses are reported for a disproportionating sulfur oxygenase/reductase and a dissimilatory sulfite reductase. Two independent papers focus on tetrathionate hydrolase, one of bacterial and one of archeal origin. Electron flow for the Sor pathway of thiosulfate oxidation has been further defined in *Sinorhizobium meliloti*. Finally, another article provides the first functional evidence in a phototrophic bacterium for the function of a quinone-interacting membrane-bound oxidoreductase that participates in the oxidation of sulfite.
- At the level of pathways and organisms, detailed reviews have been produced. For the sulfate reducing bacteria, the foci are metabolic flexibility, energy metabolism, and electron flow. In the phototrophic bacteria, putative sulfur oxidation pathways in sequenced *Chlorobi* are examined. Finally, the latest developments in microbial pathways for the degradation of DMSP, an extremely important component of the marine sulfur cycle are summarized. Three research articles focus on the regulation of sulfur oxidation genes in the purple sulfur bacterium *Allochromatium vinosum*, growth on tetrathionate vs. S(0) in *Acidithiobacillus caldus* and new *Mycobacteria* isolates from sandstone monuments that appear to grow as sulfur oxidizers.
- Multi-organism interactions and symbiosis encompass the third category. Papers on exclusively prokaryotic symbioses and those that cross domain boundaries involving microbial eukaryotes and the symbionts of marine fauna provide a broad perspective in this arena grounded in the application of traditional (label tracing experiments to examine substrate exchange) and cutting edge (transcriptomic analysis of uncultured microbial symbionts) techniques.
- Finally, this issue presents three papers on sulfur cycling at the level of ecosystems and communities. Two extreme environments are examined. Sorokin et al. (2011) summarize their long track record of work in soda lakes that combine high salinity with high pH. Both the reductive and oxidative arms of the sulfur cycle are discussed, and new insights into sulfidogenesis are presented for these fascinating systems. Yang et al. (2011) compare microbial communities and chemolithoautotrophic activity in relatively understudied freshwater hydrothermal vents in Yellowstone Lake. Finally, Luther et al. (2011) present a detailed analysis of the chemical parameters that influence abiotic oxidation of sulfide in natural environments. Sulfide oxidizing microbes must compete with this abiotic process and this report analyzes both literature and fresh experimental data to show that biotic sulfide oxidation will almost always occur at significantly faster rates due to kinetic restrictions on abiotic oxidation. Biology rules after all, as should be evident not just from this paper, but from the entire collection presented here.

Together, these papers represent the forefront of research of this field. We hope you enjoy them as much as we enjoyed working with this talented group of researchers to put this volume together.

REFERENCES

Luther, G. W., III, Findlay, A. J., MacDonald, D. J., Owings, S. M., Hanson, T. E., Beinart, R. A., and Girguis, P. R. (2011). Thermodynamics and kinetics of sulfide oxidation by oxygen: a look at inorganically controlled reactions and biologically mediated processes in the environment. *Front. Microbio.* 2:62. doi: 10.3389/fmicb.2011.00062

Sorokin, D. Y., Kuenen, J. G., and Muyzer, G. (2011). The microbial sulfur cycle at extremely haloalkaline conditions of soda lakes. *Front. Microbio.* 2:44. doi: 10.3389/fmicb.2011.00044

Wacey, D., Kilburn, M. R., Saunders, M., Cliff, J., and Brasier, M. D. (2011). Microfossils of sulphur-metabolizing cells in 3.4-billion-year-old rocks of Western Australia. *Nature Geosci.* 4, 698–702.

Yang, T., Lyons, S., Aguilar, C., Cuhel, R., and Teske, A. (2011). Microbial communities and chemosynthesis in Yellowstone Lake sublacustrine hydrothermal vent waters. *Front. Microbio.* 2:130. doi: 10.3389/fmicb.2011.00130

Received: 15 November 2011; accepted: 16 November 2011; published online: 02 December 2011.

*Citation: Klotz MG, Bryant DA and Hanson TE (2011) The microbial sulfur cycle. Front. Microbio. **2**:241. doi: 10.3389/fmicb.2011.00241*

This article was submitted to Frontiers in Microbial Physiology and Metabolism, a specialty of Frontiers in Microbiology.

frontiers in
MICROBIOLOGY

ORIGINAL RESEARCH ARTICLE
published: 10 February 2011
doi: 10.3389/fmicb.2011.00017

Sulfur metabolism in the extreme acidophile *Acidithiobacillus caldus*

Stefanie Mangold[1]*, Jorge Valdés[2,3†], David S. Holmes[2,3] and Mark Dopson[1†]

[1] *Department of Molecular Biology, Umeå University, Umeå, Sweden*
[2] *Center for Bioinformatics and Genome Biology, Fundación Ciencia para Vida, Santiago, Chile*
[3] *Departamento de Ciencias Biologicas, Andrés Bello University, Santiago, Chile*

Edited by:
Thomas E. Hanson, University of Delaware, USA

Reviewed by:
Kathleen Scott, University of South Florida, USA
Dimitry Y. Sorokin, Delft University of Technology, Netherlands

****Correspondence:***
Stefanie Mangold, Department of Molecular Biology, Umeå University, SE-901 87 Umeå, Sweden.
e-mail: stefanie.mangold@miolbiol.umu.se

†Current address:
Jorge Valdés, Bio-Computing Laboratory, Fraunhofer-Chile Research Foundation, Santiago, Chile;
Mark Dopson, Institution for Natural Sciences, Linnaeus University, 391 82 Kalmar, Sweden.

Given the challenges to life at low pH, an analysis of inorganic sulfur compound (ISC) oxidation was initiated in the chemolithoautotrophic extremophile *Acidithiobacillus caldus*. *A. caldus* is able to metabolize elemental sulfur and a broad range of ISCs. It has been implicated in the production of environmentally damaging acidic solutions as well as participating in industrial bioleaching operations where it forms part of microbial consortia used for the recovery of metal ions. Based upon the recently published *A. caldus* type strain genome sequence, a bioinformatic reconstruction of elemental sulfur and ISC metabolism predicted genes included: sulfide–quinone reductase (*sqr*), tetrathionate hydrolase (*tth*), two *sox* gene clusters potentially involved in thiosulfate oxidation (*soxABXYZ*), sulfur oxygenase reductase (*sor*), and various electron transport components. RNA transcript profiles by semi quantitative reverse transcription PCR suggested up-regulation of *sox* genes in the presence of tetrathionate. Extensive gel based proteomic comparisons of total soluble and membrane enriched protein fractions during growth on elemental sulfur and tetrathionate identified differential protein levels from the two Sox clusters as well as several chaperone and stress proteins up-regulated in the presence of elemental sulfur. Proteomics results also suggested the involvement of heterodisulfide reductase (HdrABC) in *A. caldus* ISC metabolism. A putative new function of Hdr in acidophiles is discussed. Additional proteomic analysis evaluated protein expression differences between cells grown attached to solid, elemental sulfur versus planktonic cells. This study has provided insights into sulfur metabolism of this acidophilic chemolithotroph and gene expression during attachment to solid elemental sulfur.

Keywords: *Acidithiobacillus caldus*, elemental sulfur, inorganic sulfur compounds, metabolism, attachment, proteomics

INTRODUCTION

Inorganic sulfur compounds (ISCs) in acidic, sulfide mineral environments are produced as a result of abiotic Fe(III) oxidation of sulfide minerals such as pyrite (FeS_2; initial ISC product is thiosulfate) or chalcopyrite ($CuFeS_2$; initial product is polysulfide sulfur). Their subsequent biooxidation produces sulfuric acid as the final product (Schippers and Sand, 1999; Johnson and Hallberg, 2009). As a result of sulfuric acid production, sulfide mineral environments are typically inhabited by acidophilic microorganisms. These microorganisms are exploited in the biotechnological process of "Biomining" whereby dissolution of sulfide minerals is catalyzed by the action of ISC oxidizing microorganisms as well as Fe(II) oxidizers that regenerate the Fe(III) required for the abiotic attack of sulfide minerals (Rawlings and Johnson, 2007).

A diverse range of acidophilic or neutrophilic photo- and chemolithotrophs can oxidize ISCs from sulfide (oxidation state of −2) to sulfate (+6; reviewed in Ghosh and Dam, 2009). Microorganisms utilize several systems for ISC oxidation including the *Paracoccus pantotrophus* 15 gene sulfur oxidizing (*sox*) cluster. This cluster encodes the multiple substrate Sox system that catalyzes oxidation of thiosulfate, elemental sulfur (S^0), sulfide, and sulfite to sulfate. SoxAX is composed of the dihemic and monohemic cytochromes SoxA and SoxX, respectively. SoxYZ is predicted to be able to bind ISCs in different oxidation states by the cysteine contained in the V-K-V-T-I-G-G-C-G-G conserved motif on the carboxy terminus of the protein. The SoxB subunit is predicted to have two manganese ions in the active site and works as a sulfate thiohydrolase interacting with SoxYZ (Friedrich et al., 2005). Several sulfur oxidizing bacteria (e.g., green and purple sulfur bacteria) only contain the core thiosulfate oxidizing multi-enzyme system (TOMES). The TOMES lacks the sulfur dehydrogenase $Sox(CD)_2$ and oxidizes thiosulfate to sulfate and S^0 (reviewed in Friedrich et al., 2001; Ghosh and Dam, 2009, and Sakurai et al., 2010). Due to the lack of $Sox(CD)_2$, S^0 is polymerized to form globules which can be further oxidized by proteins encoded in the dissimilatory sulfite reductase (*dsr*) gene cluster (Hensen et al., 2006).

In contrast to the well studied Sox enzyme complex, the ISC oxidations pathways in acidophiles are not very well understood. As described in recent reviews (Rohwerder and Sand, 2007; Johnson and Hallberg, 2009), S^0 is thought to be oxidized by acidophilic bacteria via sulfur dioxygenase (SDO) and by archaea via sulfur oxygenase reductase (Sor). The SDO has not been characterized although its enzyme activity has been shown (Suzuki, 1999; Rohwerder and Sand, 2003). However, the archaeal Sor has been well studied and the corresponding gene has been identified in *Acidianus tengchongensis*, *Aquifex aeolicus*, *Picrophilus torridus*, "*Ferroplasma acidarmanus*," and *Sulfolobus tokodaii* (Urich et al.,

2006). In the presence of oxygen, Sor simultaneously catalyzes oxidation and reduction of S^0 generating sulfite, thiosulfate, and sulfide (Urich et al., 2006). The enzyme does not require cofactors or external electron donors for S^0 reduction. Due to its cytoplasmic location it is believed that it does not play a role in formation of the transmembrane electron gradient but rather provide substrates for other membrane bound enzymes. Another enzyme which has recently been suggested to be involved in *Acidithiobacillus ferrooxidans* S^0 metabolism is heterodisulfide reductase (Hdr; Quatrini et al., 2009). So far no biochemical evidence for *A. ferrooxidans* S^0 oxidation by Hdr has been reported, however, transcriptomics (Quatrini et al., 2009) and proteomics data (unpublished data) strongly suggests its involvement. Hdr of methanogenic archaea has been studied (Hedderich et al., 2005) and it catalyzes the reversible reduction of the disulfide bond in heterodisulfide accompanied by the extrusion of electrons and the formation of a transmembrane electron gradient. Quatrini et al. (2009) hypothesize that Hdr works in reverse in acidophiles by utilizing the naturally existing proton gradient to oxidize disulfide intermediates originating from S^0 and donating electrons to the quinone pool. Other enzymes involved in acidophilic ISC oxidation pathways are thiosulfate:quinone oxidoreductase (Tqr) which oxidizes thiosulfate to tetrathionate, tetrathionate hydrolase (Tth), and sulfide oxidoreductase (Rohwerder and Sand, 2007; Johnson and Hallberg, 2009). Recently, the analysis of gene context has highlighted differences in ISC oxidation strategies in *A. ferrooxidans*, *Acidithiobacillus thiooxidans*, and *Acidithiobacillus caldus* (Cardenas et al., 2010). Microarray analysis suggests the *petII* (prosthetic group-containing subunits of the cytochrome bc_1 complex), *cyo* (cytochrome *o* ubiquinol oxidase), *cyd* (cytochrome *bd* ubiquinol oxidase), and *doxII* (encoding thiosulfate quinol reductase) gene clusters are up-regulated during growth on S^0 compared to Fe(II) grown cells (Quatrini et al., 2006). From these data, a model for *A. ferrooxidans* ISC metabolism has been created (Quatrini et al., 2009). *A. ferrooxidans* proteins with increased expression during growth on S^0 include an outer membrane protein (Omp40) and a thiosulfate sulfur transferase protein (Ramirez et al., 2004). Also, a high throughput study of periplasmic proteins identified 41 and 14 proteins uniquely expressed in S^0 and thiosulfate grown cells, respectively (Valenzuela et al., 2008). The genome context of these proteins suggests they are involved in ISC metabolism and possibly S^0 oxidation and Fe–S cluster construction. Secreted proteins from a pure culture of *A. thiooxidans* and from co-culture with *A. ferrooxidans* were studied by proteomics (Bodadilla Fazzini and Parada, 2009). An Omp40 like protein was identified which is suggested to be involved in attachment. Finally, S^0 induced genes in the acidophilic archaeon *Sulfolobus metallicus* include Sor (Bathe and Norris, 2007).

A. caldus is an ISC oxidizing acidophile (Hallberg et al., 1996b) often identified in biomining environments (Okibe et al., 2003; Dopson and Lindström, 2004). *A. caldus* aids in metal dissolution by removal of solid S^0 that may form a passivating layer on the mineral surface (Dopson and Lindström, 1999). The *A. caldus* draft genome contains genes for ISC oxidation (Valdes et al., 2009). The gene cluster containing the *A. caldus* tetrathionate hydrolase (*tth*) and the *doxD* component (thiosulfate:quinol oxidoreductase) has been characterized (Rzhepishevska et al., 2007). The Tth is a periplasmic homo-dimer with an optimum pH of 3 (Bugaytsova and Lindström, 2004). Previously Tth was also studied in *A. ferrooxidans* (de Jong et al., 1997).

Owing to the fact that *A. caldus* is ubiquitous in both natural and anthropogenic sulfide mineral environments, its importance in generating sulfuric acid, and in mitigating mineral passivation we have investigated its ISC metabolism. An in depth bioinformatic analysis revealed the putative genes responsible for sulfuric acid generation, that have then been verified by proteomic comparison between growth with tetrathionate and S^0 and via transcript profiling. This has generated insights into the ISC metabolism of this microorganism. Such knowledge might help to better understand the industrial processes.

MATERIALS AND METHODS

BIOINFORMATIC RECONSTRUCTION OF *A. CALDUS* ISC METABOLISM

Genes and metabolic pathways involved in ISC and S^0 oxidation/reduction were obtained from Metacyc[1] and Kegg[2]. Amino acid sequences derived from selected genes previously identified to be involved in ISC metabolism were used as a query to conduct BlastP and tBlastN (Altschul et al., 1997) searches to interrogate the *A. caldus*^{T} (ATCC51756) draft genome sequence (NZ_ACVD00000000.1). Potential gene candidates were further characterized employing the following bioinformatic tools: ClustalW (Larkin et al., 2007) for primary structure similarity relations, PSI-PRED (Bryson et al., 2005) for secondary structure predictions, Prosite (Hulo et al., 2006) for motif predictions, and ProDom (Bru et al., 2005) and Pfam (Finn et al., 2008) for domain predictions. Selected gene candidates were assigned to putative orthologous groups in order to determine potential evolutionary associations[3] (Tatusov et al., 2003). Information regarding the organization of genes in other S^0 metabolizing microorganisms was obtained from NCBI[4] and IMG–JGI[5].

MEDIA AND CULTURE CONDITIONS

A. caldus^T was cultured in mineral salts medium (MSM) with trace elements (Dopson and Lindström, 1999) at 45°C and pH 2.5 whilst sparging with 2% (vol/vol) CO_2 enriched air. Tetrathionate (5 mM; Sigma) and 5 g/L hydrophilic, biologically produced S^0 (provided by PAQUES B.V., the Netherlands) were used as substrate. Stock solutions of tetrathionate were sterile filtered and added to the autoclaved (121°C for 15 min) MSM, whereas the finely ground S^0 was added to MSM prior to autoclaving at 105°C for 30 min. The medium containing solid S^0 was stirred for 24 h to ensure fine dispersion of the S^0 particles. Biomass for the transcript profiling and proteomic comparison of growth on tetrathionate versus S^0 was produced in continuous culture with a dilution rate of 0.06 h^{-1}. The homogeneous delivery of solid substrate was ensured by continuous stirring of the feed vessel and an appropriate flow rate which did not allow S^0 to settle in the tubing. In contrast, cell mass for proteomic comparison of *A. caldus* sessile versus planktonic

[1]http://metacyc.org/

[2]http://www.genome.ad.jp/kegg/

[3]http://www.ncbi.nlm.nih.gov/COG/

[4]http://www.ncbi.nlm.nih.gov/genome/

[5]http://genome.jgi-psf.org/programs/bacteria-archaea/index.jsf

growth was grown in 1 L batch cultures with initial pH 2.5. Sessile and planktonic bacteria from batch cultures were harvested in mid exponential growth phase according to planktonic cell counts (pH at collection was 1.3–1.4). Planktonic cells from batch or continuous culture were harvested at 4750 g for 10 min followed by a washing step in MSM pH 2.5. For the continuous culture grown on S^0, the remaining S^0 particles were separated from planktonic cells by pelleting at 450 g for 30 s which only removed the S^0 but left planktonic cells in the supernatant (the solid S^0 and any attached cells were discarded). Solid S^0 with sessile bacteria attached was collected from batch cultures and washed four times with MSM pH 2.5 until no planktonic bacteria were detected in the supernatant by microscopic investigation before pelleting at 450 g for 30 s. All cell and S^0 pellets were stored at −80°C.

SEMI QUANTITATIVE RNA TRANSCRIPT PROFILES

Primers targeting selected genes putatively involved in ISC metabolism were designed for semi quantitative reverse transcription (RT-) PCR amplification (product sizes 98–530 bp; **Table 1**). RNA was extracted from 100 to 200 mL medium from the continuous cultures with TRI reagent (Ambion) according to the manufacturer's recommendations. Contaminating DNA was digested with RNase-free DNase I (Fermentas) followed by a second extraction with TRI reagent. RNA concentration and purity was measured with a NanoDrop 2000 spectrophotometer (ThermoScientific). In order to rule out DNA contamination, the RNA samples were subjected to PCR using illustra PuRE Taq Ready-To-Go PCR Beads (GE Healthcare). RT-PCR was performed in a two step reaction using RevertAid First Strand cDNA Synthesis Kit (Fermentas) for RT and AccessQuick Master Mix (Promega) for PCR. The RT reaction primed with random hexamers was performed with 1 µg total RNA for 1 h at 45°C using two independent biological samples for each condition. PCR primed with specific primers (**Table 1**) was carried out with 1 µL of RT reaction as template in 25 µL reaction volume in PTC-100 Programmable Thermal Controller (MJ Research Inc.). PCR cycling was started with initial denaturation at 95°C for 5 min, followed by 30 amplification cycles consisting of denaturation at 95°C for 30 s, annealing at primer specific temperatures (**Table 1**) for 30 s, and elongation at 72°C for 2 min 30 s and concluded with 5 min elongation at 72°C (no further increase of PCR product was observed after 31 cycles). A transcription control gene, DNA gyrase (*gyrA*), was used (Takle et al., 2007). PCR products were separated by agarose electrophoresis and quantified with QuantityOne (BioRad). For final analysis, the 2 independent RNA samples (biological replicates) were used as templates for duplicate RT-PCR reactions (technical replicates) which yielded a total of four replications. In a few cases one replicate was not considered for analysis.

Table 1 | Primers used for RNA transcript profiles.

Primer name	Primer sequence	Targeted gene	Product size [bp]	Melting temp. [°C]
ACA0302For	TTCGAGCAACTCCTGCAGACG	*sor*	271	55.5
ACA0302Rev	CGTCCGTCATACCCATGATCC	ACA_0302		
ACA1632For	GATCCAGGCGATTCATATACGG	*doxD*	337	55.5
ACA1632Rev	TGATCCCCATAGCGAAATTAGAG	ACA_1632		
ACA1633For	TTTTGCGCGTTTGTACCTACCC	*tth*	223	55.5
ACA1633Rev	AACGCCGTCTACTTGAGCTCC	ACA_1633		
ACA2312For	TGGCGATCTTACCTTGAGCGAGG	*soxA*-I	436	55.5
ACA2312Rev	TGCGCTCTGCCCCAAAAGTGG	ACA_2312		
ACA2392For	ATCTACCCTTCGACAAGTATGC	*soxA*-II	527	55.5
ACA2392Rev	TGTGCCGTCTCGCCTTGCAAG	ACA_2392		
ACA2317For	GAAGCCGGTACTGATCAACAAG	*soxB*-I	437	55.5
ACA2317Rev	CGTGTACTCCGTAACCGTAACC	ACA_2317		
ACA2394For	TCCGTCCTCAACCAGACGCCC	*soxB*-II	467	55.5
ACA2394Rev	ACAGCGATTTTGCGACCGCTG	ACA_2394		
ACA2319For	CTCGCGCCGCAAATGTTCCCG	*soxY*-I	180	55.5
ACA2319Rev	TGATCGACATCCACGGTAACCG	ACA_2319		
ACA2390For	ATCGGCACAAGCCTCGTTGCG	*soxY*-II	340	55.5
ACA2390Re2	CTGGGGTGAGATCGAACTGGC	ACA_2390		
ACA2313For	GTGCAGTTTATTTACGACCCGG	*soxX*-I	98	58
ACA2313Rev	ACCAAGCCAATCTGGTGATCCG	ACA_2313		
ACA2389For	ACTCGATACCATCGTTCGTGC	*soxX*-II	256	58
ACA2389Rev	TCTGGAACATCTGCTGGAAGG	ACA_2389		
ACA2318For	AGAGGTCCGTTCGTTGATCATG	*soxZ*-I	269	58
ACA2318Rev	TCAGGCGACGGTGATCTTTGCC	ACA_2318		
ACA2391For	ATGGCAGACAATATTGGTAACCC	*soxZ*-II	197	58
ACA2391Rev	TCGATGTCCAGCAGCTTTGCAC	ACA_2391		
ACAgyrA-F4	CAGCCTCGAAAAAGAAATGC	*gyrA*	431	55.5
ACAgyrA-R4	CCACCTCCTTCTCGTCGTAG	ACA_1592		

A. CALDUS PROTEOMICS ANALYSIS

For the preparation of the total soluble proteome, cell pellets from 200 mL culture were re-suspended in lysis buffer (7 M urea, 2 M thiourea, 30 mM Tris, 1 mM EDTA, 1.5% Triton X-100, pH 8.5), broken by sonication (2 min, 5 s pulse, 5 s break, 30% amplitude), cell debris removed by centrifugation (10 min, 10 000 rpm, 4°C), and the lysate stored at −80°C. Isoelectric focusing (IEF) was performed using pre-cast, 18 cm, Immobiline DryStrip IPG gels (GE Healthcare) with a non-linear pH gradient from 3 to 10 in an Ettan IPGphor IEF unit (GE Healthcare). Protein samples (200 μg) were applied to the IPG strip in rehydration buffer (7 M urea, 2 M thiourea, and 1.5% Triton X-100) with 1.45% dithiothreitol (DTT) and 0.5% IPG buffer (GE Healthcare). After passive rehydration for 16 h at 25°C, IEF was run for a total of 42 kVh with stepwise increasing voltage according to supplier's recommendation. Following IEF, the gel strips were equilibrated in two steps using equilibration buffer (75 mM Tris, 6 M urea, 30% glycerol, 2% SDS) with additional 100 mM DTT in the first step and equilibration buffer with 2.5% iodoacetamide in the second step. The gel strips were then applied to 12% Duracryl (NextGene Genomic Solutions) SDS-polyacrylamide gels and sealed with 1.5% (wt/vol) agarose solution containing bromophenol blue. Electrophoresis was run in an Ettan DALTsix apparatus (GE Healthcare). The gels were fixed and stained to saturation with colloidal Coomassie (Anderson, 1991). After staining was completed the gels were scanned using Image Scanner (GE Healthcare) and analyzed using image analysis software Melanie 7.03 (Genebio). The membrane enriched fractions were prepared according to Molloy (2008). In brief, crude cell extracts were obtained by sonication in Tris buffer (50 mM Tris pH 8.0, 0.5 mM EDTA) and enriched for bacterial membranes by incubation at 4°C for 1 h in 100 mM Na_2CO_3 and subsequent ultracentrifugation at 170 000 g for 70 min. This carbonate extraction in combination with membrane solubilization and 2D gel electrophoresis has been used for the recovery of outer membrane proteins of Gram-negative bacteria (Molloy et al., 2000, 2001; Phadke et al., 2001). The pellets were washed with 50 mM Tris buffer pH 8.0 and re-suspended overnight at 4°C in rehydration buffer. The protocol for 2D gels was the same as above except that 24 cm IPG strips were used and IEF was run for a total of 59 kVh. For the preparation of the soluble protein fraction from sessile bacteria it was necessary to detach the cells from the S^0 prior to protein extraction and 2D gel electrophoresis (as above). The method for cell detachment by Gehrke et al. (1998) was modified. In brief, the S^0 with sessile cells was incubated with a detergent solution pH 7.0 (0.01 mM 3-(Decyldimethylammonio)propanesulfonate inner salt (SB 3–10; Sigma), 10 mM Tris, 1 mM EDTA) for 5 min at room temperature with occasional vortexing before pelleting the S^0 by centrifuging at 450 g for 30 s. The treatment was repeated four times and supernatants containing the detached cells pooled and cells collected before proteomic analysis (as above). All gels of the same condition were run in triplicate.

Protein spots were regarded as differentially expressed if they showed the following characteristics: (i) reproducibility in all three gels of the same condition; (ii) the fold change between the two conditions was ≥2.0; and (iii) the fold change between conditions was significant with a probability of 95% according to one-way ANOVA testing. Spots of interest were excised from the gel, destained, and digested with sequencing grade modified trypsin (Promega) according to standard procedures for matrix-assisted laser desorption/ionization time-of-flight (MALDI-ToF) mass spectrometry (Shevchenko et al., 1996; Pandey et al., 2000). Subsequently, tryptic digests were spotted on a MALDI target plate and co-crystallized with α-cyana-4-hydroxy-cinnamic acid solution (Agilent Technologies). Mass spectra were acquired with a Voyager DE-STR mass spectrometer (Applied Biosystems) and analyzed using DataExplorer (Applied Biosystems). External calibration with premixed standard peptides (Sequenzyme Peptide Mass Standard Kit, Applied Biosystems) was performed. Peptide mass fingerprints (PMFs) of mass spectra were searched against a local database containing the *A. caldus*^{T} draft genome sequence (NZ_ACVD00000000.1) using Mascot with the following search parameters: (i) two missed cleavages; (ii) peptide mass tolerance of 50 ppm; and (iii) variable modifications [carbamidomethyl (C), oxidation (M), propionamide (C)]. Hits in the local database with a Mowse score > 47 were significant at a confidence level of 95%. Two samples were analyzed by Edman degradation performed at the Protein Analysis Center, Karolinska Institute, Stockholm, Sweden. For more detailed functional information of identified proteins the Biocyc database[6] was queried and InterProScan signature recognition search[7] was performed.

In order to rule out any contaminating proteins originating from the biological S^0, 2D gels were run from samples prepared by suspending the S^0 in lysis buffer and sonicating. Control gels were stained with silver (Blum et al., 1987) and no protein spots were detected (data not shown).

RESULTS

BIOINFORMATIC RECONSTRUCTION OF *A. CALDUS* ISC METABOLISM

A detailed analysis of the genes present in the draft genome sequence of *A. caldus*^{T} revealed genes for ISC oxidation that are common to *A. ferrooxidans* [sulfide quinone reductase (*sqr*), *doxD*, and *tth*] (Valdes et al., 2008) and other microbial representatives from extreme acidic environments. *A. caldus* also has gene candidates potentially encoding components of the Sox sulfur oxidizing system and Sor, which are not present in its close relative *A. ferrooxidans*. The gene clusters are presented in **Figure 1A** while the bioinformatic reconstruction of *A. caldus* ISC metabolism is presented in **Figure 1B**.

The first documented step in ISC oxidation is the transition of sulfide to S^o. In Gram-negative bacteria, this reaction is carried out by the usually membrane bound Sqr. This reaction can also be catalyzed by membrane bound FCC sulfide dehydrogenase. The enzymatic activity of Sqr (EC 1.8.5.-) has been purified from *A. ferrooxidans* membranes (Wakai et al., 2007). A sulfide oxidizing activity has been identified in *A. caldus* but the enzyme has not been identified (Hallberg et al., 1996b). Furthermore, one of the three *sqr* copies present in the *A. ferrooxidans* genome is reported to be involved in ISC metabolism (Quatrini et al., 2006, 2009). In *A. caldus*, an ortholog of the *sqr* (*sqr*-1) was identified that was divergently oriented from a gene potentially encoding Sor, that participates in the utilization of S^0 as energy source in several

[6]http://biocyc.org/

[7]http://www.ebi.ac.uk/Tools/InterProScan/

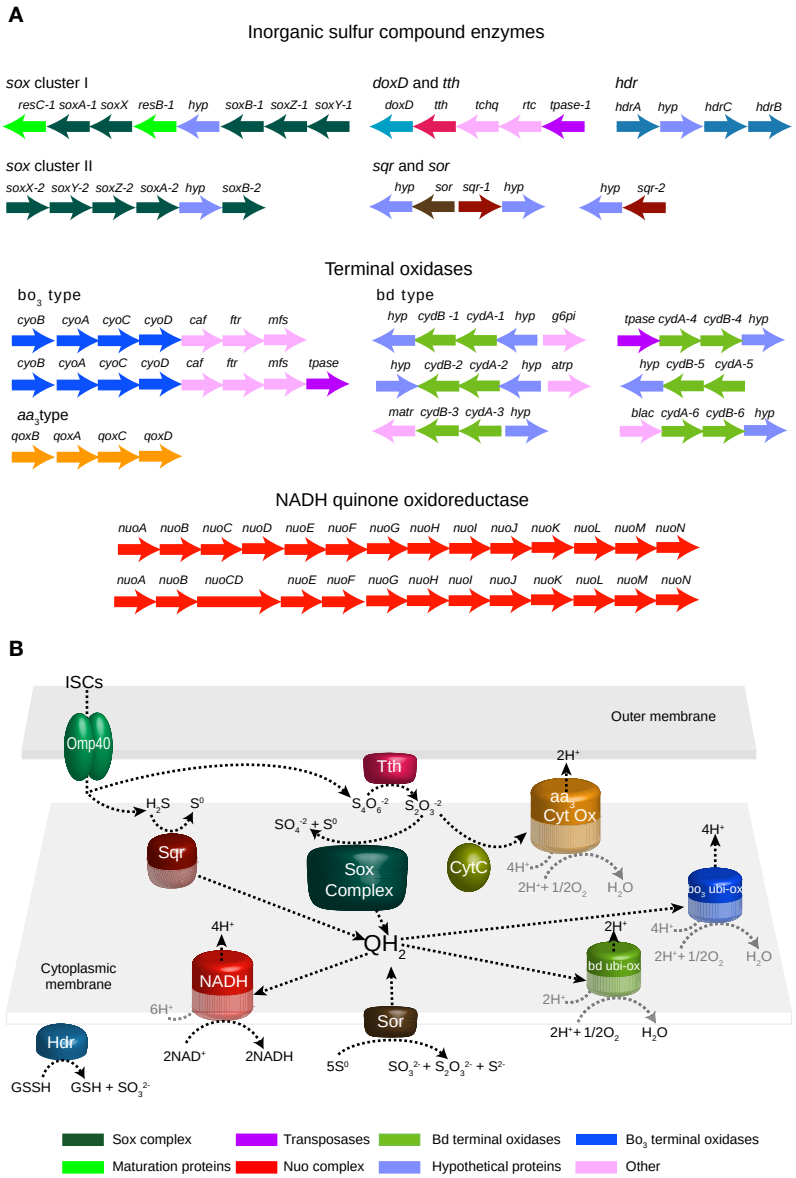

FIGURE 1 | Gene clusters of enzymes potentially involved in inorganic sulfur compound (ISC) metabolism as well as gene clusters of terminal oxidases and the NADH quinone-oxidoreductase complex as predicted by bioinformatic analysis of the *A. caldus* genome sequence (A). Suggested model for ISC metabolism in *A. caldus* (B). Abbreviations: *sox*, sulfur oxidation system; *doxD*, thiosulfate:quinol oxidoreductase; *tth*, tetrathionate hydrolase; *hdr*, heterodisulfide reductase; *sqr*, sulfide quinone reductase; *sor*, sulfur oxygenase reductase; *hyp*, hypothetical protein; *caf*, cytochrome oxidase assembly factor; *ftr*, heme O synthase, protoheme IX farnesyltranferase; *g6pi*, glucose 6-p isomerase; *mfs*, major facilitator superfamily protein; *atrp*, putative amino acid transporter; *matr*, putative malic acid transporter; *blac*, beta lactamase; *tpase*, transposase; *tchq*, two component system – histidine quinase; *rtc*, two component system – response regulator.

organisms (Urich et al., 2004). The product of the *A. caldus sqr*-1 shares 40% similarity with another putative *sqr* ortholog (*sqr*-2) identified in the draft genome sequence. This latter copy has a similar gene context to *sqr-3* from *A. ferrooxidans* and shares a 62% similarity to this protein. Although Sqr representatives belong to a large and considerably variable gene family of the pyridine nucleotide-disulfide oxido-reductases (Pfam: PF07992), the high similarity plus the conservation of gene context observed with *A. ferrooxidans* strongly suggests similar functional properties.

Another enzyme reported to be involved in ISC metabolism is Tth. The activity of this enzyme has been detected in several acidithiobacilli (Hallberg et al., 1996b; Brasseur et al., 2004). An inspection of the draft genome of *A. caldus* reveals the presence of a candidate *tth* upstream of *doxD* (**Figure 1A**). The putative Tth of *A. caldus* shares 71% similarity with the Tth of *A. ferrooxidans*, indicating their high similarity orthologous relationship. The Tth of both sequenced acidithiobacilli have a conserved pyrrolo-quinoline quinone (PQQ) domain (Pfam: PF01011). Although Tth's are

predicted to be external membrane proteins, experimental evidence showed that the *A. caldus* Tth is a soluble periplasmic protein with maximum activity at pH 3 (Bugaytsova and Lindström, 2004). Furthermore, the *tth* gene cluster has been recently studied (Rzhepishevska et al., 2007).

In contrast to the enzymes described above, the Sox sulfur oxidizing system has not been found in any microorganisms from the *Acidithiobacillus* genus. However, the bioinformatics analyses identified the presence of two gene clusters potentially encoding components of the Sox system. The *A. caldus* Sox complex is predicted to be formed by three periplasmic components (referred to as core TOMES): SoxAX, SoxYZ, and SoxB (**Figure 1A**). Our bioinformatics inspection did not identify *soxCD* orthologs in the draft genome sequence of *A. caldus*; however we cannot disregard the presence of these genes until the *A. caldus* genome sequence is finished. Nevertheless, based on the model for ISC metabolism in the green sulfur bacterium *Chlorobaculum tepidum* proposed by Sakurai et al. (2010) it can be predicted that the *A. caldus* core TOMES is able to oxidize thiosulfate with the possible accumulation of S^0 globules in the periplasm and it may be able to oxidize sulfite (Friedrich et al., 2001). No candidates for the enzymes adenylylphosphosulfate (APS) reductase or sulfate adenylyltransferases, which consecutively oxidize sulfite via an indirect pathway, have been found in the genome of *A. caldus*. However, an oxidoreductase molybdopterin-binding protein (ACA_1585) was identified as a possible sulfite oxidizing enzyme catalyzing the direct oxidation of sulfite to sulfate. ACA_1585 has a molybdopterin-binding domain (PF00174) and a twin-arginine translocation pathway signal sequence. It lacks a dimerization domain and an N-terminal heme domain. Furthermore, no additional putative subunits containing heme domains have been detected. ACA_1585 has 26% similarity with the sulfite oxidizing enzyme DraSO from *Deinococcus radiodurans* which was proposed to be a novel sulfite oxidizing enzyme without a heme domain (D'Errico et al., 2006).

Another enzyme involved in *A. caldus* ISC metabolism not found in *A. ferrooxidans* is Sor (one copy of *sor* was identified). The predicted protein shows a characteristic domain of the Sor family (Pfam: PF07682) and all activity-critical residues based on structural and experimental data (Urich et al., 2006). Furthermore, the predicted cytoplasmic location of the *A. caldus* Sor enzyme agrees with experimental data obtained from *A. tengchongensis* and *Escherichia coli* transformants (Chen et al., 2005). The *sor* was found adjacent and divergently arranged from *sqr*-1 (**Figure 1A**). This suggests the presence of potentially shared regulatory regions that could be co-regulating both enzymes, catalyzing successive reactions, and thus providing an adaptive strategy. Recently, the enzyme activity of Sor has been reported to be present in *A. caldus*-like strains (Janosch et al., 2009). However, it is still unknown how its substrate (S_8) is incorporated in to the cell or how the resulting products (S^0, H_2S, and $S_2O_3^{-2}$) are excreted. Furthermore, heterodisulfide reductase (Hdr) has been postulated to be involved in *A. ferrooxidans* S^0 oxidation (Quatrini et al., 2009) and is up-regulated during aerobic growth on solid S^0 (unpublished data). In *A. caldus* two orthologs of each HdrABC subunit have been found. Both putative HdrA subunits (ACA_1473, ACA_2418) are flavoproteins with a FAD binding site and they also contain the conserved four cysteine residues ($CXGXRDX_{6-8}CSX_2CC$) for binding of a Fe–S cluster. The putative HdrB, ACA_2421, contains two typical cysteine rich regions whereas the second putative HdrB subunit, ACA_2417, contains only one such region. The remaining subunit, HdrC, is represented by ACA_2376 and ACA_2420 both containing the 4F–4S ferredoxin iron–sulfur binding domain. ACA_2418, ACA_2421, and ACA_2420 are embedded in the gene cluster *hdrA hyp hdrC hdrB* (**Figure 1A**). All putative *A. caldus* Hdr subunits showed >90% similarity to the respective *A. ferrooxidans* Hdr subunits. As previously shown for *A. ferrooxidans* (Quatrini et al., 2009), the similarity to Hdr of other acidophilic sulfur oxidizers is significant whereas the similarity of the *A. caldus* putative HdrABC to their respective subunits of the methanogenic archaea *Methanothermobacter marburgensis* is only around 30%.

It has been shown that sulfur oxidizing bacteria which lack $Sox(CD)_2$ utilize the reverse dissimilatory sulfite reductase (DsrAB) for the oxidation of S^0 to sulfite (reviewed in Friedrich et al., 2001; Ghosh and Dam, 2009, and Sakurai et al., 2010). In *Allochromatium vinsum*, DsrAB is encoded with 13 other Dsr proteins in a cluster (Dahl et al., 2005) also containing DsrEFH and DsrC. The latter are proposed to be involved in S^0 substrate binding and transport of S^0 from the periplasmic S^0 globules to the cytoplasm (Cort et al., 2008). *Escherichia coli* DsrEFH and DsrC homologs (TusBCD and TusE) interact in a S^0 relay system during 2-thiouridine biosynthesis (Ikeuchi et al., 2006). Although no homologs of *dsr* were found in the *A. caldus* draft genome sequence, several potential DsrE-like proteins containing the characteristic DsrE/DsrF-like family features (Pfam 02635) were detected. All of those were annotated as hypothetical proteins (ACA_0867, ACA_0091, ACA_2522, ACA_0556, ACA_1583, ACA_1441, and ACA_2423) and putatively play a role in S^0 binding and transport. Additionally, several candidates for the transport of extracellular S^0 to the cytoplasm have been proposed for green sulfur bacteria (Frigaard and Bryant, 2008a,b; Sakurai et al., 2010). One possibility is that the thioredoxin SoxW acts together with thiol:disulfide interchange protein DsbD within the periplasm in transferring S^0 across the inner membrane (Sakurai et al., 2010). One candidate gene was predicted that potentially encodes a DsbC ortholog (ACA_2033) with similar functions as DsbD. DsbC thiol:disulfide interchange protein ACA_2033 exhibits a conserved N-terminal domain of the disulfide bond isomerase DsbC family (Pfam10411). It has been reported that members of this protein family are responsible for the formation of disulfide bonds and function as a disulfide bond isomerase during oxidative protein-folding in the bacterial periplasm (Hiniker et al., 2005). No homolog of SoxW has been found in *A. caldus*; however, other thioredoxins might fulfill the same function.

A. caldus is also predicted to contain two gene clusters potentially encoding components of the NADH quinone-oxidoreductase complex (EC 1.6.5.3) as has been observed in *Azotobacter vinelandii* (Bertsova et al., 2001). In addition, six *cydAB* copies possibly encoding subunits of Qox-*bd* (EC 1.10.3.-) terminal oxidase and one gene cluster that might code for a putative *aa_3-type* terminal oxidase were detected. The analysis also revealed the presence of two copies of the cytochrome *o* (*cyoBACD-caf-ftr-mfs*) gene cluster (Cyo-1 and Cyo-2), sharing 89 and 75% similarity with orthologs in *A. ferrooxidans*. This gene redundancy could have several explanations including: (i) to provide regulatory and pathway flexibility to confront environmental changes such as oxygen availability

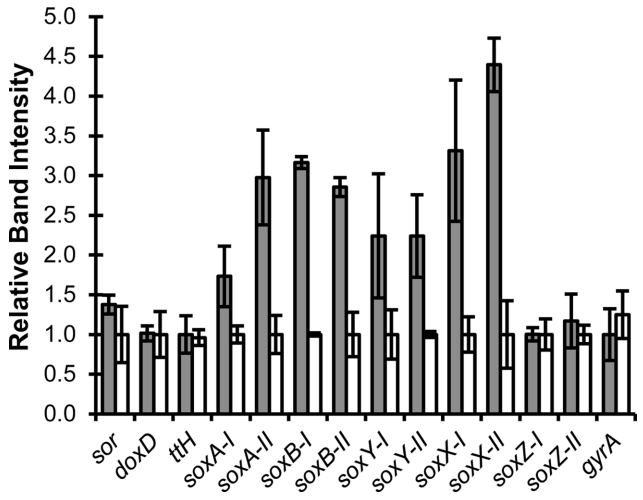

FIGURE 2 | RNA transcript profiles of selected genes predicted to be involved in *A. caldus* inorganic sulfur compound metabolism. Shown are the means of relative band intensities from semi quantitative RT-PCR products of three to four replicates with standard deviations. RNA was extracted from cells grown on tetrathionate (gray columns) or S^0 (white columns).

(*bo* and *bd* complexes have different O_2 affinities); or (ii) to manage ISC oxidizing complexes that introduce electrons at variable places in the electron transport chain (e.g., quinol-level for SQR and cytochrome *c*-level for Sox).

RNA TRANSCRIPT PROFILES OF SELECTED ISC GENES

Reverse transcription-PCR showed that all assayed genes were transcribed during growth on tetrathionate and S^0 (**Figure 2**). No significant changes in transcript levels were detected for *sor*, *doxD*, *tth*, *soxZ*-I, and *soxZ*-II. The remaining *sox* cluster genes were significantly up-regulated during growth on tetrathionate. The similar RNA levels for *soxZ*-I and *soxZ*-II during growth on tetrathionate and S^0 was unexpected as both genes would be expected to be co-transcribed with their respective gene clusters. With the exception of the *soxA* transcript, the transcript levels of both *sox* clusters followed the same trends indicating that both were involved in ISC metabolism. The control gene, *gyrA*, displayed similar transcription levels under both conditions.

PROTEIN EXPRESSION DURING GROWTH ON S^0 VERSUS TETRATHIONATE

Proteomic analysis yielded 115 identifications of differentially expressed protein spots (**Figures 3 and 4**; **Table A1** in Appendix). Forty-three proteins were up-regulated on tetrathionate (12 in soluble and 31 in membrane fraction) and 30 uniquely found on tetrathionate gels (21 in soluble and 9 in membrane fraction). During growth on S^0, 23 protein spots were up-regulated (15 in soluble and 8 in membrane fraction) and 19 were unique (11 in soluble and 8 in membrane fraction). Several protein spots yielded the same identification which indicated protein fragmentation, post translational modification, or the protein was up-regulated in both the soluble and membrane enriched fractions. Protein designations are given in parenthesis with their match ID as designated by Melanie including a capital letter S specifying soluble fraction and M for membrane enriched fractions.

No putative proteins belonging to NADH quinine-oxidoreductase or terminal oxidases were found differentially expressed in the various conditions tested. However, based on the bioinformatic reconstruction the involvement of NADH quinone-oxidoreductase complex and terminal oxidases in the *A. caldus* ISC metabolism was suggested. Therefore, these complexes were represented in the proposed model (**Figure 1B**).

Proteins involved in ISC metabolism

Proteins encoded within the two Sox clusters were up-regulated in gels from tetrathionate grown bacteria including SoxB-I (M793) and hypothetical protein ACA_2320 (S524) encoded in *sox* cluster I; as well as SoxA-II (S356, S538, S539), SoxZ-II (S10), and hypothetical protein ACA_2393 (S34) from *sox* cluster II. These findings clearly suggest an involvement of proteins encoded by both Sox clusters in ISC metabolism during growth on tetrathionate. Furthermore, both Sqr-1 (S260) and Sqr-2 (M300) were identified as up-regulated on tetrathionate. A DsrE/F-like hypothetical protein ACA_0867 (S17, S518, M13), potentially involved in S^0 binding and transport, was up-regulated on tetrathionate and subunit C of CoB–CoM heterodisulfide reductase (S543, S544; ACA_2420) was a unique protein spot on tetrathionate gels. In contrast, HdrA (S462; ACA_2418) was found as a unique protein spot in S^0 gels while the DsrE/F-like hypothetical protein ACA_1583 (S9) and DsbC thiol:disulfide interchange protein ACA_2033 (S358) were up-regulated on S^0.

General trends in the proteome of tetrathionate grown A. caldus

Several proteins relevant in signal transduction were up-regulated in tetrathionate grown cells, i.e., chemotaxis protein CheV (S151, M735), putative sensory histidine kinase YfhA (S577), nitrogen regulation protein NRI (M 776), and hypothetical protein ACA_1270 (M277) containing a PAS domain fold involved in signaling proteins. However, the signature feature of the tetrathionate grown proteome was up-regulation of proteins involved in central carbon metabolism, cell division, amino acid biosynthesis, fatty acid biosynthesis, translation, and DNA repair. The up-regulated central carbon metabolism proteins included aspartate aminotransferase (S571), dihydrolipoamide dehydrogenase (S594), fructose bisphosphate aldolase (M248), and phophoglucomutase (M368). A few proteins of central carbon metabolism were up-regulated in S^0 grown cells those including 6-phosphogluconate dehydrogenase (S154) and HAD-superfamily hydrolase (M71). Proteins involved in cell division were solely found up-regulated on gels of tetrathionate grown cells such as FtsA (M262), FtsZ (M227), and FtsH (M386, M388, M513). Four proteins involved in amino acid biosynthesis and degradation (S549, S694, M353, M755) and three involved in fatty acid biosynthesis (M179, M309, M726) were up-regulated in tetrathionate grown cells. No proteins of this group were up-regulated in S^0 grown cells. Another characteristic group consisted of translation related proteins which included two different translation elongation factors (S217, S388, M254, M521), four different tRNA synthetases (S572, S625, M431, M508), and one amidotransferase (S702) up-regulated on tetrathionate; whereas only one ribosomal protein (S338) was detected up-regulated in S^0 grown cells. Proteins involved in DNA repair included a MutS2 family protein identified in two protein spots (M344, M781) and DNA repair protein RecN (M362).

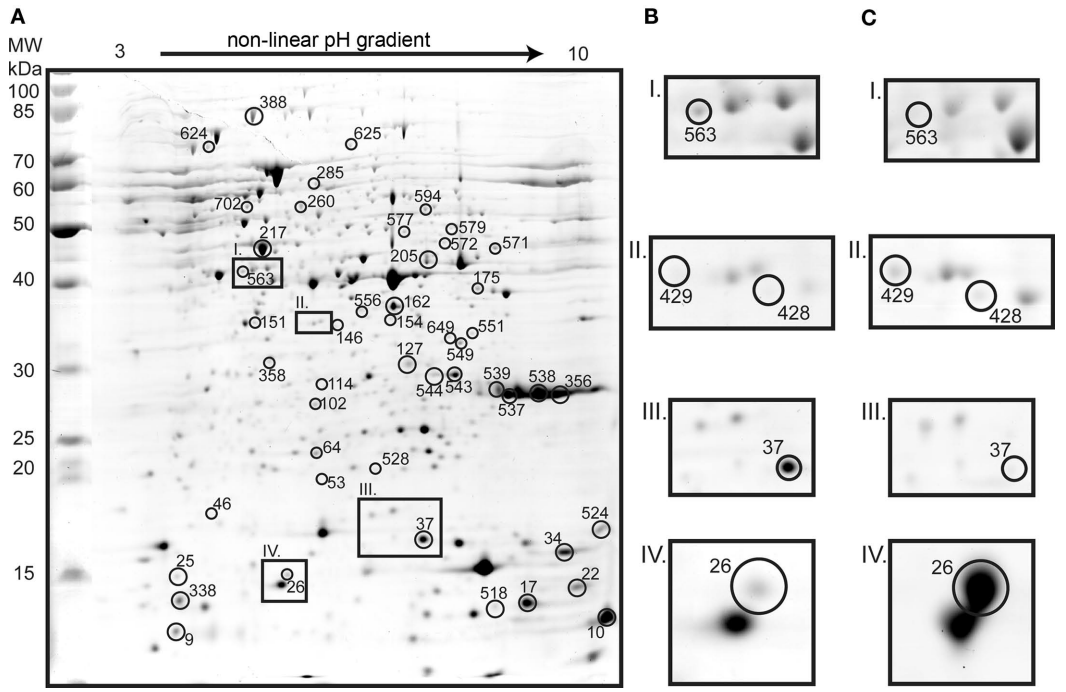

FIGURE 3 | Two dimension gel of the *A. caldus* soluble proteome from cells grown on tetrathionate (**A**; identified spots are marked with circles and the numbers indicate match IDs given without S in the figure). Inset frames show tetrathionate **(B)** and S^0 **(C)** conditions: Radical SAM domain protein (spot S563) unique in tetrathionate grown cells (I); heat shock protein GroEL (S429 and S428) unique in S^0 grown cells (II); twin-arginine translocation protein TatA (S37) which was 3.8-fold up-regulated in tetrathionate (III); and heat shock protein Hsp20 (S26) that was 8.6-fold up-regulated in S^0 grown cells (IV).

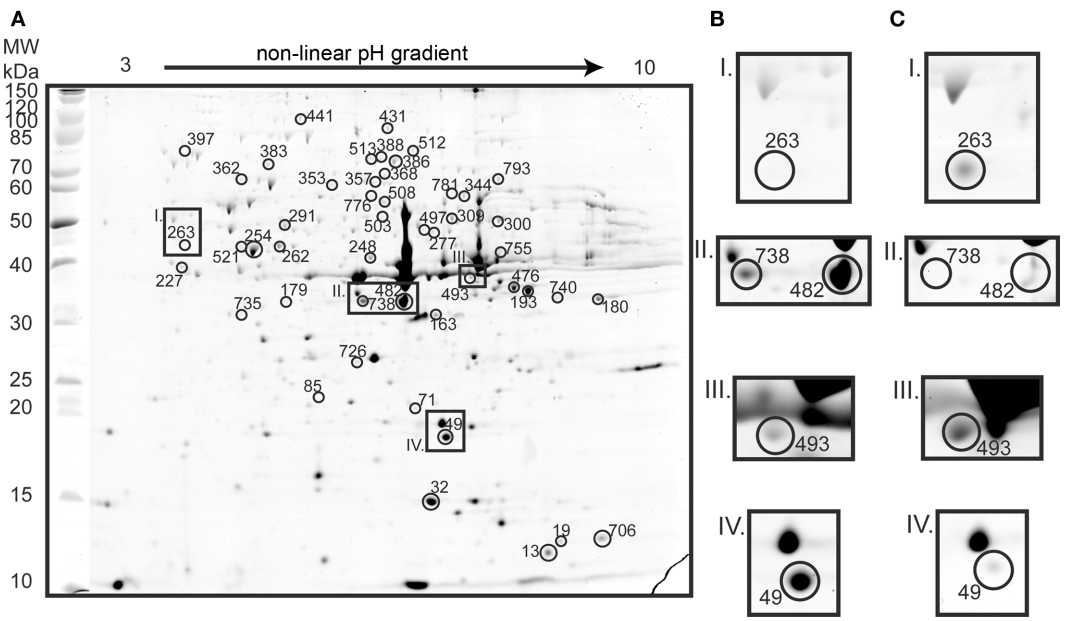

FIGURE 4 | Two dimension gel of the *A. caldus* membrane enriched proteome on tetrathionate (**A**; identified proteins indicated with circles and match IDs given without M in the figure). Inset frames are presented for tetrathionate **(B)** and for S^0 **(C)** conditions: Carboxysome shell protein CsoS1 (spot M263) that was 6.1-fold up-regulated in S^0 grown cells (I); two spots identified as hypothetical protein ACA_1144 that were unique (M738) and 10.7-fold up-regulated (M482) in gels from tetrathionate grown cells (II); type 1 secretion outer membrane protein (M493) that was 2.4-fold up-regulated in S^0 grown cells (III); and a putative lipoprotein (M49) which was 10.3-fold up-regulated on tetrathionate (IV).

Increased expression of proteins with central functions is commonly attributed to an increased growth rate. However, the samples originated from continuous cultures grown at identical dilution rates, meaning that bacteria were theoretically maintained at the same growth rate. Therefore, it was more likely that the observed trends signified down-regulation of central functions in the S^0 grown cells due to a stress response. Nevertheless, the observed results motivated the proteomic investigation of sessile and planktonic *A. caldus* grown in S^0 batch cultures as only the planktonic sub-population was investigated for the comparison of growth on tetrathionate and S^0.

General trends in the proteome of S^0 grown A. caldus

The most striking characteristic of the proteome of S^0 grown cells was the high number of up-regulated chaperones and proteases: GroEL (S114, S146, S409, S413, S416, S425, S428, S429, S435, S436), heat shock protein Hsp20 (S26, S46), DnaK (M397), ClpB (M441), and protease Do (M605). In contrast, the only chaperone up-regulated during growth on tetrathionate was HscA (S624). This indicated a stress response during growth on S^0. It should be noted that GroEL has been detected in many protein spots most of them with low molecular weight in 2D gels (**Figure 3**, **Table A1** in Appendix) indicating fragmentation of the protein. The cause of this fragmentation remains unknown. A second distinguishing feature of the S^0 grown proteome was up-regulation of proteins involved in CO_2 fixation, namely ribulose bisphosphate carboxylase large chain (M503) and carboxysome shell protein CsoS1 (M263, M530). However, the reasons for up-regulation of proteins related to CO_2 fixation remain unclear. Additionally, stringent starvation protein A (S102) and flagella basal-body rod protein FlgC (S205) were up-regulated on S^0. Stringent starvation protein A is believed to be important for stress response during stationary phase and nutrient limitation in *E. coli* (Williams et al., 1994). The up-regulation of FlgC which is part of the basal body in flagella points at an increase of flagella and the importance of cell motility in S^0 grown cells to be able to attach to the solid substrate.

Proteins up-regulated under both conditions

In one case, a two component protein was identified in both conditions whereas in other cases proteins sharing a similar function could not be clearly attributed to either condition. Those included proteins involved in protein transport such as an efflux transporter (M180, M740) and Twin-arginine translocation protein TatA (S37, M32) which were up-regulated in tetrathionate grown cells. While in S^0 grown cells protein export chaperone (S25) and Type I secretion outer membrane protein, TolC precursor (M497) were up-regulated. A two component protein was found up-regulated on tetrathionate (M291) and as a unique spot in S^0 gels (M607). The two spots were in close proximity on the gels; however the unique spot traveled with slightly larger molecular weight and more basic isoelectric point suggesting post translational modification. This protein is encoded together with the signal transduction histidine kinase up-stream of *sox* cluster II indicating that this two component system might be involved in its regulation.

PROTEIN EXPRESSION DURING PLANKTONIC VERSUS SESSILE GROWTH ON S^0

In 2D gels of planktonic *A. caldus*, three up-regulated and three unique protein spots were identified. Based on characteristic peaks in mass spectra an additional six protein spots up-regulated in planktonic cells were revealed to be the same protein. The identification of this protein could neither be determined by MALDI-ToF nor by Edman degradation. From gels of sessile cells, 22 up-regulated protein spots were identified (**Figure 5**; **Table A2** in Appendix).

Several of the proteins identified from planktonic cells were also found up-regulated in tetrathionate grown cells, i.e., TatA (64), Sqr-1 (492), and hypothetical protein ACA_0867 (826 and 827). In addition, SoxY-I (841) and hypothetical protein ACA_2219 (118) were identified. Proteins up-regulated in gels of sessile cells comprised characteristic proteins from tetrathionate grown and S^0 grown proteomes as well as proteins not identified from other gels. S^0 characteristic proteins included the chaperones GroEL and DnaK (329, 541, 543, and 556), HdrA (382; ACA_2418), and proteins involved in CO_2 fixation such as ribulose bisphosphate carboxylase large chain (258) and rubisco activation protein CbbQ (280). Tetrathionate associated proteins consisted of peptidyl-prolyl cis-trans isomerase ppiD (213), CoB–CoM HdrC (238; ACA_2420), proteins involved in amino acid biosynthesis (442, 447, 455, 515), two central carbon metabolism proteins (364, 408), and a single-stranded DNA-binding protein involved in DNA replication (70). The up-regulation of proteins involved in amino acid biosynthesis and central carbon metabolism suggests that sessile cells are less starved than planktonic cells. CoB–CoM HdrB (395; ACA_2421) was not previously detected but was found up-regulated in gels of sessile bacteria. Additionally, twitching motility protein (325) and 40-residue YVTN family β-propeller repeat protein (404) were up-regulated in gels of sessile cells. Twitching motility protein is required for twitching motility and social gliding which allows Gram-negative bacteria to move along surfaces (Merz et al., 2000). The YVTN domain is present in surface layer proteins of archaea (Jing et al., 2002) which protect cells from the environment and have been shown to be involved in cell to cell association in *Methanosarcina mazei* (Mayerhofer et al., 1998).

DISCUSSION

ISC METABOLISM IN *A. CALDUS*

A model has been constructed for ISC oxidation and electron transport based upon gene predictions and proteomics data (**Figure 1B**). Tetrathionate is hydrolyzed by a periplasmic Tth with a DoxD component (Hallberg et al., 1996b; Bugaytsova and Lindström, 2004; Rzhepishevska et al., 2007). Previously, the genes encoding Tth and DoxD were shown to be up-regulated during growth on tetrathionate as compared to growth on S^0. However, this study showed the same expression levels of *tth* and *doxD* in the semi quantitative RT-PCR. Additionally, neither protein was detected in the proteomics investigation suggesting that protein levels were also similar. A possible explanation for the discrepancy between this and the previous report (Rzhepishevska et al., 2007) is that gene transcription of *tth* and *doxD* might be different in the sub-populations of S^0 grown sessile and planktonic cells (potentially explaining the previously reported large standard deviations Rzhepishevska et al., 2007). The

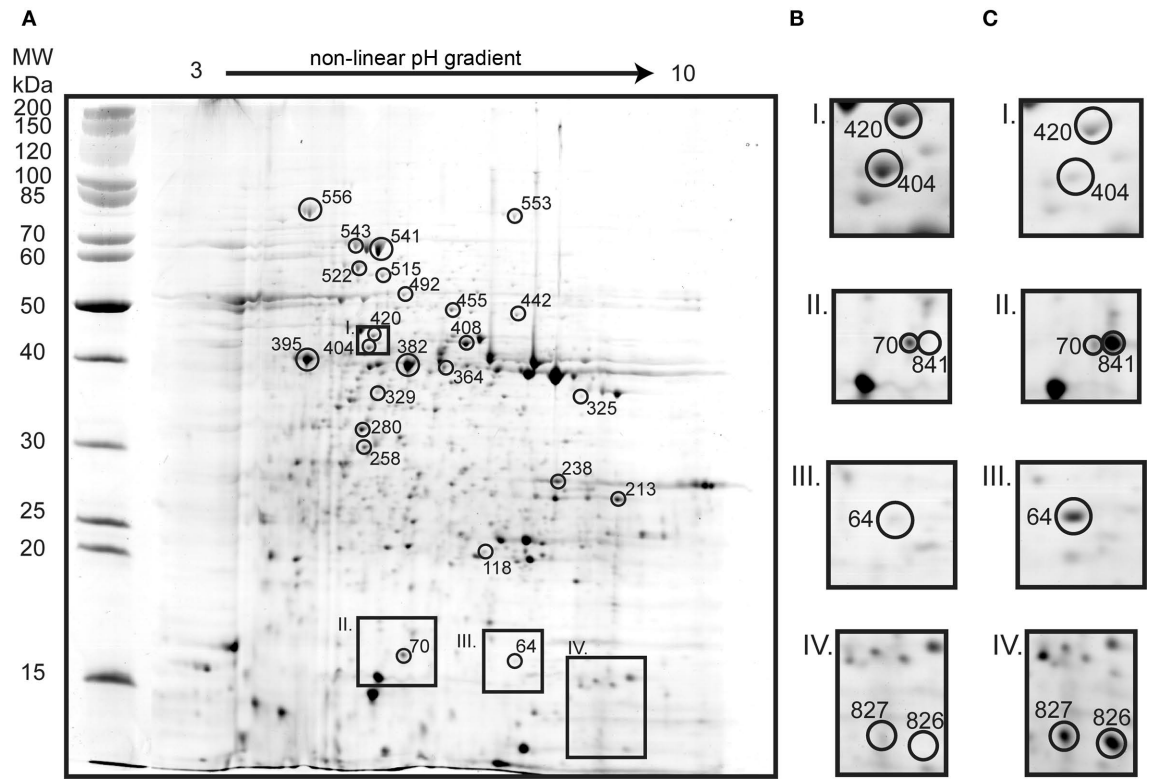

FIGURE 5 | Two dimension gel of the *A. caldus* soluble proteome of sessile cells grown on S^0 (**A**; identified proteins marked with circles and match IDs). Inset frames show sessile **(B)** and planktonic **(C)** conditions: *S*-adenosylmethionine synthetase (spot 420) and YVTN family beta-propeller repeat protein (404) that were 2.4 and spot 7.7-fold up-regulated in sessile cells (I); single-stranded DNA-binding protein (70) 3.1-fold up-regulated in sessile cells and sulfur oxidation protein SoxY (841) unique in gels from planktonic cells (II); twin-arginine translocation protein TatA (64) was up-regulated 7.9-fold in planktonic cells (III); and hypothetical protein ACA_0867 (spots 827 and 826) uniquely found in planktonic cells (IV).

role of the DoxD component is unknown as it lacks the DoxA of the thiosulfate quinine-oxidoreductase and Tth is thought to be a hydrolase (Bugaytsova and Lindström, 2004; Rzhepishevska et al., 2007). Therefore, the main product of Tth in the proposed model, thiosulfate, was suggested to be oxidized by the *A. caldus* SoxABXYZ system. The experimental data supports this view with up-regulated transcripts of both *sox* clusters as well as up-regulation of several gene products during growth on tetrathionate. As homologs of neither $Sox(CD)_2$ nor DsrAB were detected in the genome sequence of *A. caldus* to date it is proposed that the products of its core TOMES are sulfate and S^0. This aspect is further strengthened by the observation that thiosulfate oxidation has a S^0 intermediate (Hallberg et al., 1996b) and that S^0 globules have been detected in *A. caldus* when under sub-optimal conditions (Hallberg et al., 1996a). Also, sulfur globules are an obligate intermediate in *A. vinosum* thiosulfate oxidation (Pott and Dahl, 1998; Dahl et al., 2005).

The metabolism of S^0 is complicated by its hydrophobic nature which makes an activation of S^0 prior to its oxidation necessary. Potentially the DsbC (up-regulated in S^0 grown cells) was involved in transferring the S^0 equivalent from the membrane to the S^0 oxidizing enzyme as suggested for green sulfur bacteria (Sakurai et al., 2010). Additionally, it has also been suggested that sulfane sulfur is the actual substrate of the sulfur oxidizing enzyme (SDO or Hdr) in *A. ferrooxidans* (Rohwerder and Sand, 2003; Quatrini et al., 2009). The substrate for Sor is believed to be sulfur in a linear form, probably as a polysulfide. Furthermore, two hypothetical DsrE/F-like proteins were detected in the proteomics, one up-regulated on tetrathionate and the other on S^0 which might be involved in the transfer of sulfane sulfur in the course of S^0 oxidation (Dahl et al., 2005). One candidate for S^0 oxidation is Sor that catalyzes the disproportionation of S^0 to sulfite, thiosulfate, and sulfide (potentially explaining the up-regulation of Sqr in cells grown on less reduced forms of sulfur). In this study, RT-PCR data demonstrated similar levels of *sor* transcripts for growth on tetrathionate and S^0 suggesting it may be involved in ISC oxidation. A second candidate for S^0 oxidation is the trimeric complex HdrABC suggested to be involved in *A. ferrooxidans* S^0 metabolism by utilizing the proton gradient to oxidize disulfide intermediates originating from S^0 oxidation to sulfite (Quatrini et al., 2009). To date, this reverse reaction of HdrABC is purely speculative and awaits biochemical evidence. Yet, the similarities of HdrABC within acidophilic sulfur oxidizers are striking and might point to this new function of the enzyme. Additionally, *A. ferrooxidans* Hdr has been shown to be up-regulated during growth on S^0 (Quatrini et al., 2009 and unpublished data). In this study HdrA was up-regulated in S^0 grown *A. caldus*, whereas HdrC was up-regulated in tetrathionate grown cells. However, all subunits HdrABC were up-regulated in sessile compared to

planktonic cells. In our model both Sor and Hdr can oxidize S^0 and are hypothesized to comprise multiple pathways. The potential use of Hdr and/or Sor in *A. caldus* S^0 oxidation remains to be resolved. Sor or Hdr might be employed in variable growth conditions or for different (internal or external) sources of S^0. For instance, the Sor enzyme identified in *A. caldus*-like strains has an increased activity at 65°C (Janosch et al., 2009) suggesting it may be used at higher growth temperatures. The observation that DsbE-like proteins and different subunits of Hdr were up-regulated in both conditions might point to the fact that tetrathionate oxidation has a S^0 intermediate (Hallberg et al., 1996b). Following the reaction of either Sor or Hdr, the produced sulfite is oxidized to sulfate. Although no candidate for a sulfite oxidizing enzyme was detected in the proteomics a sulfite oxidase activity has been reported for *A. caldus* (Hallberg et al., 1996b) and a candidate for a sulfite oxidizing enzyme without heme domain was detected in the genome sequence. No biochemical evidence (Dopson et al., 2002) or putative gene candidates were found for involvement of the adenosine monophosphate system.

Clear trends in the protein expression of cells grown on tetrathionate versus S^0 were observed. In S^0 grown cells this included up-regulation of chaperones and a protease and down-regulation of proteins involved in central carbon metabolism, amino acid biosynthesis, fatty acid biosynthesis, cell division proteins, and DNA repair. The latter changes can be attributed to the cell's effort to conserve energy which is a feature of the general stress response.

SESSILE VERSUS PLANKTONIC *A. CALDUS*

It is believed that the stress response observed in S^0 grown sessile cells (compared to planktonic) was due to a biological phenomenon and not due to sample treatment. Several points argue in favor of this view: (i) the stress response was also apparent in S^0 grown cells when compared to tetrathionate grown cells although the treatment for both conditions was identical; and (ii) sessile cells were frozen prior to detachment which probably killed most cells conserving their proteome and making changes in the proteome of sessile cells during detachment treatment unlikely.

The *A. caldus* planktonic proteome contained up-regulated proteins similar to the expression pattern of tetrathionate grown cells; whereas, the sessile proteome contained up-regulated proteins that were described to be signature proteins of tetrathionate and S^0 grown cells. Possibly cells attached to S^0 are less starved than planktonic cells (up-regulation of proteins from central carbon metabolism) but generally more stressed than planktonic cells (up-regulation of chaperones). All three Hdr subunits were up-regulated in the sessile cells suggesting they oxidize S^0. In contrast, the planktonic sub-population may oxidize soluble ISCs (e.g., tetrathionate) potentially released from sessile cells. The growth medium of *A. caldus* grown on S^0 was tested for tetrathionate and thiosulfate. Neither compound could be detected during growth for 10 days (data not shown) potentially because the soluble ISCs were oxidized by planktonic cells before they accumulated to a detectable concentration. In addition, proteins were detected, such as a twitching motility protein involved in sessile cell motility (Merz et al., 2000) and a YVTN family beta-propeller repeat protein possibly involved in cell-to-cell interactions (Mayerhofer et al., 1998) that might also be involved in attachment to the solid substrate. Although no flagellar proteins were found up-regulated in the proteomic comparison of sessile versus planktonic cells the up-regulation of flagellar basal-body rod protein FlgC in the comparison between tetrathionate and S^0 grown cells indicated the importance of cell motility to be able to attach to the solid substrate.

Typically, planktonic and sessile sub-populations are stable (Vilain et al., 2004b) and their proteomes include many differentially expressed proteins (Vilain et al., 2004a). The proteomes and transcriptomes of biofilms have been widely studied in several neutrophilic organisms (Sauer and Camper, 2001; Oosthuizen et al., 2002; Sauer et al., 2002; Planchon et al., 2009). A transcriptomic study of biofilm and planktonic *Leptospirillum* spp. suggests acidophile biofilms are, similarly to neutrophilic biofilms, dynamic structures with distinct metabolic differences between planktonic and biofilm cells (Moreno-Paz et al., 2010). The reported differences in the proteomes between sessile and planktonic *A. caldus* sub-populations comprised a comparatively small number of differentially expressed proteins. In this case study, it may be possible that planktonic and sessile sub-populations interchanged (possibly due to vigorous stirring and shear forces exerted by the solid S^0 particles) that resulted in relatively similar proteomes.

ACKNOWLEDGMENTS

Mark Dopson wishes to thank the Swedish Research Council for financial support (Vetenskapsrådet contract number 621-2007-3537). David S. Holmes acknowledges Fondecyt 1050063, DI-UNAB 34-06, DI-UNAB 15-06/I, and a Microsoft Sponsored Research Award.

REFERENCES

Altschul, S. F., Madden, T. L., Schaffer, A. A., Zhang, J., Zhang, Z., Miller, W., and Lipman, D. J. (1997). Gapped BLAST and PSI-BLAST: a new generation of protein database search programs. *Nucleic Acids Res.* 25, 3389–3402.

Anderson, N. L. (1991). *Two Dimensional Gel Electrophoresis: Operation of the ISO-DALT System.* Rockville, MD: Large Scale Biology Press.

Bathe, S., and Norris, P. R. (2007). Ferrous iron- and sulfur-induced genes in *Sulfolobus metallicus*. *Appl. Environ. Microbiol.* 73, 2491–2497.

Bertsova, Y. V., Bogachev, A. V., and Skulachev, V. P. (2001). Noncoupled NADH:ubiquinone oxidoreductase of *Azotobacter vinelandii* is required for diazotrophic growth at high oxygen concentrations. *J. Bacteriol.* 183, 6869–6874.

Blum, H., Beier, H., and Gross, H. J. (1987). Improved silver staining of plant-proteins, RNA and DNA in polyacrylamide gels. *Electrophoresis* 8, 93–99.

Bodadilla Fazzini, R. A., and Parada, P. (2009). Analysis of sulfur metasecretome in mixed cultures of *Acidithiobacillus thiooxidans* and *Acidithiobacillus ferrooxidans*. *Adv. Mat. Res.* 71–73, 151–154.

Brasseur, G., Levican, G., Bonnefoy, V., Holmes, D., Jedlicki, E., and Lemesle-Meunier, D. (2004). Apparent redundancy of electron transfer pathways via bc_1 complexes and terminal oxidases in the extremophilic chemolithoautotrophic *Acidithiobacillus ferrooxidans*. *Biochim. Biophys. Acta* 1656, 114–126.

Bru, C., Courcelle, E., Carrère, S., Beausse, Y., Dalmar, S., and Kahn, D. (2005). The ProDom database of protein domain families: more emphasis on 3D. *Nucleic Acids Res.* 33, D212–D215.

Bryson, K., McGuffin, L. J., Marsden, R. L., Ward, J. J., Sodhi, J. S., and Jones, D. T. (2005). Protein structure prediction servers at University College London. *Nucleic Acids Res.* 33, W36–W38.

Bugaytsova, Z., and Lindström, E. B. (2004). Localization, purification and properties of a tetrathionate hydrolase from *Acidithiobacillus caldus*. *Eur. J. Biochem.* 271, 272–280.

Cardenas, J. P., Valdes, J., Quatrini, R., Duarte, F., and Holmes, D. S.

(2010). Lessons from the genomes of extremely acidophilic bacteria and archaea with special emphasis on bioleaching microorganisms. *Appl. Microbiol. Biotechnol.* 88, 605–620.

Chen, Z. W., Jiang, C. Y., She, Q., Liu, S. J., and Zhou, P. J. (2005). Key role of cysteine residues in catalysis and subcellular localization of sulfur oxygenase-reductase of *Acidianus tengchongensis*. *Appl. Environ. Microbiol.* 71, 621–628.

Cort, J. R., Selan, U., Schulte, A., Grimm, F., Kennedy, M. A., and Dahl, C. (2008). *Allochromatium vinosum* DsrC: solution-state NMR structure, redox properties, and interaction with DsrEFH, a protein essential for purple sulfur bacterial sulfur oxidation. *J. Mol. Biol.* 382, 692–707.

D'Errico, G., Di Salle, A., La Cara, F., Rossi, M., and Cannio, R. (2006). Identification and characterization of a novel bacterial sulfite oxidase with no heme binding domain from *Deinococcus radiodurans*. *J. Bacteriol.* 188, 694–701.

Dahl, C., Engels, S., Pott-Sperling, A. S., Schulte, A., Sander, J., Lubbe, Y., Deuster, O., and Brune, D. C. (2005). Novel genes of the Dsr gene cluster and evidence for close interaction of Dsr proteins during sulfur oxidation in the phototrophic sulfur bacterium *Allochromatium vinosum*. *J. Bacteriol.* 187, 1392–1404.

de Jong, G. A. H., Hazeu, W., Bos, P., and Kuenen, J. G. (1997). Polythionate degradation by tetrathionate hydrolase of *Thiobacillus ferrooxidans*. *Microbiology* 143, 499–504.

Dopson, M., and Lindström, E. B. (1999). Potential role of *Thiobacillus caldus* in arsenopyrite bioleaching. *Appl. Environ. Microbiol.* 65, 36–40.

Dopson, M., and Lindström, E. B. (2004). Analysis of community composition during moderately thermophilic bioleaching of pyrite, arsenical pyrite and chalcopyrite. *Microb. Ecol.* 48, 19–28.

Dopson, M., Lindstrom, E. B., and Hallberg, K. B. (2002). ATP generation during reduced inorganic sulfur compound oxidation by *Acidithiobacillus caldus* is exclusively due to electron transport phosphorylation. *Extremophiles* 6, 123–129.

Finn, R. D., Tate, J., Mistry, J., Coggill, P. C., Sammut, S. J., Hotz, H.-R., Ceric, G., Forslund, K., Eddy, S. R., Sonnhammer, E. L. L., and Bateman, A. (2008). The Pfam protein families database. *Nucleic Acids Res.* 36, D281–D288.

Friedrich, C. G., Bardischewsky, F., Rother, D., Quentmeier, A., and Fischer, J. (2005). Prokaryotic sulfur oxidation. *Curr. Opin. Microbiol.* 8, 253–259.

Friedrich, C. G., Rother, D., Bardischewsky, F., Quentmeier, A., and Fischer, J. (2001). Oxidation of reduced inorganic sulfur compounds by bacteria: emergence of a common mechanism? *Appl. Environ. Microbiol.* 67, 2873–2882.

Frigaard, N. U., and Bryant, D. A. (2008a). "Genomic and evolutionary perspectives on sulfur metabolism in green sulfur bacteria," in *Microbial Sulfur Metabolism*, eds C. Dahl and C. G. Friedrich (Berlin: Springer), 60–76.

Frigaard, N. U., and Bryant, D. A. (2008b). "Genomic insights into the sulfur metabolism of phototrophic green sulfur bacteria," in *Sulfur Metabolism in Phototrophic Organisms*, eds R. Hell, C. Dahl, D. B. Knaff, and T. Leustek (Berlin: Springer), 337–355.

Gehrke, T., Telegdi, J., Thierry, D., and Sand, W. (1998). Importance of extracellular polymeric substances from *Thiobacillus ferrooxidans* for bioleaching. *Appl. Environ. Microbiol.* 64, 2743–2747.

Ghosh, W., and Dam, B. (2009). Biochemistry and molecular biology of lithotrophic sulfur oxidation by taxonomically and ecologically diverse bacteria and archaea. *FEMS Microbiol. Ecol.* 33, 999–1043.

Hallberg, K. B., Dopson, M., and Lindstrom, E. B. (1996a). Arsenic toxicity is not due to a direct effect on the oxidation of reduced inorganic sulfur compounds by *Thiobacillus caldus*. *FEMS Microbiol. Lett.* 145, 409–414.

Hallberg, K. B., Dopson, M., and Lindstrom, E. B. (1996b). Reduced sulfur compound oxidation by *Thiobacillus caldus*. *J. Bacteriol.* 178, 6–11.

Hedderich, R., Hamann, N., and Bennati, M. (2005). Heterodisulfide reductase from methanogenic archaea: a new catalytic role for an iron sulfur cluster. *Biol. Chem.* 386, 961–970.

Hensen, D., Sperling, D., Truper, H. G., Brune, D. C., and Dahl, C. (2006). Thiosulphate oxidation in the phototrophic sulphur bacterium *Allochromatium vinosum*. *Mol. Microbiol.* 62, 794–810.

Hiniker, A., Collet, J. F., and Bardwell, J. C. (2005). Copper stress causes an in vivo requirement for the *Escherichia coli* disulfide isomerase DsbC. *J. Biol. Chem.* 280, 33785–33791.

Hulo, N., Bairoch, A., Bulliard, V., Cerutti, L., De Castro, E., Langendijk-Genevaux, P. S., Pagni, M., and Sigrist, C. J. (2006). The PROSITE database. *Nucleic Acids Res.* 34, D227–D230.

Ikeuchi, Y., Shigi, N., Kato, J., Nishimura, A., and Suzuki, T. (2006). Mechanistic insights into sulfur relay by multiple sulfur mediators involved in thiouridine biosynthesis at tRNA wobble positions. *Mol. Cell* 21, 97–108.

Janosch, C., Thyssen, C., Vera, M., Bonnefoy, V., Rohwerder, T., and Sand, W. (2009). Sulfur oxygenase reductase in different *Acidithiobacillus caldus*-like strains. *Adv. Mat. Res.* 71–73, 239–242.

Jing, H., Takagi, J., Liu, J. H., Lindgren, S., Zhang, R. G., Joachimiak, A., Wang, J. H., and Springer, T. A. (2002). Archaeal surface layer proteins contain beta propeller, PKD, and beta helix domains and are related to metazoan cell surface proteins. *Structure* 10, 1453–1464.

Johnson, D. B., and Hallberg, K. B. (2009). Carbon, iron and sulfur metabolism in acidophilic micro-organisms. *Adv. Microb. Physiol.* 54, 201–255.

Larkin, M. A., Blackshields, G., Brown, N. P., Chenna, R., McGettigan, P. A., McWilliam, H., Valentin, F., Wallace, I. M., Wilm, A., Lopez, R., Thompson, J. D., Gibson, T. J., and Higgins, D. G. (2007). Clustal W and Clustal X version 2.0. *Bioinformatics* 23, 2947–2948.

Mayerhofer, L. E., Conway de Macario, E., Yao, R., and Macario, A. J. (1998). Structure, organization, and expression of genes coding for envelope components in the archaeon *Methanosarcina mazei* S-6. *Arch. Microbiol.* 169, 339–345.

Merz, A. J., So, M., and Sheetz, M. P. (2000). Pilus retraction powers bacterial twitching motility. *Nature* 407, 98–102.

Molloy, M. D. (2008). Isolation of bacterial cell membrane proteins using carbonate extraction. *Methods Mol. Biol.* 424, 397–401.

Molloy, M. P., Herbert, B. R., Slade, M. B., Rabilloud, T., Nouwens, A. S., Williams, K. L., and Gooley, A. A. (2000). Proteomic analysis of the *Escherichia coli* outer membrane. *Eur. J. Biochem.* 267, 2871–2881.

Molloy, M. P., Phadke, N. D., Maddock, J. R., and Andrews, P. C. (2001). Two-dimensional electrophoresis and peptide mass fingerprinting of bacterial outer membrane proteins. *Electrophoresis* 22, 1686–1696.

Moreno-Paz, M., Gomez, M. J., Arcas, A., and Parro, V. (2010). Environmental transcriptome analysis reveals physiological differences between biofilm and planktonic modes of life of the iron oxidizing bacteria *Leptospirillum* spp. in their natural microbial community. *BMC Genomics* 11, 404. doi: 10.1186/1471-2164-11-404

Okibe, N., Gericke, M., Hallberg, K. B., and Johnson, D. B. (2003). Enumeration and characterization of acidophilic microorganisms isolated from a pilot plant stirred-tank bioleaching operation. *Appl. Environ. Microbiol.* 69, 1936–1943.

Oosthuizen, M. C., Steyn, B., Theron, J., Cosette, P., Lindsay, D., von Holy, A., and Brozel, V. S. (2002). Proteomic analysis reveals differential protein expression by *Bacillus cereus* during biofilm formation. *Appl. Environ. Microbiol.* 68, 2770–2780.

Pandey, A., Andersen, J. S., and Mann, M. (2000). Use of mass spectrometry to study signaling pathways. *Sci. STKE* 37, pl1.

Phadke, N. D., Molloy, M. P., Steinhoff, S. A., Ulintz, P. J., Andrews, P. C., and Maddock, J. R. (2001). Analysis of the outer membrane proteome of *Caulobacter crescentus* by two-dimensional electrophoresis and mass spectrometry. *Proteomics* 1, 705–720.

Planchon, S., Desvaux, M., Chafsey, I., Chambon, C., Leroy, S., Hebraud, M., and Talon, R. (2009). Comparative subproteome analysis of planktonic and sessile *Staphylococcus xylosus* C2a: new insight in cell physiology of a coagulase-negative *Staphylococcus* in biofilm. *J. Proteome Res.* 8, 1797–1809.

Pott, A. S., and Dahl, C. (1998). Sirohaem sulfite reductase and other proteins encoded by genes at the Dsr locus of *Chromatium vinosum* are involved in the oxidation of intracellular sulfur. *Microbiology* 144, 1881–1894.

Quatrini, R., Appia-Ayme, C., Denis, Y., Jedlicki, E., Holmes, D., and Bonnefoy, V. (2009). Extending the models for iron and sulfur oxidation in the extreme acidophile *Acidithiobacillus ferrooxidans*. *BMC Genomics* 10, 394. doi: 10.1186/1471-2164-10-394

Quatrini, R., Appia-Ayme, C., Denis, Y., Ratouchniak, J., Veloso, F., Valdes, J., Lefimil, C., Silver, S., Roberto, F., Orellana, O., Denizot, F., Jedlicki, E., Holmes, D., and Bonnefoy, V. (2006). Insights into the iron and sulfur energetic metabolism of *Acidithiobacillus ferrooxidans* by microarray transcriptome profiling. *Hydrometallurgy* 83, 263–272.

Ramirez, P., Guiliani, N., Valenzuela, L., Beard, S., and Jerez, C. A. (2004). Differential protein expression during growth of *Acidithiobacillus ferrooxidans* on ferrous iron, sulfur compounds, or metal sulfides. *Appl. Environ. Microbiol.* 70, 4491–4498.

Rawlings, D. E., and Johnson, D. B. (2007). The Microbiology of biomining: development and optimization of mineral-oxidizing microbial consortia. *Microbiology* 153, 315–324.

Rohwerder, T., and Sand, W. (2003). The sulfane sulfur of persulfides is the actual substrate of the sulfur-oxidizing enzymes from *Acidithiobacillus* and

Acidiphilium spp. *Microbiology* 149, 1699–1709.

Rohwerder, T., and Sand, W. (2007). Oxidation of inorganic sulfur compounds in acidophilic prokaryotes. *Engineering in Life Sciences* 7, 301-309.

Rzhepishevska, O. I., Valdés, J., Marcinkeviciene, L., Algora Gallardo, C., Meskys, R., Bonnefoy, V., Holmes, D. S., and Dopson, M. (2007). Regulation of a novel *Acidithiobacillus caldus* gene cluster involved in reduced inorganic sulfur compound metabolism. *Appl. Environ. Microbiol.* 73, 7367–7372.

Sakurai, H., Ogawa, T., Shiga, M., and Inoue, K. (2010). Inorganic sulfur oxidizing system in green sulfur bacteria. *Photosyn. Res.* 104, 163–176.

Sauer, K., and Camper, A. K. (2001). Characterization of phenotypic changes in *Pseudomonas putida* in response to surface-associated growth. *J. Bacteriol.* 183, 6579–6589.

Sauer, K., Camper, A. K., Ehrlich, G. D., Costerton, J. W., and Davies, D. G. (2002). *Pseudomonas aeruginosa* displays multiple phenotypes during development as a biofilm. *J. Bacteriol.* 184, 1140–1154.

Schippers, A., and Sand, W. (1999). Bacterial leaching of metal sulfides proceeds by two indirect mechanisms via thiosulfate or via polysulfides and sulfur. *Appl. Environ. Microbiol.* 65, 319–321.

Shevchenko, A., Wilm, M., Vorm, O., and Mann, M. (1996). Mass spectrometric sequencing of proteins silver-stained polyacrylamide gels. *Anal. Chem.* 68, 850–858.

Suzuki, I. (1999). Oxidation of inorganic sulfur compounds: chemical and enzymatic reactions. *Can. J. Microbiol.* 45, 97–105.

Takle, G. W., Toth, I. K., and Brurberg, M. B. (2007). Evaluation of reference genes for real-time RT-PCR expression studies in the plant pathogen *Pectobacterium atrosepticum*. *BMC Plant Biol.* 7, 50. doi: 10.1186/1471-2229-7-50

Tatusov, R. L., Fedorova, N. D., Jackson, J. D., Jacobs, A. R., Kiryutin, B., Koonin, E. V., Krylov, D. M., Mazumder, R., Mekhedov, S. L., Nikolskaya, A. N., Rao, B. S., Smirnov, S., Sverdlov, A. V., Vasudevan, S., Wolf, Y. I., Yin, J. J., and Natale, D. A. (2003). The COG database: an updated version includes eukaryotes. *BMC Bioinformatics* 4, 41. doi: 10.1186/1471-2105-4-41

Urich, T., Bandeiras, T. M., Leal, S. S., Rachel, R., Albrecht, T., Zimmermann, P., Scholz, C., Teixeira, M., Gomes, C. M., and Kletzin, A. (2004). The sulphur oxygenase reductase from *Acidianus ambivalens* is a multimeric protein containing a low-potential mononuclear non-haem iron centre. *Biochem. J.* 381, 137–146.

Urich, T., Gomes, C. M., Kletzin, A., and Frazao, C. (2006). X-ray Structure of a self-compartmentalizing sulfur cycle metalloenzyme. *Science* 311, 996–1000.

Wakai, S., Tsujita, M., Kikumoto, M., Manchur, M. A., Kanao, T., and Kamimura, K. (2007). Purification and characterization of sulfide:quinone oxidoreductase from an acidophilic iron-oxidizing bacterium, *Acidithiobacillus ferrooxidans*. *Biosci. Biotechnol. Biochem.* 71, 2735–2742.

Valdes, J., Pedroso, I., Quatrini, R., Dodson, R. J., Tettelin, H., Blake, R., Eisen, J. A., and Holmes, D. S. (2008). *Acidithiobacillus ferrooxidans* metabolism: from genome sequence to industrial applications. *BMC Genomics* 9, 597. doi: 10.1186/1471-2164-9-597

Valdes, J., Quatrini, R., Hallberg, K., Dopson, M., Valenzuela, P. D., and Holmes, D. S. (2009). Draft genome sequence of the extremely acidophilic bacterium *Acidithiobacillus caldus* ATCC 51756 reveals metabolic versatility in the genus *Acidithiobacillus*. *J. Bacteriol.* 191, 5877–5878.

Valenzuela, L., Chi, A., Beard, S., Shabanowitz, J., Hunt, D. F., and Jerez, C. A. (2008). "Differential-expression proteomics for the study of sulfur metabolism in the chemolithoautotrophic *Acidithiobacillus ferrooxidans*," in *Microbial Sulfur Metabolism*, eds C. Dahl and C. G. Friedrich (Berlin: Springer), 77–86.

Vilain, S., Cosette, P., Hubert, M., Lange, C., Junter, G. A., and Jouenne, T. (2004a). Comparative proteomic analysis of planktonic and immobilized *Pseudomonas aeruginosa* cells: a multivariate statistical approach. *Anal. Biochem.* 329, 120–130.

Vilain, S., Cosette, P., Zimmerlin, I., Dupont, J. P., Junter, G. A., and Jouenne, T. (2004b). Biofilm proteome: homogeneity or versatility? *J. Proteome Res.* 3, 132–136.

Williams, M. D., Ouyang, T. X., and Flickinger, M. C. (1994). Starvation-induced expression of SspA and SspB: the effects of a null mutation in sspA on *Escherichia coli* protein synthesis and survival during growth and prolonged starvation. *Mol. Microbiol.* 11, 1029–1043.

Conflict of Interest Statement: The authors declare that the research was conducted in the absence of any commercial or financial relationships that could be construed as a potential conflict of interest.

Received: 02 November 2010; accepted: 25 January 2011; published online: 10 February 2011.

Citation: Mangold S, Valdés J, Holmes DS and Dopson M (2011) Sulfur metabolism in the extreme acidophile Acidithiobacillus caldus. Front. Microbio. ***2****:17. doi: 10.3389/fmicb.2011.00017*

This article was submitted to Frontiers in Microbial Physiology and Metabolism, a specialty of Frontiers in Microbiology.

APPENDIX

Table A1 | Proteins identified from 2D gels of tetrathionate and sulfur grown *Acidithiobacillus caldus*.

Match ID[a]	Accession[b]	Protein identification	Theoretical		Experimental		Mowse score[g]	Coverage[h] (%)	Fold		
			MW (kDa)[c]	pI[d]	MW (kDa)[e]	pI[f]			E-value[i]	difference[j]	ANOVA[k]
***ACIDITHIOBACILLUS CALDUS* UP-REGULATED ON TETRATHIONATE (SOLUBLE FRACTION)**											
S10	ACA_2391	Sulfur oxidation protein SoxZ	12	9.30	12	9.32	70	60	2.6e – 04	4.0	1.5e – 02
S17	ACA_0867	Hypothetical protein ACA_0867	18	9.07	13	7.76	63	34	1.4e – 03	4.2	3.5e – 03
S37	ACA_1726	Twin-arginine translocation protein TatA	8	6.40	16	6.12	78	51	4.0e – 05	3.8	8.3e – 03
S127	ACA_2632	Pyridoxine 5′-phosphate synthase	26	6.15	29	6,05	131	54	2.2e – 10	10.5	1.6e – 03
S162	ACA_1144	Hypothetical protein ACA_1144	31	5.83	36	5.95	62	32	1.7e – 03	2.1	2.1e – 02
S217	ACA_0247	Translation elongation factor Tu	43	5.37	44	5.22	114	38	1.1e – 08	2.3	1.2e – 02
S260	ACA_0303	Sulfide-quinone reductase, sqr-1	47	5.57	54	5.44	56	17	7.6e – 03	2.2	1.2e – 03
S356	ACA_2392	Sulfur oxidation protein SoxA	32	8.77	28	8.44	49	26	3.8e – 02	2.8	2.9e – 02
S388	ACA_0248	Translation elongation factor G	64	5.12	83	5.15	150	25	2.8e – 12	3.5	1.1e – 02
S22	ACA_1957	Hypothetical protein ACA_1957	12	8.64	14	8.57	76	58	6.6e – 05	6.1	2.9e – 02
S34	ACA_2393	Protein of unknown function DUF302	19	8.96	16	8.63	89	55	3.7e – 06	6.9	4.7e – 03
S151	ACA_0832	Chemotaxis protein CheV	30	5.19	34	5.17	70	27	9.8e – 05	4.9	2.4e – 02
S518	ACA_0867	Hypothetical protein ACA_0867	18	9.07	13	7.15	59	34	3.6e – 03	unique	9.4e – 03
S524	ACA_2320	Hypothetical protein ACA_2320	17	9.15	17	9.1	73	34	1.4e – 04	unique	1.8e – 02
S528	ACA_0688	Transposase, IS4	40	9.48	19	5.85	52	16	1.6e – 02	unique	2.4e – 03
S537	ACA_1235	Peptidyl-prolyl cis-trans isomerase ppiD	28	8.54	27	7.42	61	27	2.3e – 03	unique	2.7e – 4
S538	ACA_2392	Sulfur oxidation protein SoxA	32	8.77	27	8.06	74	34	1.2e – 04	unique	1.8e – 02
S539	ACA_2392	Sulfur oxidation protein SoxA	32	8.77	28	7.23	69	24	3.7e – 04	unique	3.2e – 03
S543	ACA_2420	CoB–CoM heterodisulfide reductase subunit C	27	6.2	29	6.44	69	31	3.8e – 04	unique	1.6e – 03
S544	ACA_2420	CoB–CoM heterodisulfide reductase subunit C	27	6.2	29	6.18	68	29	4.1e – 04	unique	2.3e – 4
S549	ACA_0761	2,3,4,5-tetrahydropyridine-2,6-dicarboxylate *N*-succinyltransferase	30	6.45	31	6.57	58	21	4.0e – 03	unique	1.3e – 03
S551	ACA_2027	Methylenetetrahydrofolate dehydrogenase (NADP+)/Methenyltetrahydrofolate cyclohydrolase	32	6.62	32	6.76	101	20	2.2e – 07	unique	3.9e – 02
S556	ACA_1144	Hypothetical protein ACA_1144	31	5.83	36	5.77	58	25	4.2e – 03	unique	5.0e – 5
S563	ACA_2428	Radical SAM domain protein	43	5.17	42	5.08	66	20	7.6e – 04	unique	2.6e – 5
S571	ACA_0032	Aspartate aminotransferase	44	7.1	45	7.13	79	15	3.8e – 05	unique	2.4e – 4
S572	ACA_1795	Tyrosyl-tRNA synthetase	46	6.16	46	6.34	118	28	4.5e – 09	unique	4.5e – 4
S577	ACA_1668	Putative sensory histidine kinase YfhA	50	6.06	48	6.02	85	15	8.9e – 06	unique	2.1e – 7
S579	Mixture				49	6.43	111		2.2e – 08	unique	1.3e – 03
	ACA_0441	Fe–S protein, lactate dehydrogenase SO1521-like protein	48	6.43	49	6.43	97	30	6.2e – 07		
	ACA_0113	Serine hydroxymethyltransferase	45	6.40	49	6.43	34	18	1.2e + 00		
S594	ACA_2840	Dihydrolipoamide dehydrogenase	49	6.15	53	6.14	81	20	2.5e – 05	unique	2.0e – 7
S624	ACA_1178	Chaperone protein HscA	66	4.99	69	4.83	102	34	3.6e – 08	unique	4.2e – 4
S625	ACA_1107	Prolyl-tRNA synthetase	64	5.74	70	5.70	165	34	8.9e – 14	unique	3.4e – 02

S694	ACA_0585	2-Keto-3-deoxy-d-manno-octulosonate-8-phosphate synthase	31	6.18	32	6.39	67	22	5.9e – 04	unique	3.6e – 02
S702	ACA_0705	Aspartyl-tRNA(Asn)/Glutamyl-tRNA(Gln) amidotransferase subunit B	53	5.23	55	5.11	49	9	3.7e – 02	unique	1.5e – 4
***ACIDITHIOBACILLUS CALDUS* UP-REGULATED ON SULFUR (SOLUBLE FRACTION)**											
S9	ACA_1583	Hypothetical protein ACA_1583	13	4.68	12	4.55	110	90	2.8e – 08	2.3	2.5e – 02
S25	ACA_1132	Protein export cytoplasm chaperone protein (SecB, maintains protein to be exported in unfolded state)	16	4.68	15	4.65	60	45	3.1e – 03	3.2	2.4e – 02
S26	ACA_0889	Heat shock protein Hsp20	17	5.46	15	5.35	60	31	3.0e – 03	8.6	9.9e – 4
S46	ACA_0889	Heat shock protein Hsp20	17	5.46	17	4.86	52	31	1.7e – 02	3.5	3.4e – 02
S53	ACA_1343	Peptidoglycan-associated outer membrane lipoprotein	20	6.41	18	5.53	91	43	2.2e – 06	2.9	2.9e – 02
S64	ACA_1478	Hypothetical protein ACA_1478	20	5.52	22	5.51	62	47	1.8e – 03	3.6	4.1e – 02
S102	ACA_1210	Stringent starvation protein A	24	5.51	27	5.51	54	30	1.0e – 02	2.3	1.9e – 02
S114	ACA_2307	Heat shock protein 60 family chaperone GroEL	58	5.41	29	5.56	57	15	5.5e – 03	3.4	5.0e – 02
S146	ACA_2307	Heat shock protein 60 family chaperone GroEL	58	5.41	33	5.63	141	36	2.2e – 11	2.3	1.0e – 02
S154	ACA_0563	6-phosphogluconate dehydrogenase, NAD-binding	32	5.88	33	5.94	106	56	7.1e – 08	2.3	1.8e – 03
S175	Mixture				38	6.86	123		1.4e – 09	4.5	5.4e – 02
	ACA_2530	Membrane-fusion protein	38	7.9	38	6.86	89	40	3.3e – 06		
	ACA_2096	Glyceraldehyde-3-phosphate dehydrogenase/erythrose -4-phosphate dehydrogenase	37	7.14	38	6.86	51	33	2.5e – 02		
S205	ACA_0861	Flagellar basal-body rod protein FlgC	14	7.88	43	6.15	58	63	4.3e – 03	2.5	4.1e – 02
S285	ACA_1087	IMP cyclohydrolase/Phosphoribosylaminoimidazolecarboxamide formyltransferase	57	5.6	60	5.52	103	26	1.4e – 07	3.1	6.5e – 03
S338	ACA_0241	LSU ribosomal protein L7/L12 (L23e)	13	4.64	13	4.57	144	83	1.1e – 11	2.0	1.5e – 02
S358	ACA_2033	Thiol:disulfide interchange protein DsbG precursor	30	5.68	30	5.25	75	47	8.5e – 05	2.0	5.5e – 4
S398	ACA_1343	Peptidoglycan-associated outer membrane lipoprotein	20	6.41	16	5.55	57	30	5.5e – 03	unique	8.1e – 5
S409	ACA_2307	Heat shock protein 60 family chaperone GroEL	58	5.41	27	4.97	83	23	1.5e – 05	unique	5.7e – 03
S413	ACA_2307	Heat shock protein 60 family chaperone GroEL	58	5.41	28	5.2	50	15	3.0e – 02	unique	5.5e – 03
S416	ACA_2307	Heat shock protein 60 family chaperone GroEL	58	5.41	29	5.13	75	24	9.3e – 05	unique	1.2e – 02
S418	ACA_2632	Pyridoxine 5′-phosphate synthase	26	6.15	29	6.15	126	48	7.1e – 10	unique	3.0e – 03
S425	ACA_2307	Heat shock protein 60 family chaperone GroEL	58	5.41	33	5.17	68	24	4.2e – 04	unique	1.4e – 4
S428	ACA_2307	Heat shock protein 60 family chaperone GroEL	58	5.41	33	5.56	49	21	3.2e – 02	unique	3.2e – 03
S429	ACA_2307	Heat shock protein 60 family chaperone GroEL	58	5.41	34	5.44	56	15	6.5e – 03	unique	5.8e – 03
S435	ACA_2307	Heat shock protein 60 family chaperone GroEL	58	5.41	36	5.32	85	26	8.1e – 06	unique	2.7e – 03
S436	ACA_2307	Heat shock protein 60 family chaperone GroEL	58	5.41	37	5.33	68	22	4.6e – 04	unique	3.1e – 03
S462	ACA_2418	Heterodisulfide reductase subunit A	38	6.03	52	5.50	63	26	1.4e – 03	unique	1.9e – 02
***ACIDITHIOBACILLUS CALDUS* UP-REGULATED ON TETRATHIONATE (MEMBRANE ENRICHED FRACTION)**											
M13	ACA_0867	Hypothetical protein ACA_0867	18	9.07	12	8.69	69	34	3.6e – 04	2.3	9.9e – 03
M19	ACA_1957	Hypothetical protein ACA_1957	12	8.64	13	9.00	55	44	8.5e – 03	7.4	1.2e – 03
M32	ACA_1726	Twin-arginine translocation protein TatA	8	6.40	16	6.08	74	55	1.0e – 04	3.8	2.3e – 4
M49	ACA_1466	Putative lipoprotein	22	6.49	20	6.17	68	58	4.6e – 04	10.3	1.1e – 4

(Continued)

Table A1 | Continued

Match ID[a]	Accession[b]	Protein identification	Theoretical		Experimental		Mowse score[g]	Coverage[h] (%)	Fold		
			MW (kDa)[c]	pI[d]	MW (kDa)[e]	pI[f]			E-value[i]	difference[j]	ANOVA[k]
M163	ACA_2593	Hypothetical protein ACA_2593	39	8.71	33	6.10	49	18	3.9e – 02	5.9	3.0e – 03
M179	ACA_2091	4-hydroxy-3-methylbut-2-enyl diphosphate reductase	34	5.43	36	5.43	54	21	1.1e – 02	2.1	1.8e – 02
M180	ACA_1142	Efflux transporter, RND family, MFP subunit	39	9.39	36	9.36	78	28	4.5e – 05	15.0	2.3e – 03
M193	ACA_2096	NAD-dependent glyceraldehyde-3-phosphate dehydrogenase	37	7.14	37	8.17	99	48	3.4e – 07	2.9	6.2e – 6
M227	ACA_1229	Cell division protein FtsZ	40	4.95	41	4.98	112	28	1.8e – 08	2.2	7.7e – 4
M248	ACA_2100	Fructose-bisphosphate aldolase class II	38	5.69	43	5.74	147	35	5.6e – 12	2.1	2.6e – 4
M254	ACA_0247	Translation elongation factor Tu	43	5.37	44	5.31	101	30	2.2e – 07	4.1	3.9e – 4
	ACA_1874	Translation elongation factor Tu	21	6.21	44	5.31	72	39	1.8e – 04		
M262	ACA_1228	Cell division protein FtsA	45	5.41	46	5.41	165	40	8.9e – 14	4.5	3.1e – 4
M277	ACA_1270	Hypothetical protein ACA_1270	44	6.00	50	6.08	140	36	2.8e – 11	2.3	1.5e – 02
M291	ACA_2388	Two component, sigma54 specific, transcriptional regulator, Fis family	50	5.47	51	5.43	162	33	1.8e – 13	3.0	3.0e – 4
M300	ACA_2485	Sulfide–quinone reductase, sqr-2	48	6.53	52	7.42	108	25	4.5e – 08	2.5	2.7e – 02
M309	ACA_0933	Biotin carboxylase of acetyl-CoA carboxylase	49	6.18	53	6.22	56	20	6.6e – 03	2.1	1.5e – 02
M344	ACA_2548	MutS2 family protein	55	6.24	59	6.52	48	16	4.2e – 02	2.3	1.0e – 02
M353	ACA_2547	Acetolactate synthase large subunit	63	5.69	63	5.60	52	8	1.7e – 02	2.7	1.5e – 02
M357	ACA_2234	Uptake hydrogenase large subunit	50	6.11	64	5.76	66	21	7.8e – 04	3.1	3.2e – 02
M362	ACA_1776	DNA repair protein RecN	62	5.26	66	5.27	136	33	7.1e – 11	2.5	9.2e – 03
M368	ACA_0098	Phosphoglucomutase	59	5.88	69	5.79	56	17	7.4e – 03	3.0	1.9e – 03
M383	ACA_2179	GTPase subunit of restriction endonuclease-like protein	73	5.38	74	5.37	74	18	1.2e – 04	2.8	6.1e – 03
M386	ACA_1482	Cell division protein FtsH	69	5.98	75	5.85	114	18	1.1e – 08	4.1	6.4e – 5
M388	ACA_1482	Cell division protein FtsH	69	5.98	76	5.78	80	17	2.8e – 05	9.1	9.7e – 4
M431	ACA_2689	Phenylalanyl-tRNA synthetase beta chain	88	5.89	92	5.81	151	19	2.2e – 12	2.1	4.8e – 4
M476	ACA_2096	NAD-dependent glyceraldehyde-3-phosphate dehydrogenase	37	7.14	38	7.81	93	50	1.5e – 6	2.5	1.1e – 03
M482	ACA_1144	Hypothetical protein ACA_1144	31	5.83	35	5.91	77	32	5.1e – 05	10.7	7.9e – 5
M508	ACA_0293	Cysteinyl-tRNA synthetase	53	5.83	57	5.79	80	25	2.9e – 05	2.7	2.5e – 03
M512	ACA_0317	Chemotaxis regulator - transmits chemoreceptor signals to flagelllar motor components CheY	16	6.60	80	5.96	65	36	8.3e – 04	2.4	4.7e – 02
	ACA_0548	Hypothetical protein ACA_0548	73	6.02	80	5.96	59	14	3.8e – 03		
M513	ACA_1482	Cell division protein FtsH	69	5.98	76	5.74	128	27	4.5e – 10	3.5	1.2e – 4
M521	ACA_0247	Translation elongation factor Tu	43	5.37	46	5.27	70	22	2.9e – 04	2.1	1.4e – 03
	ACA_1874	Translation elongation factor Tu	21	6.21	46	5.27	62	40	1.8e – 03		
M706	ACA_1957	Hypothetical protein ACA_1957	12	8.64	13	9.39	71	58	2.0e – 04	unique	1.4e – 02
M726	ACA_0186	Enoyl-[acyl-carrier-protein] reductase [NADH]	27	5.70	28	5.69	122	40	1.8e – 09	unique	1.5e – 02
M735	ACA_0832	Chemotaxis protein CheV	30	5.19	34	5.27	78	24	4.7e – 05	unique	3.3e – 6
M738	ACA_1144	Hypothetical protein ACA_1144	31	5.83	36	5.72	55	34	9.8e – 03	unique	2.1e – 4
M740	ACA_1142	Efflux transporter, RND family, MFP subunit	39	9.39	36	8.90	88	23	4.7e – 06	unique	8.8e – 4

M755	ACA_2748	Aminomethyltransferase	42	6.73	45	7.45	128	49	4.5e – 10	unique	7.7e – 5
M776	ACA_1984	Nitrogen regulation protein NR(I)	54	5.84	58	5.74	104	25	1.1e – 07	unique	1.8e – 4
M781	ACA_2548	MutS2 family protein	55	6.24	60	6.23	50	13	2.9e – 02	unique	9.9e – 5
M793	ACA_2317	5′-Nucleotidase domain protein	64	6.66	66	7.41	83	11	1.3e – 05	unique	8.7e – 7
***ACIDITHIOBACILLUS CALDUS* UP-REGULATED ON SULFUR (MEMBRANE ENRICHED FRACTION)**											
M71	ACA_2067	HAD-superfamily hydrolase, subfamily IA, variant 3	24	6.08	24	5.97	160	64	2.8e – 13	2.1	1.6e – 02
M85	ACA_0146	Alkyl hydroperoxide reductase subunit C-like protein	24	5.67	26	5.55	60	23	2.8e – 03	2.6	4.1e – 02
M263	ACA_2773	Carboxysome shell protein CsoS1	10	5.52	47	5.00	58	41	4.5e – 03	6.1	6.9e – 3
M397	ACA_1454	Chaperone protein DnaK	68	5.06	79	5.01	59	18	3.9e – 03	3.6	8.4e – 03
M441	ACA_2034	ClpB protein	97	5.52	100	5.49	198	25	4.5e – 17	2.7	9.0e – 4
M493	ACA_2352	Phosphate-selective porin O and P	42	5.87	39	6.70	96	29	6.9e – 07	3.3	1.6e – 02
M497	ACA_0129	Type I secretion outer membrane protein, TolC precursor	50	6.34	50	6.02	74	23	1.1e – 04	2.4	9.4e – 03
M503	ACA_2765	Ribulose bisphosphate carboxylase large chain	53	5.96	53	5.78	121	27	2.2e – 09	2.6	8.5e – 4
M530	ACA_2773	Carboxysome shell protein CsoS1	10	5.52	10	5.39	121	62	2.2e – 09	unique	1.0e – 02
	ACA_2771	Carboxysome shell protein CsoS1	10	5.58	10	5.39	78	46	4.3e – 05		
	ACA_2772	Carboxysome shell protein CsoS1	10	5.58	10	5.39	78	46	4.3e – 05		
M539	ACA_1520	Hypothetical protein ACA_1520	12	6.52	16	8.39	91	59	2.0e – 06	unique	2.8e – 4
M550	ACA_0172	1,2-dihydroxy-3-keto-5-methylthiopentene dioxygenase	21	5.10	22	5.05	77	36	5.4e – 05	unique	1.4e – 02
M553	ACA_0993	Hypothetical protein ACA_0993	25	8.98	25	8.89	141	42	2.2e – 11	unique	1.8e – 02
M565	ACA_1527	Hypothetical protein ACA_1527	32	4.74	28	4.66	57	26	6.2e – 03	unique	1.4e – 5
M605	ACA_0109	Protease Do	53	6.98	51	6.9	54	15	1.2e – 02	unique	2.1e – 02
M607	ACA_2388	Two component, sigma54 specific, transcriptional regulator, Fis family	50	5.47	52	5.33	53	16	1.4e – 02	unique	4.0e – 4
M675	ACA_2024	Outer membrane component of tripartite multidrug resistance system	51	6.14	53	5.52	75	16	9.3e – 05	unique	4.7e – 4

[a]*Match ID was generated by Melanie and refers to protein spots in* ***Figure 3*** *(soluble fraction) and* ***Figure 4*** *(membrane fraction). Match ID in Figures is given without S or M in front of numbers.*
[b]*Annotation number is that of Genebank genome annotation NZ_ACVD01000000.1.*
[c]*Predicted Molecular weight of database entry.*
[d]*Predicted isoelectric point (pI) of database entry.*
[e]*Experimental molecular weight determined by 2D-PAGE.*
[f]*Experimental pI determined by 2D-PAGE.*
[g]*Mowse score was generated by Mascot and describes the hit of a peptide mass fingerprint (PMF) search giving the probability that the hit is not a random match in the database (scores > 47 are significant with a significance threshold of 0.05).*
[h]*Sequence coverage (generated by Mascot) presents the percentage of the database hit that was covered by the submitted peptide masses of the experimentally acquired PMF.*
[i]*Expect value (generated by Mascot) is the number of hits expected by change in a database of the same size.*
[j]*Fold change was determined with Melanie. Fold changes ≥ 2.0 were regarded as differentially expressed.*
[k]*Anova test was performed for two or three replicates of each condition and spots with p-values < 0.05 were considered to be significant.*

Table A2 | Proteins identified in 2D gels from sessile and planktonic *Acidithiobacillus caldus*.

Match ID[a]	Accession[b]	Protein identification	Theoretical		Experimental		Mowse score[g]	Coverage[h] (%)	Fold		
			MW (kDa)[c]	pI[d]	MW (kDa)[e]	pI[f]			E-value[i]	difference[j]	Anova[k]
***ACIDITHIOBACILLUS CALDUS* PLANKTONIC**											
64	ACA_1726	Twin-arginine translocation protein TatA	8	6.40	16	6.33	71	51	2.1e – 04	7.9	9.0e – 03
118	ACA_2219	Hypothetical protein ACA_2219	20	6.15	20	6.11	75	31	8.9e – 05	4.2	1.4e – -03
492	ACA_0303	Sulfide–quinone reductase, sqr-1	47	5.57	52	5.56	86	35	6.5e – 06	2.4	7.2e – 5
826	ACA_0867	Hypothetical protein ACA_0867	18	9.07	14	7.18	101	61	2.2e – 07	unique	2.9e – 6
827	ACA_0867	Hypothetical protein ACA_0867	18	9.07	14	6.95	69	53	3.2e – 04	unique	5.2e – 5
841[l]	ACA_2319	Sulfur oxidation protein SoxY			16	5.65				unique	3.3e – 4
***ACIDITHIOBACILLUS CALDUS* SESSILE**											
70	ACA_1907	Single-stranded DNA-binding protein	17	5.49	16	5.59	70	66	3.0e – 04	3.1	3.1e – 02
213	ACA_1235	Peptidyl-prolyl cis-trans isomerase ppiD	28	8.54	27	7.12	56	20	6.6e – 03	2.7	1.1e – 02
238	ACA_2420	CoB–CoM heterodisulfide reductase subunit C	27	6.20	28	6.67	113	50	1.4e – 08	2.8	7.9e – 03
258	ACA_2765	Ribulose bisphosphate carboxylase large chain	53	5.96	30	5.36	68	15	4.7e – 04	2.2	5.1e – 4
280	ACA_2783	Rubisco activation protein CbbQ mod	30	5.32	32	5.32	84	35	1.2e – 05	2.4	5.3e – 5
325	ACA_2737	Twitching motility protein	39	6.50	36	6.87	102	33	1.8e – 07	2.0	1.7e – 03
329	ACA_2307	Heat shock protein 60 family chaperone GroEL	58	5.14	37	5.4	64	18	1.2e – 03	2.2	9.5e – 03
364	ACA_0002	Pyruvate dehydrogenase E1 component beta subunit	35	5.69	39	5.8	77	20	5.5e – 05	3.0	2.5e – 02
382	ACA_2418	Heterodisulfide reductase subunit A	38	6.03	40	5.57	93	34	1.5e – 06	2.4	3.6e – 4
	ACA_1473	Heterodisulfide reductase subunit A	38	5.86	40	5.57	68	28	4.3e – 04		
395	ACA_2421	CoB–CoM heterodisulfide reductase subunit B	33	5.01	41	5.03	71	56	2.3e – 04	2.1	5.9e – 4
404	ACA_0152	40-residue YVTN family beta-propeller repeat protein	96	5.98	43	5.35	49	7	3.4e – 02	7.7	4.4e – 5
408	ACA_2100	Fructose-bisphosphate aldolase class II	38	5.69	43	5.93	76	33	7.4e – 05	2.3	1.6e – 02
420	ACA_0056	*S*-adenosylmethionine synthetase	42	5.37	45	5.38	79	21	3.3e – 05	2.4	9.0e – 6
442	ACA_0500	Gamma-glutamyl phosphate reductase	46	5.87	48	6.37	109	25	3.6e – 08	2.5	1.7e – 03
447	ACA_0113	Serine hydroxymethyltransferase	45	6.4	49	6.73	71	22	2.0e – 04	5.2	8.5e – 03
455	ACA_1035	3-isopropylmalate dehydratase large subunit	51	5.69	49	5.85	107	33	5.6e – 08	2.5	1.8e – 5
515	ACA_0148	2-isopropylmalate synthase	32	5.94	56	5.43	86	29	7.3e – 06	2.5	1.7e – 03
522	ACA_0976	ATP synthase alpha chain	56	5.32	57	5.27	68	18	4.0e – 04	2.3	1.7e – 03
541	ACA_2307	Heat shock protein 60 family chaperone GroEL	58	5.14	63	5.4	96	34	7.8e – 07	3.8	7.0e – 03
543	ACA_2307	Heat shock protein 60 family chaperone GroEL	58	5.14	67	5.26	94	28	1.2e – 06	2.4	8.1e – 4
553	ACA_2095	Transketolase	73	5.95	79	6.33	77	18	5.8e – 05	3.0	5.2e – 03
556	ACA_1454	Chaperone protein DnaK	68	5.06	82	5.02	155	36	8.9e – 13	2.6	3.4e – 03

[a]*Match ID was generated by Melanie and refers to protein spots in* ***Figure 5****.*
[b]*Annotation number is that of Genebank genome annotation NZ_ACVD01000000.1.*
[c]*Predicted Molecular weight of database entry.*
[d]*Predicted isoelectric point (pI) of database entry.*
[e]*Experimental molecular weight determined by 2D-PAGE.*
[f]*Experimental pI determined by 2D-PAGE.*
[g]*Mowse score was generated by Mascot and describes the hit of a peptide mass fingerprint (PMF) search giving the probability that the hit is not a random match in the database (scores > 47 are significant with a significance threshold of 0.05).*
[h]*Sequence coverage (generated by Mascot) presents the percentage of the database hit that was covered by the submitted peptide masses of the experimentally acquired PMF.*
[i]*Expect value (generated by Mascot) is the number of hits expected by change in a database of the same size.*
[j]*Fold change was determined with Melanie. Fold changes ≥2.0 were regarded as differentially expressed.*
[k]*Anova test was performed for two or three replicates of each condition and spots with p-values < 0.05 were considered to be significant.*
[l]*Sample was analyzed by Edman degradation.*

frontiers in
MICROBIOLOGY

ORIGINAL RESEARCH ARTICLE
published: 07 March 2011
doi: 10.3389/fmicb.2011.00037

Substrate pathways and mechanisms of inhibition in the sulfur oxygenase reductase of *Acidianus ambivalens*

Andreas Veith[1], Tim Urich[1,2†], Kerstin Seyfarth[1†], Jonas Protze[1†], Carlos Frazão[2] and Arnulf Kletzin[1]*

[1] Institute of Microbiology and Genetics, Technische Universität Darmstadt, Darmstadt, Germany
[2] Structural Biology Laboratory, Macromolecular Crystallography Unit, ITQB-UNL, Oeiras, Portugal

Edited by:
Martin G. Klotz, University of Louisville, USA

Reviewed by:
Kathleen Scott, University of South Florida, USA
Ulrike Kappler, University of Queensland, Australia

***Correspondence:**
Arnulf Kletzin, Institute of Microbiology and Genetics, Technische Universität Darmstadt, Schnittspahnstraße 10, 64287 Darmstadt, Germany.
e-mail: kletzin@bio.tu-darmstadt.de

†Present address:
Tim Urich, Department of Genetics in Ecology, University of Vienna, Vienna, Austria;
Kerstin Seyfarth, Institut für Mikrobiologie und Weinforschung, Johannes Gutenberg-Universität, Mainz, Germany;
Jonas Protze, Research Group of Structural Bioinformatics, Department of Structural Biology, Leibniz-Institut für Molekulare Pharmakologie, Berlin, Germany.

Background: The sulfur oxygenase reductase (SOR) is the initial enzyme of the sulfur oxidation pathway in the thermoacidophilic Archaeon *Acidianus ambivalens*. The SOR catalyzes an oxygen-dependent sulfur disproportionation to H_2S, sulfite and thiosulfate. The spherical, hollow, cytoplasmic enzyme is composed of 24 identical subunits with an active site pocket each comprising a mononuclear non-heme iron site and a cysteine persulfide. Substrate access and product exit occur via apolar chimney-like protrusions at the fourfold symmetry axes, via narrow polar pores at the threefold symmetry axes and via narrow apolar pores within in each subunit. In order to investigate the function of the pores we performed site-directed mutagenesis and inhibitor studies. **Results:** Truncation of the chimney-like protrusions resulted in an up to sevenfold increase in specific enzyme activity compared to the wild type. Replacement of the salt bridge-forming Arg_{99} residue by Ala at the threefold symmetry axes doubled the activity and introduced a bias toward reduced reaction products. Replacement of Met_{296} and Met_{297}, which form the active site pore, lowered the specific activities by 25–55% with the exception of an $M_{296}V$ mutant. X-ray crystallography of SOR wild type crystals soaked with inhibitors showed that Hg^{2+} and iodoacetamide (IAA) bind to cysteines within the active site, whereas Zn^{2+} binds to a histidine in a side channel of the enzyme. The Zn^{2+} inhibition was partially alleviated by mutation of the His residue. **Conclusions:** The expansion of the pores in the outer shell led to an increased enzyme activity while the integrity of the active site pore seems to be important. Hg^{2+} and IAA block cysteines in the active site pocket, while Zn^{2+} interferes over a distance, possibly by restriction of protein flexibility or substrate access or product exit.

Keywords: Archaea, sulfur metabolism, site-directed mutagenesis, structural biology, X-ray crystallography

INTRODUCTION

A large number of microorganisms oxidize sulfur and reduced inorganic sulfur compounds (ISC) for energy conservation (for review, see for example Friedrich et al., 2005; Kletzin, 2007; Frigaard and Dahl, 2009; Ghosh and Dam, 2009). Most studies on ISC oxidation were performed with soluble sulfur species like thiosulfate, sulfite and sulfide. Their mechanisms of activation and oxidation are reasonably well understood (Friedrich et al., 2005; Ghosh and Dam, 2009). Less is known how the barely soluble elemental sulfur is mobilized and oxidized (19–30 nmol/l α-S8 at 25°C, 478 nmol/l at 80°C; Kamyshny, 2009). Different enzymes and enzyme activities were described but few were analyzed in molecular detail (Rohwerder and Sand, 2003; Kletzin, 2007; Ghosh and Dam, 2009; also see Protze et al., 2011, this volume).

The best-known sulfur-oxidizing enzymes are sulfur oxygenase reductases (SOR), which were purified from two different thermoacidophilic *Acidianus* species (Emmel et al., 1986; Kletzin, 1989). In addition, SORs obtained by heterologous gene expression were studied from *Ac. ambivalens* and *Ac. tengchongensis*, from the hyperthermophilic bacterium *Aquifex aeolicus*, and from a moderately thermophilic bacterium from a bioleaching reactor (Sun et al., 2003; Urich et al., 2004; Chen et al., 2007; Pelletier et al., 2008). The SOR is the initial sulfur-oxidizing enzyme in the Archaeon *Ac. ambivalens*, which is our model organism for sulfur metabolism, and which grows optimally at 80°C and pH 1–3. The SOR or *sor* genes do not occur frequently; so far they are restricted to some thermoacidophilic Archaea and to some mesophilic and thermophilic Bacteria (**Figure 1**). The SORs catalyze an oxygen-dependent sulfur disproportionation reaction with sulfite, thiosulfate and sulfide as products (Eqs 1–3; Kletzin, 1989; Sun et al., 2003; Pelletier et al., 2008).

$$\text{Oxygenase} \quad S^0 + O_2 + H_2O \rightarrow HSO_3^- + H^+ \quad (1)$$

$$\text{Disproportionase} \quad 3S^0 + 3H_2O \rightarrow 2H_2S + HSO_3^- + H^+ \quad (2)$$

$$\text{Sum} \quad 4S^0 + O_2 + 4H_2O \rightarrow 2H_2S + 2HSO_3^- + 2H^+ \quad (3)$$

External cofactors or electron donors are not required and the two enzyme activities could not be separated. Zn^{2+}, Hg^{2+} and thiol-modifying organic agents like iodoacetamide (IAA) and *N*-ethylmaleimide (NEM) inhibit activity (Kletzin, 1989). The SORs do not catalyze sulfur disproportionation in the absence of oxygen and they have neutral or slightly acidic pH optima (5–7.4; Emmel et al., 1986; Kletzin, 1989; Sun et al., 2003).

X-ray crystallographic structures were determined of two of these enzymes, from *Ac. ambivalens* and from *Ac. tengchongensis*. Both showed that the spherical, hollow oligomers are composed

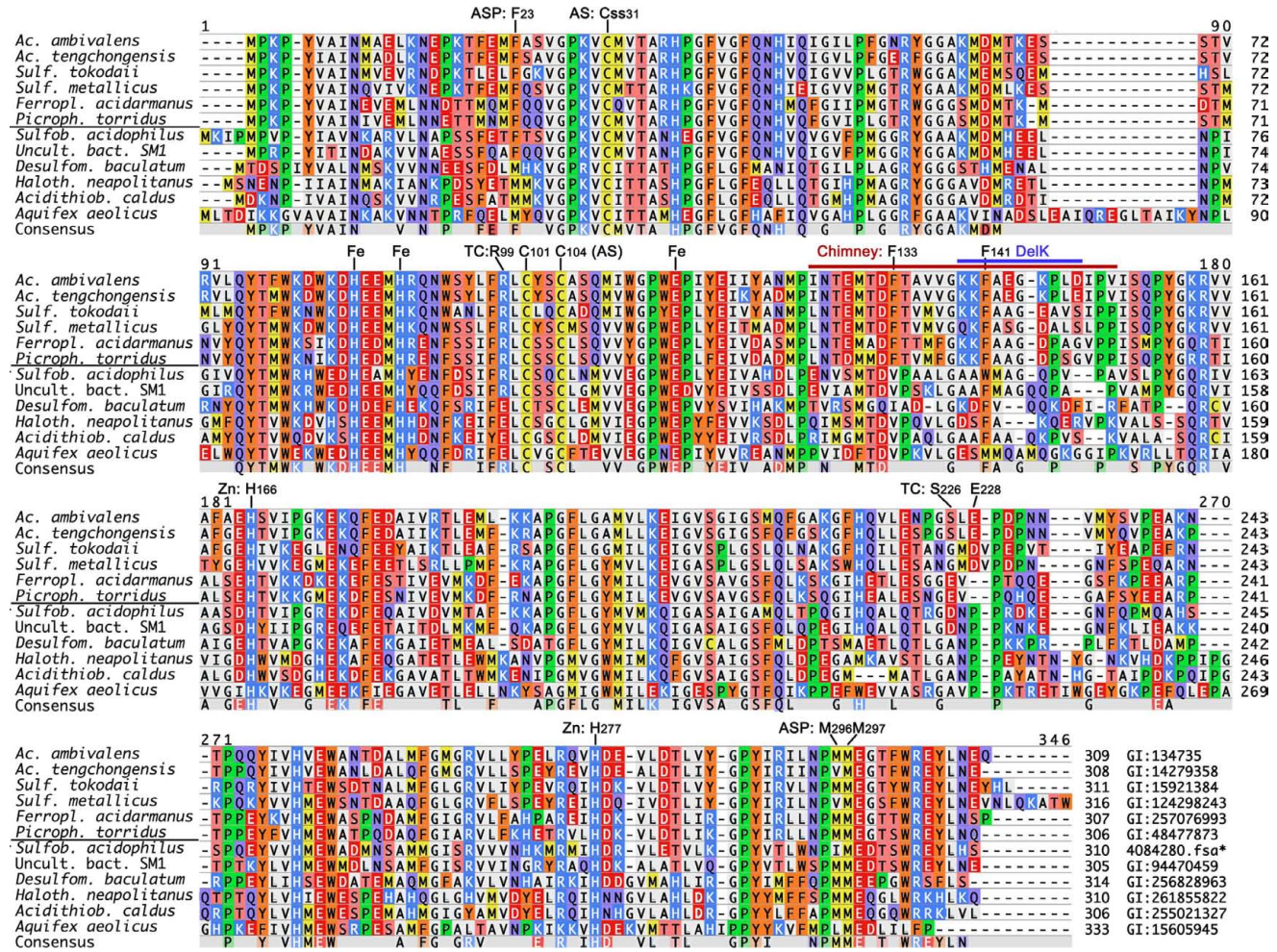

FIGURE 1 | Multiple alignments of known and complete SOR amino acid sequences from isolated proteins and from genome sequences. PCR-generated fragments with high similarity to the *Acidianus* enzymes (Chen et al., 2007) were omitted. Genbank identification (GI) numbers are given at the end; *derived from the genome sequence available at JGI[1]. The horizontal line separates Archaea from Bacteria. Abbreviations: ASP, active site pore residues (**Figure 5**); AS, active site cysteines; Css, cysteine persulfide; Fe, iron-coordinating residues; Chimney, chimney-like protrusions at the fourfold symmetry axes, identical to the DelL deletion (**Figure 2**); DelK, short deletion of the residues around the outer Phe ring (**Figure 2**); Zn, 2-His motif around the zinc-coordinating His_{277}.

of 24 identical subunits arranged in a 432 point-group symmetry (**Figure 2**; Urich et al., 2006; Li et al., 2008). The outer surfaces of the spheres are apparently smooth and impervious with the exception of very narrow pores at the four- and threefold rotational axes of the oligomers (**Figure 2**). Each subunit contains a low-potential mononuclear non-heme iron site as the putative redox-active cofactor (Urich et al., 2004, 2006). We had shown using site-directed mutagenesis that the three Fe-coordinating residues (H_{86}, H_{90} and E_{114} in *Ac. ambivalens* numbering) and a persulfurated cysteine (C_{31}) are essential for catalysis. Most likely, the cysteine persulfide is involved in sulfur binding. Mutation of the other two cysteine residues did not abolish activity, not even in a double mutant (Urich et al., 2005b). Similar results had been obtained for the *Ac. tengchongensis* SOR (Chen et al., 2005). Our current hypothesis about the reaction mechanism of the SOR predicts that the catalytic cycle is initiated by covalent sulfur binding to the active site C_{31} as a polysulfide chain (R–S_n–SH), followed by hydrolytic cleavage of the cysteine polysulfide to sulfide and a polysulfenyl moiety (R–S_n–SOH). Either Fe^{2+} or the sulfenyl group would subsequently activate oxygen (Kletzin, 2008).

The iron site and the three conserved cysteine residues (**Figure 1**) are located in an active site pocket that is connected to the inner cavity of the sphere by a narrow pore formed by two adjacent methionines and a phenylalanine (3–4 Å diameter; M_{296}/M_{297}, F_{23}; **Figures 1 and 2**). In consequence, substrate and products must pass first the outer shell of the holoenzyme into the inner cavity and then the active site pore into the pocket or *vice versa*. We had postulated that only linear polysulfane species but not circular S_8 could pass both barriers (Urich et al., 2006). Therefore, S_8-sulfur would require an initial activation step for catalysis, either by binding to a thiol group or by sulfide. The polysulfide sulfur formed in this reaction should be stable at the near-neutral pH of the cellular cytoplasm (6.5; Moll and Schäfer, 1988). In

[1]http://www.jgi.doe.gov

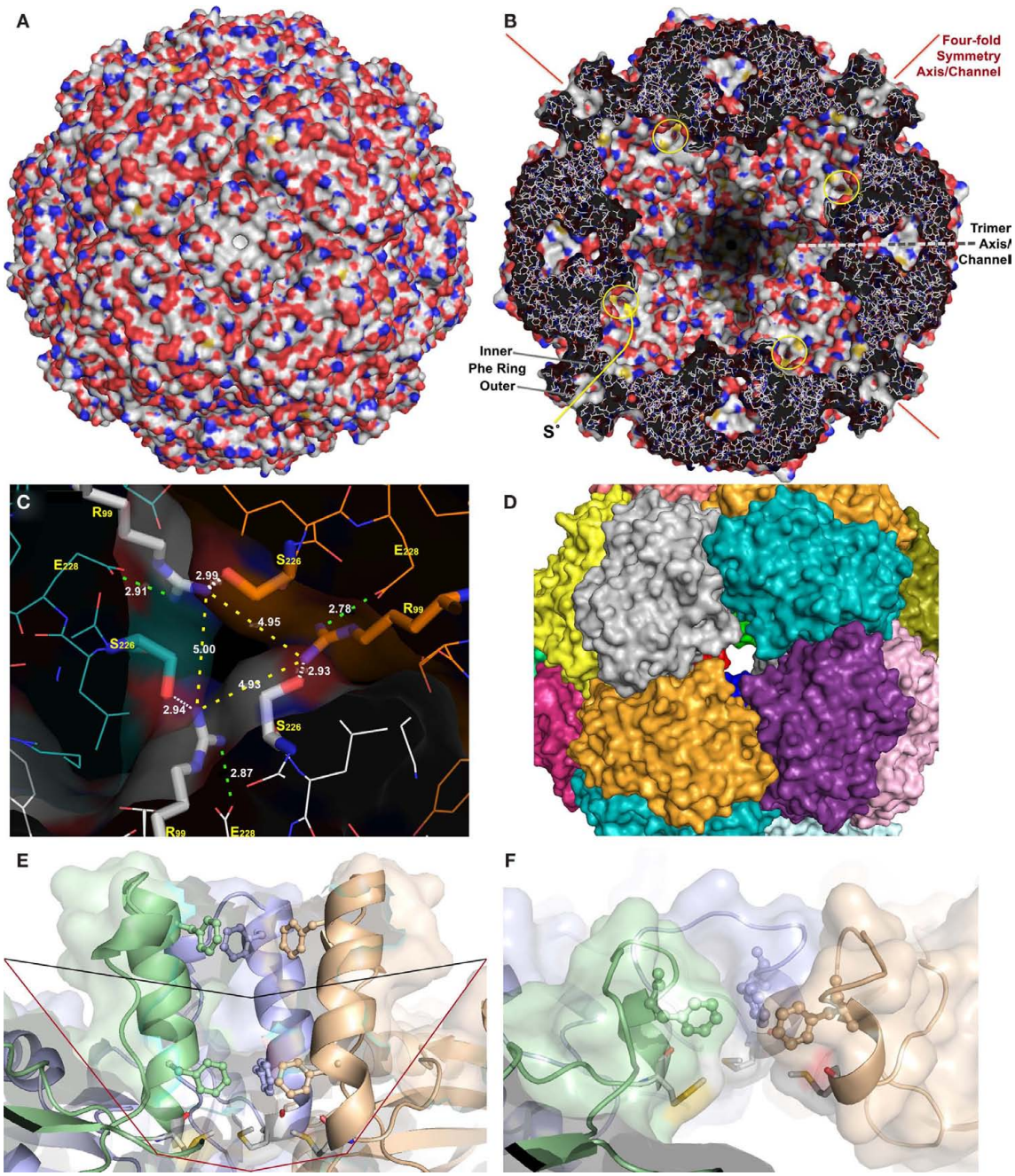

FIGURE 2 | X-ray crystallography and modeling of the SOR and its pores. (A) Surface representation of the holoenzyme centered at the chimney-like structure at the fourfold symmetry axis. **(B)** Representation of the protein structure and the inner surface of the holoenzyme sliced at the center of the fourfold symmetry axes; the position of the inner and outer phenylalanine rings are indicated, also the active site pores (yellow circles), and the approximate position of the trimer symmetry axis, which is tilted out of plane. **(C)** Channel at the threefold symmetry axis formed by R_{99} and S_{226}; distances are given between the Nη atoms of the arginines (yellow dashes), for the salt bridges to E_{228} (green dashes), and for the putative hydrogen bond to the Oγ of the S_{226} of the neighboring subunit (white dashes). **(D)** Subunit representation of the large deletion mutant at the fourfold symmetry axis DelL (**Figure 1**) modeled at the SwissModel server (Arnold et al., 2006). **(E)** Side view of the channel at the fourfold symmetry axis with outer (F_{141}) and inner phenylalanine rings (F_{133}; from top, showing three out of four subunits; wild type) and the methionine ring at its base (M_{130}); black line, approximate position of small deletion (DelK); red line, large deletion of entire chimney (DelL). **(F)** Model of the same three subunits as in panel E of the short DelK deletion, modeled at the Phyre server (Kelley and Sternberg, 2009).

contrast, polysulfides are not stable in the outside medium (pH 1–3) and disproportionate into sulfur and sulfide (Schauder and Kröger, 1993).

The question now arises how the sulfur gets inside of the enzyme and how the products get out. Two successive rings of four phenylalanine residues each form the hydrophobic pore at the

fourfold symmetry axis, followed at the inside by four methionines (**Figure 2**). In the crystallized protein, the pore is not fully open with C–C distances down to 5.0 Å in the inner Phe ring (**Figure 2**; Urich et al., 2006). Nevertheless, it is feasible that apolar molecules like the linear polysulfane species should be able to pass the pore when the protein is heated. In contrast, the polar reaction products hydrogen sulfide, sulfite and thiosulfate were proposed to exit the sphere via channels located at the threefold symmetry axes (Li et al., 2008). The narrow channel outlets are lined with hydrophilic residues such as R_{99} and S_{226}. The shortest distances between the Nη of the three arginines are ≈5 Å, or ≈6.3 Å between the Oγ of the Ser and Nη of the Arg (**Figure 2**). In addition, the arginines form salt bridges to the gamma-carboxylate group of a glutamate within the same subunit and potential hydrogen bonds to the S_{226} residues of the neighboring subunit. Nevertheless, the arginines should be able to bind transiently the anionic reaction products sulfide, sulfite and thiosulfate allowing their exit.

Here, we show by site-directed mutagenesis that opening the putative substrate and product pathways in the outer shell leads to a significant increase in specific activity and to a shift in the stoichiometry of the products. In contrast, the integrity of the inner pore seems to be important. We also show by mutagenesis studies and crystallographic analysis of inhibitor derivatives that Hg^{2+} and IAA bind in the active site as expected, whereas Zn^{2+} does not and could interfere with the movement of substrates and products.

MATERIALS AND METHODS

CONSTRUCTION OF SITE-DIRECTED MUTANTS AND HETEROLOGOUS GENE EXPRESSION IN *ESCHERICHIA COLI*

The *sor* gene (EMBL accession number X56616) was expressed heterologously using the pASK75 vector and a C-terminal Strep-tag fusion as described elsewhere (pASK-SOR.05 plasmid; Skerra, 1994; Urich et al., 2004). The site-directed mutants of several codons were constructed by using the Quikchange method with pASK-SOR.05 as a template (Stratagene; now Agilent Technologies, Böblingen, Germany; see **Table 1** for a list of the mutants and oligonucleotides used).

The PCR product was digested for 4 h with 10 U *Dpn*I (Fermentas; St. Leon-Rot, Germany), subsequently purified via the PCR Clean-Up Kit (Sigma-Aldrich; Steinheim, Germany) and eluted with 25 µl of elution buffer. After transformation of *E. coli* TOP 10' cells (Invitrogen, Darmstadt, Germany) with 6–7 µl of the purified PCR product, the resulting constructs were analyzed by restriction digestion and by sequencing. Plasmid minipreparations of 25 colonies were sequenced using the degenerated $MM_{296/297}$ primers, which resulted in the identification of the four mutants $M_{297}A$, $M_{296}V$, $MM_{296/7}VT$, and $MM_{296/7}TT$. The double mutant $F_{133}A/F_{141}$ was constructed using the $F_{141}A$ oligonucleotides with the previously constructed $F_{133}A$ mutant plasmid. In the DelL mutant (deletion, l = long), 23 chimney-forming amino acid residues were replaced by three glycines (**Figure 1**; **Table 1**). In the DelK derivative (deletion, K = kurz; German for short), 10 residues were replaced by two glycines.

Escherichia coli BL 21 Codon plus (DE3) RIL cells (Stratagene) were transformed with the mutant plasmids and the original pASK-SOR.05. The expression of the *sor* genes was induced by addition of anhydrotetracycline (200 µg/l of culture; IBA; Göttingen, Germany) to either 0.5 or 15 l cultures growing at 37°C in 2× LB medium at an OD_{600} between 0.6 and 0.8. The cultures were incubated for 20 h after induction with either vigorous shaking (0.5 l) or with vigorous aeration and stirring (15 l). In order to ensure sufficient iron incorporation, 100 µM ferric citrate was added to the media at the time of induction.

PROTEIN PURIFICATION

The harvested cells were washed once in approximately 10 volumes of 100 mM Tris–HCl/150 mM NaCl buffer pH 8 and then resuspended in five volumes of the same buffer. Cells were disrupted with a High Pressure Homogenizer (Constant Systems; 0.18 mm

Table 1 | Forward oligonucleotides used in this study for the mutagenesis of the *sor* gene; the corresponding reverse-complimentary oligonucleotides required for the Quikchange method (Stratagene) are not shown.

Oligonucleotide name	Oligonucleotide sequence*	Comment*
DelK fwd	CCGACTTCACTGCAGTTGTAggaggtggaATTC CAGTTATTTCACAACC	Replacement of aa 139-148 with two Gly residues; Addition of *Eco*RI site
DelL fwd	CAAACATGCCTATAAACACTGGGggtggaATTT CACAACCATATGGAAA	Replacement of aa 129-151 with two additional Gly residues; Removal of *Pst*I site
$R_{99}A$ fwd	GGAGTTACTTATTCgcgCTATGCTATTCATGCGC	Addition of *Bsh*1236I site
$R_{99}IL$ fwd	AACTGGAGcTACTTATTCmtcCTATGCTATTCATG	Addition of *Alu*I site
$S_{226}A$ fwd	AACCCTGGAgCACTTGAGCCcGATCCAAAT	Removal of *Psu*I site
$S_{226}T$ fwd	AACCCTGGAaCACTTGAGCCcGATCCAAAT	Removal of *Psu*I site
$S_{226}IL$ fwd	AACCCTGGamtACTTGAGCCcGATCCAAAT	Removal of *Psu*I site
$MM_{296/297}$ fwd**	ATTAAATCCAryGryGGAAGGCACcTTCTGGAG-	Addition of *Ban*I site
$F_{133}A$ fwd	TGAAATGACCGACgcaAtTGCGGTTGTA	Addition of *Mun*I site, double mutant; T134I
$F_{141}A$ fwd	GTAGGAAAGAAGgcaGCAGAAGGAAAGCCT	Removal of *Pst*I site
$H_{166}A$ fwd	GCCTTTGCAGAGgcgTCAGTAATTCC	Removal of *Bsp*1286I site
$H_{277}A$ fwd	TAAGACAAGTAgctGACGAAGTTTT	Removal of *Tat*I site

**Underlined, restriction sites specified in the comments column.*
***Multiple mutants: $M_{297}A$, $M_{296}V$, $MM_{296/7}VT$, and $MM_{296/7}TT$.*

nozzle and 1.35 MPa pressure). After a first centrifugation step (10,000 × *g* for 30 min, Sorvall, SLA-3000; Thermo Fisher Scientific, Schwerte, Germany), the soluble protein-containing supernatant was centrifuged in an ultracentrifuge (100,000 × *g* for 45 min, Beckman Instruments, 45Ti). The particle-free protein extracts from 5 to 50 g of cells (wet mass) were applied to an 8 ml Strep-Tactin super-flow column (IBA, Göttingen, Germany) connected to an ÄKTApurifier 10 (GE Healthcare Bio-Sciences AB, Uppsala, Sweden). The elution step was performed with three column volumes of washing buffer containing 2.5 mM desthiobiotin (IBA). The column was washed and regenerated according to the manufacturer's recommendations. Alternatively, the column was regenerated with three column volumes each of ddH_2O, 0.5 M NaOH, and ddH_2O instead of the regular HABA solution (IBA).

ANALYTICAL PROCEDURES

Specific activities of the wild type and mutant proteins were determined by incubation of 2–5 µg of purified enzyme/ml of Tris–HCl buffer pH 7.2 containing 2% sulfur and 0.1% of Tween 20 as described previously (Kletzin, 1989; Urich et al., 2004, 2005b). Samples were taken at appropriate time points (usually after 0, 2, 4, 6, 8, and 10 min) and the concentration of the products was determined colorimetrically. Specific activities were calculated from the linear increase of product concentrations (Kletzin, 1989). At least two activity measurements were performed for each mutant using independently purified protein preparations (see below, **Table 2**). Iron quantification was performed with pure protein preparations using the 2,4,6-tripyridyl-1,3,5-triazine method (TPTZ; Fischer and Price, 1964). Protein concentrations were determined by the Coomassie Blue method (Bradford, 1976) or using the BCA Protein Assay Kit (Novagen/Merck, Darmstadt, Germany) according to the manufacturer's instructions. Samples of purified proteins were separated by SDS-PAGE (Schägger and von Jagow, 1987) and visualized with colloidal Coomassie Blue staining (Roti-Blue; Roth, Karlsruhe, Germany).

INHIBITION ASSAYS

Zinc inhibition assays of the wild type and mutant proteins were performed by addition of a freshly prepared zinc chloride solution to the reaction buffer in concentrations ranging from 0.01 to 1 mM (Kletzin, 1989). After addition of the enzyme, the mixture was incubated for 30 min at room temperature before starting the reaction by heating to 85°C and measurement of the specific activities. A zinc/buffer mixture without protein was used as a negative control.

CRYSTALLIZATION, DATA COLLECTION, ALIGNMENT AND MODELING

Crystallization of the SOR protein was performed as described previously (Urich et al., 2005a). The mercury derivative was prepared by addition of 5 mM sodium 4-(hydroxymercury)-benzoic acid (or *p*-chloromercuribenzoic acid, *p*-CMB) for 5 days at 22°C to crystallization drops containing grown crystals. The zinc-complexed SOR was prepared by co-crystallization of the SOR in presence of 10 mM

Table 2 | Specific activities of wild type and mutant SOR, iron content, numbers (#) of preparations and assays per preparation.

Mutant	Oxygenase spec. activity (U/mg protein)	Reductase spec. activity (U/mg protein)	Fe content absolute (nmol/2.8 nmol protein)	Fe content relative (nmol/nmol subunit)	# Preps | # Assays
Wild type	3.03 ± 0.31	1.69 ± 0.44	2.8	1	4 | 2
TETRAMER CHANNEL MUTANTS					
delL	12.74	12.02	3.0	1.1	3 | 3
delK	9.89 ± 1.48	8.05 ± 3.14	3.1	1.1	4 | 3
F133A	3.89	1.48	nd*	nd*	2 | 2
F141A	4.43	1.96	4.3	1.6	2 | 2
F133A/F141A	5.88	5.87	4.8	1.72	2 | 2
ACTIVE SITE PORE MUTANTS					
M296V	3.03 ± 0.31	2.74 ± 0.71	3.9	1.4	3 | 3
M297A	1.39 ± 0.27	0.74 ± 0.05	4.3	1.5	3 | 3
MM296/297VT	1.89 ± 0.11	0.94 ± 0.09	4.0	1.4	3 | 3
MM296/297TT	2.26 ± 0.57	0.98 ± 0.05	4.4	1.6	3 | 3
TRIMER CHANNEL MUTANTS					
R99A	5.53 ± 1.21	2.55 ± 0.57	4.0	1.4	4 | 3
R99I	4.25 ± 0.72	3.82 ± 1.07	2.9	1.0	1 | 3
S226A	4.12 ± 0.92	2.21 ± 0.47	3.4	1.2	4 | 3
S226T	5.54 ± 1.34	2.64 ± 0.26	3.4	1.2	4 | 3
S226I	3.1 ± 0.98	5.15 ± 0.68	3.1	1.1	1 | 3
S226L	2.68 ± 0.35	8.39 ± 1.19	2.9	1.0	1 | 3
Zn BINDING SITE MUTANTS					
H277A	2.73 ± 0.46	1.71 ± 0.76	3.3	1.2	2 | 2
H166A	2.9 ± 0.22	1.38 ± 0.21	6.9	2.4	2 | 2

**Not determined.*

zinc acetate for 2 days at 32°C. SOR was also co-crystallized with 10 mM IAA for 2 days. After washing in a cryoprotectant solution without the reagents used for soaking, the crystals were flash-frozen in liquid nitrogen (Urich et al., 2005a). The diffraction data sets of the SOR co-crystallized with zinc and IAA were collected with a resolution of 1.7 and 1.9 Å, respectively, at the ESRF beam line 14-1. The Hg^{2+} dataset was collected with a resolution of 2.5 Å at the ESRF beam line 14-3.

Images from the three diffraction experiments were processed with DENZO and the observed intensities merged and scaled with SCALEPACK of the HKL Suite (Otwinowski and Minor, 1997). Structure factor amplitudes were then calculated with TRUNCATE and the three sets scaled together against the native data (PDB entry 2CB2-SF; Urich et al., 2006) with SCALEIT of the CCP4.2.2 suite (Collaborative Computational Project, 1994). The final model of the native structure including cysteine persulfide, Fe ions and waters molecules was used as template for structure refinement with REFMAC (Murshudov et al., 1997) or PHENIX (Adams et al., 2010). The stereochemistry of the Zn and Hg centers was refined without target geometrical restraints. After an initial rigid body refinement the models were iteratively refined, analyzed and edited with XTALVIEW-XFIT (McRee, 1999) against electron density maps, until convergence of *R*-values was achieved (Urich et al., 2006).

The sequences used for the multiple alignment (**Figure 1**) were obtained following a BLAST search at NCBI[2] with the *Ac. ambivalens* SOR sequence as input. The *Sulfobacillus acidophilus* SOR sequence was identified in the almost complete genome sequence available at the JGI genome server[3] (January 2011). The alignment was made with MAFFT using the default parameter at the Kyushu server[4]. The DelL and DelK deletion mutants were modeled using the Phyre[6] (Kelley and Sternberg, 2009) and SwissModel servers[5] (Arnold et al., 2006) with the wild type 3D structure as template. The figures were prepared in Pymol, including the qualitative surface electrostatic distribution (DeLano, 2002).

DATA DEPOSITION

The atomic coordinates of the SOR derivatives were deposited at the Protein Data Bank with identification numbers *2yav* (Zn derivative), *2yaw* (Hg) and *2yax* (IAA).

RESULTS

PROPERTIES OF THE SOR MUTANTS

SOR mutant plasmids generated via site-directed mutagenesis were sequenced and were introduced, if correct, into *E. coli* BL21 Codon Plus cells. Wild type or mutant SOR protein was obtained after overnight incubation of the induced cultures. After breaking of the cells, 10–30% of the protein was present in soluble form while ≥70% precipitated in inclusion bodies as observed previously (Urich et al., 2004). The recombinant wild type and mutant SOR proteins were purified from the soluble *E. coli* fractions in a one-step procedure using the attached *Strep*-tag and *Strep*-Tactin columns. The yields of purified protein ranged from 0.6 to 1.2 mg/l of culture volume. When analyzed with SDS-PAGE, all SOR preparations were more than 90% homogeneous. In each protein preparation one larger band with a molecular mass of 70 kDa was seen and several smaller bands (**Figure 3**), the latter of which had been shown to represent cleavage products (Urich et al., 2004). Wild type and mutant proteins were analyzed for specific enzyme activity and iron content in order to verify that altered enzyme activities reflect true mutagenesis effects and not low iron incorporation into the active site. The iron content of the purified proteins was in the range of 1–3 Fe/subunit (**Table 3**). The average values of specific wild type SOR activities were 3.03 ± 0.31 U/mg (oxygenase) and 1.69 ± 0.44 U/mg (reductase).

OPENING OF THE OUTER SPHERE INCREASES ACTIVITY

Two mutants were constructed, which feature truncated versions of the chimney-like structures located at the fourfold symmetry axes. In the DelL mutant (deletion, L = long) the 23 amino acid residues that form the protrusions including both phenylalanine rings (**Figures 1 and 2D**) are replaced by three glycines. In the DelK derivative (deletion, K = kurz; German for short) 10 residues including the outer phenylalanine ring were replaced by two glycines. When modeled into the SOR holoenzyme structure, the pore opened to a diameter of 9–10 Å in the DelL mutant. The atomic distances of the inner phenylalanine ring did not change significantly in the model of the DelK mutant, so that it does not

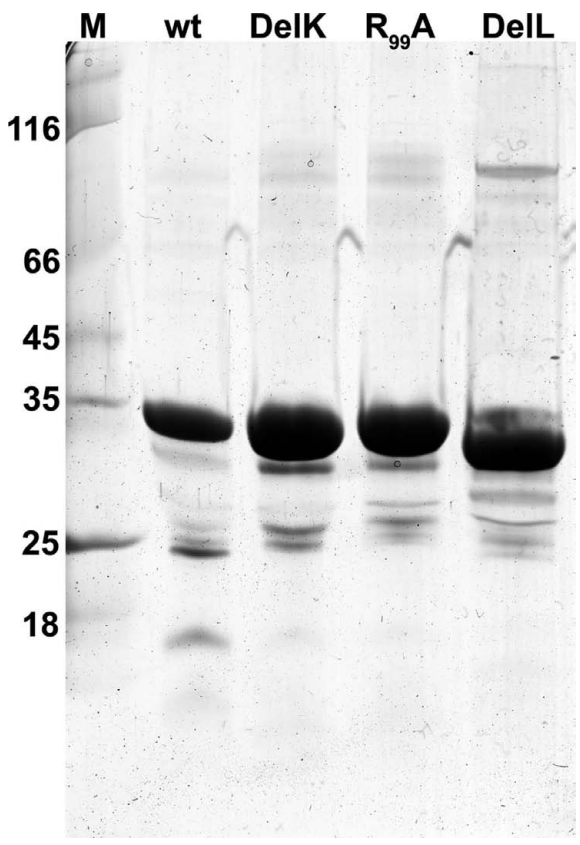

FIGURE 3 | Coomassie-stained SDS gel of SOR wild type and three of the mutants; 5 µg of protein per lane; M, molecular weight marker.

[2]http://www.ncbi.nih.gov

[3]http://mafft.cbrc.jp/alignment/server/

[4]http://www.sbg.bio.ic.ac.uk/~phyre/

[5]http://swissmodel.expasy.org/

[6]http://www.jgi.doe.gov

Table 3 | Diffraction data processing and refinement statistics.

SOR derivative	*SOR-Hg*$^{2+}$	Zn^{2+}	Iodoacetamide
Source	ESRF ID14-3	ESRF ID14-3	ESRF ID14-3
Space group	I4 (79)	I4 (79)	I4 (79)
Unit cell parameters (Å) *a*	*a* = *b* = 161.88	*a* = *b* = 162.07	*a* = *b* = 161.90
	c = 154.37	*c* = 154.24	*c* = 154.27
Wavelength (Å)	0.934	0.934	0.934
No unique intensities	68,600	213,677	172,862
Redundancy	15.0	1.9	2.8
Resolution (outer shell) (Å)	49.04–2.50 (2.53–2.50)	38.20–1.70 (1.76–1.70)	38.05–1.80 (1.85–1.80)
Completeness (outer shell) (%)	99.9 (98.9)	98.3 (94.1)	94.4
R_{merge}* (outer shell) (%)	8.1 (48.7)	6.4 (45.9)	5.5 (26.2)
$I/s(I)$ (outer shell)	33.3 (5.0)	12.0 (1.8)	16.7 (1.8)
Wilson B (Å^2)	43	19	19
REFINEMENT			
Refined structure	1842 aa	1842 aa	1842 aa
	526 waters	1382 waters	477 waters
R_{work} (%)	16.2	16.3	17.0
R_{free} (%)	18.2	19.3	19.0
R (%)	16.7	16.2	
Average ADP (Å^2)	29	21	29
Bonds RMSD (Å)	0.017	0.017	0.022
Angles RMSD (°)	0.974	1.220	1.710

*$R_{merge} = \Sigma|I_o - \langle I \rangle|/\Sigma I_o$, where $\langle I \rangle$ is the average of symmetry equivalent reflections and the summation extends over all observations I_o for all unique reflections.

display an open pore (from 5.0 Å in the wild type protein to 5.4 Å in the mutant; **Figure 2**). As expected, the apparent molecular masses of the DelL and DelK mutants were slightly smaller in SDS gels compared to the wild type enzyme (**Figure 3**).

Several-fold increased enzyme activities were observed in both cases. DelL showed 420% of the oxygenase and up to 771% of the reductase activities, while DelK showed an increase up to 326% (oxygenase) and 476% (reductase), respectively (**Figure 4**; **Table 2**). The phenylalanine residues were mutated into alanine independently ($F_{133}A$, $F_{141}A$) and as a double mutant ($F_{133}A/F_{141}A$). All three different mutants showed increased activities. The double mutant showed the highest activities (194% of the oxygenase and 347% of the reductase). Mutation of $M_{130}A$ located at the base of the channel (**Figure 2**) did not alter the catalytic properties of the enzyme (not shown).

R_{99} and S_{226}, both located at the postulated channel outlet at the threefold symmetry axis, were substituted for alanines independently. Together with an $S_{226}T$ variant, all three mutants showed elevated enzyme activities. $R_{99}A$ and $S_{226}T$ were comparable having both about 182% oxygenase and 156% reductase activities. Isoleucine and leucine variants of the pore-forming channel outlet residues were comparable to the wild type in oxygenase activity but showed a significantly increased reductase activity of up to 496% in case of $S_{226}L$ (**Figure 2**; **Table 2**).

THE INTEGRITY OF THE ACTIVE SITE PORE IS ESSENTIAL

The active site pore entrance, which provides access to the reaction center, is formed by two adjacent methionines (M_{296}/M_{297}) and one phenylalanine F_{23} (**Figure 5**). We substituted the two methionines via site-directed mutagenesis using degenerated primers that allowed for 16 variations. Twenty-five different plasmids were screened and four different mutants were obtained, two double mutants, $MM_{296/297}VT$, $MM_{296/297}TT$ and two single mutants, $M_{297}A$ and $M_{296}V$. Mutagenesis led to an opening of the active site pore as compared to the wild type with the exception of the $M_{296}V$ mutant (**Figure 5**). Both double mutants $MM_{296/297}VT$, $MM_{296/297}TT$ and also $M_{297}A$ showed a decrease to approximately 50% of wild type activity (**Figure 4**; **Table 2**). The $M_{296}V$ mutant showed an increase in reductase activity (162%) but not in oxygenase activity. The latter residue is also present in several of the naturally occurring SORs from other species (**Figure 1**).

ZINC BINDS FAR FROM THE ACTIVE SITE

Zn^{2+} had been shown to be a potent inhibitor of SOR activity as long as it is free in solution and not complexed by ligands such as EDTA (Kletzin, 1989; Urich et al., 2004). Crystals were soaked with Zn^{2+} in order to determine its binding site within the SOR. One Zn^{2+} ion was detected in the Zn-complexed structure (with 0.8 occupancy) refined at 1.7 Å resolution (**Table 3**). It was located on the opposite side of the beta barrel core of the monomer (not shown; see Urich et al., 2006) but not in close vicinity to the active site (**Figure 6**). The zinc ion was bound in a distance of 2.1 Å to His_{277} imidazole (interatomic distances from the here-presented structures are averages over of the six crystallographically independent monomers; **Figure 6**). An acetate and a chloride ion together with two water molecules completed the coordination sphere of Zn^{2+} (**Figure 6**). His_{166}, which constitutes a conserved 2-His motif together with His_{277} (**Figure 1**), had its Nε2 in hydrogen-bonding distance to the two water molecules that coordinate the zinc (**Figure 6**). Both histidines are located at the

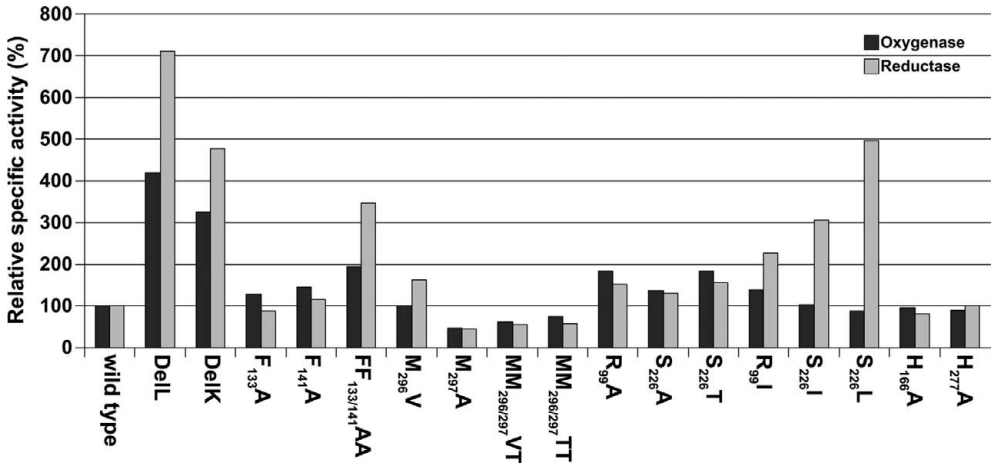

FIGURE 4 | Histogram of relative activities of wild type SOR and mutants, the wild type was set to 100% according to the values in Table 3.

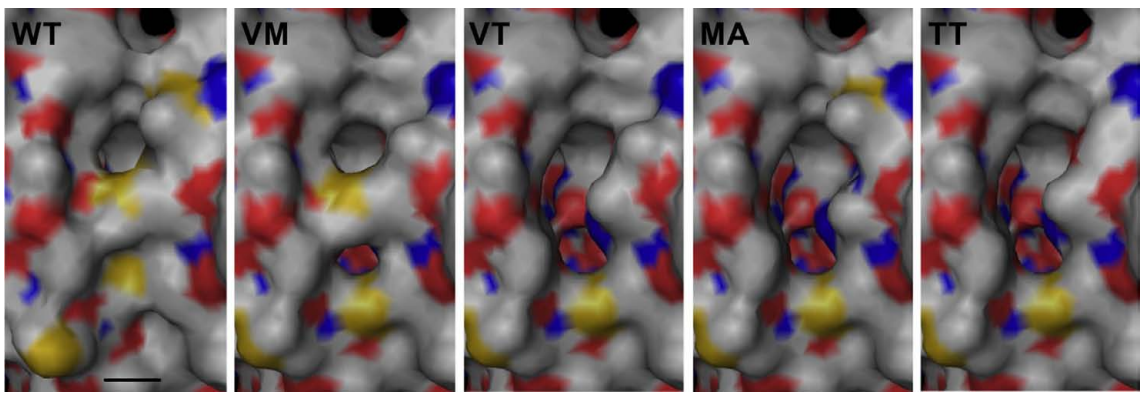

FIGURE 5 | Modeling of active site pore mutants based on the wild type (WT) structure at the SwissModel server (Arnold et al., 2006). Abbreviations and symbols: VM, $M_{296}V$; VT, $MM_{296/297}VT$; MA, $M_{297}A$; TT, $MM_{296/297}TT$; bar, 4 Å.

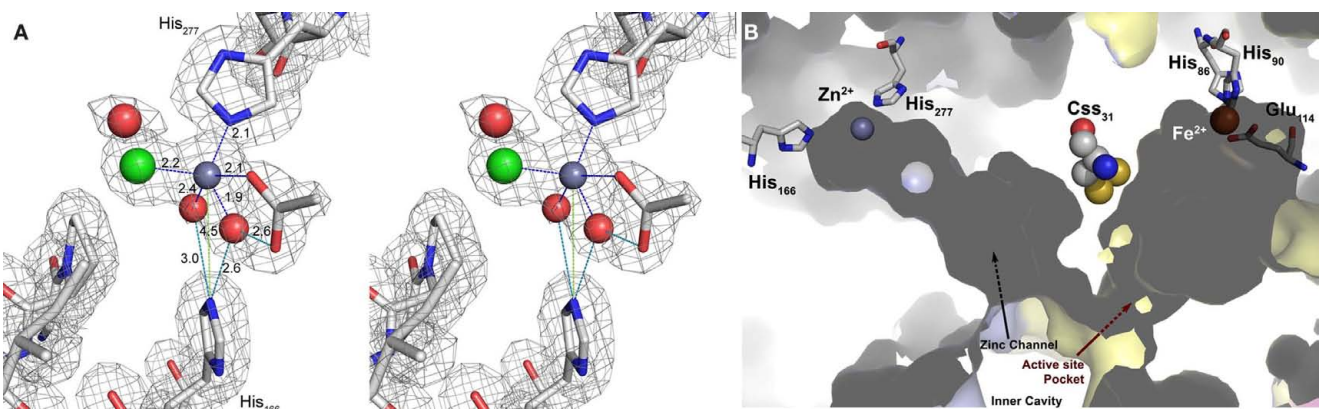

FIGURE 6 | The Zn^{2+}-binding site. (A) Electron density at the Zn^{2+}-binding site (gray mesh representing 2m|Fo| – D|Fc| map at 1 σ). Cross-eyes stereo image showing the Zn^{2+} ion coordination (dark gray sphere with blue dashed lines) with the His_{277} side chain, one acetate ion (ACT), one chloride ion (green sphere), and two waters (red spheres) that are also at hydrogen-bonding distances (cyan dashed lines) from Nε2 of the His_{166} side chain. The other acetate oxygen is at hydrogen-bonding distance (cyan dashed line) from one of the Zn^{2+} coordinating waters; light green dashes, non-bonding distances; sticks representation: carbon in gray, nitrogen in blue, oxygen in red. **(B)** Surface representation of two neighboring monomers (light blue and yellow) highlighting the positions of the Zn and Fe sites with their respective ligands and channels and the bridging cysteine persulfide. The zinc site is located at the end of a tunnel leading to the active site Css_{31} of the neighboring monomer.

bottom of a long, semi-closed channel that opens to the inner cavity of the holoenzyme next to the active site entrance of a neighboring monomer. The Fe–Zn distances were about 27 Å, both within the same subunit and with the neighboring subunit. The side chains of Css_{31} and Met_{297} separate the entrances to the active site pocket and the zinc-binding channel. We had postulated that Css_{31} is the sulfur-binding residue in the active site pocket (Urich et al., 2006). The distance between Zn^{2+} and the Sδ atom of the cysteine persulfide Css_{31} was 18 Å, so that direct interference of zinc in the catalysis is improbable.

When His_{166} and His_{277} were substituted independently for alanine, the specific activities were similar to the wild type enzyme (**Figure 4**; **Table 2**). K_i-values (half-maximal inhibitory concentration) of the wild type enzyme were 45 μM zinc chloride for the oxygenase activity and 39 μM for the reductase activity. K_i-values for $H_{166}A$ were 121 μM (oxygenase) and 150 μM (reductase). The mutant $H_{277}A$ showed comparable K_i-values of 157 μM (oxygenase) and 144 μM (reductase).

MERCURY AND IODOACETAMIDE BIND AT ACTIVE SITE CYSTEINES

Analysis of the crystallographic model of the *p*-CMB treated crystal refined at 2.5 Å resolution (**Table 3**) showed in the active site pocket two partially occupied Hg^{2+} ions per monomer. One Hg^{2+}, with 0.5 occupancy, was bound at a distance of 2.1 Å to the Sγ atom of the cysteine persulfide (Css_{31}; **Figure 7**). A putative acetate ion refined reasonably well, also with 0.5 occupancy, with one of his carboxylic oxygens coordinating Hg^{2+} at 2.0 Å distance, although the limited resolution maps also show some density noise in its neighborhood. The second mercury ion, with 0.3 occupancy, refined at 2.6 Å distance from Sγ of non-essential cysteine Cys_{101}, with the side chain in *trans* conformation for torsional angle chi1, and with occupancy 0.3. The other side chain conformation, chi1 *gauche(−)* (with occupancy 0.7) corresponds to that of the native structure. This Hg^{2+} is not too far away from the Sδ atom of Met_{108}, at 3.7 Å distance. Thus, the inhibition of the enzyme by mercury compounds (Kletzin, 1989) is caused by modification of the active site cysteine(s).

The co-crystallization with the thiol-modifying reagent IAA resulted in additional electron density resembling acetamide in covalent distance to Cys_{101} (**Figure 7**). The electron density was present with low occupancy in three out of six monomers in the asymmetric unit. No additional density was observed at Css_{31} or Cys_{104}. In consequence, it appears that Cys_{101} is the primary target for alkylation with IAA, although this conclusion is tentative due to the low reactivity between enzyme and inhibitor in this experiment.

DISCUSSION

Sulfur oxygenase reductases are uncommon sulfur-disproportionating enzymes restricted to a few species of sulfur-oxidizing Archaea and Bacteria, which are either facultative or obligatory chemolithoautotrophs (**Figure 1**). Determination the 3D structure of two of these enzymes showed that they form large hollow homomultimers with more or less secluded inner chambers. Each subunit contains a reaction pocket with conserved sites consisting of a mononuclear iron and a cysteine residue (Urich et al., 2004, 2005b, 2006; Chen et al., 2005; Li et al., 2008). The SORs thus provide enclosed reaction and/or storage compartments physically separated from the cytoplasm (**Figure 2**). Despite previous biochemical and mutagenesis studies it is still unclear how the proteins work in detail. Here, we focus on the pores in the protein and on the mode of action of important inhibitors of enzyme activity.

THE PORES AT THE FOURFOLD SYMMETRY AXIS RESTRICT ENZYME ACTIVITY

Narrow pores padded with apolar amino acids are localized at the chimney-like structures at the fourfold symmetry axes (**Figure 2**). They were already considered to be the substrate entrance points to the inner cavity of SOR (Urich et al., 2006; Li et al., 2008). Two rings of four phenylalanine side chains each define these pores in the present 3D model (**Figure 2**). Here we show that mutation of the Phe residues into Ala, which induces enlargement of the pores, gave a moderate, less than twofold increase in specific enzyme

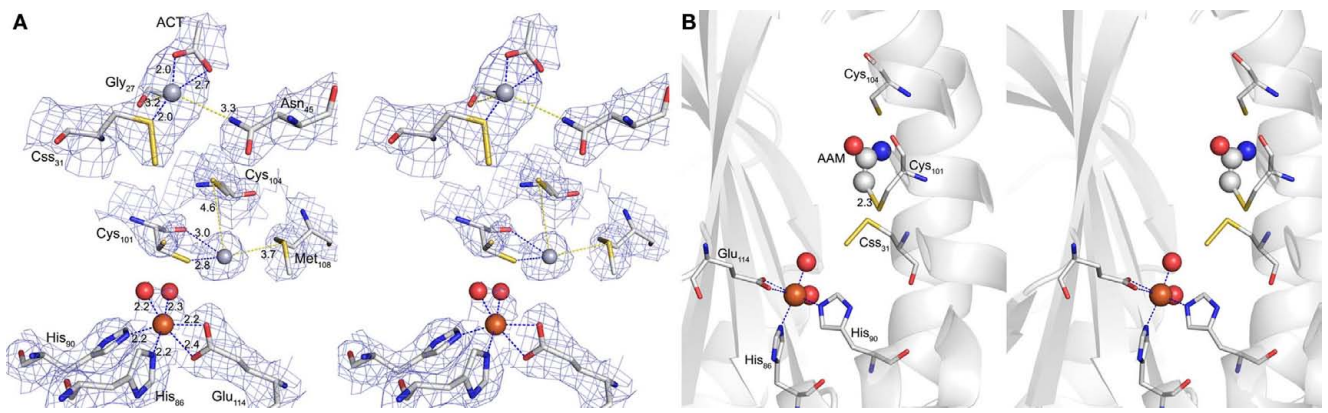

FIGURE 7 | Hg^{2+} and iodoacetamide-binding sites. (A) Electron density at the Hg^{2+}-binding sites (blue mesh representing 2m|Fo| – D|Fc| map at 1 σ). Cross-eyes stereo image of the coordination spheres of the two Hg^{2+} ions (gray spheres) and the active site Fe^{3+} (brown sphere); Hg1 at Sγ of Css_{31} with additional distances to one acetate (ACT) and the backbone oxygen of Gly_{27} (blue dashed lines) and to Nδ of Asn_{45} (yellow dashed line); Hg2 at Sγ and the backbone oxygen of Cys_{101} (blue dashed lines) and with the distances to Sγ of Cys_{104} and to Sδ of Met_{108} (yellow dashed lines); Fe^{3+} with two water ligands (red spheres), two histidine side chains and a bidentate glutamate (all blue dashed lines); sticks representation: carbon in gray, nitrogen in blue, sulfur in yellow and oxygen in red; ACT, acetate. **(B)** Cross-eyes stereo image of the acetamide (AAM) binding site with secondary structure representation of the subunit backbone; Fe site and sticks representation as above; AAM in sticks and spheres.

activity (**Figure 4**). A full deletion of the loop building the chimneys (**Figures 1 and 2**) resulted in a more than sevenfold increase in enzyme activity showing that substrate access to the active site and/or product exit is indeed limited by the outer shell of the protein. Therefore, it can be concluded that the specific activity of the wild type SOR is curbed to a lower level than optimally possible. The reasons for making the enzyme slow might be speculated upon. One option (among others) would predict that the reactive reaction products are not released uncontrollably into the cytoplasm but that they are delivered directly to the downstream oxidoreductases (Kletzin, 2008). One experimental indication for this interpretation – in the absence of known interaction partners – came from antibody/immunogold electron microscopy results of the *Ac. tengchongensis* SOR: the enzyme seemed to be attached to the inside of the cytoplasmic membrane (Chen et al., 2005). In addition, these pores might provide highly controlled access points to the active sites, preventing the oxidation of "unwanted substrates."

MUTAGENESIS AT THE THREEFOLD SYMMETRY AXIS AND REACTION MECHANISM

The amino acids Arg_{99} and Ser_{226} are central elements of the subunit interface at the threefold symmetry axis. Arg_{99} forms an intra-subunit salt bridge to Glu_{228} (**Figure 2**). The other η-nitrogen atom is in hydrogen-bonding distance (2.8 Å) to the Oγ of Ser_{226} of the neighboring subunit. Alternative hydrogen-bonding networks are also possible: Arg_{99} might link to the α-carbonyl oxygen atoms of Ser_{226} of two subunits. In addition, a hypothetical salt bridge between the ε-nitrogen of the Arg_{99} and Glu_{228} is possible, provided that an extensive charge delocalization exists in the guanidinium group. We did not obtain protein of an $E_{228}A$ mutant from *E. coli* cells, so that we cold not analyze its effects on salt bridge formation (data not shown). In contrast, mutation of Arg_{99} and Ser_{226} into Ala gave a modest, less than 1.5-fold increase in specific activity (**Figure 4**). Mutation into more hydrophobic residues changed the ratio between oxidized and reduced reaction products in favor of sulfide (**Figure 4**; **Table 2**). The same had happened in a less pronounced way in the chimney mutants DelK and DelL, suggesting that opening of the closed reaction chamber in the interior of the protein changes the ratio between the oxygenase and disproportionase partial reactions (Eqs 1 and 2).

The interpretation of the activity data is complicated by non-enzymatic reactions occurring with sulfur and ISC in aqueous solutions, which depend on the incubation temperature and the pH of the buffer. For example, sulfite reacts rapidly with excess sulfur to thiosulfate at pH ≥ 5 and 85°C so that it is still unclear whether thiosulfate is a primary or secondary reaction product of the SOR (Kletzin, 1989). The sulfur disproportionation depicted in Eq. 2 and with H_2S, polysulfides and thiosulfate (instead of sulfite) as products occurs non-enzymatically at alkaline pH (detectable above pH 7.5 at 75°C; Roy and Trudinger, 1970; Kletzin, 1989). We had concluded from previous activity assays in the presence of chemically complexed zinc (to overcome zinc inhibition and to precipitate sulfide *in situ*) that an approximate 1:1 ratio between oxidized and reduced reaction products is maintained (Eq. 3) as opposed to the 1:2 ratio for the oxygen-independent disproportionation shown in Eq. 2. We also had assumed that the sub-stoichiometric hydrogen sulfide detection in the standard assay is due to the rapid non-enzymatic re-oxidation under the aerobic assay conditions (see **Table 2**, wild type enzyme; Kletzin, 1989, 2008; Kletzin et al., 2004; Urich et al., 2004). This picture however changes with the channel mutants, which prove that the ratio between oxidized and reduced reaction products is not constant and that it depends on the integrity of the protein shell.

THE INTEGRITY OF THE ACTIVE SITE PORE SEEMS TO BE IMPORTANT

A different story resulted from the mutations at the active site pore, made from two adjacent methionines, M_{296}/M_{297} and a phenylalanine, F_{23}. M_{297} is conserved in all SORs, while M_{296} is exchanged for another hydrophobic amino acid in several naturally occurring SOR sequences (**Figure 1**). F_{23} is conserved in Archaea while Bacteria mostly use methionine at this position. The pore supposedly represents the entrance of substrate and the exit of the products; at least, we were unable to find a "back exit" in the active site pocket of the *Ac. ambivalens* enzyme as suggested for the *Ac. tengchongensis* SOR (Li et al., 2008). Expansion of the active site pore did not increase the enzyme activity, which is contrasting our observations on the tetramer and trimer channels (**Figures 4 and 5**). Replacement of the hydrophobic Met residues with the smaller and in the case of the threonine more hydrophilic residues diminished the specific activity by half, suggesting that the hydrophobic barrier and/or at least one of the methionines are essential. One could speculate that non-covalent nucleophilic interaction between the atoms of the sulfur substrate and the Sδ atom of the gate-keeping methionine residues could direct the sulfur substrate toward the active site cavity.

DIFFERENT MECHANISMS OF INHIBITOR ACTION

Zinc and the thiol-binding agents *p*-CMB, IAA and maleimide were previously shown to act as inhibitors (Kletzin, 1989). No activity had been observed in the presence of 1 mM Hg^{2+} or Zn^{2+} ions, whereas 0.1 mM resulted in 37 and 74% residual activity, respectively, for the oxidized reaction products (Kletzin, 1989). Inhibition by Zn^{2+} was neutralized by addition of at least equimolar concentrations of EDTA (Urich et al., 2004). Both Hg^{2+} and Zn^{2+} ions can theoretically bind to sulfur atoms of cysteine(s), to histidine and/or carboxylate ligands. The alkylating agents IAA and NEM were less potent inhibitors: 27% of oxygenase activity remained in the presence of 1 mM IAA (Kletzin, 1989), while 47% remained with 1 mM NEM. In order to determine the mechanisms of inhibition, we resolved the 3D structures of wild type SOR crystals soaked in *p*-CMB, IAA, and Zn^{2+}.

Two Hg^{2+} ions were found in the active site pocket of *p*-CMB treated crystals, one of them in bonding distance (2.1 Å) to the Sγ atom of the essential cysteine persulfide Css_{31}, thus explaining the inhibitory effect of Hg^{2+} (**Figure 7**). A second ligand was provided by the oxygen (at 2.0 Å distance) of a putative acetate from the crystallization media. The second Hg^{2+} ion is bound (2.6 Å) to Sγ of conserved cysteine Cys_{101}. Although unresolved, water molecules might provide additional ligands as both mercury ions face the lumen of the water-filled active site pocket. To conclude, the main mechanism of inhibition seems to be the result of mercury binding to Css_{31}, an amino acid that cannot be mutated without total loss of enzyme activity (Urich et al., 2005b). Mercury binding to Cys_{101} seems to play a less important role.

In contrast, the effect of IAA is more difficult to explain. Acetamide bound to Cys_{101} was observed only in three out of six subunits of the asymmetric unit and only with low occupancy (**Figure 7**). This observation has two implications. First it shows that the 24 subunits are not equal, minor distortions could be the result of inhibitor and/or substrate binding. Distortions were so far not seen at all because of the sheer number of subunits and the rotational symmetry of the holoenzyme. Both would average out minor distortions in the electron density and make subtle changes undetectable. We had tried to soak crystals with many different ISC without seeing additional electron density anywhere in the molecule (Urich, 2005), presumably because substrate or product binding occur only in a minority of subunits at a given time. Bound sulfur species would be averaged out within the holoenzyme. This situation is slightly different with IAA, where the low occupancy points into the same direction, supported by the observation that not all of the potential binding sites are occupied. However, the stoichiometry of inhibitor binding is high enough to facilitate the positive identification of the bound molecule. A second implication came from the binding site: Cys_{101} could be mutated to Ala with partial loss of activity (≈20%; Urich et al., 2005b). A $Cys_{101}S$ mutant had very low residual activity (≈1%) concomitant with a very low iron content (<0.1/subunit; Urich et al., 2005b). This observation showed that the chemical nature of the amino acid side chain at this position directly affects enzyme activity and active site integrity, although the cysteine itself is not essential.

Inhibition by zinc seems to follow a completely different mechanism. The Zn^{2+} ion was found in a dead-end channel, which opens next to the active site pore of the adjacent subunit. The active site Css_{31} separates the lumina of both channels (**Figure 6**). The question arises how zinc inhibits the enzyme activity over a distance of approximately 27 Å to the next iron. The zinc ion is coordinated by histidine residue H_{277}, one acetate, one chloride and two water molecules that in turn are hydrogen-bonding His_{166} (**Figure 6**). Mutation of either histidine into alanine did not alter enzyme activity significantly. However, their K_i-values for Zn^{2+} increased two- to threefold, compared to the wild type. The 2-His motif is conserved in the SOR sequences (**Figure 1**). It cannot be answered at present which role the obviously conserved zinc channel plays. In contrast, several options exist about the mechanism of inhibition at a distance. The Zn^{2+} ion might make the protein less flexible and thus block the substrate entry or product exit from the active site. In addition, it might block the important Css_{31} residue, which is located at the interface of both channels, in its movements during the catalytic cycle. Stiffening of the protein seems to be the most probable mechanism of inhibition because no further connection between the zinc channel and the active site pocket is present in the enzyme.

CONCLUSION

From these and previous findings we can propose a hypothetical model of the sulfur pathway in the SOR and the different modes of enzyme inhibition. The chimney-like structures at the fourfold symmetry axes formed by two phenylalanine rings are not essential for activity, but presumably act as restrictive elements for the access of the hydrophobic sulfur substrate to the inner hollow. Product exit might occur via hydrophilic channels, which have their outlets at the threefold symmetry axes. Enlargement of both openings increased the enzyme activity several-fold and also affected the formation of H_2S and the stoichiometry of reaction products. In contrast, the integrity of the active site pore, which provides a passage to the catalytic center, cannot be opened significantly without decreasing the specific activity of the enzyme. The inhibition of the SOR activity by Hg^{2+} and IAA occurs by binding of the compounds to different cysteine residues within the active site. In contrast, Zn^{2+} does not bind anywhere in the active site but in a separate channel. It might restrict protein flexibility and/or substrate and product movement within the protein subunits. It might also effect movements of the active site-cysteine persulfide (Css_{31}) side chain.

ACKNOWLEDGMENTS

We wish to thank Felicitas Pfeifer (Darmstadt, Germany) for her generosity and encouragement. A. Veith and A. Kletzin were supported by a grant of the Deutsche Forschungsgemeinschaft (Az Kl885-5/1). T. Urich was supported by a Marie Curie Host Fellowship (HPMT-CT-2000-00045).

REFERENCES

Adams, P. D., Afonine, P. V., Bunkoczi, G., Chen, V. B., Davis, I. W., Echols, N., Headd, J. J., Hung, L. W., Kapral, G. J., Grosse-Kunstleve, R. W., McCoy, A. J., Moriarty, N. W., Oeffner, R., Read, R. J., Richardson, D. C., Richardson, J. S., Terwilliger, T. C., and Zwart, P. H. (2010). PHENIX: a comprehensive Python-based system for macromolecular structure solution. *Acta Crystallogr. D Biol. Crystallogr.* 66, 213–221.

Arnold, K., Bordoli, L., Kopp, J., and Schwede, T. (2006). The SWISS-MODEL workspace: a web-based environment for protein structure homology modelling. *Bioinformatics* 22, 195–201.

Bradford, M. M. (1976). A rapid and sensitive method for the quantitation of microgram quantities of protein utilizing the principle of protein-dye binding. *Anal. Biochem.* 72, 248–254.

Chen, Z. W., Jiang, C. Y., She, Q., Liu, S. J., and Zhou, P. J. (2005). Key role of cysteine residues in catalysis and subcellular localization of sulfur oxygenase-reductase of *Acidianus tengchongensis*. *Appl. Environ. Microbiol.* 71, 621–628.

Chen, Z. W., Liu, Y. Y., Wu, J. F., She, Q., Jiang, C. Y., and Liu, S. J. (2007). Novel bacterial sulfur oxygenase reductases from bioreactors treating gold-bearing concentrates. *Appl. Microbiol. Biotechnol.* 74, 688–698.

Collaborative Computational Project. (1994). The CCP4 suite: programs for protein crystallography. *Acta Crystallogr. D Biol. Crystallogr.* 50, 760–763.

DeLano, W. L. (2002). *The PyMOL Molecular Graphics System*, 0.97 Edn. San Carlos, CA: DeLano Scientific.

Emmel, T., Sand, W., König, W. A., and Bock, E. (1986). Evidence for the existence of a sulfur oxygenase in *Sulfolobus brierleyi*. *J. Gen. Microbiol.* 132, 3415–3420.

Fischer, D. S., and Price, D. C. (1964). Simple serum iron method using new sensitive chromogen tripyridyl-s-triazine. *Clin. Chem.* 10, 21–25.

Friedrich, C. G., Bardischewsky, F., Rother, D., Quentmeier, A., and Fischer, J. (2005). Prokaryotic sulfur oxidation. *Curr. Opin. Microbiol.* 8, 253–259.

Frigaard, N. U., and Dahl, C. (2009). Sulfur metabolism in phototrophic sulfur bacteria. *Adv. Microb. Physiol.* 54, 103–200.

Ghosh, W., and Dam, B. (2009). Biochemistry and molecular biology of lithotrophic sulfur oxidation by taxonomically and ecologically diverse bacteria and archaea. *FEMS Microbiol. Rev.* 33, 999–1043.

Kamyshny, A. (2009). Solubility of cyclooctasulfur in pure water and sea water at different temperatures. *Geochim. Cosmochim. Acta* 73, 6022–6028.

Kelley, L. A., and Sternberg, M. J. (2009). Protein structure prediction on the Web: a case study using the Phyre server. *Nat. Protoc.* 4, 363–371.

Kletzin, A. (1989). Coupled enzymatic production of sulfite, thiosulfate, and hydrogen sulfide from sulfur:

purification and properties of a sulfur oxygenase reductase from the facultatively anaerobic archaebacterium *Desulfurolobus ambivalens*. *J. Bacteriol.* 171, 1638–1643.

Kletzin, A. (2007). "23: Metabolism of inorganic sulfur compounds in archaea," in *Archaea. Evolution, Physiology, and Molecular Biology*, eds R. A. Garrett and H.-P. Klenk (Oxford: Blackwell Publishing), 261–274.

Kletzin, A. (2008). "15. Oxidation of sulfur and inorganic sulfur compounds in *Acidianus ambivalens*," in *Microbial Sulfur Metabolism*, eds C. Dahl and C. G. Friedrich (Berlin: Springer), 184–201.

Kletzin, A., Urich, T., Müller, F., Bandeiras, T. M., and Gomes, C. M. (2004). Dissimilatory oxidation and reduction of elemental sulfur in thermophilic archaea. *J. Bioenerg. Biomembr.* 36, 77–91.

Li, M., Chen, Z., Zhang, P., Pan, X., Jiang, C., An, X., Liu, S., and Chang, W. (2008). Crystal structure studies on sulfur oxygenase reductase from *Acidianus tengchongensis*. *Biochem. Biophys. Res. Commun.* 369, 919–923.

McRee, D. E. (1999). XtalView Xfit – a versatile program for manipulating atomic coordinates and electron density. *J. Struct. Biol.* 125, 156–165.

Moll, R., and Schäfer, G. (1988). Chemiosmotic H+ cycling across the plasma membrane of the thermoacidophilic archaebacterium *Sulfolobus acidocaldarius*. *FEBS Lett.* 232, 359–363.

Murshudov, G. N., Vagin, A. A., and Dodson, E. J. (1997). Refinement of macromolecular structures by the maximum-likelihood method. *Acta Crystallogr. D Biol. Crystallogr.* 53, 240–255.

Otwinowski, Z., and Minor, W. (1997). "Processing of X-ray diffraction data collected in oscillation mode," in *Methods in Enzymology*, Vol. 276: Macromolecular Crystallography, Part A, eds C. W. Carter, Jr. and R. M. Sweet (New York: Academic Press), 307–326.

Pelletier, N., Leroy, G., Guiral, M., Giudici-Orticoni, M. T., and Aubert, C. (2008). First characterisation of the active oligomer form of sulfur oxygenase reductase from the bacterium *Aquifex aeolicus*. *Extremophiles* 12, 205–215.

Read, R. J. (1986). Improved Fourier coefficients for maps using phases from partial structures with errors. *Acta Crystallogr. A* 42, 140–149.

Rohwerder, T., and Sand, W. (2003). The sulfane sulfur of persulfides is the actual substrate of the sulfur-oxidizing enzymes from *Acidithiobacillus* and *Acidiphilium* spp. *Microbiology* 149, 1699–1710.

Roy, A. B., and Trudinger, P. A. (1970). "The chemistry of some sulphur compounds," in *The Biochemistry of Inorganic Compounds of Sulphur*, eds A. B. Roy and P. A. Trudinger (Cambridge: Cambridge University Press), 7–29.

Schägger, H., and von Jagow, G. (1987). Tricine-sodium dodecyl sulfate-polyacrylamide gel electrophoresis for the separation of proteins in the range from 1 to 100 kDa. *Anal. Biochem.* 166, 368–379.

Schauder, R., and Kröger, A. (1993). Bacterial sulphur respiration. *Arch. Microbiol.* 159, 491–497.

Skerra, A. (1994). Use of the tetracycline promoter for the tightly regulated production of a murine antibody fragment in *Escherichia coli*. *Gene* 151, 131–135.

Sun, C. W., Chen, Z. W., He, Z. G., Zhou, P. J., and Liu, S. J. (2003). Purification and properties of the sulfur oxygenase/reductase from the acidothermophilic archaeon, *Acidianus* strain S5. *Extremophiles* 7, 131–134.

Urich, T. (2005). *The Sulfur Oxygenase Reductase from Acidianus ambivalens; Functional and Structural Characterization of a Sulfur-Disproportionating Enzyme*. Ph.D. dissertation, Technische Universität, Darmstadt.

Urich, T., Bandeiras, T. M., Leal, S. S., Rachel, R., Albrecht, T., Zimmermann, P., Scholz, C., Teixeira, M., Gomes, C. M., and Kletzin, A. (2004). The sulphur oxygenase reductase from *Acidianus ambivalens* is a multimeric protein containing a low-potential mononuclear non-haem iron centre. *Biochem. J.* 381, 137–146.

Urich, T., Coelho, R., Kletzin, A., and Frazao, C. (2005a). The sulfur oxygenase reductase from *Acidianus ambivalens* is an icosatetramer as shown by crystallization and Patterson analysis. *Biochim. Biophys. Acta* 1747, 267–270.

Urich, T., Kroke, A., Bauer, C., Seyfarth, K., Reuff, M., and Kletzin, A. (2005b). Identification of core active site residues of the sulfur oxygenase reductase from *Acidianus ambivalens* by site-directed mutagenesis. *FEMS Microbiol. Lett.* 248, 171–176.

Urich, T., Gomes, C. M., Kletzin, A., and Frazao, C. (2006). X-ray structure of a self-compartmentalizing sulfur cycle metalloenzyme. *Science* 311, 996–1000.

Conflict of Interest Statement: The authors declare that the research was conducted in the absence of any commercial or financial relationships that could be construed as a potential conflict of interest.

Received: 29 December 2010; paper pending published: 10 January 2011; accepted: 17 February 2011; published online: 07 March 2011.

Citation: Veith A, Urich T, Seyfarth K, Protze J, Frazão C and Kletzin A (2011) Substrate pathways and mechanisms of inhibition in the sulfur oxygenase reductase of Acidianus ambivalens. Front. Microbio. ***2****:37. doi: 10.3389/fmicb.2011.00037*

This article was submitted to Frontiers in Microbial Physiology and Metabolism, a specialty of Frontiers in Microbiology.

frontiers in
MICROBIOLOGY

ORIGINAL RESEARCH ARTICLE
published: 25 April 2011
doi: 10.3389/fmicb.2011.00068

An extracellular tetrathionate hydrolase from the thermoacidophilic archaeon *Acidianus ambivalens* with an activity optimum at pH 1

Jonas Protze[1†], Fabian Müller[1], Karin Lauber[1], Bastian Naß[1], Reinhard Mentele[2], Friedrich Lottspeich[2] and Arnulf Kletzin[1]*

[1] *Institute of Microbiology and Genetics, Technische Universität Darmstadt, Darmstadt, Germany*
[2] *Max-Planck Institute of Biochemistry, Martinsried, Germany*

Edited by:
Martin G. Klotz, University of Louisville, USA

Reviewed by:
Biswarup Mukhpadhyay, Virginia Bioinformatics Institute, USA
Uwe Deppenmeier, University of Bonn, Germany

***Correspondence:**
Arnulf Kletzin, Institute of Microbiology and Genetics, Technische Universität Darmstadt, Schnittspahnstraße 10, 64287 Darmstadt, Germany.
e-mail: kletzin@bio.tu-darmstadt.de

[†]***Present address:***
Jonas Protze, Research Group of Structural Bioinformatics, Department of Structural Biology, Leibniz-Institut für Molekulare Pharmakologie, Robert-Rössle-Strasse 10, 13125 Berlin, Germany.
e-mail: protze@fmp-berlin.de

Background: The thermoacidophilic and chemolithotrophic archaeon *Acidianus ambivalens* is routinely grown with sulfur and CO_2-enriched air. We had described a membrane-bound, tetrathionate (TT) forming thiosulfate:quinone oxidoreductase. Here we describe the first TT hydrolase (TTH) from Archaea. **Results:** *A. ambivalens* cells grown aerobically with TT as sole sulfur source showed doubling times of 9 h and final cell densities of up to 8×10^8/ml. TTH activity (≈0.28 U/mg protein) was found in cell-free extracts of TT-grown but not of sulfur-grown cells. Differential fractionation of freshly harvested cells involving a pH shock showed that about 92% of the TTH activity was located in the pseudo-periplasmic fraction associated with the surface layer, while 7.3% and 0.3% were present in the soluble and membrane fractions, respectively. The enzyme was enriched 54-fold from the cytoplasmic fraction and 2.1-fold from the pseudo-periplasmic fraction. The molecular mass of the single subunit was 54 kDa. The optimal activity was at or above 95°C at pH 1. Neither PQQ nor divalent cations had a significant effect on activity. The gene (*tth1*) was identified following N-terminal sequencing of the protein. Northern hybridization showed that *tth1* was transcribed in TT-grown cells in contrast to a second paralogous *tth2* gene. The deduced amino acid sequences showed similarity to the TTH from *Acidithiobacillus* and other proteins from the PQQ dehydrogenase superfamily. It displayed a β-propeller structure when being modeled, however, important residues from the PQQ-binding site were absent. **Conclusion:** The soluble, extracellular, and acidophilic TTH identified in TT-grown *A. ambivalens* cells is essential for TT metabolism during growth but not for the downstream processing of the TQO reaction products in S°-grown cells. The liberation of TTH by pH shock from otherwise intact cells strongly supports the pseudo-periplasm hypothesis of the S-layer of Archaea.

Keywords: Archaea, sulfur metabolism, tetrathionate hydrolase, S4 intermediate pathway, surface layer, disproportionation

INTRODUCTION

The dissimilatory oxidation of inorganic sulfur compounds (ISC) is one of the most important sources of metabolic energy for CO_2 fixation in light-independent ecosystems like solfataras and other volcanic hot springs (reviewed for example by Kelly et al., 1997; Friedrich et al., 2005; Stetter, 2006; Kletzin, 2007; Ghosh and Dam, 2009). In addition, ISC oxidation is essential for bioleaching of precious and/or toxic metals from low-grade ores and slag heaps, regardless whether this effect is desired (metal extraction) or undesired (acid mine drainage; Sand et al., 2001; Gadd, 2010). Sulfur oxidation pathways and especially the SOX complex from neutrophilic chemo- or phototrophic bacteria are fairly well understood (for review, see Friedrich et al., 2005, 2008; Frigaard and Dahl, 2009; Sakurai et al., 2010). In contrast, there are many gaps in our knowledge concerning the mechanisms of ISC oxidation in acidophilic Bacteria and Archaea, the dominant microorganisms in volcanic hot springs and bioleaching environments (Kletzin, 2007, 2008; Ghosh and Dam, 2009).

Our model organism *Acidianus ambivalens* belongs to the Sulfolobales order within the archaeal domain (Zillig et al., 1986; Fuchs et al., 1996). *A. ambivalens* is a chemolithoautotrophic acidophile growing optimally at 80°C and pH 2.5. It oxidizes S° to sulfuric acid under aerobic conditions and uses hydrogen as the electron donor for S° reduction under anaerobic conditions. A soluble sulfur oxygenase reductase (SOR) mediates the initial step in the S° oxidation pathway of aerobically grown cells, a unique enzyme catalyzing the simultaneous S° oxygenation and disproportionation to sulfite, thiosulfate, and sulfide (Kletzin, 1989; Urich et al., 2004; Veith et al., 2011; this volume). It is not known whether thiosulfate is a primary product of the enzyme or whether it originates from a rapid non-enzymatic reaction between S° and sulfite under the assay conditions (Kletzin, 1989; Müller et al., 2004). Regardless of that, S°-grown *A. ambivalens* cells contain significant amounts of a membrane-bound thiosulfate:quinone oxidoreductase (TQO) oxidizing thiosulfate to tetrathionate (TT) and reducing quinones (Müller et al., 2004). This type of thiosulfate oxidation is known

as the S_4 intermediate pathway (Ghosh and Dam, 2009). Two observations suggest that the active site of the TQO is facing the cytoplasm. First, the SOR, which delivers thiosulfate, is a soluble and cytoplasmic enzyme. Secondly, thiosulfate is not stable at the growth conditions of *A. ambivalens* (acidic pH and high temperature; Johnston and McAmish, 1973) so that it rapidly decomposes, when being added to the medium forming sulfur and sulfite. In contrast, TT is not very stable at the near-neutral pH (6.5; Johnston and McAmish, 1973; Moll and Schäfer, 1988) and the reducing conditions in the cytoplasm. We had hypothesized that the TQO and a non-enzymatic TT reduction to thiosulfate mediated by hydrogen sulfide and sulfite in the cytoplasm ultimately feeds electrons into the respiratory chain (Müller et al., 2004; Kletzin, 2008).

As the fate of the TT produced during the TQO reaction is not clear, we initiated a search for TT-metabolizing enzymes in *A. ambivalens*. Three ways of TT metabolism are known: (1) the reduction by either multiheme or molybdenum-containing reductases enabling mesophilic proteobacteria like *Salmonella enterica* to grow anaerobically with TT as a terminal electron acceptor (Hensel et al., 1999; Price-Carter et al., 2001; Mowat et al., 2004); (2) the oxidation by still unknown subunits of SOX multienzyme complexes (Mukhopadhyaya et al., 2000; Lahiri et al., 2006); or (3) a disproportionation by tetrathionate hydrolases (TTH) forming sulfate, thiosulfate or sulfite, and sulfur or pentathionate (De Jong et al., 1997a; Bugaytsova and Lindström, 2004; Kanao et al., 2007; Rzhepishevska et al., 2007). TTHs isolated from various acidophilic *Acidithiobacillus* species and *Acidiphilium acidophilum* (formerly *Thiobacillus acidophilus*) are usually monomeric and/or homodimeric, membrane-associated, or soluble enzymes with pH optima around 2.5–4 (De Jong et al., 1997a; Bugaytsova and Lindström, 2004; Egorova et al., 2004; Kanao et al., 2007; Mangold et al., 2011; this volume). Sequence comparisons predicted that the TTHs belong to a pyrroloquinoline quinone (PQQ) containing protein family. Kanao et al. (2010) however showed that recombinant *Acidithiobacillus ferrooxidans* TTH purified from *E. coli* inclusion bodies could be refolded into the active state without PQQ and under acidic conditions.

In this contribution, we demonstrate that *A. ambivalens* grows well with TT as the sole sulfur source thereby producing a highly active TTH with an optimum at pH 1. We also show that the protein is extracellular and associated with the S-layer of the archaeon.

MATERIALS AND METHODS

ORGANISM AND GROWTH CONDITIONS

Acidianus ambivalens DSM 3772 was grown as described (Zillig et al., 1986) with slight modifications. The medium contained per liter: KH_2PO_4, 2.8 g; $(NH_4)SO_4$, 1.5 g; $MgSO_4 \times 7\ H_2O$, 0.25 g; $CaCl_2 \times 2\ H_2O$, 70 mg; $FeSO_4 \times 7\ H_2O$, 28 mg; $Na_2B_2O_7 \times 10\ H_2O$, 9 mg; $MnCl_2 \times 4\ H_2O$, 3.6 mg; $ZnSO_4 \times 7\ H_2O$, 0.44 mg; $CuCl_2 \times 2\ H_2O$, 0.1 mg; $VaSO_4 \times 5\ H_2O$, 0.07 mg; $Na_2MoO_4 \times 2\ H_2O$, 0.06 mg; $CoSO_4 \times 7\ H_2O$, 0.02 mg. The pH was adjusted to 2.5 with sterile 50% H_2SO_4. About 10 ml/l of freshly prepared and filter-sterilized 1 M $K_2S_4O_6$ solution (Merck, Darmstadt, Germany) was added as sulfur source. Additionally, the same amounts were added 24 and 48 h post-inoculation. Alternatively, elemental sulfur was used (sulfur flower, 10 g/l).

Cultures of 13–14 l were grown at 80°C in a 15-l glass bottle heated in a silicon oil bath and stirred with a magnetic stirrer at a speed of 500/min. The culture was continuously bubbled with CO_2-enriched air. The fermenter was inoculated with 500 ml of a late-exponential culture and harvested by centrifugation (10,000 × *g*) 72 h after inoculation. Cell densities were estimated by measuring both the optical density at 600 nm and the cell counts with a Hemocytometer of 10 µm depth.

ENZYME ASSAY

Tetrathionate hydrolase (TTH) activity was routinely measured following the decrease of TT concentration in the assay mixture by cyanolysis (Kelly et al., 1969). The mixture (1 ml, pH 1) contained 100 mM maleic acid, 1 mM $MgCl_2$, 1.5 or 1.8 mM $K_2S_4O_6$, and 25–190 µl of protein extracts. About 4 µM Pyrroloquinoline quinone (PQQ, methoxatin; Sigma, München, Germany), 2 mM Mg^{2+}, or 2 mM Ca^{2+} were added if appropriate. The assay mixture including the protein extracts was preheated to 80°C for 5 min prior to TT addition. Aliquots (50 µl) were taken at appropriate time points, chilled on ice water, and kept at 4°C pending cyanolysis. One unit is defined as the conversion of 1 µmol TT in 1 min. Pyrophosphatase activity was measured according to Richter and Schäfer (1992).

PROTEIN PURIFICATION FROM WHOLE CELLS

Washed cells were resuspended in 40 mM KPi pH 7.0 (10 ml/g of cells) and homogenized in a potter after addition of 1 mM $MgCl_2$, 25 µg/ml RNase A, and 10 µg/ml DNase I. Cells were disrupted by two passages through a high-pressure homogenizer at 175 MPa (Constant Cell Disruption Systems, Daventry, UK). Undisrupted cells and cell debris were removed by centrifugation at 10,000 × *g* for 30 min at 4°C. Particle fractions were removed by a second centrifugation step at 135,000 × *g* and 4°C for 60 min. The supernatant (i.e., soluble extract) was dialyzed against 40 mM KPi, 1 mM $MgCl_2$, 1 nM PQQ, pH 7.0 for 16 h.

The soluble extract was applied onto a DEAE Sepharose fast-flow column [36 ml column volume (CV); GE Healthcare Europe, Munich, Germany] equilibrated with 40 mM KPi, 1 mM $MgCl_2$, pH 7.0. Proteins were eluted with a linear gradient from 0 to 0.15 M NaCl in 6 CV followed by a linear gradient from 0.15 to 0.6 M NaCl in 6 CV. Fractions showing TTH activity were pooled and dialyzed against 50 mM Tris/HCl, pH 8.5 for 16 h at 4°C prior to addition of 2 M ammonium sulfate followed by centrifugation for 1 h at 40,000 × *g* and 4°C. The supernatant was applied onto a Phenyl-Sepharose Fast-Flow column (bed volume 24 ml; GE Healthcare). Proteins were eluted with a linear gradient from 2 to 0 M ammonium sulfate. Fractions showing TTH activity were pooled, concentrated with Centriprep YM-30 Devices (Millipore, Bedford, MA, USA), and applied on a Superdex 200 size exclusion column (30 mm × 600 mm; GE Healthcare). Elution was performed with 50 mM Tris/HCl, 150 mM NaCl, pH 8.5, and a constant flow rate of 1 ml/min. The fraction with the highest specific activity of the TTH was dialyzed against 50 mM Tris/HCl, 5 mM NaCl, pH 7.5 for 16 h at 4°C, and applied on a fast-flow Q-Sepharose column (GE Healthcare; bed volume 3.5 ml). Proteins were eluted with a linear gradient from 187.5 to 675 mM NaCl.

PROTEIN PURIFICATION FROM SPHEROBLASTS

Freshly harvested cells (wet mass 8.6 g) of a late-exponential and TT-grown *A. ambivalens* culture were split into 10 equal parts of 0.86 g and each resuspended in 10 ml spheroblast buffer of various pH values or sterile culture supernatant, followed by overnight incubation (12 h) at 4°C and centrifugation at 1000 × *g* for 15 min. The buffers were composed each of 500 mM sucrose, 100 mM NaCl, and the buffering substance, i.e., 50 mM KH_2PO_4/K_2HPO_4 (pH 5–6.5), 50 mM formic acid/NaOH (pH 3–4.5), or 50 mM maleic acid (pH 2). The supernatants containing the pseudo-periplasmic fraction were used for TTH activity assays and gel electrophoresis (**Figure 1C**).

For protein purification, the pseudo-periplasmic fraction of 6 g of *A. ambivalens* cells obtained by incubation in 500 mM sucrose, 100 mM NaCl, and 50 mM KH_2PO_4/K_2HPO_4 pH 6.5 was dialyzed against 20 mM Tris/HCl, 5 mM NaCl, pH 7.5, and applied to a fast-flow Q-Sepharose column (bed volume 3.5 ml; GE Healthcare). Proteins were eluted with a linear gradient from 187 to 675 mM NaCl. Fractions showing TTH activity were pooled and the salt concentration was adjusted to 500 mM NaCl, 1 mM $MnCl_2$, and 1 mM $CaCl_2$. This protein solution was applied to a concanavalin A column (Hi-Trap Con A 4B, GE Healthcare; bed volume 1 ml) at a flow rate of 0.1 ml/min. Proteins were eluted with 20 mM Tris/HCl, 500 mM NaCl, 500 mM methyl-D-glucoside (Acros, Fisher Scientific, Bonn, Germany) pH 7.5 with a linear gradient of 0–500 mM methyl-D-glucoside in 2.5 CV. Fractions showing TTH activity were pooled, concentrated with Centriprep YM-30 Devices (Millipore, Bedford, MA, USA), and applied to a Superdex 200 size exclusion column (30 mm × 600 mm; Amersham GE Healthcare). The elution was performed with 50 mM Tris/HCl, 150 mM NaCl, pH 8.5, and a constant flow rate of 1 ml/min.

SEQUENCE ANALYSIS

The amino acid sequence of *A. ferrooxidans* TTH was used as probe in searches of a partial genomic database of *A. ambivalens*, which resulted in the identification of two homologs (*tth1* and *tth2*). The deduced amino acid sequences were used in standard BLASTP searches conducted against the non-redundant protein database[1]. The *A. ambivalens* TTH1 and the *A. ferrooxidans* TTH were used as probes in a BLAST search against the *Sulfobacillus acidophilus* DSM 10332 genome sequence. A multiple alignment and a phylogenetic dendrogram were generated using MAFFT[2] with the L–INS–i algorithm, the BLOSUM30 similarity matrix, a gap penalty of 1.56, and an offset value of 0.1 (Katoh et al., 2005). All homologs of TTH1 and TTH2 with e-values lower than $1 \times e^{-10}$ and $1 \times e^{-20}$, respectively, were selected from the BLAST results and included in the alignment. In addition, a group of sequences from methanogenic Archaea was added for outgroup alignment. For better visualization the tree (see below; **Figure 5**) was edited with NjPlot (Perriere and Gouy, 1996).

Secondary structure predictions were done using PSIPRED[3]. Predictions of topology and signal sequences were done with TMHMM and SignalP[4] and MEMSAT (at the Psipred server). Three-dimensional models of TTH1 and TTH2 were predicted using the Phyre server[5] (Kelley and Sternberg, 2009). Energy minimization of the PHYRE models was performed using UCSF Chimera[6] (Pettersen et al., 2004). The figures were generated with Pymol (DeLano, 2002).

The nucleotide sequences of the *tth1* and *tth2* genes were submitted to EMBL database; they were assigned the accession numbers FR734215 and FR734216, respectively.

ISOLATION OF RNA AND NORTHERN ANALYSIS

Acidianus ambivalens cells were grown on tetrathionate or elemental sulfur. Samples (2 l each) were taken at 24, 48, and 72 h after inoculation and harvested by centrifugation (10 min, 6000 × *g*). RNA was prepared from these samples by the guanidinium isothiocyanide extraction method (Chomczynski and Sacchi, 1987) and quantified by UV absorption measurements. Five micrograms of each RNA preparation were separated on a denaturing agarose gel and subsequently transferred to a nylon membrane (Biodyne A; Pall Filtron; Seldon, 1988). RNA ladder mix (Invitrogen, Darmstadt, Germany) was used as a size marker.

After heat-fixation for 2 h at 80°C, the membrane was stained with methylene blue (Herrin and Schmidt, 1988). The DNA fragments used for probe synthesis were amplified with the primers TTH1_sig_fwd (ggaat catga accta aaaat cattg ttgg) and TTH1_1018_rev (attcc tcgag ataat agatg tatgc agga) for the *tth1* gene and TTH2_sig2_fwd (tctac catgg caatg aagag agag) and TTH2_442_rev (tggct cgagt gttaa acagt aaaga ggtaa) for the *tth2* gene. The primers sorn_fwd and sorc_rev (Urich et al., 2005) were used for the amplification of the *sor* gene. All primer sets amplified the entire open reading frames (ORF). The PCR products were Digoxigenin-labeled using the random hexamer labeling kit (No. 11175033910; Roche, Mannheim, Germany). The hybridization solution contained 50% formamide, 10% (w/v) dextran sulfate (Sigma, Germany), 1% (w/v) SDS, and 0.5% (w/v) skim milk powder. The detection reaction was performed using the DIG luminescence detection kit (11363514910; Roche) and Amersham hyperfilm ECL (GE Healthcare, Munich, Germany) as described by the manufacturers.

ANALYTICAL PROCEDURES

Protein concentration was determined by the bicinchoninic acid method using the BCA Protein Assay Kit (Thermo Scientific Pierce, Rockford, IL, USA). The molecular masses and subunit composition were determined by size exclusion chromatography in the course of the purification (see Protein Purification from Spheroblasts). The monomer, dimer, and trimer peaks of bovine serum albumin were used for calibration. SDS/PAGE was performed according to the method of Schägger and von Jagow (1987) using 12% (w/v) resolving and 4% (w/v) stacking gels. Samples were mixed with SDS-loading buffer (60 mM Tris/HCl, 2% SDS (v/v), 10% glycerol (v/v), 0.01% bromophenol blue (w/v), 0.015 g/ml mercaptoethanol) and incubated at 95°C for 5 min before loading onto the gel. Protein Molecular Weight Marker (SM0431, Fermentas) was used as marker. Gels

[1]www.ncbi.nih.gov

[2]http://mafft.cbrc.jp/alignment/server/index.html

[3]http://bioinf.cs.ucl.ac.uk/psipred/

[4]http://www.cbs.dtu.dk/services/

[5]http://www.sbg.bio.ic.ac.uk/phyre/html/index.html

[6]http://www.cgl.ucsf.edu/chimera

were stained with colloidal Coomassie blue (Roti Blue, Roth, Karlsruhe, Germany) or with silver nitrate (Blum et al., 1987). For N-terminal sequence analysis, the concentrated protein was run on 12% SDS gel and transferred to a PVDF (polyvinylidene difluoride) membrane using a Multiphor NovaBlot system (GE Healthcare) according to the method of Kyhse-Andersen (1984). The protein bands were visualized with conventional Coomassie brilliant blue R-250 [0.1% (w/v), 1% (v/v) acetic acid, 40% (v/v) methanol] followed by N-terminal sequence analysis by Edman degradation using a 492-cLC protein sequencer (Lifetech-Applied Biosystems, Darmstadt, Germany) according to the manufacturer's instructions.

RESULTS

ACIDIANUS AMBIVALENS IS GROWING WITH TETRATHIONATE AS SOLE SULFUR SOURCE

Acidianus ambivalens grown aerobically with 10 mM tetrathionate (TT) as sole sulfur and energy source reached cell densities of 5.9–8.0 × 10^8/ml after 72 h. Doubling times were 9 h and the final pH of the culture was 0.8–1.0. The cell yields with TT were 0.26–0.36 g/l of culture volume (wet mass). Cells grown with elemental sulfur as previously reported (Zillig et al., 1986; Teixeira et al., 1995) reached cell densities of 9.9 × 10^8/ml at doubling times of 8.4 h. Cell yields were 0.35–0.47 g/l, however, cell pellets still contained elemental sulfur. When cells were grown at TT concentrations of 20 mM or more, the cultures showed a whitish turbidity after 12 h from transiently formed hydrophilic and finely dispersed sulfur droplets. The turbidity decreased and vanished after 36–48 h due to elemental sulfur oxidation. TT concentrations of more than 40 mM were inhibitory (data not shown).

PURIFICATION OF THE TETRATHIONATE HYDROLASE FROM WHOLE CELL EXTRACTS AND IDENTIFICATION OF THE GENE

A specific TTH activity of 40 mU/mg protein was found in total cell extracts of *A. ambivalens* grown on TT. The particle-free extract showed a specific activity of 280 mU/mg protein (**Table 1**). After four chromatographic purification steps, the specific TTH activity was increased to 15 U/mg protein equaling a 54-fold purification and 0.1% recovery.

In the SDS/PAGE (**Figure 1A**) of different purification steps, a clear relation is visible between the increase of the specific TTH activity and a protein band at 54 kDa. N-terminal sequencing of this band gave the amino acids Gly-Pro-Ile-Val-Tyr-Thr-Tyr-Thr-Glu-Tyr-Asn*-Gly-Thr-Tyr with Asn* being glycosylated. These residues correspond to the amino acid sequence encoded by the *tth1* gene (Gly_{40}-Tyr_{53}) previously identified by similarity searches in a database of partial *A. ambivalens* genome sequences (5 MBp) using the amino acid sequence of the *A. ferrooxidans* TTH as a query. Residues 1–39 obviously form a signal peptide that was also predicted by the SignalP web server[7]. Another paralogous gene termed *tth2* was identified in the genome sequences as well. The smaller band with a molecular mass of ≈20 kDa seen in the SDS gel was identified as a pyrophosphatase (not shown), the larger weak protein band (approximate molecular mass of 90–100 kDa) did not give an N-terminal sequence. Specific pyrophosphatase activities (Richter and Schäfer, 1992) were up to 107 mU/mg in enrichment fractions.

Based on the TTH liberation by pH shock (see below), an alternative purification protocol was developed. The pseudo-periplasmic fraction of 6 g *A. ambivalens* cells (after incubation in pH 6.5 buffer) displayed a

[7]http://www.cbs.dtu.dk/services/

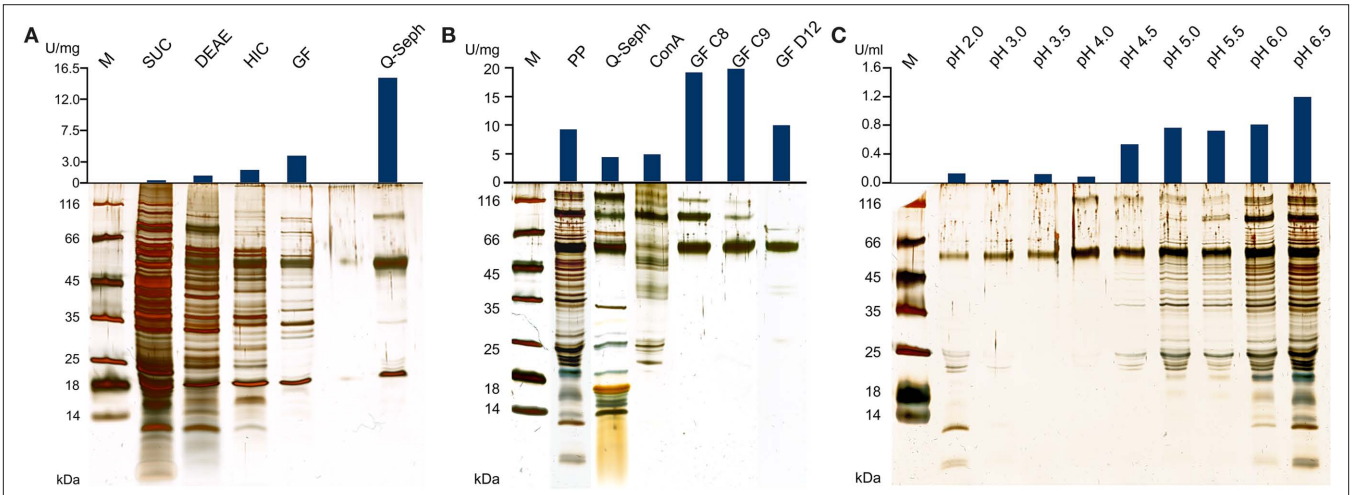

FIGURE 1 | Silver-stained SDS gels and activities of TTH fractions from *A. ambivalens*. **(A)** Purification of the TTH from soluble cell extracts and specific activities; SUC, supernatant ultracentrifugation; DEAE and HIC, active fractions of DEAE anion exchange and hydrophobic interaction chromatographies, respectively; GF, size exclusion chromatography; Q-seph, Q-sepharose chromatography. **(B)** Purification of the TTH from the pseudo-periplasmic fraction [obtained by incubation in buffer pH 6.5; see **(C)**] and specific activities; PP, pseudo-periplasmic fraction; Q-seph, Q-sepharose chromatography; Con A, concanavalin A chromatography; GF C8 and GF C9, two consecutive fractions of the dimer peak of the size exclusion chromatography; GF D12, main fraction of the monomer peak (lane from a different SDS gel). **(C)** Silver-stained SDS gel of supernatants from spheroblast formation after incubation of whole cells in buffers of the pH values given above as described in the Section "Materials and Methods" (pseudo-periplasmic fractions), 10 µl of the supernatants were separated in the gel without prior concentration; top, resulting total TTH activities per milliliter of supernatant (total: 10 ml from of 0.86 g of cells each).

specific activity of 9 U/mg and a total activity of 56 U. When being fractionated with a fast-flow Q-Sepharose column (GE Healthcare Europe, Freiburg, Germany) the TTH activity eluted at about 320 mM NaCl. A pool of the active fractions showed a specific activity of 4 U/mg and a total activity of 23 U. Lectin affinity chromatography was carried out for the removal of non-glycosylated proteins. The TTH activity eluted at a concentration of 325 mM methyl-D-glucoside. Active fractions were pooled and concentrated prior to size exclusion chromatography with a Superdex 200 column. The TTH eluted in two major 280 nm absorption peaks (not shown) with specific TTH activities of 19 U/mg (V_r = 165 ml; corresponding to a molecular mass of 105 kDa) and 10 U/mg (V_r = 190 ml; 54 kDa), respectively (**Figure 1B**). The elution pattern points to equilibrium formation between monomer and homodimer. The alternative three-step purification scheme from the pseudo-periplasmic fraction resulted in a 2.1-fold higher specific TTH activity – despite an intermediate drop – and a 62-fold higher yield of enzyme recovery compared to the purification from total soluble extracts (**Table 1**). The fractions did not have pyrophosphatase activity and the 20-kDa band was not seen in SDS gels. The 54-kDa TTH band was predominant in the dimer peak and almost homogeneous in the monomer peak (**Figure 1B**).

TTH HAS AN EXTRACELLULAR LOCATION

TTH activity was not detectable in cell-free culture supernatants (pH 1) immediately after harvesting. This changed when cells were resuspended in a 20-fold volume of spent supernatant after harvesting and incubated overnight at 4°C followed by another round of centrifugation: the TTH activity was 7.5 mU/ml (0.3 U/mg protein) in the secondary supernatant suggesting a slow release of the protein (**Table 2**). After overnight incubation of cells in pH 6.5 phosphate buffer, 92% of the TTH activity was found in the supernatant. 7.3% and 0.3% were found in the cytoplasmic and membrane fractions, respectively. In order to determine the effect of pH on the solubilization of the TTH from the cells, buffers of different pH values were used for overnight incubation after harvesting. The TTH activities in the supernatants increased significantly between pH 4 and 4.5, while the highest amount of TTH activity and the highest protein concentration were found in the pH 6.5 supernatant (**Table 2**; **Figure 1C**).

TTH IS AN EXTREMELY THERMOPHILIC AND ACIDOPHILIC ENZYME

Decrease of TT catalyzed by the TTH showed a sigmoidal behavior and an activation period whose duration is depended on the amount of enzyme in the assay mixture. The slope of the regression

Table 1 | Purification of the tetrathionate hydrolase from *A. ambivalens* cell extracts.

Fraction	Total protein (mg)	Specific activity (U/mg)	Total activity (U)	Yield (%)	Fold
A. PURIFICATION FROM SOLUBLE CELL EXTRACTS					
Cell extract	1405.7	0.28	388.0	100	1.0
DEAE	414.0	0.94	387.2	99.8	3.4
HIC	17.9	1.77	31.8	8.2	6.3
Size exclusion	1.4	3.83	5.3	1.4	13.7
Q-sepharose	0.02	14.99	0.3	0.1	53.5
B. PURIFICATION FROM THE PSEUDO-PERIPLASMIC FRACTION					
Pseudo-periplasm	6.23	8.99	55.98	100	1.0
Q-sepharose	5.57	4.17	23.2	41.5	0.5
Con A	0.71	4.65	3.30	5.9	0.5
Size exclusion GF C9	0.18	18.94	3.44	6.2	2.1

Table 2 | TTH activities in the cell-free supernatants following incubation of 0.86 g each of *A. ambivalens* cells in 10 ml of buffer of different pH values; average values from two to three enzyme assays.

pH	6.5	6.0	5.5	5.0	4.5	4.0	3.5	3.0	2.0	CS[1]
Protein conc. in supernatant (µg/ml)	177 ± 7	121 ± 4	63 ± 2	117 ± 15	49 ± 4	32 ± 1	29 ± 10	65 ± 11	48 ± 2	25 ± 5
Activity/ml in supernatant (U/ml)	1.2 ± 0.02	0.8 ± 0.02	0.7 ± 0.08	0.8 ± 0.02	0.5 ± 0.12	0.08 ± 0.10	0.12 ± 0.16	0.04 ± 0.03	0.13 ± 0.03	0.01 ± 0.002
Specific activity in supernatant (U/mg)	6.7 ± 0.10	6.7 ± 0.17	11.5 ± 1.31	6.5 ± 0.14	11 ± 2.41	2.6 ± 3.11	4.1 ± 5.36	0.6 ± 0.52	2.7 ± 0.68	0.3 ± 0.07
Total activity in supernatant (U)	11.9 ± 0.18	8.1 ± 0.21	7.2 ± 0.82	7.6 ± 0.17	5.4 ± 1.17	0.8 ± 0.99	1.2 ± 1.57	0.4 ± 0.34	1.3 ± 0.33	0.06 ± 0.02
Total activity in cellular fraction (U)	1 ± 0.41	4.9 ± 0.24	5.7 ± 0.68	5.1 ± 0.23	7.6 ± 0.98	12.3 ± 1.21	12.1 ± 0.73	12.1 ± 0.42	11.7 ± 0.13	11.4 ± 0.46
Fraction of total activity in supernatant (%)	92 ± 1.4	63 ± 1.6	56 ± 6.4	59 ± 1.3	41 ± 8.8	6 ± 7.4	9 ± 11.8	3 ± 2.6	10 ± 2.5	2 ± 0.7

[1] *Incubation in 10 ml of culture supernatant (pH ≈ 1).*

line was directly dependent on the amount of protein used for the assay (**Figure 2**). The specific activity increased in an almost linear way with the temperature with no activity at 40°C, modest activity at 50°C, and maximal activity at 95°C (**Figure 3**). The optimal and maximal temperatures were not determined for lack of suitable assay equipment. The highest enzymatic activity was recorded at pH 1. From pH 2–5, the TTH showed a specific activity of 1–0.75 U/mg (**Figure 3**). No enzyme activity was detected at pH 6. Addition of PQQ and/or Mg^{2+} or Ca^{2+} did not have a significant effect on the TTH activity (not shown). The K_M was recorded using a different TTH preparation of higher purity. At 80°C and pH 1, the K_M of the TTH was 0.8 mM TT when assayed using 2.7 µg of protein. The observed V_{max} was 43.8 nmol/min corresponding to a specific activity of 16 U/mg.

ONLY THE *tth1* GENE IS EXPRESSED IN TT-GROWN *A. AMBIVALENS* CELLS

In order to analyze expression of the two *tth* genes, total RNA was isolated from *A. ambivalens* grown aerobically with sulfur or TT at different stages of the growth curve. Northern hybridization was carried out with probes derived from the *tth1* and *tth2* genes and, as a control, with a *sor* probe from the gene encoding the sulfur oxygenase reductase (Kletzin, 1992). Hybridization signals appeared at a size of about 1500 nt with the *tth1* gene pointing toward a monocistronic transcription (**Figure 4**). Signals developed in hybridization reactions with RNA from cells grown under aerobic but not under anaerobic conditions (not shown). Signals were stronger in RNA from TT-grown cells as compared to sulfur-grown cells at late-exponential phase. The *tth2* gene did not give hybridization signals under any condition tested. The *sor* probe resulted in signals of approximately 900 nt in length with RNA from aerobically grown cells both with sulfur and TT as substrates, however signals were stronger in S°-grown cells (**Figure 4**). These results showed that the *sor* gene is expressed in TT-grown cells presumably due to transient formation of elemental sulfur.

TETRATHIONATE HYDROLASE IS SIMILAR TO PQQ-CONTAINING DEHYDROGENASES

The *tth1* gene encodes an ORF of 538 codons. The deduced amino acid sequence includes a signal sequence of 39 residues, so that the mature protein has a length of 499 aa. The calculated molecular mass of 53,642 without glycosylation corresponds well with the apparent molecular masses in SDS gels and gel filtration (54 kDa). The *tth2* gene encoded an ORF of 449 aa including a predicted signal sequence of 23–32 aa in length. Both proteins are 29–32% identical (depending on alignment parameters), which is less than the pairwise identity of TTH1 with the orthologous enzyme from *A. ferrooxidans* (40–42%).

The top hits in BLASTP searches of TTH1 at NCBI (pairwise identity >33%; e-value $<1 \times 10^{-54}$) were restricted to close homologs from acidophilic Bacteria and Archaea (TTH cluster; **Figure 5**), which seem to be true tetrathionate hydrolases. Comparable results were obtained with the TTH2 protein. Both proteins and their homologs gave distinct clades in the dendrogram. These proteins belong to a large superfamily of β-propeller proteins, whose best-known members are pyrroloquinoline quinone (PQQ) containing dehydrogenases. Secondary structure predictions confirmed that TTH1 and TTH2 are all-beta proteins except for the transmembrane helices within the signal sequences (not shown). Six copies of a PQQ enzyme β-propeller repeat are present in each protein (PFAM family PF01011)[8].

[8]http://pfam.sanger.ac.uk

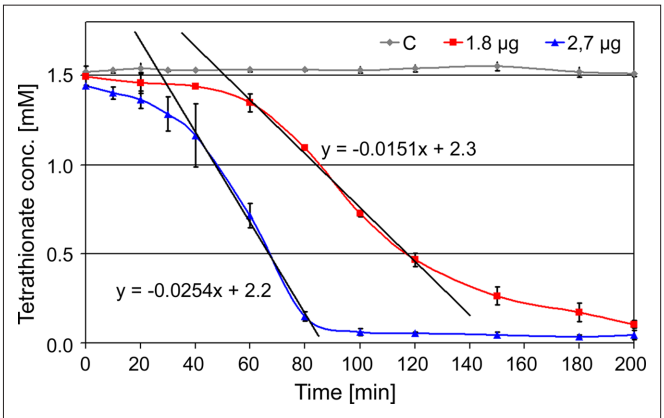

FIGURE 2 | Kinetics of TTH activity. 1.8 µg (red line) and 2.7 µg of protein (blue line) assayed at 80°C and pH 1; C: assay mixture without enzyme (control; gray line); formula, gradients of the trend lines used for activity calculation.

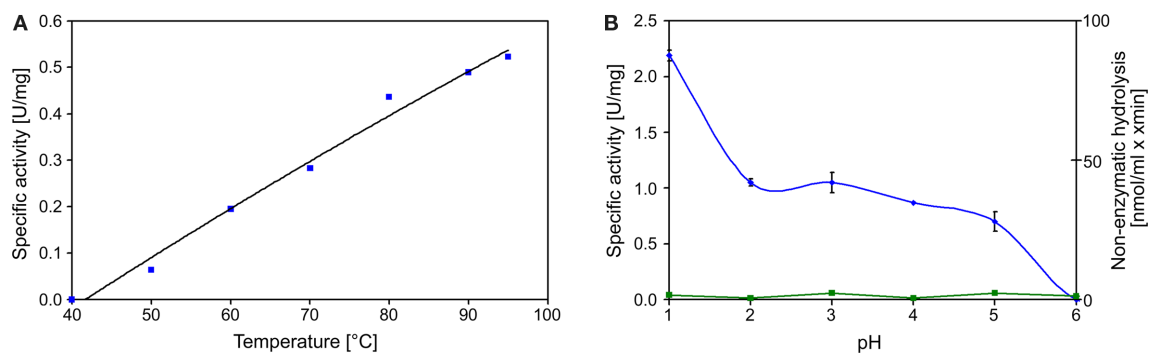

FIGURE 3 | Temperature and pH profiles of TTH activity. (A) Temperature profile of TTH activity from 40 to 95°C; **(B)** pH profile of TTH activity assayed at 80°C (blue line, left axis) and non-enzymatic TT hydrolysis (green line, right axis).

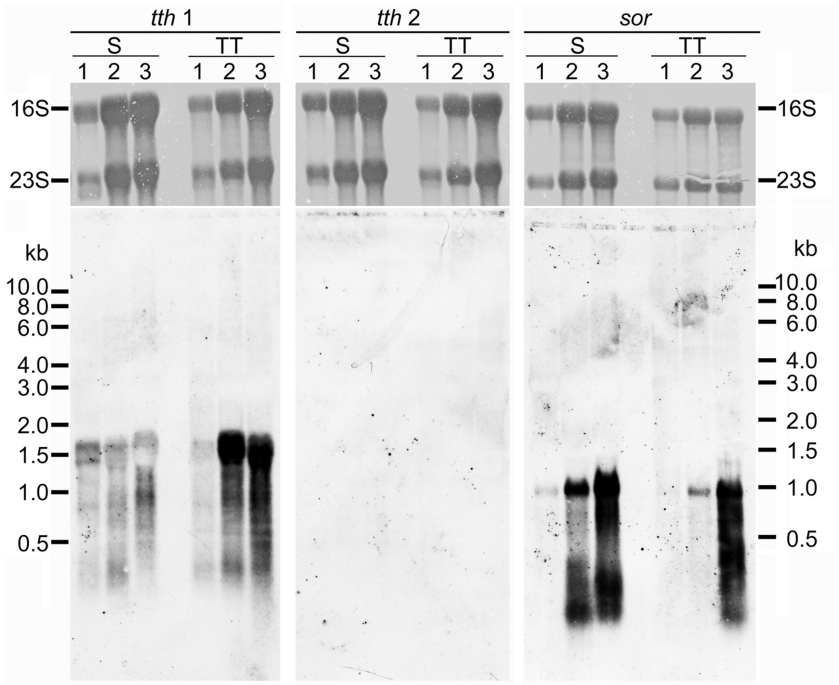

FIGURE 4 | Northern hybridization of *tth1, tth2,* and *sor* genes. All lanes with total *A. ambivalens* RNA (5 µg each) isolated from cells grown with sulfur (S) or tetrathionate (TT) after 24 h (1); 48 h (2), and 72 h (3); upper panels, methylene blue staining for 16S and 23S rRNA; lower panels, hybridization results.

Nine out of 10 top hits in homology modeling of TTH1 (and of TTH2) were PQQ-containing dehydrogenases with an eight-bladed β-propeller structure, a calcium site, and a cytochrome *c* domain (e.g., alcohol dehydrogenase from *Pseudomonas putida* HK5; PDB accession 1kv9; e-value $1 \times e^{-25}$; **Figure 6**). Homologs of the cytochrome *c* domain were missing in both TTHs. Closer examination showed that the Ca^{2+}-coordinating residues were absent as well. Likewise, a nearby disulfide from two adjacent cysteine residues was missing (**Figure 7**). The models predict that the glycosylated Asn of TTH1 is located in the center of the β-propeller.

DISCUSSION

Growth of (*Acidi-*) *Thiobacillus* species and other bacteria by TT oxidation is known for a long time. Likewise, TT-oxidizing Archaea were described previously, most of them acidophiles (Wood et al., 1987; Kurosawa et al., 2003). In contrast, most of the known TT-metabolizing enzymes come from neutrophilic proteobacteria and are molybdenum or heme-containing reductases allowing these organisms to grow anaerobically by TT respiration (Hensel et al., 1999; Price-Carter et al., 2001; Mowat et al., 2004). Although TT hydrolysis had been described already in the 1960s (Trudinger, 1964) and TT hydrolases in the 1990s (De Jong et al., 1997a), the link between purification and identification of the gene was established only recently by Kanao et al. (2007) and Rzhepishevska et al. (2007) for the TTHs from *A. ferrooxidans* and *Acidithiobacillus caldus*, respectively. Enzymes oxidizing TT to sulfate without intermediate(s) are not known, with the exception of SOX complexes from some but not all neutrophilic ISC-oxidizing bacteria (Mukhopadhyaya et al., 2000; Lahiri et al., 2006). We report here on the identification, enzyme characterization, and expression data of the first archaeal TTH described so far.

GROWTH OF *A. AMBIVALENS* ON TT, TTH GENE EXPRESSION DATA, AND ENZYME PROPERTIES

Acidianus ambivalens growth rates and yields were comparable with TT and elemental sulfur. An indication for the presence of a TTH came from the turbidity observed in cultures growing at high TT concentrations, which showed that elemental sulfur is transiently formed. TTH activity was measured in TT-grown but not in sulfur-grown cells suggesting that the protein is formed only in the presence of the substrate. This observation is supported by the Northern data, which showed a stronger signal of the *tth* gene in TT-grown cells (**Figure 4**).

The TTH activity was initially localized in the soluble fraction. The enzyme was highly enriched during various chromatographic steps but the resulting preparation was not electrophoretically homogeneous. A band of approximately 54 kDa was co-enriched with the TTH activity, whose N-terminus was identical to a protein that was previously identified by sequence similarity search with the *A. ferrooxidans* TTH. A pyrophosphatase and a protein of unknown identity were still present in the preparation (**Figure 1A**). The same 54 kDa band was enriched during purification from the pseudo-periplasmic fraction (**Figure 1B**). Again, two larger protein bands were visible in the gel but their

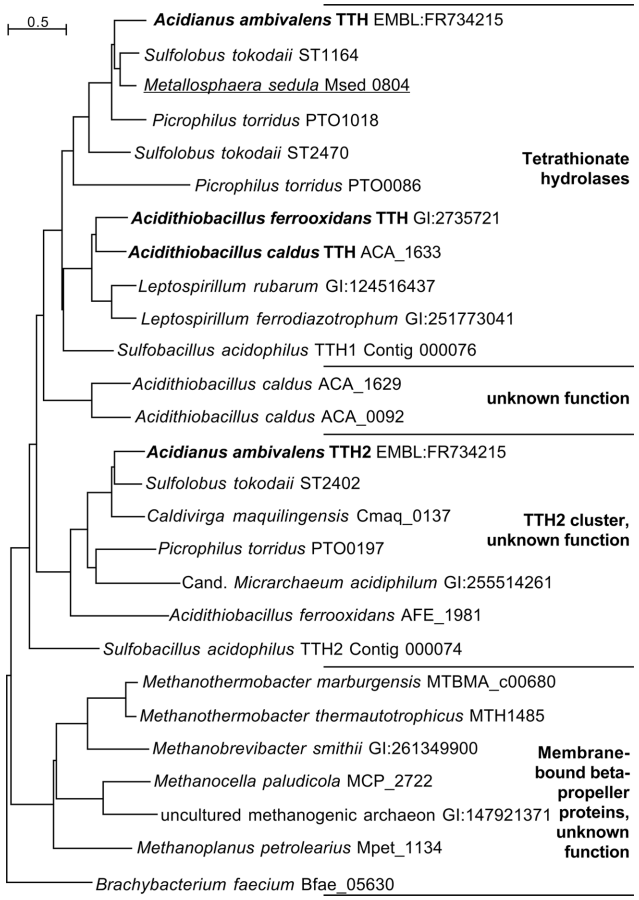

FIGURE 5 | Phylogenetic dendrogram of the TT hydrolases with 26 of the closest homologs from Archaea and Bacteria. Bold face, biochemically characterized TTH enzymes (Bugaytsova and Lindström, 2004; Kanao et al., 2007; Rzhepishevska et al., 2007); underlined, gene described in transcriptome study (Auernik and Kelly, 2008). The *Sulfobacillus* TTH homologs were identified in the draft genome sequence available at http://www.jgi.doe.gov (as of January, 2011).

stoichiometries were not constant. Therefore, we concluded that the 54-kDa protein represents the sole subunit of the TTH. This conclusion is supported by the results from the gel permeation chromatography, which showed two peaks with TTH activity, corresponding to molecular masses of 54 and 105 kDa and representing the monomer and the homodimer.

As expected, the optimal reaction temperature of the *A. ambivalens* TTH is higher (≥95°C; **Figure 3**) than for the enzymes from mesophilic species (optima 40–65°C; Sugio et al., 1996; Tano et al., 1996; De Jong et al., 1997a,b; Bugaytsova and Lindström, 2004; Kanao et al., 2007). In addition, the optimal pH was lower, being around pH 1. The protein was glycosylated at Asn_{50} and probably other residues as well. Glycosylation seems to be a common protection mechanism of membrane-bound and extracellular proteins from *A. ambivalens* and other Sulfolobales species: the TQO, the terminal oxidase, and the large S-layer protein could be stained with glycosylation-specific dyes (Müller et al., 2004; Veith et al., 2009; Peyfoon et al., 2010).

TTH IS FOUND IN THE PSEUDO-PERIPLASMIC SPACE OF TT-GROWN CELLS

Cell pellets had been washed with pH 6.5 buffer prior to disruption in order to remove excess acid (not shown). It turned out that this procedure releases the enzyme from the cells (**Figure 1C**). Treatment of freshly harvested cells with buffers of increasing pH values resulted in the liberation of almost all of the TTH activity in buffers of pH 4.5 and above. A 54-kDa protein band is constantly present in all of the supernatant, that showed TTH activity. Although the amount and the number of proteins seen in the SDS gel are increasing with the pH (**Figure 1B**) the cells apparently remained intact under the microscope (not shown). Therefore, we think that the protein is liberated by pH shock presumably due to changes in S-layer topology but not by (partial) cell lysis. The TTH has a canonical signal sequence but no membrane anchor according to the analysis of the deduced amino acid sequence of the protein. Therefore, an extracytoplasmic location was expected.

As most Archaea including *Acidianus* have proteinaceous S-layers (Baumeister et al., 1988; Baumeister and Lembcke, 1992; König et al., 2007; Veith et al., 2009) as their sole cell wall component, the question arises whether the TTH is secreted into the medium or whether it is somehow attached to the S-layer. As we were unable to detect activity in spent growth medium, the TTH must be attached to the outside of the cytoplasmic membrane or to the S-layer. S-layers consist of a proteinaceous canopy supported by stalks at a constant and species-specific distance above the archaeal cytoplasmic membrane. Baumeister et al. (1988) and Baumeister and Lembcke (1992) proposed from electron microscopic images that S-layers form a space equivalent to the periplasm of Gram-negative Bacteria. Narrow pores in the S-layer connect the medium with the so-called quasi- or pseudo-periplasmic space as porins do in the outer membrane of bacteria. It had been speculated that the electron-light pseudo-periplasmic space in between the electron-dense stalks might accommodate secreted proteins, which are prevented from diffusion into the medium by the porous protein canopy (Baumeister and Lembcke, 1992). We showed here that the TTH is liberated from the cells by pH shift alone. We deduced from these results that the shift in pH causes a rearrangement of the S-layer thereby liberating the TTH. Alternatively, the TTH might be attached to the S-layer by ionic and/or hydrophobic interactions, however, the total lack of TTH activity in the medium argues against this hypothesis. Therefore, we conclude that our results support the pseudo-periplasm hypothesis and that the TTH is one of few enzymes so far shown to be located in this compartment. This conclusion is consistent with the acidic pH optimum of the *A. ambivalens* TTH (around pH 1) corresponding to the media conditions.

ACIDITHIOBACILLUS AND *ACIDIANUS* TTHs ARE SIMILAR ENZYMES

The extracellular location of the *A. ambivalens* enzyme is consistent with bacterial TTHs, which were localized in the periplasm or attached to the membrane. The localization was verified experimentally in the case of the *A. caldus* TTH (Bugaytsova and Lindström, 2004). In most other cases the localization was inferred by the acidic pH optima of the enzymes (pH 2.5–4; Sugio et al., 1996; Tano et al., 1996; De Jong et al., 1997a,b). Comparison of the amino acid sequences showed that almost all of the TTHs

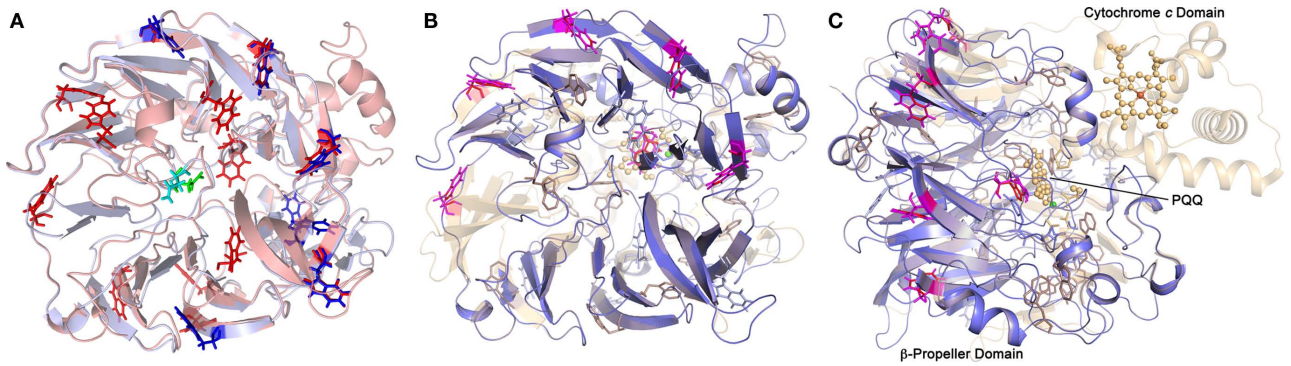

FIGURE 6 | Predictions of the 3D structures of *A. ambivalens* TTH1 and TTH2 modeled with the quinoprotein alcohol dehydrogenase from *Pseudomonas putida* as template (PDB accession number 1kv9). (A) TTH1 model (red) overlaid with TTH2 (blue); tryptophane residues characteristic of the β-propeller wings (see text) are highlighted in sticks representation; the glycosylated Asn resdidue of TTH1 is highlighted in green, the corresponding Asn of TTH2 in cyan. **(B,C)** Overlay of the TTH1 model (blue) with the 1kv9 template (red), top and side views; spheres, PQQ and cytochrome *c* molecules; green sphere, Ca^{2+} ion; brown sphere, iron ion; the tryptophane residues are highlighted as above.

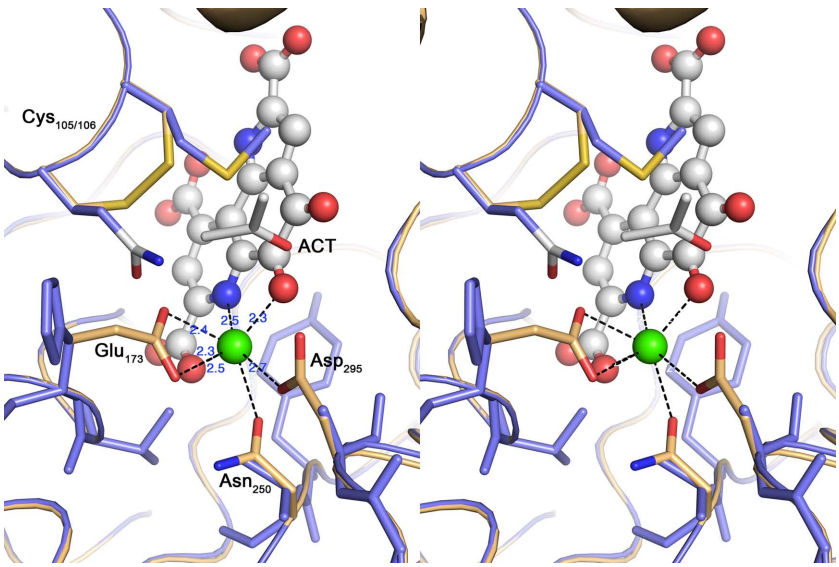

FIGURE 7 | Cross-eyed stereo view of the active site of the quinoprotein alcohol dehydrogenase from *Pseudomonas putida* (beige) overlayed with the TTH1 model (blue). Spheres represent the Calcium–PQQ moiety (carbon, gray; oxygen, red; nitrogen, blue; calcium, green); sticks acetone (ACT) and amino acid side chains. The calcium-coordinating side chains and the disulfide bridge characteristic for this type of proteins are highlighted; note the absence of the equivalent residues in the TTH model.

including TTH2 contain a canonical signal sequence (not shown) thereby confirming the presumed or verified periplasmic or extracellular location. The molecular masses of the TTHs purified so far are fairly similar and differ from the only known trithionate hydrolase, which is a homotrimeric enzyme with a subunit mass of 34 kDa (Meulenberg et al., 1992). Meulenberg's results suggest that trithionate hydrolases represent separate and unrelated entities, however, this cannot be confirmed because the genes are not known.

The sequence analysis and comparisons of the TTH genes showed that they are rare and present only in obligatory or facultative chemolithoautotrophs. In addition, most of the species represented in the dendrogram (**Figure 5**) harbor at least two *tth* genes. The gene products fall into two separate phylogenetic clades. The clade around the TTH1 encompasses true tetrathionate hydrolases from their similarity and from the known enzyme activities. The TTH2 proteins are paralogous proteins with a different and unknown function, however, they also contain a signal sequence and should therefore be secreted (**Figure 5**).

TTH IN LITHOAUTOTROPHIC AND ORGANOHETEROTROPHIC SULFOLOBALES SPECIES

The absence of *tth* genes in many organoheterotrophic Sulfolobales species is of particular interest as for example *Sulfolobus acidocaldarius* had originally been described as a facultatively chemolithoautotrophic, sulfur-dependent species (Brock et al., 1972).

Neither *S. acidocaldarius* nor *Sulfolobus solfataricus/Sulfolobus islandicus* species have *tth* genes suggesting that they are unable to grow at the expense of TT oxidation. An analogous observation was made with the sulfur oxygenase reductase (SOR): (facultatively) chemolithoautotrophs like *Sulfolobus metallicus*, *Metallosphaera sedula*, and *Sulfolobus tokodaii* possess *sor* genes, while *S. acidocaldarius*, *S. solfataricus*, and *S. islandicus* lack the gene and corresponding enzyme activities (Kletzin, 1989; Veith et al., 2011; this volume). Both observations suggest that the colony-isolated, heterotrophic Sulfolobales species are not sulfur-dependent at all and unable to grow oxidatively with sulfur or tetrathionate.

TTH: β-PROPELLER STRUCTURE WITHOUT PQQ

It can be concluded from sequence analysis and structure prediction that the TTHs are all-beta and also β-propeller-forming proteins with a conserved 3D structure similar but not identical to PQQ-containing dehydrogenases. These proteins, e.g., type II alcohol dehydrogenases and glucose dehydrogenases, consist of a PQQ domain, composed of seven to eight conserved, propeller-forming PQQ repeats (PFAM family PF01011; **Figure 6**; Oubrie et al., 1999; Chen et al., 2002). The alcohol dehydrogenases contain an additional heme *c* domain (Chen et al., 2002). The PQQ repeats contain a conserved motif of amino acids (Ala-x_5-Gly-x_3-Trp) thought to stabilize the structure (Chen et al., 2002).

The model of the *A. ambivalens* TTH1 and the sequence alignments used for dendrogram calculation (**Figure 5**; alignment not shown) contain five to six of these tryptophane motifs, whereas TTH2 contains four (**Figure 6**). In contrast, the heme *c* domain and conserved PQQ-binding site residues are missing including the disulfide-forming cysteines and the calcium-coordinating amino acids (**Figure 7**). The glycosylated Asn of TTH1 sits in the middle of the β-propeller and far from the region where the dehydrogenases bind PQQ. The alignments did not show a conserved cysteine residue – the usual suspect for sulfur binding – so that the reaction mechanism remains enigmatic at present, especially in the absence of PQQ and metal ions.

CONCLUSION

Some final conclusions for the *A. ambivalens* sulfur metabolism can be drawn: One of the initial questions was, how TT produced in the TQO reaction is metabolized (Müller et al., 2004). The TTH found here does not give an answer to this question because the protein was found only in TT-grown cells and the gene is poorly expressed in sulfur-grown cells. The localization and pH optimum of the TTH argue against a role in the oxidative metabolism of elemental sulfur. In contrast, the SOR does seem to play an important role in TT-grown cells, presumably by disproportionation of the sulfur generated by the TTH.

The TTH itself seems to be a monomeric or homodimeric enzyme with an overall β-propeller structure. The enzyme has a high temperature optimum and very low pH optimum, both of which are in accordance with the extracellular location shown by the pH shock-mediated enzyme liberation.

ACKNOWLEDGMENTS

We wish to thank Felicitas Pfeifer (Darmstadt, Germany) for her generosity and encouragement. This work was supported by grants of the Deutsche Forschungsgemeinschaft (Az Kl885-3/3 and Kl885-5/1).

REFERENCES

Auernik, K. S., and Kelly, R. M. (2008). Identification of components of electron transport chains in the extremely thermoacidophilic crenarchaeon *Metallosphaera sedula* through iron and sulfur compound oxidation transcriptomes. *Appl. Environ. Microbiol.* 74, 7723–7732.

Baumeister, W., and Lembcke, G. (1992). Structural features of archaebacterial cell envelopes. *J. Bioenerg. Biomembr.* 24, 567–575.

Baumeister, W., Wildhaber, I., and Engelhardt, H. (1988). Bacterial surface proteins. Some structural, functional and evolutionary aspects. *Biophys. Chem.* 29, 39–49.

Blum, H., Beier, H., and Gross, H. J. (1987). Improved silver staining of plant proteins, RNA and DNA in polyacylamide gels. *Electrophoresis* 8, 93–99.

Brock, T. D., Brock, K. M., Belly, R. T., and Weiss, R. L. (1972). *Sulfolobus*: a new genus of sulfur-oxidizing bacteria living at low pH and high temperature. *Arch. Microbiol.* 84, 54–68.

Bugaytsova, Z., and Lindström, E. B. (2004). Localization, purification and properties of a tetrathionate hydrolase from *Acidithiobacillus caldus*. *Eur. J. Biochem.* 271, 272–280.

Chen, Z. W., Matsushita, K., Yamashita, T., Fujii, T. A., Toyama, H., Adachi, O., Bellamy, H. D., and Mathews, F. S. (2002). Structure at 1.9 Å resolution of a quinohemoprotein alcohol dehydrogenase from *Pseudomonas putida* HK5. *Structure* 10, 837–849.

Chomczynski, P., and Sacchi, N. (1987). Single-step method of RNA isolation by acid guanidinium thiocyanate-phenol-chloroform extraction. *Anal. Biochem.* 162, 156–159.

De Jong, G. A., Hazeu, W., Bos, P., and Kuenen, J. G. (1997a). Isolation of the tetrathionate hydrolase from *Thiobacillus acidophilus*. *Eur. J. Biochem.* 243, 678–683.

De Jong, G. A. H., Hazeu, W., Bos, P., and Kuenen, J. G. (1997b). Polythionate degradation by tetrathionate hydrolase of *Thiobacillus ferrooxidans*. *Microbiology* 143, 499–504.

DeLano, W. L. (2002). *The PyMOL Molecular Graphics System. 0.97 ed.* San Carlos, CA: DeLano Scientific.

Egorova, M. A., Tsaplina, I. A., Zakharchuk, L. M., Bogdanova, T. I., and Krasil'nikova, E. N. (2004). Effect of cultivation conditions on the growth and activities of sulfur metabolism enzymes and carboxylases of *Sulfobacillus thermosulfidooxidans* subsp. *asporogenes* strain 41. *Prikl. Biokhim. Mikrobiol.* 40, 448–454.

Friedrich, C. G., Bardischewsky, F., Rother, D., Quentmeier, A., and Fischer, J. (2005). Prokaryotic sulfur oxidation. *Curr. Opin. Microbiol.* 8, 253–259.

Friedrich, C. G., Quentmeier, A., Bardischewsky, F., Rother, D., Orawski, G., Hellwig, P., and Fischer, J. (2008). "Redox control of chemotrophic sulfur oxidation of *Paracoccus pantotrophus*," in *Microbial Sulfur Metabolism*, eds C. Dahl and C. G. Friedrich (Berlin: Springer Verlag), 139–150.

Frigaard, N. U., and Dahl, C. (2009). Sulfur metabolism in phototrophic sulfur bacteria. *Adv. Microb. Physiol.* 54, 103–200.

Fuchs, T., Huber, H., Burggraf, S., and Stetter, K. O. (1996). 16S rDNA-based phylogeny of the archaeal order *Sulfolobales* and reclassification of *Desulfurolobus ambivalens* as *Acidianus ambivalens* comb. nov. *Syst. Appl. Microbiol.* 19, 56–60.

Gadd, G. M. (2010). Metals, minerals and microbes: geomicrobiology and bioremediation. *Microbiology* 156, 609–643.

Ghosh, W., and Dam, B. (2009). Biochemistry and molecular biology of lithotrophic sulfur oxidation by taxonomically and ecologically diverse bacteria and archaea. *FEMS Microbiol. Rev.* 33, 999–1043.

Hensel, M., Hinsley, A. P., Nikolaus, T., Sawers, G., and Berks, B. C. (1999). The genetic basis of tetrathionate respiration in *Salmonella typhimurium*. *Mol. Microbiol.* 32, 275–287.

Herrin, D. L., and Schmidt, G. W. (1988). Rapid, reversible staining of northern blots prior to hybridization. *BioTechniques* 6, 196–197, 199–200.

Johnston, F., and McAmish, L. (1973). Study of rates of sulfur production in acid thiosulfate solutions using S-35. *J. Colloid Interface Sci.* 42, 112–119.

Kanao, T., Kamimura, K., and Sugio, T. (2007). Identification of a gene encoding a tetrathionate hydrolase

in *Acidithiobacillus ferrooxidans*. *J. Biotechnol.* 132, 16–22.

Kanao, T., Matsumoto, C., Shiraga, K., Yoshida, K., Takada, J., and Kamimura, K. (2010). Recombinant tetrathionate hydrolase from *Acidithiobacillus ferrooxidans* requires exposure to acidic conditions for proper folding. *FEMS Microbiol. Lett.* 309, 43–47.

Katoh, K., Kuma, K., Miyata, T., and Toh, H. (2005). Improvement in the accuracy of multiple sequence alignment program MAFFT. *Genome Inform.* 16, 22–33.

Kelley, L. A., and Sternberg, M. J. (2009). Protein structure prediction on the web: a case study using the Phyre server. *Nat. Protoc.* 4, 363–371.

Kelly, D. P., Chambers, L. A., and Trudinger, P. A. (1969). Cyanolysis and spectrophotometric determination of trithionate in mixtures with thiosulfate and tetrathionate. *Anal. Chem.* 41, 898–901.

Kelly, D. P., Shergill, J. K., Lu, W. P., and Wood, A. P. (1997). Oxidative metabolism of inorganic sulfur compounds by bacteria. *Antonie Van Leeuwenhoek* 71, 95–107.

Kletzin, A. (1989). Coupled enzymatic production of sulfite, thiosulfate, and hydrogen sulfide from sulfur: purification and properties of a sulfur oxygenase reductase from the facultatively anaerobic archaebacterium *Desulfurolobus ambivalens*. *J. Bacteriol.* 171, 1638–1643.

Kletzin, A. (1992). Molecular characterization of the sor gene, which encodes the sulfur oxygenase reductase of the thermoacidophilic archaeon *Desulfurolobus ambivalens*. *J. Bacteriol.* 174, 5854–5859.

Kletzin, A. (2007). "Metabolism of inorganic sulfur compunds in Archaea," in *Archaea. Evolution, Physiology, and Molecular Biology*, eds R. A. Garrett and H.-P. Klenk (Oxford: Blackwell Publishing), 261–274.

Kletzin, A. (2008). "Oxidation of sulfur and inorganic sulfur compounds in *Acidianus ambivalens*," in *Microbial Sulfur Metabolism*, eds C. Dahl and C. G. Friedrich (Berlin: Springer), 184–201.

König, H., Rachel, R., and Claus, H. (2007). "Proteinaceous surface layers of Archaea: ultrastructure and biochemistry," in *Archaea. Molecular and Cellular Biology*, ed. R. Cavicchioli (Washington, DC: ASM Press), 315–340.

Kurosawa, N., Itoh, Y. H., and Itoh, T. (2003). Reclassification of *Sulfolobus hakonensis* Takayanagi et al. 1996 as *Metallosphaera hakonensis* comb. nov. based on phylogenetic evidence and DNA G + C content. *Int. J. Syst. Evol. Microbiol.* 53, 1607–1608.

Kyhse-Andersen, J. (1984). Electroblotting of multiple gels: a simple apparatus without buffer tank for rapid transfer of proteins from polyacrylamide to nitrocellulose. *J. Biochem. Biophys. Methods* 10, 203–209.

Lahiri, C., Mandal, S., Ghosh, W., Dam, B., and Roy, P. (2006). A novel gene cluster soxSRT is essential for the chemolithotrophic oxidation of thiosulfate and tetrathionate by *Pseudaminobacter salicylatoxidans* KCT001. *Curr. Microbiol.* 52, 267–273.

Mangold, S., Valdés, J., Holmes, D. S., and Dopson, M. (2011). Sulfur metabolism in the extreme acidophile *Acidithiobacillus caldus*. *Front. Microbiol.* 2:17. doi: 10.3389/fmicb.2011.00017

Meulenberg, R., Pronk, J. T., Frank, J., Hazeu, W., Bos, P., and Kuenen, J. G. (1992). Purification and partial characterization of a thermostable trithionate hydrolase from the acidophilic sulphur oxidizer *Thiobacillus acidophilus*. *Eur. J. Biochem.* 209, 367–374.

Moll, R., and Schäfer, G. (1988). Chemiosmotic H+ cycling across the plasma membrane of the thermoacidophilic archaebacterium *Sulfolobus acidocaldarius*. *FEBS Lett.* 232, 359–363.

Mowat, C. G., Rothery, E., Miles, C. S., McIver, L., Doherty, M. K., Drewette, K., Taylor, P., Walkinshaw, M. D., Chapman, S. K., and Reid, G. A. (2004). Octaheme tetrathionate reductase is a respiratory enzyme with novel heme ligation. *Nat. Struct. Mol. Biol.* 11, 1023–1024.

Mukhopadhyaya, P. N., Deb, C., Lahiri, C., and Roy, P. (2000). A *soxA* gene, encoding a diheme cytochrome *c*, and a *sox* locus, essential for sulfur oxidation in a new sulfur lithotrophic bacterium. *J. Bacteriol.* 182, 4278–4287.

Müller, F. H., Bandeiras, T. M., Urich, T., Teixeira, M., Gomes, C. M., and Kletzin, A. (2004). Coupling of the pathway of sulphur oxidation to dioxygen reduction: characterization of a novel membrane-bound thiosulphate:quinone oxidoreductase. *Mol. Microbiol.* 53, 1147–1160.

Oubrie, A., Rozeboom, H. J., Kalk, K. H., Olsthoorn, A. J., Duine, J. A., and Dijkstra, B. W. (1999). Structure and mechanism of soluble quinoprotein glucose dehydrogenase. *EMBO J.* 18, 5187–5194.

Perriere, G., and Gouy, M. (1996). WWW-query: an on-line retrieval system for biological sequence banks. *Biochimie* 78, 364–369.

Pettersen, E. F., Goddard, T. D., Huang, C. C., Couch, G. S., Greenblatt, D. M., Meng, E. C., and Ferrin, T. E. (2004). UCSF Chimera – a visualization system for exploratory research and analysis. *J. Comput. Chem.* 25, 1605–1612.

Peyfoon, E., Meyer, B., Hitchen, P. G., Panico, M., Morris, H. R., Haslam, S. M., Albers, S. V., and Dell, A. (2010). The S-layer glycoprotein of the crenarchaeote *Sulfolobus acidocaldarius* is glycosylated at multiple sites with chitobiose-linked *N*-glycans. *Archaea* 2010, Article ID 754101. doi: 10.1155/2010/754101

Price-Carter, M., Tingey, J., Bobik, T. A., and Roth, J. R. (2001). The alternative electron acceptor tetrathionate supports B12-dependent anaerobic growth of *Salmonella enterica* serovar typhimurium on ethanolamine or 1,2-propanediol. *J. Bacteriol.* 183, 2463–2475.

Richter, O.-M., and Schäfer, G. (1992). Purification and enzymic characterization of the cytoplasmic pyrophosphatase from the thermoacidophilic archaebacterium *Thermoplasma acidophilum*. *Eur. J. Biochem.* 209, 343–349.

Rzhepishevska, O. I., Valdes, J., Marcinkeviciene, L., Gallardo, C. A., Meskys, R., Bonnefoy, V., Holmes, D. S., and Dopson, M. (2007). Regulation of a novel *Acidithiobacillus caldus* gene cluster involved in metabolism of reduced inorganic sulfur compounds. *Appl. Environ. Microbiol.* 73, 7367–7372.

Sakurai, H., Ogawa, T., Shiga, M., and Inoue, K. (2010). Inorganic sulfur oxidizing system in green sulfur bacteria. *Photosyn. Res.* 104, 163–176.

Sand, W., Gehrke, T., Jozsa, P. G., and Schippers, A. (2001). (Bio) chemistry of bacterial leaching – direct vs. indirect bioleaching. *Hydrometallurgy* 59, 159–175.

Schägger, H., and von Jagow, G. (1987). Tricine-sodium dodecyl sulfate-polyacrylamide gel electrophoresis for the separation of proteins in the range from 1 to 100 kDa. *Anal. Biochem.* 166, 368–379.

Seldon, R. F. (1988). "Preparation and analysis of RNA: 4.9, analysis of RNA by northern hybridization," in *Current Protocols in Molecular Biology*, eds F. M. Ausubel, R. Brent, R. E. Kingston, D. D. Moore, J. G. Seidman, J. A. Smith and K. Struhl (New York: Greene Publishing Associates and Wiley-Interscience), 4.9.1–4.9.8.

Stetter, K. O. (2006). Hyperthermophiles in the history of life. *Philos. Trans. R. Soc. Lond. B Biol. Sci.* 361, 1837–1842; discussion 1842–1833.

Sugio, T., Kanao, T., Furukawa, H., Nagasawa, T., and Blake, R. C. (1996). Isolation and identification of an iron-oxidizing bacterium which can grow on tetrathionate medium and the properties of a tetrathionate-decomposing enzyme isolated from the bacterium. *J. Ferment. Bioeng.* 82, 233–238.

Tano, T., Kitaguchi, H., Harada, M., Nagasawa, T., and Sugio, T. (1996). Purification and some properties of a tetrathionate decomposing enzyme from *Thiobacillus thiooxidans*. *Biosci. Biotech. Biochem.* 60, 224–227.

Teixeira, M., Batista, R., Campos, A. P., Gomes, C., Mendes, J., Pacheco, I., Anemüller, S., and Hagen, W. R. (1995). A seven-iron ferredoxin from the thermoacidophilic *Desulfurolobus ambivalens*. *Eur. J. Biochem.* 227, 322–327.

Trudinger, P. A. (1964). Effects of thiosulphate and oxygen concentration on tetrathionate oxidation by *Thiobacillus* X and *Thiobacillus thioparus*. *Biochem. J.* 90, 640–646.

Urich, T., Bandeiras, T. M., Leal, S. S., Rachel, R., Albrecht, T., Zimmermann, P., Scholz, C., Teixeira, M., Gomes, C. M., and Kletzin, A. (2004). The sulphur oxygenase reductase from *Acidianus ambivalens* is a multimeric protein containing a low-potential mononuclear non-haem iron centre. *Biochem. J.* 381, 137–146.

Urich, T., Kroke, A., Bauer, C., Seyfarth, K., Reuff, M., and Kletzin, A. (2005). Identification of core active site residues of the sulfur oxygenase reductase from *Acidianus ambivalens* by site-directed mutagenesis. *FEMS Microbiol. Lett.* 248, 171–176.

Veith, A., Klingl, A., Zolghadr, B., Lauber, K., Mentele, R., Lottspeich, F., Rachel, R., Albers, S.-V., and Kletzin, A. (2009). *Acidianus*, *Sulfolobus* and *Metallosphaera* surface layers: structure, composition and gene expression. *Mol. Microbiol.* 73, 58–72.

Veith, A., Urich, T., Seyfarth, K., Protze, J., Frazão, C., and Kletzin, A. (2011). Substrate pathways and mechanisms of inhibition in the sulfur oxygenase reductase of *Acidianus ambivalens*. *Front. Microbiol.* 2:37. doi: 10.3389/fmicb.2011.00037

Wood, A. P., Kelly, D. P., and Norris, P. R. (1987). Autotrophic growth of 4 *Sulfolobus* strains on tetrathionate and the effect of organic nutrients. *Arch. Microbiol.* 146, 382–389.

Zillig, W., Yeats, S., Holz, I., Böck, A., Rettenberger, M., Gropp, F., and Simon, G. (1986). *Desulfurolobus*

ambivalens gen. nov., sp. nov., an autotrophic archaebacterium facultatively oxidizing and reducing sulfur. *Syst. Appl. Microbiol.* 8, 197–203.

Conflict of Interest Statement: The authors declare that the research was conducted in the absence of any commercial or financial relationships that could be construed as a potential conflict of interest.

Received: 03 January 2011; paper pending published: 21 January 2011; accepted: 25 March 2011; published online: 25 April 2011.

Citation: Protze J, Müller F, Lauber K, Naß B, Mentele R, Lottspeich F and Kletzin A (2011) An extracellular tetrathionate hydrolase from the thermoacidophilic archaeon Acidianus ambivalens with an activity optimum at pH 1. Front. Microbio. ***2****:68. doi: 10.3389/fmicb.2011.00068*

This article was submitted to Frontiers in Microbial Physiology and Metabolism, a specialty of Frontiers in Microbiology.

frontiers in
MICROBIOLOGY

ORIGINAL RESEARCH ARTICLE
published: 18 April 2011
doi: 10.3389/fmicb.2011.00079

Growth of *Acidithiobacillus ferrooxidans* ATCC 23270 in thiosulfate under oxygen-limiting conditions generates extracellular sulfur globules by means of a secreted tetrathionate hydrolase

Simón Beard[1†], Alberto Paradela[2], Juan P. Albar[2] and Carlos A. Jerez[1]*

[1] *Faculty of Sciences, Laboratory of Molecular Microbiology and Biotechnology, Department of Biology, Millenium Institute for Cell Dynamics and Biotechnology, University of Chile, Santiago, Chile*

[2] *Servicio de Proteómica, Centro Nacional de Biotecnología, Consejo Superior de Investigaciones Científicas, Madrid, España*

Edited by:
Thomas E. Hanson, University of Delaware, USA

Reviewed by:
Biswarup Mukhpadhyay, Virginia Bioinformatics Institute, USA
John Stolz, Duquesne University, USA

***Correspondence:**
Carlos A. Jerez, Facultad de Ciencias, Departamento de Biología, Universidad de Chile, Santiago 1, Casilla 653, Santiago, Chile.
e-mail: cjerez@uchile.cl

†Present address:
Simón Beard, Biotecnologías Antofagasta S.A., Las Araucarias 9080-9110 módulo C, Quilicura, Santiago, Chile.
e-mail: sbeard@bta-sa.cl

Production of sulfur globules during sulfide or thiosulfate oxidation is a characteristic feature of some sulfur bacteria. Although their generation has been reported in *Acidithiobacillus ferrooxidans*, its mechanism of formation and deposition, as well as the physiological significance of these globules during sulfur compounds oxidation, are currently unknown. Under oxygen-sufficient conditions (OSC), *A. ferrooxidans* oxidizes thiosulfate to tetrathionate, which accumulates in the culture medium. Tetrathionate is then oxidized by a tetrathionate hydrolase (TTH) generating thiosulfate, elemental sulfur, and sulfate as final products. We report here a massive production of extracellular conspicuous sulfur globules in thiosulfate-grown *A. ferrooxidans* cultures shifted to oxygen-limiting conditions (OLC). Concomitantly with sulfur globule deposition, the extracellular concentration of tetrathionate greatly diminished and sulfite accumulated in the culture supernatant. *A. ferrooxidans* cellular TTH activity was negligible in OLC-incubated cells, indicating that this enzymatic activity was not responsible for tetrathionate disappearance. On the other hand, supernatants from both OSC- and OLC-incubated cells showed extracellular TTH activity, which most likely accounted for tetrathionate consumption in the culture medium. The extracellular TTH activity described here: (i) gives experimental support to the TTH-driven model for hydrophilic sulfur globule generation, (ii) explains the extracellular location of *A. ferrooxidans* sulfur deposits, and (iii) strongly suggests that the generation of sulfur globules in *A. ferrooxidans* corresponds to an early step during its adaptation to an anaerobic lifestyle.

Keywords: *Acidithiobacillus ferrooxidans*, sulfur globules, extracellular tetrathionate hydrolase, thiosulfate oxidation

INTRODUCTION

During oxidation of reduced inorganic sulfur compounds (RISCs), by some microaerophilic chemotrophic sulfur bacteria and by anoxygenic phototrophic microorganisms, the deposition of intracellular or extracellular conspicuous sulfur globules as an important (and sometimes obligatory) intermediary occurs. It has been proposed that production of obligated intracellular sulfur deposits, during anoxygenic sulfide and thiosulfate oxidation in photolithotrophic and facultative anaerobic chemolithotrophic bacteria, correlates with the lack of sulfur dehydrogenase (SoxCD), normally present in the thiosulfate-oxidizing multi-enzyme system (TOMES; Friedrich et al., 2005). The latter is a characteristic feature of microorganisms that oxidize RISCs by using the branched *Paracoccus* sulfur oxidation (PSO) pathway (Grimm et al., 2008; Ghosh and Dam, 2009, and references therein). The mechanisms for production of sulfur globules by sulfur bacteria that do not use the branched-PSO pathway are currently unknown. *Acidithiobacillus ferrooxidans* is a facultative anaerobe, chemolithoautotroph gram negative γ-proteobacterium that obtains its energy from the oxidation of ferrous iron, elemental sulfur, or RISCs, amongst other compounds (Pronk et al., 1990; Rohwerder and Sand, 2003; Rawlings, 2005). Due to its ability to solubilize metal sulfides, this bacterium has been successfully applied in biomining operations (Olson et al., 2003; Rawlings, 2005). In *A. ferrooxidans*, thiosulfate is oxidized through the S4-intermediary pathway (S4I; Pronk et al., 1990; Kelly et al., 1997; Ghosh and Dam, 2009). The first step in the S4I-pathway is the condensative oxidation of two molecules of thiosulfate to generate the four sulfur atoms intermediate tetrathionate, a reaction catalyzed by a thiosulfate dehydrogenase (TD). The second step in the S4I-pathway is tetrathionate hydrolysis by a tetrathionate hydrolase (TTH), generating sulfate and disulfane monosulfonic acid ($HS_2SO_3^-$) as direct hydrolysis products. Due to the high reactivity of the last compound, *A. ferrooxidans* TTH generates sulfate, thiosulfate, and elemental sulfur as final products (de Jong et al., 1997). This enzyme has been purified and its corresponding coding gene (*tetH*; BAF03501) was identified (Buonfiglio et al., 1999; Kanao et al., 2007). A cyclic thiosulfate-oxidizing pathway has been proposed in thiobacilli, in which disulfane monosulfonic acid is biologically oxidized to trithionate ($S_3O_6^{2-}$), and then hydrolyzed to thiosulfate and sulfate by means of a trithionate hydrolase without the production of long-chain polythionates or elemental sulfur (Pronk et al., 1990; Ghosh and Dam, 2009). However, the production of long-chain polythionates and elemental sulfur has been reported

in aerated *A. ferrooxidans* suspensions incubated with tetrathionate (Steudel et al., 1987). Based on these results, a set of reactions involving the highly reactive disulfane monosulfonic acid were proposed, in which this compound reacts with itself in successive elongation chain reactions leading to the production elemental sulfur and sulfite ($2HS_2SO_3^- \leftrightarrow HS_4SO_3^- + HSO_3^-$; $2HS_4SO_3^- \leftrightarrow HS_8SO_3^- + HSO_3^-$; $HS_8SO_3^- \leftrightarrow S_8^\circ + HSO_3^-$; **Figure 1**).

The hydrophobic elemental sulfur generated can be "solubilized" by polythionates in a micelle-like structure, forming hydrophilic sulfur globules (Steudel et al., 1987). Due to the reversibility of the reactions involved in the higher polythionates pathway and because their formation does not explain oxidation of the sulfane-sulfur moiety from thiosulfate, the physiological significance of polythionates (and hence of hydrophilic sulfur globules) as intermediates during sulfur oxidation remains obscure (Kelly et al., 1997; Ghosh and Dam, 2009). The appearance of visible sulfur (sulfur globules) during *A. ferrooxidans* growth in a substrate-limited chemostat on tetrathionate under high substrate concentrations (above 400 μM) has been reported. Transmission electron microscopy (TEM) micrographs of these cells showed tiny globules located between the inner and outer membranes or in a discrete cytoplasmic vacuole-like structure (Hazeu et al., 1988). Despite the low concentration and small size of sulfur globules produced by thiosulfate-grown *A. ferrooxidans*, it was possible to identify polythionates as the main sulfur species present in them by using sulfur K-edge X-ray absorption near-edge spectroscopy (XANES) analysis (Prange et al., 2002). However, some controversy exist regarding the methodological approach used by Prange et al. (2002) in their sulfur K-edge XANES analysis (George et al., 2008) and other researchers have found elemental sulfur as the main sulfur species in *A. ferrooxidans* sulfur globules (He et al., 2010).

Sulfur globule deposition is a characteristic feature amongst anoxygenic sulfur bacteria. In the proposed model for hydrophilic sulfur globule production, TTH is the key enzyme involved and it does not use molecular oxygen during tetrathionate hydrolysis. The reaction proceeds under both aerobic and anaerobic conditions (de Jong et al., 1997). Moreover, disulfane monosulfonic acid can lead to the formation of polythionates both in aerobic and anaerobic conditions ($2HS_2SO_3^- + \frac{1}{2}O_2 \rightarrow S_6O_6^{2-} + H_2O$; $2HS_2SO_3^- \leftrightarrow S_5O_6^{2-} + H_2S$; **Figure 1**; Steudel et al., 1987), indicating that hydrophilic sulfur globule forming reactions may proceed under anoxygenic conditions. Therefore, the effect of oxygen availability during thiosulfate oxidation by *A. ferrooxidans* was studied in the present communication. Thiosulfate-grown *A. ferrooxidans* cultures shifted to oxygen-limiting conditions (OLC) produced extracellular sulfur globules. In addition, extracellular TTH activity was detected in the growth medium of OLC-incubated *A. ferrooxidans* cells and the corresponding protein was identified by mass spectrometry analysis. Extracellular sulfur globules formed under OLC contained elemental sulfur and concomitantly with their production sulfite was also accumulated in the growth medium. Therefore, the extracellular TTH activity and the chemical by-products detected here give experimental support to the TTH-driven hydrophilic sulfur globule production model proposed by Steudel et al. (1987) and suggest for the first time a mechanism for extracellular sulfur globule deposition by an S4I-pathway-using microorganism. Furthermore, our results suggest that deposition of sulfur globules might be an early step of a physiological response to a decrease in oxygen availability.

MATERIALS AND METHODS

BACTERIAL STRAINS AND GROWTH CONDITIONS

Acidithiobacillus ferrooxidans strain ATCC 23270 was grown in batch cultures by using thiosulfate-containing DSMZ medium 71 [in grams per liter: KH_2PO_4, 3.0; $MgSO_4 \cdot 7H_2O$, 0.5; $(NH_4)_2SO_4$, 3.0; $CaCl_2 \cdot 2H_2O$, 0.25; $Na_2S_2O_3 \cdot 5H_2O$, 5.0; pH 4.4–4.7]. No ferrous sulfate was added to the medium according to the instructions given by DSMZ. *A. ferrooxidans* cells were washed with basal salts DSMZ 71 medium solution and inoculated at a density of 2.5×10^6 cells/mL in Erlenmeyer flasks (2 L) containing 500 mL of DSMZ 71 medium (flask to culture volume ratio of 0.25) followed by incubation at 30°C with shaking (150 RPM). Once the culture reached the mid to late-exponential-phase, shifts to OLC were achieved by

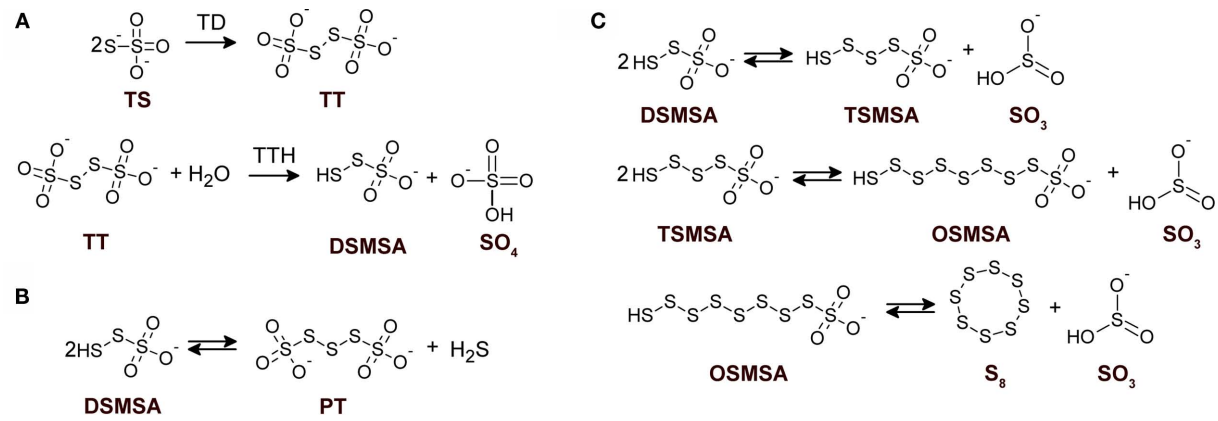

FIGURE 1 | Detailed structures of relevant sulfur compounds and reactions proposed for sulfur globules production. (A) Enzymatically catalyzed reactions. TD, thiosulfate dehydrogenase; TTH, tetrathionate hydrolase. **(B)** Anoxygenic condensation of disulfane monosulfonic acid that leads to polythionates generation. **(C)** Successive condensation reactions of sulfane monosulfonic acids that leads to elemental sulfur production. TS, thiosulfate; TT, tetrathionate; DSMSA, disulfane monosulfonic acid; SO_4, sulfate; SO_3, sulfite; PT, pentathionate; TSMSA, tetrasulfane monosulfonic acid; OSMSA, octosulfane monosulfonic acid; S_8, elemental sulfur. Reactions according to Steudel et al. (1987).

trespassing 200–250 mL of the grown culture to a 250-mL flask (culture to flask volume ratio of 0.8:1.0) followed by incubation at 30°C without shaking. The remaining *A. ferrooxidans* culture was kept in the 2-L Erlenmeyer flask (culture to flask volume ratio of 0.1:0.125) and was further incubated at 30°C with shaking. These cultures were used as the oxygen-sufficient condition (OSC). Cell and sulfur globule counting was carried out by using a Petroff-Hausser chamber in a phase-contrast Olympus BX50 microscope. Sulfur globules were identified as extracellular refringent structures viewed at a 600 × magnification. After centrifugation of OLC- and OSC-cultures (5,000 × *g* at 4°C for 20 min) media supernatants were filtered through a 0.22-μm nitrocellulose filter and were used to determine presence of different thiols and enzymatic activities.

PREPARATION OF CELL-FREE EXTRACTS

Acidithiobacillus ferrooxidans cells were washed three times by centrifugation with 1 M ammonium sulfate pH 3.0 and finally resuspended in 500 μL of 1 M ammonium sulfate pH 3.0. To obtain cell-free extracts, cells were disrupted by sonication on ice (Misonix XL2020, Farmingdale, NY, USA; 20% intensity cycles of 20 s on, 40 s off for 10 min total time). Unbroken cells and cellular debris were removed by centrifugation at 15,000 × *g* at 4°C for 10 min.

ANALYSIS OF SULFUR COMPOUNDS

Thiosulfate was determined by the decoloration of methylene-blue at 670 nm in acidic conditions (Kletzin, 1989). Tetrathionate was determined by a cold-cyanolysis protocol (Kelly et al., 1969). Production of extracellular sulfur in *A. ferrooxidans* cultures was estimated by the increase in absorbance at 430 nm (Hazeu et al., 1988). Elemental sulfur was quantitatively determined by extraction with acetone/water (19:1) followed by cyanolysis (Kelly and Wood, 1998) and normalized by the amount of total protein content of the cell pellet extracted. Analysis of low molecular thiols present in *A. ferrooxidans* growth medium supernatants was carried out by using HPLC after sample derivatization with THIOLYTE® monobromobimane reagent (Calbiochem, La Jolla, CA, USA) as previously described (Rethmeier et al., 1997).

OXYGEN DETERMINATION

Oxygen measurements were carried out in a liquid-phase oxygraph (Hansatech Instruments, Ltd., Norfolk, UK). The electrode cell was filled with 2.5 mL of a mid to late-exponential-phase culture of *A. ferrooxidans* and the oxygen concentration in the medium was recorded. To mimic oxygen-suficient conditions, the electrode chamber lid was removed and 1.0 mL of the *A. ferrooxidans* culture was kept in the cell chamber. At different times, 0.1 mL aliquots were taken and the absorbance at 430 nm was measured.

ENZYMATIC ASSAYS

Thiosulfate dehydrogenase activity was determined spectrophotometrically by using ferricyanide as an artificial electron acceptor. The reaction was followed by the thiosulfate-dependent decrease in ferricyanide absorbance at 420 nm. The TD reaction mixture contained (in 1 mL final volume): 150 mM potassium acetate buffer pH 5.0, 1 mM ferricyanide, 10 mM sodium thiosulfate, and 50 μg mL^{-1} of cell-free extract protein. One unit of activity (U) was defined as the amount of enzyme that catalyzes the reduction of 1 μmol ferricyanide min^{-1}. Tetrathionate hydrolase activity was determined in a continuous assay, measuring the increase in absorbance at 290 nm due to the production of long-chain sulfur intermediates derived from tetrathionate hydrolysis (de Jong et al., 1997). The reaction mixture contained (in 0.1 mL final volume): 1 M ammonium sulfate pH 3.0, 1 mM sodium tetrathionate, and 50 μg mL^{-1} of cell-free extract protein. TTH activity was determined in aliquots of filtrated growth medium supernatants from *A. ferrooxidans* cultures incubated under OLC and OSC. Units for TTH activity were expressed as ΔAbs 290 nm min^{-1}. All enzymatic reactions were carried out at room-temperature. Data presented for sulfur compounds and enzymatic activities correspond to the mean values and SD of at least three independent experiments.

RNA MANIPULATIONS

Acidithiobacillus ferrooxidans total RNA was prepared as previously reported for qRT-PCR analysis (Navarro et al., 2009). Primers tetHFw (TGCTGTTCCAATGGATTCAA) and tetHR1 (TGATACGCCGTTCCTTATCC) were used for *tetH* amplification and 16SFw (TGGTGCCTAGCGTACTGAGTG) and 16SR (CCGAAGGGCACTTCCGCA) for *A. ferrooxidans* 16S rRNA. Absolute copy numbers for *tetH* and 16S rRNA were determined by using standard curves obtained by serial dilutions of *A. ferrooxidans* genomic DNA. Copy numbers of *tetH* relative to 16S rRNA were determined at each OLC-incubation time from three independent experiments and the mean values and SD are shown.

PRECIPITATION OF EXTRACELLULAR PROTEINS AND THEIR IDENTIFICATION BY MASS SPECTROMETRY ANALYSIS

Acidithiobacillus ferrooxidans cells were separated from their growth medium (400 mL) by centrifugation at 5,000 × *g* at 4°C for 20 min. Proteins present in the filtered supernatants were precipitated by using the PRMM method (Caldwell and Lattemann, 2004) as applied to *A. ferrooxidans* cells (Pagliai and Jerez, 2009). Precipitated proteins were electrophoresed on a Tris/Glycine SDS polyacrylamide gel and stained with Coomassie Blue G-250. Bands of interest were excised manually from the gels and the proteins present in them were identified by MALDI peptide mass fingerprinting and MALDI–TOF/TOF MS analysis as described before (Varela et al., 2010). Possible subcellular localization of identified proteins was predicted by using the SubCell 1.0 server at Center for Biological Sequence Analysis, BioCentrum-DTU, The Technical University of Denmark (http://www.cbs.dtu.dk/services/SubCell/). Protein measurements were carried out by using Bradford's method (PIERCE, Rockford, IL, USA) and crystalline BSA as standard.

RESULTS

GROWTH OF *A. FERROOXIDANS* IN THIOSULFATE AS ENERGY SOURCE

As it has been previously shown (Hazeu et al., 1986) during thiosulfate oxidation by *A. ferrooxidans*, tetrathionate was accumulated in the culture medium, and in our experimental conditions it reached a maximum concentration of c.a. 5 mM (**Figure 2A**). The ratio between the rates of thiosulfate consumption and tetrathionate increase in the culture medium was c.a. 4:1. This ratio, and the stoichiometric relationship involved in tetrathionate formation by means of thiosulfate oxidation by TD, suggests that half of the tetrathionate formed from thiosulfate oxidation diffuses out of the cells and into the culture medium. Tetrathionate concentration

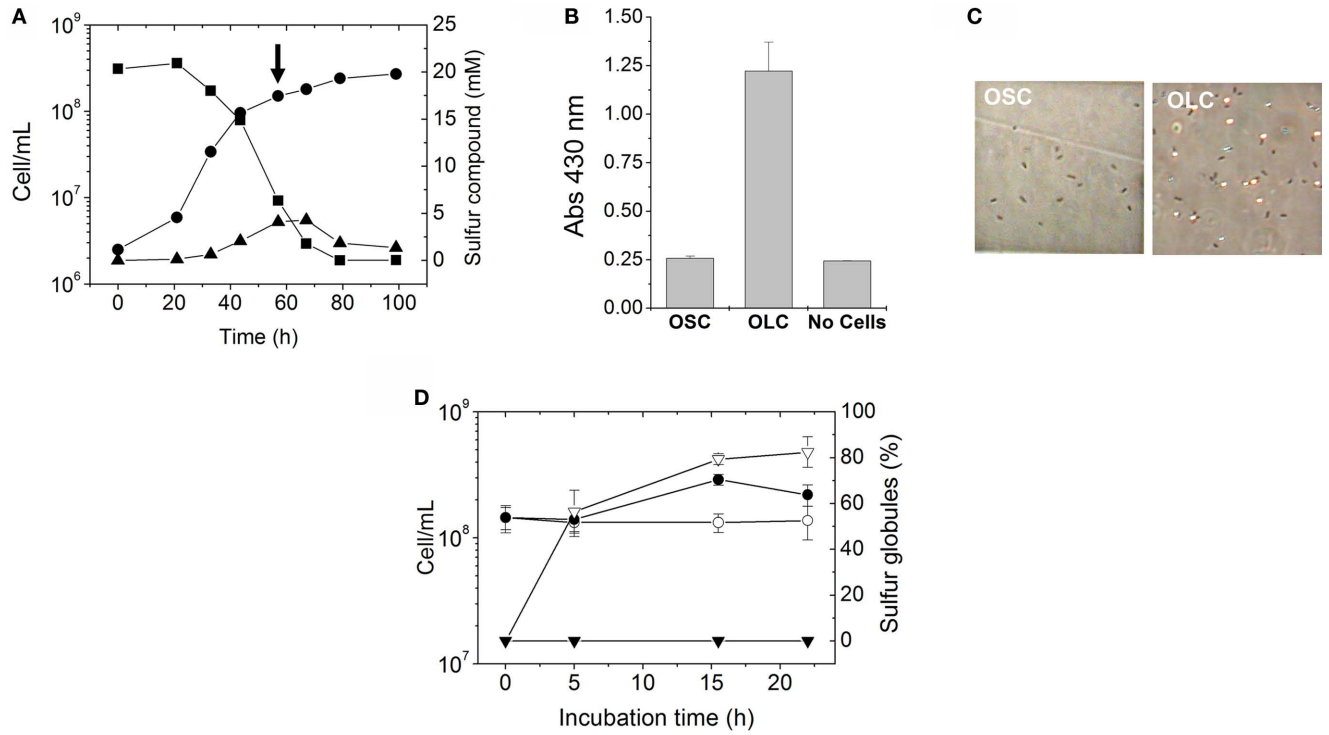

FIGURE 2 | Production of extracellular sulfur globules by *A. ferrooxidans* during incubation under oxygen-limiting conditions. (A) *A. ferrooxidans* was grown in thiosulfate under OSC and the changes in concentrations of thiosulfate (■) and tetrathionate (▲) during *A. ferrooxidans* cell growth (●) were determined. To study the effect of oxygen limitation, thiosulfate-grown *A. ferrooxidans* cultures were either shifted to OLC or kept under OSC at the point of the growth curve shown by an arrow. **(B)** Generation of elemental sulfur as detected by the increase in the absorbance at 430 nm in *A. ferrooxidans* cultures. Three *A. ferrooxidans* cultures were grown in thiosulfate until the late-exponential-phase. One culture was subjected for 16 h to OSC and another one to OLC. The third culture was filtered (0.22 µm-filter) and the medium obtained was incubated for 16 h under OLC and was used as the "No Cells" control. **(C)** Phase-contrast micrographies (600 × magnification) of *A. ferrooxidans* cells from OLC- and OSC-incubated cultures shown in **(B)**. **(D)** Cell growth of *A. ferrooxidans* cultures (●,○) and percentages of sulfur globules produced (▼,▽) during OSC- (●,▼) or OLC- (○,▽) incubations.

began to decrease only when thiosulfate was almost completely consumed (**Figure 2A**). Most likely, tetrathionate starts being oxidized by cells due to the lack of thiosulfate as an energy source.

EFFECT OF OXYGEN AVAILABILITY IN THIOSULFATE-GROWN *A. FERROOXIDANS* CULTURES

When mid to late-exponential-phase thiosulfate-grown *A. ferrooxidans* cultures were shifted to OLC, their media became white and their absorbance at 430 nm was significantly increased compared to OSC-incubated cultures (**Figure 2B**). The increment in absorbance at 430 nm suggests the production of elemental sulfur in OLC-incubated cultures. This change in absorbance was not observed when cells were removed by filtration before shifting the culture to OLC (**Figure 2B**), indicating that the increase in absorbance was not due to the chemical reactivity of the thiosulfate/tetrathionate mixture present in the culture medium when the OLC-incubation started, but rather to a cell-dependent phenomenon. Moreover, after 20 h incubation of *A. ferrooxidans* under OSC or OLC pH values of culture supernatants were 2.30 ± 0.51 and 3.23 ± 0.44, respectively, indicating that the increment in absorbance at 430 nm observed was not due to a low pH-dependent decomposition of thiosulfate. Inspection of cells under the phase-contrast microscope showed a massive production of extracellular globular-shaped refringent structures (sulfur globules) only in OLC-incubated cultures (**Figure 2C**). Cell growth and production of sulfur globules were both directly counted under the phase-contrast microscope at different times during OSC- or OLC-incubations. 50% of the total specimens (bacteria and sulfur globules) counted by phase-contrast microscopy corresponded to sulfur globules after incubating cells for 5 h under OLC. They reached a maximum of 80% after incubating for 15 h. On the other hand, production of sulfur globules was not observed at all in cultures incubated under OSC (**Figure 2D**).

EXTRACELLULAR *A. FERROOXIDANS* SULFUR GLOBULES CONTAIN ELEMENTAL SULFUR

The increase in absorbance at 430 nm observed in *A. ferrooxidans* cultures shifted to OLC (**Figure 2B**) suggests the production of elemental sulfur in the medium. To determine whether the extracellular globules produced by *A. ferrooxidans* contained elemental sulfur, *A. ferrooxidans* cells pelleted together with globules were extracted with acetone and sulfur was determined by cyanolysis. During incubation under OLC, the amount of sulfur extracted increased, whereas under OSC sulfur amounts remained unchanged (**Figure 3A**). Moreover, visual inspection of acetone-extracted *A. ferrooxidans* cells by phase-contrast microscopy showed that sulfur globules were completely extracted from OLC-incubated cultures

after acetone treatment (**Figure 3B**). These results confirm that the refringent structures produced during OLC-incubations corresponded to elemental sulfur-containing globules.

SULFUR GLOBULE PRODUCTION DEPENDS ON OXYGEN CONCENTRATION

To correlate extracellular sulfur globule production with the availability of oxygen, the concentration of oxygen dissolved in a thiosulfate-grown culture of *A. ferrooxidans* was determined by using a liquid-phase oxygraph. The absorbance at 430 nm of the culture incubated in the oxygraph-cell was recorded and used as an indicator of the production of sulfur globules. Oxygen initially dissolved in the culture medium dropped within the first 15 min of incubation, most likely due to its consumption by *A. ferrooxidans* cells. After the medium was depleted of oxygen absorbance at 430 nm begun to increase (**Figure 4**). Moreover, when oxygen concentration increased again (by opening the oxygraph-cell lid), a concomitant decrease in absorbance at 430 nm was obtained (**Figure 4**). This suggests that sulfur compounds accumulated during OLC-incubation were readily oxidized most likely by *A. ferrooxidans* cells once oxygen was restored.

ANALYSIS OF SULFUR COMPOUNDS OXIDATION DURING SULFUR GLOBULES PRODUCTION

To determine the mechanisms underlying extracellular sulfur globule production under OLC-incubations, concentrations of thiosulfate and tetrathionate in culture media, and enzymatic activities related to its oxidation (TD and TTH) under OLC- and OSC-incubations were measured. Thiosulfate was completely depleted from the culture medium after 25 h OSC-incubation (**Figure 5A**), almost certainly due to its consumption by the cells. Under OLC-incubation, thiosulfate concentration slightly increased within the first 5 h, and after that period it remained unchanged (**Figure 5A**). TD activity of cells incubated under OLC was c.a. six times lower than that of cells incubated under OSC (0.15 ± 0.06 and 0.99 ± 0.08 U mg protein^{-1}, respectively; **Figure 5C**). This result was expected since thiosulfate oxidation was not observed in the OLC-incubated culture and Northern-Blot analysis indicated the downregulation of both *doxDA1* and *doxDA2* genes in OLC-incubated cells (Beard and Jerez, results not shown). *doxDA1* and *doxDA2* coded in *A. ferrooxidans* ATCC 23270 genome are ortholog genes of *Acidianus ambivalens* thiosulfate:quinone oxidoreductase (TQO; Müller et al., 2004). On the other hand, tetrathionate concentration in the culture media decreased both in OSC- and OLC-incubated cultures (**Figure 5B**). Surprisingly, TTH activity found in OLC-cells was c.a. 25 times lower than the one in the OSC-incubated cells (0.007 ± 0.004 and 0.167 ± 0.05 U mg protein^{-1}, respectively; **Figure 5D**). To assess whether the decrease in TTH activity was due to a possible transcriptional regulation of *tetH* gene, its transcription was determined by qRT-PCR. Transcriptional levels of *tetH* were highly downregulated in *A. ferrooxidans* cells subjected to OLC-incubations during 5–20 h (**Figure 5E**). A set of housekeeping genes has been proposed for qRT-PCR transcriptome analysis in *A. ferrooxidans* (Nieto et al., 2009). However, none of those genes have been tested under the OSC/OLC-conditions used in this study. Although 16S rRNA transcript levels can vary due to growth conditions, we have normalized the qRT-PCR values by using 16S rRNA as previously reported (Vera et al., 2008; Navarro et al., 2009). The very low TTH activity and expression level of the TTH coding gene in OLC-incubated microorganisms suggest cells do not have enough TTH activity to account for either the decrease in extracellular tetrathionate concentration or the sulfur globule production observed. Since hydrolysis of tetrathionate by a TTH is proposed as the key step during biological formation of hydrophillic sulfur globules (Steudel, 2003), lack of TTH activity in OLC-incubated cells was unexpected and suggests the existence of a mechanism independent of cellular TTH activity for generation of sulfur globules by *A. ferrooxidans*.

TTH ACTIVITY IS PRESENT IN *A. FERROOXIDANS* CULTURE SUPERNATANTS

Due to the extracellular nature of sulfur globules produced by *A. ferrooxidans*, supernatant fractions from OSC- and OLC-incubated cultures were further investigated. To determine the low molecular weight thiol composition of supernatants from *A. ferrooxidans*

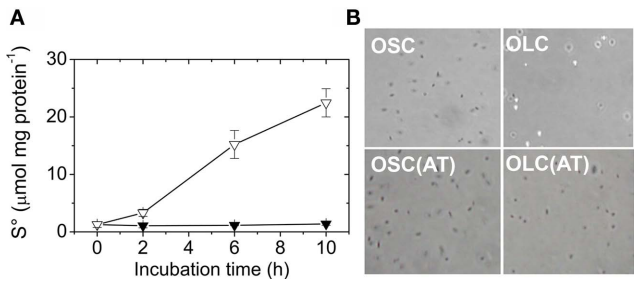

FIGURE 3 | Extracellular *A. ferrooxidans* deposits contain elemental sulfur. (A) Time course of elemental sulfur production by *A. ferrooxidans* cultures subjected to OSC- (▼) or OLC- (▽) incubations. Aliquots of *A. ferrooxidans* cultures were taken at the times indicated and cells and sulfur were sedimented by centrifugation. Sulfur was extracted from the pellets with acetone and determined by cyanolysis. **(B)** Phase-contrast micrographies of *A. ferrooxidans* cells (600 × magnification) after 10 h OLC- or OSC-incubation. Panels labeled AT correspond to cells obtained after resuspending acetone-treated pellets in DSMZ 71 medium (without thiosulfate).

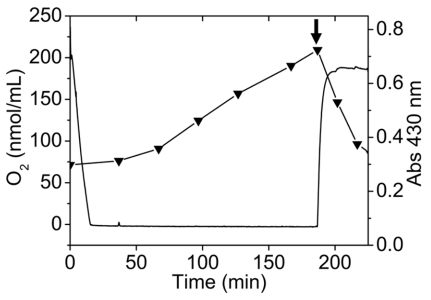

FIGURE 4 | Production of sulfur globules depend on oxygen concentration present in the culture medium. Oxygen concentration (continuous line) was determined by using a liquid-phase oxygraph and absorbance at 430 nm (▼) of aliquots taken at the indicated times was measured in a spectrophotometer. The oxygraph-cell was filled with 2.5 mL of a thiosulfate-grown *A. ferrooxidans* culture and OLC-incubation was started by closing the oxygraph-cell lid. OSC was obtained by removing the oxygraph-cell lid and leaving 1.0 mL of the *A. ferrooxidans* culture in the oxygraph-cell (shown by an arrow). Oxygraph stirrer was set at 100 RPM.

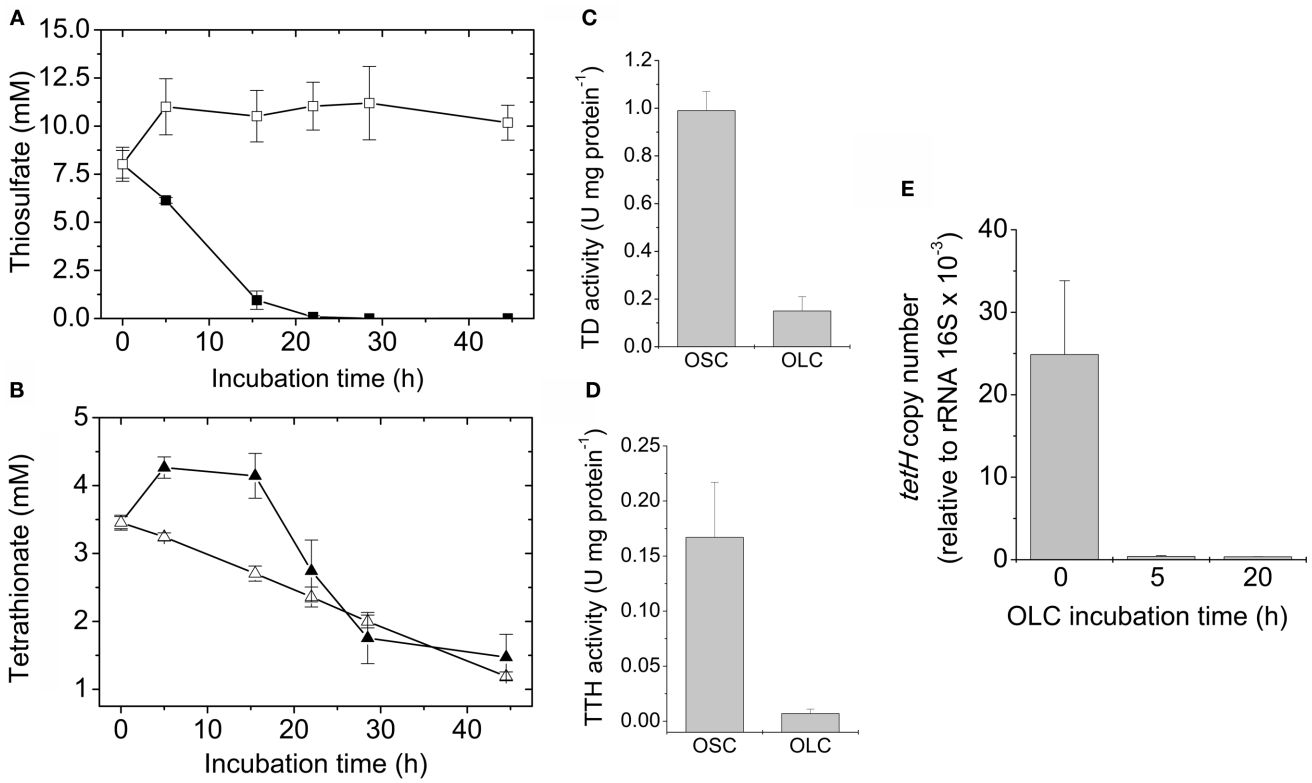

FIGURE 5 | Sulfur compounds oxidation during sulfur globule production. Changes in thiosulfate (■, □) **(A)** and tetrathionate (▲, △) **(B)** concentrations in the culture medium were determined during OSC- (filled symbols) or OLC- (open symbols) incubations. The corresponding TD **(C)** and TTH activities **(D)** of *A. ferrooxidans* cells subjected to 16 h OSC- or OLC-incubation conditions were also determined. **(E)** Determination of *tetH* mRNA copy numbers by qRT-PCR. For cDNA synthesis, 200 ng of total RNA obtained from *A. ferrooxidans* after 0, 5, and 20 h OLC-incubations were used. Copy numbers were expressed relative to 16S rRNA copies present in each sample.

cultures subjected to OLC-incubation, they were directly derivatized with monobromobimane and analyzed by HPLC. Unlike OSC culture supernatants, the OLC-incubated *A. ferrooxidans* supernatants showed the presence of sulfite (**Figure 6A**). During the incubation of *A. ferrooxidans* cultures under OLC sulfite accumulated in the supernatants (**Figure 6B**). Due to the oxygen requirement for sulfur-oxidizing enzymes from thiobacilli (Suzuki, 1994) it is not likely that sulfite arose from elemental sulfur oxidation under OLC-incubation. TTH activity was detected both in OSC- and OLC-incubated culture supernatants (**Figure 6C**). The proteins present in the growth medium of OLC-incubated cells were precipitated and analyzed by SDS-PAGE (**Figure 6D**). Two of the three main protein bands present in the SDS-PAGE could be correctly identified by MALDI–TOF/MS (**Table 1**).

Protein band No. 1 corresponded to TetH protein of *A. ferrooxidans* ATCC 53993, which is identical to TetH from *A. ferrooxidans* ATCC 23270 used in this study and actually corresponds to *A. ferrooxidans* TTH (Buonfiglio et al., 1999; Kanao et al., 2007). Although TetH has a predicted Sec-type signal peptide, to date its subcellular location is not clear.

Protein band No. 2 was identified as the phosphate-binding protein PstS2 of *A. ferrooxidans* ATCC 23270. This protein belongs to the phosphate starvation responding Pho regulon of this microorganism (Seeger and Jerez, 1993; Vera et al., 2003). Phosphate-binding proteins have also been reported in the medium of other bacteria (Tjalsma et al., 2004; Diaz et al., 2005; Meneses et al., 2010). Besides its obvious role in phosphate uptake, its possible relationship with extracellular TetH function in *A. ferrooxidans* cannot be anticipated at present.

The evidence presented here suggests that the TetH protein found in *A. ferrooxidans* culture supernatants corresponded to an active TTH and its activity would be related to extracellular sulfur globule production under OLC-incubations.

DISCUSSION

Thiosulfate is relatively unstable at pH values below 4.0. As the culture medium becomes acid due to thiosulfate oxidation, sulfite, and elemental sulfur formation is usually observed. For this reason it has been suggested that batch cultures are not adequate to study growth of thiobacilli on thiosulfate (Pronk et al., 1990). However, when washed *A. ferrooxidans* cells are used as inoculum at low cell densities (2.5×10^6 cells/mL), neither the precipitation of elemental sulfur nor the formation of sulfur globules take place in batch cultures. Therefore, we have used these conditions to study the effect of oxygen availability in thiosulfate-grown *A. ferrooxidans* cells.

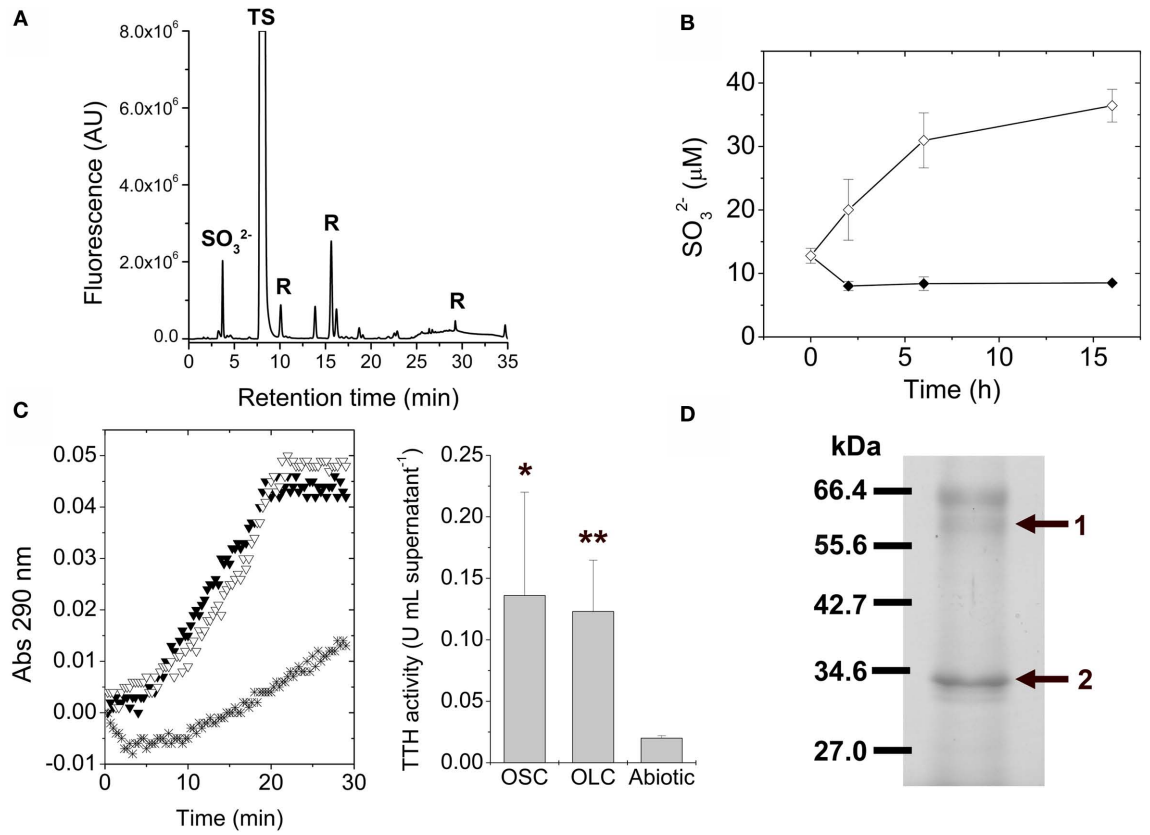

FIGURE 6 | Tetrathionate hydrolase activity is present in *A. ferrooxidans* culture supernatants. **(A)** Identification of low molecular weight thiols in *A. ferrooxidans* culture supernatants by HPLC. Thiols present in the culture supernatants from *A. ferrooxidans* subjected to 5 h OLC-incubation were derivatized with the monobromobimane reagent and separated by using HPLC. SO_3^{2-}, sulfite; TS, thiosulfate; R, reagent or water-derived peaks. **(B)** Changes in sulfite concentrations in thiosulfate-grown *A. ferrooxidans* culture supernatants during OSC- (♦) or OLC- (◊) incubations. Aliquots were taken from cultures at the indicated times, derivatized with monobromobimane reagent, and analyzed by HPLC. Sulfite concentrations were determined by integration of the area corresponding to the sulfite peak on each chromatogram. **(C)** (Left panel) Cells were separated from their growth medium by centrifugation and the filtered supernatants were used directly for TTH activity measurements. Spectrophotometer original traces [**(A)**, 290 nm] from representative continuous TTH activity assays of supernatants from thiosulfate-grown *A. ferrooxidans* cultures subjected to 16 h OSC-(▼) or OLC-(▽) incubations. The Abiotic control (*) corresponds to the tetrathionate-dependent increase in absorbance at 290 nm when sterile DSMZ 71 medium (without thiosulfate) was used instead of culture supernatants in the TTH assay. (Center panel), TTH activity (expressed as U mL supernatant^{-1}) from *A. ferrooxidans* culture supernatants. Statistically significative differences (Student's *t*-test; $n = 3$; *, p value < 0.05; **, p value < 0.005) are indicated. **(D)** Identification of TetH protein in supernatants from *A. ferrooxidans* cultures incubated under OLC. Proteins precipitated by the PRMM method were separated by SDS-PAGE and stained with Coomassie Blue G-250. The bands obtained were isolated from the gel and identified by mass spectrometry analysis. The protein band corresponding to the *tetH* gene product is indicated by an arrow.

Table 1 | Proteins present in OLC-incubated *A. ferrooxidans* growth media identified by MALDI–TOF/MS.

Band[a]	Protein	Description	Mascot score	Mascot *E*-value	Coverage (%)	MW (kDa)[b]	pI[b]	Predicted localization[c]
1	TetH	YP_002218499 pyrrolo-quinoline quinone (*A. ferrooxidans* ATCC 53993)	218	6.16e – 016	19	53.16	9.15	SIGNALP (sec-type signal peptide)
2	PstS2	YP_002426348 phosphate ABC transporter, periplasmic phosphate-binding protein PstS (*A. ferrooxidans* ATCC 23270)	718	6.6e – 66	45	37.9	9.21	SIGNALP (sec-type signal peptide)

[a] *Band numbers according to* ***Figure 6D***.
[b] *Deduced from aminoacidic sequences.*
[c] *Subcellular localization predicted by using the SubCell 1.0 server (http://www.cbs.dtu.dk/services/SubCell/).*

Cell densities did not change under OLC, indicating that cells did not grow or lyse during the conditions used in the experiments. Therefore, it is not likely that sulfur globules were released to the culture medium by a cell-lysis mechanism, as it has been proposed in *Thermoanaerobacterium sulfurigignens* JW/SL-NZ826^T (Lee et al., 2007). To assess whether the lack of oxygen affects in general the gene expression pattern in *A. ferrooxidans* during OLC-incubations, transcriptional levels of a group of genes related to stress response and other cellular processes were measured by using a DNA-microarray system as described before (Orell et al., 2010). Levels of transcripts of most *A. ferrooxidans* genes measured showed no significant differences. The only significant change observed in *A. ferrooxidans* cultures subjected to OLC-incubations was the downregulation of the *cydA* gene coding for a subunit of a *bd*-type terminal quinol-oxidase, suggesting that cells were actually responding rather specifically to changes in the availability of oxygen under the experimental set-up used (results not shown).

To date the subcellular location of TetH is not clear. It has been previously described as an outer membrane protein (Buonfiglio et al., 1999), a soluble and probably periplasmic protein (de Jong et al., 1997; Chi et al., 2007), and as a membrane-associated protein (Kanao et al., 2007). The gene coding for TetH contains a Sec-secretion signal (Kanao et al., 2007), strongly suggesting that it is a protein secreted into the periplasm (**Table 1**). The extracellular location of TetH reported here corresponds to a new finding and opens the question about the mechanism involved in its secretion from the periplasm into the growth medium. The sequence of the N-terminal end of the protein was not obtained during its identification by mass spectrometry in our studies. Therefore the cleavage site of the Sec-type signal peptide could not be confirmed in the extracellular TetH. Nevertheless, bioinformatic analyses have shown that *A. ferrooxidans* ATCC 23270 genome contains genes coding for six of the eight secretion systems known in bacteria (Pagliai and Jerez, 2009), several of which would be capable of secreting proteins by using the Sec system.

The current model for thiosulfate oxidation by the S4I-pathway (Pronk et al., 1990; Ghosh and Dam, 2009) explains intracellular sulfur globule production as some of the disulfane monosulfonic acid derived from periplasmic tetrathionate oxidation can follow the "higher polythionates pathway" that leads to the formation of intracellular sulfur deposits (Hazeu et al., 1988; **Figure 7**). However, this model does not explain the deposition of extracellular sulfur by *A. ferrooxidans* shown in this report. Since TTH activity was found in the extracellular medium of both OSC- and OLC-conditions, sulfur deposition was expected in both kinds of cultures. However, sulfur globule formation was seen only under OLC-conditions. The extracellular TTH activity could account for tetrathionate disappearance from the growth medium. The concomitant extracellular sulfur globule production in OLC-incubated *A. ferrooxidans* cells could be explained by the negligible periplasmic TD and TTH activities. Under these conditions, the only reaction that could take place is the extracellular hydrolysis of tetrathionate (**Figure 7**). An additional possible explanation for the lack of sulfur globules in OSC-incubated cells is that sulfur is indeed produced by extracellular TTH but is followed by its immediate oxidation by the cells.

To understand the significance of sulfur globule generation under OLC-incubations, some issues regarding enzymatic activities as well as some physiological considerations must be taken into account. The lack of TD activity in OLC-incubated cells is probably due to the fact that in *A. ferrooxidans* this activity should be directly coupled to molecular oxygen reduction by a terminal oxidase, as it has been shown in *A. ambivalens* (Müller et al., 2004). *A. ferrooxidans* is a facultative anaerobe bacterium and can use ferric iron as an electron acceptor during anaerobic oxidation of elemental sulfur (Pronk et al., 1992). Moreover, it was recently reported that *A. ferrooxidans* TTH has ferric iron reductase activity (Sugio et al., 2009). Although ferric iron may act as an alternative electron acceptor in anoxygenic tetrathionate oxidation, the physiological electron acceptors for this reaction are unknown. Once *A. ferrooxidans* cells switch to anaerobic metabolism, elemental sulfur stored into sulfur globules may be further oxidized by means of ferric iron respiration.

Our preliminary observations indicate that TetH protein is also present in supernatants obtained from elemental sulfur and pyrite-grown *A. ferrooxidans* cultures, suggesting that extracellular TTH activity may play a role during elemental sulfur oxidation and bioleaching of sulfide ores. In this regard, it is noteworthy that during pyrite oxidation in acidic environments and in excess ferric iron, thiosulfate is formed as the key intermediary (Schippers et al., 1996). The rate of chemical oxidation of thiosulfate is several orders of magnitude faster than that for tetrathionate oxidation. Therefore, tetrathionate can persist in the environment and may be metabolized by sulfur-oxidizing microorganisms (Druschel et al., 2003). This gives a geochemical relevance to the biochemical pathways related to tetrathionate oxidation. Interestingly, the production of colloidal sulfur particles within *A. ferrooxidans* capsule was observed during incubation of cells grown on synthetic pyrite films (Rojas-Chapana et al., 1996).

To the best of our knowledge, the present report is the first evidence for an enzymatic activity existing in *A. ferrooxidans* culture supernatants. Furthermore, this finding suggests a mechanism for extracellular sulfur globule deposition in a microorganism that does not use the branched-PSO pathway for thiosulfate oxidation. In addition, a physiological role for *A. ferrooxidans* extracellular sulfur globule production is proposed as a response allowing cells to overcome a

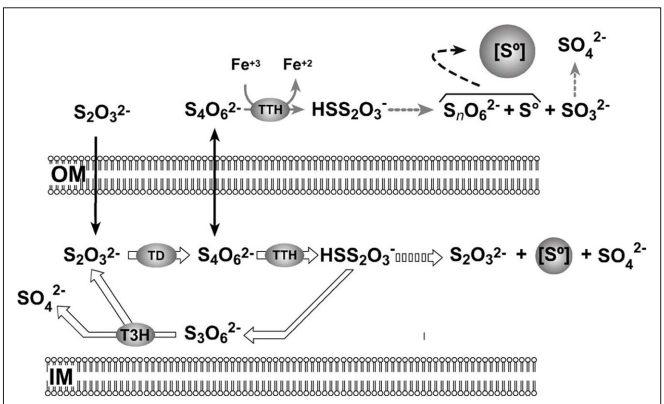

FIGURE 7 | Proposed model for *A. ferrooxidans* extracellular sulfur globules production. OM, outer membrane; PE, periplasmic space; IM, inner membrane; [S°], sulfur globule; TD, thiosulfate dehydrogenase; TTH, tetrathionate hydrolase; T3H, trithionate hydrolase. Diffusion of substrates across the outer membrane is shown by black arrows. Continuous arrows show enzymatic steps and broken arrows show non-enzymatic steps. Reactions that do not proceed in OLC-incubated cells are indicated by thick empty arrows. See text for details.

momentary decrease in oxygen availability, probably as an early step during the metabolic switch to anaerobic lifestyle. Further investigation using non-invasive methods for *in situ* analysis of sulfur globules (such as sulfur K-edge XANES or Laser Raman spectroscopy) will be needed in order to unveil the exact chemical nature of the sulfur species generated by *A. ferrooxidans* in its extracellular sulfur globules and whether they are different from the composition previously reported for *A. ferrooxidans* globules (Prange et al., 2002). In this regard, a recent study on sulfur speciation using sulfur K-edge XANES shows that the extracellular globules from thiosulfate-grown *A. ferrooxidans* are composed mainly of elemental sulfur rings (He et al., 2010), which is consistent with the results reported here.

CONCLUSION

Acidithiobacillus ferrooxidans produce extracellular sulfur globules when thiosulfate-grown cultures are shifted to OLC. The finding of TetH protein in the *A. ferrooxidans* growth medium represent a novel issue regarding both the subcellular location and the function of this enzyme, suggesting its involvement in an extracellular sulfur globule deposition mechanism in a microorganism that does not use the branched-PSO pathway for RISCs oxidation. Although demonstration of the mechanism proposed here will require further studies with purified TTH, we believe it may have a physiological as well as geochemical relevance during sulfur compounds cycling in microaerophilic metal sulfide rich environments, in which *A. ferrooxidans* can be normally found.

ACKNOWLEDGMENTS

This work was supported by ICM-P05-001-F project and a doctoral fellowship from CONICYT to Simón Beard. We thank A. Hokeer for her help with the English language and S. Rubio and F. Perez (Laboratory of Vegetal Biochemistry, Faculty of Sciences, University of Chile) for their support in the oxygraph measurements and A. Banderas for encouraging us to start this work.

REFERENCES

Buonfiglio, V., Polidoro, M., Soyer, F., Valenti, P., and Shively, J. (1999). A novel gene encoding a sulfur-regulated outer membrane protein in *Thiobacillus ferrooxidans*. *J. Biotechnol.* 72, 85–93.

Caldwell, R. B., and Lattemann, C. T. (2004). Simple and reliable method to precipitate proteins from bacterial culture supernatant. *Appl. Environ. Microbiol.* 70, 610–612.

Chi, A., Valenzuela, L., Beard, S., Mackey, A. J., Shabanowitz, J., Hunt, D. F., and Jerez, C. A. (2007). Periplasmic proteins of the extremophile *Acidithiobacillus ferrooxidans*: a high throughput proteomics analysis. *Mol. Cell. Proteomics* 6, 2239–2251.

de Jong, G. A. H., Hazeu, W., Bos, P., and Kuenen, J. G. (1997). Polythionate degradation by tetrathionate hydrolase of *Thiobacillus ferrooxidans*. *Microbiology* 143, 499–504.

Diaz, M., Esteban, A., Fernandez-Abalos, J. M., and Santamaria, R. I. (2005). The high-affinity phosphate-binding protein PstS is accumulated under high fructose concentrations and mutation of the corresponding gene affects differentiation in *Streptomyces lividans*. *Microbiology* 151, 2583–2592.

Druschel, G. K., Hamers, R. J., and Banfield, J. F. (2003). Kinetics and mechanism of polythionate oxidation to sulfate at low pH by O2 and Fe^{3+}. *Geochim. Cosmochim. Acta* 67, 4457–4469.

Friedrich, C. G., Bardischewsky, F., Rother, D., Quentmeier, A., and Fischer, J. (2005). Prokaryotic sulfur oxidation. *Curr. Opin. Microbiol.* 8, 253–259.

George, G. N., Gnida, M., Bazylinski, D. A., Prince, R. C., and Pickering, I. J. (2008). X-ray absorption spectroscopy as a probe of microbial sulfur biochemistry: the nature of bacterial sulfur globules revisited. *J. Bacteriol.* 190, 6376–6383.

Ghosh, W., and Dam, B. (2009). Biochemistry and molecular biology of lithotrophic sulfur oxidation by taxonomically and ecologically diverse bacteria and archaea. *FEMS Microbiol. Rev.* 33, 999–1043.

Grimm, F., Franz, B., and Dahl, C. (2008). "Thiosulfate and sulfur oxidation in purple sulfur bacteria," in *Microbial Sulfur Metabolism*, eds C. Dahl and C. G. Friedrich (Berlin: Springer), 101–116.

Hazeu, W., Batenburg-van der Vegte, W. H., Bos, P., van der Pas, R. K., and Kuenen, J. G. (1988). The production and utilization of intermediary elemental sulfur during the oxidation of reduced sulfur compounds by *Thiobacillus ferrooxidans*. *Arch. Microbiol.* 150, 574–579.

Hazeu, W., Bijleveld, W., Grotenhuis, J. T. C., Kakes, E., and Kuenen, J. G. (1986). Kinetics and energetics of reduced sulfur oxidation by chemostat cultures of *Thiobacillus ferrooxidans*. *Antonie Van Leeuwenhoek* 52, 507–518.

He, H., Xia, J.-L., Jiang, H.-C., Yan, Y., Liang, C.-L., Ma, C.-Y., Zheng, L., Zhao, Y.-D., and Qiu, G.-Z. (2010). Sulfur species investigation in extra- and intracellular sulfur globules of *Acidithiobacillus ferrooxidans* and *Acidithiobacillus caldus*. *Geomicrobiol. J.* 27, 707–713.

Kanao, T., Kamimura, K., and Sugio, T. (2007). Identification of a gene encoding a tetrathionate hydrolase in *Acidithiobacillus ferrooxidans*. *J. Biotechnol.* 132, 16–22.

Kelly, D. P., Chambers, L. A., and Trudinger, P. A. (1969). Cyanolysis and spectrophotometric estimation of trithionate in mixture with thiosulfate and tetrathionate. *Anal. Chem.* 41, 898–902.

Kelly, D. P., Shergill, J. K., Lu, W. P., and Wood, A. P. (1997). Oxidative metabolism of inorganic sulfur compounds by bacteria. *Antonie Van Leeuwenhoek* 71, 95–107.

Kelly, D. P., and Wood, A. P. (1998). "Microbes of the sulfur cycle," in *Techniques in Microbial Ecology*, eds R. S. Burlage, R. Atlas, D. Stahl, G. Geesey, and G. Sayler (New York: Oxford University Press), 31–57.

Kletzin, A. (1989). Coupled enzymatic production of sulfite, thiosulfate, and hydrogen sulfide from sulfur: purification and properties of a sulfur oxygenase reductase from the facultatively anaerobic archaebacterium *Desulfurolobus ambivalens*. *J. Bacteriol.* 171, 1638–1643.

Lee, Y. J., Prange, A., Lichtenberg, H., Rohde, M., Dashti, M., and Wiegel, J. (2007). In situ analysis of sulfur species in sulfur globules produced from thiosulfate by *Thermoanaerobacter sulfurigignens* and *Thermoanaerobacterium thermosulfurigenes*. *J. Bacteriol.* 189, 7525–7529.

Meneses, N., Mendoza-Hernandez, G., and Encarnacion, S. (2010). The extracellular proteome of *Rhizobium etli* CE3 in exponential and stationary growth phase. *Proteome Sci.* 8, 51.

Müller, F. H., Bandeiras, T. M., Urich, T., Teixeira, M., Gomes, C. M., and Kletzin, A. (2004). Coupling of the pathway of sulphur oxidation to dioxygen reduction: characterization of a novel membrane-bound thiosulphate:quinone oxidoreductase. *Mol. Microbiol.* 53, 1147–1160.

Navarro, C. A., Orellana, L. H., Mauriaca, C., and Jerez, C. A. (2009). Transcriptional and functional studies of *Acidithiobacillus ferrooxidans* genes related to survival in the presence of copper. *Appl. Environ. Microbiol.* 75, 6102–6109.

Nieto, P. A., Covarrubias, P. C., Jedlicki, E., Holmes, D. S., and Quatrini, R. (2009). Selection and evaluation of reference genes for improved interrogation of microbial transcriptomes: case study with the extremophile *Acidithiobacillus ferrooxidans*. *BMC Mol. Biol.* 10, 63. doi: 10.1186/1471-2199-10-63

Olson, G. J., Brierley, J. A., and Brierley, C. L. (2003). Bioleaching review part B: progress in bioleaching: applications of microbial processes by the minerals industries. *Appl. Microbiol. Biotechnol.* 63, 249–257.

Orell, A., Navarro, C. A., Arancibia, R., Mobarec, J. C., and Jerez, C. A. (2010). Life in blue: copper resistance mechanisms of bacteria and archaea used in industrial biomining of minerals. *Biotechnol. Adv.* 28, 839–848.

Pagliai, F. A., and Jerez, C. A. (2009). The secretome of the extremophilic *Acidithiobacillus ferrooxidans* ATCC 23270. *Adv. Mat. Res.* 71–73, 183–186.

Prange, A., Chauvistre, R., Modrow, H., Hormes, J., Truper, H. G., and Dahl, C. (2002). Quantitative speciation of sulfur in bacterial sulfur globules: X-ray absorption spectroscopy reveals at least three different species of sulfur. *Microbiology* 148, 267–276.

Pronk, J. T., de Bruyn, J. C., Bos, P., and Kuenen, J. G. (1992). Anaerobic growth of *Thiobacillus ferrooxidans*. *Appl. Environ. Microbiol.* 58, 2227–2230.

Pronk, J. T., Meulenberg, R., Hazeu, Z., Bos, P., and Kuenen, J. G. (1990). Oxidation of inorganic sulphur compounds by acidophilic thiobacilli. *FEMS Microbiol. Rev.* 75, 293–306.

Rawlings, D. E. (2005). Characteristics and adaptability of iron- and

sulfur-oxidizing microorganisms used for the recovery of metals from minerals and their concentrates. *Microb. Cell Fact.* 4, 13.

Rethmeier, J., Rabenstein, A., Langer, M., and Fischer, U. (1997). Detection of traces of oxidized and reduced sulfur compounds in small samples by combination of different high-performance liquid chromatography methods. *J. Chromatogr. A* 760, 295–302.

Rohwerder, T., and Sand, W. (2003). The sulfane sulfur of persulfides is the actual substrate of the sulfur-oxidizing enzymes from *Acidithiobacillus* and *Acidiphilium* spp. *Microbiology* 149, 1699–1710.

Rojas-Chapana, J. A., Giersig, M., and Tributsch, H. (1996). The path of sulfur during the bio-oxidation of pyrite by *Thiobacillus ferrooxidans*. *Fuel* 75, 923–930.

Schippers, A., Jozsa, P., and Sand, W. (1996). Sulfur chemistry in bacterial leaching of pyrite. *Appl. Environ. Microbiol.* 62, 3424–3431.

Seeger, M., and Jerez, C. A. (1993). Phosphate-starvation induced changes in *Thiobacillus ferrooxidans*. *FEMS Microbiol. Lett.* 108, 35–41.

Steudel, R. (2003). Aqueus sulfur sols. *Top. Curr. Chem.* 230, 153–166.

Steudel, R., Holdt, G., Göbel, T., and Hazeu, W. (1987). Chromatographic separation of higher polythionates SnO62- (n = 3…22) and their detection in cultures of *Thiobacillus ferrooxidans*: molecular composition of bacterial sulfur secretion. *Angew. Chem. Int. Ed. Engl.* 26, 151–153.

Sugio, T., Taha, T. M., and Takeuchi, F. (2009). Ferrous iron production mediated by tetrathionate hydrolase in tetrathionate-, sulfur-, and iron-grown *Acidithiobacillus ferrooxidans* ATCC 23270 cells. *Biosci. Biotechnol. Biochem.* 73, 1381–1386.

Suzuki, I. (1994). Sulfur-oxydazing enzymes. *Meth. Enzymol.* 243, 455–462.

Tjalsma, H., Antelmann, H., Jongbloed, J. D., Braun, P. G., Darmon, E., Dorenbos, R., Dubois, J. Y., Westers, H., Zanen, G., Quax, W. J., Kuipers, O. P., Bron, S., Hecker, M., and van Dijl, J. M.. (2004). Proteomics of protein secretion by *Bacillus subtilis*: separating the "secrets" of the secretome. *Microbiol. Mol. Biol. Rev.* 68, 207–233.

Varela, C., Mauriaca, C., Paradela, A., Albar, J. P., Jerez, C. A., and Chávez, F. P. (2010). New structural and functional defects in polyphosphate deficient bacteria: a cellular and proteomic study. *BMC Microbiol.* 10, 7. doi: 10.1186/1471-2180-10-7

Vera, M., Guiliani, N., and Jerez, C. A. (2003). Proteomic and genomic analysis of the phosphate starvation response of *Acidithiobacillus ferrooxidans*. *Hydrometallurgy* 71, 125–132.

Vera, M., Pagliai, F., Guiliani, N., and Jerez, C. A. (2008). The chemolithoautotroph *Acidithiobacillus ferrooxidans* can survive under phosphate-limiting conditions by expressing a C-P lyase operon that allows it to grow on phosphonates. *Appl. Environ. Microbiol.* 74, 1829–1835.

Conflict of Interest Statement: The authors declare that the research was conducted in the absence of any commercial or financial relationships that could be construed as a potential conflict of interest.

Received: 05 January 2011; accepted: 04 April 2011; published online: 18 April 2011.
Citation: Beard S, Paradela A, Albar JP and Jerez CA (2011) Growth of Acidithiobacillus ferrooxidans ATCC 23270 in thiosulfate under oxygen-limiting conditions generates extracellular sulfur globules by means of a secreted tetrathionate hydrolase. Front. Microbio. ***2****:79. doi: 10.3389/fmicb.2011.00079*
This article was submitted to Frontiers in Microbial Physiology and Metabolism, a specialty of Frontiers in Microbiology.

frontiers in
MICROBIOLOGY

ORIGINAL RESEARCH ARTICLE
published: 10 May 2011
doi: 10.3389/fmicb.2011.00104

Mycobacteria isolated from Angkor monument sandstones grow chemolithoautotrophically by oxidizing elemental sulfur

Asako Kusumi, Xian Shu Li† and Yoko Katayama*

Graduate School of Agriculture, Tokyo University of Agriculture and Technology, Tokyo, Japan

Edited by:
Thomas E. Hanson, University of Delaware, USA

Reviewed by:
Masaharu Ishii, University of Tokyo, Japan
Koji Mori, National Institute of Technology and Evaluation, Japan

***Correspondence:**
Yoko Katayama, Graduate School of Agriculture, Tokyo University of Agriculture and Technology, 3-5-8 Saiwai-cho, Fuchu-shi, Tokyo 183-8509, Japan.
e-mail: katayama@cc.tuat.ac.jp

†Present address:
Xian Shu Li, Division of Environmental Biotechnology, Fujimix Co., Ltd., 4-44-1 Kohoku-cho, Minato-ku, Nagoya-shi, Aichi 455-0067, Japan.

To characterize sulfate-producing microorganisms from the deteriorated sandstones of Angkor monuments in Cambodia, strains of *Mycobacterium* spp. were isolated from most probable number-positive cultures. All five strains isolated were able to use both elemental sulfur (S^0) for chemolithoautotrophic growth and organic substances for chemoorganoheterotrophic growth. Results of phylogenetic and phenotypic analyses indicated that all five isolates were rapid growers of the genus *Mycobacterium* and were most similar to *Mycobacterium cosmeticum* and *Mycobacterium pallens*. Chemolithoautotrophic growth was further examined in the representative strain THI503. When grown in mineral salts medium, strain THI503 oxidized S^0 to thiosulfate and sulfate; oxidation was accompanied by a decrease in the pH of the medium from 4.7 to 3.6. The link between sulfur oxidation and energy metabolism was confirmed by an increase in ATP. Fluorescence microscopy of DAPI-stained cells revealed that strain THI503 adheres to and proliferates on the surface of sulfur particles. The flexible metabolic ability of facultative chemolithoautotrophs enables their survival in nutrient-limited sandstone environments.

Keywords: facultative sulfur-oxidizing bacteria, *Mycobacterium*, biodeterioration, Angkor monuments

INTRODUCTION

Many stone monuments suffer from various kinds of degradation; biodeterioration caused by algae, cyanobacteria, bacteria, archaea, fungi, and lichens is among the most destructive (Warscheid and Braams, 2000; Scheerer et al., 2009). The ancient structures of Angkor, Cambodia, one of the most famous cultural heritage sites in the world are suffering from serious biodeterioration. For example, the Bayon temple, known for its intricately carved bas-reliefs, are being lost due to exfoliation and the formation of biofilms, which are microbial layers of various colors formed on the stone surface. Exfoliate weathering where sandstone flakes off in large, flat pieces, is also damaging historical cathedrals and churches in Europe (Hirsch et al., 1995).

Sulfur-oxidizing bacteria that excrete sulfuric acid are the dominant group of microorganisms involved in exfoliate weathering of sandstone at the Angkor site (Pochon and Jaton, 1967). However, sulfur-oxidizing bacteria have not been detected on the historic monuments in northern Europe. Therefore, they are considered to play a major role in stone decay only under warm and wet conditions (Warscheid and Braams, 2000), such as in Southeast Asia. The Angkor site has a tropical climate with high humidity. The density of sulfur-oxidizing microorganisms at Angkor, estimated annually using the most probable number (MPN) method, ranged from 10^1 to 10^5 MPN g^{-1} of deteriorated stone sample over a 10-year period. This data indicated their possible involvement of sulfur-oxidizing microorganisms in the deterioration of sandstone in this area (Li et al., 2008).

Sulfur-oxidizing fungal strains, including *Fusarium solani* strain THIF01, have been isolated from the MPN-positive cultures inoculated with the deteriorated sandstone collected at Angkor monuments. Strain THIF01 exhibited both chemolithoautotrophic sulfur-oxidizing activity and chemoorganoheterotrophic growth using organic substances (Li et al., 2010). Strain THIF01 was able to degrade carbonyl sulfide (COS), the most abundant sulfur compound in the atmosphere, suggesting that ambient COS could provide a source of sulfur for fungi colonizing on stone surfaces. Thus, COS may also be a source of sulfur for sulfur-oxidizing bacteria.

Sulfur-oxidizing ability is a characteristic of many phylogenetically diverse bacteria, including members of the phyla *Aquificae*, *Chlorobi*, *Proteobacteria*, and *Firmicutes* (Friedrich et al., 2001). Knowledge of this diversity continues to expand. For example, chemolithoautotrophic thiosulfate-oxidizing bacteria that were isolated from rhizosphere soils were identified as belonging to five genera not previously known to be sulfur-oxidizers (Anandham et al., 2008). Furthermore, the well-known soil bacterium *Bradyrhizobium japonicum* strain USDA110 recently demonstrated the ability to grow chemolithoautotrophically, using thiosulfate as an electron donor (Masuda et al., 2010). Thus, the genes required for sulfur-oxidizing ability may occur in bacteria and fungi that are not currently known to be sulfur-oxidizing microorganisms.

In the present study, five strains of sulfur-oxidizing bacteria of the genus *Mycobacterium* (phylum *Actinobacteria*) were isolated from MPN-positive cultures inoculated with samples from Angkor monuments. All five isolates were able to grow both chemolithoautotrophically using elemental sulfur (S^0) and chemoorganoheterotrophically using organic substances. Autotrophic growth with hydrogen (Lukins and Foster, 1963; Park and Decicco, 1974) and the ability to use either methanol or carbon monoxide as a sole source of carbon and energy has been reported for several mycobacteria (Park et al., 2003). Structural genes encoding a novel

form of ribulose 1,5-bisphosphate carboxylase/oxygenase were identified in *Mycobacterium* strain JC1 (Park et al., 2009). The role of assimilatory sulfur metabolism in the virulence, antibiotic resistance, and anti-oxidant defense of pathogenic *Mycobacterium* spp. has been examined (Schelle and Bertozzi, 2006). However, this is the first study to suggest a link between sulfur oxidation, energy production, and chemolithoautotrophic growth in the mycobacteria. The results have important implications for the role of sulfur-oxidizing bacteria in the deterioration of sandstone in Angkor site.

MATERIALS AND METHODS

SAMPLING OF DETERIORATED SANDSTONE

Sandstone samples were collected from deteriorated walls and near-ground sections of pillars at Angkor Wat, Bayon, and Phnom Krom temples, Angkor, Cambodia during August 2003. Details of the sampling sites and the densities of sulfur-oxidizing microorganisms, enumerated by the MPN method, were previously reported (Li et al., 2008).

ISOLATION OF SULFUR-OXIDIZING BACTERIA

Sulfur-oxidizing bacteria were isolated from MPN-positive cultures, grown in a liquid WS5 medium (3.0 g L^{-1} KH_2PO_4, 0.2 g L^{-1} $(NH_4)_2SO_4$, 0.5 g L^{-1} $MgSO_4$ $7H_2O$, 0.01 g L^{-1} $FeSO_4$ $7H_2O$, 0.25 g L^{-1} $CaCl_2$ $2H_2O$, 10 g L^{-1} S^0, pH 5.0; Li et al., 2008). Oxidation of S^0 was monitored by measuring the decrease in pH of the culture medium, due to the production of sulfuric acid, with a pH meter (Twin pH, Type B-212, Horiba, Kyoto, Japan). Sulfur-oxidizing bacteria from the most dilute MPN-positive cultures were isolated on agar plates of WS5 medium (Li et al., 2010) by serial streaking, and the colonies were then transferred to agar plates of PYG medium [2.0 g L^{-1} Polypepton (Nihon Pharmaceutical, Tokyo, Japan), 1.0 g L^{-1} Bacto yeast extract (Difco Laboratories, Detroit, MI, USA), 0.5 g L^{-1} glucose, pH 7.2] to which 15 g L^{-1} of Bacto agar (Difco Laboratories) was supplemented.

MORPHOLOGICAL AND PHYSIOLOGICAL CHARACTERIZATION

Morphological characteristics of the cultured bacteria were observed after Gram-staining. Catalase and oxidase activities were determined for all isolates. Catalase activity was tested in the presence of 3% hydrogen peroxide and oxidase activity was determined by a Pourmedia oxidase test (Eiken Chemical, Tokyo, Japan). To observe growth of strain THI503, cells were grown for 9 day in liquid medium of WS5 at 30°C with reciprocal shaking at 120 rpm, in the dark. The cells were stained with 4,6-diamidino-2-phenylindole (DAPI), and microphotographs were taken by single z-stack steps, using a BZ-8000 fluorescence microscope (KEYENCE, Osaka, Japan).

PHYLOGENETIC IDENTIFICATION

For phylogenetic analysis, isolates were cultured for 3 day in liquid PYG medium at 30°C with reciprocal shaking at 120 rpm, and genomic DNA was isolated from the harvested cells according to the procedure described by Saito and Miura (1963). The DNA concentration was determined using a NanoDrop ND-1000 spectrophotometer (NanoDrop Technologies, Wilmington, DE, USA). The 16S rRNA gene was amplified with primers 27F (5′-AGAGTTTGATCCTGGCTCAG-3′) and 1525R (5′-AAAGGAGGTGATCCAGCC-3′; Lane, 1991), and then sequenced using a 3130x genetic analyzer (Applied Biosystems, CA, USA) as previously described (Li et al., 2010). Sequence data were compiled with the GENETYX-MAC/ATSQ program version 4.2.1 (GENETYX Corporation, Tokyo, Japan) and compared with sequences in the GenBank database using BLAST version 2.2.24 (Altschul et al., 1990). The data were then analyzed using the Clustal W Program version 1.83 (Thompson et al., 1994) with Kimura's (1980) distance method. A multiple sequence alignment was performed, and bootstrapping analysis with MEGA version 4 (Tamura et al., 2007) was used to generate a neighbor-joining phylogenetic tree (Felsenstein, 1985), which was viewed with MEGA. The 16S rRNA gene sequences obtained have been deposited in the DNA Data Bank of Japan (DDBJ) under the following accession numbers: AB605019 for strain THI501, AB605020 for strain THI502, AB605021 for strain THI503, AB605022 for strain THI504, and AB605023 for strain THI505.

OXIDATION OF S^0 BY STRAIN THI503

Oxidation of S^0 was examined by measuring concentrations of thiosulfate and sulfate ions, and the decrease of medium pH in sulfate-free WS5 (WS5-S) medium (Li et al., 2010). The sulfate salts in WS5 medium were replaced with chloride salts, and the production of sulfuric acid was measured. Strain THI503 was pre-incubated for 7 day in three 50-mL conical polypropylene tubes, each containing 15 mL of WS5-S medium, with reciprocal shaking at 120 rpm, at 30°C in the dark. The contents of the three tubes were then combined, and three 225-mL polypropylene conical tubes containing 50 mL of WS5-S medium were each inoculated with 5 mL of the pre-incubation culture. The tubes were incubated at 30°C with reciprocal shaking at 120 rpm in the dark. Medium that was not inoculated, and medium with strain THI503 but no S^0, served as negative controls. pH and concentrations of thiosulfate and sulfate ions in the medium were measured periodically. Thiosulfate and sulfate concentrations were measured using an ion chromatograph (Model 861 Advanced Compact IC, Metrohm, Switzerland) as previously reported (Li et al., 2010). All experiments were done in triplicate.

EXTRACTION AND MEASUREMENT OF ATP

To evaluate bacterial growth, ATP was measured by the bioluminescence method (Stanley and Williams, 1969). Strain THI503 was cultured as described in section Oxidation of S^0 by strain THI503 except for using WS5 medium. ATP was extracted as reported (Rakotonirainy et al., 2003) and assayed using ATP assay mix (FLAAM, Sigma-Aldrich, MO, USA) and a LUMI-COUNTER 700 (Microtec, Chiba, Japan) at room temperature. ATP disodium salt hydrate (FLAAS, Sigma-Aldrich, MO, USA) was used to prepare the standard curve.

DEGRADATION OF COS BY STRAIN THI503

Degradation of COS by strain THI503 was measured according to the procedure described by Kato et al. (2008). Strain THI503 was pre-incubated for 3 day in a test tube containing 10 mL of PYG medium, with reciprocal shaking at 120 rpm at 30°C in the dark. The pre-culture was then added to a 500-mL Sakaguchi flask containing 100 mL of PYG medium and incubated for 24 h.

Cells were collected by centrifugation at 5,000 × *g* for 15 min, and then rinsed three times with autoclaved 25 mM phosphate buffer (PB, pH 7.0). The aqueous phase was discarded, and fresh PB was added to prepare the cell suspension. Volumes of 10 mL were dispensed into Pyrex test tubes (180 mm × 18 mm), which were sealed with butyl rubber caps. We then added 11.5 μL 10.5% COS gas with N_2 as the balance gas (Nissan Tanaka, Saitama, Japan) to headspace to make a final COS mixing ratio of 25 parts per million by volume (ppmv). As a control, 10 mL of sterile PB was dispensed into test tubes. A gas-tight microsyringe was used to obtain 50 μL of headspace gas, which was injected into a gas chromatograph (GC-14B, Shimadzu, Kyoto, Japan) with a flame photometric detector and a glass column packed with Porapak QS (50-80 mesh, Waters Associates, MA, USA) as described previously (Katayama et al., 1992). Organic carbon was measured by using a wet oxidation-non-dispersive infrared gas analyzer (Seto and Tange, 1980).

RESULTS

ISOLATION AND PHYLOGENETIC ANALYSIS OF SULFUR-OXIDIZING BACTERIA

Bacterial colonies on WS5 agar plates were around 0.1 mm in diameter, circular, entire, convex, and transparent. Five strains – THI501, THI502, THI503, THI504, and THI505 – were isolated from the deteriorated stone samples from the Angkor Wat, Bayon, and Phnom Krom temples (**Table 1**). On PYG agar medium, all isolates formed colonies within 3 day at 30°C in the dark that were approximately 1 mm diameter, circular, smooth, entire, and convex. Color of the colonies of strains THI501, THI504, and THI505 were pale yellow, and that of strains THI502 and THI503 were creamy white. All isolates were catalase positive and oxidase negative. Microscopic observation revealed that all isolates were Gram-positive rods and acid-fast positive.

Phylogenetic analysis of 16S rRNA gene sequences showed that all isolates belonged to the rapid grower group of the genus *Mycobacterium* (**Figure 1**). Strains THI501, THI504, and THI505 were most closely related to *Mycobacterium pallens* (DQ370008; Hennessee et al., 2009), and strains THI502 and THI503 to *Mycobacterium cosmeticum* (AY449728; Cooksey et al., 2004). Because all isolates grew in both the mineral salts medium supplemented with S^0 and the PYG medium, they were considered to be facultative chemolithoautotrophic bacteria.

SULFUR-OXIDIZING ABILITY OF STRAIN THI503

Strain THI503 was selected for further analysis because it originated in a deteriorated sandstone wall in the Bayon temple where sulfur-oxidizing microbes were found every year through the observation (Li et al., 2008). Epifluorescence microscopy of DAPI-stained cells showed that strain THI503 cultivated in WS5 liquid medium grew on the surface S^0 particles (**Figures 2A,B**). Planktonic cells of strain THI503 were much less abundant than attached cells (data not shown). Growth of cells adhering to solid surfaces, particularly to insoluble substrates, such as S^0, have been reported for *Thiobacillus thiooxidans* (now *Acidithiobacillus thiooxidans*; Schaeffer et al., 1963), *Ferrobacillus ferrooxidans* and *Thiobacillus ferrooxidans* (now *Acidithiobacillus ferrooxidans*; Dugan and Lundgren, 1964; McGoran et al., 1969), and *Sulfolobus acidocaldarius* (Brock et al., 1972; Shivvers and Brock, 1973).

S^0 is hydrophobic. When incubated with strain THI503 for 7 day, however, the sulfur became "wet" (**Figure 2C**) and easily diffused in the WS5 medium (**Figure 2D**), indicating that being covered with bacterial cells reduced its hydrophobicity. S^0 in the non-inoculated tube remained floating on the medium, due to hydrophobicity (**Figure 2E**). Adherence of strain THI503 cells may promote solubilization of S^0 and help the bacteria acquire nutrients (Knickerbocker et al., 2000). When strain THI503 was incubated in mineral salts medium with S^0 as the sole energy source, the pH of the medium decreased from 4.7 to 3.6, and 1.1 ± 0.3 mol thiosulfate and 0.1 ± 0.1 mol sulfate accumulated in 50 mL culture after 22 day (**Figure 3**).

ATP MEASUREMENT

Estimating the growth of strain THI503 in mineral salts medium with S^0 after DAPI staining and epifluorescence microscopy was difficult, because solid particles of S^0 impeded microscopic observation and the cells adhered so tightly to the surface of S^0 that detaching them was problematic. Therefore, an increase in ATP was used to confirm growth in the mineral salts medium, assuming that the energy was produced through the oxidation of S^0. ATP reached a maximum of 300 pmol in 50 mL culture after 12 day (**Figure 4**). Control culture without added sulfur reached only around half that ATP concentration; the increased ATP probably derived from ~1 g L^{-1} S^0 transferred from the pre-culture medium. By comparing to the reported data on the content of ATP in *Mycobacterium bovis* (1.014 fg per a colony-forming unit,

Table 1 | Phylogenetic affiliation by 16S rRNA gene sequences and some phenotypic characteristics of the five sulfur-oxidizing isolates.

Strain	Phylogenetic affiliation	Similarity (%)	Color of colony	Cell size, length × width (μm)	Cell shape	Sampling site	Sampling location†
THI502	*M. cosmeticum*	1369/1369 (100)	Cream	1.2 × 0.5	Rod	P, AW	AW2
THI503	*M. cosmeticum*	1438/1438 (100)	Cream	0.8 × 0.4	Rod	W, BY	BYc
THI501	*M. pallens*	1415/1416 (99)	Pale yellow	1.1 × 0.8	Short rod	P, AW	AW1
THI504	*M. pallens*	1343/1350 (99)	Pale yellow	0.7 × 0.5	Short rod	W, PK	PK2
THI505	*M. pallens*	1415/1416 (99)	Pale yellow	0.8 × 0.6	Short rod	P, PK	PK3

P, near-ground sections of deteriorated pillars; W, deteriorated wall; AW, Angkor Wat; BY, Bayon; PK, Phnom Krom.
†Li et al. (2008).
All strains were Gram positive, acid-fast positive, catalase positive, and oxidase negative.

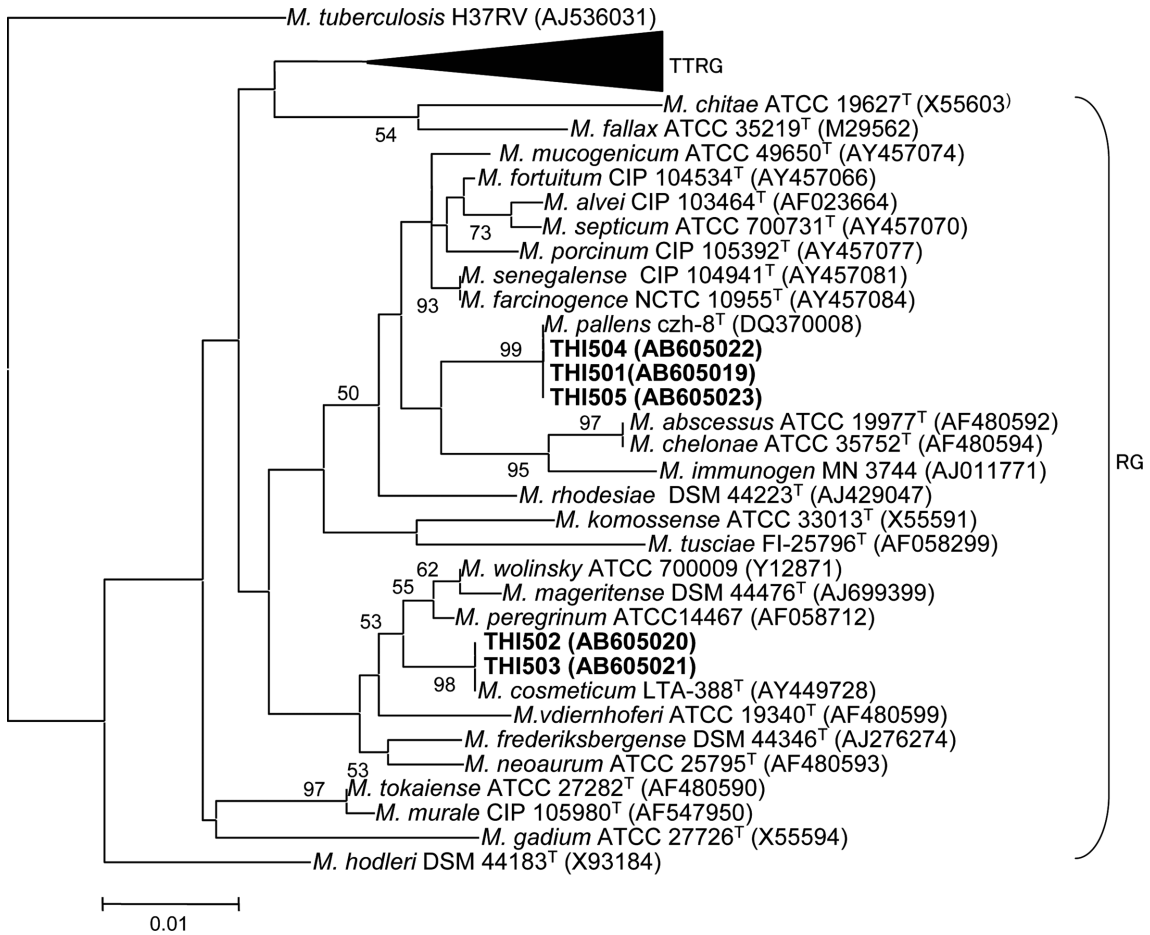

FIGURE 1 | Phylogenetic relationship between the five sulfur-oxidizing isolates and other rapid growing *Mycobacterium* species based on a comparison of their 16S rRNA gene sequences. A slow-growing species, *M. tuberculosis*, was included as the outgroup. GenBank accession numbers are shown in parentheses. Numbers at the branch nodes are bootstrap values per 1000 trials; only values greater than 50% are shown. The scale bar corresponds to 1% estimated sequence divergence. TTRG, thermotolerant rapid growers; RG, rapid growers.

CFU; Prioli et al., 1985), bacterial density in WS5-S medium was calculated to be 1.5×10^7 CFU tube^{-1} at the maximum of 300 pmol ATP (1.5×10^7 fg).

DEGRADATION OF COS BY STRAIN THI503

Degradation of COS by strain THI503 was analyzed to know of the possibility whether COS is one of the sources of sulfur for sulfuric acid in the deteriorated sandstone. COS in the headspace of the liquid cultures with no bacterial inoculation decreased from 24 ppmv (39 nmol) to 18 ppmv (30 nmol) during the 6.5-h incubation (**Figure 5**). The decrease indicated that COS gas dissolved into the liquid medium, because the solubility of COS in water is 1.15 g kg^{-1} (19 nmol mL^{-1}; Yaws, 1999). In contrast, test tubes inoculated with strain THI503 showed a decrease in COS in the headspace from 25 ppmv (40 nmol) to 1 ppmv (2 nmol) in 6.5 h. Thus, COS degraded by strain THI503 was 29 nmol in 6.5 h. At the same time, total organic carbon increased to 1.86 ± 0.03 mg C in the inoculated tubes, while only 0.24 ± 0.04 mg C was found in the non-inoculated tube. Total organic carbon from strain THI503 was estimated to be 1.62 mg C. By comparing to the reported data on the carbon content of cell in *Pseudomonas putida* (1.1×10^{-13} to 3.1×10^{-13} g of carbon cell^{-1}, Bratbak, 1985), bacterial cell in the test tube was calculated as 4.8×10^9 to 1.4×10^{10} cells and estimated COS degraded per cell per hour was estimated as 3.3×10^{-10} to 9.2×10^{-10} nmol COS cell^{-1} h^{-1}. **Figure 5** showed that 25 ppmv COS was degraded by strain THI503, however, at ambient atmospheric levels (500 pptv; Torres et al., 1980; Bandy et al., 1992; Chin and Davis, 1995), COS was not degraded by strain THI503 under experimental condition used (data not shown).

DISCUSSION

Analysis of morphological and physiological characteristics indicated that all five strains isolated as sulfur-oxidizing bacteria were closely related to the genus *Mycobacterium*. Comparison of 16S rRNA gene sequences supported this conclusion (**Figure 1**; **Table 1**). All five strains isolated in the present study developed visible colo-

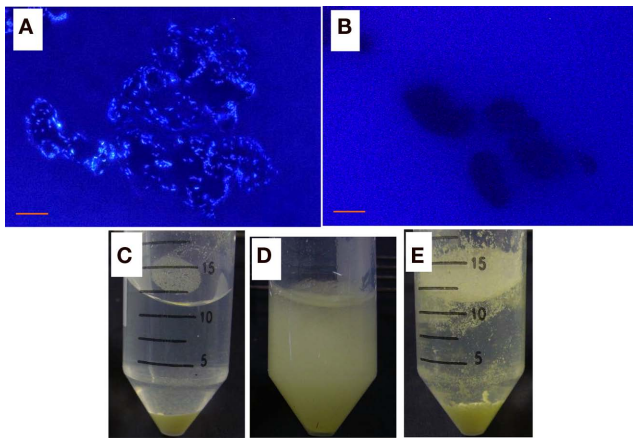

FIGURE 2 | Growth of strain THI503 with S^0. (A,B) Fluorescence microphotographs of WS5 liquid medium culture with S^0 after 9 day. **(A)** with strain THI503 and **(B)** without strain THI503. Bar indicates 10 μm. **(C,D,E)** S^0 in WS5 media after 7 day of incubation. **(C,D)** With or **(E)** without strain THI503. Cultures were allowed to stand for 5 min **(C)**, followed by brief shaking **(D)**. In the absence of strain THI503, some S^0 remained floating on the surface of WS5 medium **(E)**.

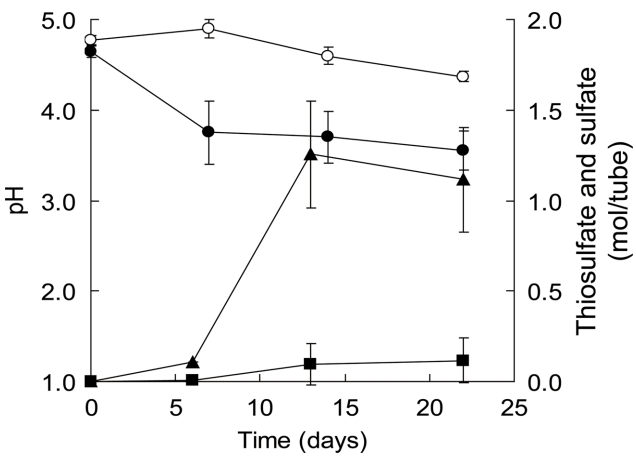

FIGURE 3 | Changes in the medium pH and thiosulfate and sulfate ions during growth of strain THI503 in WS5-S medium with S^0 as the sole energy source. Cells were grown in a 225-mL conical tube containing 50 mL culture. Error bars indicates SD, $n = 3$. Symbols: *circles*, pH; *triangles*, thiosulfate; *square*, sulfate, *filled symbols*, +THI503 + S^0; *empty symbols*, –THI503 + S^0.

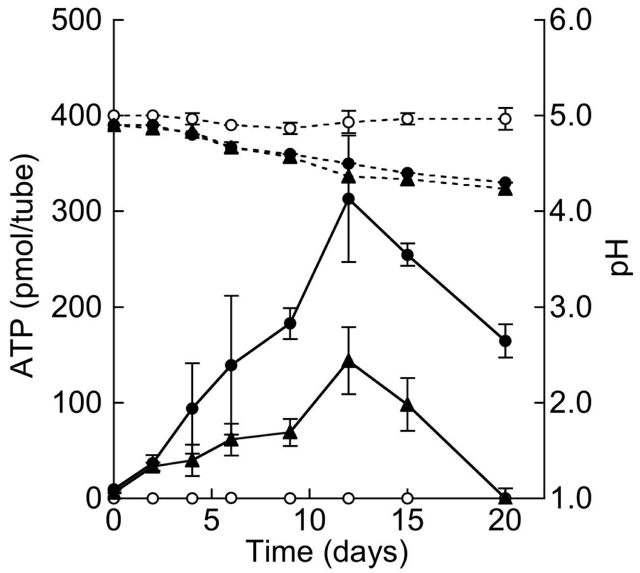

FIGURE 4 | Growth of strain THI503 in WS5 medium with S^0 as the sole energy source. Growth of strain THI503 was assessed based on ATP of the culture in a 225-mL conical tube containing 50 mL culture. Error bars indicate SD, $n = 3$. Symbols: solid line, ATP, dashed line, medium pH, *filled circles*, +THI503 + 10 g S^0 L^{-1}; *triangles*, +THI503 – S^0 (final concentration of S^0 was 1 g L^{-1} due to the carry-over from pre-culture); *empty circles*, –THI503 + 10 g S^0 L^{-1}.

nies within 7 day on PYG agar media, which is characteristic of rapid-growth species in the genus. Although, both sulfur-oxidizing bacteria and *Mycobacterium* spp. have been found by means of MPN and DGGE, respectively from corroded concrete sewer pipes (Vincke et al., 2001), no sulfur-oxidizing *Mycobacterium* had previously been cultured. The present study provides the first evidence of facultative chemolithoautotrophic ability of sulfur oxidation species of the genus *Mycobacterium*.

All five strains isolated in the present study were found to be facultative sulfur-oxidizing bacteria, able to grow in both mineral salts medium with S^0 and chemoorganoheterotrophic PYG medium. *Mycobacterium* spp. are known to produce sulfated metabolites, such as sulfated glycolipids (Mougous et al., 2002); however, a link between sulfur oxidation and energy metabolism has not been reported. Sulfates were found in most of the samples of the salts and deteriorated sandstones taken from Angkor Wat, Bayon, and Phnom Krom temples. The primary source of sulfur in deteriorated sandstone was assumed to be bat dropping, based on stable isotope analysis (Hosono et al., 2006). Since low concentrations of sulfur compounds can limit survival and growth of sulfur-oxidizing bacteria (Graff and Stubner, 2003; Anandham et al., 2008), the ability to switch between chemolithotrophy and chemoorganotrophy, or to use sulfur compounds by co-oxidation in addition to organic substrates, would be advantageous in nutrient-limited environments such as sandstone surfaces. Strain THI503 degraded COS when it was provided at 25 ppmv, but not at 500 pptv under the experimental conditions employed here. Considering that *Mycobacterium* spp. isolated from soils (Kato et al., 2008) and sulfur-oxidizing fungi isolated from deteriorated sandstones in Angkor site (Li et al., 2010) degraded COS at both high (30 ppmv) and ambient (500 pptv) levels, it is unclear whether strain THI503 can use COS as a sulfur source under ambient conditions. Experiments to test the utilization of other reduced sulfur compounds such as sulfide, thiosulfate, sulfite, and tetrathionate by these *Mycobacterium* spp. isolates are in progress.

Although pathogenic species have been reported in the rapid-growth group of *Mycobacterium* (Brown-Elliott and Wallace, 2002), none of the isolates were closely related to those species. All five isolates fell into either *M. pallens* or *M. cosmeticum* by 16S

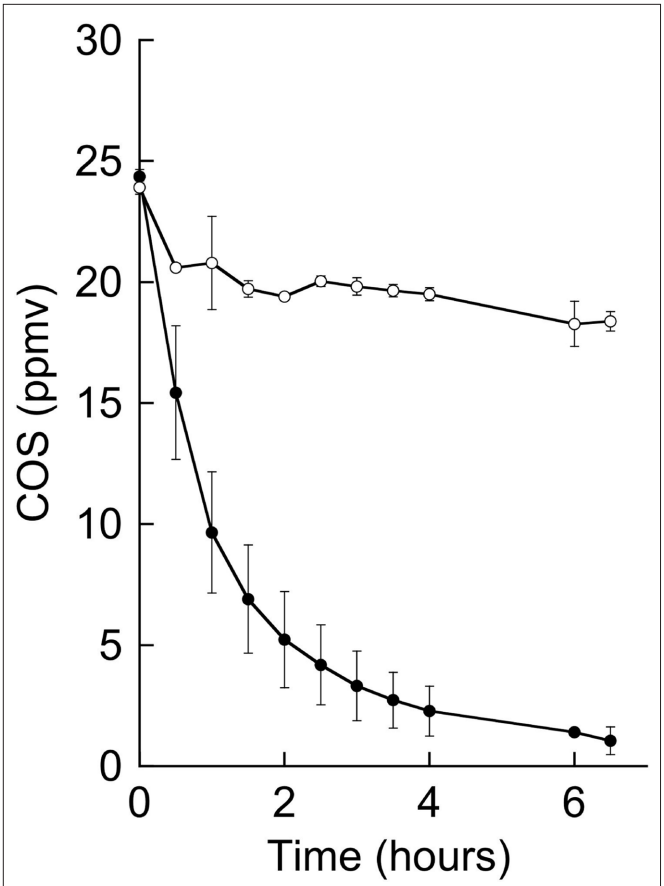

FIGURE 5 | Degradation of 25 ppmv of COS by strain THI503. Cells were suspended in PB. Error bars indicate SD, $n = 3$. Symbols: Filled circles, +THI 503; empty circles, –THI503.

rRNA sequences. *M. pallens* was isolated from a soil as a bacterium degrading polycyclic aromatic hydrocarbons (Hennessee et al., 2009); *M. cosmeticum* was isolated from a cosmetic and nail salon (Cooksey et al., 2004).

Strain THI503 achieved a density of around 1.5×10^7 CFU (50 mL culture)$^{-1}$ in mineral salts medium with S^0, with accumulations of 1.1 ± 0.3 mol thiosulfate and 0.1 ± 0.1 mol sulfate. The higher amount of thiosulfate suggests that the sulfate formed was rapidly used for biosynthesis in the sulfate-free medium, WS5-S. Although little is known about the oxidation of sulfur compounds in Gram-positive bacteria, activities of sulfur dioxygenase (SDO) and other relevant enzymes were reported for *Sulfobacillus thermosulfidooxidans* (Egorova et al., 2004; Rohwerder and Sand, 2007). In mesophilic Gram-negative sulfur-oxidizing bacteria, such as *Acidithiobacillus ferrooxidans* and *Acidithiobacillus thiooxidans*, S^0 is thought to be oxidized by SDO, resulting in the formation of sulfite: $[S] + O_2 + H_2O \rightarrow SO_3^{2-} + 2H^+$. Much of the sulfite is further oxidized to sulfate by the sulfite:acceptor oxidoreductase (SAR). The sulfite can also react abiotically with excess S^0 to produce thiosulfate. Another metabolic pathway of S^0 found in archaea is the formation of thiosulfate by sulfur oxygenase reductase (SOR): $5[S] + O_2 + 4OH^- \rightarrow HSO_3^- + S_2O_3^{2-} + 2HS^- + H^+$ (Chen et al., 2005). SOR activity results in the concomitant formation of sulfite and sulfide; the sulfite can either react abiotically with excess S^0 or be oxidized by SAR (Rohwerder and Sand, 2007). *Sor* genes have been identified in a novel mesophilic *Acidithiobacillus* sp. strain SM-1, as well as in archaea (Chen et al., 2007; Kletzin, 2008). Based on the higher accumulation of thiosulfate compared to sulfate, strain THI503 probably oxidizes S^0 by the SOR pathway. The search for a gene relevant to sulfur oxidation by strain THI503 is in progress.

CONCLUSION

The MPN approach used to isolate the bacterial strains reported here indicated that the sulfur-oxidizing microorganisms occurred at 10^3–10^4 cells g^{-1} of deteriorated sandstone in the Angkor monuments. All five isolates were characterized as facultative chemolithoautotrophic sulfur-oxidizing bacteria by growth in both mineral salts medium with S^0 and chemoorganoheterotrophic PYG medium. The isolates were most closely related to *M. pallens* or *M. cosmeticum* by 16S rRNA gene sequence comparisons. Thus, the present study provides the first evidence of facultative chemolithoautotrophic sulfur oxidation with S^0 in the species of the genus *Mycobacterium*.

ACKNOWLEDGMENTS

The authors thank APSARA Authority and Ministry on Environment, Kingdom of Cambodia, for permission to collect stone samples from monuments and transport to Japan, and Plant Protection Station of Japanese Ministry of Agriculture, Forestry, and Fisheries, for permission to import the stone samples. This research was supported by Japanese Government Team for Safeguarding Angkor and by a Grant-in-aid for Scientific Research (No.19251001) from the Ministry of Education, Culture, Sports, and Technology of Japan. Assistance of Hideo Arai, and Ichita Shimoda in sampling is appreciated.

REFERENCES

Altschul, S. F., Gish, W., Miller, W., Myers, E. W., and Lipman, D. J. (1990). Basic local alignment search tool. *J. Mol. Biol.* 215, 403–410.

Anandham, R., Indiragandhi, P., Medhaiyan, M., Ryu, K. Y., Jee, H. J., and Sa, T. M. (2008). Chemolithoautotrophic oxidation of thiosulfate and phylogenetic distribution of sulfur oxidation gene (*soxB*) in rhizobacteria isolated from crop plants. *Res. Microbiol.* 159, 579–589.

Bandy, A. R., Thornton, D. C., Scott, D. L., Lalevic, M., Lewin, E. E., and Driedger, A. R. III. (1992). A time series for carbonyl sulfide in the northern hemisphere. *J. Atmos. Chem.* 14, 527–534.

Bratbak, G. (1985). Bacterial biovolume and biomass estimations. *Appl. Environ. Microbiol.* 49, 1488–1493.

Brock, T. D., Brock, K. M., Belly, R. T., and Weiss, R. L. (1972). *Sulfolobus*: a new genus of sulfur-oxidizing bacteria living at low pH and high temperature. *Arch. Microbiol.* 84, 54–68.

Brown-Elliott, B. A., and Wallace, R. J. Jr. (2002). Clinical and taxonomic status of pathogenic nonpigmented or late-pigmenting rapidly growing mycobacteria. *Clin. Microbiol. Rev.* 15, 716–746.

Chen, Z.-W., Jiang, C.-Y., She, Q., Liu, S.-J., and Zhou, P.-J. (2005). Key role of cysteine residues in catalysis and subcellular localization of sulfur oxygenase-reductase of *Acidianus tengchongensis*. *Appl. Environ. Microbiol.* 71, 621–628.

Chen, Z.-W., Liu, Y.-Y., Wu, J.-F., She, Q., Jiang, C.-Y., and Liu, S.-J. (2007). Novel bacterial sulfur oxygenase reductases from bioreactors treating gold-bearing concentrates. *Appl. Microbiol. Biotechnol.* 74, 688–698.

Chin, M., and Davis, D. D. (1995). A reanalysis of carbonyl sulfide as a source of stratospheric background sulfur aerosol. *J. Geophys. Res.* 100, 8993–9005.

Cooksey, R. C., de Waard, J. H., Yakrus, M. A., Rivera, I., Chopite, M., Toney, S. R., Morlock, G. P., and Butler, W.

R. (2004). *Mycobacterium cosmeticum* sp. nov., a novel rapidly growing species isolated from a cosmetic infection and from a nail salon. *Int. J. Syst. Evol. Microbiol.* 54, 2385–2391.

Dugan, P. R., and Lundgren, D. G. (1964). Acid production by *Ferrobacillus ferrooxidans* and its relation to water pollution. *Develop. Ind. Microbiol.* 5, 250–257.

Egorova, M. A., Tsaplina, I. A., Zakharchuk, L. M., Bogdanova, T. I., and Krasil'nikova, E. N. (2004). Effect of cultivation conditions on the growth and activities of sulfur metabolism enzymes and carboxylases of *Sulfobacillus thermosulfidooxidans* subsp. *asporogenes* strain 41. *Appl. Biochem. Microbiol.* 40, 381–387.

Felsenstein, J. (1985). Confidence limits on phylogenies: an approach using the bootstrap. *Evolution* 39, 783–791.

Friedrich, C. G., Rother, D., Bardischewsky, F., Quentmeier, A., and Fischer, J. (2001). Oxidation of reduced inorganic sulfur compounds by bacteria: emergence of a common mechanism? *Appl. Environ. Microbiol.* 67, 2873–2882.

Graff, A., and Stubner, S. (2003). Isolation and molecular characterization of thiosulfate-oxidizing bacteria from an Italian rice field soil. *System. Appl. Microbiol.* 26, 445–452.

Hennessee, C. T., Seo, J.-S., Alvarez, A. M., and Li, Q. X. (2009). Polycyclic aromatic hydrocarbon-degrading species isolated from Hawaiian soils: *Mycobacterium crocinum* sp. nov., *Mycobacterium pallens* sp. nov., *Mycobacterium rutilum* sp. nov., *Mycobacterium rufum* sp. nov. and *Mycobacterium aromaticivorans* sp. nov. *Int. J. Syst. Evol. Microbiol.* 59, 378–387.

Hirsch, P., Eckhardt, F. E. W., and Palmer, R. J. Jr. (1995). Methods for the study of rock-inhabiting microorganisms – a mini review. *J. Microbiol. Meth.* 23, 143–167.

Hosono, T., Uchida, E., Suda, C., Ueno, A., and Nakagawa, T. (2006). Salt weathering of sandstone at the Angkor monuments, Cambodia: identification of the origins of salts using sulfur and strontium isotopes. *J. Archaeol. Sci.* 33, 1541–1551.

Katayama, Y., Narahara, Y., Inoue, Y., Amano, F., Kanagawa, T., and Kuraishi, H. (1992). A thiocyanate hydrolase of *Thiobacillus thioparus*. A novel enzyme catalyzing the formation of carbonyl sulfide from thiocyanate. *J. Biol. Chem.* 267, 9170–9175.

Kato, H., Saito, M., Nagahata, Y., and Katayama, Y. (2008). Degradation of ambient carbonyl sulfide by *Mycobacterium* spp. in soil. *Microbiology* 154, 249–255.

Kimura, M. (1980). A simple method for estimating evolutionary rates of base substitutions through comparative studies of nucleotide sequences. *J. Mol. Evol.* 16, 111–120.

Kletzin, A. (2008). "Oxidation of sulfur and inorganic sulfur compounds in *Acidianus ambivalens*," in *Microbial Sulfur Metabolism*, eds C. Dahl and C. G. Friedrich (Berlin: Springer), 184–201.

Knickerbocker, C., Nordstrom, D. K., and Southam, G. (2000). The role of "blebbing" in overcoming the hydrophobic barrier during biooxidation of elemental sulfur by *Thiobacillus thiooxidans*. *Chem. Geol.* 169, 425–433.

Lane, D. J. (1991). "16S/23S rRNA sequencing," in *Nucleic Acid Techniques in Bacterial Systematics*, eds E. Stackebrandt and M. Goodfellow (New York: John Wiley & Sons), 115–175.

Li, X., Arai, H., Shimoda, I., Kuraishi, H., and Katayama, Y. (2008). Enumeration of sulfur-oxidizing microorganisms on deteriorating stone of the Angkor monuments, Cambodia. *Microbes Environ.* 23, 293–298.

Li, X. S., Sato, T., Ooiwa, Y., Kusumi, A., Gu, J.-D., and Katayama, Y. (2010). Oxidation of elemental sulfur by *Fusarium solani* strain THIF01 harboring endobacterium *Bradyrhizobium* sp. *Microb. Ecol.* 60, 96–104.

Lukins, H. B., and Foster, J. W. (1963). Utilization of hydrocarbons and hydrogen by mycobacteria. *Z. Allg. Mikrobiol.* 3, 251–264.

Masuda, S., Eda, S., Ikeda, S., Mitsui, H., and Minamisawa, K. (2010). Thiosulfate-dependent chemolithoautotrophic growth of *Bradyrhizobium japonicum*. *Appl. Environ. Microbiol.* 76, 2402–2409.

McGoran, C. J. M., Duncan, D. W., and Walden, C. C. (1969). Growth of *Thiobacillus ferrooxidans* on various substrates. *Can. J. Microbiol.* 15, 135–138.

Mougous, J. D., Leavell, M. D., Senaratne, R. H., Leigh, C. D., Williams, S. J., Riley, L. W., Leary, J. A., and Bertozzi, C. R. (2002). Discovery of sulfated metabolites in mycobacteria with a genetic and mass spectrometric approach. *Proc. Natl. Acad. Sci. U.S.A.* 99, 17037–17042.

Park, S. S., and Decicco, B. T. (1974). Autotrophic growth with hydrogen of *Mycobacterium gordonae* and another scotochromogenic mycobacterium. *Int. J. Syst. Bacteriol.* 24, 338–345.

Park, S. W., Hwang, E. H., Jang, H. S., Lee, J. H., Kang, B. S., Oh, J. I., and Kim, Y. M. (2009). Presence of duplicate genes encoding a phylogenetically new subgroup of form I ribulose 1,5-bisphosphate carboxylase/oxygenase in *Mycobacterium* sp. strain JC1 DSM 3803. *Res. Microbiol.* 160, 159–165.

Park, S. W., Hwang, E. H., Park, H., Kim, J. A., Heo, J., Lee, K. H., Song, T., Kim, E., Ro, Y. T., Kim, S. W., and Kim, Y. M. (2003). Growth of mycobacteria on carbon monoxide and methanol. *J. Bacteriol.* 185, 142–147.

Pochon, J., and Jaton, C. (1967). The role of microbiological agencies in the deterioration of stone. *Chem. Ind.* 9, 1587–1589.

Prioli, R. P., Tanna, A., and Brown, I. N. (1985). Rapid methods for counting mycobacteria – comparison of methods for extraction of mycobacterial adenosine triphosphate (ATP) determined by firefly luciferase assay. *Tubercle.* 66, 99–108.

Rakotonirainy, M. S., Héraud, C., and Lavédrine, B. (2003). Detection of viable fungal spores contaminant on documents and rapid control of the effectiveness of an ethylene oxide disinfection using ATP assay. *Luminescence* 18, 113–121.

Rohwerder, T., and Sand, W. (2007). Oxidation of inorganic sulfur compounds in acidophilic prokaryotes. *Eng. Life. Sci.* 7, 301–309.

Saito, H., and Miura, K.-I. (1963). Preparation of transforming deoxyribonucleic acid by phenol treatment. *Biochim. Biophys. Acta* 72, 619–629.

Schaeffer, W. I., Holbert, P. E., and Umbreit, W. W. (1963). Attachment of *Thiobacillus thiooxidans* to sulfur crystals. *J. Bacteriol.* 85, 137–140.

Scheerer, S., Ortega-Morales, O., and Gaylarde, C. (2009). Microbial deterioration of stone monuments – an updated overview. *Adv. Appl. Microbiol.* 66, 97–139.

Schelle, M. W., and Bertozzi, C. R. (2006). Sulfate metabolism in mycobacteria. *ChemBioChem* 7, 1516–1524.

Seto, M., and Tange, I. (1980). Rapid and sensitive method for the determination of total organic carbon in soil by potassium persulfate-nondispersive infrared gas analyzer. *Jap. J. Soil Sci. Plant Nutr.* 51, 27–30 (in Japanese).

Shivvers, D. W., and Brock, T. D. (1973). Oxidation of elemental sulfur by *Sulfolobus acidocaldarius*. *J. Bacteriol.* 114, 706–710.

Stanley, P. E., and Williams, S. G. (1969). Use of the liquid scintillation spectrometer for determining adenosine triphosphate by the luciferase enzyme. *Anal. Biochem.* 29, 381–392.

Tamura, K., Dudley, J., Nei, M., and Kumar, S. (2007). MEGA4: molecular evolutionary genetics analysis (MEGA) software version 4.0. *Mol. Biol. Evol.* 24, 1596–1599.

Thompson, J. D., Higgins, D. G., and Gibson, T. J. (1994). CLUSTAL W: improving the sensitivity of progressive multiple sequence alignment through sequence weighting, position-specific gap penalties and weight matrix choice. *Nucleic Acids Res.* 22, 4673–4680.

Torres, A. L., Maroulis, P. J., Goldberg, A. B., and Bandy, A. R. (1980). Atmospheric OCS measurements on project Gametag. *J. Geophys. Res.* 85, 7357–7360.

Vincke, E., Boon, N., and Verstraete, W. (2001). Analysis of the microbial communities on corroded concrete sewer pipes – a case study. *Appl. Microbiol. Biotechnol.* 57, 776–785.

Warscheid, T., and Braams, J. (2000). Biodeterioration of stone: a review. *Int. Biodeter. Biodegr.* 46, 343–368.

Yaws, C. L. (1999). "Solubility in water and octanol-water partition coefficient," in Chemical Properties Handbook: Physical, Thermodynamic, Environmental, Transport, Safety, and Health Related Properties for Organic and Inorganic Chemicals, ed. C. L. Yaws (New York: McGraw-Hill), 364–388.

Conflict of Interest Statement: The authors declare that the research was conducted in the absence of any commercial or financial relationships that could be construed as a potential conflict of interest.

Received: 17 January 2011; accepted: 27 April 2011; published online: 10 May 2011. Citation: Kusumi A, Li XS and Katayama Y (2011) Mycobacteria isolated from Angkor monument sandstones grow chemolithoautotrophically by oxidizing elemental sulfur. Front. Microbio. ***2****:104. doi: 10.3389/fmicb.2011.00104*

This article was submitted to Frontiers in Microbial Physiology and Metabolism, a specialty of Frontiers in Microbiology.

frontiers in
MICROBIOLOGY

ORIGINAL RESEARCH ARTICLE
published: 25 March 2011
doi: 10.3389/fmicb.2011.00058

How are "atypical" sulfite dehydrogenases linked to cell metabolism? Interactions between the SorT sulfite dehydrogenase and small redox proteins

Louie Low, James Ryan Kilmartin, Paul V. Bernhardt and Ulrike Kappler*

School of Chemistry and Molecular Biosciences, Centre for Metals in Biology, The University of Queensland, St. Lucia, QLD, Australia

Edited by:
Martin G. Klotz, University of Louisville, USA

Reviewed by:
Martin G. Klotz, University of Louisville, USA
Christiane Dahl, Rheinische Friedrich-Wilhelms-Universität Bonn, Germany

***Correspondence:**
Ulrike Kappler, School of Chemistry and Molecular Bioscience, The University of Queensland, St. Lucia, QLD 4072, Australia.
e-mail: u.kappler@uq.edu.au

Sulfite dehydrogenases (SDHs) are enzymes that catalyze the oxidation of the toxic and mutagenic compound sulfite to sulfate, thereby protecting cells from adverse effects associated with sulfite exposure. While some bacterial SDHs that have been characterized to date are able to use cytochrome *c* as an electron acceptor, the majority of these enzymes prefer ferricyanide as an electron acceptor and have therefore been termed "atypical" SDHs. Identifying the natural electron acceptor of these enzymes, however, is crucial for understanding how the "atypical" SDHs are integrated into cell metabolism. The SorT sulfite dehydrogenase from *Sinorhizobium meliloti* is a representative of this enzyme type and we have investigated the interactions of SorT with two small redox proteins, a cytochrome *c* and a Cu containing pseudoazurin, that are encoded in the same operon and are co-transcribed with the *sorT* gene. Both potential acceptor proteins have been purified and characterized in terms of their biochemical and electrochemical properties, and interactions and enzymatic studies with both the purified SorT sulfite dehydrogenase and components of the respiratory chain have been carried out. We were able to show for the first time that an "atypical" sulfite dehydrogenase can couple efficiently to a cytochrome *c* isolated from the same organism despite being unable to efficiently reduce horse heart cytochrome *c*, however, at present the role of the pseudoazurin in SorT electron transfer is unclear, but it is possible that it acts as an intermediate electron shuttle between. The SorT system appears to couple directly to the respiratory chain, most likely to a cytochrome oxidase.

Keywords: sulfite dehydrogenase, sulfite oxidation, molybdoenzyme, cytochrome, redox protein, pseudoazurin

INTRODUCTION

Sulfite dehydrogenases (SDHs) are enzymes that catalyze the oxidation of sulfite, which can cause damage to important cellular components such as proteins, DNA, and lipids, to the inert and non-toxic compound sulfate (Kappler and Dahl, 2001; Kappler, 2011). They belong to the sulfite oxidase family of molybdenum enzymes that comprises three distinct groups of enzymes, two of which are largely unstudied, while the third and best studied group contains the sulfite oxidases (SO) and SDHs that oxidize sulfite to sulfate (Kappler, 2008).

One of the distinctive features of molybdenum enzymes is that they can catalyze the transfer of an oxygen atom to a substrate using water as the oxygen donor (Hille, 1996). The reaction catalyzed by SOs and SDHs proceeds according to the general equation

$$SO_3^{2-} + H_2O \rightarrow SO_4^{2-} + 2H^+ + 2e^- \quad (1)$$

For SO [EC1.8.3.1], such as the enzyme from *Arabidopsis thaliana* (Eilers et al., 2001), oxygen serves as the electron acceptor, leading to the production of hydrogen peroxide, while for most SDHs [EC1.8.2.1], which include the vertebrate "SO," two molecules of cytochrome *c* serve as the natural electron acceptor (Rajagopalan, 1980; Kappler, 2011).

Sulfite-oxidizing enzymes (SOEs) have been studied for over 40 years in vertebrates and humans, where SOEs are essential and their absence causes the lethal sulfite oxidase deficiency syndrome, however, significant progress in studying bacterial SOEs has only been made in the last 10 years (Kappler and Dahl, 2001; Kappler, 2011). SOEs have been identified in a wide variety of bacteria including sulfur-oxidizing chemolithotrophs, organosulfonate degraders, pathogenic, and extremophilic bacteria (Kappler and Dahl, 2001; Myers and Kelly, 2005; Di Salle et al., 2006; D'Errico et al., 2006; Denger et al., 2008; Wilson and Kappler, 2009; Kappler, 2011), suggesting an important role for these enzymes outside dissimilatory sulfur metabolism.

Vertebrate SOEs occur in the mitochondrial intermembrane space and appear to have a uniform overall structure. They are homodimers with a mobile heme *b* domain fused to the main body of the enzyme which consists of a molybdenum binding and a dimerization domain. As far as is known, this combination of domains is the common "core structure" of all SOEs, and, e.g., the plant SO are homodimers of this core structure (Schrader et al., 2003).

In contrast to the conserved architecture of the vertebrate and plant enzymes, bacterial SOEs are much more diverse in terms of their overall structure. Of the bacterial SOEs studied in sufficient detail to date one is a heterodimer of the core Moco/dimer subunit and a cytochrome *c* subunit (Kappler et al., 2000; Kappler and Bailey, 2005), while SOEs from other bacteria are either homodimers or even monomers of the core two domain structure (Denger et al., 2008; D'Errico et al., 2006; Di Salle et al., 2006; Wilson and Kappler, 2009; Kappler, 2011).

Intriguingly however, with the exception of the heterodimeric, cytochrome *c* containing enzyme isolated from the soil bacterium *Starkeya novella* (Kappler et al., 2000), almost all the bacterial SOEs isolated to date display higher activities when assayed with the artificial electron acceptor ferricyanide than when assayed with cytochrome *c* (Kappler, 2011), which raises the question how these enzymes are integrated into cell metabolism.

This is of particular interest as bacterial SOEs have been found in bacteria with widely differing lifestyles, including thermophilic bacteria, pathogens, and environmental bacteria, and thus might be fulfilling very different metabolic roles. The ferricyanide-linked bacterial SOEs have, in fact, been referred to as "atypical" SOEs due to their low activity with cytochrome *c* and were first described in organosulfonate degrading bacteria (Reichenbecher et al., 1999). In contrast, bacterial SOEs that prefer cytochrome *c* as the natural electron acceptor are directly linked to the respiratory chain and thus energy generation via the natural electron acceptor cytochromes (mitochondrial cytochrome *c* in vertebrates, a cytochrome c_{550} in *Starkeya novella*; Kappler et al., 2000) that are able to transfer electrons directly to the respective cytochrome *c* oxidases (Rajagopalan, 1980; Yamanaka et al., 1981).

As "atypical" SDHs, like any other redox enzyme, require an electron acceptor in order to retain their functionality, a variety of possibilities exist that could explain the high activity of these SDHs, with the artificial electron acceptor ferricyanide. The natural electron acceptor could be molecular oxygen, however, this would lead to the formation of hydrogen peroxide that would then have to be detoxified in additional enzymatic reactions. Alternatively, the natural acceptor could be an electron transfer protein occurring within the cells, but this protein might have redox properties that differ from those of horse heart cytochrome *c* (e.g., a different redox potential might be required), or might have different structural properties that enable efficient docking to these SDHs (Wilson and Kappler, 2009). Another option would be that the "atypical" SDHs can transfer electrons directly to, e.g., the cytochrome oxidase, thus by passing the need for a separate electron carrier.

We have recently purified a ferricyanide-linked SOE from the plant symbiontic soil bacterium *Sinorhizobium meliloti* grown on the organosulfonate taurine. The SorT SDH is a periplasmic, homodimeric SOEs with a clear preference for ferricyanide over horse heart cytochrome *c* in *in vitro* assays (Wilson and Kappler, 2009). The SorT SDH also displayed some interesting catalytic properties, including an almost pH invariant $K_{M\ sulfite}$, which differs clearly from all the well studied cytochrome *c* linked SDHs, where $K_{M\ sulfite}$ increases almost exponentially above pH 8–8.5 (Wilson and Kappler, 2009). The *sorT* gene was found to be co-transcribed with two genes encoding for redox proteins, namely a cytochrome *c* (*smc04048*) and a pseudoazurin, *azu2* (Wilson and Kappler, 2009). The *smc04048* gene encodes a single heme cytochrome and, same as the pseudoazurin, did not appear to be part of the purified enzyme, but it was postulated that one or both of these proteins might be natural electron acceptors for SorT.

Using the SorT SDH from *S. meliloti* as the model system, we have investigated how atypical SDHs might be linked to cell metabolism (**Figure 1**). There are a variety of options, including the direct interaction of SorT with the respiratory chain, involvement of either or both of Smc04048 and Azu2. We have already shown previously

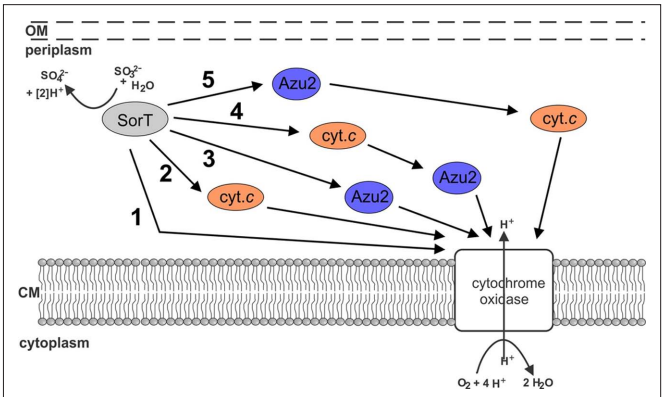

FIGURE 1 | Schematic representation of potential electron transfer pathways between SorT and the respiratory chain. 1 direct transfer of electron transfer between SorT and the cytochrome oxidase 2 using the Smc04048 cytochrome *c* as an electron carrier, 3 using the pseudoazurin Azu2 as an electron carrier, 4 + 5 using both the Smc04048 cytochrome *c* and pseudoazurin Azu2 the as electron carriers.

that native SorT does not have sulfite oxidase activity (Wilson and Kappler, 2009), and thus investigations focused on the interactions of SorT with the two redox proteins that are co-transcribed with it the enzyme's structural gene.

MATERIALS AND METHODS

BACTERIAL STRAINS AND GROWTH MEDIA *SINORHIZOBIUM MELILOTI*

Rm 1021 was routinely grown on liquid or solidified DSMZ medium 69 supplemented with 20 mM taurine or TYS medium (Beringer, 1974) at 30°C. Liquid or solidified LB medium was used to cultivate *Escherichia coli* strains DH5α (Invitrogen), TP1000 (Palmer et al., 1996), and BL21(DE3; Novagen) at 37°C. Growth media were supplemented with antibiotics where appropriate: ampicillin 100 μg/mL, kanamycin 50 μg/mL, chloramphenicol 25 μg/mL, *S. meliloti* streptomycin 25 μg/mL.

MOLECULAR BIOLOGICAL METHODS

Standard methods were used throughout (Ausubel et al., 2005). Standard PCR reactions used GoTaqGreen Mastermix (Promega), restriction enzymes were from Invitrogen. Protein expression plasmids were constructed using pProex Htb (Invitrogen) for the *sorT* gene, and pET22b+ (Novagen) for the *Smc04048*, *azu2*, and *Snovc550* (acc.no ADH88353) genes. The genes were amplified using the listed primers (SM_SDH4049f_bam AAAA*GGATCC*AAGGAGACGAAGCCTCTGCC; SM_SDH4049r_pst AAAA*CTGCAG*TCAGGCAACGGTGAGTTTGACG; SM_04048F_nco AAAA*CCATGG*AAGAAGACAAGCTTGCGCT; SM_4048r_tag AAAA*GAATTC*TTGGCTTTTCCGGCGAC; SM_azu2f-nco AAAA*CCATGG*AGGAATATCGTGTCGAAATGCTG; SM_azu2r_tag AAAA*GAATTC*TCGCCGCCGCTCTCGATTTC; SNc550petF AAAA*CCATGG*CACAGAGCCCGGCCGGCGATC; SNc550pETrevtag AAAA*AAGCTT*CTTCTTGGTGCCGTCGGCG) and Phusion HF polymerase (Finnzymes) before cloning into the appropriate expression vectors. Plasmids pProex-SorT, pET22b-Smc04048tag, pET22b-SNCtag, and pET22b-azu2tag were verified by DNA sequencing. The plasmid pProex-SorT contains only the coding region for the mature SorT enzyme but lacks the coding

region for the signal peptide, leading to a cytoplasmic expression of recombinant SorT (rSorT). In contrast, the constructs pET-Smc04048tag, pET22b-SNCtag, and pEt22b-azu2tag contain the coding regions for the mature proteins (sequence parts encoding native signal peptides have been removed) fused to a sequence encoding the *E. coli*-specific PelB signal peptide, leading to protein expression in the periplasm. The choice of cytoplasmic and periplasmic expression was made depending on which cellular compartment the target protein matures in, i.e., folds and has its cofactor inserted. The location of production for the recombinant proteins should have no influence on the protein interaction studies, all of which used purified proteins.

PROTEIN EXPRESSION PROTOCOLS

pProex-SorT was transformed into *E. coli* TP1000. Expression cultures (4 × 1 L in 2.5 L flasks) were grown at 37°C, 200 rpm in LB medium supplemented with ampicillin, kanamycin, and 1 mM sodium molybdate. At an OD_{600} of ~0.8, protein expression was induced by the addition of 250 μM IPTG and cultures were grown overnight at 30°C before being harvested by centrifugation at 4°C and 5000 × *g*.

pET22b-Smc04048tag and pET22b-SNCtag were transformed into *E. coli* BL21(DE3) carrying plasmid pEC86 (Arslan et al., 1998). Expression cultures (4 × 1 L in 2 L flasks) were grown in autoinduction medium (Hill et al., 2007) in the presence of ampicillin and chloramphenicol at 20°C, 200 rpm for 48 h before harvesting by centrifugation. pET22b-azu2Tag was transformed into *E. coli* BL21(DE3) and expression cultures grown on LB medium supplemented with 1 mM copper(II) sulfate and ampicillin at 37°C, 200 rpm until an OD_{600} of 0.6–0.8 was reached. Protein expression was induced by addition of 50 μM IPTG and cultures incubated at 30°C for 3 h before harvesting by centrifugation and isolation of periplasmic proteins using the osmotic shock method (Ausubel et al., 2005).

PROTEIN PURIFICATION METHODS

Native SorT was purified from *S. meliloti* as in Wilson and Kappler (2009). For the purification of recombinant proteins, cell extracts from whole cells were prepared by passing the resuspended cells three times through a French Pressure Cell (Thermo) at 14000 psi. Cell debris was removed by centrifugation at 15000 × *g*, 4°C, 20 min resulting in a crude extract. rSorT was purified by preparing the crude extract in 20 mM potassium phosphate, 0.5 M NaCl pH 7.4, 4 mM Pefabloc SC (Roche) and, after adding imidazole (final conc. 20 mM), loading this extract onto a 5-mL HisTrap column (GE Healthcare Biosciences) equilibrated in the same buffer containing 20 mM imidazole. rSorT was eluted in a linear gradient from 20 to 500 mM imidazole. SorT containing fractions were pooled and desalted using a HiPrep 26/10 column (GE Healthcare Biosciences) equilibrated in 20 mM Tris–Cl pH 7.8, 5% (w/v) glycerol before concentrating the samples (Vivaspin 20 concentrators, MWCO 30 kDa, GE Healthcare Biosciences) and further purification on a Superdex75 16/60 column (GE Healthcare Biosciences) equilibrated in 20 mM Tris–Cl pH 7.8, 150 mM NaCl, 2.5% (w/v) glycerol.

Recombinant Smc04048 and SNCtag were purified from crude extracts using a 5-mL HisTrap column and the buffer system already described above. Cytochrome *c* containing fractions were pooled, 15% (w/v) ammonium sulfate was added and samples separated on a Phenyl Sepharose column (1.6 cm × 21 cm) equilibrated in 20 mM Tris–Cl, pH 7.8, 15% (w/v) ammonium sulfate using a linear, decreasing gradient of ammonium sulfate (100-0%, 5 CV). Fractions were pooled according to protein purity and desalted using dialysis before storing. If necessary, proteins were subjected to size exclusion chromatography on a Superdex 75 (16/60) column for further purification.

Following isolation of the periplasmic protein fraction recombinant Azu2 was purified using anion exchange chromatography (DEAE-Sepharose, buffer: 20 mM Tris–Cl pH 8.8) and a linear elution gradient (0–25% NaCl, 7 CV). Azu2 containing fractions were pooled and 0.5 mM $CuSO_4$ added before concentrating of samples and separation on a Superdex 75 (16/60) in 20 mM Tris–Cl pH 7.8, 150 mM NaCl). If necessary, size exclusion chromatography was repeated to improve protein purity.

BIOCHEMICAL METHODS

SDS PAGE used the method of (Laemmli, 1970). Protein determinations were performed using either the BCA kit (Sigma-Aldrich) or 2D Quant kit (GE Healthcare Biosciences). Hemochrome spectra were carried out as described in (Berry and Trumpower, 1987), in gel heme stains used the method of (Thomas et al., 1976). UV–Vis electronic absorption spectra and kinetic assay data were recorded on a Cary50 spectrophotometer (Varian) at 25°C unless otherwise specified. Sulfite dehydrogenase activity assays were performed as in (Wilson and Kappler, 2009) and data fitted using SigmaPlot 9.0 (Sysstat). Temperature stability of SorT was tested by pre-incubating samples of purified SorT in the presence (1 mM) or absence of sulfite for 0, 5, 10, and 20 min at temperatures between 20 and 60°C before quick-chilling the sample on ice, followed by brief centrifugation and determination of SDH activity. pH stability of rSorT was determined by a similar method, where purified, concentrated rSorT was incubated in buffers between pH 6 and 11 and samples were taken after 5, 10, and 20 min and immediately assayed for SDH activity under standard conditions (pH 8.0, 25°C). Interaction assays used a combination of electronic absorption spectra and kinetic assays, in brief electronic absorption spectra were recorder between 700 and 250 nm before the start of the kinetic run ("oxidized"), immediately following the end of the kinetic run ("part reduced") and after addition of dithionite ("fully reduced"). Experiments involving an oxygen electrode used a Hansatech Oxygraph, membrane fractions for use in these experiments were isolated from *S. meliloti* cells grown on medium 69 supplemented with taurine by subjecting a crude extract to ultracentrifugation (145,000 × *g*, 4°C, 90 min) and resuspension of the membrane pellet in 20 mM Tris–Cl pH 8.0. Mass fingerprints of tryptic peptides and whole proteins were determined as in Wilson and Kappler (2009).

CYCLIC VOLTAMMETRY

All electrochemical experiments were performed with a BAS100B/W potentiostat coupled to a BAS C3 cell stand. The reference electrode was Ag/AgCl and the counter electrode was a Pt wire. The electrolyte solution comprised phosphate buffer (0.1 M) titrated to the desired pH with dilute NaOH or AcOH solution. The two proteins rAzu2 and SMC04048 were examined at different working electrodes as described below.

rAzu2: a Au disk working electrode was cleaned and polished as described (Tkac and Davis, 2008) and then chemically modified by immersion in a 1-mM ethanolic solution of 11-mercaptoundecanoic acid using standard procedures (Kalimuthu et al., 2010). To the inverted thiol-modified Au working electrode was added a 10-μL aliquot of rAzu2 (56 μM). The droplet was allowed to dry to a film. To prevent protein loss, the electrode surface was carefully covered with a perm-selective dialysis membrane (MW cutoff *ca.* 3.5 kDa), presoaked in water. The membrane was fastened with a rubber O-ring to prevent leakage. The pH-dependence of the rAzu2 redox potential was modeled with Eq. 1 which is applicable for a coupled single electron/single proton redox reaction where only the reduced (Cu^{I}) form exhibits a pK_a.

$$E_m(H^+) = E^o + \frac{RT}{F}\ln\left(K_a(rAzu2_{red}) + [H^+]\right) \quad (2)$$

rSmc04048: A glassy carbon disk electrode was polished with alumina suspension (50 nm). Eastman AQ 29D polymer (28% w/v) was diluted 1:20 v/v and a 10-μL droplet of this solution was carefully deposited onto the inverted electrode surface and allowed to dry to a film at room temperature (*ca.* 1 h). A solution of rSmc04048 (40 μL, 250 μM) was diluted 1:10 v/v with 0.1 M phosphate buffer to give a volume of *ca.* 0.5 mL. The polymer-coated glassy carbon electrode was inserted into the protein solution and allowed to stand for approximately 3 h prior to measurement to allow the protein to accumulate within the polymer modified electrode. Voltammograms were recorded in the presence of dioxygen but at potentials above that at which dioxygen reduction is significant.

Phylogenetic analyses BLASTP was used to identify sequences related to either SorT, Azu2, or SMC04048. Phylogenetic relationships were analyzed using MEGA4.0 (Tamura et al., 2007) using neighbor-joining, maximum parsimony and minimum evolution algorithms. Bootstrap analysis was carried out with 500 replicates.

RESULTS

CHARACTERIZATION OF RECOMBINANT SorT

The *S. meliloti* SDH, SorT, can only be purified with very low yields as several proteins co-purify with SorT (Wilson and Kappler, 2009), and this precludes detailed characterization of this protein both in terms of enzyme kinetics and structure as well as spectroscopic characterization of the protein. rSorT was produced in *E. coli* TP1000 as a cytoplasmic protein and purified to homogeneity using a combination of affinity chromatography and size exclusion chromatography. Molybdoenzymes are known to undergo folding and cofactor-insertion in the cytoplasm, which means that in the case of periplasmic enzymes such as SorT, the enzyme is fully functional before it is exported to the periplasmic space, allowing for expression of these enzymes in the *E. coli* cytoplasm. This type of expression strategy has been used successfully for other molybdenum enzymes located in extracytoplasmic cell compartments (Hilton et al., 1999; Temple et al., 2000).

The purified rSorT protein had a subunit mol. mass of 42669 ± 2 Da as determined by mass spectrometry. The small difference between the observed mass and the calculated molecular mass of rSorT (42791 Da) could indicate the loss of the N-terminal methionine residue. rSorT can appear as a double band when analyzed by gel electrophoresis during purification, and this is due to the loss of the cleavable His-Tag in some protein subunit during the early stages of purification as shown by mass fingerprinting (data not shown), use of protease inhibitor during purification minimizes this effect. rSorT contained 0.69 molecules of Mo per protein subunit, which is comparable to the value of 0.59 obtained for the native SorT by (Wilson and Kappler, 2009). Using size exclusion chromatography, the molecular mass of rSorT was estimated to be 71 kDa, indicating that just like the native SorT (est. mol mass 68 kDa by gel filtration, calculated subunit mol mass 39.42 kDa; Wilson and Kappler, 2009), the recombinant protein forms a homodimeric complex. Optical spectra of rSorT showed features typically associated with molybdenum proteins (**Figure 2**), with the "as prepared" protein being mostly in the oxidized state.

At pH 8.0, rSorT had a $K_{M\ sulfite\ app}$ of 13.4 ± 0.5 μM and a k_{cat} of 338 ± 3/s, which is in very good agreement with the values obtained for the native SorT ($K_{M\ sulfite\ app}$: 15.5 ± 1.1 μM; k_{cat}: 343 ± 11/s). At pH 7 and pH 6, rSorT had $K_{M\ sulfite\ app}$ values of 23.4 ± 1.2 and 33.3 ± 6.5 μM, which is also very close to what was reported for the native enzyme (Wilson and Kappler, 2009). In addition, the rSorT activity profile between pH 6 and 12 also closely resembles the profile of the native SorT (**Figure 2**). To ascertain that changes in kinetic parameters and the enzyme's catalytic performance were not caused by enzyme inactivation during the assay (duration: ~2 min), the pH stability of rSorT was determined. rSorT was stable for at least 20 min between pH 6 and 10. At pH 11 the enzyme lost about

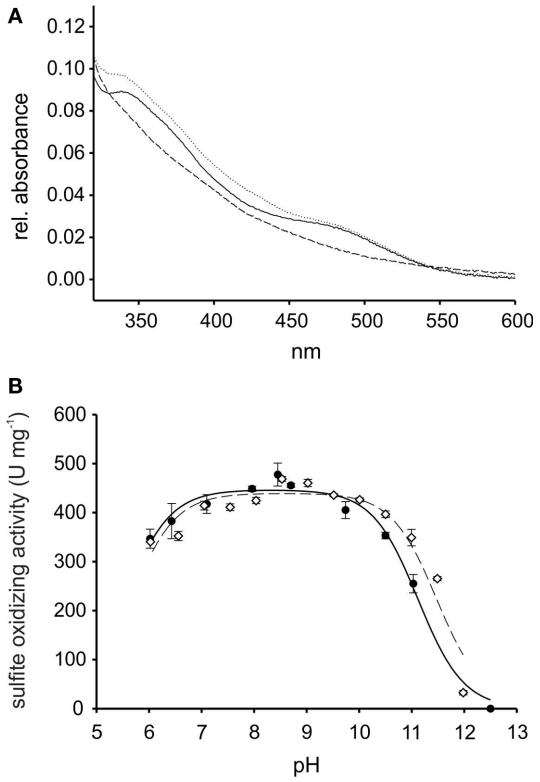

FIGURE 2 | Properties of recombinant SorT (rSorT) (A) electronic absorption spectra of rSorT (solid line: as prepared, dotted line: oxidized and dashed line: sulfite reduced) (B) comparison of the pH dependency of SorT activity for the native and rSorT.

25% of activity within the first 5 min, and after 20 min an activity loss of ~50% was apparent. Although typical SorT enzyme assays only take about 2 min to complete it therefore cannot be excluded that the significantly lower activities recorded at pH 11 (**Figure 2**) are at least in part due to enzyme inactivation.

SorT occurs in a mesophilic microorganism and standard assays are therefore carried out at 25°C, however, many of the Mo-containing SDHs are known to be resistant to thermal inactivation by temperature well above the growth temperature of the source organism (Kappler, 2011). To determine the temperature stability of rSorT, the enzyme was preincubated at temperatures between 20 and 60°C for up to 20 min followed by activity assays under standard conditions at 25°C and pH 8. In these experiments rSorT was stable for at least 20 min at temperatures of up to 40°C, while at 50 and 60°C the enzyme had a half-life of 2 min and under 1 min respectively (**Figure 3**). Interestingly, if rSorT was reduced by addition of sulfite before incubation, no significant loss of activity was observed at 50°C after 10 min of incubation, and at 60°C the half-life improved to an estimated 20–25 min (**Figure 3**). This effect is similar to what has been observed for both the bacterial SorAB SDH and for vertebrate SO (Southerland and Rajagopalan, 1978; Kappler et al., 2000). While for the latter the effect was explained by a tighter packing of the two mobile domains of the reduced vertebrate sulfite oxidase, it is unclear what is causing the increased temperature stability of the reduced bacterial enzymes neither of which has any mobile domains.

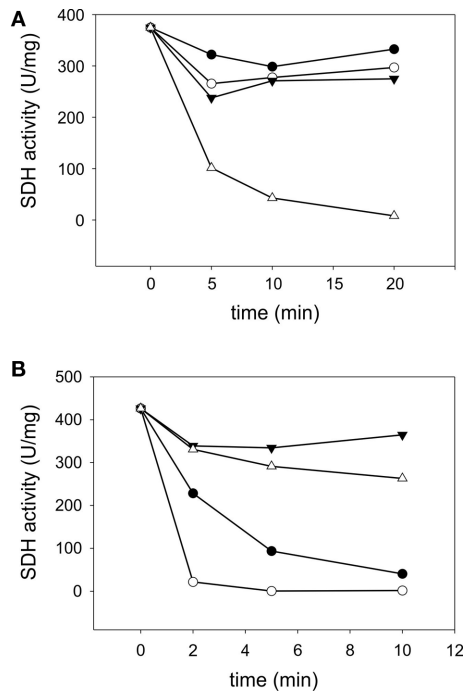

FIGURE 3 | Temperature stability of rSorT (A) changes in rSorT activity following incubation at 20°C (● closed circles), 30°C (○ open circles), 40°C (▼ closed triangles), and 50°C (△ open triangles) for 5, 10, and 20 min. (B) rSorT inactivation at 50 (● closed circles) and 60°C (○ open circles) and protective effect of sulfite reduction on rSorT temperature stability at these temperatures. 50°C + sulfite (▼ closed triangles) and 60°C + sulfite (△ open triangles).

PROPERTIES OF PURIFIED RECOMBINANT CYTOCHROMES AND Azu2

Both recombinant Smc04048 (rSmc04048) and recombinant Snc_{550} ($rSnc_{550}$) were expressed in *E. coli* as a periplasmic protein using the helper plasmid pEC86 (Arslan et al., 1998) and purified to homogeneity from whole cell extracts. Purified rSmc04048 had a molecular mass of 12004 ± 2 Da, which corresponds to the calculated mass of the protein. rSmc04048 eluted from a calibrated gel filtration column in two peaks corresponding to 19.5 and 41 kDa, indicating that this cytochrome exists both as a monomer and as a dimer. rSmc04048 contained a full complement of the redox cofactor as determined by hemochrome spectra.

Redox potentiometry of rSmc04048 gave inconsistent results and protein precipitation during the experiment was a particular problem. Therefore, we turned to cyclic voltammetry as a means of determining the heme redox potential. A number of different working electrodes were tried including an Au electrode modified with several different long chain thiols but none gave a redox response. Pyrolytic graphite electrodes similarly were ineffective in facilitating a redox signal. Finally, we turned to using a polymer-coated glassy carbon electrode into which the protein had been soaked over a period of hours. This method has been successful with cyclic voltammetry of other cytochromes we have studied in the past (Santini et al., 2007; Creevey et al., 2008). A pair of well defined redox peaks were identified with an average peak potential of +205 mV vs NHE at pH 6.8 (**Figure 4**). This technique is limited to relatively slow sweep rates (<20 mV/s) to ensure that the protein is able to diffuse through the polymer matrix. At higher sweep rates the waves became distorted. In the range 2–20 mV/s the average peak potential remained the same (**Figure 4**).

In contrast to the two cytochromes which could be purified with high yields, the pseudoazurin Azu2 was much more difficult to produce in soluble and cofactor-containing form. Most of the recombinant *S. meliloti* Azu2 was found in inclusion bodies, however, with optimized expression conditions some soluble protein could be obtained from periplasmic extracts (total yield of purified

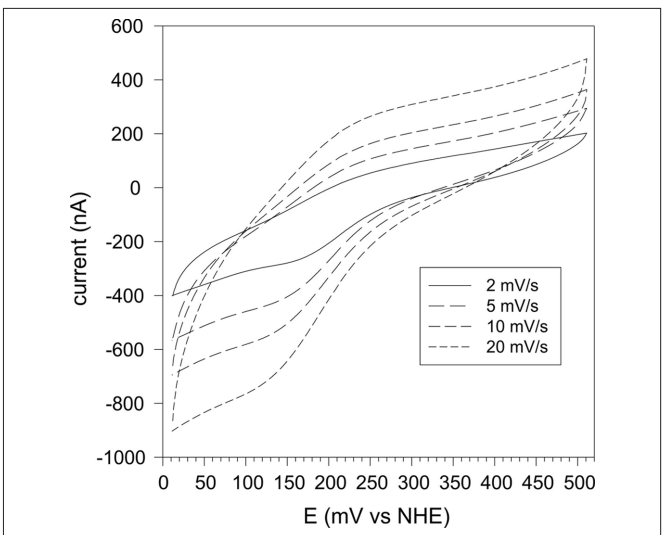

FIGURE 4 | Cyclic voltammetry of rSmc04048 at sweep rates of 2, 5, 10, and 20 mV/s and at pH 6.9. The protein was soaked into a polymer film cast on a glassy carbon electrode (see Materials and Methods).

protein: ~2 mg). Fractions containing purified rAzu2 had a blue color, and rAzu2 was found to be a monomeric protein with a molecular mass of 21 kDa as estimated by gel filtration and optical spectra reminiscent of other azurin proteins with peaks at 452, 591, and 758 nm. The relatively low ratio of the 591-nm absorbance peak to the protein peak at 280 nm (~0.1) suggests however, that only some of the purified rAzu2 protein contained the copper cofactor. The calculated molecular mass of mature, Histidine-tagged rAzu2 is 15677.85 Da, mass spectrometry revealed a molecular mass of 15678.26 ± 2 Da for rAzu2.

Cyclic voltammetry of rAzu2 was straightforward. After a range of different thiol modifiers were trialed, the most successful one was the long chain acid 11-mercaptoundecanoic acid which forms a self-assembled monolayer on the Au surface which is highly biocompatible with terminal carboxylic acid/carboxylate groups interacting with the surface of the protein. At this electrode surface a pair of anodic and cathodic peaks were observed (**Figure 5A**) whose potentials were markedly pH-dependent (**Figure 5B**). Between pH 8.3 and 6.8 this potential was invariant at *ca.* +200 mV vs NHE, however, below pH 6.8 the redox potential became pH-dependent with a −59/pH variation in potential. This is indicative of a proton coupled redox reaction (single electron/single proton; Clark, 1960). The pH-dependence was fit to such a model with a pK_a for the reduced (Cu^I) form of 6.3 (**Figure 4B**). It is also noteworthy that the redox response became weaker at the pH was raised above *ca.* 6.5. This is indicative of a weakening of the interaction between the terminal carboxylate groups at the electrode and the protein rAzu2 due to deprotonation. Presumably these key surface amino acid residues that undergo deprotonation (and are then repelled by the negatively charged electrode) are in proximity to the Cu center.

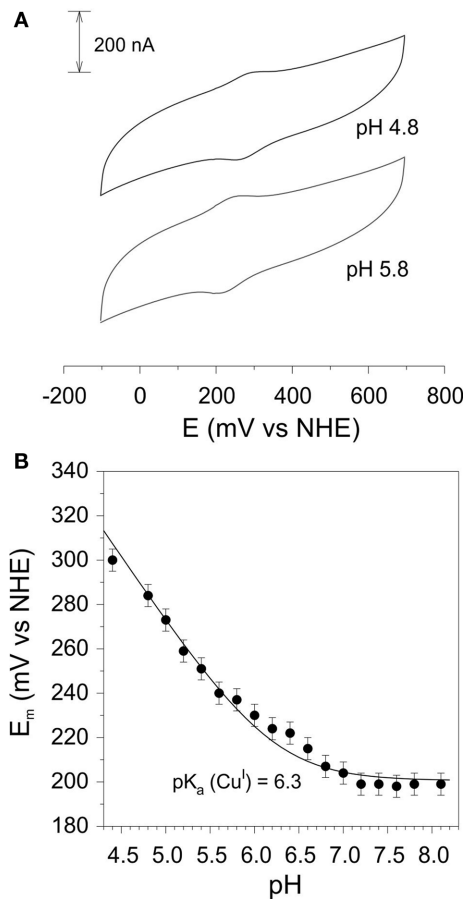

FIGURE 5 | (A) Cyclic voltammograms of rAzu2 at a 11-mercaptoundecanoic acid-modified Au working electrode at pH 4.5 and 5.5 (sweep rate 50 mV/s) **(B)** pH-dependence of the redox potential. Curve is the best fit to the data using Eq. 2 which gave a pK_a of 6.3 for the reduced (Cu^I) form of rAzu2. Experimental conditions: sweep rate 50 mV/s, 0.1 M phosphate titrated with NaOH or acetic acid to the desired pH.

INTERACTIONS BETWEEN SorT AND POTENTIAL ELECTRON ACCEPTORS

It had been previously reported that at pH 8.0 the native SorT only showed ~13% of the activity observed with ferricyanide when horse heart cytochrome was used as the electron acceptor. The activity of rSorT was tested with three different cytochromes, horse heart cytochrome *c*, the *S. meliloti* cytochrome rSmc04048 and the recombinant *Starkeya novella* cytochrome *c* $rSnc_{550}$, which is known to be the natural electron acceptor for the SorAB sulfite dehydrogenase (Kappler et al., 2000). Under standard assay conditions at pH 8.0, rSorT had activities of 7.4 ± 0.7, 33.4 ± 1.9, and 0.6 U/mg respectively with the three cytochromes. However, in all three cases only about 40% of the cytochrome added to the assay was reduced during the assay, which is in contrast to the reaction of the SorAB sulfite dehydrogenase which leads to a near complete reduction of the horse heart or *S. novella* cytochrome *c* present in the assay. For rSmc04048 the fraction of cytochrome reduced in the assay could be increased to >95% if the monomeric form of the protein was separated from the dimeric form by size exclusion chromatography, indicating that the rSmc04048 monomeric form interacts with rSorT. As the horse heart and *S. novella* cytochromes were in monomeric form, this excludes dimerization as a cause of their poor interaction with rSorT.

Further investigations of the interaction of rSmc04048 with rSorT showed that activity increased at lower pH with activities of 44.9 ± 3.7 and 57.7 ± 1.5 U/mg being observed at pH 7.0 and 6.0 respectively. This is in clear contrast to what is observed with ferricyanide as the electron acceptor, where activities are nearly pH invariant between pH 6.5 and 10, and then decrease at the extreme ends of the pH range tested.

No reduction of rAzu2 by rSorT was observed when rAzu2 was substituted for cytochrome *c* in assays conducted at pH 8.0, however, only low concentrations of rAzu2 could be used in these assays (standard: 8 μM, max: 56 μM) due to the limited amounts of protein available. Using a 56-μM protein solution, reduction of rAzu2 by sulfite (0.4 mM), and a combination of sulfite (0.4 mM) and rAzu2T was tested. Addition of sulfite produced no change in the rAzu2 absorption spectrum after incubation for 5 min, while following incubation with sulfite and rAzu2 for 5 min a 22% reduction of the absorption at 591 nm was observed, indicating that some reduction of rAzu2 had occurred. However, the absorbance change per minute for this reduction was only −0.002 ΔE_{595}/min Reduction of rAzu2 with dithionite led to a marked change in the absorbance spectrum with all absorbance features being significantly reduced to near baseline levels (data not shown).

DOES SorT REQUIRE MORE THAN ONE REDOX PROTEIN FOR EFFICIENT ELECTRON TRANSFER?

To investigate whether more than one redox carrier was required for efficient electron removal from rSorT the effect of inclusion of ferricyanide or purified rAzu2 in cytochrome *c* containing assay mixtures on enzyme activities was investigated. Inclusion of 50 μM ferricyanide in assays 40 μM containing any of the three cytochromes tested resulted in complete reduction of each cytochrome and reduction rates that increased ~15–20 times over the rates detected without ferricyanide. A small (1–8 s) initial lag that was not seen in assays that did not contain ferricyanide was observed in these assays.

This indicated that that ferricyanide might be acting as the primary electron acceptor and in turn could be reducing the cytochrome *c*. Another explanation could be that, like *Rhodobacter sphaeroides* DMSO reductase expressed in *E. coli* (Hilton et al., 1999), rSorT needs to undergo "redox cycling" to become fully active. If ferricyanide treatment of rSorT were required for full activity, this would not be apparent in the ferricyanide containing activity assays routinely used for SorT enzymes as an excess of the activating agent would always be present.

To test whether rSorT required redox activation, an aliquot of the enzyme was incubated in the presence of 16 μM ferricyanide for 10 min, before assaying activity (ferricyanide concentration in the assay: 0.08 μM). For horse heart cytochrome *c*, the activity with redox cycled rSorT showed very limited increase from 7 to 10 U/mg, however, addition of 50 μM ferricyanide to such an assay mixture immediately increased the cytochrome reduction rate to values similar to those observed with untreated rSorT. rSmc04048 based assays using redox treated SorT did not show increased cytochrome reduction rates. This suggests that ferricyanide may have acted as a primary electron acceptor, and then subsequently transferred electrons to the different cytochromes *c.* The apparent "preference" of rSorT for ferricyanide over the cognate rSmc04048 cytochrome could be due to the difference in molecular mass of the two electron acceptors.

Inclusion of 8 μM Azu2 in the assays did not change the rSmc04048 reduction rates relative to the rates observed when only rSmc04048 was present at either pH 6, 7, or 8. Due to the strong absorbance of the heme group in rSmc04048 it was not possible to monitor whether absorbance changes occur in the rAzu2 spectrum, and it could therefore not be determined whether the cytochrome or rAzu2 is reduced first, or whether rAzu2 participates in the reaction at all (**Figure 1**).

INTERACTIONS OF rSorT WITH COMPONENTS OF THE RESPIRATORY CHAIN

In addition to using a small redox protein as its natural electron acceptor, it is also possible that rSorT might either use molecular oxygen as an electron acceptor or interact directly with the cytochrome *c* oxidase or other respiratory complexes present in the cell membrane (**Figure 1**). We investigated these possibilities using an oxygen electrode and cell membranes isolated from *S. meliloti* grown on taurine-containing medium.

Addition of sulfite to the buffer in the oxygen electrode chamber led to a background oxygen consumption rate of −1.05 ± 0.07 nmol/mL/min. This rate was subtracted from all "enzymatic" oxygen consumption rates observed. With this correction, rSorT gave rise to a negligible oxygen consumption rate of −0.2 ± 0.21 nmol/mL/min, indicating that like the native enzyme, rSorT does not have significant sulfite oxidase activity.

When sulfite was added to membrane preparations a corrected respiratory rate of −1.81 ± 0.5 nmol/min/mL was observed while membrane preparations with sulfite and rSorT added resulted in a rate of −1.21 ± 0.07 nmol/mL/min. This suggests that in the presence of its substrate, sulfite, rSorT did not enhance respiratory activity, indicating that it was unlikely that rSorT interacted directly with any respiratory chain complexes.

When either rSmc04048 or rAzu2 were added to assays containing membrane preparations and sulfite at concentrations similar to those used in standard assays, oxygen consumption rates of −64 ± 6 nmol/min/mL and −62 nmol/min/mL were recorded. This clearly shows that both redox proteins were capable of interaction with the *S. meliloti* respiratory chain components, although we were unable to demonstrate an increase in the observed oxygen consumption rates following addition of purified rSorT to rSmc04048 containing assays. As the only substrate added to the assay was sulfite, and neither rSmc04048 nor rAzu2 are reduced by sulfite in standard photometric assays at a significant rate. These results suggest that some component of the membrane preparation must have been able to use sulfite as a substrate and then to reduce either the azurin or the cytochrome, which in turn were passing on electrons to a respiratory chain component, most likely a cytochrome oxidase. It is possible that the membrane preparations may have contained some SorT, as this protein is highly abundant in *S. meliloti* grown on taurine and some soluble proteins may have been present in the preparation. During the purification of SorT from *S. melioti* no SorT-independent SOE activity was noted (Wilson and Kappler, 2009).

DISCUSSION

With the exception of the plant sulfite oxidase, which is a true sulfite oxidase, all sulfite-oxidizing molybdenum enzymes for which the natural electron acceptor is known couple sulfite oxidation to the reduction of a cytochrome *c*. Although the SorT sulfite dehydrogenase from *S. meliloti* is a representative of the "atypical" bacterial SDHs that show highest activities with the artificial electron acceptor ferricyanide, our data suggest that *in vivo* the reaction of SorT is coupled to a cognate cytochrome *c* that is found in the *sorT* operon.

In order to carry out this work it was first necessary to establish an efficient overexpression system for SorT, which increased the yields of purified protein from about 70 μg for the native enzyme to over 15 mg/L of bacterial culture for the rSorT. The low yields for the native enzyme are not due to a low abundance of SorT in *S. meliloti*, but to the fact that several proteins co-purify with SorT and cannot be removed from the majority of the enzyme present in cell extracts (Wilson and Kappler, 2009). Our data show that rSorT is fully active and its subunit structure and catalytic properties are very similar to those of the native enzyme, demonstrating that the cytoplasmic expression system used for the production of rSorT does not have an impact on enzyme performance or structure. In *S. meliloti* the mature SorT and the two acceptor proteins are located in the periplasmic space, i.e., in the same, extracellular compartment.

Like the native enzyme, rSorT had low activity (7 U/mg) with horse heart cytochrome *c*, however, rSorT showed good activities with the cognate rSmc04048 cytochrome (33.4 U/mg). In contrast, rSorT only showed negligible activity (0.6 U/mg) with the *S. novella* cytochrome c_{550}, which is known to be the natural electron acceptor of the SorAB sulfite dehydrogenase.

A possible cause of this could be differences in the redox potentials of the three cytochromes. As SorT interacts very well with ferricyanide, which has a very high redox potential of +430 mV vs NHE, it could be possible that SorT requires an acceptor protein with a very high redox potential. The reported redox potentials for horse heart cytochrome *c* and the *S. novella* cytochrome c_{550} are relatively high with +263 and +302 mV vs NHE respectively (Kappler et al., 2000; Battistuzzi et al., 2002), however, the redox potential of rSmc04048 was only +205 mV (pH 6.8). It thus appears that rSorT interaction with the three cytochromes is not governed primarily by the redox potential of the acceptor protein.

Analysis of the three cytochromes on a molecular level uncovered further. Both the horse heart cytochrome and the *S. novella* cytochrome have basic isoelectric points (computed pI 9.59 and 8.86, respectively) and thus are positively charged at pH 7. In contrast, the Smc04048 cytochrome has an isoelectric point of 4.29 (pI 4.78 for His-tagged rSmc04048), and thus is negatively charged at physiological pH values. This difference in the charge state is likely to be a major factor in determining the interactions of rSorT with the cytochromes. However, in addition to the overall charge of the protein, structural determinants likely also play a role in shaping the interactions of rSorT with the cytochromes, as activity with horse heart cytochrome *c* which has the highest pI and is strongly positively charged (calculated total charge of +9 at pH 7) was 7 U/mg, while with the less strongly charged *S. novella* cytochrome (computed charge state +3.45 at pH 7) SDH activity was only 0.6 U/mg. The differences in the cytochrome fold and surface charge distribution should be investigated further in the future.

An interesting observation was that inclusion of ferricyanide in cytochrome *c* based assays led to a very strong increase of reduction rates for all three cytochromes tested, with the small lag observed initially being likely to indicate that ferricyanide was being reduced first, before cytochrome reduction started to take place. Ferricyanide is clearly not a natural electron acceptor for this enzyme, however, relative to any electron accepting proteins it is a very small compound, which leads to faster diffusion rates which in turn would enable a more efficient interaction with SorT relative to the cytochromes. The positive redox potential of ferricyanide (+430 mV vs NHE) could also contribute to a favorable interaction with SorT, however, it does not explain how subsequently the cytochromes, all of which have less positive redox potentials, are being reduced. We suggest that the interaction between the cytochromes and ferrocyanide might be charge-driven. In this case, interaction between positively charged cytochrome molecules and the strongly negatively charged ferricyanide would lead to the formation of a strong outer sphere complex that would favor the reduction of the cytochromes despite the unfavorable redox potentials. This has been experimentally observed for ferrocyanide and cobalt complexes (Bernhardt et al., 2002, 2005). However, studies of the electron transfer pathways in SorT and the respective sites of interaction with the acceptor cytochrome and ferri-/ferrocyanide will be required to fully understand this phenomenon.

The physiological role of the pseudoazurin, Azu2, which is also part of the *sorT* operon, remains, at this stage, elusive, which is partly due to the low protein yield obtained for rAzu2 that prevented more extensive investigations. rAzu2 did not appear to be reduced directly by rSorT at pH 8.0, and caused no significant changes in observed rSorT activity when it was added to assays in addition to rSmc04048. If anything, rSorT activities were slightly lower in assays containing rAzu2 as well as rSmc04048 although this difference was within the experimental error. If rAzu2 were participating in electron transfer within the SorT system, this might be indicative of rAzu2 accepting electrons from rSmc04048, which would lead to an apparent lowering of the cytochrome *c* reduction rate through reoxidation of reduced cytochrome molecules. However, insufficient rAzu2 was available to investigate this possibility in detail.

Based on our results we propose that SorT uses the Smc04048 cytochrome *c* as its *in vivo* electron acceptor, and that electrons get passed on to the cytochrome oxidase either directly or potentially via Azu2 (**Figure 6**).

DO ALL FERRICYANIDE-LINKED SDHs USE Smc04048-LIKE CYTOCHROMES AS ELECTRON ACCEPTORS?

SorT is a representative of the "atypical," "ferricyanide-linked" SDHs which have been isolated from a variety of microorganisms including extremophiles such as *Thermus thermophilus, Deinococcus radiodurans* and organosulfonate degraders such as *Cupriavidus necator*, *Delftia acidovorans* (Kappler, 2011). Since SorT is the first SDH of its type for which a natural electron acceptor has been identified we investigated whether Smc04048 and Azu2-like protein were associated with any of the other ferricyanide-linked SOEs. With the exception of the enzyme from *Deinococcus radiodurans*, all genes encoding characterized SDHs are found upstream of genes encoding *c*-type cytochromes (Kappler, 2011), however, only the cytochrome *c* encoded downstream of the *Delftia acidovorans* SDH (Daci_0054) showed significant homology to Smc04048 (52% amino acid sequence similarity). For all other SDH associated cytochromes amino acid sequence similarities with Smc04048 were between 18 and 24%.

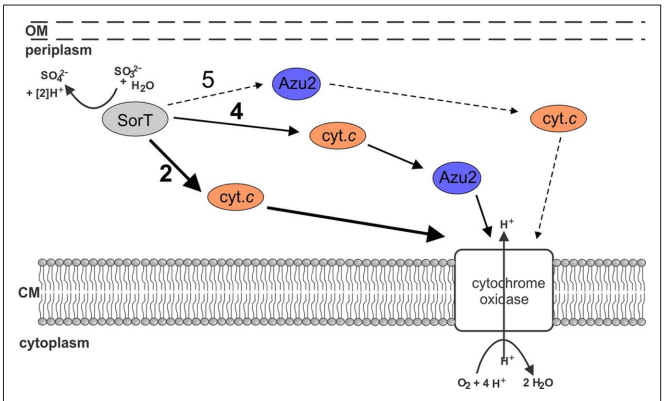

FIGURE 6 | Current working model of electron transfer pathways between SorT and the respiratory chain. The main pathway appears to be no. 2 using the Smc04048 cytochrome *c* as an electron carrier. It is also possible that both Smc04048 and Azu2 participate in electron transfer (pathways 4 + 5), however, based on present data it seems unlikely that pathway 5 would play a significant role in electron transfer.

Protein sequences related to Smc04048 were identified using BLASTP searches (**Figure 7**). In some cases, Smc04048 related sequences were observed as domains of larger proteins (e.g., *Ixodes scapularis*, *Conexibacter woesei*), and such fusion proteins were excluded from further analysis. The only fusion proteins that were retained in later analyses were from the marine gamma Proteobacteria HTCC2080 and HTCC2148, where the Smc04048-like protein had been fused to a SorT-like protein. Smc04048 is distantly related to cytochrome c_6 from *Synechococcus* sp. JA-2-3Ba(2-13) and to the SoxX cytochromes. Twenty-two of the Smc04048-like proteins were encoded by genes that were located adjacent to genes encoding SorT-like proteins (**Figure 7**). In some other cases, e.g., *Marinobacter hydrocarbonoclasticus* and *Marinosulfomonas methylotropha* only limited sequence data was available, and thus it could not be ascertained whether a similar gene arrangement exists in these organisms. For *Verminephrobacter eiseniae* a pseudogene (Veis_1600) encoding an Smc04048 related cytochrome was identified adjacent to the gene encoding the SorT-like SDH (Veis_1599) from this organism, however, this protein sequence was not included in the analysis due to its classification as a pseudogene.

Phylogenetic analysis of the SorT and Smc04048 related sequences clearly shows the similarity of the respective clades (**Figure 7**). In contrast, Azu2-like proteins only occurred in *sorT* operons of species of *Sinorhizobium*; although many other Azu2 related sequences were found in the database these genes did not occur in operons also containing SDH-encoding genes (data not shown).

This analysis confirms what had already been observed as part of a general analysis of the SO enzyme family (Kappler, 2008, 2011), namely that while the majority of the genes encoding the SOE Mo-binding subunits occur adjacent to genes encoding *c*-type cytochromes, these *c*-type cytochromes are specific to particular subtypes of SDHs and are not conserved outside their immediate phylogenetic grouping. Examples of this are the genes encoding the SorB subunit of the SorAB-type SDH from *S. novella*, the *soxC* and *soxD* subunits of the sulfur dehydrogenases (Kappler, 2008) and those encoding SorT and Smc04048 that were studied here. Our results also underline the catalytic and structural plasticity of the SDH proteins, as it should be extremely interesting to study the SDH/cytochrome fusion proteins found in the two marine bacteria and to observed the structural and kinetic properties of these proteins.

CONCLUSION

We have for the first time identified a natural electron acceptor for one of the "atypical," ferricyanide-linked SDHs, and found it to be a cytochrome *c* that is capable of transferring electrons to the respiratory chain and most likely directly to the cytochrome oxidase. Although this may seem unsurprising as other SDHs have been shown to interact with *c*-type cytochromes in this manner, the Smc04048 cytochrome was shown to have molecular properties that differed significantly from those of other characterized SDH electron acceptor cytochromes in terms of its charge state. The function of the Azu2 protein for the

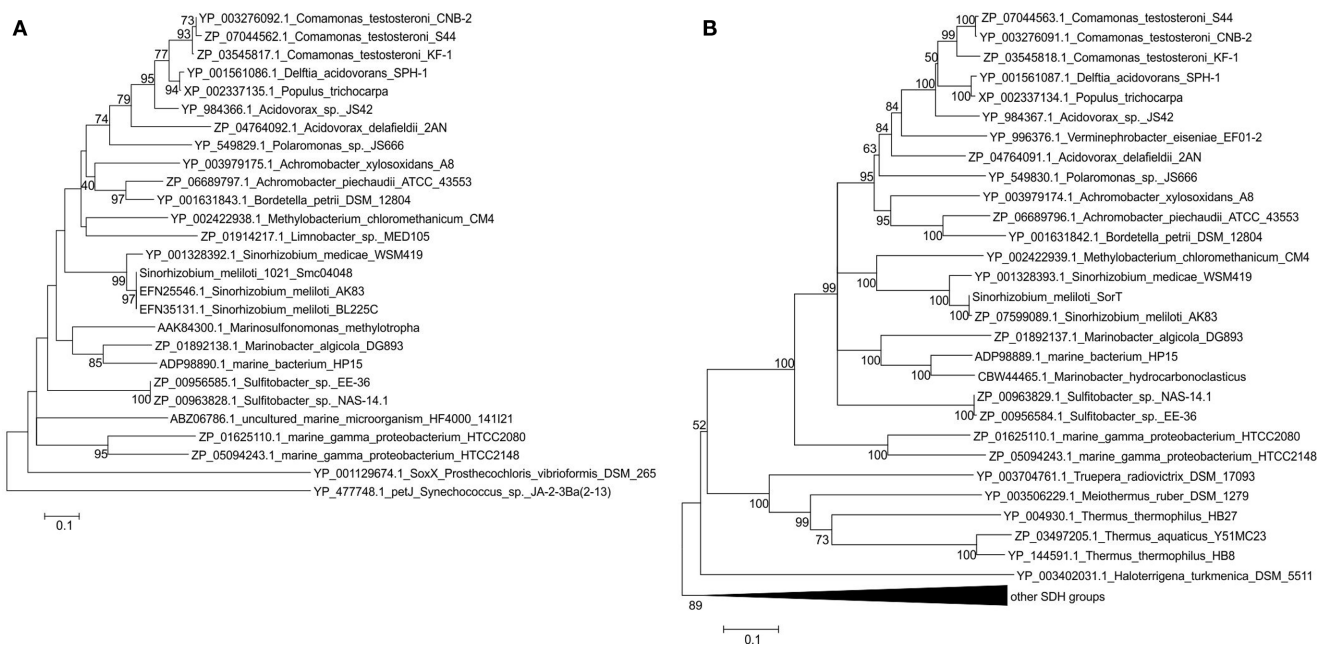

FIGURE 7 | Phylogenetic analysis of Smc04048 and SorT related protein sequences available in the database. (A) Neighbor-joining tree or Smc04048 related protein sequences **(B)** neighbor-joining tree of SorT (Smc04049). Bootstrapping used 500 samples, for clarity bootstrap values below 40 are not shown. Minimum Evolution and Maximum Parsimony algorithms were also used and generated trees with the same topology and very similar bootstrap values for both sequences setc. Sequence accession numbers are shown in the figure. The sequences from the two marine gamma Proteobacteria are fusions between a *smc04048* and a *sorT* genes, the cytochromes from *Sulfitobacter* species are diheme cytochromes. The pseudogene Veis_1600 that encodes an Smc04048 related protein from *Verminephrobacter eiseniae* was not included in the dataset.

SDH reaction remains unclear at this stage and its role needs to be investigated further, especially as Azu2 proteins are only encoded in SDH operons of *Sinorhizobium* species. Future work will focus on the kinetics of the cytochrome linked SorT activity will also be studied in more detail, including the significance of the Smc04048 monomer/dimer interconversion. Furthermore the structures of these proteins will be determined to enable the identification of surface areas involved in the SorT/Smc04048 interactions, and to reveal any structural differences that may exist between Smc04048 and other cytochromes known to accept electrons from SOEs.

ACKNOWLEDGMENTS

This work was supported by a grant (DP0878525) and fellowship from the Australian Research Council to UK and grant DP0880288 to Paul V. Bernhardt.

REFERENCES

Arslan, E., Schulz, H., Zufferey, R., Kunzler, P., and Thony-Meyer, L. (1998). Overproduction of the *Bradyrhizobium japonicum c*-type cytochrome subunits of the *cbb(3)* oxidase in *Escherichia coli*. *Biochem. Biophys. Res. Comm.* 251, 744–747.

Ausubel, F. M., Brent, R., Kingston, R. E., Moore, D. D., Seidman, J. G., Smith, J. A., and Struhl, K. (2005). *Current Protocols in Molecular Biology*, ed. K Janssen. Hoboken, NJ: John Wiley & Sons Inc.

Battistuzzi, G., Borsari, M., Cowan, J. A., Ranieri, A., and Sola, M. (2002). Control of cytochrome *c* redox potential: axial ligation and protein environment effects. *J. Am. Chem. Soc.* 124, 5315–5324.

Beringer, J. E. (1974). R factor transfer in *Rhizobium leguminosarum*. *J. Gen. Microbiol.* 84, 188–198.

Bernhardt, P. V., Bozoglian, F., Macpherson, B. P., and Martinez, M. (2005). Molecular mixed-valence cyanide bridged coiii-feii complexes. *Coord. Chem. Rev.* 249, 1902–1916.

Bernhardt, P. V., Macpherson, B. P., and Martinez, M. (2002). The influence of cis/trans isomerism on the physical properties of a cyano-bridged dinuclear mixed valence complex. *J. Chem. Soc. Dalton Trans.* 1435–1441.

Berry, E. A., and Trumpower, B. L. (1987). Simultaneous determination of hemes a, b and c from pyridine hemochrome spectra. *Anal. Biochem.* 161, 1–15.

Clark, W. M. (1960). *The Oxidation-Reduction Potentials of Organic Systems*. Baltimore: The Williams and Wilkins Company.

Creevey, N. L., McEwan, A. G., Hanson, G. R., and Bernhardt, P. V. (2008). Thermodynamic characterization of the redox centers within dimethylsulfide dehydrogenase. *Biochemistry* 47, 3770–3776.

D'Errico, G., Di Salle, A., La Cara, F., Rossi, M., and Cannio, R. (2006). Identification and characterization of a novel bacterial sulfite oxidase with no heme binding domain from *Deinococcus radiodurans*. *J. Bacteriol.* 188, 694–701.

Denger, K., Weinitschke, S., Smits, T. H. M., Schleheck, D., and Cook, A. M. (2008). Bacterial sulfite dehydrogenases in organotrophic metabolism: separation and identification in *Cupriavidus necator* h16 and in *Delftia acidovorans* sph-1. *Microbiology* 154, 256–263.

Di Salle, A., D'Errico, G., La Cara, F., Cannio, R., and Rossi, M. (2006). A novel thermostable sulfite oxidase from *Thermus thermophilus*: characterization of the enzyme, gene cloning and expression in *Escherichia coli*. *Extremophiles* 10, 587–598.

Eilers, T., Schwarz, G., Brinkmann, H., Witt, C., Richter, T., Nieder, J., Koch, B., Hille, R., Haensch, R., and Mendel, R. R. (2001). Identification and biochemical characterization of *Arabidopsis thaliana* sulfite oxidase – a new player in plant sulfur metabolism. *J. Biol. Chem.* 276, 46989–46994.

Hill, J. M., Kobe, B., Guss, M., and Huber, T. (2007). "Nmr screening for rapid protein characterisation in structural proteomics," in *Structural Proteomics: High-Throughput Methods*, eds B. Kobe, M. Guss and T. Huber (Totowa, NJ: Humana Press).

Hille, R. (1996). The mononuclear molybdenum enzymes. *Chem. Rev.* 96, 2757–2816.

Hilton, J. C., Temple, C. A., and Rajagopalan, K. V. (1999). Re-design of *Rhodobacter sphaeroides* dimethyl sulfoxide reductase. Enhancement of adenosine n1-oxide reductase activity. *J. Biol. Chem.* 274, 8428–8436.

Kalimuthu, P., Tkac, J., Kappler, U., Davis, J. J., and Bernhardt, P. V. (2010). Highly sensitive and stable electrochemical sulfite biosensor incorporating a bacterial sulfite dehydrogenase. *Anal. Chem.* 82, 7374–7379.

Kappler, U. (2008). "Bacterial sulfite dehydrogenases – enzymes for chemolithtrophs only?" in *Microbial Sulfur Metabolism*, eds C. Dahl and C. G. Friedrich (Berlin: Springer), 151–169.

Kappler, U. (2011). Bacterial sulfite-oxidizing enzymes. *Biochim. Biophys. Acta* 1807, 1–10.

Kappler, U., and Bailey, S. (2005). Molecular basis of intramolecular electron transfer in sulfite-oxidizing enzymes is revealed by high resolution structure of a heterodimeric complex of the catalytic molybdopterin subunit and a *c*-type cytochrome subunit. *J. Biol. Chem.* 280, 24999–25007.

Kappler, U., Bennett, B., Rethmeier, J., Schwarz, G., Deutzmann, R., McEwan, A. G., and Dahl, C. (2000). Sulfite: cytochrome *c* oxidoreductase from *Thiobacillus novellus* – purification, characterization and molecular biology of a heterodimeric member of the sulfite oxidase family. *J. Biol. Chem.* 275, 13202–13212.

Kappler, U., and Dahl, C. (2001). Enzymology and molecular biology of prokaryotic sulfite oxidation. *FEMS Microbiol. Lett.* 203, 1–9.

Laemmli, U. K. (1970). Cleavage of structural protein during the assembly of the head of bacteriophage t4. *Nature* 227, 680–685.

Myers, J. D., and Kelly, D. J. (2005). A sulphite respiration system in the chemoheterotrophic human pathogen *Campylobacter jejuni*. *Microbiology* 151, 233–242.

Palmer, T., Santini, C. L., Iobbi Nivol, C., Eaves, D. J., Boxer, D. H., and Giordando, G. (1996). Involvement of the narj and mob gene products in distinct steps in the biosynthesis of the molybdoenzyme nitrate reductase in *Escherichia coli*. *Mol. Microbiol.* 20, 875–884.

Rajagopalan, K. V. (1980). "Sulfite oxidase (sulfite: ferricytochrome c oxidoreductase)," in *Molybdenum and Molybdenum-Containing Enzymes*, ed. M. P. Coughlan (Oxford: Pergamon Press), 243–272.

Reichenbecher, W., Kelly, D. P., and Murrell, J. C. (1999). Desulfonation of propanesulfonic acid by *Comamonas acidovorans* strain p53: evidence for an alkanesulfonate sulfonatase and an atypical sulfite dehydrogenase. *Arch. Microbiol.* 172, 387–392.

Santini, J. M., Kappler, U., Ward, S. A., Honeychurch, M. J., vanden Hoven, R. N., and Bernhardt, P. V. (2007). The nt-26 cytochrome *c*552 and its role in arsenite oxidation. *Biochim. Biophys. Acta* 1767, 189–196.

Schrader, N., Fischer, K., Theis, K., Mendel, R. R., Schwarz, G., and Kisker, C. (2003). The crystal structure of plant sulfite oxidase provides insights into sulfite oxidation in plants and animals. *Structure* 11, 1251–1263.

Southerland, W. M., and Rajagopalan, K. V. (1978). Domain interactions in oxidized and reduced forms of rat liver sulfite oxidase. *J. Biol. Chem.* 253, 8753–8758.

Tamura, K., Dudley, J., Nei, M., and Kumar, S. (2007). Mega4: molecular evolutionary genetics analysis (mega) software version 4.0. *Mol. Biol. Evol.* 24, 1596–1599.

Temple, C. A., Graf, T. N., and Rajagopalan, K. V. (2000). Optimization of expression of human sulfite oxidase and its molybdenum domain. *Arch. Biochem. Biophys.* 383, 281–287.

Thomas, P. E., Ryan, D., and Levit, M. (1976). An improved staining procedure for the detection of peroxidase activity of cytochrome p-450 on sodium dodecyl sulfate polyacrylamide gels. *Anal. Biochem.* 75, 168–176.

Tkac, J., and Davis, J. J. (2008). An optimised electrode pre-treatment for sam formation on polycrystalline gold. *J. Electroanal. Chem.* 621, 117–120.

Wilson, J. J., and Kappler, U. (2009). Sulfite oxidation in *Sinorhizobium meliloti*. *Biochim. Biophys. Acta* 1787, 1516–1525.

Yamanaka, T., Yoshioka, T., and Kimura, K. (1981). Purification of sulphite cytochrome *c* reductase of *Thiobacillus novellus* and reconstitution of its sulphite oxidase system with the purified constituents. *Plant Cell Physiol.* 22, 613–622.

Conflict of Interest Statement: The authors declare that the research was conducted in the absence of any commercial or financial relationships that could be construed as a potential conflict of interest.

Received: 01 February 2011; paper pending published: 13 March 2011; accepted: 15 March 2011; published online: 25 March 2011.

Citation: Low L, Kilmartin JR, Bernhardt PV and Kappler U (2011) How are "atypical" sulfite dehydrogenases linked to cell metabolism? Interactions between the SorT sulfite dehydrogenase and small redox proteins. Front. Microbio. ***2****:58. doi: 10.3389/fmicb.2011.00058*

This article was submitted to Frontiers in Microbial Physiology and Metabolism, a specialty of Frontiers in Microbiology.

frontiers in MICROBIOLOGY

ORIGINAL RESEARCH ARTICLE
published: 13 April 2011
doi: 10.3389/fmicb.2011.00071

Structural insights into dissimilatory sulfite reductases: structure of desulforubidin from *Desulfomicrobium norvegicum*

Tânia F. Oliveira[1,2], Edward Franklin[2], José P. Afonso[3], Amir R. Khan[2], Neil J. Oldham[3], Inês A. C. Pereira[1]* and Margarida Archer[1]*

[1] Instituto de Tecnologia Química e Biológica, Universidade Nova de Lisboa, Oeiras, Portugal
[2] School of Biochemistry and Immunology, Trinity College, Dublin, Ireland
[3] School of Chemistry, University of Nottingham, Nottingham, UK

Edited by:
Martin G. Klotz, University of Louisville, USA

Reviewed by:
John Robert Cort, Pacific Northwest National Laboratory, USA
Vilmos Fulop, University of Warwick, UK

***Correspondence:**
Margarida Archer, Membrane Protein Crystallography Laboratory, Instituto de Tecnologia Química e Biológica, Universidade Nova de Lisboa, Avenida da República EAN, 2780-157 Oeiras, Portugal.
e-mail: archer@itqb.unl.pt;
Inês A. C. Pereira, Bacterial Energy Metabolism Laboratory, Instituto de Tecnologia Química e Biológica, Universidade Nova de Lisboa, Avenida da República EAN, 2780-157 Oeiras, Portugal.
e-mail: ipereira@itqb.unl.pt

Dissimilatory sulfite reductases (dSiRs) are crucial enzymes in bacterial sulfur-based energy metabolism, which are likely to have been present in some of the earliest life forms on Earth. Several classes of dSiRs have been proposed on the basis of different biochemical and spectroscopic properties, but it is not clear whether this corresponds to actual physiological or structural differences. Here, we describe the first structure of a dSiR from the desulforubidin class isolated from *Desulfomicrobium norvegicum*. The desulforubidin (Drub) structure is assembled as $\alpha_2\beta_2\gamma_2$, in which two DsrC proteins are bound to the core $[DsrA]_2[DsrB]_2$ unit, as reported for the desulfoviridin (Dvir) structure from *Desulfovibrio vulgaris*. Unlike Dvir, four sirohemes and eight [4Fe–4S] clusters are present in Drub. However, the structure indicates that only two of the Drub coupled siroheme-[4Fe–4S] cofactors are catalytically active. Mass spectrometry studies of purified Drub and Dvir show that both proteins present different oligomeric complex forms that bind two, one, or no DsrC proteins, providing an explanation for conflicting spectroscopic and biochemical results in the literature, and further indicating that DsrC is not a subunit of dSiR, but rather a protein with which it interacts.

Keywords: sulfite reductases, sulfur metabolism, sulfate reducing bacteria, siroheme, iron–sulfur clusters, X-ray structure

INTRODUCTION

Microorganisms play an important role in sulfur transformations and are a critical component of sulfur cycling on our planet. Many Bacteria and Archaea have the ability to use sulfur compounds in a series of oxidation or reduction reactions, thereby generating metabolic energy in the process of dissimilatory metabolism. Data from isotopic analysis suggests that dissimilatory reduction of sulfur compounds is an extremely ancient process which began 3.5 billion years ago (Canfield and Raiswell, 1999; Canfield et al., 2006). After sulfate concentrations increased significantly in the Precambrian oceans approximately 2.5 billion years ago, reduction of sulfate also became of global significance (Canfield et al., 2006). A key enzyme in the reduction of sulfate/sulfite is the dissimilatory sulfite reductase (dSiR), which is responsible for the six electron reduction of sulfite to sulfide. dSiRs belong to a redox enzyme super family, characterized by the presence of a coupled siroheme-[4Fe–4S] cluster cofactor, which include assimilatory sulfite (aSiRs) and nitrite reductases, and other types of sulfite reductases (Crane and Getzoff, 1996; Dhillon et al., 2005; Loy et al., 2007). The dSiR is composed of two subunits, DsrA and DsrB, in a ~200 kDa $\alpha_2\beta_2$ arrangement. The *dsrA* and *dsrB* genes are paralogous and probably originated from duplication of an early *dsr* gene before the separation of the Archaea and Bacteria domains (Dahl et al., 1993; Molitor et al., 1998; Wagner et al., 1998). aSiRs, which generate sulfide for incorporation into amino-acids and cofactors, are monomeric enzymes with an internal two-fold symmetry of a unit related to DsrA/DsrB, which suggests gene duplication, followed by gene fusion of an ancestral sulfite reductase gene present in a very early life form (Crane et al., 1995, 1996; Dhillon et al., 2005). After the early divergence of the aSiR and dSiR genes there was incorporation of a ferredoxin domain in the *dsr* gene before separation into the *dsrA* and *dsrB* genes (Dahl et al., 1993). Evolutionary analysis of the *dsrAB* genes indicates they were mainly inherited via vertical transmission, except for a few events of lateral gene transfer, namely in the archaeal genus *Archaeoglobus*, which has *dsrAB* genes of bacterial origin, in the thermophilic genus *Thermodesulfobacterium*, and Gram-positive bacteria of the *Firmicutes* phylum like *Desulfotomaculum* species (Wagner et al., 1998; Klein et al., 2001; Zverlov et al., 2005; Loy et al., 2007). In contrast to aSiRs, which reduce sulfite directly to sulfide, the *in vitro* product of dSiRs is not only sulfide, but a mixture of products including also trithionate and thiosulfate (Peck and LeGall 1982), suggesting other proteins may be required for the complete reduction to sulfide. Thus, the mechanism and physiological products of dissimilatory reduction by dSiRs is still a matter of debate.

Biochemical studies of dSiRs led to their categorization into four different classes based on UV/visible absorption and other molecular characteristics (Rabus et al., 2007): Desulfoviridin (Dvir), a green protein (characteristic absorption peak at 628 nm) present in *Desulfovibrio* spp. (Lee and Peck, 1971; Moura et al., 1988; Pierik and Hagen, 1991; Steuber et al., 1994; Wolfe et al., 1994); Desulforubidin (Drub), a reddish-brown protein (characteristic absorption peak at 545 nm) present in *Desulfomicrobium* and *Desulfosarcina* spp. (Lee et al., 1973; Moura et al., 1988; Arendsen et al., 1993; DerVartanian, 1994); Desulfofuscidin (characteristic absorption peak at 576 nm) present in *Thermodesulfobacterium* spp. (Hatchikian and Zeikus, 1983; Hatchikian, 1994); and the brown colored P-582 protein (characteristic absorption peak at 582 nm) present in *Desulfotomaculum* spp. (Akagi et al., 1974). All these dSiRs are proposed to assemble as $\alpha_2\beta_2$, but the type and content of the cofactors has been the subject of some controversy (Rabus et al., 2007).

After many years of failed attempts, the first X-ray structures of dSiRs were determined, including the Dvir from *Desulfovibrio vulgaris* Hildenborough at 2.10 Å (Oliveira et al., 2008a), and dSiR from *Archaeoglobus fulgidus* at 2.04 Å resolution (Schiffer et al., 2008), showing an $\alpha_2\beta_2$ arrangement with similar overall folds, and finally shedding light on the cofactor composition of these proteins. Four sirohemes and eight [4Fe–4S] clusters are present in *A. fulgidus* dSiR, whereas two sirohemes, two sirohydrochlorins (the metal-free form of siroheme), and eight [4Fe–4S] clusters are present in *D. vulgaris* Dvir. Nevertheless, only two sirohemes per $\alpha_2\beta_2$ unit are proposed to be catalytically active in both proteins. The sequence-based predictions of a similar fold to aSiRs, and of a separate ferredoxin domain containing a [4Fe–4S] cluster that transfers electrons to the active site, were confirmed by these structures. In addition, the crystal structure of *D. vulgaris* Dvir provided important functional information, because it comprised the DsrAB subunits complexed with the DsrC protein in a $\alpha_2\beta_2\gamma_2$ arrangement. DsrC was originally thought to constitute a third subunit of dSiR (Pierik et al., 1992), but has subsequently been recognized as an independent protein that interacts with DsrAB (Steuber et al., 1995; Cort et al., 2001, 2008; Dahl et al., 2005; Mander et al., 2005; Pires et al., 2006), and is homologous to the TusE protein involved in biosynthetic sulfur-relay reactions (Ikeuchi et al., 2006; Numata et al., 2006). In the structure of the *D. vulgaris* DsrAB–DsrC complex, the strictly conserved Cys at the C-terminus of DsrC is positioned right next to the substrate-binding site pointing to the involvement of DsrC in the reduction of sulfite (Oliveira et al., 2008a).

More recently, the crystal structure of the Dvir from *Desulfovibrio gigas* has been reported in two active forms (Dvir-I and Dvir-II; Hsieh et al., 2010), also including the DsrAB and DsrC proteins. The overall structure of the two *D. gigas* Dvir forms are very similar to *D. vulgaris* Dvir, and the C-terminal tail of DrsC from both forms is either inserted into the channel formed between DsrA and DsrB or swung away from the catalytic siroheme (Hsieh et al., 2010). *D. gigas* Dvir belongs to the Dvir class, and comprises eight iron–sulfur clusters, two sirohemes, and two sirohydrochlorins, as reported for Dvir. However, Dsr-II contains a [3Fe–4S] cluster associated with the siroheme instead of the usual [4Fe–4S] center, observed in all the other structures analyzed so far. Additionally, the *A. fulgidus* DsrAB structure has been characterized in complex with several ligands (Parey et al., 2010).

In this work we report the 3D structure of a dSir from a different class, the Drub isolated from *Desulfomicrobium norvegicum*, at 2.5 Å resolution. Moreover, we report mass spectrometry studies of both Drub and Dvir that provide important insights into the quaternary structures of these proteins in solution.

MATERIALS AND METHODS

PROTEIN PURIFICATION

Desulfomicrobium norvegicum (formerly known as *Desulfovibrio desulfuricans* strain Norway 4 and *Desulfovibrio baculatus* strain Norway 4) was grown in lactate/sulfate medium and cell extracts prepared as previously described (Pereira et al., 2006). The purification protocol was performed aerobically at 6°C. The soluble fraction was loaded on a DEAE-Sepharose fast flow XK50/30 column (GE Healthcare) equilibrated with 20 mM Tris–HCl pH 7.6 buffer. A stepwise gradient of increasing NaCl concentration (0 to 1 M, incremental steps of 0.05 M) was performed. The fraction eluted with 300 mM NaCl was dialyzed against 20 mM Tris–HCl pH 7.6. The protein was then concentrated and loaded onto a Q-Sepharose 26/10 ion-exchange column (GE Healthcare), and a similar procedure was performed. The protein sample was then subjected to size exclusion chromatography on a Sephacryl S-200 HR (GE Healthcare). Finally, the protein was dialyzed in 20 mM Tris–HCl pH 7.6 and loaded onto a Mono Q 5/50 GL column (GE Healthcare) and eluted using the same NaCl step gradient as outlined above. All purification steps were monitored by Sodium Dodecyl Sulfate Polyacrylamide Gel Electrophoresis (SDS-PAGE) and UV–visible spectroscopy analysis.

CRYSTALLIZATION

The protein was concentrated with Amicon (100 kDa cutoff) to 8 mg ml^{-1} in 20 mM Tris–HCl pH 7.6 and was further used for crystallization trials with a TTP LabTech's mosquito nanoliter pipetting crystallization robot. Many screens were tested (PEG I and II from Qiagen; Structure Screen, Pact Premier I and II, and JSCG from Molecular Dimensions; Wizard I and II and JBS screen HTS L I and II from Jena Biosciences) with some initial crystals being obtained. Crystal optimization was complicated due to poor crystal reproducibility between different batches of purified protein, and protein degradation over time. Thin needle crystals were obtained using the hanging drop vapor diffusion method at 291 K with a reservoir volume of 500 µl of 20% PEG 3350 (w/v), 0.1 M BisTris Propane pH 7.5, and 0.2 M K/Na Tartrate. Crystals grew using a protein: precipitant ratio of 2:1 (total volume of 3 µl) over 2 months with dimensions of 0.15 mm × 0.03 mm × 0.03 mm. Prior to X-ray data collection, crystals were cryo-protected by being briefly dipped into a reservoir solution supplemented with 25% glycerol, and immediately flash-cooled in liquid nitrogen.

DATA COLLECTION AND STRUCTURE DETERMINATION

X-ray diffraction data were collected at 0.933 Å at ID14-2 beamline, ESRF – Grenoble, France, to 2.5 Å resolution. A total of 340 images were measured with an oscillation range of 0.6° and exposure time

of 10 s per image. Data were processed with *MOSFLM* (Leslie, 1992); and scaled with *SCALA* from the *CCP4* program suite (Collaborative Computational project, Number 4, 1994). The sequence information for *D. norvegicum dsrAB* genes is incomplete at their termini. They do however share 99% sequence identity with the corresponding genes of *Desulfomicrobium baculatum* (strain DSM 4028). This high identity allowed completion of the Drub *dsrAB* sequences based on those from *D. baculatum*: 62 amino-acid residues were added at the N-terminus of DsrA and 115 residues at the C-terminus of DsrB.

Molecular Replacement was done with *PHASER* (McCoy et al., 2007) using the *D. vulgaris* Dvir (PDB code: 2V4J; Oliveira et al., 2008a) as a search model. One *PHASER* run was performed searching independently for two molecules of each Dsr-A, B, and C subunits. A solution was obtained with rotation (RFZ) and translation functions (TFZ) of 22.9 and 23.1, respectively, and a refinement log-likelihood gain LLG of 662.90.

A first model building cycle was performed with *BUCANEER* (Cowtan, 2006). Electron-density map inspection and manual model building were carried out using *COOT* (Emsley and Cowtan, 2004). Further refinement was done with *REFMAC5* (Murshudov et al., 1997) within the *CCP4* program suite. For the refinement a subset (5%) of the reflections were randomly excluded for cross validation (R_{free} calculation). All structural figures were drawn with *PyMOL* (DeLano, 2002).

The atomic coordinates and structure factors of Drub isolated from *D. norvegicum* were deposited in the RCSB Protein Data Bank with accession number 2XSJ.

MASS SPECTROMETRY STUDIES

Purified *D. norvegicum* Drub and *D. vulgaris* Dvir were subjected to preparative 9% native gel electrophoresis. Each band was excised from the gel and the protein extracted by electro-elution as described in (Oliveira et al., 2008b). Nanoflow electrospray ionization-mass spectrometry was performed on the proteins thus obtained. Experiments were conducted on a Waters Synapt High Definition Mass Spectrometer (Manchester, UK) – a hybrid quadrupole/ion mobility/orthogonal acceleration time of flight (oa–TOF) instrument – equipped with a nanospray source and operated in TOF mode. Protein samples were buffer-exchanged into 1 M ammonium acetate pH 7.5 buffer using Vivaspin 500 centrifugal filters with 10 kDa molecular weight cutoff (Sartorius, Göttingen, Germany), diluted to a final concentration of 5 μM and electrosprayed from thin wall Nanoflow Probe Tips (Waters, Manchester, UK). Experiments were conducted at a capillary voltage of 1.5 kV, nanoflow gas pressure of 0.3 Bar, source temperature of 323 K, and sample cone voltage of 30 V, with the source operating in positive ion mode. Backing pressure was maintained between 5.0 and 6.0 mBar to provide collisional cooling of ions in the intermediated vacuum region of the instrument. The collisional energies were 50–70 V in the trap and 30–50 V in the transfer, with a trap gas flow of 10 ml min^{-1} resulting in a pressure of 5.2×10^{-2} mBar. Tandem mass spectrometry experiments were performed with trap voltages between 60 and 120 V. The oa-TOF-MS was operated over the scanning range of m/z 500–15000. Spectra were acquired and processed using Masslynx 4.1 software (Waters, Manchester, UK).

ELECTRON TRANSFER ASSAYS

Desulfoviridin from *D. vulgaris* Hildenborough was used in experiments to test potential electron donors, since it can be purified with much higher yields than Drub from *D. norvegicum*. Direct protein–protein interactions were probed using the surface plasmon resonance technique (Biacore T100 GE Healthcare). Two possible electron donors were tested: ferredoxin-I (FDX; DVU3276) isolated from *D. vulgaris* Hildenborough, and pyruvate–ferredoxin oxidoreductase (PFOR) isolated from *Desulfovibrio africanus* (as the *D. vulgaris* one is very unstable and shows 69/82% sequence identity/homology with *D. vulgaris* protein). A CM5 (carboxymethylated dextran) chip from GE Healthcare was used for the immobilization of dSiR *D. vulgaris*, and FDX and PFOR were tested as analytes. In one of the cases, the reverse experiment was performed, with FDX being coupled to the CM5 chip and *D. vulgaris* dSiR used as analyte.

Reduction of sulfite by Dvir with pyruvate/PFOR as electron donors was followed by spectroscopic measurement of hydrogen sulfide, using an adaptation of the methylene blue (MB) method (Fogo and Milton, 1949). MB is produced when sulfide reacts with *N*,*N*′-dimethyl-*p*-phenylenediamine (DPD) and ferric chloride under acidic conditions. For the assay, the reaction mixture contained 10 mM sodium pyruvate, 100 μM coenzyme A, 22.5 nM PFOR, 625 nM Dvir, and 200 μM sodium sulfite in a total volume of 200 μl and was started with the addition of sulfite and stopped at various time points (30min, 1 h, 2 h, 3 h, 4 h, and 12 h) on addition of 50 μl of the DPD/$FeCl_3$ mixture (prepared in 50% HCl). The color was allowed to develop by incubating at room temperature for 10 min before the absorbance was measured at 670 nm in a 96 well plate on a SpectraMax Plus384 spectrophotometer.

RESULTS AND DISCUSSION

DRUB CRYSTAL STRUCTURE

The purified sample of *D. norvegicum* Drub showed three bands in SDS-PAGE analysis corresponding to DsrA, DsrB, and DsrC protein, as also reported for other dSiRs (Pierik et al., 1992; Steuber et al., 1995). Crystals of Drub were obtained using PEG3350 as precipitant (pH ~7.5) and diffracted to ~2.5 Å at a synchrotron source. Drub crystals belonged to the orthorhombic space group ($P2_12_12_1$) with unit cell dimensions $a = 99.3$, $b = 135.1$, and $c = 178.0$ Å. The Matthews coefficient (Matthews, 1968) was 2.7 $Å^3$ Da^{-1}, consistent with the presence of one molecule ($\alpha_2\beta_2\gamma_2$) in the asymmetric unit and 53.3% of solvent content. The structure of Drub was determined by molecular replacement using the coordinates of *D. vulgaris* Dvir as search model.

The final crystallographic model of Drub comprised 1850 amino-acid residues out of 1856, 4 sirohemes and 8 [4Fe–4S] clusters, 2 sulfite ions, 1 glycerol, and 1051 water molecules (**Figure 1**). Final refinement values for R and R_{free} are 15.6 and 20.8%, respectively, with the entire model fitting the generally well defined electron-density map.

The deposited sequences for *D. norvegicum dsrA* and *dsrB* genes are incomplete at the N-terminal of *dsrA* and C-terminal of *dsrB*. However, due to the very high sequence identity (~99%) with *D. baculatum dsrAB* genes, the sequences of *D. norvegicum dsrA* and *dsrB* were completed. On inspection of the inserted residues extrapolated from the sequence of *D. baculatum*, six residues were observed which did not fit the electron-density and thus were not

conserved in the *D. norvegicum* sequences. Amino-acid residues at positions 33A, 57A, and 59A were refined manually with serine providing the best fit, residue 35A was refined as Gln, 323B as Ser and 364B as Ile, taking also into account their chemical environments. These predictions are expected to be robust, but nevertheless potential mis-assignments will not have major implications for the structural model due to the nature and position of these residues. Structure analysis and validation of the model was achieved using *PROCHECK* (Laskowski et al., 1993) from CCP4 indicating good stereochemistry. The relevant statistics for data processing and structure refinement are displayed in **Table 1**.

OVERALL DRUB ARCHITECTURE AND COFACTORS

The overall structure of *D. norvegicum* Drub (**Figure 1**) forms a dimer of αβγ units with a MW of 200 kDa. The $\alpha_2\beta_2\gamma_2$ unit corresponding to $[DsrA]_2[DsrB]_2[DsrC]_2$ is composed of the α subunit comprising residues 2–437 of chains A and D, the β subunit consisting of residues 2–386 from chains B and E, and the γ subunit containing residues 2–105 of chains C and F. In some dSiRs, namely Dvirs, the small DsrC protein copurifies with DsrAB (Pierik et al., 1992; Steuber et al., 1995), whereas in other dSiRs it does not (Dahl et al., 1993; Molitor et al., 1998).

The C-terminal arm of DsrA (405–437 of chains A/D) extends toward DsrB from the other monomer (DsrB*, chains E/B), and establishes several hydrogen-bonds with amino-acid residues from this subunit, important for dimer stabilization. Both DsrA and DsrB proteins are formed by three domains ($A_1A_2A_3/B_1B_2B_3$) as observed in *D. vulgaris* (Oliveira et al., 2008a), *A. fulgidus* (Schiffer et al., 2008), and *D. gigas* (Hsieh et al., 2010) dSiRs. The Drub structure comprises a conserved four domain core ($A_1A_2B_1B_2$, where A_1 corresponds to residues 19A–168A, A_2 to 169A–241A and 135B–207B, B_1 to residues 24B–134B, and B_2 to residues 323A–402A and 283B–370B) that is homologous to the structures of aSiRs and aNiR (Crane et al., 1995; Schnell et al., 2005; Swamy et al., 2005).

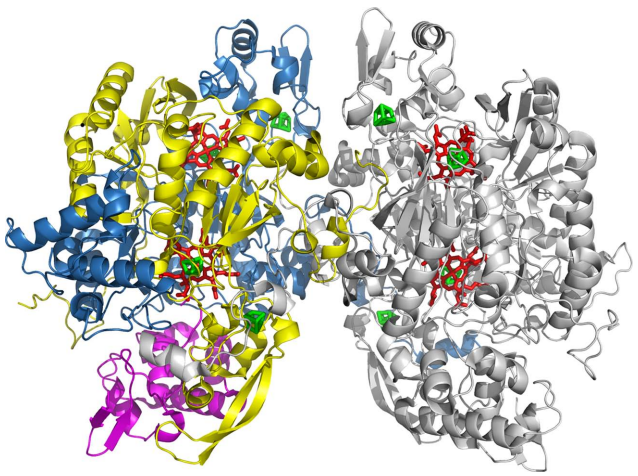

FIGURE 1 | Cartoon representation of the overall $\alpha_2\beta_2\gamma_2$ structure of Drub from *D. norvegicum*. α (DsrA) is colored in blue, β (DsrB) in yellow, and γ (DsrC) in magenta for one αβγ unit (chains D, E, and F), whereas the other is displayed in gray (chains A, B, and C). Sirohemes and [4Fe–4S] clusters and are represented in sticks and colored respectively red and green.

A third ferredoxin domain A_3/B_3 is present in both DsrA and DsrB, where A_3 consists of residues 242A–322A, and B_3 refers to residues 208B–282B.

Table 1 | Data collection and refinement statistics.

Data collection and processing	
Beamline	ID14-2 ESRF, Grenoble
Wavelength (Å)	0.933
Resolution range (Å)	45.10–2.53 (2.67–2.53)
No of images	340
Space group	$P2_12_12_1$
Unit cell parameters (Å)	a = 99.3, b = 135.1, c = 178.0
Mosaicity (°)	0.4
No. of complexes in asymmetric unit	1 ($\alpha_2\beta_2\gamma_2$)
R_{merge} (%)[a]	11.4 (28.6)
R_{pim} (%)[b]	4.2 (11.1)
$I/\sigma(I)$	12.8 (5.8)
Multiplicity	8.1 (7.4)
Completeness (%)	99.4 (96.9)
Total reflections	649457 (82716)
Unique reflections	79925 (11215)
Wilson B (Å^2)	33.5
Refinement	
No. of amino-acid residues	1850
Other molecules	
Siroheme (SRM)	4
[4Fe–4S]	8
SO_3^{2-}	2
Glycerol	1
Water molecules	1051
R (working set) (%)	15.6
R_{free} (%)	20.8
Ramachandran plot, residues in	
Most favored regions (%)	88.5
Additional allowed regions (%)	11.0
Generously allowed regions (%)	0.3
Disallowed regions (%)	0.3
Average B-factor (Å^2)	
Main chain	
DsrAB	13.6
DsrC	26.7
Side-chain	
DsrAB	14.9
DsrC	28.7
Solvent molecules	18.0
r.m.s. deviation from ideal values	
Bond length (Å)	0.015
Bond angle (°)	1.56

Values in parentheses are for the outer shell.

(a) $R_{merge} = \sum_{hkl}\sum_i \left| I_i(hkl) - \overline{I(hkl)} \right| \Big/ \sum_{hkl}\sum_i I_i(hkl)$

(b) $R_{pim} = \sum_{hkl}\left[1/(N-1) \right]^{1/2} \sum_i \left| I_i(hkl) - \overline{I(hkl)} \right| \Big/ \sum_{hkl}\sum_i I_i(hkl)$

Calculated with the program SCALA, R_{merge}, and R_{pim} are indicators of the precision of the final merged and averaged data-set, where $I_i(hkl)$ is the observed intensity of the ith measurement, $\overline{I(hkl)}$ is the average intensity of multiple observations of symmetry-related reflections and N is redundancy.

Each of the A_2/B_2 domains binds a saddle-shaped siroheme-[4Fe–4S] cofactor, giving a total of four sirohemes per $\alpha_2\beta_2$ unit as described for the dSiR of *A. fulgidus* (**Figure 2**). In contrast, dSiRs from *D. vulgaris* and *D. gigas* contain two sirohemes and two flat sirohydrochlorins per $\alpha_2\beta_2$ unit. The [4Fe–4S] cluster of the coupled siroheme cofactor in A_2 is coordinated by the strictly conserved Cys-X_5-Cys-X_n-Cys-X_3-Cys motif (Cys residues 177A, 183A, 221A, and 225A), whereas a different cysteine motif (C-X_n-C-C-X_3-C) is observed in the B_2 domain (Cys residues 151B, 188B, 189B, and 193B). In each motif two cysteine residues (225A and 193B) share the coordination of the [4Fe–4S] cluster and the siroheme. In the A_3/B_3 ferredoxin domains the [4Fe–4S] cluster is coordinated by cysteines 283A, 303A, 306A, and 309A; and 231B, 263B, 266B, and 269B, respectively. Previous cofactor quantifications of dSiRs from the Drub class indicated a content of 2.2 ± 0.3 mol of siroheme and 21 ± 2 mol of iron per mol of *D. baculatum* Drub (Moura et al., 1988), and 2 sirohemes and approximately 15 irons for *Desulfosarcina variabilis* Drub (Arendsen et al., 1993). The present structure indicates these values were underestimated with a total of 4 sirohemes, 36 irons, and 32 sulfurs present in the *D. norvegicum* Drub $\alpha_2\beta_2$ unit.

The structure of DsrC is mainly helical and comprises 104 residues out of 105. The C-terminal arm of DsrC (Leu98C–Val105C) is inserted into a cleft between DsrA and DsrB, which leads into the active site, with the conserved terminal cysteine (Sγ Cys104C/E) covalently linked to the catalytic siroheme (20′-*meso* carbon of the porphyrin ring; **Figure 2**). This covalent interaction was also observed in *D. vulgaris* (Oliveira et al., 2008a) and more recently in *D. gigas* Dvirs (Hsieh et al., 2010). We proposed that the covalent Cys104C-siroheme bond is non-physiological and forms as a result of porphyrin oxidation to give a π-cation radical that is quenched by the nearby Cys (Oliveira et al., 2008a). The presence of this bond probably stabilizes the DsrAB–DsrC complex and facilitates crystallization.

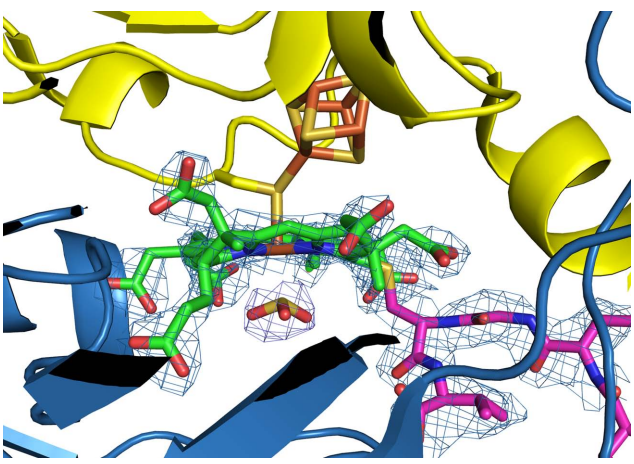

FIGURE 2 | Zoomed view of siroheme B – [4Fe–4S] cluster bridged by a cysteine residue (Cys193B). The covalent bond between Cys104C (DrsC is magenta) and siroheme B is displayed. A SO_3^{2-} is observed at the distal site of the catalytic siroheme. The 2Fo–Fc electron-density map is contoured at 1.5σ. DsrA is displayed in blue and DsrB in yellow. Atom color code: C, green; N, blue; Fe, orange; S, gold, and O, red.

Interestingly, two other DsrC conformations are observed in the recently reported *D. gigas* Dvir structure: in one there is no covalent bond between Cys104C and the siroheme and the cysteine side-chain is closer to the sulfite present in the active site; in the other one, the DsrC C-terminal arm is swung away from the siroheme in a way that brings Cys104C close to Cys93C (3.4–4.0 Å apart), but not forming a disulfide bond (Hsieh et al., 2010). In 70% of the molecules the DsrC arm is in the extended configuration, and in 30% in the retracted one, but both conformations are proposed to be in dynamic equilibrium (Hsieh et al., 2010). Previous crystal and solution structures of isolated DsrC proteins have also shown flexibility around the C-terminal tail, with either extended or retracted conformations (Cort et al., 2001, 2008; Weiss et al., 2004; Mander et al., 2005). Structural analysis of *D. gigas* Dvir reveals that Pro101C suffers significant conformational changes between these two conformations, functioning as a hinge, and being responsible for the different positions of the C-terminal arm (Pro-Thr-Gly-Cys-Val). There is enough space around the C-terminal tail in the DsrAB cleft to accommodate such structural rearrangements, while the rest of the DsrC globular domain and the DsrAB structure remain basically the same regardless of the DsrC C-terminal segment conformation. The presence of these two alternative conformations of the DsrC arm in the *D. gigas* Dvir structure provide supporting evidence for our proposal that the DsrC penultimate Cys is involved in the catalytic cycle and that a disulfide bond is ultimately formed between the two conserved DsrC cysteines (Oliveira et al., 2008a).

THE CATALYTIC SITE

The catalytic siroheme-bound by DsrB is buried in the protein interior and sits at the interface between DsrA and DsrB (**Figure 2**). DsrA provides the basic residues for substrate-binding at the distal site, whereas DrsB supplies the residues at the proximal site including Cys193B. This cysteine residue is covalently bound to the siroheme iron (~2.3 Å) and a cluster iron (~2.5 Å), where both irons are *ca.* 4.3 Å apart. The [4Fe–4S] cluster is bound exclusively by residues from DsrB subunit. A blob of electron-density with a trigonal pyramidal shape is observed at the distal site of the siroheme iron suggesting an axial ligand bound to it. A sulfite ion (SO_3^{2-}) was modeled into the blob with its sulfur pointing toward the siroheme moiety (sulfur atom is at a distance of ~2.3 Å to the siroheme iron, **Figure 2**). Arg101A, Arg172A, Lys213A, and Lys215A are strictly conserved residues that interact directly with the substrate. These residues together with other basic residues, such as arginines (83A, 231A, 376A, 378A, and 71B), lysine 217A, and histidines (150B and 152B) form a positively charged pocket with a favorable environment for binding the negatively charged sulfite and compensate the negative charges of the siroheme carboxylate groups (propionates and acetates substituents). The identification of the substrate channel leading to the catalytic siroheme is not consensual. A 15-Å long channel was identified in *A. fulgidus* dSiR (DsrAB), involving Arg80A, Arg358A, His64A, and His141B, with a size of 10 × 15 Å at its entrance and *ca* 6 × 9 Å at its substrate-binding pocket (Schiffer et al., 2008), This large cavity is however almost completely occupied by the C-terminal arm of DsrC, which is not present in *A. fulgidus* dSiR. Beside this channel, a narrower funnel is observed in Drub with a positive electrostatic potential which makes the distal side of the catalytic siroheme solvent accessible. The entrance is formed by Tyr212A, Arg376A, Glu381A

Leu226B, and is not blocked by the DsrC binding. This putative substrate funnel is also present in the other dSiR structures. In *D. gigas* Dvir, two other possible entry points are proposed: channel A, where Lys100C can bind a sulfite at the surface and transfer it to the active site through a swing of the DsrC C-terminal arm; and channel B which can connect the sirohydrochlorin and siroheme within each monomer, with Cys198B and Arg231A located in the middle of the channel (Hsieh et al., 2010). More structural and functional information is needed to clarify this issue.

Despite the presence of four siroheme-[4Fe–4S] cofactors in Drub, the sirohemes bound by DsrA should not be catalytically active, because they are not solvent accessible, and several basic residues important for substrate-binding are missing at the distal side of the heme. *D. vulgaris* and *D. gigas* Dvirs contain sirohydrochlorin at this site in DsrA, whereas *A. fulgidus* also has a siroheme. Interestingly, in aSiRs this second cofactor-binding site is empty.

STRUCTURAL COMPARISON OF DRUB WITH OTHERS dSiRs

Superposition of Drub with other dSiR structures from *D. vulgaris*, *D. gigas*, and *A. fulgidus* with PDBeFold (Krissinel and Henrick, 2004) yielded root-mean-square (r.m.s.) deviations of 0.74, 0.8, and 1.37Å for 1830, 1837, and 1500 aligned Cα atoms, respectively. Drub shares 74, 72, and 53% of amino-acid sequence identity with *D. vulgaris*, *D. gigas*, and *A. fulgidus* dSiRs, respectively.

Although the overall fold of dSiRs is quite conserved, there are some relevant localized differences (**Figure 3**). In Drub, DsrB has an inserted loop formed by residues 239B and 254B (5 residues longer than in *D. vulgaris* and *D. gigas* Dvirs, and 11 residues longer than *A. fulgidus* dSiR), which corresponds to a longer two stranded anti-parallel β-sheet followed by a three-residue-H-bonded turn. This loop extends outward in between the N-terminal of DsrA* (chain D) and DsrC. Moreover, the DsrB N-terminus of Drub is 11-residues longer than in *A. fulgidus* dSiR, but similar to *D. vulgaris* and *D. gigas* Dvir. It adopts an extended conformation toward DsrA residues: 39A–41A (located in a bending loop, e.g., the distance between the Cαs of 3B–41A is 5.9 Å), and 147A–151A (sited in a α-helix, Cα distance of 6B–151A is 5.3 Å); and DsrC (e.g., O atom of Pro10B is 5.9 Å apart from Oε1 Glu35C, Cγ of Pro13B is 4.7 Å away from Cα Gly38C). The O atom of Val4B and Asn16B are establishing hydrogen-bonds with the side-chain atoms of Arg125A and His158A, respectively. Interestingly, both of these inserted segments, not present in *A. fulgidus* dSiR, are flanking DsrC in Drub, *D. vulgaris* and *D. gigas* Dvir (**Figure 3**), and may play a role in the interaction between DsrAB and DsrC in these proteins.

In Drub, *D. vulgaris* and *D.gigas* Dvir, DsrA shows a 16-residue-insertion (257A–274A), which is partially overlapped by a five-residue longer loop in *A. fulgidus* (119B–125B: *A. fulgidus* numbering). In spite of similar length, the C-terminus of DsrA of both Drub and Dvirs show a different conformation compared to *A. fulgidus* dSiR. In Drub the DsrA C-terminal arm extends along DsrB* (chain E, e.g., distances between Cα atoms: 404A–378E is 4.0 Å, 414A–264E is 4.9 Å, 435A–86D is 5.4 Å) until it reaches DsrA* (chain D) and close to DsrC* (chain F), whereas in *A. fulgidus* the C-terminal arm is more "wrapped" around itself and only in closer contact with DsrB*. These C-terminal tails start diverging after residue 420A (Drub numbering).

Although no 3D structure is yet available for dSiRs belonging to either Desulfofuscidin or P582 classes, we expect similar overall folds for these proteins based on the high sequence identity (ranging from ~50 to 70%) and similarity (ranging from ~65 to 80%) among them. *D. norvegicum* Drub shows highest sequence identity to *D. vulgaris* Dvir (73%), followed by P582 proteins (~65%), and lastly *A. fulgidus* dSiR and Desulfofuscidins (~50%). The DsrA and DsrB cysteine motifs

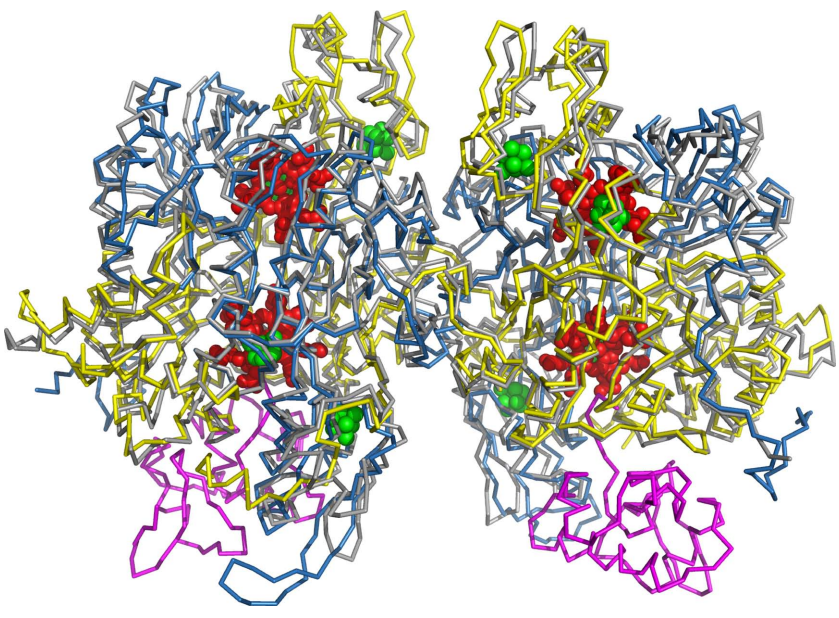

FIGURE 3 | Cα superposition of *D. norvegicum* Drub (DrsA-yellow, DsrB-blue, and DsrC. magenta) and *A. fulgidus* dSiR (gray), structures. For sake of clarity and due to high homology with Drub, the structures of *D. vulgaris* and *D. gigas* Dvirs were not represented. Sirohemes (red) and [4Fe–4S] clusters (green) are drawn in cpk mode (spheres).

required for binding the [4Fe–4S] cluster of the coupled cofactor, as well as the cysteine residues coordinating the ferredoxin domain [4Fe–4S] cluster, are strictly conserved among the analyzed Desulfofuscidin or P582 dSiRs. In addition, most positively charged residues around the catalytic siroheme and surrounding the substrate channel are also conserved in these proteins. Furthermore, the non-conservation of some substrate interacting residues around the non-catalytic DsrA siroheme is also observed in the Desulfofuscidin or P582 dSiRs, which indicates that the presence of a single catalytically active siroheme is a shared characteristic of the different classes of dSirs.

ANALYSIS OF *D. VULGARIS* AND *D. NORVEGICUM* dSiR OLIGOMERIC STATES

As previously reported for *D. vulgaris* Dvir (Lee et al., 1973; Seki et al., 1979; Wolfe et al., 1994; Marritt and Hagen, 1996), as well as recently for *D. gigas* (Hsieh et al., 2010) we observed that purification of Dvir (Oliveira et al., 2008b) and Drub by ion-exchange chromatography originates two or three peaks that cannot be distinguished by several analytical techniques including SDS-PAGE, UV–Visible spectroscopy, and enzyme activity. However, they also originate distinct bands on native gel electrophoresis, which together with the separation by ion-exchange chromatography indicates that they have quite different isoelectric points (Oliveira et al., 2008b).

Native gel of the purified *D. norvegicum* Drub showed three distinct bands, indicating the protein is also present in different states (**Figure 4B**). In *D. vulgaris* Dvir only two bands were observed (**Figure 4A**; Seki et al., 1979; Oliveira et al., 2008b), and crystals could only be obtained from the faster migrating band 1. In order to clarify the difference between the different forms, nanoflow electrospray ionization-mass spectrometry studies of the bands isolated from preparative native gel electrophoresis of *D. vulgaris* and *D. norvegicum* dSiRs were carried out.

The MS spectrum for *D. vulgaris* Dvir band 1 produced well defined peaks corresponding to a MW of 213.8 kDa, indicating the presence of a single species (**Figure 5A**). Analysis of Dvir band 2 from the same gel, provided less definition across the peaks, and a mixture of three species with MW of 213.4, 200.5, and 105.9 kDa is observed (**Figure 5B**). Molecular weight calculations for the different possible stoichiometries between *D. vulgaris* DsrA, DsrB, and DsrC, including cofactors, gives a theoretical MW of 213.3 kDa for the *D. vulgaris* $\alpha_2\beta_2\gamma_2$ form, 200.5 kDa for $\alpha_2\beta_2\gamma$, and 106.6 kDa for $\alpha\beta\gamma$ forms (**Table 2**). From these theoretical masses we can conclude that the fast migrating band 1 of Dvir comprises a single $\alpha_2\beta_2\gamma_2$ species, which is in agreement with the crystal structure obtained. In contrast, the slower migrating Dvir band 2 includes a mixture of three different forms, $\alpha_2\beta_2\gamma_2$ and $\alpha_2\beta_2\gamma$ and $\alpha\beta\gamma$.

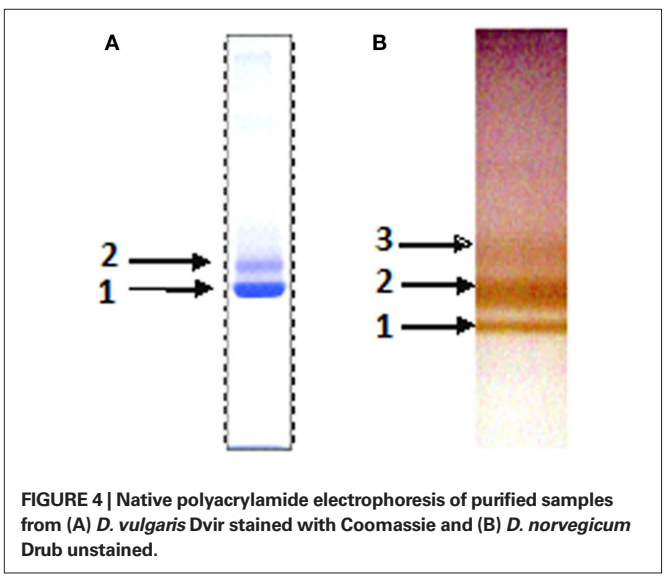

FIGURE 4 | Native polyacrylamide electrophoresis of purified samples from (A) *D. vulgaris* Dvir stained with Coomassie and (B) *D. norvegicum* Drub unstained.

For *D. norvegicum* Drub, bands 1 and 2 produced well defined peaks at 215.1 and 202.0 kDa, respectively, corresponding to single $\alpha_2\beta_2\gamma_2$ (band 1) and $\alpha_2\beta_2\gamma$ (band 2) forms (**Figures 5C,D**). In the slower migrating band 3 (**Figure 5E**), a mixture of peaks at 215.1, 202.3, 189.1, 107.2, and 94.5 kDa is observed, suggesting the presence of an heterogeneous sample corresponding to $\alpha_2\beta_2\gamma_2$, $\alpha_2\beta_2\gamma$, $\alpha_2\beta_2$, $\alpha\beta\gamma$, and $\alpha\beta$ complex compositions. Interestingly, in both Dvir and Drub the dissociation of DsrC is associated with loss of the corresponding siroheme.

Tandem MS experiments were then carried out to try to test dissociation of DsrC from DsrAB in the single species samples, by gradually increasing the trap voltage (**Figure 6**). At 60 V no dissociation is observed, whereas from 80 to 120 V we can detect dissociation of free DsrC, siroheme-bound DsrC as well as siroheme, from the $\alpha_2\beta_2\gamma_2$ and $\alpha_2\beta_2\gamma$ forms of Drub and the $\alpha_2\beta_2\gamma_2$ form of Dvir. The presence of DsrC ions without attached siroheme indicate sub-stoichiometric covalent bonding of this protein to the porphyrin, or disruption of the bond under conditions of collisional activation in the mass spectrometer.

These results are important because they clearly show that the purified dSiRs from *D. vulgaris* and *D. norvegicum*, which seem homogeneous by SDS-PAGE analysis, are in fact a mixture of oligomeric states, even after purification. A similar situation is likely to occur for other purified dSiRs described in the literature, which may explain the disparate results in terms of cofactor content and spectroscopic properties (Rabus et al., 2007), the appearance of several peaks with different pIs in ion-exchange chromatography, and also why this protein resisted attempts to crystallize for so long. The major species present in both Dvir and Drub are the $\alpha_2\beta_2\gamma_2$ and $\alpha_2\beta_2\gamma$ forms. These forms can be separated on ion-exchange chromatography, but the resulting fractions still have some of the other form, probably due to an equilibrium between dissociation and association of the DsrC protein. In addition, the MS results indicate that the crystallization process selects for the $\alpha_2\beta_2\gamma_2$ form with a covalent bond between DsrC and the siroheme, since other forms are present in the Drub protein solution used for crystallization. The presence of the covalent bond is likely to make the whole structure more stable and enable crystallization. Forms of the $\alpha_2\beta_2\gamma_2$ complex without a covalent bond are also likely to be present in the *D. vulgaris* Dvir solution, which did not crystallize. This was confirmed in the *D. gigas* Dvir X-ray structure where non-covalently bonded DsrC is observed, either in a stretched or retracted conformation (Hsieh et al., 2010). In this work the authors could crystallize two of the Dvir forms that are separated by ion-exchange chromatography. In the second form (Dvir-II) one Fe atom is missing, turning the siroheme-associated [4Fe–4S] cluster into a [3Fe–4S] one, and the authors attribute the difference in pI between the two Dvir forms to this fact. We have also observed by EPR that a [3Fe–4S] cluster is present in the slow form of *D. vulgaris* Dvir. However, we consider that this difference alone is

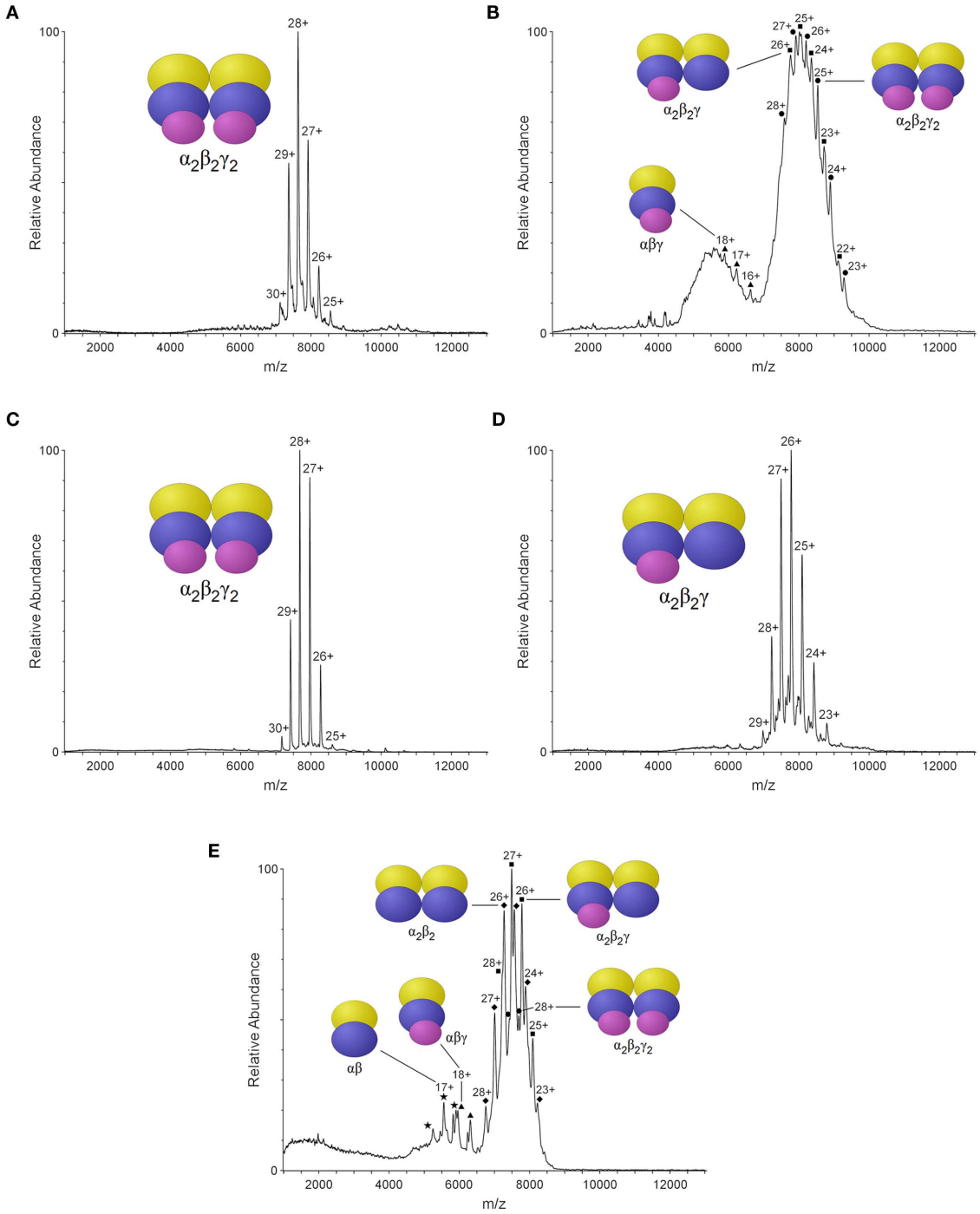

FIGURE 5 | Nano-ESI/MS spectra of the purified dSiRs bands after native gel electrophoresis; *D. vulgaris* Dvir (A) band 1, (B) band 2; *D. norvegicum* (C) band 1, (D) band 2, and (E) band 3. Schematic representation of the different chains as ovals colored as in **Figure 1**.

unlikely to explain the large difference in charge between the two Dvir forms, as the $\alpha_2\beta_2$ complex has a highly negative charge. Rather, it is likely that *D. gigas* Dvir-II separated by ion-chromatography is still a mixture of $\alpha_2\beta_2\gamma$ and $\alpha_2\beta_2\gamma_2$ forms, but the crystallization procedure has selected for the less flexible conformation in the $\alpha_2\beta_2\gamma_2$ form, which is observed in the crystal structure.

SEARCH FOR THE DSIR ELECTRON DONOR

The direct involvement of DsrC in the reduction of sulfite by DsrAB, as revealed by the *D. vulgaris* Dvir structure, led us to propose a mechanism for sulfite reduction in which reduced DsrC is a co-substrate of DsrAB, with oxidized DsrC (with a disulfide bond between the two C-terminal conserved Cys) being

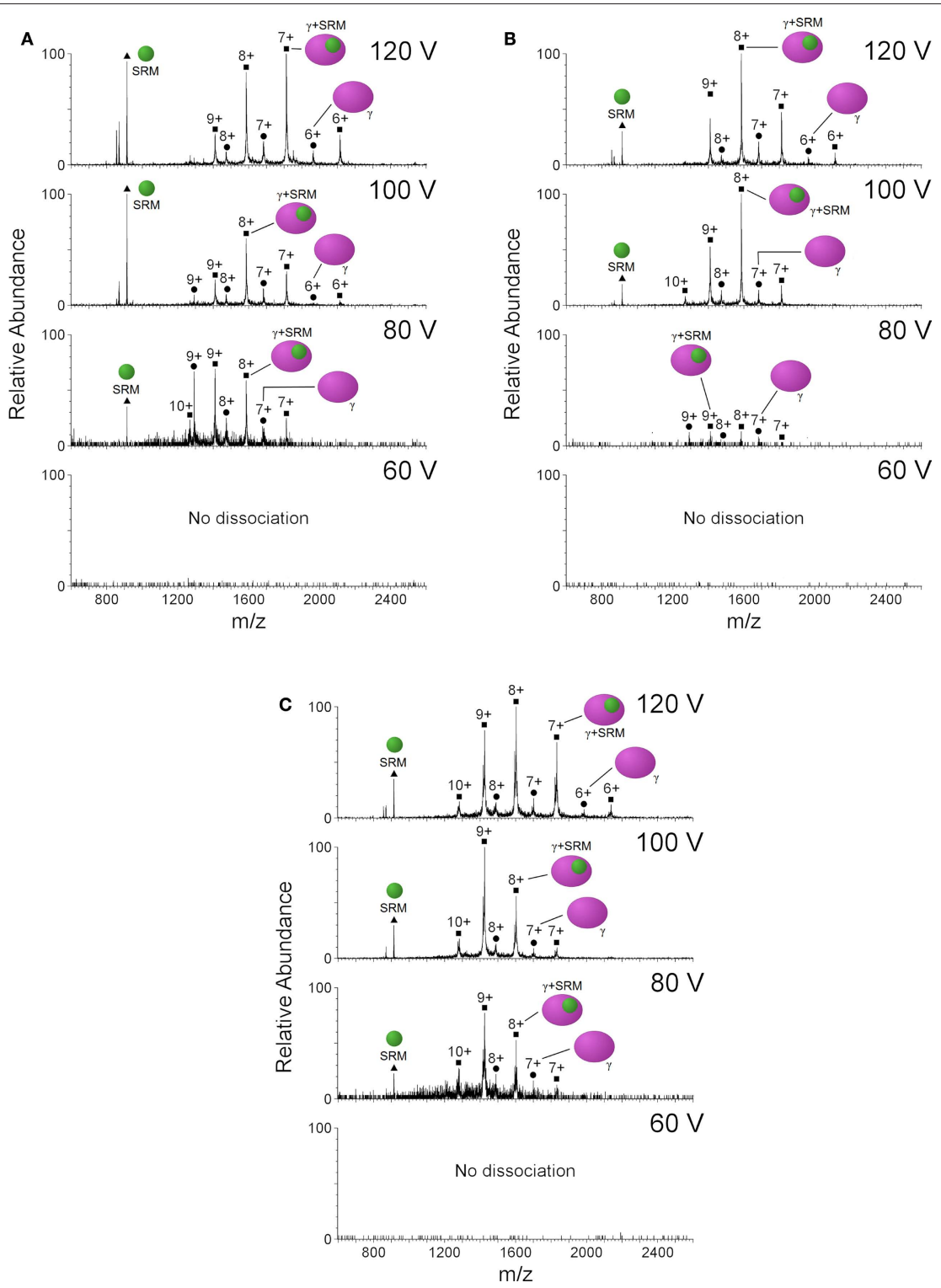

FIGURE 6 | Nano-ESI/MS spectra of (A) band 1 and (B) band 2 from dSiR *D. norvegicum* and for (C) band 1 from *D. vulgaris*, showing the presence of isolated DsrC and SRM and DsrC-SRM complex. Schematic representation of (DsrC) as magenta and siroheme (SRM) as green ovals.

formed as a product (Oliveira et al., 2008a). The oxidized DsrC is proposed to be reduced by the membrane-bound DsrMKJOP complex, with the result that two of the six electrons required for sulfite reduction probably originate from the quinone pool. This still leaves a requirement for another electron donor to deliver the remaining four electrons to dSiR, but this donor has not yet

Table 2 | Predicted and observed molecular weight of the different oligomeric forms of *D. vulgaris* Dvir and *D. norvegicum* Drub.

	Predicted complex stoichiometry	Predicted cofactors	Theoretical MW (kDa)	Obtained MW (kDa)
Dvir band 1	$\alpha_2\beta_2\gamma_2$	2 SRM + 2 SRHC + 8 [4Fe–4S]	213.3	213.8
Dvir band 2	$\alpha_2\beta_2\gamma_2$	2 SRM + 2 SRHC + 8 [4Fe–4S]	213.3	213.4
	$\alpha_2\beta_2\gamma$	1 SRM + 2 SRHC + 8 [4Fe–4S]	200.5	200.5
	$\alpha\beta\gamma$	1 SRM + 1 SRHC + 4 [4Fe–4S]	106.7	105.9
Drub band 1	$\alpha_2\beta_2\gamma_2$	4 SRM + 8 [4Fe–4S]	215.5	215.1
Drub band 2	$\alpha_2\beta_2\gamma$	3 SRM + 8 [4Fe–4S]	202.8	202.0
Drub band 3	$\alpha_2\beta_2\gamma_2$	4 SRM + 8 [4Fe–4S]	215.5	215.1
	$\alpha_2\beta_2\gamma$	3 SRM + 8 [4Fe–4S]	202.8	202.3
	$\alpha_2\beta_2$	2 SRM + 8 [4Fe–4S]	190.0	189.1
	$\alpha\beta\gamma$	2 SRM + 4 [4Fe–4S]	107.8	107.2
	$\alpha\beta$	1 SRM + 4 [4Fe–4S]	95.0	94.5

been identified. It is known that ferredoxin is the electron donor for the aSiRs and nitrite reductases. However, in dSir structures, a ferredoxin domain was incorporated in DsrA and DsrB during dSir evolution (Dahl et al., 1993; Dhillon et al., 2005). This incorporation suggests that the external electron donor may be a ferredoxin-reducing protein.

Using biochemical and biophysical techniques we have tried to examine two potential electron donors to dSiRs: PFOR, and ferredoxin-I. We first generated a model for the *D. vulgaris* Hildenborough PFOR based on the structure of PFOR from *D. africanus* (PDB code 1BOP; Chabriere et al., 2001), since the proteins share 69% sequence identity. The surface electrostatic potential was calculated for both *D. vulgaris* Dvir and PFOR structures, to detect possible interaction sites. On the *D. vulgaris* Dvir surface, a negatively charged region is observed in the ferredoxin domain of chain B, which is a likely region for interaction with an electron donor. In contrast, an overall positive charge along the surface of the ferredoxin domain is observed in PFOR. Using modeling tools in Pymol, the PFOR ferredoxin domain can be placed in the vicinity of the *D. vulgaris* Dvir ferredoxin domain positioning the iron–sulfur clusters of the two domains at ~15 Å from each other. This suggests that electron transfer from the PFOR [4Fe–4S] cluster to the Dvir ferredoxin [4Fe–4S] cluster is possible, so PFOR looks like a plausible candidate electron donor.

We analyzed protein–protein interactions between the *D. vulgaris* Dvir and potential donors using surface plasmon resonance. However, we could detected no direct binding between immobilized Dvir and either PFOR or Fd-I. We cannot exclude that this technique may be hampered by the transient nature of the interaction between PFOR and Dvir. In addition to the direct protein–protein interaction assays, we also tested an activity-based assay for reduction of sulfite by Dvir with pyruvate/PFOR as electron donors. The assay was based on the measurement of sulfide production using the MB method. Again, we could detect no reduction of sulfite from pyruvate. These results do not suggest that PFOR or Fd-I may be physiological electron donors to dSiRs, or alternatively, the system may need other components to allow the enzyme to complete the catalytic cycle. Further work is necessary to elucidate the nature of the electron donor to dSiR.

CONCLUSION

In conclusion, the structure of a Drub determined herein shows that it is similar to the structure of Dvirs. The difference in spectral properties that led to its classification as a different protein is explained by the presence of both sirohydrochlorin and siroheme in Dvir, whereas only siroheme is present in Drub. Since the Drub sirohemes corresponding to the sirohydrochlorins are nonetheless not catalytic, there seems to be little justification for classifying Drub and Dvir as two different classes of dSiRs. The presence of two non-catalytic cofactors in the dSiRs has been confirmed in the four structures reported, where in the *A. fulgidus* dSiR and in the Drub structure reported herein these two cofactors are sirohemes, and in the *D. vulgaris* and *D.gigas* Dvirs they are sirohydrochlorins. The actual function of this cofactor is uncertain. It obviously results from the gene duplication event that gave rise to the homologous DsrA and DsrB subunits, but whereas in the aSiRs this event was followed by loss of this second cofactor (Crane and Getzoff, 1996), in dSiRs this cofactor has been retained. This may either mean that dSiRs are still at an intermediate stage of evolution, which will eventually lead to complete loss of the second cofactor, or that this cofactor has been kept because it is actually performing a valuable function. Since Fe is not required for this function, we tend to favor a structural role for the sirohydrochlorin/siroheme group, which probably serves to stabilize the whole molecule. From sequence and structural analysis we could not identify differences among the dSiRs that could explain why in some cases the Fe is lost, while in others it is retained. Elucidation of the dSiR cofactor insertion and maturation processes may in the future provide further clues to this issue. Schiffer et al. (2008) have also suggested that optimization of the catalytic siroheme site was achieved at the expense of the loss of catalytic activity at the second heme.

Using MS studies we established that purified Dvir and Drub are present in different oligomeric forms with two, one, or no DsrC molecules bound. The relative proportions of these species are likely to be highly dependent on the preparation, finally providing an explanation for the conflicting results in terms of cofactor content and spectroscopy results for these proteins. In addition, we obtained evidence for the fact that not all DsrC molecules in the DsrABC complexes have a covalent bond to the siroheme (as was recently confirmed by the *D. gigas* Dvir structures), which further

supports the involvement of the DsrC penultimate Cys in the sulfite reduction mechanism. Our preliminary attempts to discover the physiological electron donor to dSir have proved unsuccessful, and future studies are necessary to elucidate this important question.

ACKNOWLEDGMENTS

This work was supported by research grant PTDC/QUI-BIQ/100591/2008 to Inês A. C. Pereira and PTDC/BIA-PRO/103718/2008 to Margarida Archer funded by Fundação para a Ciência e Tecnologia (FCT, MCTES, Portugal); and by a Science Foundation Ireland Investigator grant (07/IN.1/B975) to Amir R. Khan, Edward Franklin and Tânia F. Oliveira. FCT is acknowledged for the fellowship to Tânia F. Oliveira (SFRH/BD/29519/2006) and ESRF for financial and technical support for X-ray diffraction data collection. We thank Dr. Pedro Matias for help in refinement and fruitful discussions. We acknowledge Dr. Chun-Jung Chen (Taiwan) for providing us the coordinates of *D. gigas* Dvir with the retracted DsrC C-terminal arm.

REFERENCES

Akagi, J. M., Chan, M., and Adams, V. (1974). Observations on the bisulfite reductase (P582) isolated from *Desulfotomaculum nigrificans*. *J. Bacteriol.* 120, 240–244.

Arendsen, A. F., Verhagen, M. F., Wolbert, R. B., Pierik, A. J., Stams, A. J., Jetten, M. S., and Hagen, W. R. (1993). The dissimilatory sulfite reductase from *Desulfosarcina variabilis* is a desulforubidin containing uncoupled metalated sirohemes and S = 9/2 iron-sulfur clusters. *Biochemistry* 32, 10323–10330.

Canfield, D. E., and Raiswell, R. (1999). The evolution of the sulfur cycle. *Am. J. Sci.* 299, 627–723.

Canfield, D. E., Rosing, M. T., and Bjerrum, C. (2006). Early anaerobic metabolisms. *Philos. Trans. R. Soc. Lond. B Biol. Sci.* 361, 1819–1834; discussion 1835–1836.

Chabriere, E., Vernede, X., Guigliarelli, B., Charon, M. H., Hatchikian, E. C., and Fontecilla-Camps, J. C. (2001). Crystal structure of the free radical intermediate of pyruvate:ferredoxin oxidoreductase, *Science* 294, 2559–2563.

Collaborative Computational Project, Number 4. (1994). The CCP4 suite: programs for protein crystallography. *Acta Crystallogr. D Biol. Crystallogr.* 50, 760–763.

Cort, J. R., Mariappan, S. V., Kim, C. Y., Park, M. S., Peat, T. S., Waldo, G. S., Terwilliger, T. C., and Kennedy, M. A. (2001). Solution structure of *Pyrobaculum aerophilum* DsrC, an archaeal homologue of the gamma subunit of dissimilatory sulfite reductase. *Eur. J. Biochem.* 268, 5842–5850.

Cort, J. R., Selan, U., Schulte, A., Grimm, F., Kennedy, M. A., and Dahl, C. (2008). *Allochromatium vinosum* DsrC: solution-state NMR structure, redox properties, and interaction with DsrEFH, a protein essential for purple sulfur bacterial sulfur oxidation. *J. Mol. Biol.* 382, 692–707.

Cowtan, K. (2006). The Buccaneer software for automated model building. 1. Tracing protein chains. *Acta Crystallogr. D Biol. Crystallogr.* 62, 1002–1011.

Crane, B. R., and Getzoff, E. D. (1996). The relationship between structure and function for the sulfite reductases. *Curr. Opin. Struct. Biol.* 6, 744–756.

Crane, B. R., Siegel, L. M., and Getzoff, E. D. (1995). Sulfite reductase structure at 1.6 A: evolution and catalysis for reduction of inorganic anions. *Science* 270, 59–67.

Dahl, C., Engels, S., Pott-Sperling, A. S., Schulte, A., Sander, J., Lubbe, Y., Deuster, O., and Brune, D. C. (2005). Novel genes of the dsr gene cluster and evidence for close interaction of Dsr proteins during sulfur oxidation in the phototrophic sulfur bacterium *Allochromatium vinosum*. *J. Bacteriol.* 187, 1392–1404.

Dahl, C., Kredich, N. M., Deutzmann, R., and Truper, H. G. (1993). Dissimilatory sulphite reductase from *Archaeoglobus fulgidus*: physico-chemical properties of the enzyme and cloning, sequencing and analysis of the reductase genes. *J. Gen. Microbiol.* 139, 1817–1828.

DeLano, W. L. (2002). *The PyMOL Molecular Graphics System*. San Carlos, CA: DeLano Scientific.

DerVartanian, D. V. (1994). Desulforubidin: dissimilatory, high-spin sulfite reductase of *Desulfomicrobium* species. *Meth. Enzymol.* 243, 270–276.

Dhillon, A., Goswami, S., Riley, M., Teske, A., and Sogin, M. (2005). Domain evolution and functional diversification of sulfite reductases. *Astrobiology* 5, 18–29.

Emsley, P., and Cowtan, K. (2004). Coot: model-building tools for molecular graphics. *Acta Crystallogr. D Biol. Crystallogr.* 60, 2126–2132.

Fogo, J. K., and Milton, P. (1949). Spectrophotometric determination of hydrogen sulfide. *Anal. Chem.* 21, 732–734.

Hatchikian, E. C. (1994). Desulfofuscidin: dissimilatory, high-spin sulfite reductase of thermophilic, sulfate-reducing bacteria. *Meth. Enzymol.* 243, 276–295.

Hatchikian, E. C., and Zeikus, J. G. (1983). Characterization of a new type of dissimilatory sulfite reductase present in *Thermodesulfobacterium commune*. *J. Bacteriol.* 153, 1211–1220.

Hsieh, Y. C., Liu, M. Y., Wang, V. C., Chiang, Y. L., Liu, E. H., Wu, W. G., Chan, S. I., and Chen, C. J. (2010). Structural insights into the enzyme catalysis from comparison of three forms of dissimilatory sulphite reductase from *Desulfovibrio gigas*. *Mol. Microbiol.* 78, 1101–1116.

Ikeuchi, Y., Shigi, N., Kato, J., Nishimura, A., and Suzuki, T. (2006). Mechanistic insights into multiple sulfur mediators sulfur relay by involved in thiouridine biosynthesis at tRNA wobble positions. *Mol. Cell* 21, 97–108.

Klein, M., Friedrich, M., Roger, A. J., Hugenholtz, P., Fishbain, S., Abicht, H., Blackall, L. L., Stahl, D. A., and Wagner, M. (2001). Multiple lateral transfers of dissimilatory sulfite reductase genes between major lineages of sulfate-reducing prokaryotes. *J. Bacteriol.* 183, 6028–6035.

Krissinel, E., and Henrick, K. (2004). Secondary-structure matching (SSM), a new tool for fast protein structure alignment in three dimensions. *Acta Crystallogr. D Biol. Crystallogr.* 60, 2256–2268.

Laskowski, R. A., MacArthur, M. W., Moss, D. S., and Thornton, J. M. (1993). PROCHECK: a program to check the stereochemical quality of protein structures. *J. Appl. Crystallogr.* 26, 283–291.

Lee, J. P., and Peck, H. D. (1971). Purification of the enzyme reducing bisulfite to trithionate from *Desulfovibrio gigas* and its identification as desulfoviridin. *Biochem. Biophys. Res. Commun.* 45, 583–589.

Lee, J. P., Yi, C.-S., LeGall, J., and Peck, H. D. (1973). Isolation of a new pigment, desulforubidin, from *Desulfovibrio desulfuricans* (Norway strain) and its role in sulfite reduction. *J. Bacteriol.* 115, 453–455.

Leslie, A. G. W. (1992). *Joint CCP4+ESF-EAMBC Newsletter on Protein Crystallography 26*.

Loy, A., Duller, S., and Wagner, M. (2007). "Evolution and ecology of microbes dissimilating sulfur compounds: insights from siroheme sulfite reductases," in *Microbial Sulfur Metabolism*, eds C. Dahl and C. Friedrich (Berlin: Springer), 46–59.

Mander, G. J., Weiss, M. S., Hedderich, R., Kahnt, J., Ermler, U., and Warkentin, E. (2005). X-ray structure of the gamma-subunit of a dissimilatory sulfite reductase: fixed and flexible C-terminal arms. *FEBS Lett.* 579, 4600–4604.

Marritt, S. J., and Hagen, W. F. (1996). Dissimilatory sulfite reductase revisited. The desulfoviridin molecule does contain 20 iron ions, extensively demetallated siroheme, and an S = 9/2 iron-sulfur cluster. *Eur. J. Biochem.* 238, 724–727.

Matthews, B. W. (1968). Solvent content of protein crystals. *J. Mol. Biol.* 33, 491–497.

McCoy, A. J., Grosse-Kunstleve, R. W., Adams, P. D., Winn, M. D., Storoni, L. C., and Read, R. J. (2007). Phaser crystallographic software. *J. Appl. Crystallogr.* 40, 658–674.

Molitor, M., Dahl, C., Molitor, I., Schafer, U., Speich, N., Huber, R., Deutzmann, R., and Truper, H. G. (1998). A dissimilatory siroheme-sulfite-reductase-type protein from the hyperthermophilic archaeon *Pyrobaculum islandicum*. *Microbiology* 144(Pt 2), 529–541.

Moura, I., LeGall, J., Lino, A. R., Peck, H. D., Fauque, G., Xavier, A. V., DerVartanian, D. V., Moura, J. J. G., and Huynh, B. H. (1988). Characterization of two dissimilatory sulfite reductases (desulforubidin and desulfoviridin) from the sulfate-reducing bacteria. Mössbauer and EPR Studies. *J. Am. Chem. Soc.* 110, 1075–1082.

Murshudov, G. N., Vagin, A. A., and Dodson, E. J. (1997). Refinement of macromolecular structures by the maximum-likelihood method. *Acta Crystallogr. D Biol. Crystallogr.* 53, 240–255.

Numata, T., Fukai, S., Ikeuchi, Y., Suzuki, T., and Nureki, O. (2006). Structural basis for sulfur relay to RNA mediated by heterohexameric TusBCD complex. *Structure* 14, 357–366.

Oliveira, T. F., Vonrhein, C., Matias, P. M., Venceslau, S. S., Pereira, I. A., and Archer, M. (2008a). The crystal structure of *Desulfovibrio vulgaris* dissimilatory sulfite reductase bound to DsrC provides novel insights into the mechanism of sulfate respiration. *J. Biol. Chem.* 283, 34141–34149.

Oliveira, T. F., Vonrhein, C., Matias, P. M., Venceslau, S. S., Pereira, I. A., and Archer, M. (2008b). Purification, crystallization and preliminary crystallographic analysis of a dissimilatory DsrAB sulfite reductase in complex with DsrC. *J. Struct. Biol.* 164, 236–239.

Parey, K., Warkentin, E., Kroneck, P. M., and Ermler, U. (2010). Reaction cycle of the dissimilatory sulfite reductase from *Archaeoglobus fulgidus*. *Biochemistry* 49, 8912–8921.

Peck, H. D. Jr., and LeGall, J. (1982). Biochemistry of dissimilatory sulphate reduction. *Philos. Trans. R. Soc. Lond. B Biol. Sci.* 298, 443–466.

Pereira, P. M., Teixeira, M., Xavier, A. V., Louro, R. O., and Pereira, I. A. C. (2006). The Tmc complex from *Desulfovibrio vulgaris* Hildenborough is involved in transmembrane electron transfer from periplasmic hydrogen oxidation. *Biochemistry* 45, 10359–10367.

Pierik, A. J., Duyvis, M. G., van Helvoort, J. M., Wolbert, R. B., and Hagen, W. R. (1992). The third subunit of desulfoviridin-type dissimilatory sulfite reductases. *Eur. J. Biochem.* 205, 111–115.

Pierik, A. J., and Hagen, W. R. (1991). S = 9/2 EPR signals are evidence against coupling between the siroheme and the Fe/S cluster prosthetic groups in *Desulfovibrio vulgaris* (Hildenborough) dissimilatory sulfite reductase. *Eur. J. Biochem.* 195, 505–516.

Pires, R. H., Venceslau, S. S., Morais, F., Teixeira, M., Xavier, A. V., and Pereira, I. A. C. (2006). Characterization of the *Desulfovibrio desulfuricans* ATCC 27774 DsrMKJOP complex – a membrane-bound redox complex involved in sulfate respiration. *Biochemistry* 45, 249–262.

Rabus, R., Hansen, T., and Widdel, F. (2007). "Dissimilatory sulfate- and sulfur-reducing prokaryotes," in *The Prokaryotes*, ed. M. E. A. Dworkin (New York: Springer-Verlag), 659–768.

Schiffer, A., Parey, K., Warkentin, E., Diederichs, K., Huber, H., Stetter, K. O., Kroneck, P. M., and Ermler, U. (2008). Structure of the dissimilatory sulfite reductase from the hyperthermophilic archaeon *Archaeoglobus fulgidus*. *J. Mol. Biol.* 379, 1063–1074.

Schnell, R., Sandalova, T., Hellman, U., Lindqvist, Y., and Schneider, G. (2005). Siroheme- and [Fe4-S4]-dependent NirA from *Mycobacterium tuberculosis* is a sulfite reductase with a covalent Cys-Tyr bond in the active site. *J. Biol. Chem.* 280, 27319–27328.

Seki, Y., Kobayashi, K., and Ishimoto, M. (1979). Biochemical studies on sulfate-reducing bacteria. XV. Separation and comparison of two forms of desulfoviridin. *J. Biochem.* 85, 705–711.

Steuber, J., Arendsen, A. F., Hagen, W. R., and Kroneck, P. M. (1995). Molecular properties of the dissimilatory sulfite reductase from *Desulfovibrio desulfuricans* (Essex) and comparison with the enzyme from *Desulfovibrio vulgaris* (Hildenborough). *Eur. J. Biochem.* 233, 873–879.

Steuber, J., Cypionka, H., and Kroneck, P. M. H. (1994). Mechanism of dissimilatory sulfite reduction by *Desulfovibrio desulfuricans* – purification of a membrane-bound sulfite reductase and coupling with cytochrome C(3) and hydrogenase. *Arch. Microbiol.* 162, 255–260.

Swamy, U., Wang, M., Tripathy, J. N., Kim, S. K., Hirasawa, M., Knaff, D. B., and Allen, J. P. (2005). Structure of spinach nitrite reductase: implications for multi-electron reactions by the iron-sulfur:siroheme cofactor. *Biochemistry* 44, 16054–16063.

Wagner, M., Roger, A. J., Flax, J. L., Brusseau, G. A., and Stahl, D. A. (1998). Phylogeny of dissimilatory sulfite reductases supports an early origin of sulfate respiration. *J. Bacteriol.* 180, 2975–2982.

Weiss, M. S., Mander, G., Hedderich, R., Diederichs, K., Ermler, U., and Warkentin, E. (2004). Determination of a novel structure by a combination of long-wavelength sulfur phasing and radiation-damage-induced phasing. *Acta Crystallogr. D Biol. Crystallogr.* 60, 686–695.

Wolfe, B. M., Lui, S. M., and Cowan, J. A. (1994). Desulfoviridin, a multimeric-dissimilatory sulfite reductase from *Desulfovibrio vulgaris* (Hildenborough). Purification, characterization, kinetics and EPR studies. *Eur. J. Biochem.* 223, 79–89.

Zverlov, V., Klein, M., Lucker, S., Friedrich, M. W., Kellermann, J., Stahl, D. A., Loy, A., and Wagner, M. (2005). Lateral gene transfer of dissimilatory (bi) sulfite reductase revisited. *J. Bacteriol.* 187, 2203–2208.

Conflict of Interest Statement: The authors declare that the research was conducted in the absence of any commercial or financial relationships that could be construed as a potential conflict of interest.

Received: 09 February 2011; paper pending published: 25 February 2011; accepted: 28 March 2011; published online: 13 April 2011.

Citation: Oliveira TF, Franklin E, Afonso JP, Khan AR, Oldham NJ, Pereira IAC and Archer M (2011) Structural insights into dissimilatory sulfite reductases: structure of desulforubidin from Desulfomicrobium norvegicum. Front. Microbio. ***2****:71. doi: 10.3389/fmicb.2011.00071*

This article was submitted to Frontiers in Microbial Physiology and Metabolism, a specialty of Frontiers in Microbiology.

frontiers in
MICROBIOLOGY

REVIEW ARTICLE
published: 19 April 2011
doi: 10.3389/fmicb.2011.00069

A comparative genomic analysis of energy metabolism in sulfate reducing bacteria and archaea

Inês A. Cardoso Pereira*, Ana Raquel Ramos, Fabian Grein, Marta Coimbra Marques, Sofia Marques da Silva and Sofia Santos Venceslau

Instituto de Tecnologia Química e Biológica, Universidade Nova de Lisboa, Oeiras, Portugal

Edited by:
Martin G. Klotz, University of Louisville, USA

Reviewed by:
Kathleen Scott, University of South Florida, USA
Donald A. Bryant, The Pennsylvania State University, USA

****Correspondence:***
Inês A. Cardoso Pereira, Instituto de Tecnologia Química e Biológica, Avenida da Republica – Estação Agronómica Nacional, 2780-157 Oeiras, Portugal.
e-mail: ipereira@itqb.unl.pt

The number of sequenced genomes of sulfate reducing organisms (SRO) has increased significantly in the recent years, providing an opportunity for a broader perspective into their energy metabolism. In this work we carried out a comparative survey of energy metabolism genes found in 25 available genomes of SRO. This analysis revealed a higher diversity of possible energy conserving pathways than classically considered to be present in these organisms, and permitted the identification of new proteins not known to be present in this group. The *Deltaproteobacteria* (and *Thermodesulfovibrio yellowstonii*) are characterized by a large number of cytochromes *c* and cytochrome *c*-associated membrane redox complexes, indicating that periplasmic electron transfer pathways are important in these bacteria. The Archaea and *Clostridia* groups contain practically no cytochromes *c* or associated membrane complexes. However, despite the absence of a periplasmic space, a few extracytoplasmic membrane redox proteins were detected in the Gram-positive bacteria. Several ion-translocating complexes were detected in SRO including H^+-pyrophosphatases, complex I homologs, Rnf, and Ech/Coo hydrogenases. Furthermore, we found evidence that cytoplasmic electron bifurcating mechanisms, recently described for other anaerobes, are also likely to play an important role in energy metabolism of SRO. A number of cytoplasmic [NiFe] and [FeFe] hydrogenases, formate dehydrogenases, and heterodisulfide reductase-related proteins are likely candidates to be involved in energy coupling through electron bifurcation, from diverse electron donors such as H_2, formate, pyruvate, NAD(P)H, β-oxidation, and others. In conclusion, this analysis indicates that energy metabolism of SRO is far more versatile than previously considered, and that both chemiosmotic and flavin-based electron bifurcating mechanisms provide alternative strategies for energy conservation.

Keywords: energy metabolism, sulfate reducing bacteria, membrane complexes, electron bifurcation, hydrogenase, formate dehydrogenase, cytochrome, *Desulfovibrio*

INTRODUCTION

Sulfate reducing organisms (SRO) are anaerobic prokaryotes found ubiquitously in nature (Rabus et al., 2007; Muyzer and Stams, 2008). They employ a respiratory mechanism with sulfate as the terminal electron acceptor giving rise to sulfide as the major metabolic end-product. These organisms play an important role in global cycling of sulfur and carbon in anaerobic environments, particularly in marine habitats due to the high sulfate concentration, where they are responsible for up to 50% of carbon remineralization (Jørgensen, 1982). Sulfate reduction is a true respiratory process, which leads to oxidative phosphorylation through a still incompletely understood electron-transfer pathway. This electron transport chain links dehydrogenases to the terminal reductases, which are located in the cytoplasm, and therefore, not directly involved in charge translocation across the membrane and generation of transmembrane electrochemical potential. In recent years, the advent of genomic information coupled with biochemical and genetic studies has provided significant advances in our understanding of sulfate respiration, but several important questions remain to be answered including the sites and mechanisms of energy conservation. These studies revealed that sulfate reduction is associated with a set of unique proteins. Some of these proteins are also present in sulfur-oxidizing organisms, whereas others are shared with anaerobes like methanogens. Most biochemical studies have focused on mesophilic sulfate reducers of the *Deltaproteobacteria*, mostly *Desulfovibrio* spp. (Matias et al., 2005; Rabus et al., 2007), but previous analyses indicated that the composition of energy metabolism proteins can vary significantly between different SRO (Pereira et al., 2007; Rabus et al., 2007; Junier et al., 2010). The increasing number of SRO genomes available from different classes of both Bacteria and Archaea prompted us to perform a comparative analysis of energy metabolism proteins. In this work we report the analysis of 25 genomes of SRO available at the Integrated Microbial Genomes website. This includes 3 Archaea, 17 *Deltaproteobacteria* (of the *Desulfovibrionacae*, *Desulfomicrobiacae*, *Desulfobacteraceae*, *Desulfohalobiacae*, *Desulfobulbaceae*, and *Syntrophobacteraceae* families), 4 *Clostridia* (of the *Peptococcaceae* and *Thermoanaerobacterales* families), and *T. yellowstonii* DSM 11347 of the Nitrospira phylum (**Table 1**). This analysis extends a previous one in which only the *Deltaproteobacteria Desulfovibrio vulgaris* Hildenborough, *Desulfovibrio desulfuricans* G20, and *Desulfotalea psychrophila* were considered (Pereira et al., 2007). Genes/proteins involved in carbon

Table 1 | Analysis of Hase distribution in the SRO genomes.

	N_T	N_P	Periplasmic [NiFe]				Periplasmic [FeFe]		Cytoplasmic [NiFe]							Cytoplasmic [FeFe]			
			Soluble		Memb		Sol	Memb	Soluble					Memb		Soluble			
			HynAB	HysAB	Hyn ABC	Hyn ABC_3	HydAB	$[FeFe]_{mem}$	HdrA-Mvh	HdrABC-Mvh	Mvh	Hox	Sens.	Ech	Coo	$[FeFe]_{bif}$	$[FeFe]_{mon}$	FHL_s	HsfB
ARCHAEA																			
Archaeoglobus fulgidus	2	1			1					1									
Archaeoglobus profundus	2	1			1					1									
Caldivirga maquilingensis																			
DELTAPROTEOBACTERIA																			
Desulfovibrionacae																			
Desulfovibrio aespoeensis	3	2	1				1							1					
Desulfovibrio desulfuricans G20	6	4	1	1		1	1										1	1	
Desulfovibrio desulfuricans ATCC 27774	5	3	1		1		1							1	1				
Desulfovibrio magneticus RS-1	8	3	2				1							1		2		1	1
Desulfovibrio piger	4	2	1	1											1		1		
Desulfovibrio salexigens	5	3	1	1			1							1				1	
Desulfovibrio sp. FW1012B	5	2	1				1							1		1			1
Desulfovibrio vulgaris Hildenborough	7	4	1	1		1	1							1	1	1			
Desulfomicrobiacae																			
Desulfomicrobium baculatum	2	2	1	1															
Desulfobacteraceae																			
Desulfatibacillum alkenivorans	3	1	1						1				1						
Desulfobacterium autotrophicum HRM2	6	2	1	1					1							1		1	1
Desulfococcus oleovorans Hxd3																			
Desulfohalobiacae																			
Desulfohalobium retbaense DSM 5692	2	1	1						1										
Desulfonatronospira thiodismutans ASO3-1	3								1	1			1						
Desulfobulbaceae																			
Desulfotalea psychrophila	6	2	1		1				1			1					1	1	
Desulfurivibrio alkaliphilus	4	2	1		1						1	1							
Syntrophobacteraceae																			
Syntrophobacter fumaroxidans MPOB	9	2	1				1		2		1	1				1	1		1

	N_T	N_P	Periplasmic [NiFe]				Periplasmic [FeFe]		Cytoplasmic [NiFe]						Cytoplasmic [FeFe]			
			Soluble		Memb		Sol	Memb	Soluble					Memb	Soluble			
			HynAB	HysAB	HynABC	$HynABC_3$	HydAB	$[FeFe]_{mem}$	HdrA-MvhHdrABC-MvhMvhHoxSens.EchCooo						$[FeFe]_{bif}$	$[FeFe]_{mon}$	FHL_s	HsfB
CLOSTRIDIA																		
Peptococcaceae																		
Desulfotomaculum acetoxidans DSM 771	4	1						1							1	1		1
Desulfotomaculum reducens	7	1						1							3	2		1
C. Desulforudis audaxviator MP104C	7	1						1			1			1	1	3		
Thermoanaerobacterales																		
Ammonifex degensii KC4	5	2		1				1			1					2		
NITROSPIRA																		
Thermodesulfovibrio yellowstonii	5	1		1						1	1					2		
No. of organisms			15	8	5	2	8	4	6	4	5	3	2	7	3	8	9	5	6

N_T, total number of Hases; N_P, number of periplasmic Hases; $[FeFe]_{mem}$, membrane-associated [FeFe] Hase; $[FeFe]_{bif}$, cytoplasmic NAD(P)-dependent Hases; $[FeFe]_{mon}$, monomeric Fd-dependent Hases.

metabolism are not discussed, with the exception of lactate and formate dehydrogenases. The loci for all genes analyzed can be found in Supplementary Material. A general scheme depicting most of the proteins discussed is presented in **Figure 1**.

PROTEINS ESSENTIAL FOR SULFATE REDUCTION

As expected, all organisms analyzed contain genes for those proteins long known to be directly involved in sulfate reduction (Rabus et al., 2007), including sulfate transporters, ATP sulfurylase (*sat*), APS reductase (*aprAB*), and dissimilatory sulfite reductase (*dsrAB*; Supplementary Material). The hydrolysis of pyrophosphate is carried out by soluble inorganic pyrophosphatases in most cases, but in a few organisms a membrane-associated proton-translocating pyrophosphatase (Serrano et al., 2007) is present, which may allow energy conservation from hydrolysis of pyrophosphate. These include the Gram-positive bacteria (Junier et al., 2010), *Syntrophobacter fumaroxidans*, *Desulfococcus oleovorans*, *Desulfatibacillum alkenivorans*, and *Caldivirga maquilingensis*. F_1F_0-ATP synthases are also present in all the SRO analyzed. Other strictly conserved proteins include ferredoxins, which are very abundant proteins in sulfate reducers (Moura et al., 1994). Their crucial role in anaerobic metabolism has gained increasing evidence in recent years (Meuer et al., 2002; Herrmann et al., 2008; Thauer et al., 2008; see Cytoplasmic Electron Transfer section below). All organisms analyzed contain ferredoxin I, which in some cases is present in multiple copies, and most contain also ferredoxin II.

One of the remaining important questions about sulfate reduction is the nature of the electron donors to the terminal reductases AprAB and DsrAB. Two membrane complexes, QmoABC and DsrMKJOP (**Figures 1 and 2**) have been proposed to perform this function (Pereira, 2008).

THE QmoABC COMPLEX

QmoABC (for *Q*uinone-interacting *m*embrane-bound *o*xidoreductase complex) was first described in *D. desulfuricans* ATCC 27774 (Pires et al., 2003). It includes three subunits binding two hemes *b*, two FAD groups and several iron–sulfur centers. QmoA and QmoB are both soluble proteins homologous to HdrA, a flavin-containing subunit of the soluble heterodisulfide reductases (HDRs; Hedderich et al., 2005). HDRs are key enzymes in methanogens that catalyze the reduction of the CoM-S-S-CoB heterodisulfide, formed in the last step of methanogenesis, to the corresponding thiols (Hedderich et al., 2005). The function of HdrA is still not clear, but it has been proposed to be involved in flavin-based electron bifurcation by an HdrABC/MvhADG complex, where the endergonic reduction of ferredoxin by H_2 is coupled to the exergonic reduction of the CoM-S-S-CoB heterodisulfide by H_2 (Thauer et al., 2008). QmoC is a fusion protein that contains a cytochrome *b* transmembrane domain related to HdrE and a hydrophilic iron–sulfur domain related to HdrC. QmoB includes also a domain similar to MvhD, a subunit of F420-non-reducing hydrogenase (Mvh; Thauer et al., 2010). Since the *qmo* genes are usually adjacent to *aprAB*, and both QmoC hemes are reduced by a menaquinol analog, it has been proposed that Qmo transfers electrons from the quinone pool to AprAB, in a process that may result in energy conservation (Pires et al., 2003; Venceslau et al., 2010). Although direct electron transfer has not been reported, it was recently shown that in *D. vulgaris*

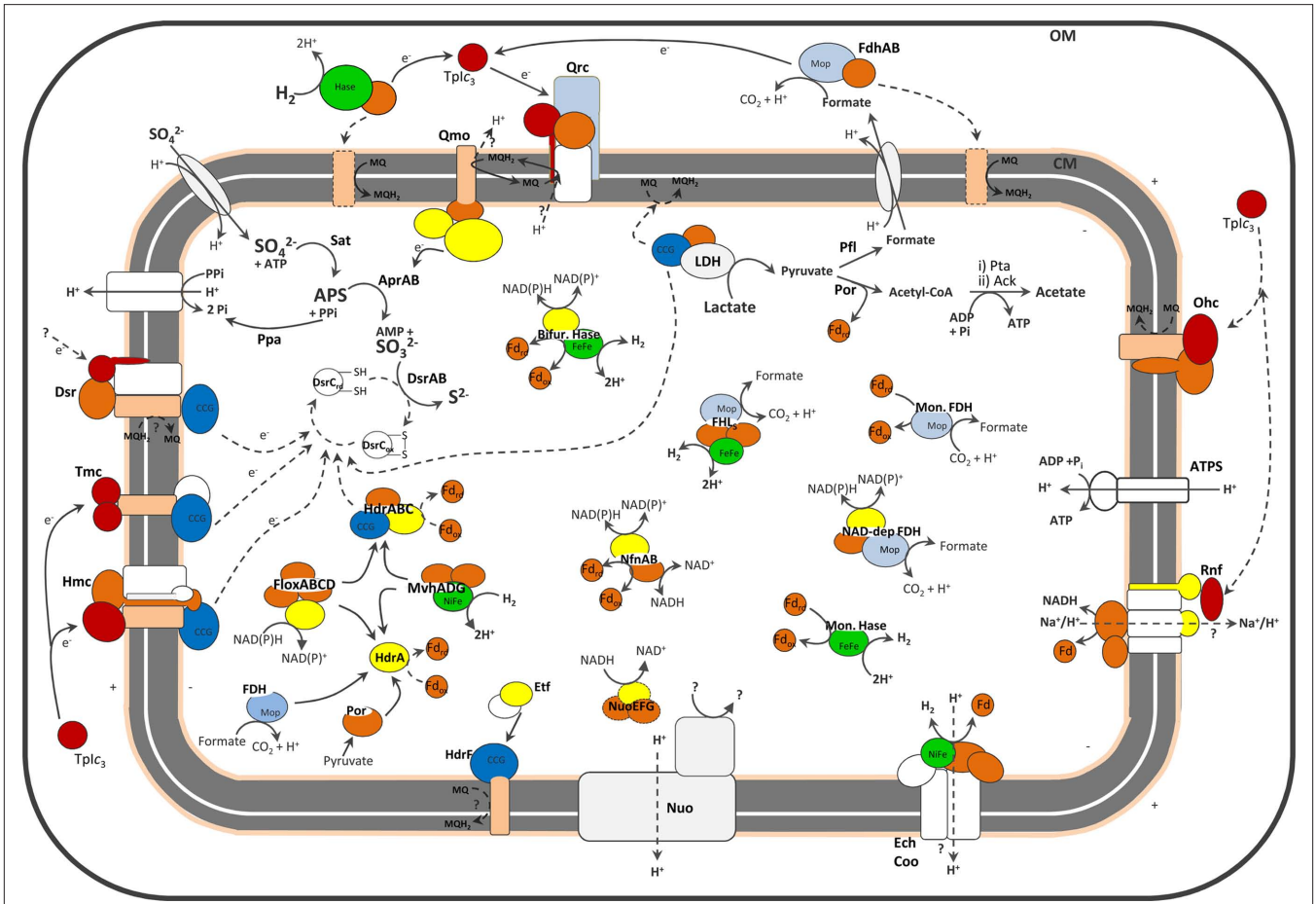

FIGURE 1 | Schematic representation of the cellular location of SRO main energy metabolism proteins. No single organism is represented. For the exact distribution of proteins in each organism please refer to the Tables. The dashed lines represent hypothetical pathways, or (in the case of periplasmic Hases and FDHs) pathways present in only a few organisms. For the sake of clarity a few proteins discussed are not represented. Color code is red for cytochromes *c*, pale orange for cytochromes *b*, yellow for flavoproteins, dark orange for FeS proteins, light blue for proteins of molybdopterin family, dark blue for CCG proteins and green for catalytic subunits of Hases.

Hildenborough the Qmo complex is essential for sulfate, but not for sulfite, reduction (Zane et al., 2010). Our analysis confirmed that a gene locus containing *sat*, *aprAB* and the *qmoABC* genes is present in the majority of SRO analyzed. The exceptions are the archaeon *C. maquilingensis* for which no *qmo* genes are detected, and the Gram-positive bacteria where the *qmoC* gene is absent. In *Desulfotomaculum acetoxidans* and *Candidatus Desulforudis* audaxviator the *qmoC* gene is replaced by the *hdrBC* genes that code for soluble subunits of HDRs (Junier et al., 2010). This suggests that in Gram-positive bacteria the reduction of APS reductase may derive from soluble pathways, rather than quinones, and not be coupled to energy conservation.

THE DsrMKJOP COMPLEX

The *dsrMKJOP* genes were first reported in the sulfur-oxidizing bacterium *Allochromatium vinosum* as part of a *dsr* locus encoding also the *dsrAB* and *dsrC* genes, among others (Pott and Dahl, 1998). The DsrMKJOP complex was isolated from *Archaeoglobus fulgidus* (Mander et al., 2002; where it was named Hme) and *D. desulfuricans* ATCC 27774 (Pires et al., 2006). It is a transmembrane complex with redox subunits in the periplasm – the triheme cytochrome *c* DsrJ, and the iron–sulfur protein DsrO; in the membrane – the cytochrome *b* DsrM (NarI family), and DsrP (NrfD family); and in the cytoplasm – the iron–sulfur protein DsrK that is homologous to HdrD, the catalytic subunit of the membrane-bound HdrED. DsrK and HdrD are both members of the CCG protein family, named after the CysCysGly residues present in the conserved cysteine-rich sequence (CX_nCCGX_mCXXC), which includes over 2000 archaeal and bacterial proteins (Hedderich et al., 1999; Hamann et al., 2007). This Cys sequence binds a special [4Fe4S] cluster, which in HDR is responsible for heterodisulfide reduction (Hedderich et al., 2005), and is also present in Dsr (Pires et al., 2006). Sequence analysis suggests that there may be two modules in the Dsr complex. One module, formed by DsrMK (based on its similarity to HdrED), may be involved in menaquinol oxidation and reduction of a cytoplasmic substrate, probably the DsrC disulfide (Oliveira et al., 2008);

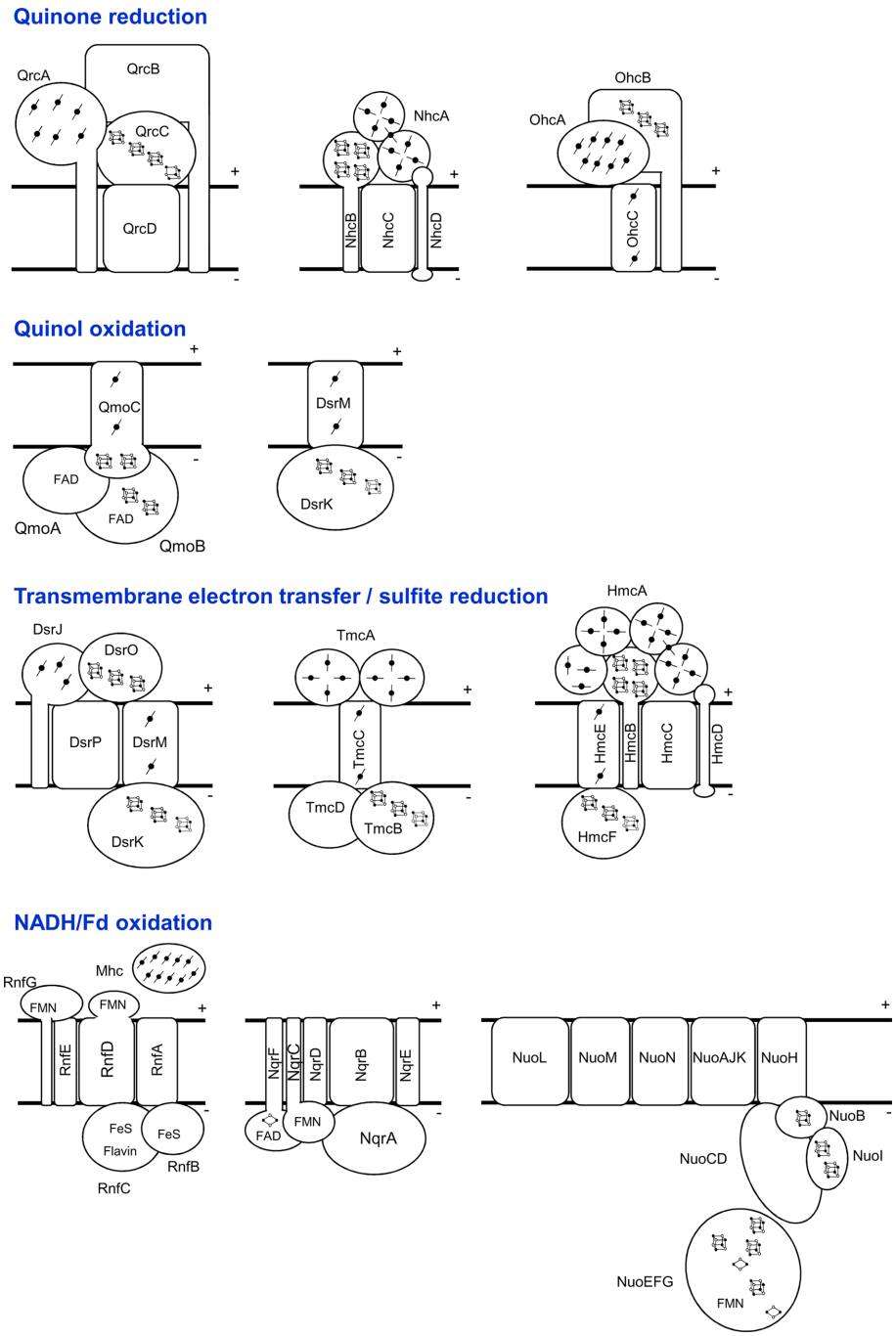

FIGURE 2 | Schematic representation of the SRO membrane-bound electron-transfer complexes, grouped in different categories according to expected function. The NuoEFG proteins are shown as one module, which is not always present.

a second module formed by DsrJOP may be involved in electron transfer between the menaquinone pool and a periplasmic component, but it is not clear in which direction. The *dsrMKJOP* genes are present in all SRO genomes analyzed, with the exception of the Gram-positive bacteria (Junier et al., 2010) and *C. maquilingensis*, for which only *dsrMK* are present. This indicates that only these two proteins are essential for sulfite reduction. Gram-positive bacteria lack a periplasmic space, which may explain the absence of DsrJO, and in these organisms DsrMK must transfer electrons between the menaquinone pool and the cytoplasm, whereas in organisms with DsrMKJOP electron transfer likely involves also periplasmic components. Several SRO contain both *dsrMKJOP* and one or more copies of *dsrMK*. A DsrMK protein was isolated from *Archaeoglobus profundus* (Mander et al., 2004).

DsrC

The *dsrC* gene is also strictly conserved in all SRO. It is one of the most highly expressed genes in *D. vulgaris* Hildenborough (Haveman et al., 2003; Wall et al., 2008) and also environmental samples (Canfield et al., 2010), pointing to an important role in sulfur metabolism. All organisms encoding a *dsrAB* sulfite reductase (sulfate/sulfite reducers or sulfur oxidizers) also contain the *dsrC* and *dsrMK* genes. DsrC is a small protein with a C-terminal swinging arm containing two strictly conserved cysteines (Cort et al., 2001; Mander et al., 2005). It belongs to a larger family of proteins, present also in organisms that do not perform dissimilatory sulfur metabolism (e.g., *E. coli* TusE), where they are involved in sulfur-transfer reactions (Ikeuchi et al., 2006). In these cases, a single cysteine, the penultimate residue of the C-terminal arm, is conserved. This suggests the involvement of a disulfide bond between the two DsrC cysteines as a redox-active center in the sulfite reduction pathway. DsrC was initially described as a subunit of DsrAB, with which it forms a tight complex (Pierik et al., 1992). However, DsrC is not a subunit, but rather a protein with which DsrAB interacts. The crystal structure of the DsrAB–DsrC complex from *D. vulgaris* revealed that the DsrC swinging arm inserts into a cleft between DsrA and DsrB, such that its penultimate cysteine comes in close proximity to the sulfite binding site at the catalytic siroheme (Oliveira et al., 2008). A mechanism for sulfite reduction involving DsrC was proposed, in which a DsrC persulfide is formed and gives rise to oxidized DsrC ($DsrC_{ox}$) with a disulfide bond between the two cysteines (Oliveira et al., 2008). $DsrC_{ox}$ is then proposed to be reduced by the DsrK subunit of the Dsr complex, which contains a catalytic iron–sulfur center for putative reduction of disulfide bonds, as described in HDRs (Pires et al., 2006). The involvement of the Dsr complex provides a link between membrane quinol oxidation and sulfite reduction that may explain the fact that proton translocation is associated with this reduction (Kobayashi et al., 1982). *In vitro* sulfite reduction by desulfoviridin, the dissimilatory sulfite reductase of *Desulfovibrio* spp. does not produce sulfide as observed in the assimilatory enzymes, but a mixture of products including thiosulfate and trithionate (Rabus et al., 2007). This led to the proposal that sulfite reduction in SRO proceeds with thiosulfate and trithionate as intermediates (Akagi, 1995). In *Desulfovibrio gigas*, flavoredoxin was implicated in thiosulfate reduction (Broco et al., 2005). However, flavoredoxin is not conserved across the SRO analyzed and there is also no evidence for enzymes to handle trithionate. Most likely the *in vitro* polythionate products observed originate from the absence of other proteins required for physiological sulfite reduction, namely DsrC (Oliveira et al., 2008).

Our genomic analysis of SRO supports the interaction between DsrC, DsrAB and the DsrMKJOP complex: In *A. profundus* and *T. yellowstonii dsrC* is in the same gene cluster as *dsrMKJOP*, and in the three Gram-positive organisms and *Ammonifex degensii*, a *dsrMK–dsrC* gene cluster is present (**Figure 3**). Strikingly, this cluster is preceded by a gene encoding a ferredoxin (Fd), and a Fd gene is also present after the *dsrMKJOP* genes and in close proximity to *dsrAB* in three *Deltaproteobacteria*. This suggests that a Fd may also be involved in the electron transfer pathway between the Dsr complex, DsrC, and DsrAB. The involvement of Fd provides a link between the sulfite reduction step and other soluble electron transfer pathways.

PERIPLASMIC ELECTRON TRANSFER

One of the most discussed models for energy conservation in SRO is the hydrogen-cycling mechanism proposed by Odom and Peck (1981). In this mechanism the reducing power from lactate

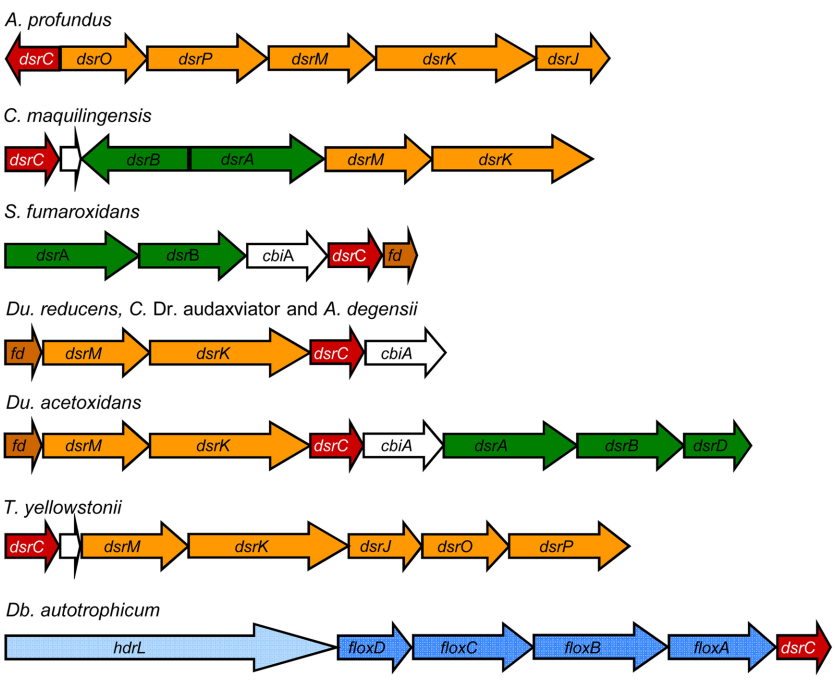

FIGURE 3 | Examples of neighborhood gene organization of the *dsrC* gene.

oxidation is transferred to a cytoplasmic hydrogenase to generate H_2 that diffuses to the periplasm. There its reoxidation generates electrons that are transferred back across the membrane for the cytoplasmic reduction of sulfate, resulting in a transmembrane proton gradient to drive ATP synthesis. This intracellular redox cycling proposal has been extended to include other possible intermediates like formate and CO (Voordouw, 2002). Hydrogen and formate are also important energy sources for SRO in natural habitats. Oxidation of these substrates by periplasmic enzymes contributes to a proton gradient as electrons are transferred to the quinone pool or directly across the membrane for cytoplasmic sulfate reduction. The common bacterial uptake hydrogenases (Hases) and formate dehydrogenases (FDHs) are composed of three subunits: a large catalytic subunit, a small electron-transfer subunit and a membrane-associated protein responsible for quinone reduction. *Desulfovibrio* organisms are unusual in that most of their periplasmic Hases and FDHs lack the membrane subunit, and instead transfer electrons to one or several cytochromes *c* (Heidelberg et al., 2004; Matias et al., 2005).

PERIPLASMIC-FACING HYDROGENASES

Two of the SRO analyzed contain no Hases at all: the archaeon *C. maquilingensis* and the *Deltaproteobacterium Dc. oleovorans*. In addition, *Desulfonatronospira thiodismutans* contains no periplasmic Hases (**Table 1**). The total absence of Hases in two SRO was unexpected and indicates that hydrogen metabolism is not essential for sulfate reduction. The other SRO contain from one to four periplasmic enzymes, the most common of which is the soluble [NiFe] HynAB. All *Deltaproteobacteria* contain at least one copy of HynAB. In two archaea and three *Deltaproteobacteria* this protein is membrane-anchored by an additional subunit for quinone reduction (HynABC). Eight organisms also contain the [NiFeSe] HysAB Hase (Valente et al., 2005). The HynAB and HysAB enzymes use as electron acceptor the Type I cytochrome c_3 ($TpIc_3$; Matias et al., 2005). Finally, only two organisms contain a copy of a HynABC3, in which another dedicated cytochrome c_3 is encoded next to the *hynAB* genes. A periplasmic [FeFe] Hase is present in all *Desulfovibrio* organisms, except *D. piger*, and is also found in *S. fumaroxidans*. This enzyme is soluble and also uses $TpIc_3$ as electron acceptor. A membrane-anchored [FeFe] Hase is present in the four *Clostridial* organisms. A Tat signal peptide present in the catalytic subunit indicates that the enzyme is translocated to the extracytoplasmic side of the cellular membrane, which is somewhat unexpected for the Gram-positive organisms that lack a periplasmic compartment. The enzyme is anchored to the membrane through a NrfD-like transmembrane protein that should transfer electrons to the menaquinone pool.

Overall, the analysis indicates that a periplasmic Hase is found in most SRO, which functions in the uptake of H_2. The *Desulfovibrionacae* organisms contain a higher number of periplasmic enzymes compared to the others. In *D. vulgaris* Hildenborough, which has four periplasmic Hases, it has been shown that expression of these enzymes is fine tuned to respond to metal availability (Valente et al., 2006) and hydrogen concentration (Caffrey et al., 2007). The Clostridial organisms contain a novel membrane-anchored [FeFe] Hase.

PERIPLASMIC-FACING FORMATE DEHYDROGENASES

As in the case of Hases, the periplasmic FDHs can be either soluble, comprising only the catalytic and small subunits (FdhAB; Almendra et al., 1999) or additionally a dedicated cytochrome c_3 (FdhABC3; Sebban et al., 1995), or they can be of the typical membrane-associated form, in which a subunit for quinone reduction is present. This can either be a NarI-like cytochrome *b* (FdhABC) or a larger protein of the NrfD family (FdhABD). The physiological electron acceptor for FdhAB is also likely to be the soluble $TpIc_3$ (ElAntak et al., 2003; Venceslau et al., 2010). Of the SRO analyzed, two Archaea contain neither periplasmic or cytoplasmic FDHs (**Table A1** in Appendix), again indicating that formate metabolism is not essential for sulfate reduction. All other SRO analyzed contain from one to three periplasmic FDHs, the most widespread of which is FdhAB. Six organisms contain one FdhABC3. Only three organisms contain FdhABC. Two Gram-positive bacteria contain FdhABD where FdhB has a twin-arginine signal peptide, indicating that these enzymes are translocated to outside of the cellular membrane, as observed for the [FeFe] Hase. In *D. vulgaris* Hildenborough the gene locus for FdhABD includes also two cytochromes *c*. Several of the FDHs contain selenocysteine (Sec), and in some organisms only Sec-containing FDHs are present, whereas others contain also Cys-containing enzymes.

CYTOCHROMES *c*

The *Desulfovibrionacae* organisms are characterized by a very high level of multiheme cytochromes *c*, the most abundant and well studied of which is the $TpIc_3$ (Matias et al., 2005). The genome of *D. vulgaris* Hildenborough first revealed that a pool of cytochromes *c* is present in the periplasm (Heidelberg et al., 2004), some of which belong to the cytochrome c_3 family, but not all (Matias et al., 2005; Pereira et al., 2007). Several multiheme cytochromes *c* are associated with membrane complexes, and these will be discussed in the following section. Most SRO analyzed contain a high number of multiheme cytochromes *c* (**Table A2** in Appendix) but several exceptions are observed: *C. maquilingensis*, *Dm. acetoxidans*, and *Desulfotomaculum reducens* contain no cytochromes *c* at all; *A. profundus* contains only DsrJ; *A. fulgidus* contains DsrJ and an octaheme cytochrome, and *Dm. reducens* contains only the NrfHA proteins (Rodrigues et al., 2006), both with signal peptides again indicating an extracytoplasmic location. In general terms, the *Deltaproteobacteria* and *T. yellowstonii* have multiple cytochromes *c*, contrary to the Archaea, Gram-positive SRO, and *A. degensii*. The $TpIc_3$ is present in all the *Deltaproteobacteria* (except *Dt. psychrophila* and *Dv. alkaliphilus*) and in *T. yellowstonii*. Often there are two to four copies of monocistronic cytochromes c_3, whereas others are associated with periplasmic Hases and FDHs. Tetraheme cytochromes of the c_{554} family (Iverson et al., 1998) are also present in several organisms, including one associated with a methyl-accepting chemotaxis sensory transducer protein, suggesting an involvement in regulation. The monoheme cytochrome c_{553} is only present in five *Deltaproteobacteria*, often in the same locus as cytochrome *c* oxidase, suggesting it acts as its electron donor. The nitrite reductase complex formed by the two cytochromes NrfH and NrfA (Rodrigues et al., 2006) is one of the more widespread cytochromes in SRO. Nitrite is a powerful inhibitor of SRO and NrfHA acts as a detoxifying enzyme (Greene et al., 2003).

Table 2 | Analysis of membrane redox complexes distribution in the SRO genomes.

	H^+-PPi	Dsr	Qmo	Periplasmic		TpIc_3	Qrc	Tmc	Hmc	Nhc	Ohc	Rnf	Nuo	Nqr	bc_1
				Hase	Fdh										
ARCHAEA															
Archaeoglobus fulgidus		1 + 2MK	1										1‡		
Archaeoglobus profundus		1	1										1‡		
Caldivirga maquilingensis	2	MK											?		1
DELTAPROTEOBACTERIA															
Desulfovibrionacae															
Desulfovibrio aespoeensis		1	1	+	+	2	1	1	1	1		1	1*		
Desulfovibrio desulfuricans G20		1	1	+	+	2	1	1	1			1			
Desulfovibrio desulfuricans ATCC 27774		1	1	+	+	1		1		1		1	1*		
Desulfovibrio magneticus RS-1		1	1	+	+	2	1	1	1		1		1*+1		
Desulfovibrio piger		1	1	+	+	1				1		1			
Desulfovibrio salexigens		1	1	+	+	3	1	1	1		1	2	1*	1	
Desulfovibrio sp. FW1012B		1	1	+	+	2	1	1	1				1*+1		
Desulfovibrio vulgaris Hildenborough		1	1	+	+	1	1	1	1		1	1			
Desulfomicrobiacae															
Desulfomicrobium baculatum		1	1	+	+	2	1	1	1		1	1			
Desulfobacteraceae															
Desulfatibacillum alkenivorans	1	1	1	+		2	1			1	1	1			
Desulfobacterium autotrophicum HRM2		1	1	+	+	1	2	2				1 + 1↔		1	
Desulfococcus oleovorans Hxd3	1	1	1		+	2	1	2	1		1	1 + 1↔		1	
Desulfohalobiacae															
Desulfohalobium retbaense DSM 5692		1	1	+	+	4	1	1	1		1	1↔			
Desulfonatronospira thiodismutans ASO3-1		1	1		+	3		2		1			1*		
Desulfobulbaceae															
Desulfotalea psychrophila		1	1	+								1↔	1*	1	
Desulfurivibrio alkaliphilus		1	1	+		2							1*	1	
Syntrophobacteraceae															
Syntrophobacter fumaroxidans MPOB	2	1	1	+	+	1	1				1	1↔	1		1
CLOSTRIDIA															
Peptococcaceae															
Desulfotomaculum acetoxidans DSM 771	1	MK	1†										1*		
Desulfotomaculum reducens	1	MK	1†										1*		

	H^+-PPi	Dsr	Qmo	Periplasmic		$TpIc_3$	Qrc	Tmc	Hmc	Nhc	Ohc	Rnf	Nuo	Nqr	bc_1
				Hase	Fdh										
C. Desulforudis audaxviator MP104C	1	MK	1[†]												
Thermoanaerobacterales															
Ammonifex degensii KC4		MK	1	+	+										
NITROSPIRA															
Thermodesulfovibrio yellowstonii		1	1	+	+	1			1				1*		1
No. of organisms	7	20/5	24	17	16	17	12	12	10	5	8	13	15	5	3

*The presence of periplasmic soluble Hases and FDHs, and $Tplc_3$, is also indicated. MK, only dsrMK genes present; [†]only qmoAB present; [↔]rnf gene cluster without the multiheme cytochrome gene; $^{+}F_{420}H_2$:quinone oxidoreductase; *nuo gene cluster lacking nuoEFG; 1 – nuo gene cluster located separately from nuoEFG genes.*

MEMBRANE REDOX COMPLEXES

Tmc, Hmc, Nhc, AND Ohc COMPLEXES

A family of transmembrane redox complexes that include a multiheme cytochrome *c* subunit has been described in *Desulfovibrio* (Pereira, 2008). The first complex identified was the Hmc complex composed of HmcABCDEF (Rossi et al., 1993). The subunit composition of Hmc is strikingly similar to the Dsr complex in terms of the type of proteins present: a cytoplasmic CCG protein related to HdrD, two integral membrane proteins of the NarI and NrfD families, a periplasmic ferredoxin-like protein and a periplasmic cytochrome *c* (**Figures 1 and 2**). This suggests that both complexes have related functions, but the sequence identity between subunits is very low. The cytochrome *c* subunit is a large 16 heme cytochrome in Hmc (HmcA) and a small triheme cytochrome in Dsr (DsrJ). HmcA can accept electrons from periplasmic hydrogenases via the $TpIc_3$ (Pereira et al., 1998; Matias et al., 2005), but this is not observed for DsrJ (Pires et al., 2006). This cytochrome has a heme with unusual histidine/cysteine ligation, but its function has not been elucidated (Pires et al., 2006; Grein et al., 2010). It is not clear if Hmc exchanges electrons with the quinone pool, or directly between the periplasm and cytoplasm. Some studies have indicated that the function of Hmc is in electron transfer to the cytoplasm during growth with hydrogen (Dolla et al., 2000; Voordouw, 2002), but the *hmc* genes are downregulated under these conditions (Caffrey et al., 2007; Pereira et al., 2008). More recently this complex was shown to play a role during syntrophic growth of *D. vulgaris*, where it was proposed to be implicated in electron transfer from the cytoplasm to the periplasm (Walker et al., 2009).

The TmcABCD complex seems to be a simplified version of Hmc. It includes a tetraheme cytochrome c_3 (TmcA, first described as acidic cytochrome c_3 or Type II c_3, Valente et al., 2001), a CCG protein homologous to HmcF (TmcB), a cytochrome *b* (TmcC), and a tryptophan-rich protein (TmcD; Pereira et al., 2006). TmcA is an efficient electron acceptor of the periplasmic Hase/$TpIc_3$ couple (Valente et al., 2001, 2005; Pieulle et al., 2005). All redox centers of the Tmc complex are reduced with H_2 (Pereira et al., 2006), and the *tmc* genes are upregulated in growth with hydrogen *versus* lactate (Pereira et al., 2008), indicating that Tmc acts to transfer electrons from periplasmic H_2 oxidation to the cytoplasm.

Two other complexes related to Tmc and Hmc are present in the genomes of SRO. One includes a nine-heme cytochrome and is designated as Nhc complex (for *n*ine-*h*eme cytochrome *c*omplex; Saraiva et al., 2001), and the other includes an eight-heme cytochrome and was designated as Ohc (for *o*cta*h*eme cytochrome *c*omplex; Pereira et al., 2007). The structure of the NhcA cytochrome is similar to the C-terminal domain of the HmcA, and it is also reduced by the Hase/$TpIc_3$ couple (Matias et al., 1999), whereas OhcA belongs to a different cytochrome family. OhcC is a cytochrome *b* of the NarI family, whereas NhcC membrane subunit is of the NrfD family. The subunits of the Hmc, Tmc, Nhc, and Ohc complexes are homologous to each other, indicating they belong to the same family. However, the Nhc and Ohc complexes lack the cytoplasmic CCG protein, so they should transfer electrons from the periplasm to the quinone pool. In contrast, both Hmc and Tmc include the CCG protein related to DsrK and HdrD, containing

a binding site for a putative catalytic [4Fe4S] center, which hints that they are implicated in similar thiol/disulfide redox chemistry as DsrK possibly involving $DsrC_{ox}$.

The genomic analysis indicates that the Hmc, Tmc, Nhc, and Ohc complexes (**Table 2**) are present in *Deltaproteobacteria*, with the exception of the two members of the *Desulfobulbaceae* family. They are not present in the Archaea organisms or members of *Clostridia*, and *T. yellowstonii* has only Hmc. This distribution correlates well with the presence of their putative electron donor, $TpIc_3$. All organisms that have Hmc, usually also have Tmc, and some organisms have two copies of Tmc. In *D. desulfuricans* ATCC 27774 a three-subunit complex is found including a triheme cytochrome c_7, homologous to the N-terminal part of Hmc. Although its subunits are more similar to Hmc, the subunit composition is more characteristic of a Tmc. The Nhc complex has a more limited distribution, and in some organisms the cytochrome subunit has 13 hemes. In *Dt. thiodismutans* the cytochrome subunit is not present.

Qrc COMPLEX

Recently, a new membrane complex named Qrc (for *q*uinone *r*eductase *c*omplex) was isolated from *D. vulgaris* (Venceslau et al., 2010). It is composed of four subunits, QrcABCD, including a hexaheme cytochrome *c* (QrcA), a large protein of the molybdopterin-containing family, but which does not bind molybdenum (QrcB), a periplasmic iron–sulfur protein (QrcC) and an integral membrane protein of the NrfD family (QrcD). The Qrc complex accepts electrons from periplasmic Hases and FDHs through $TpIc_3$ and has activity as a $TpIc_3$:menaquinone oxidoreductase (Venceslau et al., 2010). A *D. desulfuricans* G20 mutant lacking the *qrcB* gene was selected from a library of transposon mutants by its inability to grow syntrophically with a methanogen on lactate (Li et al., 2009). This mutant is unable to grow with H_2 or formate as electron donors but grows normally with lactate, confirming the role of Qrc in H_2 and formate oxidation. It has been proposed that the Qrc and Qmo complexes constitute the two arms of an energy conserving redox loop (Simon et al., 2008), contributing to proton motive force generation during sulfate reduction with H_2 or formate (Venceslau et al., 2010). This previous study showed that the *qrc* genes are present in sulfate reducers that have periplasmic Hases and/or FDHs that lack a membrane subunit for quinone reduction. Our present analysis confirms this and shows that the *qrc* genes are found in many *Deltaproteobacteria*, but not in other SRO (**Table 2**). *D. piger* and *Dt. thiodismutans* both have soluble periplasmic Hases and FDHs but lack a Qrc. In both cases an alternative complex for quinone reduction is present, like Nhc and Ohc. An exception is *T. yellowstonii* that also has soluble periplasmic Hases and FDHs and for which only the Hmc complex was identified. In this case maybe electrons go directly to the cytoplasm through Hmc or this is also capable of quinone reduction.

Rnf, Nqr, AND Nuo COMPLEXES FOR NADH AND FERREDOXIN OXIDATION

Although it has long been known that NADH and ferredoxin (Fd) are important cytoplasmic components of energy metabolism in SRO, it is still not clear what role they play in the electron-transfers chains of these organisms. The membrane-bound Rnf complex mediates electron transfer between NADH and Fd and is found in numerous organisms (Li et al., 2006; McInerney et al., 2007; Müller et al., 2008; Seedorf et al., 2008). It was first described in *Rhodobacter capsulatus* where it is proposed to catalyze the reverse electron transport from NADH to Fd driven by the transmembrane proton potential (Schmehl et al., 1993). In other organisms it is proposed to carry out electron transport from reduced Fd to NAD^+, coupled to electrogenic Na^+ or H^+ translocation (Müller et al., 2008). The Rnf complexes are constituted by six to eight subunits (**Figures 1 and 2**), which show similarity to Na^+-translocating NADH:quinone oxidoreductases (Nqr; Steuber, 2001). There is yet no direct biochemical confirmation that Rnf translocates ions, but recent inhibitor studies obtained with membrane vesicles of the acetogenic bacterium *Acetobacterium woodii* are consistent with the proposal that Rnf catalyzes reduction of NAD^+ from Fd coupled to electrogenic Na^+ transport (Biegel and Müller, 2010). Both Rnf and Nqr are small complexes compared to the usual 14 subunits of the Nuo NADH:quinone oxidoreductases (Complex I; Efremov et al., 2010).

Our analysis shows that most organisms analyzed contain one, or more, of the Nuo, Rnf, and Nqr complexes (except *C. Dr.* audaxviator and *A. degensii*; **Table 2**). A surprisingly high number of SRO contain the *nuo* genes for complex I. Only Nuo is detected in the four *Clostridia* organisms, and $F_{420}H_2$:quinone oxidoreductase in the case of the Archaea (Kunow et al., 1994). In most cases the NuoEFG subunits that form the NADH dehydrogenase module are absent, as observed for the complex from cyanobacteria and chloroplasts (Friedrich and Scheide, 2000), suggesting that NADH is not the actual electron donor. It is tempting to speculate that these complexes also oxidize Fd. In *Desulfovibrio magneticus* and *Desulfovibrio* sp. FW1012B two clusters of *nuo* genes are present, one of which includes the *nuoEFG* genes.

The Rnf complex is present in most organisms, with the exception of the *Clostridia* and Archaea, suggesting it plays a key role in the energy conservation strategies of many sulfate reducers. In most cases a multiheme cytochrome *c* encoding gene (with 4–10 hemes) is found next to the *rnf* genes as reported for *Methanosarcina acetivorans* (Li et al., 2006). Interestingly, *Desulfobacterium autotrophicum* and *Dc. oleovorans* have two copies of the *rnf* genes, and only one includes the cytochrome *c* gene. The presence of this cytochrome provides an electron input/output module in the periplasm, which may link the cytochrome *c* pool with NAD(H) and/or Fd. The Nqr complex has a more limited distribution and is detected in only 5 of the 25 genomes analyzed. Of these, four are marine organisms and the other (*Desulfurivibrio alkaliphilus*) is a haloalkaliphilic bacterium isolated from soda lakes, and thus all are likely to have Na^+-based bioenergetics. Two of these organisms have genes for all three complexes (Nuo, Rnf, and Nqr).

H^+-PYROPHOSPHATASES AND OTHERS

The Gram-positive organisms, *C. maquiligensis* and a few *Deltaproteobacteria* contain ion-translocating pyrophosphatases, which are probably involved in energy conservation (**Table 2**). This is likely to compensate for the absence of other transmembrane complexes in some of these organisms. A bc_1 complex is also present

in *C. maquiligensis*, *S. fumaroxidans*, and *T. yellowstonii*. A *bd* quinol oxidase is present in 19 of the 25 organisms, and 7 contain a cytochrome *c* oxidase (**Table A2** in Appendix).

Ech AND Coo HYDROGENASES

The Ech Hases belong to the energy-conserving membrane-bound [NiFe] Hases that are closely related to complex I (Hedderich and Forzi, 2005; Hedderich et al., 2005). They catalyze the reduction of H^+ with Fd coupled to chemiosmotic energy conservation, or reduction of Fd with H_2 driven by reverse electron transport. Thus, Ech Hases and Rnf constitute the two complexes in SRO capable of performing endergonic reduction of Fd based on chemiosmotic coupling. A closely related group are the CooMKLXUH CO-induced Hases of chemolithoautotrophic bacteria that oxidize CO to CO_2 with reduction of H^+ to H_2 (Hedderich et al., 2005; Singer et al., 2006). The presence of an Ech Hase in SRO was first reported in *Desulfovibrio gigas*, where it was proposed to constitute the cytoplasmic Hase required for the hydrogen-cycling hypothesis (Rodrigues et al., 2003). The genome of *D. vulgaris* Hildenborough encodes both an Ech and Coo Hase (Heidelberg et al., 2004), and it was shown that this organism produces CO transiently from pyruvate during growth on sulfate (Voordouw, 2002). In *D. vulgaris* the *ech* genes are very upregulated during growth with H_2, and also upregulated with pyruvate as electron donors relative to lactate, whereas the *coo* genes are downregulated in H_2 (Pereira et al., 2008). This agrees with an expected higher level of CO during growth with lactate, leading to production of the Coo Hase, and suggests that Ech may work bidirectionaly, to reduce Fd for carbon fixation during growth with H_2 or to produce H_2 from reduced Fd during growth with pyruvate. Recently, the *coo* genes were shown to be upregulated during syntrophic growth of *D. vulgaris* on lactate with a methanogen (Walker et al., 2009). In addition, mutation of the *coo* genes severely impaired syntrophic growth while not affecting sulfate respiration, suggesting that Coo is an essential Hase to produce H_2 from lactate in these conditions.

Despite these interesting results the Ech and Coo Hases are restricted to *Desulfovibrio* organisms, with a single exception of *C. Dr.* audaxviator that has a set of *ech* genes (**Table 1**). In contrast, the other organisms have soluble cytoplasmic Hases that are not present in *Desulfovibrio*.

CYTOPLASMIC ELECTRON TRANSFER

In recent years several studies unraveled a novel process of coupling endergonic to exergonic redox reactions in anaerobic organisms, through a flavin-based electron bifurcation mechanism involving only soluble proteins (Herrmann et al., 2008; Li et al., 2008; Thauer et al., 2008; Schut and Adams, 2009). This mechanism involves the two-step reduction/oxidation of a flavin cofactor, through a flavin-semiquinone intermediate, in which each step is associated with a different reductant/oxidant (Thauer et al., 2008), in analogy to the quinone-based electron bifurcating mechanism of the bc_1 complex (Xia et al., 2007). Five examples have been described including: (i) the coupling of Fd reduction with NADH to reduction of butyryl-CoA with NADH by the butyryl-CoA dehydrogenase-EtfAB complex (Herrmann et al., 2008; Li et al., 2008), (ii) coupling of Fd reduction with H_2 to the reduction of the methanogenic CoM-S-S-CoB heterodisulfide with H_2 catalyzed by the MvhADG/HdrABC complex (Thauer et al., 2008, 2010), (iii) coupling of Fd reduction with formate to the reduction of the methanogenic CoM-S-S-CoB heterodisulfide with formate catalyzed by a FdhAB/HdrABC complex (Costa et al., 2010), (iv) coupling of H_2 formation from NADH with H_2 formation from reduced Fd catalyzed by the multimeric [FeFe] Hases (Schut and Adams, 2009), and (v) coupling of $NADP^+$ reduction with reduced Fd with $NADP^+$ reduction with NADH catalyzed by NfnAB (Wang et al., 2010). These cases stress the important role Fd plays in anaerobic metabolism. The reduced Fd produced through a bifurcating reaction may be oxidized by membrane-associated ion-translocating complexes (such as Rnf or Ech), resulting in energy conservation, or it may be used as electron donor in other metabolic reactions. Our genomic analysis of SRO revealed there are several examples of soluble proteins in these organisms with the potential to carry out electron bifurcation from H_2, formate or other carbon-based electron donors. In particular, a very high number of proteins related to HDRs were identified (see below).

CYTOPLASMIC HASES

An unexpectedly high number of soluble cytoplasmic hydrogenases, of both [NiFe] and [FeFe] families, were detected in the present analysis (**Table 1**). Most organisms contain a cytoplasmic-facing Hase, either soluble or membrane-bound, except the two organisms that contain no Hases at all and *Desulfomicrobium baculatum*. In numerous cases, the gene organization indicates that the cytoplasmic Hases are likely to be involved in electron bifurcation mechanisms, either involving NADH dehydrogenases or HdrA-like proteins. A large number of the [NiFe] Hases detected are related to the MvhADG Hases of methanogens (Thauer et al., 2010). In these organisms MvhADG reduces the cytoplasmic heterodisulfide reductase HdrABC, and the two proteins have been shown to form a large complex (Stojanowic et al., 2003). The activity of this complex is increased in the presence of Fd, and MvhADG/HdrABC are proposed to couple the endergonic reduction of Fd with H_2 to the exergonic reduction of the heterodisulfide with H_2 by electron bifurcation, probably involving the FAD group of HdrA (Thauer et al., 2008, 2010). In the SRO analyzed the *mvhADG* genes are found next to an *hdrA* gene (six organisms) or *hdrABC* genes (four organisms), suggesting these act as electron acceptors in a process that may involve electron bifurcation. In five organisms no *hdr* genes are close by. Another type of closely related [NiFe] Hase, of the Hox type, is present only in three organisms. Hox Hases are bidirectional NAD(P)-linked Hases common in cyanobacteria, and also found in other organisms (Vignais and Billoud, 2007). In the three SRO the Hox gene cluster includes *hoxHY* coding for the catalytic and small subunits, and *hoxEFG* that are homologous to *nuoEFG*, and code for the diaphorase module of the Hase. It is striking that in all SRO analyzed, with a single exception (*C. Dr.* audaxviator), the organisms that contain the energy-conserving Hases Ech or Coo do not contain other cytoplasmic [NiFe] Hases, and organisms that contain cytoplasmic [NiFe] Hases do not contain either Ech or Coo. This suggests that in SRO energy coupling through [NiFe] Hases involves either a chemiosmotic or an electron bifurcating mechanism. In the Archaea, only MvhADG/HdrABC is

detected, and in the *Clostridia* only two isolated MvhADG Hases are present. In two organisms, genes for another [NiFe] Hase are found next to genes encoding sensor/response-regulator proteins and histidine kinases, suggesting they are regulatory Hases.

Many cytoplasmic [FeFe] Hases are also present in the SRO analyzed, and are particularly abundant in the *Clostridia* class. Many of these are monomeric Fd-dependent Hases (**Table 1**). Another large group of [FeFe] Hases detected is formed by multimeric NAD(P)-dependent Hases similar to the tetrameric Hases from *D. fructosovorans* (Malki et al., 1995) and *Thermoanaerobacter tengcongensis* (Soboh et al., 2004). These enzymes include one flavoprotein subunit that binds NAD(P). Another member of this group is the trimeric Hase of *Thermotoga maritima* that was shown to use Fd and NADH synergistically as electron donors for production of H_2 (Schut and Adams, 2009). This is proposed to be also an electron bifurcating mechanism in which the exergonic oxidation of Fd is coupled to the unfavorable oxidation of NADH to give H_2. In *D. fructosovorans* cell extracts no NAD^+-reducing activity was detected and it was proposed that the enzyme functions as a $NADP^+$-reducing H_2-uptake Hase (Malki et al., 1995). The enzyme from *T. tengcongensis* was isolated and shown to work bidirectionally with NAD(H), but not with NADP(H) (Soboh et al., 2004). In the organisms analyzed the enzyme may be tetrameric, trimeric and in two organisms (*D. vulgaris* and *Db. autotrophicum*) dimeric. At this point it is not clear if the function of these Hases in the SRO is of H_2 production from Fd/NAD(P)H, the reverse, or both depending on the metabolic conditions.

A novel and interesting group of [FeFe] Hases genes is found next to a gene coding for a type I FDH (Matson et al., 2010), suggesting the two units may form a soluble formate–hydrogen lyase complex (FHL_s). This gene cluster is present only in five *Deltaproteobacteria*, and includes minimally the gene coding for the iron-only Hase, the gene for the catalytic subunit of FDH and two four-cluster electron-transfer proteins related to HydN. All subunits are soluble in contrast to the *E. coli* FHL complex (Sawers, 2005). In some organisms, the iron–sulfur protein encoded next to the *hydA* gene has a predicted signal peptide, but this is absent in other organisms. This raises doubts about the cellular location of the Hase. It is possible that this sequence is not cleaved and acts as a membrane anchor. This putative FHL_s complex is equivalent of the one recently described to be present in the termite gut acetogen *Treponema primitia*, where it is proposed to carry out H_2-dependent CO_2 reduction (Matson et al., 2010). However, the function of these proteins in SRO remains for now unknown.

Finally, in six organisms an [FeFe] Hase including a PAS sensor domain was identified, which is very similar to the HsfB protein recently reported in *Thermoanaerobacterium saccharolyticum* (Shaw et al., 2009). This Hase is likely to be involved in H_2 sensing and regulation.

CYTOPLASMIC FORMATE DEHYDROGENASES

A cytoplasmic FDH is present in many, but not all SRO (**Table A1** in Appendix). It is absent in the Archaea, for which a single periplasmic FDH is detected. A NAD(P)H-linked FDH is present in many organisms, but not in *Desulfovibrionacae* and *Desulfobacteraceae*. In these cases the catalytic FDH gene is found next to two *nuoEF*-like genes. Another noteworthy group is that of the putative soluble FHL_s described above. Only in two organisms (*Df. alkenivorans* and *Db. autotrophicum*) is an isolated *fdhA* gene present that may encode a Fd-dependent FDH. In other cases an *fdhA* gene is part of a more complex gene cluster, including in some cases *hdr* genes (see below).

ELECTRON BIFURCATING TRANSHYDROGENASE

A heterodimeric transhydrogenase was recently reported from *Clostridium kluyveri* (Wang et al., 2010). The enzyme, named NfnAB, catalyzes the reversible NADH-dependent reduction of $NADP^+$ by reduced Fd, or the NAD^+-dependent reduction of Fd by NADPH. It is another example of a bifurcating reaction as it couples the exergonic reduction of $NADP^+$ with reduced Fd to the endergonic reduction of $NADP^+$ with NADH. The *nfnAB* genes, both encoding iron–sulfur flavoproteins, are present in several organisms (Wang et al., 2010). They are often annotated as sulfide dehydrogenase, as this enzyme was initially reported in *Pyrococcus furiosus* to act as sulfide dehydrogenase (Ma and Adams, 1994), but later described to act physiologically as a Fd:$NADP^+$ oxidoreductase (Ma and Adams, 2001). We found that the *nfnAB* genes are also present in the great majority of SRO, with the exception of the Archaea, and three bacteria (**Table A3** in Appendix), suggesting it plays an important role also in the metabolism of SRO.

HETERODISULFIDE REDUCTASE-LIKE PROTEINS

In methanogens without cytochromes the HDR enzyme is soluble and composed of three subunits, HdrABC, whereas in methanogens with cytochromes it is membrane-associated and formed by two subunits, HdrDE (Hedderich et al., 2005; Thauer et al., 2008). HdrA is an iron–sulfur flavoprotein, HdrC is a small iron–sulfur protein and HdrB contains two CCG domains and harbors a special [4Fe4S] catalytic site. HdrE is a membrane-bound cytochrome *b* and HdrD has both HdrB- and HdrC-like domains and includes a similar catalytic cofactor to HdrB. The HdrDE protein receives electrons from methanophenazine and reduction of the heterodisulfide is coupled to energy conservation by a redox loop mechanism involving also the membrane-associated VhoACG Hase (Hedderich et al., 2005; Thauer et al., 2008). The soluble HdrABC enzyme forms a complex with the soluble MvhADG Hase that catalyzes heterodisulfide reduction with H_2. This exergonic reaction is proposed to be coupled to the endergonic reduction of Fd by flavin-based electron bifurcation involving HdrA (Thauer et al., 2008). As discussed above, the membrane complexes Qmo, Dsr, Tmc, and Hmc all include subunits related to HDRs (Pereira, 2008). The abundance of HDR-like proteins in SRO has been highlighted in recent genomes of SRO (Strittmatter et al., 2009; Junier et al., 2010). Recently, Strittmatter et al. (2009) proposed two new types of HDR subunits, based on proteins encoded in the *Db. autotrophicum* genome. The first, HdrF includes HdrB- and HdrC-like domains fused to a third transmembrane domain. Thus, HdrF is like a fusion of HdrE and HdrD. The second, HdrL, is a large protein containing an HdrA domain and one or two NADH-binding domains (Strittmatter et al., 2009). We have analyzed genes coding for HdrA-, HdrB-, and HdrD-like proteins as these are the most relevant subunits of HDRs. In general, we found few HdrB-like proteins and they are either associated with HdrAs or they are domains of HdrDs. In contrast, we found a very high number of HdrA- and HdrD-related proteins in the genomes of SRO, so our analysis focuses on these two protein families.

HdrA

The majority of HdrA-like proteins are encoded in two types of gene loci (**Figure 4**; **Table 3**). In the first type an *hdrA* gene or a set of *hdrABC* genes are found next to *mvhDGA* genes coding for a soluble Mvh [NiFe] Hase as discussed above. In the second type, again a single *hdrA* gene or a set of *hdrABC* genes are found next to four genes that we named *floxABCD* genes (for *fl*avin *ox*idoreductase). The *floxABCD/hdrABC* gene cluster was first identified in *D. vulgaris* Hildenborough as encoding a putative Hase–HDR complex (Haveman et al., 2003), as the *flox* genes are annotated as putative Hase genes because they code for proteins related to subunits of *P. furiosus* NAD(P)-dependent soluble Hases (SH) I and II (Jenney and Adams, 2008). However, a gene coding for a catalytic Hase subunit is not present, so Flox is not a Hase. The *floxA* gene codes for a protein with both FAD and NAD(P)-binding domains and is similar to *P. furiosus* SH subunit γ. The *floxB* and *floxC* genes are related to *rnfC* and both code for iron–sulfur proteins similar to *P. furiosus* SH subunit β. The *floxD* gene codes for a protein similar to MvhD, which in methanogens is involved in electron transfer from Mvh Hase to Hdr (Stojanowic et al., 2003). In several organisms the *floxCD* genes are fused into a single gene. Thus, the Flox proteins are likely to oxidize NAD(P)H and transfer electrons to the HdrABC proteins. In *D. vulgaris* and other organisms the *floxABCD/hdrABC* genes are found next to a co-regulated *adh* gene coding for an alcohol dehydrogenase (Haveman et al., 2003). The Adh may reduce NAD^+ to NADH, which will be oxidized by Flox. The *floxABCD/hdrA* or *floxABCD/hdrABC* genes are present in the majority of the SRO analyzed. This suggests they play an important physiological role, and indeed these genes have been reported in several gene expression and proteomic studies of *D. vulgaris* energy metabolism (Haveman et al., 2003; Zhang et al., 2006a,b; Caffrey et al., 2007; Pereira et al., 2008; Walker et al., 2009). The HdrA-associated Mvh and Flox proteins probably constitute parallel pathways for HdrA reduction from H_2 or NAD(P)H. It seems likely that these proteins may be involved in electron bifurcating reactions involving HdrA as previously suggested (Thauer et al., 2008). We further propose that the electron acceptor of the HdrBC proteins may be $DsrC_{ox}$, also thought to be a substrate for DsrK (Oliveira et al., 2008). Thus, in SRO the HdrABC/MvhDGA and HdrABC/FloxABCD complexes may provide a soluble route of electron transfer to sulfite reduction through DsrC, where energy coupling occurs through electron bifurcation rather than chemiosmotically through DsrMK. In support of this hypothesis the *dsrC* gene of *Db. autotrophicum* is found next to a *hdrA(L)/floxACBD* gene cluster (**Figure 3**).

Other gene loci in SRO containing *hdrA*-like genes include a *fdhA* gene (and an *hdrL*) or genes for a pyruvate:Fd oxidoreductase (Por), suggesting that formate and pyruvate may also be the source of electrons for HdrA reduction.

HdrD

The analysis of *hdrD*-like genes also provided interesting results, one of which was the identification of the iron–sulfur subunit of three putative lactate dehydrogenases (LDH) as belonging to the CCG family (**Figure 4**; **Table 3**). One of the LDH gene clusters

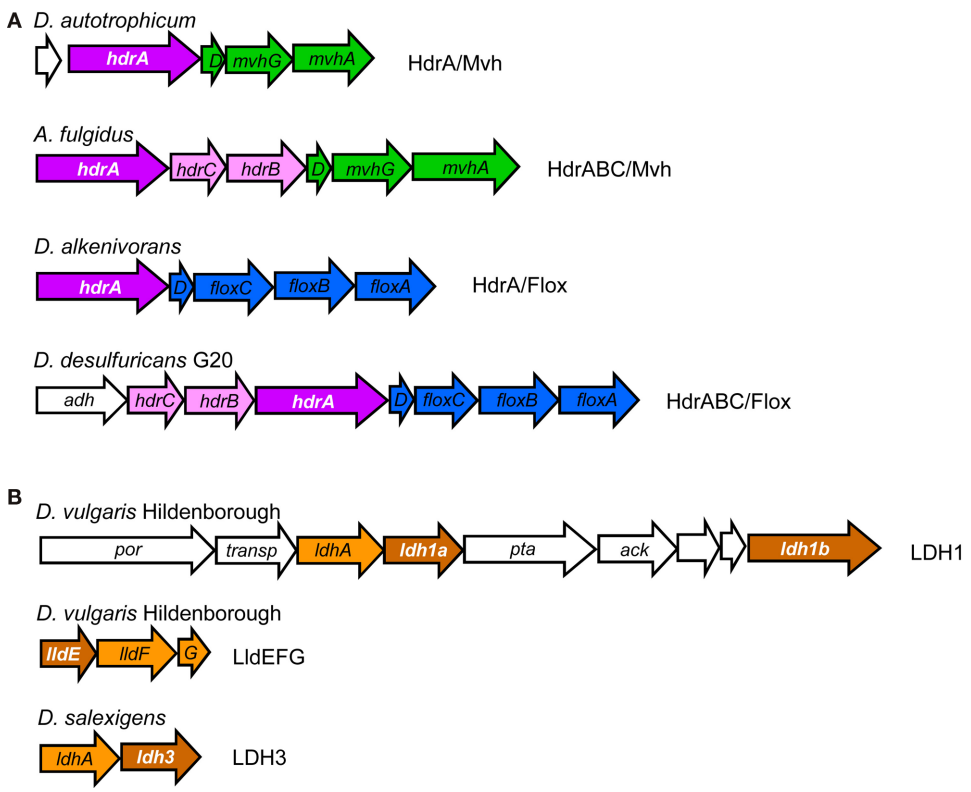

FIGURE 4 | Examples of gene loci for (A) *hdrA*-related genes (in white lettering) and (B) *hdrD*-related genes (in white lettering).

Table 3 | Analysis of HdrA-like and HdrD-like proteins in the SRO genomes.

	Hdr/Mvh		Hdr/Flox		HdrA/other			LDH				Other HdrD-like		
	HdrABC/ Mvh	HdrA/ Mvh	HdrABC/ Flox	HdrA/ Flox	HdrAL/ Fdh	HdrA/ Fdh	HdrAL/ POR	LDH 1a	LDH 1b	Lld EFG	LDH3	HdrD-FAD	HdrD/ Etf	HdrD/ Mop
ARCHAEA														
Archaeoglobus fulgidus	1													
Archaeoglobus profundus	1													
Caldivirga maquilingensis														
DELTAPROTEOBACTERIA														
Desulfovibrionacae														
Desulfovibrio aespoeensis					1			1	1		1	1		
Desulfovibrio desulfuricans G20			2					1	1	1	1	1		1
Desulfovibrio desulfuricans ATCC 27774			1					1	1		1	1		1
Desulfovibrio magneticus RS-1			1					1	1	1	1	1		1
Desulfovibrio piger			1					1	1			1		1
Desulfovibrio salexigens			1					1	1		1	1		1
Desulfovibrio sp. FW1012B			1					1	1	1	1	1		1
Desulfovibrio vulgaris Hildenborough			1					1	1	1	1	1		1
Desulfomicrobiacae														
Desulfomicrobium baculatum			1		1			1		1	1	1		1
Desulfobacteraceae														
Desulfatibacillum alkenivorans		1		1			1			1	1		2	1
Desulfobacterium autotrophicum HRM2		1		1	1	3		1	1	1		1	1	1
Desulfococcus oleovorans Hxd3											1		1	
Desulfohalobiacae														
Desulfohalobium retbaense DSM 5692		1	2		1			1	1		1	1		1
Desulfonatronospira thiodismutans ASO3-1	1	1	1					1	1			1		
Desulfobulbaceae														
Desulfotalea psychrophila		1						1	1	1			1	1
Desulfurivibrio alkaliphilus						1								
Syntrophobacteraceae														
Syntrophobacter fumaroxidans MPOB		2		2	1		1	1	1	1				1

	Hdr/Mvh		Hdr/Flox		HdrA/other			LDH			Other HdrD-like		
	HdrABC/Mvh	HdrA/Mvh	HdrABC/Flox	HdrA/Flox	HdrAL/Fdh	HdrA/Fdh	HdrAL/POR	LDH 1a	LDH 1b	Lld EFG	LDH3	HdrD-FAD	HdrD/Etf	HdrD/Mop
CLOSTRIDIA														
Peptococcaceae														
Desulfotomaculum acetoxidans DSM 771			2	1	2						1		1	1
Desulfotomaculum reducens				1	1						1		1	
C. Desulforudis audaxviator MP104C			1											
Thermoanaerobacterales														
Ammonifex degensii KC4			1					1	1					
NITROSPIRA														
Thermodesulfovibrio yellowstonii	1							1	1					
No. of organisms	4	6	13	5	7	2	2	16	15	9	13	12	6	14

Ldh1a/b – HdrD-like proteins in LDH operon; FAD–HdrD, HdrD-like protein with FAD-binding site; HdrD/Etf, HdrD-like protein encoded next to etfAB genes; HdrD/Mop, HdrD-like protein encoded next to molybdo-containing aldehyde oxidoreductase gene.

was previously identified as an "organic acid oxidation region" in the genome of *D. vulgaris* and *D. desulfuricans* G20 (Pereira et al., 2007; Wall et al., 2008). It includes genes for pyruvate:Fd oxidoreductase (*por*), putative lactate permease, the putative LDH catalytic subunit, a putative LDH iron–sulfur subunit that has two CCG domains, phosphate acetyl transferase (*pta*) and acetate kinase (*ack*). A larger HdrD-related protein is also present in this gene cluster. A novel three-subunit L-lactate dehydrogenase that was named LldEFG (or LutABC) was recently identified in *Bacillus subtilis* (Chai et al., 2009), *Shewanella oneidensis* (Pinchuk et al., 2009), and *Campylobacter jejuni* (Thomas et al., 2011). LldEFG is also present in several of the SRO genomes analyzed and the LldE protein is a small HdrD-related iron–sulfur protein with one CCG domain. The LldEFG enzyme is membrane-associated although no transmembrane helices are present in any of its subunits. A third putative LDH with an HdrD-like subunit was also identified. The role of the LDH HdrD-like subunits is uncertain, as the electron acceptor for LDH has not been identified.

Other proteins related to HdrD include one membrane-associated HdrF protein found next to the *etfAB* genes coding for electron-transfer flavoprotein, a large flavoprotein with two CCG domains and a putative FAD-binding site, and a protein encoded next to a gene for a molybdenum-containing aldehyde oxidoreductase. These HdrD-related proteins suggest the presence of different electron-transfer pathways (from lactate, β-oxidation, and others) as possible donors for reduction of the menaquinone pool or $DsrC_{ox}$.

CONCLUDING REMARKS

The comparative genomic analysis reported in this work provides new insights into the energy metabolism of SRO. By comparing phylogenetically distinct organisms capable of sulfate reduction we identified the proteins that can be considered as comprising the minimal set required for this metabolic activity: a sulfate transporter, Sat, a pyrophosphatase, AprAB, DsrAB, DsrC, DsrMK, and Fd. The QmoAB proteins are also present in most organisms, being absent only in *C. maquiligensis*. In addition, we identified a higher diversity of possible energy conserving pathways than classically has been considered to be present in these organisms. The intracellular redox cycling of metabolites (like H_2, formate or CO) is not a universal mechanism, but should play a role in bioenergetics of *Deltaproteobacteria* and *T. yellowstonii*, which are characterized by a large number of cytochromes *c* and cytochrome *c*-associated membrane redox complexes. A large number of cytochromes *c* has previously been correlated with increased respiratory versatility in anaerobes (Thomas et al., 2008), and such versatility is also suggested by the apparent redundancy of periplasmic redox proteins and membrane complexes found in many *Deltaproteobacteria*. Redox cycling is associated with energy conservation though charge separation or redox loop mechanisms. In contrast, the Archaea and *Clostridia* groups contain practically no cytochromes *c* or associated membrane complexes. The Gram-positive organisms analyzed present some unique traits including the absence of QmoC and DsrJOP proteins. Despite the absence of a periplasmic space, three extracytoplasmic proteins are predicted for these organisms, namely NrfHA and membrane-anchored [FeFe] Hase and FDH.

Overall, this analysis suggests that all SRO use diverse processes for energy conservation involving membrane-based chemiosmotic mechanisms, or soluble flavin-based electron bifurcation ones. Many organisms include *nuo* genes for an ion-translocating complex I, which in most cases uses a still unidentified electron donor. Another widespread ion-translocating complex is Rnf, which together with Ech and Coo Hases, provides coupling sites for Fd-associated processes such as electron bifurcation. Regarding soluble processes, we identified a surprisingly high number of cytoplasmic Hases and FDHs as likely candidates for electron bifurcation coupling involving NAD(P)/H, Fd, or HDRs. A large number of HDR-related proteins were also detected. We propose that these proteins are part of electron-transfer pathways involving energy coupling through electron bifurcation, from diverse electron donors such as H_2, formate, pyruvate, NAD(P)H, β-oxidation, and others. These pathways may constitute alternatives to Dsr and other transmembrane complexes for reduction of $DsrC_{ox}$, the protein we propose is central to the sulfite reduction step.

A few novel redox proteins were identified in SRO, including a FloxABCD/HdrA(BC) complex proposed to perform electron bifurcation with NAD(P)H, Fd, and $DsrC_{ox}$, a new type of membrane-anchored periplasmic [FeFe] Hase, and a putative soluble FHL also comprising an [FeFe] Hase. In conclusion, this analysis indicates that energy metabolism of SRO is far more versatile than previously considered; both chemiosmotic and flavin-based electron bifurcating mechanisms provide alternative strategies for energy conservation. An interesting aspect of (at least some) SRO is their ability to grow syntrophically in the absence of sulfate. In such situation some modules of this versatile redox machinery may operate in the opposite direction to that of respiratory conditions. Finally, it should be stressed that although drawing theories based on comparative genomic analysis is an attractive and even convincing exercise, no definite conclusions can be drawn until experimental evidence is provided. Thus, much work remains to be carried out to elucidate the bioenergetic mechanisms of SRO.

ACKNOWLEDGMENT

This work was supported by grant QUI-BIQ/10059/2008 funded by FCT, Portugal.

SUPPLEMENTARY MATERIAL

The locus tags for all genes can be found in http://www.frontiersin.org/Microbial_Physiology_and_Metabolism/10.3389/fmicb.2011.00069/abstract

REFERENCES

Akagi, J. M. (1995). "Respiratory sulfate reduction," in *Sulfate-Reducing Bacteria*, ed. L. L. Barton (New York: Plenum Press), 89–111.

Almendra, M. J., Brondino, C. D., Gavel, O., Pereira, A. S., Tavares, P., Bursakov, S., Duarte, R., Caldeira, J., Moura, J. J. G., and Moura, I. (1999). Purification and characterization of a tungsten-containing formate dehydrogenase from *Desulfovibrio gigas*. *Biochemistry* 38, 16366–16372.

Biegel, E., and Müller, V. (2010). Bacterial Na+-translocating ferredoxin: NAD+ oxidoreductase. *Proc. Natl. Acad. Sci. U.S.A.* 107, 18138–18142.

Broco, M., Rousset, M., Oliveira, S., and Rodrigues-Pousada, C. (2005). Deletion of flavoredoxin gene in *Desulfovibrio gigas* reveals its participation in thiosulfate reduction. *FEBS Lett.* 579, 4803–4807.

Caffrey, S. A., Park, H. S., Voordouw, J. K., He, Z., Zhou, J., and Voordouw, G. (2007). Function of periplasmic hydrogenases in the sulfate-reducing bacterium *Desulfovibrio vulgaris* Hildenborough. *J. Bacteriol.* 189, 6159–6167.

Canfield, D. E., Stewart, F. J., Thamdrup, B., De Brabandere, L., Dalsgaard, T., Delong, E. F., Revsbech, N. P., and Ulloa, O. (2010). A cryptic sulfur cycle in oxygen-minimum-zone waters off the chilean coast. *Science* 330, 1375–1378.

Chai, Y. R., Kolter, R., and Losick, R. (2009). A widely conserved gene cluster required for lactate utilization in *Bacillus subtilis* and its involvement in biofilm formation. *J. Bacteriol.* 191, 2423–2430.

Cort, J. R., Mariappan, S. V., Kim, C. Y., Park, M. S., Peat, T. S., Waldo, G. S., Terwilliger, T. C., and Kennedy, M. A. (2001). Solution structure of *Pyrobaculum aerophilum* DsrC, an archaeal homologue of the gamma subunit of dissimilatory sulfite reductase. *Eur. J. Biochem.* 268, 5842–5850.

Costa, K. C., Wong, P. M., Wang, T., Lie, T. J., Dodsworth, J. A., Swanson, I., Burn, J. A., Hackett, M., and Leigh, J. A. (2010). Protein complexing in a methanogen suggests electron bifurcation and electron delivery from formate to heterodisulfide reductase. *Proc. Natl. Acad. Sci. U.S.A.* 107, 11050–11055.

Dolla, A., Pohorelic, B. K. J., Voordouw, J. K., and Voordouw, G. (2000). Deletion of the hmc operon of *Desulfovibrio vulgaris* subsp. *vulgaris* Hildenborough hampers hydrogen metabolism and low-redox-potential niche establishment. *Arch. Microbiol.* 174, 143–151.

Efremov, R. G., Baradaran, R., and Sazanov, L. A. (2010). The architecture of respiratory complex I. *Nature* 465, 441–445.

ElAntak, L., Morelli, X., Bornet, O., Hatchikian, C., Czjzek, M., Alain, D. A., and Guerlesquin, F. (2003). The cytochrome *c*3-[Fe]-hydrogenase electron-transfer complex: structural model by NMR restrained docking. *FEBS Lett.* 548, 1–4.

Friedrich, T., and Scheide, D. (2000). The respiratory complex I of bacteria, archaea and eukarya and its module common with membrane-bound multisubunit hydrogenases. *FEBS Lett.* 479, 1–5.

Greene, E. A., Hubert, C., Nemati, M., Jenneman, G. E., and Voordouw, G. (2003). Nitrite reductase activity of sulphate-reducing bacteria prevents their inhibition by nitrate-reducing, sulphide-oxidizing bacteria. *Environ. Microbiol.* 5, 607–617.

Grein, F., Venceslau, S. S., Schneider, L., Hildebrandt, P., Todorovic, S., Pereira, I. A. C., and Dahl, C. (2010). DsrJ, an essential part of the DsrMKJOP transmembrane complex in the purple sulfur bacterium *Allochromatium vinosum*, is an unusual triheme cytochrome *c*. *Biochemistry* 49, 8290–8299.

Hamann, N., Mander, G. J., Shokes, J. E., Scott, R. A., Bennati, M., and Hedderich, R. (2007). Cysteine-rich CCG domain contains a novel [4Fe-4S] cluster binding motif as deduced from studies with subunit B of heterodisulfide reductase from *Methanothermobacter marburgensis*. *Biochemistry* 46, 12875–12885.

Haveman, S. A., Brunelle, V., Voordouw, J. K., Voordouw, G., Heidelberg, J. F., and Rabus, R. (2003). Gene expression analysis of energy metabolism mutants of *Desulfovibrio vulgaris* Hildenborough indicates an important role for alcohol dehydrogenase. *J. Bacteriol.* 185, 4345–4353.

Hedderich, R., and Forzi, L. (2005). Energy-converting [NiFe] hydrogenases: more than just H2 activation. *J. Mol. Microbiol. Biotechnol.* 10, 92–104.

Hedderich, R., Hamann, N., and Bennati, M. (2005). Heterodisulfide reductase from methanogenic archaea: a new catalytic role for an iron-sulfur cluster. *Biol. Chem.* 386, 961–970.

Hedderich, R., Klimmek, O., Kröger, A., Dirmeier, R., Keller, M., and Stetter, K. O. (1999). Anaerobic respiration with elemental sulfur and with disulfides. *FEMS Microbiol. Rev.* 22, 353–381.

Heidelberg, J. F., Seshadri, R., Haveman, S. A., Hemme, C. L., Paulsen, I. T., Kolonay, J. F., Eisen, J. A., Ward, N., Methe, B., Brinkac, L. M., Daugherty, S. C., Deboy, R. T., Dodson, R. J., Durkin, A. S., Madupu, R., Nelson, W. C., Sullivan, S. A., Fouts, D., Haft, D. H., Selengut, J., Peterson, J. D., Davidsen, T. M., Zafar, N., Zhou, L. W., Radune, D., Dimitrov, G., Hance, M., Tran, K., Khouri, H., Gill, J., Utterback, T. R., Feldblyum, T. V., Wall, J. D., Voordouw, G., and Fraser, C. M. (2004). The genome sequence of the anaerobic, sulfate-reducing bacterium *Desulfovibrio vulgaris* Hildenborough. *Nat. Biotechnol.* 22, 554–559.

Herrmann, G., Jayamani, E., Mai, G., and Buckel, W. (2008). Energy conservation via electron-transferring flavoprotein in anaerobic bacteria. *J. Bacteriol.* 190, 784–791.

Ikeuchi, Y., Shigi, N., Kato, J., Nishimura, A., and Suzuki, T. (2006). Mechanistic insights into multiple sulfur mediators

sulfur relay by involved in thiouridine biosynthesis at tRNA wobble positions. *Mol. Cell* 21, 97–108.

Iverson, T. M, Arciero, D. M., Hsu, B. T., Logan, M. S. P., Hooper, A. B., and Rees, D. C. (1998). Heme packing motifs revealed by the crystal structure of the tetra-heme cytochrome *c*554 from *Nitrosomonas europaea*. *Nat. Struct. Mol. Biol.* 5, 1005–1012.

Jenney, F. E., and Adams, M. W. W. (2008). Hydrogenases of the model hyperthermophiles. *Ann. N. Y. Acad. Sci.* 1125, 252–266.

Jørgensen, B. B. (1982). Mineralization of organic matter in the sea-bed – the role of sulphate reduction. *Nature* 390, 364–370.

Junier, P., Junier, T., Podell, S., Sims, D. R., Detter, J. C., Lykidis, A., Han, C. S., Wigginton, N. S., Gaasterland, T., and Bernier-Latmani, R. (2010). The genome of the Gram-positive metal- and sulfate-reducing bacterium *Desulfotomaculum reducens* strain MI-1. *Environ. Microbiol.* 12, 2738–2754.

Kobayashi, K., Hasegawa, H., Takagi, M., and Ishimoto, M. (1982). Proton translocation associated with sulfite reduction in a sulfate-reducing bacterium, *Desulfovibrio vulgaris*. *FEBS Lett.* 142, 235–237.

Kunow, J., Linder, D., Stetter, K. O., and Thauer, R. K. (1994). F420H2: quinone oxidoreductase from *Archaeoglobus fulgidus*. Characterization of a membrane-bound multisubunit complex containing FAD and iron-sulfur clusters. *Eur. J. Biochem.* 223, 503–511.

Li, F., Hinderberger, J., Seedorf, H., Zhang, J., Buckel, W., and Thauer, R. K. (2008). Coupled ferredoxin and crotonyl coenzyme A (CoA) reduction with NADH catalyzed by the butyryl-CoA dehydrogenase/Etf complex from *Clostridium kluyveri*. *J. Bacteriol.* 190, 843–850.

Li, Q., Li, L., Rejtar, T., Lessner, D. J., Karger, B. L., and Ferry, J. G. (2006). Electron transport in the pathway of acetate conversion to methane in the marine archaeon *Methanosarcina acetivorans*. *J. Bacteriol.* 188, 702–710.

Li, X., Luo, Q., Wofford, N. Q., Keller, K. L., McInerney, M. J., Wall, J. D., and Krumholz, L. R. (2009). A molybdopterin oxidoreductase is involved in H2 oxidation in *Desulfovibrio desulfuricans* G20. *J. Bacteriol.* 191, 2675–2682.

Ma, K., and Adams, M. W. (2001). Ferredoxin:NADP oxidoreductase from *Pyrococcus furiosus*. *Meth. Enzymol.* 334, 40–45.

Ma, K., and Adams, M. W. W. (1994). Sulfide dehydrogenase from the hyperthermophilic archaeon *Pyrococcus furiosus* – a new multifunctional enzyme involved in the reduction of elemental sulfur. *J. Bacteriol.* 176, 6509–6517.

Malki, S., Saimmaime, I., De Luca, G., Rousset, M., Dermoun, Z., and Belaich, J. P. (1995). Characterization of an operon encoding an NADP-reducing hydrogenase in *Desulfovibrio fructosovorans*. *J. Bacteriol.* 177, 2628–2636.

Mander, G. J., Duin, E. C., Linder, D., Stetter, K. O., and Hedderich, R. (2002). Purification and characterization of a membrane-bound enzyme complex from the sulfate-reducing archaeon *Archaeoglobus fulgidus* related to heterodisulfide reductase from methanogenic archaea. *Eur. J. Biochem.* 269, 1895–1904.

Mander, G. J., Pierik, A. J., Huber, H., and Hedderich, R. (2004). Two distinct heterodisulfide reductase-like enzymes in the sulfate-reducing archaeon *Archaeoglobus profundus*. *Eur. J. Biochem.* 271, 1106–1116.

Mander, G. J., Weiss, M. S., Hedderich, R., Kahnt, J., Ermler, U., and Warkentin, E. (2005). X-ray structure of the gamma-subunit of a dissimilatory sulfite reductase: fixed and flexible C-terminal arms. *FEBS Lett.* 579, 4600–4604.

Matias, P. M., Coelho, R., Pereira, I. A., Coelho, A. V., Thompson, A. W., Sieker, L. C., Gall, J. L., and Carrondo, M. A. (1999). The primary and three-dimensional structures of a nine-haem cytochrome *c* from *Desulfovibrio desulfuricans* ATCC 27774 reveal a new member of the Hmc family. *Structure* 7, 119–130.

Matias, P. M., Pereira, I. A., Soares, C. M., and Carrondo, M. A. (2005). Sulphate respiration from hydrogen in *Desulfovibrio* bacteria: a structural biology overview. *Prog. Biophys. Mol. Biol.* 89, 292–329.

Matson, E. G., Zhang, X. N., and Leadbetter, J. R. (2010). Selenium controls transcription of paralogous formate dehydrogenase genes in the termite gut acetogen, *Treponema primitia*. *Environ. Microbiol.* 12, 2245–2258.

McInerney, M. J., Rohlin, L., Mouttaki, H., Kim, U., Krupp, R. S., Rios-Hernandez, L., Sieber, J., Struchtemeyer, C. G., Bhattacharyya, A., Campbell, J. W., and Gunsalus, R. P. (2007). The genome of *Syntrophus aciditrophicus*: life at the thermodynamic limit of microbial growth. *Proc. Natl. Acad. Sci. U.S.A.* 104, 7600–7605.

Meuer, J., Kuettner, H. C., Zhang, J. K., Hedderich, R., and Metcalf, W. W. (2002). Genetic analysis of the archaeon *Methanosarcina barkeri* Fusaro reveals a central role for Ech hydrogenase and ferredoxin in methanogenesis and carbon fixation. *Proc. Natl. Acad. Sci. U.S.A.* 99, 5632–5637.

Moura, J. J., Macedo, A. L., and Palma, P. N. (1994). Ferredoxins. *Meth. Enzymol.* 243, 165–188.

Müller, V., Imkamp, F., Biegel, E., Schmidt, S., and Dilling, S. (2008). Discovery of a ferredoxin:NAD+-oxidoreductase (Rnf) in *Acetobacterium woodii*: a novel potential coupling site in acetogens. *Ann. N. Y. Acad. Sci.* 1125, 137–146.

Muyzer, G., and Stams, A. J. (2008). The ecology and biotechnology of sulphate-reducing bacteria. *Nat. Rev. Microbiol.* 6, 441–454.

Odom, J. M., and Peck, H. D. Jr. (1981). Hydrogen cycling as a general mechanism for energy coupling in the sulfate-reducing bacteria, *Desulfovibrio* sp. *FEMS Microbiol. Lett.* 12, 47–50.

Oliveira, T. F., Vonrhein, C., Matias, P. M., Venceslau, S. S., Pereira, I. A., and Archer, M. (2008). The crystal structure of *Desulfovibrio vulgaris* dissimilatory sulfite reductase bound to DsrC provides novel insights into the mechanism of sulfate respiration. *J. Biol. Chem.* 283, 34141–34149.

Pereira, I. A. C. (2008). "Membrane complexes in *Desulfovibrio*," in *Microbial Sulfur Metabolism*, eds C. Friedrich and C. Dahl (Berlin: Springer-Verlag), 24–35.

Pereira, I. A. C., Haveman, S. A., and Voordouw, G. (2007). "Biochemical, genetic and genomic characterization of anaerobic electron transport pathways in sulphate-reducing delta-proteobacteria," in *Sulphate-Reducing Bacteria: Environmental and Engineered Systems*, eds L. L. Barton and W. A. Allan Hamilton (Cambridge: Cambridge University Press), 215–240.

Pereira, I. A. C., Romão, C. V., Xavier, A. V., LeGall, J., and Teixeira, M. (1998). Electron transfer between hydrogenases and mono and multiheme cytochromes in *Desulfovibrio* spp. *J. Biol. Inorg. Chem.* 3, 494–498.

Pereira, P. M., He, Q., Valente, F. M. A., Xavier, A. V., Zhou, J. Z., Pereira, I., A. C., and Louro, R. O. (2008). Energy metabolism in *Desulfovibrio vulgaris* Hildenborough: insights from transcriptome analysis. *Antonie Van Leeuwenhoek* 93, 347–362.

Pereira, P. M., Teixeira, M., Xavier, A. V., Louro, R. O., and Pereira, I. A. (2006). The Tmc complex from *Desulfovibrio vulgaris* Hildenborough is involved in transmembrane electron transfer from periplasmic hydrogen oxidation. *Biochemistry* 45, 10359–10367.

Pierik, A. J., Duyvis, M. G., van Helvoort, J. M., Wolbert, R. B., and Hagen, W. R. (1992). The third subunit of desulfoviridin-type dissimilatory sulfite reductases. *Eur. J. Biochem.* 205, 111–115.

Pieulle, L., Morelli, X., Gallice, P., Lojou, E., Barbier, P., Czjzek, M., Bianco, P., Guerlesquin, F., and Hatchikian, E. C. (2005). The type I/type II cytochrome *c*3 complex: an electron transfer link in the hydrogen-sulfate reduction pathway. *J. Mol. Biol.* 354, 73–90.

Pinchuk, G. E., Rodionov, D. A., Yang, C., Li, X. Q., Osterman, A. L., Dervyn, E., Geydebrekht, O. V., Reed, S. B., Romine, M. F., Collart, F. R., Scott, J. H., Fredrickson, J. K., and Beliaev, A. S. (2009). Genomic reconstruction of *Shewanella oneidensis* MR-1 metabolism reveals a previously uncharacterized machinery for lactate utilization. *Proc. Natl. Acad. Sci. U.S.A.* 106, 2874–2879.

Pires, R. H., Lourenco, A. I., Morais, F., Teixeira, M., Xavier, A. V., Saraiva, L. M., and Pereira, I. A. (2003). A novel membrane-bound respiratory complex from *Desulfovibrio desulfuricans* ATCC 27774. *Biochim. Biophys. Acta* 1605, 67–82.

Pires, R. H., Venceslau, S. S., Morais, F., Teixeira, M., Xavier, A. V., and Pereira, I. A. (2006). Characterization of the *Desulfovibrio desulfuricans* ATCC 27774 DsrMKJOP complex-A membrane-bound redox complex involved in the sulfate respiratory pathway. *Biochemistry* 45, 249–262.

Pott, A. S., and Dahl, C. (1998). Sirohaem sulfite reductase and other proteins encoded by genes at the dsr locus of *Chromatium vinosum* are involved in the oxidation of intracellular sulfur. *Microbiology* 144, 1881–1894.

Rabus, R., Hansen, T., and Widdel, F. (2007). "Dissimilatory sulfate- and sulfur-Reducing prokaryotes," in *The Prokaryotes*, ed. M. Dworkin (New York: Springer-Verlag), 659–768.

Rodrigues, M. L., Oliveira, T. F., Pereira, I. A., and Archer, M. (2006). X-ray structure of the membrane-bound cytochrome *c* quinol dehydrogenase NrfH reveals novel haem coordination. *EMBO J.* 25, 5951–5960.

Rodrigues, R., Valente, F. M., Pereira, I. A., Oliveira, S., and Rodrigues-Pousada, C. (2003). A novel membrane-bound Ech [NiFe] hydrogenase in *Desulfovibrio gigas*. *Biochem. Biophys. Res. Commun.* 306, 366–375.

Rossi, M., Pollock, W. B. R., Reij, M. W., Keon, R. G., Fu, R., and Voordouw, G. (1993). The hmc operon of *Desulfovibrio vulgaris* subsp. *vulgaris* Hildenborough encodes a potential transmembrane redox protein complex. *J. Bacteriol.* 175, 4699–4711.

Saraiva, L. M., da Costa, P. N., Conte, C., Xavier, A. V., and LeGall, J. (2001). In the facultative sulphate/nitrate reducer *Desulfovibrio desulfuricans* ATCC 27774, the nine-haem cytochrome *c* is part of a membrane-bound redox complex mainly expressed in sulphate-grown cells. *Biochim. Biophys. Acta* 1520, 63–70.

Sawers, R. G. (2005). Formate and its role in hydrogen production in *Escherichia coli*. *Biochem. Soc. Trans.* 33, 42–46.

Schmehl, M., Jahn, A., Meyer zu Vilsendorf, A., Hennecke, S., Masepohl, B., Schuppler, M., Marxer, M., Oelze, J., and Klipp, W. (1993). Identification of a new class of nitrogen fixation genes in *Rhodobacter capsulatus*: a putative membrane complex involved in electron transport to nitrogenase. *Mol. Gen. Genet.* 241, 602–615.

Schut, G. J., and Adams, M. W. (2009). The iron-hydrogenase of *Thermotoga maritima* utilizes ferredoxin and NADH synergistically: a new perspective on anaerobic hydrogen production. *J. Bacteriol.* 191, 4451–4457.

Sebban, C., Blanchard, L., Bruschi, M., and Guerlesquin, F. (1995). Purification and characterization of the formate dehydrogenase from *Desulfovibrio vulgaris* Hildenborough. *FEMS Microbiol. Lett.* 133, 143–149.

Seedorf, H., Fricke, W. F., Veith, B., Bruggemann, H., Liesegang, H., Strittmatter, A., Miethke, M., Buckel, W., Hinderberger, J., Li, F., Hagemeier, C., Thauer, R. K., and Gottschalk, G. (2008). The genome of *Clostridium kluyveri*, a strict anaerobe with unique metabolic features. *Proc. Natl. Acad. Sci. U.S.A.* 105, 2128–2133.

Serrano, A., Perez-Castineira, J. R., Baltscheffsky, M., and Baltscheffsky, H. (2007). H+-PPases: yesterday, today and tomorrow. *IUBMB Life* 59, 76–83.

Shaw, A. J., Hogsett, D. A., and Lynd, L. R. (2009). Identification of the [FeFe]-hydrogenase responsible for hydrogen generation in *Thermoanaerobacterium saccharolyticum* and demonstration of increased ethanol yield via hydrogenase knockout. *J. Bacteriol.* 191, 6457–6464.

Simon, J., van Spanning, R. J., and Richardson, D. J. (2008). The organisation of proton motive and non-proton motive redox loops in prokaryotic respiratory systems. *Biochim. Biophys. Acta* 1777, 1480–1490.

Singer, S. W., Hirst, M. B., and Ludden, P. W. (2006). CO-dependent H2 evolution by Rhodospirillum rubrum: role of CODH:CooF complex. *Biochim. Biophys. Acta* 1757, 1582–1591.

Soboh, B., Linder, D., and Hedderich, R. (2004). A multisubunit membrane-bound [NiFe] hydrogenase and an NADH-dependent Fe-only hydrogenase in the fermenting bacterium *Thermoanaerobacter tengcongensis*. *Microbiology* 150, 2451–2463.

Steuber, J. (2001). Na(+) translocation by bacterial NADH:quinone oxidoreductases: an extension to the complex-I family of primary redox pumps. *Biochim. Biophys. Acta* 1505, 45–56.

Stojanowic, A., Mander, G. J., Duin, E. C., and Hedderich, R. (2003). Physiological role of the F420-non-reducing hydrogenase (Mvh) from *Methanothermobacter marburgensis*. *Arch. Microbiol.* 180, 194–203.

Strittmatter, A. W., Liesegang, H., Rabus, R., Decker, I., Amann, J., Andres, S., Henne, A., Fricke, W. F., Martinez-Arias, R., Bartels, D., Goesmann, A., Krause, L., Pühler, A., Klenk, H. P., Richter, M., Schüler, M., Glöckner, F. O., Meyerdierks, A., Gottschalk, G., and Amann, R. (2009). Genome sequence of *Desulfobacterium autotrophicum* HRM2, a marine sulfate reducer oxidizing organic carbon completely to carbon dioxide. *Environ. Microbiol.* 11, 1038–1055.

Thauer, R. K., Kaster, A. K., Goenrich, M., Schick, M., Hiromoto, T., and Shima, S. (2010). Hydrogenases from methanogenic archaea, nickel, a novel cofactor, and H2 storage. *Annu. Rev. Biochem.* 79, 507–536.

Thauer, R. K., Kaster, A. K., Seedorf, H., Buckel, W., and Hedderich, R. (2008). *Methanogenic archaea*: ecologically relevant differences in energy conservation. *Nat. Rev. Microbiol.* 6, 579–591.

Thomas, M. T., Shepherd, M., Poole, R. K., van Vliet, A. H., Kelly, D. J., and Pearson, B. M. (2011). Two respiratory enzyme systems in *Campylobacter jejuni* NCTC 11168 contribute to growth on L-lactate. *Environ. Microbiol.* 13, 48–61.

Thomas, S. H., Wagner, R. D., Arakaki, A. K., Skolnick, J., Kirby, J. R., Shimkets, L. J., Sanford, R. A., and Löffler, F. E. (2008). The mosaic genome of *Anaeromyxobacter dehalogenans* strain 2CP-C suggests an aerobic common ancestor to the delta-proteobacteria. *PLoS ONE* 3, e2103. doi: 10.1371/journal.pone.0002103

Valente, F. A. A., Almeida, C. C., Pacheco, I., Carita, J., Saraiva, L. M., and Pereira, I. A. C. (2006). Selenium is involved in regulation of periplasmic hydrogenase gene expression in *Desulfovibrio vulgaris* Hildenborough. *J. Bacteriol.* 188, 3228–3235.

Valente, F. M. A., Oliveira, A. S. F., Gnadt, N., Pacheco, I., Coelho, A. V., Xavier, A. V., Teixeira, M., Soares, C. M., and Pereira, I. A. C. (2005). Hydrogenases in *Desulfovibrio vulgaris* Hildenborough: structural and physiologic characterisation of the membrane-bound [NiFeSe] hydrogenase. *J. Biol. Inorg. Chem.* 10, 667–682.

Valente, F. M. A., Saraiva, L. M., LeGall, J., Xavier, A. V., Teixeira, M., and Pereira, I. A. C. (2001). A membrane-bound cytochrome *c*3: a type II cytochrome *c*3 from *Desulfovibrio vulgaris* Hildenborough. *Chembiochem* 2, 895–905.

Venceslau, S. S., Lino, R. R., and Pereira, I. A. (2010). The Qrc membrane complex, related to the alternative complex III, is a menaquinone reductase involved in sulfate respiration. *J. Biol. Chem.* 285, 22774–22783.

Vignais, P. M., and Billoud, B. (2007). Occurrence, classification, and biological function of hydrogenases: an overview. *Chem. Rev.* 107, 4206–4272.

Voordouw, G. (2002). Carbon monoxide cycling by *Desulfovibrio vulgaris* Hildenborough. *J. Bacteriol.* 184, 5903–5911.

Walker, C. B., He, Z. L., Yang, Z. K., Ringbauer, J. A., He, Q., Zhou, J. H., Voordouw, G., Wall, J. D., Arkin, A. P., Hazen, T. C., Stolyar, S., and Stahl, D. A. (2009). The electron transfer system of syntrophically grown *Desulfovibrio vulgaris*. *J. Bacteriol.* 191, 5793–5801.

Wall, J. D., Arkin, A. P., Balci, N. C., and Rapp-Giles, B. (2008). "Genetics and genomics of sulfate respiration in *Desulfovibrio*," in *Microbial Sulfur Metabolism*, eds C. Dahl and C. G. Friedrich (Heidelbeg: Springer-Verlag), 1–12.

Wang, S., Huang, H., Moll, J., and Thauer, R. K. (2010). NADP+ reduction with reduced ferredoxin and NADP+ reduction with NADH are coupled via an electron-bifurcating enzyme complex in *Clostridium kluyveri*. *J. Bacteriol.* 192, 5115–5123.

Xia, D., Esser, L., Yu, L., and Yu, C. A. (2007). Structural basis for the mechanism of electron bifurcation at the quinol oxidation site of the cytochrome bc1 complex. *Photosyn. Res.* 92, 17–34.

Zane, G. M., Yen, H. C., and Wall, J. D. (2010). Effect of the deletion of qmoABC and the promoter-distal gene encoding a hypothetical protein on sulfate reduction in *Desulfovibrio vulgaris* Hildenborough. *Appl. Environ. Microbiol.* 76, 5500–5509.

Zhang, W. W., Culley, D. E., Scholten, J. C. M., Hogan, M., Vitiritti, L., and Brockman, F. J. (2006a). Global transcriptomic analysis of *Desulfovibrio vulgaris* on different electron donors. *Antonie Van Leeuwenhoek* 89, 221–237.

Zhang, W. W., Gritsenko, M. A., Moore, R. J., Culley, D. E., Nie, L., Petritis, K., Strittmatter, E. F., Camp, D. G., Smith, R. D., and Brockman, F. J. (2006b). A proteomic view of *Desulfovibrio vulgaris* metabolism as determined by liquid chromatography coupled with tandem mass spectrometry. *Proteomics* 6, 4286–4299.

Conflict of Interest Statement: The authors declare that the research was conducted in the absence of any commercial or financial relationships that could be construed as a potential conflict of interest.

Received: 03 February 2011; paper pending published: 07 March 2011; accepted: 25 March 2011; published online: 19 April 2011.

*Citation: Pereira IAC, Ramos AR, Grein F, Marques MC, Marques da Silva S and Venceslau SS (2011) A comparative genomic analysis of energy metabolism in sulfate reducing bacteria and archaea. Front. Microbio. **2**:69. doi: 10.3389/fmicb.2011.00069*

This article was submitted to Frontiers in Microbial Physiology and Metabolism, a specialty of Frontiers in Microbiology.

APPENDIX

Table A1 | Analysis of FDH distribution in the SRO genomes.

	N_T	N_P	Periplasmic				Cytoplasmic		
			Soluble		Membrane-associated				
			FdhAB	FdhABC3	FdhABC	FdhABD	NAD-	FHL_s	Others
ARCHAEA									
Archaeoglobus fulgidus	0	0							
Archaeoglobus profundus	1	1			1				
Caldivirga maquilingensis	0	0							
DELTAPROTEOBACTERIA									
Desulfovibrionacae									
Desulfovibrio aespoeensis	2	2	2						
Desulfovibrio desulfuricans G20	4	3	3					1	
Desulfovibrio desulfuricans ATCC 27774	3	2		1		1			1
Desulfovibrio magneticus RS-I	4	3	3					1	
Desulfovibrio piger	2	1		1					1
Desulfovibrio salexigens	3	2	1	1				1	
Desulfovibrio sp. FW1012B	2	2	2						
Desulfovibrio vulgaris Hildenborough	3	3	1	1		1			
Desulfomicrobiacae									
Desulfomicrobium baculatum	3	2	2				1		
Desulfobacteraceae									
Desulfotomaculum alkenivorans	3	1				1			2
Desulfobacterium autotrophicum HRM2	8	3	2	2				1	4
Desulfococcus oleovorans Hxd3	2	1	1						1
Desulfohalobiacae									
Desulfohalobium retbaense DSM 5692	1	1	1						
Desulfonatronospira thiodismutans AS03-1	4	2	2				2		
Desulfobulbaceae									
Desulfotalea psychrophila	4	2			2		1	1	
Desulfurivibrio alkaliphilus	4	1			1				3
Syntrophobacteraceae									
Syntrophobacter fumaroxidans MPOB	8	3	3				1		4

(Continued)

Table A1 | Continued

	N_T	N_P	Periplasmic				Cytoplasmic		
			Soluble		Membrane-associated				
			FdhAB	FdhABC3	FdhABC	FdhABD	NAD-	FHL_s	Others
CLOSTRIDIA									
Peptococcaceae									
Desulfotomaculum acetoxidans DSM 771	2	0					2		
Desulfotomaculum reducens	2	1				1	1		
C. Desulforudis audaxviator MP104C	3	1				1			2
Thermoanaerobacterales									
Ammonifex degensii KC4	2	1		1			1		
NITROSPIRA									
Thermodesulfovibrio yellowstonii	1	1	1						
No. of organisms			13	6	3	5	7	5	8

N_T, total number of FDHs; N_P, number of periplasmic FDHs; NAD, NAD(H)-dependent FDH; FHLS, putative soluble formate:hydrogen lyase complex.

Table A2 | Analysis of distribution of selected cytochromes *c* in the SRO genomes.

	N_T	Tplc_3	c_{554}-like	split-Soret	NrfHA	c_{553}	Cyt oxid	*bd* oxid
ARCHAEA								
Archaeoglobus fulgidus	1							
Archaeoglobus profundus	1							
Caldivirga maquilingensis	0							
DELTAPROTEOBACTERIA								
Desulfovibrionacae								
Desulfovibrio aespoeensis	13	2	1		1			1
Desulfovibrio desulfuricans G20	14	1	1	1		1	1	1
Desulfovibrio desulfuricans ATCC 27774	11	1		1	1	1		1
Desulfovibrio magneticus RS-1	14	2	3		1	1	1	1
Desulfovibrio piger	7	1		1	1			1
Desulfovibrio salexigens	14	3	1		1			1
Desulfovibrio sp. FW1012B	11	2	2		1	1	1	1
Desulfovibrio vulgaris Hildenborough	18	1	2		1	2	1	1
Desulfomicrobiacae								
Desulfomicrobium baculatum	15	2	1		1	1	1	1
Desulfobacteraceae								
Desulfatibacillum alkenivorans	14	2	1					1
Desulfobacterium autotrophicum HRM2	15	1	1				1	1
Desulfococcus oleovorans Hxd3	14	2		1				1
Desulfohalobiacae								
Desulfohalobium retbaense DSM 5692	13	4		1				1
Desulfonatronospira thiodismutans AS03-1	11	3	1	1	1			1
Desulfobulbaceae								
Desulfotalea psychrophila	5				1			1
Desulfurivibrio alkaliphilus	22	?	4	1	1		1	1
Syntrophobacteraceae								
Syntrophobacter fumaroxidans M POB	10	1	1		1			1
CLOSTRIDIA								
Peptococcaceae								
Desulfotomaculum acetoxidans DSM 771	0							

(Continued)

Table A2 | Continued

	N_T	$TpIc_3$	c_{554}-like	split-Soret	NrfHA	c_{553}	Cyt oxid	*bd* oxid
Desulfotomaculum reducens	2				1			1
C. Desulforudis audaxviator MP104C	0							
Thermoanaerobacterales								
Ammonifex degensii KC4	3				1			
NITROSPIRA								
Thermodesulfovibrio yellowstonii	10	1	1	1	1			1
No. of organisms		17	13	8	15	6	7	19

N_T, total number of multiheme cytochromes c detected. The presence of cytochrome c oxidases and bd quinol oxidases is also indicated.

Table A3 | Analysis of nfnAB gene distribution in the SRO genomes.

	nfnA	nfnB
ARCHAEA		
Archaeoglobus fulgidus		
Archaeoglobus profundus		
Caldivirga maquilingensis		
DELTAPROTEOBACTERIA		
Desulfovibrionacae		
Desulfovibrio aespoeensis		
Desulfovibrio desulfuricans G20	1	1
Desulfovibrio desulfuricans ATCC 27774	1	1
Desulfovibrio magneticus RS-1	1	1
Desulfovibrio piger	1	1
Desulfovibrio salexigens	1	1
Desulfovibrio sp. FW1012B	1	1
Desulfovibrio vulgaris Hildenborough	1	1
Desulfomicrobiacae		
Desulfomicrobium baculatum	1	1
Desulfobacteraceae		
Desulfatibacillum alkenivorans	1	1
Desulfobacterium autotrophicum HRM2	1	1
Desulfococcus oleovorans Hxd3	1	1
Desulfohalobiacae		
Desulfohalobium retbaense DSM 5692	1	1
Desulfonatronospira thiodismutans AS03-1	1	1
Desulfobulbaceae		
Desulfotalea psychrophila		
Desulfurivibrio alkaliphilus	1	1
Syntrophobacteraceae		
Syntrophobacter fumaroxidans MPOB	1	1
CLOSTRIDIA		
Peptococcaceae		
Desulfotomaculum acetoxidans DSM 771	1	1
Desulfotomaculum reducens	1	1
C. Desulforudis audaxviator MP104C	1	1
THERMOANAEROBACTERALES		
Ammonifex degensii KC4	1	1
NITROSPIRA		
Thermodesulfovibrio yellowstonii		
No. of organisms	19	19

frontiers in
MICROBIOLOGY

REVIEW ARTICLE
published: 29 June 2011
doi: 10.3389/fmicb.2011.00135

Genetics and molecular biology of the electron flow for sulfate respiration in *Desulfovibrio*

Kimberly L. Keller [1,2] ***and Judy D. Wall*** [1,2,3] ***

[1] *Department of Biochemistry, University of Missouri, Columbia, MO, USA*
[2] *Virtual Institute of Microbial Stress and Survival, Berkeley, CA, USA*
[3] *Ecosystems and Networks Integrated with Genes and Molecular Assemblies, Berkeley, CA, USA*

Edited by:
Thomas E. Hanson, University of Delaware, USA

Reviewed by:
Larry L. Barton, University of New Mexico, USA
David A. Stahl, University of Washington, USA

***Correspondence:**
Judy D. Wall, Department of Biochemistry, University of Missouri, Columbia, MO 65211, USA.
e-mail: wallj@missouri.edu

Progress in the genetic manipulation of the *Desulfovibrio* strains has provided an opportunity to explore electron flow pathways during sulfate respiration. Most bacteria in this genus couple the oxidation of organic acids or ethanol with the reduction of sulfate, sulfite, or thiosulfate. Both fermentation of pyruvate in the absence of an alternative terminal electron acceptor, disproportionation of fumarate and growth on H_2 with CO_2 during sulfate reduction are exhibited by some strains. The ability to produce or consume H_2 provides *Desulfovibrio* strains the capacity to participate as either partner in interspecies H_2 transfer. Interestingly the mechanisms of energy conversion, pathways of electron flow and the parameters determining the pathways used remain to be elucidated. Recent application of molecular genetic tools for the exploration of the metabolism of *Desulfovibrio vulgaris* Hildenborough has provided several new datasets that might provide insights and constraints to the electron flow pathways. These datasets include (1) gene expression changes measured in microarrays for cells cultured with different electron donors and acceptors, (2) relative mRNA abundances for cells growing exponentially in defined medium with lactate as carbon source and electron donor plus sulfate as terminal electron acceptor, and (3) a random transposon mutant library selected on medium containing lactate plus sulfate supplemented with yeast extract. Studies of directed mutations eliminating apparent key components, the quinone-interacting membrane-bound oxidoreductase (Qmo) complex, the Type 1 tetraheme cytochrome c_3 (Tp1-c_3), or the Type 1 cytochrome c_3:menaquinone oxidoreductase (Qrc) complex, suggest a greater flexibility in electron flow than previously considered. The new datasets revealed the absence of random transposons in the genes encoding an enzyme with homology to Coo membrane-bound hydrogenase. From this result, we infer that Coo hydrogenase plays an important role in *D. vulgaris* growth on lactate plus sulfate. These observations along with those reported previously have been combined in a model showing dual pathways of electrons from the oxidation of both lactate and pyruvate during sulfate respiration. Continuing genetic and biochemical analyses of key genes in *Desulfovibrio* strains will allow further clarification of a general model for sulfate respiration.

Keywords: *Desulfovibrio*, sulfate respiration, sulfite reduction, Coo hydrogenase, cytochrome c_3

INTRODUCTION

The ability to obtain energy from substrate oxidation coupled with sulfate reduction is a unique mechanism that is shared by a heterogeneous group of microbes that include proteobacteria, firmicutes and archaea; mesophiles, thermophiles, and psychrophiles. While this means of energy generation is restricted to anaerobes, these sulfate-reducing microbes (SRM) are found in a wide variety of environments including oxic waters and soils. Whereas oxygen at high concentrations is toxic to SRM, large variations in sensitivity are observed (Sass and Cypionka, 2007). Oxygen is reduced by many SRM perhaps as a protective mechanism because sustained growth supported through oxygenic respiration has not been demonstrated (Marschall et al., 1993; Hansen, 1994a).

Of this group of microbes, members of the δ-proteobacterial genus *Desulfovibrio* have been most intensively studied because of their rapid growth and ease of manipulation. *Desulfovibrio vulgaris* Hildenborough was the first of the sulfate-reducing bacteria to have its genome sequenced (Heidelberg et al., 2004). *D. vulgaris* was also the first to be genetically manipulated through conjugation (Powell et al., 1989; van den Berg et al., 1989) and the second to be modified by marker exchange mutagenesis (Fu and Voordouw, 1997), after *Desulfovibrio fructosovorans* (Rousset et al., 1991). Genome sequences of many more SRM are now available.[1]

[1] http://www.ncbi.nlm.nih.gov/sites/entrez

Improved genetic tools have been developed (Wall et al., 1993; Rousset et al., 1998; Bender et al., 2007; Keller et al., 2009; Zane et al., 2010), transposon mutant libraries have been generated (Groh et al., 2005; Deutschbauer, personal communication, and this lab) and systems biology tools have been applied (Mukhopadhyay et al., 2006; Redding et al., 2006; Tang et al., 2007; Pereira et al., 2008; He et al., 2010). Therefore this chapter will focus on the contributions of molecular genetics to our understanding of energy conversion in the *Desulfovibrio* strains. Confirmation that these insights might be applicable to other SRM genera remain to be established.

Our discussion will consider energy conversion by *Desulfovibrio* strains grown with lactate as carbon and electron source and sulfate as electron acceptor. Because electron flow from lactate oxidation with sulfate reduction provides robust growth of *Desulfovibrio*, data from systems biology approaches are now available from cells grown on these substrates. Strengthening relevance, the released fermentation products, lactate and H_2, are likely to be the sources of electrons found in natural environments where these bacteria flourish. Currently many transcriptomic data and some proteomic data have been generated[2] and transposon libraries have been selected with cells grown on these substrates (Deutschbauer, personal communication, and Wall lab).

As a terminal electron acceptor, sulfate has four properties that together give the SRM access to growth niches unavailable to other microbes. First, sulfate is a thermodynamically stable oxidized form of sulfur and must be activated prior to being reduced. Second, sulfate is reduced by soluble enzymes in the cytoplasm making active transport of the sulfate necessary because it is an ionized species at physiological pHs (H_2SO_4; pKa1, −3; pKa2, 2). Third, sulfide, HS^- (H_2S, pKa 6.9) the reduced product, is toxic at elevated concentrations (Caffrey and Voordouw, 2010) and must be transported out of the cell or defense systems invoked. Fourth, the fact that the reductive enzymes are soluble and not membrane-bound suggests that reduction of sulfate may not be uniquely or tightly associated with an electron transport system in the membrane.

The common sources of carbon and electrons used by SRM are fermentation products from facultative anaerobes. Most *Desulfovibrio* strains are incomplete oxidizers of organic acids and alcohols producing acetate in quantities nearly stoichiometric to the added substrate (Postgate, 1984a; Rabus et al., 2006). Therefore, about 95% of the carbon substrate oxidized by *Desulfovibrio* strains is used for energy generation and the residual used to produce cell material (Noguera et al., 1998; Rabus et al., 2006). The inability of these strains to oxidize acetate has been suggested to result from the high reduction potential of the fumarate/succinate couple ($E^{0\prime} = 33$ mV, Eq. 1, from Thauer et al., 1977) in the standard TCA cycle (Thauer, 1989). Therefore, reduction of the activated form of sulfate, adenosine 5′-phosphosulfate (APS, Eq. 2) or bisulfite (Eq. 3) cannot be coupled with succinate oxidation.

$$\text{Fumarate} + 2e^- + 2H^+ = \text{Succinate} \qquad E^{0\prime} = 33\ \text{mV} \qquad (1)$$

$$APS^{2-} + 2e^- + H^+ = HSO_3^- + AMP^{2-} \qquad E^{0\prime} = -60\ \text{mV} \qquad (2)$$

$$HSO_3^- + 6e^- + 6H^+ = HS^- + 3H_2O \qquad E^{0\prime} = -116\ \text{mV} \qquad (3)$$

[2]www.microbesonline.org

For those strains of the genus *Desulfobacter* or *Desulfobacterium* that do completely oxidize organic acids to CO_2 with sulfate as electron acceptor, the standard TCA cycle is not used (Hansen, 1994a).

The *Desulfovibrio* pathway for lactate oxidation is through pyruvate to acetyl-CoA and from acetyl-CoA to acetate via acetylphosphate which is of sufficient energy to generate ATP by substrate-level phosphorylation (See Eqs 4–8). Early researchers believed that the SRM were restricted to substrate-level phosphorylation for ATP generation. However, the demonstration that *Desulfovibrio* strains could grow with H_2 oxidation, with carbon supplied by CO_2 and acetate, and sulfate as terminal electron acceptor (Butlin et al., 1949; Peck, 1960) firmly established the capacity for electron transport-linked phosphorylation. In addition, Peck (1966) convincingly argued that a mechanism, in addition to substrate-level phosphorylation, was essential during lactate plus sulfate growth. Peck pointed out that the two moles of ATP generated during the oxidation of two moles of lactate would be consumed during sulfate activation. Therefore, energy to support growth must be provided by an additional mechanism.

HYDROGEN CYCLING MODEL

Odom and Peck (1981a) proposed an unusual and controversial model for increasing the energy budget called the "hydrogen cycle." This model was proposed, in part, as an explanation for the observation of a H_2 transient seen in cultures of *Desulfovibrio* inoculated into medium with lactate or pyruvate as electron donors and sulfate as electron acceptor. They proposed that electrons and protons generated from organic acid oxidation could serve as substrates for a cytoplasmically located hydrogenase. The resulting H_2 could diffuse through the cytoplasmic membrane and be reoxidized by periplasmic hydrogenases. The electrons produced by the H_2 oxidation would be delivered to the *c*-type cytochrome pool for return to the cytoplasm through transmembrane protein complexes and used for sulfate reduction. The protons released would contribute to the chemiosmotic potential.

In contrast, Lupton et al. (1984) proposed that trace H_2 was produced and consumed in the initial growth phases of *Desulfovibrio* cultures on organic acids plus sulfate to control redox state of electron carriers. These researchers also provided evidence that they interpreted as eliminating the argument that the purpose of the transient H_2 production was to allow fermentation to make ATP for sulfate activation and reduction in growth initiation. They showed that with thiosulfate as terminal electron acceptor, a substrate that does not require activation prior to reduction, H_2 was still produced and consumed when cells were introduced into fresh medium.

Evidence both for and against the hydrogen cycling model has been published. Odom and Peck (1981a) demonstrated that spheroplasts produced from *Desulfovibrio gigas* were unable to oxidize lactate and reduce sulfate without the restoration of the periplasmic proteins, hydrogenase and the type I cytochrome c_3 (Tp1-c_3). From this result it was inferred that electrons were routed from lactate through the periplasm and back to sulfate. In addition, Peck et al. (1987) were able to trap and measure H_2 released by *D. vulgaris* from pyruvate oxidation coupled to sulfate reduction with membrane-inlet mass spectrometry. On the other hand, the existence of free H_2, predicted by the model to be a periplasmic

intermediate in the oxidation of lactate or pyruvate, would lead to the expectation that a H_2 atmosphere would strongly inhibit oxidation of these substrates. Lupton et al. (1984) showed that there was no inhibition of lactate or pyruvate oxidation by H_2 during sulfate respiration. This lack of inhibition of substrate oxidation by H_2 was confirmed by Pankhania et al. (1986) for cells with lactate. Also, a mutant of *Desulfovibrio desulfuricans* ATCC27774 was isolated that could grow on lactate plus sulfate but not H_2 plus sulfate (Odom and Wall, 1987). This result is incongruent with periplasmic H_2 as an intermediate in lactate oxidation during sulfate reduction. In addition, if the cycling process – H_2 production, membrane diffusion and H_2 oxidation – were essential for sulfate respiration with organic acids, SRM should all have hydrogenases. *Desulfovibrio sapovorans* is one example that lacks hydrogenase (Postgate, 1984b).

More recent reviews have diminished the putative role of hydrogen cycling in the metabolism of the SRM. Widdel and Hansen (1991) suggested that H_2 production is simply an accident of having constitutive hydrogenases active in the cell. Rabus et al. (2006) proposed that constitutive hydrogenases would produce hydrogen whenever there was an imbalance between reductant produced or consumed by the cells. An alternative suggestion of the latter researchers derived from the postulation that in natural environments the SRM participate routinely in interspecies H_2 transfer when sulfate is absent. As a result, SRM might not be able to redirect electrons completely when sulfate was available, thus driving the release of electrons as H_2 (Rabus et al., 2006). In contrast to these theories, Noguera et al. (1998) elegantly generated and tested a model for H_2 production and consumption by *D. vulgaris* growing on lactate plus sulfate. These researchers proposed that dual pathways were operating, simultaneously, for electron flow and that the free energy available determined the distribution of electron flow. Their model predicted 52% of the electron flow would move from lactate through H_2 and finally to sulfate; whereas, 48% would move to sulfate without H_2 formation. After subtraction of the reductant moving to biomass, their experiments showed that 47% of the remaining electrons were directly coupled to sulfate reduction and 53% formed H_2 before being used for sulfate reduction (Noguera et al., 1998).

SULFATE REDUCTION AND LACTATE OXIDATION

REACTIONS

The predicted pathways of sulfate reduction and lactate oxidation are presented in the equations below (Eqs 4–16). Dissimilatory sulfate reduction occurs by a two step process requiring a minimum of four enzymes (**Table 1A**). First sulfate is activated to form APS at the expense of two ATP equivalents by sulfate adenylyltransferase. Two electrons are then used by APS reductase to reduce APS to HSO_3^- (Eqs 10 and 12). The activation reaction is pulled by the hydrolysis of the released pyrophosphate (Eq. 11). Then bisulfite reductase reduces HSO_3^- with six electrons to HS^-, in one step (Eq. 13). The equations show protonated species considering the published pKa's of the compounds[3] and assuming that the internal pH is ca. 7.5 (Cypionka, 1995). It should be noted that the pKa's of HSO_3^{2-}, H_2S, and $H_2PO_4^-$ are 7.2, 7.0, and 7.2, respectively, and therefore the protonated and deprotonated forms were considered to be present in about equal quantities. The net result for sulfate reduction (Eq. 14) indicates a consumption of eight moles of electrons with eight and a half moles of protons.

Lactate oxidation by the incomplete oxidizers in the *Desulfovibrio* genus, proceeds with pyruvate and acetyl-CoA as intermediates. Reductant is generated from lactate through lactate dehydrogenase and pyruvate:ferredoxin oxidoreductase (Eqs 4 and 5), while acetyl-CoA is the source for substrate-level phosphorylation producing ATP (Eqs 6 and 7). Seven protons were produced in the reactions as shown (Eq. 8). By interconversion of the adenylate nucleotides (Eq. 15) and summing Eqs 8, 9, 14, and 15, the combined oxidation/reduction reaction for growth with lactate plus sulfate is shown as Eq. 16. With the assumptions made here, 0.5 mole of protons are produced in excess of those consumed during reduction of one mole of sulfate. Clearly nitrogen metabolism, biomass production, transport functions and/or small variations in internal pH that affect the concentrations of protonated species will all affect the actual balance of electrons and protons (Hooper and DiSpirito, 1985).

EQUATIONS

Lactate oxidation:

$$2CH_3CHOHCOO^- = 2CH_3COCOO^- + 4e^- + 4H^+$$
Lactate dehydrogenase (4)

$$2CH_3COCOO^- + 2CoASH = 2CH_3CO \sim SCoA + CO_2 + 4e^- + 2H^+$$ Pyruvate:ferredoxin oxidoreductase (5)

$$2CH_3CO \sim SCoA + H_2PO_4^- + HPO_4^{2-} = 2CH_3CO \sim OPO_3^{2-} + 2CoASH + H^+$$ Phosphotransacetylase (6)

$$2CH_3CO \sim OPO_3^{2-} + 2ADP^{3-} = 2CH_3COO^- + 2ATP^{4-}$$
Acetate kinase (7)

$$2CH_3CHOHCOO^- + 2ADP^{3-} + H_2PO_4^{2-} = 2CH_3COO^- + 2ATP^{4-} + 2CO_2 + 8e^- + 7H^+$$ Lactate oxidation summary (8)

Dissolved CO_2:

$$2CO_2 + 2H_2O = 2HCO_3^- + 2H^+$$ Carbonic anhydrase (9)

Sulfate reduction:

$$SO_4^{2-} + ATP^{4-} + H^+ = APS^{2-} + HP_2O_7^{3-}$$
Sulfate adenylyltransferase (10)

$$HP_2O_7^{3-} + H_2O = H_2PO_4^- + HPO_4^{2-}$$
Inorganic pyrophosphatase (11)

$$APS^{2-} + 2e^- + 0.5H^+ = 0.5\ HSO_3^- + 0.5\ SO_3^{2-} + AMP^{2-}$$
APS reductase (12)

$$0.5\ HSO_3^- + 0.5\ SO_3^{2-} + 6e^- + 7H^+ = 0.5\ HS^- + 0.5\ H_2S + 3\ H_2O$$ Bisulfite reductase (13)

$$SO_4^{2-} + ATP^{4-} + 8e^- + 8.5H^+ = 0.5\ HS^- + 0.5\ H_2S + AMP^{2-} + H_2PO_4^- + HPO_4^{2-} + 2\ H_2O$$ Sulfate reduction summary (14)

[3]http://chemweb.unp.ac.za/Chemistry/Physical_data/pKa_complilation.pdf

Table 1 | Expression of genes encoding enzymes putatively involved in Lactate/Sulfate growth of *Desulfovibrio vulgaris* Hildenborough.

Locus DVU No.	Gene	Annotation[a]	Microarray data (Log_2 R)[b]			Average Log_2 RNA/DNA[f]	Tn in gene[g]
			Stat/Expo[c]	LThio/LS[d]	PS/LS[e]		
A. SULFATE REDUCTION ENZYMES							
1295	*sat*	Sulfate adenylyltransferase (ATP-sulfurylase)	0.45	−1.07	−0.33	4.44	N
1636	*ppaC*	Pyrophosphatase	0.52	−1.17	−0.24	2.52	N
h 0846	*apsB*	Adenylsulfate reductase ß subunit	−0.56	−0.99	0.39	4.90	N
↓ 0847	*aspA*	Adenylsulfate reductase a subunit	−0.58	−1.81	0.04	4.72	N
0402	*dsrA*	Dissimilatory sulfite reductase alpha subunit	−0.07	−0.33	0.69	4.32	N
0403	*dsrB*	Dissimilatory sulfite reductase beta subunit	−1.23	−0.18	0.88	4.19	N
↓ 0404	*dsrD*	Dissimilatory sulfite reductase D	−1.88	0.91	0.47	4.89	N
2776	*dsrC*	Dissimilatory sulfite reductase, gamma subunit	3.48	0.07	−0.87	3.39	N
B. CARBON METABOLISM ENZYMES							
0253	*D-ldh*	Lactate dehydrogenase, Glycolate oxidoreductase, FAD/iron-sulfur cluster-binding domain protein	−0.16	0.33	0.39	2.09	Y
0390	*glcD*	FAD/FMN-containing dehydrogenase, glycolate oxidase, subunit GlcD, putative	−0.97	0.28	0.26	0.11	Y
0600	*ldh*	L-lactate dehydrogenase	1.20	0.22	−0.14	−1.32	Y
↑ 0826	NA[i]	Glycolate oxidase, iron-sulfur subunit, putative	0.47	−0.51	−0.28	−0.05	Y
0827	NA	Glycolate oxidase, subunit GlcD, putative, GO:0009339 glycolate oxidase complex	−0.19	−0.58	−0.02	−0.05	Y
1412	NA	D-isomer specific 2-hydroxyacid dehydrogenase family protein	0.15	−0.42	−0.36	0.42	Y
↑ 1782	NA	Iron-sulfur cluster-binding protein	0.29	−0.22	−0.21	−0.02	Y
1783	NA	Cysteine-rich domain protein; GO:0009339 glycolate oxidase complex	1.19	0.02	−0.61	0.40	Y
2784	*L-ldh*	Dehydrogenase, FMN-dependent family	−0.84	−1.10	−0.45	0.07	Y
3071	NA	Oxidoreductase, FAD/iron-sulfur cluster-binding domain protein	−0.71	1.02	0.39	0.25	N
3025	*por*	Pyruvate:ferredoxin oxidoreductase	−0.57	−0.26	0.37	2.83	N
3027	*glcD*	D-lactate dehydrogenase, glycolate oxidase subunit	1.10	0.25	−0.01	1.99	Y
3028	*glpC*	D-lactate dehydrogenase, iron-sulfur cluster-binding protein	1.39	0.47	−0.34	1.44	Y
3029	*pta*	Phosphotransacetylase	−0.33	−0.50	−0.29	1.80	N
↓ 3030	*ackA*	Acetate kinase	−0.97	−0.78	−0.30	1.79	N
2824	*pfl-I*	Pyruvate formate lyase	0.36	−0.40	−0.41	−1.44	Y
1569	*porA*	Pyruvate-ferredoxin-oxidoreductase, alpha subunit	0.80	−0.56	−0.12	0.53	Y
↓ 1570	*porB*	Pyruvate-ferredoxin-oxidoreductase, beta subunit	−0.02	−0.25	−0.06	−0.81	N
C. PERMEASES AND TRANSPORTERS							
0053	*sulP-1*	Sulfate permease, putative	1.49	−0.23	−0.12	−0.21	Y
0279	*sulP-1*	Sulfate permease family protein	−2.28	−0.46	0.38	0.40	Y
1999	*sul-1*	Sulfate transporter family protein	−0.13	−0.06	−0.01	−0.75	Y
2110	*b2975*	L-lactate permease	0.79	0.65	−0.13	−0.85	Y
2285	*lctP-1*	L-lactate permease family protein	−2.34	−0.31	−0.20	0.13	Y
2451	*lctP-2*	L-lactate permease family protein	−1.05	−0.07	0.28	0.69	Y
2683	*lldP-1*	L-lactate permease family protein	−1.41	−0.27	0.25	0.47	Y

(Continued)

Table 1 | Continued

Locus DVU No.	Gene	Annotation[a]	Microarray data (Log_2 R)[b]			Average Log_2 RNA/DNA[f]	Tn in gene[g]
			Stat/Expo[c]	LThio/LS[d]	PS/LS[e]		
3026	*lldP-2*	L-lactate permease	0.23	0.11	0.13	0.74	Y
3284	*b2975*	L-lactate permease	1.28	1.07	0.51	−1.68	Y
0446	*dhlC*	Sodium/solute symporter family protein	1.51	−0.09	0.23	−1.98	Y
0088	*panF*	Sodium/pantothenate symporter	1.16	0.61	0.07	−0.09	Y
D. MEMBRANE-BOUND ELECTRON TRANSFER COMPLEXES							
0848	*qmoA*	Quinone-interacting membrane-bound oxidoreductase, Flavin protein	−0.49	−1.30	0.46	2.64	N
0849	*qmoB*	Quinone-interacting membrane-bound oxidoreductase, Flavin protein	−1.25	−1.30	0.004	1.62	N
0850	*qmoC*	Quinone-interacting membrane-bound oxidoreductase, Membrane FeS protein	−0.15	−1.26	0.42	0.83	N
1286	*dsrP*	Integral membrane protein	1.40	−1.07	0.66	2.06	N
1287	*dsrO*	Periplasmic (Tat), binds 2[4Fe-4S]	−1.57	−1.47	0.81	1.43	N
1288	*dsrJ*	Periplasmic (Sec) triheme cytochrome *c*	−1.31	−1.47	0.46	1.42	N
1289	*dsrK*	Cytoplasmic, binds 2 [4Fe-4S]	−1.98	−1.46	0.58	1.04	N
1290	*dsrM*	Inner membrane protein binds 2 heme *b*	−1.84	ND[j]	ND	1.37	N
0692	*qrcD*[k]	Molybdopterin oxidoreductase, transmembrane subunit	−0.46	−0.81	0.47	1.11	Y
0693	*qrcC*	Molybdopterin oxidoreductase, iron sulfur cluster binding subunit, containing cytochrome *c* heme	−1.65	−0.67	0.05	1.10	N
0694	*qrcB*	Molybdopterin oxidoreductase, molybdopterin binding subunit	−0.95	−0.35	0.10	1.06	Y
0695	*qrcA*	Cytochrome *c*, (six hemes)	−0.72	0.06	0.34	1.34	N
0263	*tmcA*	Transmembrane complex, tetraheme cytochrome c_3	−0.31	−0.17	0.28	1.69	N
0264	*tmcB*	Transmembrane complex, ferredoxin, 2 [4Fe-4S]	0.5	−0.44	0.39	2.21	Y
0265	NA	Membrane protein, putative	0.58	−0.50	0.26	1.41	Y
0531	*hmcF*	52.7 kd protein in *hmc* operon	0.59	0.29	−1.49	−1.90	Y
0532	*hmcE*	25.3 kd protein in *hmc* operon	0.19	1.53	0.35	−1.54	Y
0533	*hmcD*	5.8 kd protein in *hmc* operon	0.78	−0.55	−1.1	−1.97	N
0534	*hmcC*	43.2 kd protein in *hmc* operon	2.33	0.16	−0.33	−1.07	Y
0535	*hmcB*	40.1 kd protein in *hmc* operon	1.55	1.79	ND	−1.21	Y
0536	*hmcA*	High-molecular-weight cytochrome *c*	0.14	1.61	−0.3	−1.44	N
2791	*dhcA*	Decaheme cytochrome *c* associated with Rnf complex	−0.19	−0.14	0.96	1.03	Y
2792	*rnfC*	NADH:quinone oxidoreductase subunit RnfC	−0.37	−0.26	0.91	0.21	Y
2793	*rnfD*	Electron transport complex protein RnfD, putative	1.10	−0.57	1.00	−0.43	Y
2794	*rnfG*	NADH:quinone oxidoreductase subunit RnfG	0.14	−0.60	0.94	−0.05	Y
2795	*rnfE*	NADH:quinone oxidoreductase subunit RnfE	1.08	−0.71	0.38	−1.03	N
2796	*rnfA*	NADH:quinone oxidoreductase subunit RnfA	1.38	−0.52	1.09	−0.75	N
2797	*rnfB*	NADH:quinone oxidoreductase subunit RnfB	−0.13	−0.03	0.73	0.05	Y
3143	*ohcB*	Iron-sulfur cluster-binding protein	1.36	−0.11	0.59	−2.33	N
3144	*ohcA*	Cytochrome *c* family protein	1.12	−0.15	0.54	−1.74	Y
3145	*ohcC*	Hydrogenase, *b*-type cytochrome subunit, putative	0.78	0.48	0.64	−1.75	Y

(Continued)

Table 1 | Continued

Locus DVU No.	Gene	Annotation[a]	Microarray data (Log_2 R)[b]			Average Log_2 RNA/DNA[f]	Tn in gene[g]
			Stat/Expo[c]	LThio/LS[d]	PS/LS[e]		
E. PERIPLASMIC HYDROGENASES							
1769	*hydA*	Periplasmic [Fe] hydrogenase, large subunit	−0.47	1.27	−0.003	−0.06	Y
1770	*hydB*	Periplasmic [Fe] hydrogenase, small subunit	−0.42	1.86	0.74	−0.29	Y
1917	*hysB*	Periplasmic [NiFeSe] hydrogenase, small subunit	−0.93	0.25	0.31	1.88	Y
1918	*hysA*	Periplasmic [NiFeSe] hydrogenase, large subunit, selenocysteine-containing	−1.32	ND	ND	2.43	Y
1921	*hynB-1*	Periplasmic [NiFe] hydrogenase, small subunit, isozyme 1	0.82	−0.56	0.74	0.74	Y
1922	*hynA-1*	Periplasmic [NiFe] hydrogenase, large subunit, isozyme 1	0.57	−0.57	0.84	0.39	Y
2524	NA	[NiFe] hydrogenase	−0.23	−1.79	−0.34	−2.22	Y
2525	*hynB-2*	Periplasmic [NiFe] hydrogenase, small subunit, isozyme 2	−0.1	−1.46	−0.49	−0.96	Y
2526	*hynA-2*	Periplasmic [NiFe] hydrogenase, large subunit, isozyme 2	2.02	−1.36	−0.64	−0.44	Y
F. CYTOPLASMIC HYDROGENASES AND CARBON MONOXIDE DEHYRDOGENASES							
0429	*echF*	Ech hydrogenase, subunit EchF, putative	0.55	0.65	1.34	−1.30	Y
0430	*echE*	Ech hydrogenase, subunit EchE, putative	ND	ND	ND	ND	Y
0431	*echD*	Ech hydrogenase, subunit EchD, putative	−0.07	0.64	1.23	−1.14	N
0432	*echC*	Ech hydrogenase, subunit EchC, putative	1.35	0.25	0.77	−0.83	N
0433	*echB*	Ech hydrogenase, subunit EchB, putative	0.51	0.33	1.44	−1.33	Y
0434	*echA*	Ech hydrogenase, subunit EchA, putative	−0.08	−0.18	0.63	−0.34	Y
2286	*cooM*	Hydrogenase, CooM subunit, putative	−1.59	0.25	−0.10	1.30	N
2287	*cooK*	Hydrogenase, CooK subunit, selenocysteine-containing, putative	−0.47	−0.01	−0.78	1.52	N
2288	*cooL*	Hydrogenase, CooL subunit, putative	−0.70	−0.11	−0.73	1.69	N
2289	*cooX*	Hydrogenase, CooX subunit, putative	−0.91	0.09	−0.54	1.73	N
2290	*cooU*	Hydrogenase, CooU subunit, putative	−0.10	−0.21	−0.51	2.10	N
2291	*cooH*	Carbon monoxide-induced hydrogenase CooH, putative	−0.88	−0.34	−0.70	1.82	N
2292	*hypA*	Hydrogenase nickel insertion protein	1.09	0.50	−0.44	2.82	N
2293	*cooF*	Iron-sulfur protein	1.04	0.21	−0.74	2.70	N
2098	*cooS*	Carbon monoxide dehydrogenase	ND	ND	ND	0.54	Y
2099	*cooC*	Carbon monoxide dehydrogenase	0.19	1.52	1.52	−1.58	Y
G. PERIPLASMIC FORMATE DEHYDROGENASES							
0587	*fdnG-1*	Formate dehydrogenase, alpha subunit, selenocysteine-containing	1.87	ND	ND	0.29	Y
0588	*hybA*	Formate dehydrogenase, beta subunit	0.93	1.31	0.39	−0.27	N
2481	*fdoH*	Formate dehydrogenase, beta subunit	0.49	−0.17	−0.52	0.65	Y
2482	*fdnG-2*	Formate dehydrogenase, alpha subunit, selenocysteine-containing	0.34	ND	ND	0.00	Y
2483	*cfdE*	Formate dehydrogenase, cytochrome *c* family protein	0.09	−0.55	−0.27	0.54	Y
2484	*cfdD*	Formate dehydrogenase, cytochrome *c* family protein	−0.18	−0.59	−0.08	−0.62	N
2485	*cfdC*	Formate dehydrogenase, membrane protein, putative	0.53	−0.35	−0.33	0.15	Y

(Continued)

Table 1 | Continued

Locus DVU No.	Gene	Annotation[a]	Microarray data (Log_2 R)[b]			Average Log_2 RNA/DNA[f]	Tn in gene[g]
			Stat/Expo[c]	LThio/LS[d]	PS/LS[e]		
↑2809	NA	Cytochrome c_3	−0.83	−0.09	0.84	−1.51	Y
2810	*fdhE*	Formate dehydrogenase formation protein FdhE, putative	0.16	0.06	0.77	−1.70	Y
2811	*COG-HybA*	Formate dehydrogenase, beta subunit	−0.16	−0.82	0.66	−1.95	Y
2812	*fdnG-3*	Formate dehydrogenase, alpha subunit, selenocysteine-containing	−0.03	−0.33	0.70	−1.75	Y
H. PERIPLASMIC CYTOCHROMES							
3107	*occ*	Cytochrome *c* family protein (eight hemes)	2.63	−2.33	0.14	−0.10	Y
3171	*cycA*	Cytochrome c_3 (TpI-c_3; four hemes)	0.29	−0.73	0.81	4.30	N
1817	*cyf*	c_{553}cytochrome (one heme)	0.90	−0.04	−0.12	2.54	Y
3041	NA	c_{553} cytochrome (one heme)	−0.13	0.89	−0.10	0.13	N
0702	NA	c_{554} cytochrome (four hemes)	−0.30	0.26	−0.17	0.99	N
0922	NA	c_{554} cytochrome (four hemes)	0.20	−0.05	0.14	−1.60	Y
0624	*nrfH*	Cytochrome *c* nitrate reductase, small subunit (four hemes)	−0.34	0.08	−0.01	−0.58	Y
↓0625	*nrfA*	Cytochrome *c* nitrite reductase, catalytic subunit (five hemes)	−0.49	−0.90	0.46	−2.37	Y
I. OTHER							
1777	*cynT*	Carbonic anhydrase	−1.08	0.15	−0.39	0.50	Y
2013	*HCP*	Hybrid cluster protein	ND	ND	ND	0.74	Y
2543	*b0873*	Hybrid cluster protein	0.67	0.07	0.01	0.66	Y
↑2402	*hdrA*	Heterodisulfide reductase, A subunit	−0.3	−0.36	0.23	1.61	Y
2403	*hdrB*	Heterodisulfide reductase, B subunit	−0.1	−0.17	0.54	2.14	Y
2404	*hdrC*	Heterodisulfide reductase, C subunit	0.8	−0.30	−0.11	2.48	N

[a] *Gene annotation was obtained from http://www.microbesonline.org*

[b] *Log_2 R, where R is the ratio of transcripts in the experimental versus the control.*

[c] *Stat/Expo is the ratio of transcripts from cells grown in lactate/sulfate (60 mM/50 mM) comparing stationary cells to exponentially growing cells (samples T5/T1 as presented in Clark et al., 2006).*

[d] *LThio/LS is the ratio of transcripts from cultures growing exponentially ($OD_{600} \approx 0.3$) on lactate/thiosulfate (60 mM/30 mM) compared to those from lactate/sulfate (60 mM/30 mM) grown cells.*

[e] *PS/LS is the ratio of transcripts from cultures growing exponentially ($OD_{600} \approx 0.3$) on pyruvate/sulfate (60 mM/15 mM) compared to those from lactate/sulfate (60 mM/30 mM) grown cells.*

[f] *Average Log_2 RNA/DNA hybridization is a measure of the relative abundance of transcripts present for a given gene in an exponentially growing lactate/sulfate culture ($OD_{600} \approx 0.3$; Wall et al., 2009). Abundances were averaged from 173 data points with an average standard deviation of ± 1.54. The average gene expression was arbitrarily given a Log_2 R value of 0.*

[g] *Tn in gene, 'Y' indicates that at least one transposon insertion has been recovered in the gene and 'N', that a transposon insertion has not been recovered. The transposon used is the modified Tn5-RL27 (Oh et al., 2010).*

[h] *Arrows in the first column indicate the direction of transcription of the genes within a predicted operon.*

[i] *NA = Not annotated with a gene name.*

[j] *ND = No data, insufficient useable data for given condition.*

[k] *Most current annotation of DVU0692–0695 was used (Venceslau et al., 2010).*

Adenylate nucleotide interchange:

$$AMP^{2-} + ATP^{4-} = 2ADP^{3-} \text{ Adenylate kinase} \quad (15)$$

Summary lactate plus sulfate metabolism:

$$2\ CH_3CHOHCOO^- + SO_4^{2-} = 2\ CH_3COO^- + 2\ HCO_3^- + 0.5\ HS^- + 0.5\ H_2S + 0.5H^+ \quad (16)$$

TRANSPORT FUNCTIONS

Transport functions of substrates and products have been addressed experimentally in variable detail. Cypionka (1995) has summarized his detailed work on sulfate transport in SRM. In freshwater SRM strains, sulfate was shown to be symported with protons, two if sulfate were in excess and three electrogenically if sulfate were limited. Since the genetic experiments to be described here with *D. vulgaris* were carried out with excess sulfate, transport

of sulfate likely occurs with the electroneutral symport of two electrons. Energy for the sulfate transport, i.e., the two protons used, is compensated by the diffusion of H_2S from the cell. However, in the slightly alkaline pH of the cell much of the sulfide would be ionized, HS^-. Little is known about the export of this charged ion. Cypionka (1995) suggests that it may be impermeable or symported with one proton. If true, energy spent transporting sulfate into the cell would be balanced by the electroneutral export of sulfide or diffusion of the protonated form.

Transport of the monocarboxylates, lactate and acetate, into and out of the cell, respectively, is likely to be by symport with one proton (Dong et al., 1993). Thus, the reciprocal transport of these compounds will not affect the proton balance of the cell. Although acetic acid in its protonated form can apparently diffuse across the cell membrane (Thauer and Morris, 1984), its continued production against a chemical gradient of acetate during oxidation of lactate or pyruvate would suggest an energy linked export process. Six genes have been annotated as lactate permeases in *D. vulgaris*, five for L-lactate and one for D-lactate (**Table 1**); whereas, no genes were annotated as acetate transporters. BLAST analysis[4] of the *D. vulgaris* genome showed that DVU0446 is 61% identical and DVU0088 is 23% identical to the acetate permease (*actP*, b4067) from *Escherichia coli* str. K-12 substr. MG1655. Further experimentation will be needed to establish whether these genes encode transporters for acetate and whether they might be essential.

THERMODYNAMICS

The model of Noguera et al. (1998) is predicated on the existence of two routes for electron flow during lactate plus sulfate growth and controlled by a thermodynamic switch that responds to free energy availability. This is consistent with the differences in reduction potential for the two oxidation steps generating electrons from lactate. For the first oxidation step, the $E^{0\prime}$ (mV) of the pyruvate/lactate couple is -190 mV; whereas, for pyruvate oxidation, the acetyl-CoA + CO_2/pyruvate couple is -498 mV. When sulfate is terminal electron acceptor, the $E^{0\prime}$ (mV) of SO_4^{2-}/HS^- is -200 (calculated for [HS^-] of 0.1 mM; Thauer et al., 2007). The standard reduction potential of the lactate dehydrogenases is above that of the H^+/H_2 couple ($E^{0\prime}$ of -414 mV), even if H_2 at more environmental concentrations is considered ($E^{0\prime}$ of -270 mV at 1 Pa:H_2), and would require energy-driven reverse electron flow to accomplish H_2 generation. In contrast, pyruvate oxidation with ferredoxin reduction has sufficient redox potential to generate H_2. Thus it is tempting to suggest that the two pathways for electron transport coincide with electrons from lactate and those from pyruvate.

It is clear that the lactate dehydrogenases are membrane-bound flavoproteins capable of delivering electrons directly to the menaquinone pool in the membrane (Reed and Hartzell, 1999; Thauer et al., 2007). In contrast, the pyruvate:ferredoxin oxidoreductase is a soluble enzyme in the cytoplasm that delivers electrons to the soluble electron carrier, ferredoxin (Kletzin and Adams, 1996; Garczarek et al., 2007). Indeed, these electron pools must mix when the SRM grow on lactate in coculture with hydrogenotrophic methanogens, since lactate can be completely oxidized without the production of detectable pyruvate (Walker et al., 2009). During this syntrophic growth by *D. vulgaris*, the Coo membrane-bound hydrogenase has been shown to be needed, although it was not essential for monoculture on lactate plus sulfate (Walker et al., 2009). Interestingly, this protein complex belongs to a family of transmembrane complexes that function as proton (or sodium) – translocating hydrogenases and that use reduced ferredoxin as electron donors (Welte et al., 2010; **Figure 1**). The recently proposed mechanism of flavin-based electron bifurcation (Herrmann et al., 2008) could offer a possible solution to the necessity of lactate supported hydrogen production. This mechanism would suggest that, when concentrations of H_2 are maintained at very low levels, the exergonic reduction of protons to form H_2 from the reduced ferredoxin ($E^{0\prime} \leq 420$ mV) could be coupled with the endergonic formation of hydrogen with electrons from menaquinone ($E^{0\prime}$ -75 mV). The Coo membrane-bound hydrogenase complex is a flavoprotein that could allow bifurcation of electrons from the two sources, reduced ferredoxin and menaquinone. This model (**Figure 1**) would also provide an explanation for the decrease or cessation of electron flow in this pathway as hydrogen concentrations increased. Currently no experiments have been conducted to explore electron bifurcation during lactate oxidation and sulfate reduction in *Desulfovibrio*.

GENOMES

In 2004, the genome sequence of *D. vulgaris* (Heidelberg et al., 2004) became available. In the ensuing few years, several additional SRM genomes have become accessible. If hydrogen cycling were a major mechanism for augmenting the energy budget of the SRM, one might predict that conserved hydrogenases would be found among these bacteria for this process. By making the simple comparison of the genomes of two species that from physiological analyses were thought to be closely related, *D. vulgaris* and *Desulfovibrio alaskensis* G20 (Hauser et al., 2011), it can be seen that the candidate cytoplasmic hydrogenases from *D. vulgaris* (Ech hydrogenase, DVU0429–0434, and Coo hydrogenase, DVU2286–2293) are not conserved in the G20 strain. However, that does not preclude the existence of multiple electron pathways to sulfate in the SRM.

EXPRESSION AND MUTANT ANALYSIS OF GENES FOR CENTRAL REDOX PATHWAYS OF D.VULGARIS HILDENBOROUGH

Here we examine *D. vulgaris* gene expression data from microarrays of cells grown under different nutrient conditions, the relative abundance of transcripts from cells grown on lactate plus sulfate, and a random transposon mutant library to determine whether genes important for enzymes needed for energy generation in this growth mode become evident (**Table 1**).

MICROARRAY DATA

Microarray data provide information about the changes in expression of genes in response to environmental changes but do not allow absolute levels of gene expression to be determined. Changes in gene expression for *D. vulgaris* have been generated through

[4]http://blast.ncbi.nlm.nih.gov/Blast.cgi

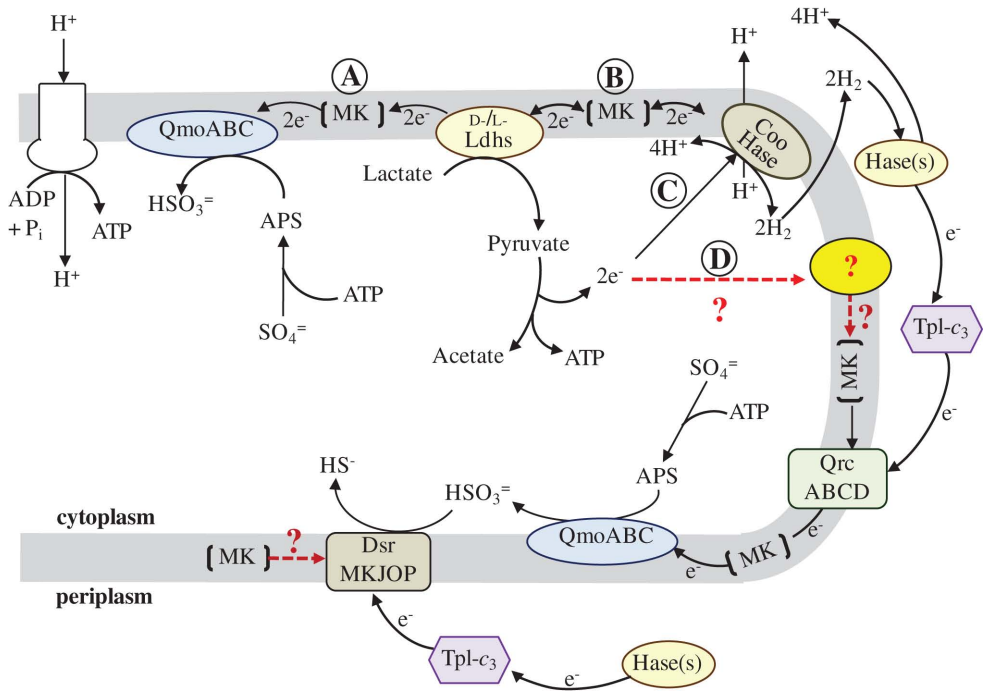

FIGURE 1 | Proposed model for the flow of electrons during sulfate respiration in *D. vulgaris* Hildenborough. Abbreviations: QmoABC, Quinone-interacting membrane-bound oxidoreductase (DVU0848–0850); Ldhs, lactate dehydrogenases (nine annotated); Coo Hase, CO-induced membrane-bound hydrogenase (DVU2286–2293); Hase(s), periplasmic hydrogenases (four annotated); Tpl-c_3, Type-1 tetraheme cytochrome c_3 (DVU3171); QrcABCD, Type-1 cytochrome c_3:menaquinone oxidoreductase, formerly molybdopterin oxidoreductase (DVU0692–0695); DsrMKJOP, (DVU1290–1286); and MK, Menaquinone pool. Red, dashed lines and (?) indicate metabolic pathways for which less evidence is available. The reaction arrows were drawn as unidirectional for clarity of the model and electron flow. Pathway description is given in text.

the Virtual Institute for Microbial Stress and Survival (VIMSS) program[5] supported by the US Department of Energy and are available at www.microbesonline.org (Dehal et al., 2010). These data are $\log_2$ ratios of experimental versus control transcript abundances from gene probe microarrays with 12 replicates for each ratio. All transcript preparations were made from cells that were in the mid-exponential growth phase (OD_{600} of ca. 0.3) with the exception of the experiment following gene expression changes throughout the growth curve (Clark et al., 2006).

Our simple interpretations of the differential expression of genes in microarrays (**Table 1**) are as follows. Comparison of transcripts from cultures in stationary phase versus exponential phase for cells growing with lactate (60 mM) plus sulfate (50 mM; Clark et al., 2006) represent a lactate-limiting condition and preparation for a non-growing state. We have assumed that an indicator for gene importance in the metabolism of lactate plus sulfate as cells enter stationary phase, at the substrate concentrations given, would be an increase in expression of carbon acquisition genes. A decrease in those genes needed for sulfate reduction and energy generation might also be expected since the cells are slowing growth and sulfate is plentiful. For cultures grown to mid-exponential phase with thiosulfate versus sulfate as electron acceptor, we would predict that transcript changes would reflect a decrease for the sulfate-reducing enzymes but that sulfite reduction and carbon and electron metabolism would remain unchanged. For cultures growing exponentially with pyruvate as carbon and electron source compared to lactate, the genes differentially transcribed should include those required for lactate transport and oxidation. Clearly a direct connection between transcript changes and enzyme levels is often not evident (Torres-García et al., 2009). However, because energy conversion is such a large proportion of the metabolism of these bacteria, the possibility of correlated changes was tacitly assumed.

RELATIVE ABUNDANCE OF TRANSCRIPTS

All microarray experiments in the database of the VIMSS program have been normalized to DNA signals on the microarrays. As a result, a robust measure of the relative abundance of mRNA for each gene has been accumulated during microarray experiments, with 173 data points in the calculation for each (Wall et al., 2009). We determined an average expression level from the mRNA/DNA signals and arbitrarily set the average for all genes to 1 or $\log_2 = 0 \pm 1.54$. Thus a transcript value that is one SD above the average is a gene expressed approximately three fold more highly than average and is in the top 16% expression level of all genes. Because so much of the metabolic capacity of anaerobes is devoted to energy conversion, we assumed that the genes for the proteins and enzymes responsible would likely be among those above the average in expression.

[5]http://VIMSS.lbl.gov

RANDOM TRANSPOSON MUTANTS

To reveal genes needed for growth of *D. vulgaris* on lactate plus sulfate, the final information source comes from mutation analysis. The creation of a random transposon library in this bacterium with a modified Tn*5*-RL27 transposon (Larsen et al., 2002; Oh et al., 2010) has been initiated. To date, the Wall lab has 8,869 *D. vulgaris* mutants in which the insertion site of the transposon has been identified by sequencing that can be seen on the following website http://desulfovibriomaps.biochem.missouri.edu/mutants/. Most mutants were selected on lactate (60 mM) plus sulfate (30 mM) medium supplemented with yeast extract to avoid loss of auxotrophs. The library currently has mutations in 2208 unique genes or 62% of the ca. 3500 genes predicted in the genome. Our assumption for interpreting these data was that if a gene were essential for this growth mode, no mutations would be found in the gene. Of course, essential genes not specific to lactate/sulfate growth would also be identified among those not mutated. Conversely, genes actually needed, but whose loss could be compensated by expression of others, would likely be found to be mutated. As yet the library is not saturating for non-essential genes and the data must be interpreted with that caveat in mind.

Figure 2 provides two examples of the transposon mutant analysis. The enzymes for sulfate reduction have been biochemically confirmed (Peck and LeGall, 1994) and, as a result, the gene annotations are firm (**Table 1A**). There are apparently single copies of these genes in the genome and we would not expect mutations to be found in cells growing by sulfate respiration. In **Figure 2A**, a section of the genome with the genes for the bisulfite reductase is illustrated with the insertion sites of the transposon indicated. There are no mutations in *dsrABD* while the flanking genes were successfully mutated. In the second example (**Figure 2B**), the genes putatively encoding the cytoplasmic hydrogenase associated with carbon monoxide dehydrogenase, *cooMKLXUH*, also lack insertions of the transposon, a result not entirely expected. This is a region is about 8.2 kb. With 8869 transposon insertions, on average we should expect an insertion about every 425 bp (with the conservative assumption that the entire genome is an appropriate target). Interestingly the region in which transposon mutations have not been recovered is precisely congruent with the Coo hydrogenase operon. It is probable that this region is needed for growth on lactate/sulfate or to survive the manipulations of the mutagenesis process.

INFLUENCE OF GROWTH CONDITIONS ON THE EXPRESSION OF GENES

SULFATE UTILIZATION GENES

The molecular information about genes potentially involved in lactate/sulfate growth of *D. vulgaris* – differential expression in defined culture conditions, relative abundance of mRNA and essentiality during growth with lactate/sulfate – are considered for the different categories of functions (**Table 1**). First, the genes known to encode APS reductase (*apsBA*) and bisulfite reductase (*dsrABD*), tended to decrease in expression in stationary phase cells limited for electron donor where growth rate was decreasing (**Table 1A**). The expression levels of *apsBA* were also decreased when thiosulfate replaced sulfate. This result might be predicted since the substrate for the APS reductase was absent. Also as expected, *dsrABD* mRNA did not decrease with thiosulfate, since the initial two electron reduction of thiosulfate generates sulfide and bisulfite (Thauer et al., 2007). Measurements of the dissimilatory bisulfite reductase genes in *Desulfobacterium autotrophicum* grown in lactate/sulfate compared to lactate/thiosulfate (lactate limiting in both media) showed that early exponential phase expression of the *dsrAB* genes with sulfate was slightly higher than that observed with bisulfite (Neretin et al., 2003). As these *D. autotrophicum* cells entered stationary phase, the *dsrAB* expression in bisulfite medium exceeded that with sulfate. Major changes were not seen in the production of *dsrAB* transcripts in *D. vulgaris* with alternative electron acceptors consistent with the report of constitutive expression of these genes (Brusseau, 1998, as reported in Neretin et al., 2003).

Neither *apsBA* nor *dsrABD* was responsive to the change in electron donor from lactate to pyruvate. The predictions of abundant mRNAs for these genes (**Table 1A**) and the absence of transposon mutations in the library (**Figure 2A**) were accurate and serve as the proof of principle for the use of these features as predictive measures. The transcript abundances for these genes were among the top 1% of all *D. vulgaris* genes.

For the highly expressed genes encoding sulfate adenylyltransferase and pyrophosphatase, *sat* and *ppaC*, the microarray data showed that transcription decreased with thiosulfate as terminal electron acceptor (**Table 1A**). Because these enzymes function primarily for sulfate utilization, the mRNA decrease for the encoding genes might reflect a control by sulfate concentrations. No transposon mutations in these genes were isolated from cells grown on lactate/sulfate medium consistent with an essential function.

Because sulfate carries two charges at physiological pHs, transport functions would be expected. However, all growth conditions from which molecular and genetic information were obtained had plentiful sulfate, where electroneutral uptake with two protons might be expected (Cypionka, 1995). Three candidate sulfate permease genes were annotated, but no single one was apparently essential since transposon mutants lacking each were recovered (**Table 1C**). The abundance level of the mRNA of each was near that of the average for *D. vulgaris* genes. Microarray changes also did not indicate a unique ortholog among the genes, although DVU0279 was strongly decreased in expression in stationary phase when carbon and electron flow was limited.

CANDIDATE GENES FOR LACTATE METABOLISM

For genes encoding possible enzymes for lactate transport and oxidation, the story is not clear. While some biochemical analysis for lactate dehydrogenase has been accomplished (Odom and Peck, 1981b; Ogata et al., 1981; Stams and Hansen, 1982), the genes encoding the enzyme(s) responsible for either oxidation or transport have not been identified. Of the six genes annotated as putative lactate permeases, only two showed increases in transcription as the cells were being limited for carbon, DVU2110 and DVU3284. Neither of these was essential alone since mutations were found in each in lactate/sulfate grown cells and the mRNA abundance of both was well below average (**Table 1C**). The two most highly transcribed orthologs were still only 1.6–1.7 times the average gene in expression.

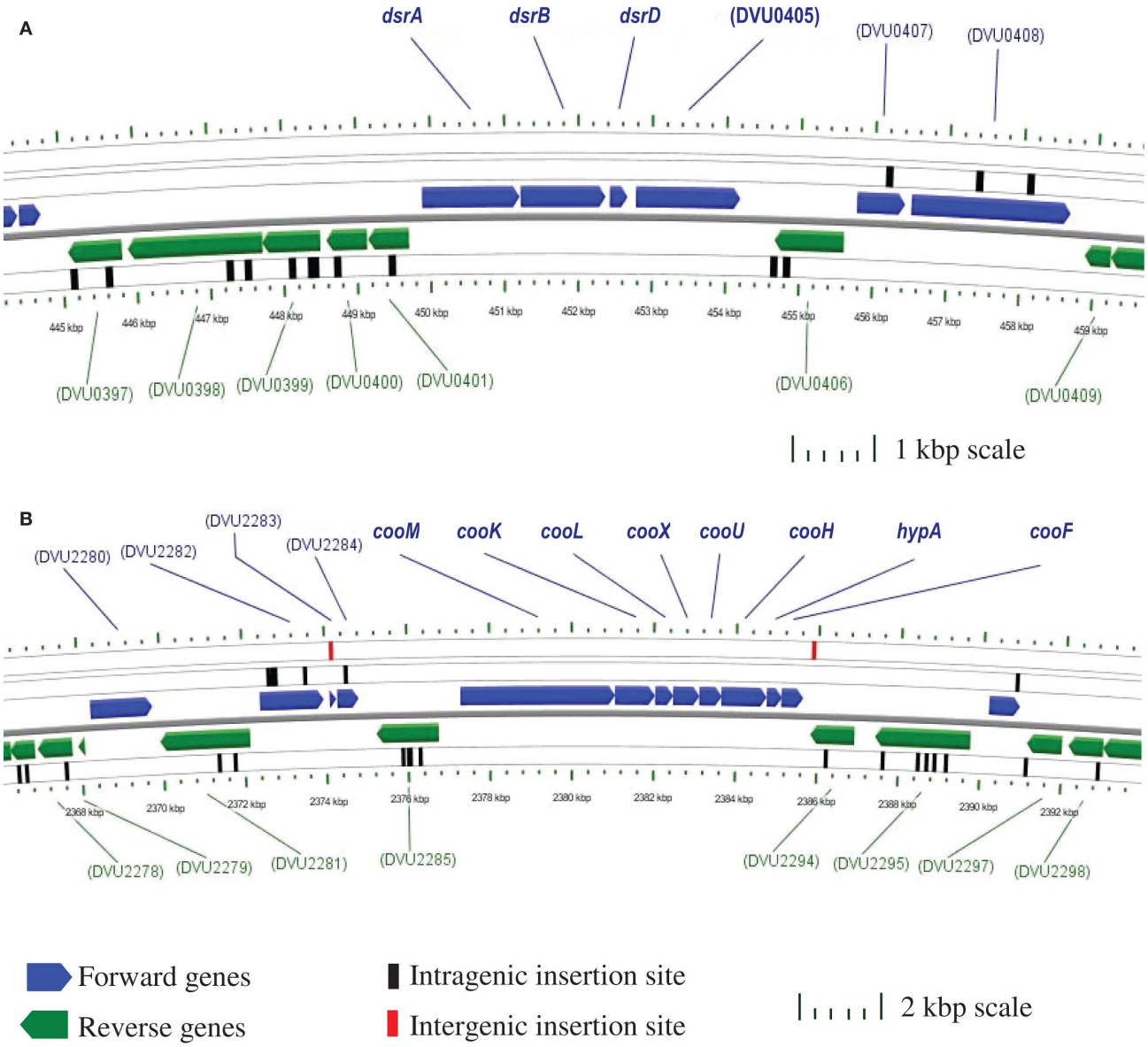

FIGURE 2 | Chromosomal maps generated with CGView (Stothard and Wishart, 2004) indicating the location of transposon insertions in the *Desulfovibrio vulgaris* Hildenborough genome. Open reading frames are designated by TIGR DVU numbers. **(A)** No intragenic transposons are within the 4.2 kb four gene dissimilatory bisulfite reductase (*dsr*) operon; however within the 5 kb regions flanking the operon there are 14 intragenic insertions. **(B)** No intragenic transposons are within the 8.2 kb eight gene putative CO-induced membrane-bound hydrogenase (*coo*) operon. Also, there are 21 intragenic transposon insertions within the 10 kb regions up- and down-stream of the operon, as well as two intergenic transposon insertions.

The number of candidate genes encoding the lactate dehydrogenase (LDH) activities that have been annotated is about nine (**Table 1B**), including those annotated as glycolate oxidases. Because many *Desulfovibrio* strains can readily use both L- and D-lactate (Stams and Hansen, 1982), at least two enzymes would seem to be necessary. Biochemical analysis of the LDHs showed that all are membrane-bound and NAD(P)$^+$-independent (Hansen, 1994b). However, the L- and D-LDH differ in their sensitivity to oxygen with the L-LDH from *Desulfovibrio baculatus* HL21 DSM 2555 (formerly, *Desulfovibrio desulfuricans* HL21) being extremely unstable (Stams and Hansen, 1982; Hansen, 1994a); whereas, the D-LDH from *D. vulgaris* Miyazaki is apparently much more stable when exposed to oxygen (Ogata et al., 1981).

Of the nine *ldh* orthologs and paralogs in *D. vulgaris*, none was increased in response to a change in electron donor from lactate to pyruvate (**Table 1B**). Genes for three enzymes were increased from 2.1 to 2.6 fold upon entering stationary phase presumably because of carbon and electron donor limitation, DVU0600, DVU1783, and the complex DVU3027–3028. Of the three, only the latter complex had more abundant transcripts than the average gene.

This complex is also part of a nine gene operon that includes *por,* encoding the primary pyruvate:ferredoxin oxidoreductase; *pta*, phosphotransacetylase; and *ackA*, the acetate kinase; and is preceded by a gene annotated as a lactate permease, DVU3026. Interestingly, *por*, *pta*, and *ackA* have not been mutated by the insertion of the transposon; whereas, seven transposon insertion sites have been identified within the coding sequences of the putative permease and lactate dehydrogenase, DVU3026, 3027, and 3028. We suggest that the transposon data mean that these genes are either not involved in lactate metabolism or that there are other enzymes able to compensate for the mutations in these genes.

TRANSMEMBRANE COMPLEX OPERONS

The genes encoding the transmembrane electron transport complexes (TMC) that are proposed to function with APS reductase and bisulfite reductase are *qmoABC* and *dsrMKJOP*, respectively (**Table 1D**; Matias et al., 2005; Pereira et al. (2007)). They are strictly conserved among sulfate reducers, underscoring their importance for sulfate reduction. The assignment of QmoABC and DsrMKJOP as electron carriers to their respective reductases also receives support from the location of their encoding genes (Pereira et al., 2007). *qmoABC* are immediately adjacent to and downstream of *apsBA*. Although the *dsrMKJOP* operon is not in the proximity of the structural genes for bisulfite reductase in *D. vulgaris*, it is contiguous with orthologs of the structural genes in the sulfur oxidizer, *Allochromatium vinosum* (Dahl et al., 2005). The genes for both of these TMCs were down regulated when *D. vulgaris* entered stationary growth phase caused by electron donor limitation (**Table 1D**), as suggested for genes encoding functions involved in energy generation. Curiously both are also decreased in expression when thiosulfate replaced sulfate as terminal electron acceptor, even though DsrMKJOP would be predicted to be essential for thiosulfate use (Thauer et al., 2007). A change in electron donor did not appear to impact the transcription of the genes for either of the TMCs importantly. The relative mRNA abundances for these genes were among the top 20% of all genes in the bacterium and no transposon mutants were identified, supporting the supposition that their function is essential for growth on lactate plus sulfate.

A deletion of the *qmoABC*-DVU0851 was recently constructed by marker exchange mutagenesis in *D. vulgaris* (Zane et al., 2010). This mutant confirmed the essential role of the encoded complex in sulfate reduction. The deletion mutant was unable to grow with sulfate as terminal electron acceptor with any electron donor including H_2 or formate, although growth with sulfite or thiosulfate was unimpaired. The hypothetical gene, DVU0851, was shown not to be necessary for sulfate reduction. Interestingly no other TMC of *D. vulgaris* was able to compensate for the loss of QmoABC.

Recently an additional four protein transmembrane complex, QrcDCBA or Type 1 cytochrome c_3:menaquinone oxidoreductase, has been proposed to be essential to carry electrons coming from H_2 or formate to the cytoplasmic membrane for delivery to APS reductase in *D. vulgaris* (Venceslau et al., 2010). The Qrc complex was suggested to be necessary because the QmoABC complex apparently has no periplasmic interface that would allow electrons from the soluble cytochrome *c* matrix to traverse the membrane to reach the sulfate-reducing enzymes. Curiously 10 of 12 fully sequenced *Desulfovibrio* strains have highly conserved *qrc* operons[2]; however, *D. desulfuricans* ATCC 27774 and *Desulfovibrio piger* do not. Because these two species still have a conserved Qmo complex, another complex may be needed to serve the Qrc function of delivery of periplasmic electrons to the membrane for sulfate reduction (Venceslau et al., 2010).

A transposon mutation in the *D. alaskensis* G20 gene Dde_2933 corresponding to *qrcB*, was unable to grow with H_2 or formate as electron donor (Li et al., 2009). In *D. vulgaris*, QrcDCBA was also decreased in expression during stationary phase when energy generation was decreased (**Table 1D**) and was found to have above average transcript abundance. Surprisingly, transposon insertions in the genes for this complex were isolated in cells growing on lactate plus sulfate, showing that either this complex was not required for electrons from all donors or that compensation for this complex was possible.

A deletion of DVU0692–0694, Δ*qrcBCD*, has been constructed in *D. vulgaris* (Wall lab, unpublished). Preliminary experiments showed that this mutant was capable of growing on lactate plus sulfate but the rate was slower and the yield was about 40% less than that of wild-type cells. As for the *D. alaskensis* G20 mutant, the *D. vulgaris* deletion could not grow with H_2 or formate with sulfate as electron acceptor, consistent with the predicted role for this complex by Venceslau et al. (2010). A need for the Qrc complex should be bypassed if electrons from the periplasmic cytochrome pool could be transferred to bisulfite reductase through a cytochrome *c* containing complex. Because DsrJ of the DsrMKJOP complex is a periplasmic cytochrome *c* and the complex is predicted to be the electron conduit to bisulfite reductase, this complex would be predicted to be able to accept periplasmically generated electrons from H_2 or formate carried by the abundant Tp1-c_3. Sulfite does support growth of the *qrc* mutant on formate. The inability of the Δ*qmoABC* mutant to grow on lactate, H_2 or formate during sulfate respiration would suggest that the Qrc complex acts prior to Qmo. The possible role of QrcABCD must be further investigated.

Of the remaining TMCs characterized or recognized in the *D. vulgaris* genome, the High molecular weight cytochrome (Hmc) complex has been proposed by many researchers to be a conduit for electrons from H_2 to sulfate (Peck, 1993; Dolla et al., 2000; Pereira et al., 2007). A mutant deleted for *hmcBCDE* was impaired in syntrophic growth with *Methanococcus maripaludis* (Walker et al., 2009). The low level of transcript abundance for this complex during growth on lactate/sulfate (**Table 1D**) would not appear compatible with a primary role for Hmc for energy conversion on these substrates. In addition, the presence of multiple transposon insertions within the Hmc coding sequences in the mutant library casts doubt on its importance. The inference that a functional Hmc is not essential for *D. vulgaris* in lactate plus sulfate medium is consistent with monoculture growth, albeit slower, of the deletion mutant (Dolla et al., 2000; Walker et al., 2009). These observations support a role for this TMC when H_2 must be maintained at a low level.

A role for the decaheme cytochrome *c* and the RnfCDGEAB complex in *Desulfovibrio* has not been established. This complex was first identified in *Rhodobacter capsulatus* as complex required

for nitrogen fixation (Schmehl et al., 1993). It is also in the family of electron bifurcating flavoproteins that are NADH ferredoxin oxidoreductases (Herrmann et al., 2008).Transcript changes and abundances were not particularly informative. However, several transposon mutations have been identified in the encoding genes indicating that the complex is not essential to *D. vulgaris* cells growing on lactate plus sulfate. A deletion of *rnfC* constructed by marker replacement confirmed a role for this complex in the ability of *D. vulgaris* to grow with molecular nitrogen as the sole nitrogen source (Wall lab, unpublished).

Finally, *tmcABCD* and *ohcABC* (Pereira et al., 2007) have been identified as encoding TMCs but a role for each is not yet known. The *tmc* genes are expressed at about the same level as the *dsrMKJOP* operon suggesting a role in the metabolism (**Table 1D**), but preliminary characterization of a mutant deleted for the genes had no apparent phenotype (Wall lab, unpublished). This was consistent with finding transposon mutations within the structural genes for the complex. In contrast, *ohcABC* transcripts were in the lower 15% abundance of all *D. vulgaris* genes, perhaps indicating a non-critical role in energy metabolism in cells growing with lactate plus sulfate.

HYDROGENASE OPERONS

The presence and activity of cytoplasmic hydrogenases were predicted to be necessary for energy augmentation by hydrogen cycling in sulfate reducers (Odom and Peck, 1981a). Although the distribution of cytoplasmic hydrogenases in *Desulfovibrio* strains is not conserved, there are candidate enzymes that could function in most cases. *D. vulgaris* has two putative energy-converting hydrogenases with subunits related to the proton-pumping NADH:ubiquinone oxidoreductase (complex I), Ech hydrogenase (Friedrich and Scheide, 2000) and the Coo hydrogenase, CooH, originally described in *Rhodospirillum rubrum* (Kerby et al., 1992). These enzyme complexes are reversible, oxidizing reduced ferredoxin with the production of H_2 while generating an electrochemical proton potential or using reversed electron transport to catalyze reduced ferredoxin from H_2 (Thauer et al., 2007). These complexes are encoded in DVU0429–0434 and DVU2286–2293, respectively (**Table 1F**). Transcription expression changes were not dramatic for these complexes, but the transcript abundance difference between the two was striking. The *cooMKLZUHhypAcooF* operon is among the top 15% of expressed genes; whereas, the *echABCDEF* operon is well below average in expression. As seen earlier in **Figure 1**, mutations in this *coo* operon were not recovered in cells grown with lactate/sulfate, suggesting that this cytoplasmic hydrogenase is needed for this growth mode. It should be noted that the putative structural genes for the CO dehydrogenase enzyme, *cooSC,* were found to carry transposon insertions, as did the *ech* operon.

Through examination of a mutation in *cooL,* the Coo hydrogenase has also been shown to be essential for syntrophic growth of *D. vulgaris* with *Methanococcus* on lactate but not pyruvate (Walker et al., 2009). However, there was no requirement for this hydrogenase for respiration of lactate with sulfate. This observation is curiously in conflict with the absence of transposon mutations in these genes when selection was carried out on lactate/sulfate medium. Interestingly, Coo hydrogenase belongs to a family of transmembrane complexes that function as proton (or sodium) – translocating hydrogenases and that use reduced ferredoxin as electron donors (Welte et al., 2010; **Figure 1**). The recently proposed mechanism of flavin-based electron bifurcation (Herrmann et al., 2008) could offer a possible solution to the necessity of lactate supported hydrogen production. This mechanism would suggest that, when concentrations of H_2 are maintained at very low levels, the exergonic reduction of protons to form H_2 from the reduced ferredoxin ($E^{0\prime} \leq 420$ mV) could be coupled with the endergonic formation of hydrogen with electrons from menaquinone ($E^{0\prime}$ -75 mV). The Coo membrane-bound hydrogenase complex is a flavoprotein potentially allowing bifurcation of electrons from the two sources, reduced ferredoxin and menaquinone. While the energy available for pumping a proton (or sodium ion) might be dissipated through the bifurcation, the overall contribution to the proton gradient from the oxidation of the additional H_2 might compensate. This model (**Figure 1**) would also provide an explanation for the cessation of electron flow in this pathway as hydrogen concentrations increased. Currently no experiments have been conducted to explore electron bifurcation function during lactate oxidation and sulfate reduction in *Desulfovibrio*.

While the four periplasmic hydrogenases have been well characterized (Fontecilla-Camps et al., 1997; Vignais and Billoud, 2007), no single enzyme has been shown to be essential for uptake or production of H_2 (Casalot et al., 2002; Caffrey et al., 2007). While the transcript abundance of the [NiFeSe] hydrogenase appears to be the highest of the four, this may reflect the inclusion of selenium in the medium trace elements which strongly increases the production of the [NiFeSe] hydrogenase while repressing the [FeFe] and [NiFe]-1 hydrogenases (Valente et al., 2006). Multiple deletions and various combinations will be needed to determine the roles of these enzymes.

GENES FOR *c*-TYPE CYTOCHROMES

Of the annotated *c*-type cytochromes that are not apparently associated with large TMCs, the Type I tetraheme cytochrome c_3 (Tp1-c_3, DVU3171) and the monoheme c_{553} cytochrome (DVU1817) have highly abundant transcripts (**Table 1H**) suggesting a major role in electron flow during energy conversion. The high expression levels are congruent with the abundance of the cytochromes as well (Moura et al., 1991; Pollock and Voordouw, 1994; Aubert et al., 1998). Tp1-c_3 has been suggested to be the electron acceptor for each of the periplasmic hydrogenases and to serve as a capacitor for electrons in the periplasm of the SRM (Heidelberg et al., 2004). Interestingly, there is little expression modulation of the gene encoding, Tp1-c_3, *cycA*, upon entry into stationary phase or in response to altered electron acceptors or donors as has previously been reported (Payne et al., 2002). No transposon mutations have been recovered that would eliminate Tp1-c_3, although the small size of *cycA* may be a factor in mutant isolation. However, the successful construction of a marker exchange deletion of the encoding gene (Semkiw et al., 2010), showed that Tp1-c_3 is not essential for growth on lactate/sulfate. Similar mutants have been generated in *D. alaskensis* G20 (Rapp-Giles et al., 2000; Li et al., 2009). The *D. vulgaris* Δ*cycA* mutant was unable to grow

with H_2 or formate with sulfate or sulfite as electron acceptor (Semkiw et al., 2010). Growth was slowed with lactate plus sulfate or sulfite but the biomass produced was not different from wild-type. For cells growing with sulfate respiration, the observations mirror those for the Δ*qrc* mutant of this bacterium or transposon interruptions in the homologs found in *D. alaskensis* G20 (Li et al., 2009). These results suggest a pathway for periplasmically generated electrons through Tp1-c_3 and the Qrc complex to the Qmo. Whether both the cytochrome and the Qrc complex are needed to transfer electrons for bisulfite reduction remains to be established.

The gene for the abundant cytochrome c_{553} (*cyf*, DVU1817) is located just upstream of the cytochrome *c* oxidase, a putative heme-copper oxygen reductase. It has been suggested that the cytochrome c_{553} might serve as an electron donor to that membrane-bound complex (Dolla et al., 2007). No major differences in expression were apparent in the microarray data. It might be predicted that constitutive expression could be advantageous if this cytochrome plays a role in oxygen protection. A deletion of *cyf* grew well on lactate plus sulfate (Wall lab, unpublished) confirming that this cytochrome is not a key electron carrier for energy conversion under these conditions. A possible role in oxygen tolerance will require further experimentation.

The function of other *c*-type cytochromes is still undetermined and will likely require multiple deletions and biochemical analysis to gain insight. The lack of transposon mutations in a number of the encoding genes may simply reflect the small size of the genes and the lack of saturation in the library of mutants.

SUMMARY OF KEY OBSERVATIONS FROM TRANSCRIPTS AND MUTANTS

In summary, the data in **Table 1** show that the transcriptional changes in the microarray data suggest that genes for both sulfate and sulfite reduction are not constitutively expressed but respond to the energy demands of the cell, decreasing in expression in stationary phase and when thiosulfate is provided as electron acceptor. The operons for the proposed transmembrane complexes for donating electrons to APS reductase and that for bisulfite reductase were similarly decreased under these conditions; whereas, operons for other putative transmembrane complexes were not uniformly changed in transcription in these conditions. The genes and operons for sulfate and sulfite reduction were among the most highly transcribed genes in the cells and, as would be predicted while growing with lactate plus sulfate, transposon insertions in these genes were not recovered. Transposons were recovered in almost all other operons and genes listed with the interesting exception of the Coo hydrogenase complex which showed a surprisingly low number of insertions. This complex has been shown not to be essential for growth on lactate plus sulfate but it appears to be needed for syntrophic growth with *Methanococcus maripaludis* with lactate as sole source of carbon and reductant (Walker et al., 2009 and for the efficient recovery of transposon mutants. Because this complex is a member of the energy-converting [NiFe] hydrogenases (Hedderich, 2004), it is predicted that this complex is integral to the energy budget at some stage of culturing for single colony formation on medium with lactate as electron donor and sulfate as electron acceptor.

MUTAGENESIS TOOL DEVELOPED FOR *DESULFOVIBRIO*

Important information about electron carriers has been gained from constructed deletions and from transposon insertions. However, the genes encoding a number of the enzymes believed to be needed for electron flow in *D. vulgaris* have not been specifically identified in part because multiple ORFs have been similarly annotated. Examples include the periplasmic hydrogenases, formate dehydrogenases, lactate permeases, lactate dehydrogenases, and others. When multiple genes encode isozymes, the loss of one enzyme by mutation of its encoding gene may be compensated by others. This compensation or suppression could explain why transposon mutations are observed in genes for what would be predicted to be key enzymes (**Table 1**). To elucidate the function of individual members of protein families, multiple genes will likely need to be eliminated simultaneously. Until recently, the number of sequential deletions in the same strain of *D. vulgaris* was limited by the number of reliable antibiotic resistant markers available to use for marker exchange deletion construction. A markerless deletion system has now been developed based on the counterselection of the gene for uracil phosphoribosyltransferase, *upp*, by resistance to the toxic uracil analog 5-fluorouracil (Keller et al., 2009). This method allows the generation of in-frame deletions without a residual antibiotic resistance gene. The application of this technique may contribute critical information about any unique roles of the four periplasmic hydrogenases. The flexible electron flow pathways and mechanisms of energy conversion in *D. vulgaris* will require the combined application of genetic, biochemical and systems biology approaches.

MODEL OF ELECTRON TRANSPORT FOR *D. VULGARIS* HILDENBOROUGH

To provide a framework for organizing the information obtained to date for electron flow from lactate to sulfate, a model is presented in **Figure 1**. This scheme draws heavily from the models presented by Noguera et al. (1998) and Walker et al. (2009) and is driven by the observations of two proteins putatively involved in the electron pathways, the Tp1-c_3 and the Coo hydrogenase. First, the phenotype of a deletion of the *cycA* gene encoding the Tp1-c_3 indicates that electrons from periplasmic H_2 (or formate) are exclusively dependent on this cytochrome for reaching sulfate. Thus the ability of the Δ*cycA* mutant to grow on organic acids with sulfate and produce sulfide means that some proportion of the electrons generated from substrate oxidation must not cycle as molecular H_2. Thus the hydrogen cycling hypothesis may contribute but is not essential to the energy budget of SRM grown with organic acids. Second, a mutant in the Coo hydrogenase complex *cooL*::Tn*5*-RL27 was unable to grow by syntrophy with a methanogen on lactate but could grow in monoculture with lactate plus sulfate (Walker et al., 2009). An interpretation of these observations is that the mutation in the Coo hydrogenase complex prevented H_2 generation from lactate but did not block electron flow to sulfate. With pyruvate as electron donor, syntrophy was established as well as growth of monocultures (Walker et al., 2009). Thus a path for H_2 production is available for electrons from pyruvate that is not available to electrons from lactate. In addition, the apparent lack of recovery of transposon mutations in the *cooMKLXUHhypAcooF* genes in the recently generated library, points to Coo hydrogenase

as potentially important, but not necessarily essential, player in electron flow from lactate to sulfate.

The model accommodates these seemingly contradictory observations by suggesting two pathways for the electrons from lactate (**Figure 1A and B**) and from pyruvate (**Figure 1C, and D**). In each case, one pathway has the potential for transfer of electrons into the menaquinone pool for delivery to the membrane associated complex, Qmo, that is dedicated for the first step in sulfate reduction (pathways A and D). Whereas the DsrMKJOP complex is thought to be the transmembrane complex for electron donation to bisulfite reductase, it may also receive electrons directly from the menaquinone pool. The second path in each case, B and C, provides a route for the electrons to generate H_2. The model is already too simple for electron flow from pyruvate since H_2 generation in the absence of a functional Coo hydrogenase is documented (Walker et al., 2009). The question marks in the model indicate the components that have a high uncertainty, including the membrane associated component(s) accepting electrons from pyruvate oxidation.

A future effort will be to determine the gatekeepers for directing electrons into one path or another. Will this be just the availability of acceptors or will the rate of flux through the pathways determine the choices? The complexity of this simple system continues to impress. It is already evident that there will not be a single wiring circuit for electron flow from these substrates in the SRM as it does not extend to the physiologically similar *D. alaskensis* G20 strain that lacks orthologs encoding the cytoplasmic hydrogenases of *D. vulgaris*.

ACKNOWLEDGMENTS

This work, conducted by ENIGMA, was supported by the Office of Science, Office of Biological and Environmental Research, of the US Department of Energy under Contract No. DE-AC02-05CH11231. A portion of the work was supported by the Office of Science, Office of Biological and Environmental Research, Genomics Program:GTL BioHydrogen Production and BioEthanol contract DE-FG02-083464691. In addition, some of this work was supported as part of the Virtual Institute for Microbial Stress and Survival (http://VIMSS.lbl.gov) supported by the US Department of Energy, Office of Science, Office of Biological and Environmental Research, Genomics Program:GTL through contract DE-AC02-05CH11231 between Lawrence Berkeley National Laboratory and the US Department of Energy. We thank Barbara J. Rapp-Giles, Elizabeth S. Semkiw, and Grant M. Zane from the Wall lab for graciously sharing their unpublished data and Adam Deutschbauer and Jennifer Kuehl for their contributions to the transposon library.

REFERENCES

Aubert, C., Leroy, G., Bianco, P., Forest, E., Bruschi, M., and Dolla, A. (1998). Characterization of the cytochromes *c* from *Desulfovibrio desulfuricans* G201. *Biochem. Biophys. Res. Commun.* 242, 213–218.

Bender, K. S., Yen, H.-C. B., Hemme, C. L., Yang, Z., He, Z., He, Q., Zhou, J., Huang, K. H., Alm, E. J., Hazen, T. C., Arkin, A. P., and Wall, J. D. (2007). Analysis of a ferric uptake regulator (fur) mutant of *Desulfovibrio vulgaris* Hildenborough. *Appl. Enivron. Microbiol.* 73, 5389–5400.

Brusseau, G. A. (1998). *The Role of Syntrophy in the Expression of key Metabolic Enzymes in Sulfate-Reducing Bacteria.* Ph.D. dissertation, Northwestern University, Evanston, IL.

Butlin, K. R., Adams, M. E., and Thomas, M. (1949). The isolation and cultivation of *sulphate*-reducing bacteria. *J. Gen. Microbiol.* 3, 46–59.

Caffrey, S. M., Park, H. S., Voordouw, J. K., He, Z., Zhou, J., and Voordouw, G. (2007). Function of periplasmic hydrogenases in the sulfate-reducing bacterium *Desulfovibrio vulgaris* Hildenborough. *J. Bacteriol.* 189, 6159–6167.

Caffrey, S. M., and Voordouw, G. (2010). Effect of sulfide on growth physiology and gene expression of *Desulfovibrio vulgaris* Hildenborough. *Antonie van Leeuwenhoek* 97, 11–20.

Casalot, L., Valette, O., De Luca, G., Dermoun, Z., Rousset, M., and de Philip, P. (2002). Construction and physiological studies of hydrogenase depleted mutants of *Desulfovibrio fructosovorans*. *FEMS Microbiol. Lett.* 214, 107–112.

Clark, M. E., He, Q., He, Z., Huang, K. H., Alm, E. J., Wan, X. F., Hazen, T. C., Arkin, A. P., Wall, J. D., Zhou, J. Z., and Fields, M.W. (2006). Temporal transcriptomic analysis as *Desulfovibrio vulgaris* Hildenborough transitions into stationary phase during electron donor depletion. *Appl. Environ. Microbiol.* 72, 5578–5588.

Cypionka, H. (1995). "Solute transport and cell energetic," in *Sulfate-Reducing Bacteria*, ed. L. L. Barton (New York, NY: Plenum Press), 151–184.

Dahl, C., Engels, S., Pott-Sperling, A. S., Schulte, A., Sander, J., Lübbe, Y., Deuster, O., and Brune, D. C. (2005). Novel genes of the *dsr* gene cluster and evidence for close interaction of Dsr proteins during sulfur oxidation in the phototrophic sulfur bacterium *Allochromatium vinosum*. *J. Bacteriol.* 187, 1392–1404.

Dehal, P. S., Joachimiak, M. P., Price, M. N., Bates, J. T., Baumohl, J. K., Chivian, D., Friedland, G. D., Huang, K. H., Keller, K., Novichkov, P. S., Dubchak, I. L., Alm, E. J., and Arkin, A. P. (2010). MicrobesOnline: an integrated portal for comparative and functional genomics. *Nucleic Acids Res.* 38(Suppl. 1), D396–D400.

Dolla, A., Kurtz, D. M Jr., Teixeira, M., and Voordouw, G. (2007). "Biochemical, proteomic and genetic characterization of oxygen survival mechanisms in *sulphate*-reducing bacteria of the genus Desulfovibrio," in *Sulphate-Reducing Bacteria: Environmental and Engineered Systems*, eds L. L. Barton and W. A. Hamilton (Cambridge: Cambridge University Press), 185–213.

Dolla, A., Pohorelic, B. K., Voordouw, J. K., and Voordouw, G. (2000). Deletion of the hmc operon of *Desulfovibrio vulgaris* subsp. *vulgaris* Hildenborough hampers hydrogen metabolism and low-redox-potential niche establishment. *Arch. Microbiol.* 174, 143–151.

Dong, J. M., Taylor, J. S., Latour, D. J., Iuchi, S., and Lin, E. C. C. (1993). Three overlapping *ict* genes involved in L-lactate utilization by *Escherichia coli*. *J. Bacteriol.* 175, 6671–6678.

Fontecilla-Camps, J. C., Frey, M., Garcin, E., Hatchikian, C., Montet, Y., Piras, C., Vernède, X., and Volbeda, A. (1997). Hydrogenase: a hydrogen-metabolizing enzyme. What do the crystal structures tell us about its mode of action? *Biochimie* 79, 661–666.

Friedrich, T., and Scheide, D. (2000). The respiratory complex I of bacteria, archaea and eukarya and its module common with membrane-bound multisubunit hydrogenases. *FEBS Lett.* 479, 1–5.

Fu, R., and Voordouw, G. (1997). Targeted gene-replacement mutagenesis of *dcrA*, encoding an oxygen sensor of the sulfate-reducing bacterium *Desulfovibrio vulgaris* Hildenborough. *Microbiology* 143, 1815–1826.

Garczarek, F., Dong, M., Typke, D., Witkowska, H. E., Hazen, T. C., Nogales, E., Biggin, M. D., and Glaeser, R. M. (2007). Octomeric pyruvate:ferredoxin oxidoreductase from *Desulfovibrio vulgaris*. *J. Struct. Biol.* 159, 9–18.

Groh, J. L., Luo, Q., Ballard, J. D., and Krumholz, L. R. (2005). A method adapting microarray technology for signature-tagged mutagenesis of *Desulfovibrio desulfuricans* G20 and *Shewanella oneidensis* MR-1 in anaerobic sediment survival experiments. *Appl. Environ. Microbiol.* 71, 7064–7074.

Hansen, T. A. (1994a). Metabolism of sulfate-reducing prokaryotes. *Antonie Van Leeuwenhoek* 66, 165–185.

Hansen, T. A. (1994b). "NAD(P)-independent lactate dehydrogenase from sulfate-reducing prokaryotes," in *Methods in Enzymology: Inorganic Microbial Sulfur Metabolism*, eds H. D. Peck Jr. and J. LeGall (New York: Academic Press), 21–23.

Hauser, L. J., Land, M. L., Brown, S. D., Larimer, F., Keller, K. L., Rapp-Giles, B. J., Price, M. N., Lin, M., Bruce, D. C., Detter, J. C., Tapia, R., Han, C. S., Goodwin, L. A., Cheng, J.-F., Pitluck, S., Copeland, A., Lucas, S., Nolan, M.,. Lapidus, A. L, Palumbo, A. V., and Wall, J. D. (2011). The complete genome sequence and updated annotation of *Desulfovibrio alaskensis* G20. *J. Bacteriol.* doi: 10.1128/JB.05400–11. [Epub ahead of print].

He, Z., Zhou, A., Baidoo, E., He, Q., Joachimiak, M. P., Benke, P., Phan, R., Mukhopadhyay, A., Hemme, C. L., Huang, K., Alm, E. J., Fields, M. W., Wall, J., Stahl, D., Hazen, T. C., Keasling, J. D., Arkin, A. P., and Zhou, J. (2010). Global transcriptional, physiological, and metabolite analyses of the responses of *Desulfovibrio vulgaris* Hildenborough to salt adaptation. *Appl. Environ. Microbiol.* 76, 1574–1586.

Hedderich, R. (2004). Energy-converting [NiFe] hydrogenases from Archaea and extremophiles: ancestors of complex I. *J. Bioenerg. Biomembr.* 36, 65–75.

Heidelberg, J. F., Seshadri, R., Haveman, S. A., Hemme, C. L., Paulsen, I. T., Kolonay, J. F., Eisen, J. A., Ward, N., Methe, B., Brinkac, L. M., Daugherty, S. C., Deboy, R. T., Dodson, R. J., Durkin, A. S., Madupu, R., Nelson, W. C., Sullivan, S. A., Fouts, D., Haft, D. H., Delengut, J., Peterson, J. D., Davidsen, T. M., Zafar, N., Zhou, L., Radune, D., Dimitrov, G., Hance, M., Tran, K., Khouri, H., Gill, J., Utterback, T. R., Feldblyum, T. V., Wall, J. D., Voordouw, G., and Fraser, C. M. (2004). The genome sequence of the anaerobic sulfate-reducing bacterium *Desulfovibrio vulgaris* Hildenborough. *Nat. Biotechnol.* 22, 554–559.

Herrmann, G., Jayamani, E., Mai, G., and Buckel, W. (2008). Energy conservation via electron-transferring flavoprotein in anaerobic bacteria. *J. Bacteriol.* 190,784–791.

Hooper, A. B., and DiSpirito, A. A. (1985). In bacteria which grow on simple reductants, generation of a proton gradient involves extracytoplasmic oxidation of substrate. *Microbiol. Rev.* 49, 140–157.

Keller, K. L., Bender, K. S., and Wall, J. D. (2009). Development of a markerless genetic exchange system in *Desulfovibrio vulgaris* Hildenborough and its use in generating a strain with increased transformation efficiency. *Appl. Environ. Microbiol.* 75, 7682–7691.

Kerby, R. L., Hong, S. S., Ensign, S. A., Coppoc, L. J., Ludden, P. W., and Roberts, G. P. (1992). Genetic and physiological characterization of the *Rhodospirillum rubrum* carbon monoxide dehydrogenase system. *J. Bacteriol.* 174, 5284–5294.

Kletzin, A., and Adams, M. W. (1996). Molecular and phylogenetic characterization of pyruvate and 2-ketoisovalerate ferredoxin oxidoreductases from *Pyrococcus furiosus* and pyruvate ferredoxin oxidoreductase from *Thermotoga maritima*. *J. Bacteriol.* 178, 248–257.

Larsen, R. A., Wilson, M. M., Guss, A. M., and Metcalf, W. W. (2002). Genetic analysis of pigment biosynthesis in *Xanthobacter autotrophicus* Py2 using a new, highly efficient transposon mutagenesis system that is functional in a wide variety of bacteria. *Arch. Microbiol.* 178, 193–201.

Li, X., Luo, Q., Wofford, N. Q., Keller, K. L., McInerney, M. J., Wall, J. D., and Krumholz, L. R. (2009). A molybdopterin oxidoreductase is involved in H_2 oxidation in *Desulfovibrio desulfuricans* G20. *J. Bacteriol.* 191, 2675–2682.

Lupton, F. S., Conrad, R., and Zeikus, J. G. (1984). Physiological function of hydrogen metabolism during growth of sulfidogenic bacteria on organic substrates. *J. Bacteriol.* 159, 843–849.

Marschall, C., Frenzel, P., and Cypionka, H. (1993). Influence of oxygen on sulfate reduction and growth of sulfate-reducing bacteria. *Arch. Microbiol.* 159, 168–173.

Matias, P. M., Pereira, I. A., Soares, C. M., and Carrondo, M. A. (2005). Sulphate respiration from hydrogen in *Desulfovibrio* bacteria: a structural biology overview. *Prog. Biophys. Mol. Biol.* 89, 292–329.

Moura, J. J., Costa, C., Liu, M. Y., Moura, I., and LeGall, J. (1991). Structural and functional approach toward a classification of the complex cytochrome c system found in sulfate-reducing bacteria. *Biochim. Biophys. Acta* 1058, 61–66.

Mukhopadhyay, A., He, Z., Alm, E. J., Arkin, A. P., Baidoo, E. E., Borglin, S. C., Chen, W., Hazen, T. C., He, Q., Holman, H. Y., Huang, K., Huang, R., Joyner, D. C., Katz, N., Keller, M., Oeller, P., Redding, A., Sun, J., Wall, J., Wei, J., Yang, Z., Yen, H. C., Zhou, J., and Keasling, J. D. (2006). Salt stress in *Desulfovibrio vulgaris* Hildenborough: an integrated genomics approach. *J. Bacteriol.* 188, 4068–4078.

Neretin, L. N., Schippers, A., Pernthaler, A., Hamann, K., Amann, R., and Jørgensen, B. B. (2003). Quantification of dissimilatory (bi)sulphite reductase gene expression in *Desulfobacterium autotrophicum* using real-time RT-PCR. *Environ. Microbiol.* 5, 660–671.

Noguera, D. R., Brusseau, G. A., Rittmann, B. E., and Stahl, D. A. (1998). A unified model describing the role of hydrogen in the growth of *Desulfovibrio vulgaris* under different environmental conditions. *Biotechnol. Bioeng.* 59, 732–746.

Odom, J. M., and Peck, H. D. Jr. (1981a). Hydrogen cycling as a general mechanism for energy coupling in the sulfate reducing bacteria, *Desulfovibrio* sp. *FEMS Microbiol. Lett.* 12, 47–50.

Odom, J. M., and Peck, H. D. Jr. (1981b). Localization of dehydrogenases, reductases, and electron transfer components in the sulfate-reducing bacterium *Desulfovibrio gigas*. *J. Bacteriol.* 147, 161–169.

Odom, J. M., and Wall, J. D. (1987). Properties of a hydrogen-inhibited mutant of *Desulfovibrio desulfuricans* ATCC 27774. *J. Bacteriol.* 169, 1335–1337.

Ogata, M., Arihara, K., and Yagi, T. (1981). D-lactate dehydrogenase of *Desulfovibrio vulgaris*. *J. Biochem.* 89, 1423–1431.

Oh, J., Fung, E., Price, M. N., Dehal, P. S., Davis, R.W., Giaever, G., Nislow, C., Arkin, A. P., Deutschbauer, A. (2010). A universal TagModule collection for parallel genetic analysis of microorganisms. *Nuc. Acids Res.* 38, e146.

Pankhania, I. P., Gow, L. A., and Hamilton, W. A. (1986). The effect of hydrogen on the growth of *Desulfovibrio vulgaris* Hildenborough on lactate. *J. Gen. Microbiol.* 132, 3349–3356.

Payne, R. B., Gentry, D. M., Rapp-Giles, B. J., Casalot, L., and Wall, J. D. (2002). Uranium reduction by *Desulfovibrio desulfuricans* strain G20 and a cytochrome c_3 mutant. *Appl. Environ. Microbiol.* 268, 3129–3132.

Peck, H. D. Jr. (1960). Evidence for oxidative phosphorylation during the reduction of sulfate with hydrogen by *Desulfovibrio desulfuricans*. *J. Biol. Chem.* 235, 2734–2738.

Peck, H. D. Jr. (1966). Phosphorylation coupled with electron transfer in extracts of the sulfate reducing bacterium, *Desulfovibrio gigas*. *Biochem. Biophys. Res. Comm.* 22, 112–118.

Peck, H. D. Jr. (1993). "Bioenergetics strategies of the sulfate-reducing bacteria," in *The Sulfate-Reducing Bacteria: Contemporary Perspectives*, eds J. M. Odom and R. Jr. Singleton (New York, NY: Springer), 41–76.

Peck, H. D. Jr., and LeGall, J. (1994). *Methods in Enzymology: Inorganic Microbial Sulfur Metabolism.* New York: Academic Press.

Peck, H. D. Jr., LeGall, J., Lespinat, P. A., Berlier, Y., and Fauque, G. (1987). A direct demonstration of hydrogen cycling by *Desulfovibrio vulgaris* employing membrane-inlet mass spectrometry. *FEMS Microbiol. Lett.* 40, 295–299.

Pereira, I. A. C., Haveman, S. A., and Voordouw, G. (2007). "Biochemical, genetic and genomic characterization of anaerobic electron transport pathways in sulphate-reducing "*Deltaproteobacteria*," in *Sulphate-Reducing Bacteria*, eds L. L. Barton and W. A. Hamilton (Cambridge: Cambridge University Press), 215–240.

Pereira, P. M., He, Q., Valente, F. M., Xavier, A. V., Zhou, J., Pereira, I. A., and Louro, R. O. (2008). Energy metabolism in *Desulfovibrio vulgaris* Hildenborough: insights from transcriptome analysis. *Antonie Van Leeuwenhoek* 93, 347–362.

Pollock, W. B., and Voordouw, G. (1994). Molecular biology of *c*-type cytochromes from *Desulfovibrio vulgaris* Hildenborough. Biochimie 76, 554–560.

Postgate, J. R. (1984a). *The Sulphate-Reducing Bacteria*, 2nd Edn. New York: Cambridge University Press.

Postgate, J. R. (1984b). "Genus *Desulfovibrio*," in *Bergey's Manual of Systematic Bacteriology*, eds N. R. Krieg and J. G. Holt (Baltimore, MD: Williams & Wilkins), 666–672.

Powell, B., Mergeay, M., and Christofi, N. (1989). Transfer of broad host-range plasmids to sulphate-reducing bacteria. *FEMS Microbiol. Lett.* 59, 269–273.

Rabus, R., Hansen, T. A., and Widdel, F. (2006). "Dissimilatory sulfate- and sulfur-reducing prokaryotes," in *The Prokaryotes*, eds M. Dworkin, S. Falkow, E. Rosenberg, K.-H. Schleifer, and E. Stackebrandt (New York, NY: Springer-Verlag), 659–768.

Rapp-Giles, B. J., Casalot, L., English, R. S., Ringbauer, J. A. Jr., Dolla, A., and Wall, J. D. (2000). Cytochrome c_3 mutants of *Desulfovibrio desulfuricans*. *Appl. Environ. Microbiol.* 66, 671–677.

Redding, A. M., Mukhopadhyay, A., Joyner, D. C., Hazen, T. C., and Keasling, J. D. (2006). Study of nitrate stress in *Desulfovibrio vulgaris* Hildenborough using iTRAQ proteomics. *Brief Funct. Genomic. Proteomic.* 2,133–143.

Reed, D. W., and Hartzell, P. L. (1999). The *Archaeoglobus fulgidus* D-lactate dehydrogenase is a Zn^{2+} flavoprotein. *J. Bacteriol.* 181, 7580–7587.

Rousset, M., Casalot, L., Rapp-Giles, B. J., Dermoun, Z., de Philip, P., Bélaich, J-P., and Wall, J. D. (1998). New shuttle vectors for the introduction of cloned DNA in *Desulfovibrio*. *Plasmid* 39, 114–122.

Rousset, M., Dermoun, Z., Chippaux, M., and Bélaich, J. P. (1991). Marker exchange mutagenesis of the *hydN* genes in *Desulfovibrio fructosovorans*. *Mol. Microbiol.* 7, 1735–1740.

Sass, H., and Cypionka, H. (2007). "Response of sulphate-reducing bacteria to oxygen," in *Sulphate-Reducing Bacteria*, eds L. L. Barton and W. A. Hamilton (Cambridge: Cambridge University Press), 167–183.

Schmehl, M., Jahn, A., Meyer zu Vilsendorf, A., Hennecke, S., Masepohl, B., Schuppler, M., Marxer, M., Oelze, J., and Klipp, W. (1993). Identification of a new class of nitrogen fixation genes in *Rhodobacter capsulatus*: a putative membrane complex involved in electron transport to nitrogenase. *Mol. Gen. Genet.* 241, 602–615.

Semkiw, E. S., Zane, G. M., and Wall, J. D. (2010). "The role of the type-1 tetraheme cytochrome c_3 in *Desulfovibrio vulgaris* Hildenborough metabolism (Abstract)," in *110th General Meeting of American Society For Microbiology*, San Diego, CA, K-773.

Stams, A. J. M., and Hansen, T. A. (1982). Oxygen-labile L(+) lactate dehydrogenase activity in *Desulfovibrio desulfuricans*. *FEMS Microbiol. Lett.* 13, 389–394.

Stothard, P., and Wishart, D. S. (2004). Circular genome visualization and exploration using CGView. *Bioinformatics* 21, 537–539.

Tang, Y., Pingitore, F., Mukhopadhyay, A., Phan, R., Hazen, T. C., and Keasling, J. D. (2007). Pathway confirmation and flux analysis of central metabolic pathways in *Desulfovibrio vulgaris* Hildenborough using gas chromatography-mass spectrometry and Fourier transform-ion cyclotron resonance mass spectrometry. *J. Bacteriol.* 189, 940–949.

Thauer, R. K. (1989). "Energy metabolism of sulfate-reducing bacteria," in *Autotrophic Bacteria*, eds H. G. Schegel and B. Bowien (Berlin: Springer-Verlag), 397–413.

Thauer, R.K., Jungermann, K., and Decker, K. (1977). Energy conservation in chemotrophic anaerobic bacteria. *Bacteriol. Rev.* 41, 100–180.

Thauer, R. K., and Morris, J. G. (1984). "Metabolism of chemotrophic anaerobes: old views and new aspects," in *The Microbe 1984. Part II. Prokaryotes and Eukaryotes*, eds D. P. Kelly and N. G. Carr (Cambridge: Cambridge University Press), 123–168.

Thauer, R. K., Stackebrandt, E., and Hamilton, W. A. (2007). "Energy metabolism of sulphate reducing bacteria," in Sulphate-Reducing Bacteria, eds L. L. Barton and W. A. Hamilton (Cambridge: Cambridge University Press), 1–37.

Torres-García, W., Zhang, W., Runger, G. C., Johnson, R. H., and Meldrum, D. R. (2009). Integrative analysis of transcriptomic and proteomic data of *Desulfovibrio vulgaris*: a non-linear model to predict abundance of undetected proteins. *Bioinformatics* 25, 1905–1914.

Valente, F. M., Almeida, C. C., Pacheco, I., Carita, J., Saraiva, L. M., and Pereira, I. A. (2006). Selenium is involved in regulation of periplasmic hydrogenase gene expression in *Desulfovibrio vulgaris* Hildenborough. *J. Bacteriol.* 188, 3228–3235.

van den Berg, W. A. M., Stevens, A. A. M., Verhagen, M. F. J. M., van Dongen W. M. A. M., and Hagen, W. R. (1989). Overproduction of the prismane protein from *Desulfovibrio desulfuricans* ATCC 27774 in *Desulfovibrio vulgaris* (Hildenborough) and EPR spectroscopy of the [6Fe-6S] cluster in different redox states. *Biochim. Biophys. Acta-Protein Struct. M.* 1206, 240–246.

Venceslau, S. S., Lino, R. R., and Pereira, I. A. (2010). The Qrc membrane complex, related to the alternative complex III, is a menaquinone reductase involved in sulfate respiration. *J. Biol. Chem.* 285, 22774–22783.

Vignais, P. M., and Billoud, B. (2007). Occurrence, classification, and biological function of hydrogenases: an overview. *Chem. Rev.* 107, 4206–42072.

Walker, C. B., He, Z., Yang, Z. K., Ringbauer, J. A. Jr., He, Q., Zhou, J., Voordouw, G., Wall, J. D., Arkin, A. P., Hazen, T. C., Stoylar, S., and Stahl, D. A. (2009). The electron transfer system of syntrophically grown *Desulfovibrio vulgaris*. *J. Bacteriol.* 191, 5793–5801.

Wall, J. D., Arkin, A. P., Balci, N. C., and Rapp-Giles, B. (2009). "Genetics and genomics of sulfate respiration in *Desulfovibrio*," in *Microbial Sulfur Metabolism*, eds C. Dahl and C. G. Friedrich (Berlin: Springer-Verlag.), 1–12.

Wall, J. D., Rapp-Giles, B. J., and Rousset, M. (1993). Characterization of a small plasmid from *Desulfovibrio desulfuricans* and its use for shuttle vector construction. *J. Bacteriol.* 175, 4121–4128.

Welte, C., Krätzer, C., and Deppenmeier, U. (2010). Involvement of Ech hydrogenase in energy conservation of *Methanosarcina mazei*. *FEBS J.* 277, 3396–3403.

Widdel, F., and Hansen, T. A. (1991). "The dissimilatory sulfate- and sulfur-reducing bacteria," in *The Prokaryotes*, eds A. Balows, H. G. Truper, M. Dworkin, W. Harder, and K.-H. Schleifer (New York, NY: Springer-Verlag), 659–768.

Zane, G. M., Yen, H.-C., and Wall, J. D. (2010). Effect of the deletion of *qmoABC* and the promoter-distal gene encoding a hypothetical protein on sulfate reduction in *Desulfovibrio vulgaris* Hildenborough. *Appl. Environ. Microbiol.* 76, 5500–5509.

Conflict of Interest Statement: The authors declare that the research was conducted in the absence of any commercial or financial relationships that could be construed as a potential conflict of interest.

Received: 22 January 2011; accepted: 10 June 2011; published online: 29 June 2011.

Citation: Keller KL and Wall JD (2011) Genetics and molecular biology of the electron flow for sulfate respiration in Desulfovibrio. Front. Microbio. ***2****:135. doi: 10.3389/fmicb.2011.00135*

This article was submitted to Frontiers in Microbial Physiology and Metabolism, a specialty of Frontiers in Microbiology.

frontiers in
MICROBIOLOGY

REVIEW ARTICLE
published: 02 May 2011
doi: 10.3389/fmicb.2011.00081

Metabolic flexibility of sulfate-reducing bacteria

Caroline M. Plugge[1]*, Weiwen Zhang[2], Johannes C. M. Scholten[3] and Alfons J. M. Stams[1]

[1] *Laboratory of Microbiology, Wageningen University, Wageningen, Netherlands*
[2] *Center for Ecogenomics, Biodesign Institute, Arizona State University, Tempe, AZ, USA*
[3] *230 King Fisher Court, Harleysville, PA, USA*

Edited by:
Thomas E. Hanson, University of Delaware, USA

Reviewed by:
Lee Krumholz, University of Oklahoma, USA
Ralf Rabus, University Oldenburg, Germany

****Correspondence:***
Caroline M. Plugge, Laboratory of Microbiology, Wageningen University, Dreijenplein 10, 6703 HB Wageningen, Netherlands.
e-mail:caroline.plugge@wur.nl

Dissimilatory sulfate-reducing prokaryotes (SRB) are a very diverse group of anaerobic bacteria that are omnipresent in nature and play an imperative role in the global cycling of carbon and sulfur. In anoxic marine sediments sulfate reduction accounts for up to 50% of the entire organic mineralization in coastal and shelf ecosystems where sulfate diffuses several meters deep into the sediment. As a consequence, SRB would be expected in the sulfate-containing upper sediment layers, whereas methanogenic archaea would be expected to succeed in the deeper sulfate-depleted layers of the sediment. Where sediments are high in organic matter, sulfate is depleted at shallow sediment depths, and biogenic methane production will occur. In the absence of sulfate, many SRB ferment organic acids and alcohols, producing hydrogen, acetate, and carbon dioxide, and may even rely on hydrogen- and acetate-scavenging methanogens to convert organic compounds to methane. SRB can establish two different life styles, and these can be termed as sulfidogenic and acetogenic, hydrogenogenic metabolism. The advantage of having different metabolic capabilities is that it raises the chance of survival in environments when electron acceptors become depleted. In marine sediments, SRB and methanogens do not compete but rather complement each other in the degradation of organic matter. Also in freshwater ecosystems with sulfate concentrations of only 10–200 μM, sulfate is consumed efficiently within the top several cm of the sediments. Here, many of the δ-Proteobacteria present have the genetic machinery to perform dissimilatory sulfate reduction, yet they have an acetogenic, hydrogenogenic way of life. In this review we evaluate the physiology and metabolic mode of SRB in relation with their environment.

Keywords: sulfate-reducing bacteria, metabolic flexibility, syntrophy, metabolic interactions

Dissimilatory sulfate-reducing prokaryotes (SRB) are a diverse group of anaerobic bacteria that are widespread in nature and play an essential role in the global cycling of carbon and sulfur. The SRB mainly use sulfate, the most oxidized form of sulfur, as the terminal electron acceptor in the oxidation of hydrogen and various organic compounds (Widdel and Hansen, 1991; Rabus et al., 2006; Muyzer and Stams, 2008). Some SRB can use nitrate as electron acceptor, and their possible microaerophilic nature has also been discussed (Cypionka, 2000).

The anaerobic food chain changes largely when sulfate enters the methanogenic zone. In that case sulfate-reducing bacteria will outcompete methanogenic archaea for hydrogen, formate and acetate, and syntrophic methanogenic communities for substrates like propionate and butyrate (Stams, 1994; Muyzer and Stams, 2008). Interestingly, sulfate reducers can also grow without sulfate and in some cases they grow only in syntrophic association with methanogens or other hydrogen-scavengers. Thus, sulfate reducers may compete with methanogens and grow in syntrophy with methanogens depending on the prevailing environmental conditions (Muyzer and Stams, 2008). Already in the 1970s, the metabolic flexibility of SRB was investigated. Bryant et al. (1977) demonstrated growth of *Desulfovibrio* on lactate in the absence of sulfate but in the presence of a methanogen. They concluded that the sulfate reducer produced H_2 which is used by the methanogen, acting as an alternative electron sink in the absence of sulfate. Therefore, in sulfate-depleted environments, it is possible that sulfate reducers may be metabolically active by living in association with methanogenic bacteria instead of reducing sulfate (Bryant et al., 1977; McInerney et al., 1981). This symbiotic process is known as "syntrophy" and is a widespread type of microbial interaction especially in methanogenic environments (Bryant et al., 1967; Schink, 1997; Stams and Plugge, 2009). Two major life styles are thus performed by some SRB: the sulfidogenic and the syntrophic metabolism. The advantage of having different metabolic potentials is that it enhances the chance of survival of communities of SRB in environments when electron acceptors become depleted.

In sulfate-depleted marine sediments, SRB and methanogens do not compete but rather complement each other in the degradation of organic matter. Also in sulfate-rich marine sediments, SRB and methanogens co-exist, but presumably by competing for common substrates, such as H_2 (Oremland et al., 1982; Winfrey and Ward, 1983; Kuivila et al., 1990; Holmer and Kristensen, 1994). Recently, it was found that sulfate reducers were still abundant in the methanogenic zones of Aarhus Bay (Leloup et al., 2009).

In the past decades significant progress has been made through extensive studies of pure cultures, in SRB particularly with its model species *Desulfovibrio vulgaris*. Genomic analysis gave insight how the utilization of H_2 and organic acids (formate and lactate) as electron donors is coupled to sulfate reduction, ATP synthesis and growth (Heidelberg et al., 2004). Lactate is oxidized through several

enzymatic steps to acetate resulting in ATP synthesis (Heidelberg et al., 2004). Besides substrate-level ATP synthesis, additional ATP is generated from a proton gradient according to a chemiosmotic model (Peck, 1966), in which the protons and electrons produced during lactate oxidation react with cytoplasmic hydrogenases to form H_2, which then diffuses across the membrane where it is re-oxidized by periplasmic hydrogenases to form a proton gradient (Odom and Peck, 1981; Heidelberg et al., 2004). The electrons generated during lactate oxidation are channeled to sulfate through a vast network of hemes that is created by various interconnected *c*-type cytochromes and involving several transmembrane complexes (Aubert et al., 2000; Heidelberg et al., 2004). Nowadays, research efforts with SRB are significantly aided by the availability of over 20 genome sequences of which 12 representatives of the genus *Desulfovibrio* (http://img.jgi.doe.gov; Integrated Microbial Genomes). Numerous research groups have since then reported global transcriptomic and proteomic analyses of *D. vulgaris* under various growth or stress conditions (Chhabra et al., 2006; Clark et al., 2006; He et al., 2006; Mukhopadhyay et al., 2006, 2007; Zhang et al., 2006a,b,c; Bender et al., 2007; Tang et al., 2007; Pereira et al., 2008; Walker et al., 2009; Plugge et al., 2010). As a result, there has been a better understanding of the electron transfer and energy conservation mechanisms of *D. vulgaris* mainly associated with lactate oxidation during sulfidogenic growth. Yet, the energy metabolism of *D. vulgaris* is very complex and flexible and as such deserves further study (Pereira et al., 2008).

While the physiology of the symbiotic/syntrophic relationship has been studied for more than 40 years (Bryant et al., 1967, 1977; Stams, 1994; Schink, 1997; Stams and Plugge, 2009), relatively little is known about the metabolic and regulatory networks involved in syntrophic interactions. This may be due to the technical difficulties to establish stable mixed-culture systems and lack of analytical tools for direct large-scale measurement of various biological components (i.e., RNA, proteins or metabolites). However, availability of complete genome sequences and various functional genomics tools in recent years have provided the most needed methodologies to analyze mixed-culture systems. In a recent study, a syntrophic pair, *D. vulgaris* and a hydrogenotrophic methanogen *Methanococcus maripaludis*, was cultured syntrophically on lactate in the absence of sulfate (Stolyar et al., 2007). Syntrophic associations were initiated by mixing equal volumes of stationary phase *D. vulgaris* and *M. maripaludis* cultures. Experimental measurements with the co-culture were used to test predictions derived from the first multi-species stoichiometric metabolic model involving the two species (Stolyar et al., 2007). The *D. vulgaris* and *M. maripaludis* flux-balance models were combined to form one model describing growth and metabolite accumulation when the organisms were growing together. To model the interaction between the two species, a system of three "compartments" was proposed. The first two compartments each contained the metabolite fluxes for one of the single-species models analyzed above. These species' compartments could each represent the action of single cells, or the combined flux of many cells of the same species. To model the interaction between the two species, a third compartment was added to the model, through which metabolites could be transferred between organisms. Exchange fluxes were added to the model in this compartment. With this modification, species could take up metabolites excreted by the other species. The results of these initial model simulations predicted that *D. vulgaris*, growing optimally, converts the majority of the carbon contained in the substrate lactate into acetate, and that only 4.8% of the carbon is directed to biomass. The remaining carbon is lost as CO_2 or formate. To maintain redox balance in the absence of an external electron acceptor, evolution of a reduced compound, either formate or hydrogen, is predicted. The model shows that when acetate is available, it is the preferred source of biomass carbon for *M. maripaludis* over the CO dehydrogenase pathway to fix carbon dioxide. This prediction is consistent with published data and the experimental results showed that *M. maripaludis* consumes acetate and presumably uses it as a carbon source (Stolyar et al., 2007).

Comparative transcriptomic analysis to investigate syntrophic systems was done recently. In one study, comparative transcriptional analysis of *D. vulgaris* in two culture conditions was performed: syntrophic co-cultures with *M. maripaludis* strain S2 (without sulfate) and sulfate-limited monocultures (Walker et al., 2009). During syntrophic growth on lactate with a hydrogenotrophic methanogen, numerous genes involved in electron transfer and energy generation were up-regulated in *D. vulgaris* compared with their expression in sulfate-limited pure cultures. In another study, whole-genome *D. vulgaris* microarrays were used to determine relative transcript levels when *D. vulgaris* shifted its lifestyle from syntroph in a lactate-oxidizing co-culture with *Methanosarcina barkeri* to a sulfidogenic lifestyle (Plugge et al., 2010). In the study, syntrophic co-cultures were grown in two independent chemostats and perturbation was introduced after six volume changes with the addition of sulfate. Functional analyses revealed that genes involved in cell envelope and energy metabolism were the most regulated when comparing syntrophic and sulfidogenic metabolism. These two studies are similar in many ways, however, there are four major differences in experimental design between the two studies: (i) the methanogenic partner in the study of Walker et al. (2009) was *M. maripaludis*, whereas it was *M. barkeri* in the study of Plugge et al. (2010); (ii) the *D. vulgaris* and *M. maripaludis* co-culture and the *D. vulgaris* monoculture were cultivated in parallel in different chemostats by Walker et al. (2009), while a perturbation experiment by adding sulfate was performed to the chemostat co-culture to produce the *D. vulgaris* sulfidogenic metabolism in Plugge et al. (2010); (iii) the sulfidogenic monoculture of Walker et al. (2009) was sulfate-limited, whereas the *D. vulgaris* sulfidogenic metabolism was lactate-limited (Plugge et al., 2010); and (iv) the cell ratio (between *D. vulgaris* and *M. maripaludis*) during steady-state co-culture growth was higher (4:1) compared with the 1:1 in the *D. vulgaris M. barkeri* co-culture. Nevertheless, some similar results were obtained. These included the identification of a five-gene cluster encoding several lipo- and membrane-bound proteins which was down-regulated when cells were shifted to a sulfidogenic metabolism (**Figure 1**). Interestingly, this gene cluster has orthologs found only in the syntrophic bacterium *Syntrophobacter fumaroxidans* and four recently sequenced *Desulfovibrio* strains, suggesting that these genes are possible "syntrophic genes." Both studies demonstrated that syntrophic growth and sulfate respiration use mostly independent energy generation pathways, implying that the molecular mechanism of microbial syntrophic processes cannot be fully interpreted by studying only

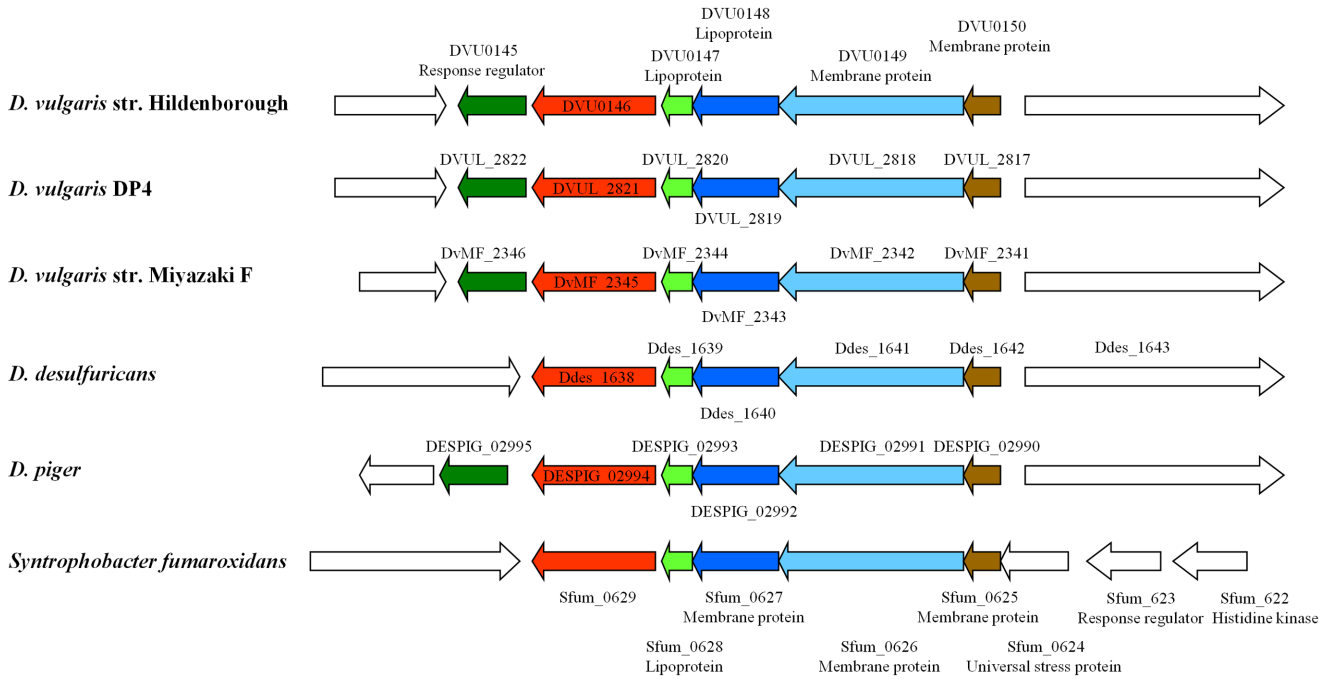

FIGURE 1 | A gene cluster with orthologs only in *Syntrophobacter fumaroxidans* and four recently sequences *Desulfovibrio* strains was significantly down-regulated during shift from syntrophic to sulfidogenic metabolism (Printed from Plugge et al., 2010, with permission of SGM).

pure cultures (Walker et al., 2009; Plugge et al., 2010). In addition, the studies also identified the upregulation during the *D. vulgaris* syntrophic metabolism of the high-molecular-mass cytochrome complex (DVU0533, encoding Hmc protein 4), the DVU0145–0150 cellular membrane gene cluster of unknown function and heterodisulfide reductase (*hdrAB*), and the downregulation of genes involved in iron transport (*feoB* and *feoA*; Walker et al., 2009; Plugge et al., 2010).

Among the SRB members of the genus *Desulfovibrio* are easy to grow and they grow rapidly. Therefore, they have been the subject of the most intensive biochemical and molecular research (Postgate, 1984; Peck, 1993; Voordouw, 1993). However, multiple studies have described physiology and metabolic mode of SRB in relation with their environment. In the following paragraphs we will review a variety of these SRB-containing communities and their role in anaerobic biodegradation.

METABOLIC FLEXIBILITY OF *DESULFOTOMACULUM* CLUSTER IH

Members of the Gram-positive *Desulfotomaculum* cluster I are commonly considered as regular sulfate-reducing bacteria. However, in the last decade new representatives have been isolated that lack the ability of sulfate reduction, all phylogenetically grouping in *Desulfotomaculum* cluster Ih. These representatives are isolated from environments typically low in sulfate and producing methane: anaerobic bioreactors and rice paddy soils. Syntrophic propionate-oxidizing species of the genus *Pelotomaculum* are *Pelotomaculum schinkii, P. thermopropionicum,* and *P. propionicicum* (de Bok et al.,2005; Imachi et al., 2002, 2006, 2007). Additional members of *Desulfotomaculum* cluster Ih are *P. terephthalicum* sp. nov., and *P. isophthalicum* sp. nov. (Qiu et al., 2006) involved in syntrophic degradation of phthalate isomers and also lacking the ability of sulfate reduction. Imachi et al. (2006) demonstrated that none of these species was able to use sulfate, sulfite, or organosulfonates as electron acceptors. A PCR-based screening for *dsr*AB genes (key genes of the sulfate respiration pathway encoding the alpha and beta subunits of the dissimilatory sulfite reductase) of all cultures tested was negative with the exception of *P. propionicicum.* Based on these results it was proposed that subcluster Ih bacteria have adapted to anoxic, low-sulfate conditions and thus constitute a significant fraction of the *Desulfotomaculum* cluster I population in methanogenic microbial communities in a wide variety of methanogenic environments, highlighting its ecological impact in anoxic environments low in sulfate (Imachi et al., 2006; **Figure 2**). As a consequence of this evolutionary process, they have lost the capability of dissimilatory sulfate reduction and adopted the syntrophic life style, in close proximity to hydrogen- and formate-consuming methanogens. In such a way they can maintain an energetically favorable, low-hydrogen partial pressure that is necessary for the syntrophic oxidation of organic substrates. Given their recognized phenotypes and wide occurrence in low-sulfate, methanogenic environments, descendants of the *Desulfotomaculum* subcluster Ih branch most likely function as non-sulfate-reducing, syntrophic degraders of organic substrates *in situ.* This hypothesis received further support from a study that showed, by using rRNA-based stable-isotope probing, that *Pelotomaculum* species were not only dominant, but also actively involved in syntrophic propionate oxidation in a rice paddy soil (Lueders et al., 2004). Interestingly, the recently sequenced genome of *P. thermopropionicum* (Kosaka et al., 2008) points out the presence of *dsr* and *aps* genes (*aps* is coding for

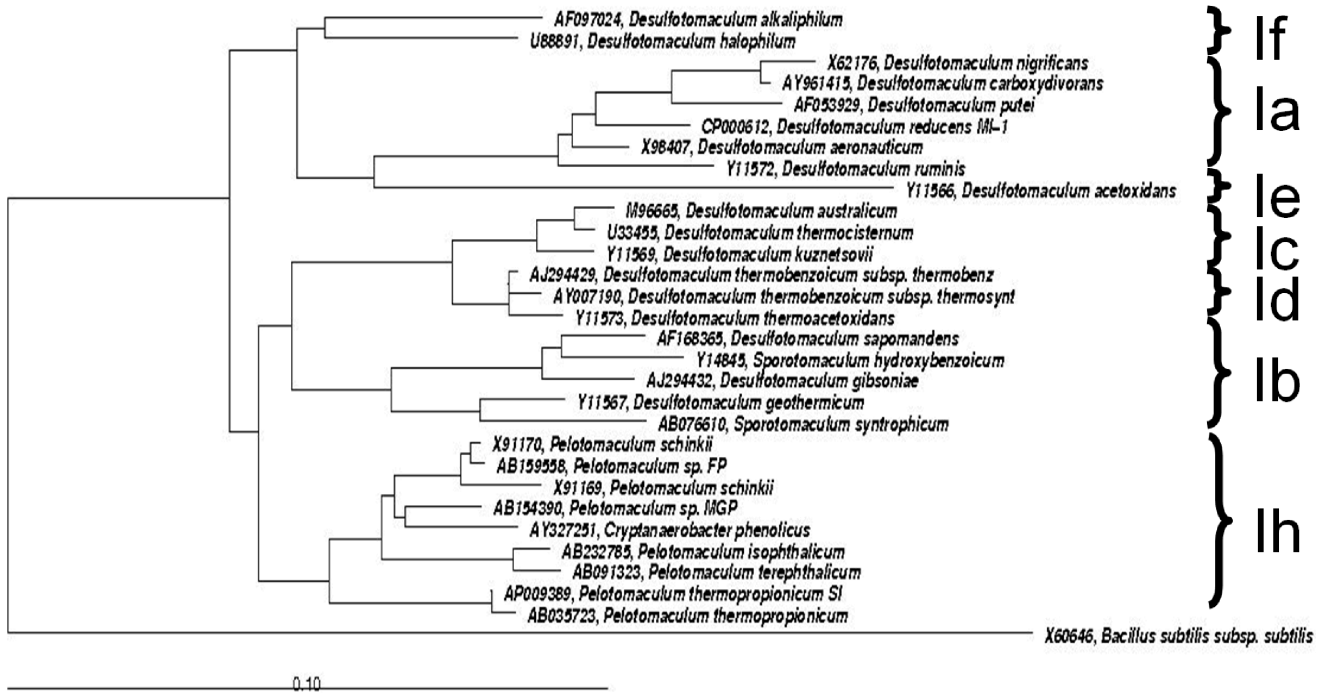

FIGURE 2 | Phylogenetic tree of *Desulfotomaculum* cluster I, showing the grouped phylogeny of *Pelotomaculum* ssp. The tree is based on comparative analyses of 16S rRNA gene sequences. The tree was constructed with sequences greater than 1,000 nucleotides using the latest released version of ARB (ARB 5.2, September 5, 2010). *Bacillus subtilis* was set as root. The reference bar indicates 10% sequence divergence.

adenylyl sulfate reductase, another important enzyme in the sulfate respiration pathway that consists of an alpha and beta subunit). The genes are clustered in an operon (PTH_0235 to PTH_0242).

Gene clusters necessary for dissimilatory sulfate reduction, such as those for transmembrane electron transport complexes (Haveman et al., 2004), were not found in the genome of *P. thermopropionicum*. This is consistent with previous physiological observations showing that this bacterium could not utilize sulfate as an electron acceptor (Imachi et al., 2002). The PCR-based screening for *dsr*AB genes by Imachi et al. (2006) that tested negative for *P. thermopropionicum* may have used primer sets that did not amplify the *dsr*AB genes in *P. thermopropionicum*. It is also possible that some of these *dsrAB*-carrying non-sulfate reducers use organosulfonates as electron acceptors for anaerobic respiration instead. e.g., *Bilophila wadsworthia* degradestaurine to sulfite, which is the actual substrate for its dissimilatory sulfite reductase (Cook et al., 1998). However, a whole range of organosulfonates did not support growth of the thermophilic spore-forming, low-G+C bacteria belonging to the genus *Pelotomaculum* (Imachi et al., 2006). An alternative explanation is that the real substrate for the dissimilatory sulfite reductase in syntrophic bacteria has not yet been identified.

Desulfotomaculum cluster Ih related species are also involved in the anaerobic mineralization of benzene in the presence of sulfate (Kleinsteuber et al., 2008; Laban et al., 2009; Herrmann et al., 2010). Identification of the benzene-degrading, sulfate-reducing communities was in all three studies based on culture-independent methods. A *Pelotomaculum/Cryptanaerobacter*-like phylotype represented a syntrophic community responsible for the initiation of the anaerobic benzene degradation in the studies by Kleinsteuber et al. (2008) and Herrmann et al. (2010). Benzene was completely mineralized in the presence of sulfate by a consortium consisting of syntrophs, hydrogenotrophic sulfate reducers and to a minor extent aceticlastic methanogens. Also Laban et al. (2009) showed that organisms phylogenetically related to the Gram-positive genus *Pelotomaculum* were responsible for benzene degradationcoupled to sulfate reduction. However, the 16S rRNA gene-based sequence similarity to the next cultivated representative of *Desulfotomaculum* cluster Ih constituted only 95%. These sequences could be clustered between the genera *Desulfotomaculum* and *Pelotomaculum*. The similarity of the sequences of the *Pelotomaculum*-related phylotypes described by Kleinsteuber et al. (2008) to those identified by Laban et al. (2009) range from 88.8 to 95.7% indicating that these phylotypes are indeed different.

Based on their results with a highly enriched culture, where only one dominant species was present, Laban et al. (2009) proposed that these bacteria with *Pelotomaculum*-related 16S rRNA gene sequences oxidize benzene directly coupled to sulfate reduction.

Clearly we cannot exclude that members of the *Desulfotomaculum* subcluster 1 h are capable of sulfate reduction, but apparently they can not be easily adapted to do so. The information presented here is based on our present knowledge.

METABOLIC FLEXIBILITY BY MEMBERS OF THE ORDER SYNTROPHOBACTERALES

The Syntrophobacterales are an order of the δ-Proteobacteria, with three families, the Syntrophaceae, Syntrophobacteraceae, and Syntrophorhabdaceae (McInerney et al., 2008). Many of

the members of these families are SRB, but also representatives of these families have been isolated that lack the ability for anaerobic sulfate respiration, or can grow as SRB or fermentative organism, depending on the environmental conditions (Wallrabenstein et al., 1994, 1995; Van Kuijk and Stams, 1995; Liu et al., 1999; Chen et al., 2005). With respect to 16S rRNA phylogeny, no predictions can be made on their metabolic flexibility.

Research has focused on propionate-degrading bacteria from the order Syntrophobacterales, specifically members that were enriched and isolated in the absence of sulfate. All species studied (**Table 1**) were capable of propionate degradation in syntrophic co-culture with a syntrophic partner but also as a pure culture coupled to dissimilatory sulfate reduction.

It remains unknown why some bacteria have actively expressed *dsrAB* genes, but cannot utilize sulfate, sulfite, and/or organosulfonates for anaerobic respiration. One might speculate that these microbes were formerly active sulfate reducers, but have lost this trait since they have to deal with low-sulfate and/or sulfite levels in methanogenic environments (Imachi et al., 2006). For this reason, the presence of *dsrAB* in these bacteria, which most often live in close association with hydrogen-consuming microorganisms for the syntrophic oxidation of substrates, would be a genetic remnant and thus indicative of an ancient sulfate/sulfite-respiring potential. The physiological data on syntrophs from the Syntrophobacterales order, which are abundantly present in methanogenic environments (Loy et al., 2004; Lueders et al., 2004; Stams and Plugge, 2009), indicate that all have retained their sulfate-reducing capability (Wallrabenstein et al., 1994; Van Kuijk and Stams, 1995). Syntrophic *dsrAB*-containing non-SRBs, syntrophic SRBs, and real sulfate reducers are phylogenetically fused, indicating an evolutionary connection between the sulfate-reducing and syntrophic lifestyle.

Table 1 | Growth rates of selected propionate-degrading bacteria with and without sulfate.

	Growth rate (day^{-1})		References
	Propionate	**Propionate + sulfate**	
Syntrophobacter fumaroxidans	0.17	0.024	Van Kuijk and Stams (1995), Harmsen et al. (1998)
Syntrophobacter pfennigii	0.066	0.063	Wallrabenstein et al. (1995)
Syntrophobacter sulfatireducens	n.d.*	0.12	Chen et al. (2005)
Syntrophobacter wolinii	6.7**	0.062	Wallrabenstein et al. (1994)
Smithella propionica	n.d.*	n.d.***	Liu et al. (1999)

*Capable of syntrophic growth on propionate, but growth rate not determined.
**Only a doubling time (days) was determined.
***Capable of sulfate reduction, but growth rate not reported.

NON-EXISTING METABOLIC FLEXIBILITY BY BUTYRATE OXIDIZERS

Bacteria that grow on butyrate syntrophically with methanogens can only be found within the Gram-positive genera *Syntrophomonas* and *Syntrophus*. None of the members of these genera has the ability to reduce sulfate. The recently sequenced genomes of *Syntrophomonas wolfei* and *Syntrophus aciditrophicus* clearly show the lack of *dsr* and *aps* genes which explains on a molecular basis the inability of these organisms to do so. On the other hand, Gram-positive and Gram-negative butyrate-degrading sulfate-reducing genera have been described (e.g., *Desulfobacterium*, *Desulfosarcina*, and *Desulfoarculus*). None of the isolated sulfate-reducing species was ever shown to be able to grow in the absence of sulfate in syntrophy with methanogens (Rabus et al., 2006; Muyzer and Stams, 2008). This suggests that butyrate-degrading communities have a different response to changes in sulfate availability than propionate-degrading communities. In granular sludge butyrate-degrading bacteria that grow in syntrophy with methanogens are not easily outcompeted by sulfate-reducing bacteria (Oude Elferink et al., 1994). Instead, hydrogen-consuming methanogens seem to be replaced by hydrogen-consuming sulfate reducers, while propionate-degrading communities are easily outcompeted by typical propionate-degrading sulfate-reducing bacteria. Recently, it was observed that in communities that degrade long-chain fatty acids *Syntrophomonas* sp. persisted when methanogenic sludge was exposed to increasing levels of sulfate, but the hydrogen-consuming archaea were outcompeted by hydrogen-consuming sulfate-reducing bacteria (Sousa et al., 2009).

METABOLIC FLEXIBILITY OF SRB IN MARINE ENVIRONMENTS

In sulfate-rich marine sediments, sulfate-reducing bacteria typically use all the products of primary fermentations and oxidize them to CO_2 coupled to sulfate reduction (Muyzer and Stams, 2008). Therefore, fermentation by syntrophic communities is thought to be unimportant. However, when sulfate becomes limited the organic matter is no longer mineralized coupled to sulfate reduction, but through methanogenesis. Kendall et al. (2006) described marine syntrophic propionate- and butyrate-degrading cultures. This study implied that syntrophic communities contribute to the vast methane reservoirs in marine sediments. Microbial populations identified in shallow methanogenic sediments in the Gulf of Mexico revealed the presence of members of *Syntrophobacteriaceae* (Lloyd et al., 2006; McInerney et al., 2008). Cultured members of this family include syntrophic propionate oxidizers that can also reduce sulfate and as such have the capability to switch from sulfate-reducing life style to syntrophic life style as was discussed in paragraph "metabolic flexibility by members of the order Syntrophobacterales" (McInerney et al., 2008). Members of the *Syntrophobacteriaceae* were also found in the sulfate–methane transition zone in the Black Sea (Leloup et al., 2007, 2009). It was speculated that in these sediments, sulfate-reducing bacteria and methanogens do not compete but rather co-exist when mineralizing organic matter. In the absence of sulfate the reducing equivalents produced (hydrogen or formate) by SRB can be shuttled to a methanogen, serving as the syntrophic partner. More recently in Aarhus Bay it was found, that sulfate reducers were still very abundant in the methanogenic zones (Leloup et al., 2009). It is still

unclear which type of metabolism sulfate reducers encompass in the methane zone and *vice versa*. Non-competitive substrates in marine environments (used by methanogens but not by sulfate reducers) methanol and methylamine were indeed converted by methanogens in sulfate-containing sediments from Aarhus Bay. However, sulfate reducers could scavenge the nanomolar hydrogen that leaked from the methanogenic cells (Finke et al., 2007), once more illustrating the complexity of metabolic interactions.

EVOLUTION OF STABILITY AND PRODUCTIVITY AT THE ORIGIN OF A SYNTROPHIC COMMUNITY OF AN SRB AND METHANOGEN

A syntrophic community was established by combining the *D. vulgaris* Hildenborough with the methanogenic archaeon *M. maripaludis* S2 (Hillesland and Stahl, 2010). Both members in the community could be grown in pure culture with appropriate substrates, but under the conditions of the experiments they could grow only through syntrophic cooperation. In the absence of hydrogen and sulfate, the species feed together by cooperating to complete the following energy-yielding reaction:

$$2\,\text{Lactate}^- + \text{H}_2\text{O} \rightarrow 2\,\text{Acetate}^- + \text{CH}_4 + \text{H}^+ + \text{HCO}_3^-$$

Twenty-four independent pairings(co-cultures) of the bacterium *D. vulgaris* and the archaeon *M. maripaludis* were established and followed for 300 community doublings in two environments, one allowing for the development of a heterogeneous distribution of resources and the other not. Evolved co-cultures grew up to 80% faster and were up to 30% more productive (biomass yield per mole of substrate) than the ancestors. Unfortunately, the authors did not include quantitative data on substrate depletion, product formation, and biomass production in the evolved co-cultures to support their hypothesis.

Unlike eukaryotes that evolve principally through the modification of existing genetic information, bacteria can obtain a significant proportion of their genetic diversity through the acquisition of sequences from distantly related organisms (Scholten et al., 2007). Horizontal gene transfer produces extremely dynamic genomes in which substantial amounts of DNA are introduced into and deleted from the chromosome. These lateral transfers have effectively changed the ecological and pathogenic character of bacterial species (Ochman et al., 2000). Previous studies indicated that the scale of horizontal gene transfer may have previously been underestimated and that horizontal gene transfer may be a major force in the evolution of prokaryotic genomes (Boucher and Doolittle, 2000; Calteau et al., 2005). In a more recent study, a combination of transcriptomics and phylogenomics, codon, and amino acid usage analyses of the syntrophic interaction between *D. vulgaris* and *M. barkeri* has led to the discovery of a functionally unknown gene set in the genome of *D. vulgaris*. This may be the result of ancient horizontal gene transfer from an archaeal methanogen. The gene set consists of three closely located genes on the chromosome, DVU2103 and DVU2104 encoding iron–sulfur cluster-binding/ATPase domain proteins and DVU2108 encoding an MTH1175-like domain family protein (Scholten et al., 2007). Similar lateral gene transfer was also reported between other syntrophic bacteria and methanogenic archaea (Kosaka et al., 2008; Fournier, 2009), suggesting that lateral gene transfer among microorganisms whose niches are closely associated is a common and important evolutionary process (Kato and Watanabe, 2010).

FUTURE PERSPECTIVES

The metabolic flexibility of syntrophs and SRBs deserves future attention. The analysis of available and future genome sequences of SRBs, syntrophs and their partners in more detail will provide more insight into horizontal gene transfer, loss of genes (such as *dsr* and *aps*), genotypic and phenotypic similarities and its consequences for their ecological specialization. Dedicated physiological studies will unravel the occurrence and significance of less obvious metabolic capabilities of microorganisms in general and of more specifically syntrophic and sulfate-reducing bacteria. Molecular ecological studies such as comparative metagenomics on environments with fluctuating sulfate levels may reveal the *in situ* metabolism of the microorganisms present.

ACKNOWLEDGMENTS

The authors were financially supported by the Earth and Life Sciences division (ALW) and Chemical Science division (CW) of the Netherlands Organization for Scientific Research (NWO). The authors thank Tom van den Bogert for beautification of the phylogenetic tree.

REFERENCES

Aubert, C., Brugna, M., Dolla, A., Bruschi, M., and Giudici-Orticoni, M. T. (2000). A sequential electron transfer from hydrogenases to cytochromes in sulfate-reducing bacteria. *Biochim. Biophys. Acta* 1476, 85–92.

Bender, K. S., Yen, H. C., Hemme, C. L., Yang, Z., He, Z., He, Q., Zhou, J., Huang, K. H., Alm, E. J., Hazen, T. C., Arkin, A. P., and Wall, J. D. (2007). Analysis of a ferric uptake regulator (Fur) mutant of *Desulfovibrio vulgaris* Hildenborough. *Appl. Environ. Microbiol.* 73, 5389–5400.

Boucher, Y., and Doolittle, W. F. (2000). The role of lateral gene transfer in the evolution of isoprenoid biosynthesis pathways. *Mol. Microbiol.* 37, 703–716.

Bryant, M. P., Campbell, L. L., Reddy, C. A., and Crabill, M. R. (1977). Growth of *Desulfovibrio* in lactate or ethanol media low in sulfate in association with H2-utilizing methanogenic bacteria. *Appl. Environ. Microbiol.* 33, 1162–1169.

Bryant, M. P., Wolin, E. A., Wolin, M. J., and Wolfe, R. S. (1967). *Methanobacillus omelianskii* a symbiotic association of two species of bacteria. *Arch. Microbiol.* 59, 20–31.

Calteau, A., Gouy, M., and Perriere, G. (2005). Horizontal transfer of two operons coding for hydrogenases between bacteria and archaea. *J. Mol. Evol.* 60, 557–565.

Chen, S. Y., Liu, X. L., and Dong, X. Z. (2005). *Syntrophobacter sulfatireducens* sp. nov., a novel syntrophic, propionate-oxidizing bacterium isolated from UASB reactors. *Int. J. Syst. Evol. Microbiol.* 55, 1319–1324.

Chhabra, S. R., He, Q., Huang, K. H., Gaucher, S. P., Alm, E. J., He, Z., Hadi, M. Z., Hazen, T. C., Wall, J. D., Zhou, J., Arkin, A. P., and Singh, A. K. (2006). Global analysis of heat shock response in *Desulfovibrio vulgaris* Hildenborough. *J. Bacteriol.* 188, 1817–1828.

Clark, M. E., He, Q., He, Z., Huang, K. H., Alm, E. J., Wan, X. F., Hazen, T. C., Arkin, A. P., Wall, J. D., Zhou, J. Z., and Fields, M. W. (2006). Temporal transcriptomic analysis as *Desulfovibrio vulgaris* Hildenborough transitions into stationary phase during electron donor depletion. *Appl. Environ. Microbiol.* 72, 5578–5588.

Cook, A. M., Laue, H., and Junker, F. (1998). Microbial desulfonation. *FEMS Microbiol. Rev.* 22, 399–419.

Cypionka, H. (2000). Oxygen respiration in *Desulfovibrio* species. *Ann. Rev. Microbiol.* 54, 827–848.

de Bok, F. A. M., Harmsen, H. J. M., Plugge, C. M., deVries, M. C., Akkermans, A. D. L., deVos, W. M., and Stams, A. J. M. (2005). *Pelotomaculum schinkii* sp. nov., an obligate syntrophic propionate-oxidizing spore-forming bacterium isolated in co-culture with

Methanospirillum hungatei. *Int. J. Syst. Evol. Microbiol.* 55, 1697–1703.

Finke, N., Hoehler, T. M., and Jørgensen, B. B. (2007). Hydrogen leakage during methanogenesis from methanol and methylamine: implications for anaerobic carbon degradation pathways in aquatic sediments. *Environ. Microbiol.* 9, 1060–1071.

Fournier, G. (2009). Horizontal gene transfer and the evolution of methanogenic pathways. *Methods Mol. Biol.* 532, 163–179.

Harmsen, H. J. M., van Kuijk, B. L. M., Plugge, C. M., Akkermans, A. D. L., de Vos, W. M., and Stams, A. J. M. (1998). *Syntrophobacter fumaroxidans* sp. nov., a syntrophic propionate-degrading sulfate-reducing bacterium. *Int. J. Syst. Bacteriol.* 48, 1383–1387.

Haveman, S. A., Greene, E. A., Stilwell, C. P., and Voordouw, J. K., and Voordouw, G. (2004). Physiological and gene expression analysis of inhibition of *Desulfovibrio vulgaris* Hildenborough by nitrite. *J. Bacteriol.* 186, 7944–7950.

He, Q., Huang, K. H., He, Z., Alm, E. J., Fields, M. W., Hazen, T. C., Arkin, A. P., Wall, J. D., and Zhou, J. (2006). Energetic consequences of nitrite stress in *Desulfovibrio vulgaris* Hildenborough inferred from global transcriptional analysis. *Appl. Environ. Microbiol.* 72, 4370–4381.

Heidelberg, J. F., Seshadri, R., Haveman, S. A., Hemme, C. L., Paulsen, I. T., Kolonay, J. F., Eisen, J. A., Ward, N., Methe, B., Brinkac, L. M., Daugherty, S. C., Deboy, R. T., Dodson, R. J., Durkin, A. S., Madupu, R., Nelson, W. C., Sullivan, S. A., Fouts, D., Haft, D. H., Selengut, J., Peterson, J. D., Davidsen, T. M., Zafar, N., Zhou, L., Radune, D., Dimitrov, G., Hance, M., Tran, K., Khouri, H., Gill, J., Utterback, T. R., Feldblyum, T. V., Wall, J. D., Voordouw, G., and Fraser, C. M. (2004). The genome sequence of the anaerobic sulfate-reducing bacterium *Desulfovibrio vulgaris* Hildenborough. *Nat. Biotechnol.* 22, 554–559.

Herrmann, S., Kleinsteuber, S., Chatzinotas, A., Kuppardt, S., Lueders, T., Richnow, H.-H., and Vogt, C. (2010). Functional characterization of an anaerobic benzene-degrading enrichment culture by DNA stable isotope probing. *Environ. Microbiol.* 12, 401–411.

Hillesland, K. L., and Stahl, D. A. (2010). Rapid evolution of stability and productivity at the origin of a microbial mutualism. *Proc. Natl. Acad. Sci. U.S.A.* 107, 2124–2129.

Holmer, M., and Kristensen, E. (1994). Co-existence of sulfate reduction and methane production in an organic-rich sediment. *Mar. Ecol. Prog. Ser.* 107, 177–184.

Imachi, H., Sakai, S., Ohashi, A., Harada, H., Hanada, S., Kamagata, Y., and Sekiguchi, Y. (2007). *Pelotomaculum propionicicum* sp. nov., an anaerobic, mesophilic, obligately syntrophic, propionate-oxidizing bacterium. *Int. J. Syst. Evol. Microbiol.* 57, 1487–1492.

Imachi, H., Sekiguchi, Y., Kamagata, Y., Hanada, S., Ohashi, A., and Harada, H. (2002). *Pelotomaculum thermopropionicum* gen. nov., sp. nov., an anaerobic, thermophilic, syntrophic propionate-oxidizing bacterium. *Int. J. Syst. Evol. Microbiol.* 52, 1729–1735.

Imachi, H., Sekiguchi, Y., Kamagata, Y., Loy, A., Qiu, Y.-L., Hugenholtz, P., Kimura, N., Wagner, M., Ohashi, A., and Harada, H. (2006). Non-sulfate-reducing, syntrophic bacteria affiliated with *Desulfotomaculum* Cluster I are widely distributed in methanogenic environments. *Appl. Environ. Microbiol.* 72, 2080–2091.

Kato, S., and Watanabe, K. (2010). Ecological and evolutionary interactions in syntrophic methanogenic consortia. *Microbes Environ.* 25, 145–151.

Kendall, M. M., Liu, Y., and Boone, D. R. (2006). Butyrate- and propionate-degrading syntrophs from permanently cold marine sediments in Skan Bay, Alaska, and description of *Algorimarina butyrica* gen. nov., sp. nov. *FEMS Microbiol. Lett.* 262, 107–114.

Kleinsteuber, S., Schleinitz, K. M., Breitfeld, J., Harms, H., Richnow, H.-H., and Vogt, C. (2008). Molecular characterization of bacterial communities mineralizing benzene under sulfate-reducing conditions. *FEMS Microbiol. Ecol.* 66, 143–157.

Kosaka, T., Kato, S., Shimoyama, T., Ishii, S., Abe, T., and Watanabe, K. (2008). The genome of *Pelotomaculum thermopropionicum* reveals niche-associated evolution in anaerobic microbiota. *Genome Res.* 18, 442–448.

Kuivila, K. M., Murray, J. W., and Devol, A. H. (1990). Methane production in the sulfate depleted sediments of two marine basins. *Geochim. Cosmochim. Acta* 54, 403–411.

Laban, N. A., Selesi, D., Jobelius, C., and Meckenstock, R. U. (2009). Anaerobic benzene degradation by Gram-positive sulfate-reducing bacteria. *FEMS Microbiol. Ecol.* 68, 300–311.

Leloup, J., Fossing, H., Kohls, K., Holmkvist, L., and Jørgensen, B. B. (2009). Sulfate-reducing bacteria in marine sediment (Aarhus Bay, Denmark): abundance and diversity related to geochemical zonation. *Environ. Microbiol.* 11, 1278–1291.

Leloup, J., Loy, A., Knab, N. J., Borowski, C., Wagner, M., and Jørgensen, B. B. (2007). Diversity and abundance of sulfate-reducing microorganisms in the sulfate and methane zones of a marine sediment, Black Sea. *Environ. Microbiol.* 9, 131–142.

Liu, Y., Balkwill, D. L., Aldrich, H. C., Drake, G. R., and Boone, D. R. (1999). Characterization of the anaerobic propionate-degrading syntrophs *Smithella propionica* gen. nov., sp. nov. and *Syntrophobacter wolinii*. *Int. J. Syst. Bacteriol.* 49, 545–556.

Lloyd, K. G., Lapham, L., and Teske, A. (2006). An anaerobic methane-oxidizing community of ANME-1b archaea in hypersaline Gulf of Mexico sediments. *Appl. Environ. Microbiol.* 72, 7218–7230.

Loy, A., Küsel, K., Lehner, A., Drake, H. L., and Wagner, M,. (2004). Microarray and functional gene analyses of sulfate-reducing prokaryotes in low sulfate, acidic fens reveal co-occurence of recognized genera and novel lineages. *Appl. Environ. Microbiol.* 70, 6998–7009.

Lueders, T., Pommerenke, B., and Friedrich, M. W. (2004). Stable-isotope probing of microorganisms thriving at thermodynamic limits: syntrophic propionate oxidation in flooded soil. *Appl. Environ. Microbiol.* 70, 5778–5786.

McInerney, M. J., Mackie, R. I., and Bryant, M. P. (1981). Syntrophic association of a butyrate-degrading bacterium and *Methanosarcina* enriched from bovine rumen fluid. *Appl. Environ. Microbiol.* 41, 826–828.

McInerney, M. J., Struchtemeyer, C. G., Sieber, J., Mouttaki, H., Stams, A. J. M., Schink, B., Rholin, L., and Gunsalus, R. P. (2008). Physiology, ecology, phylogeny, and genomics of microorganisms capable of syntrophic metabolism. *Ann. N. Y. Acad. Sci.* 1125, 58–72.

Mukhopadhyay, A., He, Z., Alm, E. J., Arkin, A. P., Baidoo, E. E., Borglin, S. C., Chen, W., Hazen, T. C., He, Q., Holman, H. Y., Huang, K., Huang, R., Joyner, D. C., Katz, N., Keller, M., Oeller, P., Redding, A., Sun, J., Wall, J., Wei, J., Yang, Z., Yen, H. C., Zhou, J., and Keasling, J. D. (2006). Salt stress in *Desulfovibrio vulgaris* Hildenborough: an integrated genomics approach. *J. Bacteriol.* 188, 4068–4078.

Mukhopadhyay, A., Redding, A. M., Joachimiak, M. P., Arkin, A. P., Borglin, S. E., Dehal, P. S., Chakraborty, R., Geller, J. T., Hazen, T. C., He, Q., Joyner, D. C., Martin, V. J., Wall, J. D., Yang, Z. K., Zhou, J., and Keasling, J. D. (2007). Cell-wide responses to low-oxygen exposure in *Desulfovibrio vulgaris* Hildenborough. *J. Bacteriol.* 189, 5996–6010.

Muyzer, G., and Stams, A. J. M. (2008). The ecology and biotechnology of sulphate-reducing bacteria. *Nat. Microbiol. Rev.* 6, 441–454.

Ochman, H., Lawrence, J. G., and Groisman, E. A. (2000). Lateral gene transfer and the nature of bacterial innovation. *Nature* 405, 299–304.

Odom, J. M., and Peck, H. D. Jr. (1981). Hydrogen cycling as a general mechanism for energy coupling in the sulfate-reducing bacteria *Desulfovibrio* sp. *FEMS Microbiol. Lett.* 12, 47–50.

Oremland, R. S., Marsh, L. M., and Polcin, S. (1982). Methane production and simultaneous sulfate reduction in anoxic saltmarsh sediments. *Nature* 296, 143–145.

Oude Elferink, S. J. W. H., Visser, A., Hulshoff Pol, L. W., and Stams, A. J. M. (1994). Sulfate reduction in methanogenic bioreactors. *FEMS Microbiol. Rev.* 15, 119–136.

Peck, H. D. Jr. (1966). Phosphorylation coupled with electron transfer in extracts of the sulfate reducing bacterium *Desulfovibrio* gigas. *Biochem. Biophys. Res. Commun.* 22, 112–118.

Peck, H. D. Jr. (1993). "Bioenergetics strategies of the sulfate-reducing bacteria," in *The Sulfate-Reducing Bacteria: Contemporary Perspectives*, eds J. M. Odom and R. Singleton, Jr (New York: The Springer Verlag), 41–76.

Pereira, P. M., He, Q., Valente, F. M. A., Xavier, A. V., Zhou, J., Pereira, I. A. C., and Louro, R. O. (2008). Energy metabolism in *Desulfovibrio vulgaris* Hildenborough: insights from transcriptome analysis. *Antonie Van Leeuwenhoek* 93, 347–362.

Plugge, C. M., Scholten, J. C. M., Culley, D. E., Nie, L., Brockman, F. J., and Zhang, W. (2010). Global transcriptomics analysis of *Desulfovibrio vulgaris* lifestyle change from syntrophic growth with *Methanosarcina barkeri* to sulfate reducer. *Microbiology* 156, 2746–2756.

Postgate, J. R. (1984). *The Sulphate-Reducing Bacteria*. Cambridge: Cambridge University Press.

Qiu, Y.-L., Sekiguchi, Y., Hanada, S., Imachi, H., Tseng, I.-C., Cheng, S.-S., Ohashi, A., Harada, H., and Kamagata, Y. (2006). *Pelotomaculum terephthalicum* sp. nov. and *Pelotomaculum isophthalicum* sp. nov.: two anaerobic bacteria that degrade phthalate isomers in syntrophic association with hydrogenotrophic methanogens. *Arch. Microbiol.* 185, 172–182.

Rabus, R., Hansen, T. A., and Widdel, F. (2006). "Dissimilatory sulfate- and sulfur-reducing prokaryotes," in *The Prokaryotes*, Vol. 2, eds M. Dworkin, S. Falkow, E. Rosenberg, K.-H. Schleifer, and E. Stackebrandt (New York: Springer), 659–768.

Schink, B. (1997). Energetics of syntrophic cooperation in methanogenic degradation. *Microbiol. Mol. Biol. Rev.* 61, 262–280.

Scholten, J. C., Culley, D. E., Brockman, F. J., Wu, G., and Zhang, W. (2007). Evolution of the syntrophic interaction between *Desulfovibrio vulgaris* and *Methanosarcina barkeri*: Involvement of an ancient horizontal gene transfer. *Biochem. Biophys. Res. Commun.* 352, 48–54.

Sousa, D. Z., Alves, J. I., Alves, M. M., Smidt, H., and Stams, A. J. M. (2009). Effect of sulfate on methanogenic communities that degrade unsaturated and saturated long chain fatty acids (LCFA). *Environ. Microbiol.* 11, 68–80.

Stams, A. J. M. (1994). Metabolic interactions between anaerobic bacteria in methanogenic environments. *Antonie Van Leeuwenhoek* 66, 271–294.

Stams, A. J. M., and Plugge, C. M. (2009). Electron transfer in syntrophic communities of anaerobic bacteria and archaea. *Nat. Rev. Microbiol.* 7, 568–577.

Stolyar, S., Van Dien, S., Hillesland, K. L., Pinel, N., Lie, T. J., Leigh, J. A., and Stahl, D. A. (2007). Metabolic modeling of a mutualistic microbial community. *Mol. Syst. Biol.* 3, 92.

Tang, Y., Pingitore, F., Mukhopadhyay, A., Phan, R., Hazen, T. C., and Keasling, J. D. (2007). Pathway confirmation and flux analysis of central metabolic pathways in *Desulfovibrio vulgaris* Hildenborough using gas chromatography-mass spectrometry and Fourier transform-ion cyclotron resonance mass spectrometry. *J. Bacteriol.* 189, 940–949.

Van Kuijk, B. L. M., and Stams, A. J. M. (1995). Sulfate reduction by a syntrophic propionate- oxidizing bacterium. *Antonie Van Leeuwenhoek* 68, 293–296.

Voordouw, G. (1993). "Molecular biology of the sulfate-reducing bacteria," in *The Sulfate-Reducing Bacteria: Contemporary Perspectives*, eds J. M. Odom and R. Singleton, Jr (New York: The Springer Verlag), 88–130.

Walker, C. B., He, Z., Yang, Z. K., Ringbauer, J. A. Jr, He, Q., Zhou, J., Voordouw, G., Wall, J. D., Arkin, A. P., Hazen, T. C., Stolyar, S., and Stahl, D. A. (2009). The electron transfer system of syntrophically grown *Desulfovibrio vulgaris*. *J. Bacteriol.* 191, 5793–5801.

Wallrabenstein, C., Hauschild, E., and Schink, B. (1994). Pure culture and cytological properties of *Syntrophobacter wolinii*. *FEMS Microbiol. Lett.* 123, 249–254.

Wallrabenstein, C., Hauschild, E., and Schink, B. (1995). *Syntrophobacter pfennigii* sp. nov., new syntrophically propionate-oxidizing anaerobe growing in pure culture with propionate and sulfate. *Arch. Microbiol.* 164, 346–352.

Widdel, F., and Hansen, T. A. (1991). "The sulphate and sulphur-reducing prokaryotes," in *The Prokaryotes*, 2nd Edn, Vol. II, eds M. Dworkin, S. Falkow, E. Rosenberg, K.-H. Schleifer, and E. Stackebrandt (New York: Springer), 583–624.

Winfrey, M. R., and Ward, D. M. (1983). Substrates for sulfate reduction and methane production in intertidal sediments. *Appl. Environ. Microbiol.* 45, 193–199.

Zhang, W., Culley, D. E., Scholten, J. C., Hogan, M., Vitiritti, L., and Brockman, F. J. (2006a). Global transcriptomic analysis of *Desulfovibrio vulgaris* on different electron donors. *Antonie Van Leeuwenhoek* 89, 221–237.

Zhang, W., Culley, D. E., Hogan, M., Vitiritti, L., and Brockman, F. J. (2006b). Oxidative stress and heat-shock responses in *Desulfovibrio vulgaris* by genome-wide transcriptomic analysis. *Antonie Van Leeuwenhoek* 90, 41–55.

Zhang, W., Gritsenko, M. A., Moore, R. J., Culley, D. E., Nie, L., Petritis, K., Strittmatter, E., Camp, D. G. II, Smith, R. D., and Brockman, F. J. (2006c). A proteomic view of *Desulfovibrio vulgaris* metabolism as determined by liquid chromatography coupled with tandem mass spectrometry. *Proteomics* 6, 4286–4299.

Conflict of Interest Statement: The authors declare that the research was conducted in the absence of any commercial or financial relationships that could be construed as a potential conflict of interest.

Received: 18 January 2011; paper pending published: 21 March 2011; accepted: 05 April 2011; published online: 02 May 2011.
Citation: Plugge CM, Zhang W, Scholten JCM and Stams AJM (2011) Metabolic flexibility of sulfate reducing bacteria. Front. Microbio. ***2****:81. doi: 10.3389/fmicb.2011.00081*
This article was submitted to Frontiers in Microbial Physiology and Metabolism, a specialty of Frontiers in Microbiology.

frontiers in
MICROBIOLOGY

ORIGINAL RESEARCH ARTICLE
published: 22 March 2011
doi: 10.3389/fmicb.2011.00051

Regulation of dissimilatory sulfur oxidation in the purple sulfur bacterium *Allochromatium vinosum*

Frauke Grimm, Bettina Franz† and Christiane Dahl*

Institut für Mikrobiologie und Biotechnologie, Rheinische Friedrich-Wilhelms-Universität Bonn, Bonn, Germany

Edited by:
Martin G. Klotz, University of Louisville, USA

Reviewed by:
Niels-Ulrik Frigaard, University of Copenhagen, Denmark
Jan Kuever, Bremen Institute for Materials Testing, Germany

***Correspondence:**
Christiane Dahl, Institut für Mikrobiologie und Biotechnologie, Rheinische Friedrich-Wilhelms-Universität Bonn, Meckenheimer Allee 168, D-53115 Bonn, Germany.
e-mail: chdahl@uni-bonn.de
†Present address:
Bettina Franz, Institut für Medizinische Mikrobiologie und Krankenhaushygiene, Klinikum der Goethe-Universität, Paul-Ehrlich-Straße 40, D-60596 Frankfurt/Main, Germany

In the purple sulfur bacterium *Allochromatium vinosum*, thiosulfate oxidation is strictly dependent on the presence of three periplasmic Sox proteins encoded by the *soxBXAK* and *soxYZ* genes. It is also well documented that proteins encoded in the dissimilatory sulfite reductase (*dsr*) operon, *dsrABEFHCMKLJOPNRS*, are essential for the oxidation of sulfur that is stored intracellularly as an obligatory intermediate during the oxidation of thiosulfate and sulfide. Until recently, detailed knowledge about the regulation of the *sox* genes was not available. We started to fill this gap and show that these genes are expressed on a low constitutive level in *A. vinosum* in the absence of reduced sulfur compounds. Thiosulfate and possibly sulfide lead to an induction of *sox* gene transcription. Additional translational regulation was not apparent. Regulation of *soxXAK* is probably performed by a two-component system consisting of a multi-sensor histidine kinase and a regulator with proposed di-guanylate cyclase activity. Previous work already provided some information about regulation of the *dsr* genes encoding the second important sulfur-oxidizing enzyme system in the purple sulfur bacterium. The expression of most *dsr* genes was found to be at a low basal level in the absence of reduced sulfur compounds and enhanced in the presence of sulfide. In the present work, we focused on the role of DsrS, a protein encoded by the last gene of the *dsr* locus in *A. vinosum*. Transcriptional and translational gene fusion experiments suggest a participation of DsrS in the post-transcriptional control of the *dsr* operon. Characterization of an *A. vinosum* Δ*dsrS* mutant showed that the monomeric cytoplasmic 41.1-kDa protein DsrS is important though not essential for the oxidation of sulfur stored in the intracellular sulfur globules.

Keywords: *Allochromatium vinosum*, *sox* genes, thiosulfate oxidation, anoxygenic phototrophic sulfur bacteria, *dsr* genes, regulation, dissimilatory sulfite reductase, sulfur globules

INTRODUCTION

The ability to utilize reduced sulfur compounds as electron donors for anaerobic phototrophic and aerobic or anaerobic chemotrophic growth is phylogenetically wide-spread (Dahl et al., 2008a). It occurs in organisms residing in environments abundant with sulfide like organic nutrient-rich anoxic sediments or hydrothermal vents. Many environmentally important photo- and chemotrophic sulfur-oxidizing bacteria accumulate globules of polymeric, water-insoluble sulfur as an intermediary product during the oxidation of reduced sulfur compounds such as thiosulfate or sulfide. These sulfur globules are deposited intracellularly, inside the periplasm in many chemotrophic sulfur oxidizers (e.g., *Beggiatoa* species or the bacterial endosymbionts of marine invertebrates like *Riftia pachyptila* or *Calyptogena okutanii*) and also in phototrophic purple sulfur bacteria of the family Chromatiaceae. *Allochromatium vinosum*, a representative of the latter, has been especially well characterized on a molecular genetic level (Dahl, 2008; Frigaard and Dahl, 2009).

It is established that thiosulfate oxidation in this organism is strictly dependent on the presence of three periplasmic Sox proteins encoded by the *soxB*, *soxXAK*, and *soxYZ* genes (Hensen et al., 2006; Welte et al., 2009). These genes are organized in three different transcriptional units (Hensen et al., 2006) within the genome of *A. vinosum* (Acc. No. NC_013851). It is also well documented that proteins encoded by the *A. vinosum* dissimilatory sulfite reductase (*dsr*) genes, *dsrABEFHCMKLJOPNRS*, are essential for the oxidation of sulfur stored intracellularly as an obligatory intermediate during the oxidation of sulfide and thiosulfate (Pott and Dahl, 1998; Dahl et al., 2005; Sander et al., 2006).

Until recently, detailed knowledge about the regulation of these two important enzyme systems was not available. We started to fill this gap and showed that the *dsr* genes are expressed in a reduced sulfur compound-dependent manner (Grimm et al., 2010b). In *A. vinosum*, the expression of most of the 15 *dsr* genes is at a low basal level in the absence of reduced sulfur compounds and greatly enhanced in the presence of sulfide. Real-time-PCR experiments suggested that the genes *dsrC* and *dsrS* are not only expressed from the main *dsr* promoter but also from secondary internal promoters, pointing at a special function of the encoded proteins. DsrC was identified as a potential DNA-binding protein (Grimm et al., 2010b). An *A. vinosum* Δ*dsrR* deletion strain showed a significantly reduced sulfur oxidation rate that was fully restored upon complementation with *dsrR in trans*. Immunoblot analyses revealed a reduced level of DsrE and DsrL in the Δ*dsrR* strain. These proteins are absolutely essential for sulfur oxidation. Transcriptional and translational gene fusion experiments suggested a participation of DsrR in the post-transcriptional control of the *dsr* operon (Grimm et al., 2010a).

Much less is currently known about regulation of thiosulfate oxidation. The most detailed information regarding *sox* gene regulation is available for the chemotrophic sulfur oxidizer *Paracoccus pantotrophus*. It should be noted that in this organism thiosulfate oxidation does not proceed along exactly the same pathway as in *A. vinosum*. *P. pantotrophus* contains an additional Sox protein, the sulfane dehydrogenase SoxCD (Zander et al., 2010), and oxidizes thiosulfate to sulfate without the formation of sulfur globules as an intermediate. In *P. pantotrophus*, two genes, *soxR* and *soxS*, are divergently oriented to the other *sox* genes, *soxVWXYZA–H*. SoxR, a transcriptional regulator of the ArsR family, has been shown to act as a repressor of *sox* gene expression in the absence of thiosulfate. SoxS appears to be a periplasmic thioredoxin and is essential for full *sox* gene expression (Rother et al., 2005). In *A. vinosum* neither *soxR* nor *soxS* homologs are present. Information on *sox* gene regulation in this model organism has so far been restricted to the finding by Hensen et al. (2006) that SoxA is produced in higher amounts during photolithoautotrophic as compared to photoorganoheterotrophic growth.

In the present work, we therefore set out to provide more detailed information on *sox* gene regulation in a purple sulfur bacterium at the molecular biological level via RT-PCR and translational gene fusions. Furthermore, we analyzed *dsr* gene regulation in *A. vinosum* in more detail and assessed the role of the *dsrS* encoded protein in this context.

MATERIALS AND METHODS

BACTERIAL STRAINS, PLASMIDS, MEDIA, AND GROWTH CONDITIONS

The strains and plasmids used in this study are listed in **Table 1**. *A. vinosum* was grown and harvested as described (Dahl et al., 2008b). Antibiotics were used at the following concentrations (in μg mL^{-1}): for *Escherichia coli*, kanamycin, 50; ampicillin, 100; for *A. vinosum*, kanamycin, 10; rifampicin, 50.

OVERPRODUCTION AND PURIFICATION OF RECOMBINANT DsrS

DsrS was overproduced with an amino-terminal His-tag in *E. coli* BL21(DE3) cells containing pDsrS-N (**Table 1**). The cells were cultured in 500 mL LB medium containing 100 μg ampicillin mL^{-1} at 25°C and 180 r.p.m. At an $OD_{600\,nm}$ of 0.5, 2 μM IPTG was added and the cells were harvested after 3 h. The pellet was resuspended in 50 mM NaH_2PO_4, 300 mM NaCl, and 10 mM imidazole, pH 7.5, including Complete protease inhibitor cocktail, EDTA-free (Roche), and 1 mg lysozyme mL^{-1}. The cells were disrupted by sonication (2 min mL^{-1}, Cell Disruptor B15, Branson) and centrifuged at 10000*g* for 30 min at 4°C. The N-terminally His-tagged DsrS was mainly found in the pellet, though solubility was improved by a low growth temperature (25°C). The supernatant containing soluble DsrS was purified using a nickel agarose column (Qiagen) followed by dialysis against 50 mM Tris–HCl (pH 7.5), 300 mM NaCl. The protein was concentrated to a final volume of no more than 2 mL via Centriprep-10 (Amicon). The state of oligomerization of the protein was investigated by gel filtration chromatography on a Superdex-200 column (GE Healthcare) equilibrated with 50 mM Tris–HCl (pH 7.5), 300 mM NaCl.

CONSTRUCTION, CHARACTERIZATION, AND COMPLEMENTATION OF AN *A. VINOSUM* Δ*dsrS IN FRAME* DELETION STRAIN

All general molecular genetic techniques, as well as the method for achieving and complementing *in frame* deletions in *A. vinosum*, were described earlier (Dahl et al., 2008b). The primers SXbaf1, srev1, Sfor1, and sXbar1 were utilized for the construction of the *dsrS* deletion and the primer pair DsrSNhef1 and TermDsrXbar1 was used to amplify the *dsrS* gene for the complementation of the deletion strain (**Table 2**). Photolithoautotrophic growth of *A. vinosum* strains was examined in batch culture under continuous illumination essentially as described by Prange et al. (2004) in a medium containing sulfide as the sole sulfur compound. 250 mL of a photoheterotrophically grown stationary-phase culture were harvested (5900*g*, 10 min) and the cell material was used to inoculate 1 L of modified Pfennig's medium (Dahl et al., 2008b) in a thermostatted fermenter. Sulfur compounds were determined as described in (Dahl et al., 2008b). Sodium dodecyl sulfate-polyacrylamide gel electrophoresis (SDS-PAGE) and Immunoblot (Western) analyses were performed as described in Dahl et al. (2005).

EXPRESSION STUDIES BY RT-PCR

Cells were harvested in the stationary growth phase and used to inoculate the modified "Pfennig's" medium described in Dahl et al. (2008b) supplemented with either 2 mM malate, 2 mM sulfide, 2 mM thiosulfate, or 5 mM sulfite. In case of the experiments concerning *dsr* genes, cells were harvested for RNA isolation 3 h after inoculation. At that time the maximum content of intracellular sulfur is achieved and its oxidation commences (Grimm et al., 2010b). For experiments concerning *sox* genes, cells were harvested 30 min, 1 h, and 3 h after inoculation into medium containing sulfide, thiosulfate, and sulfite, respectively because cells exhibited high and constant substrate oxidation rates around these time points. Total RNA of *A. vinosum* Rif50, *A. vinosum* Δ*dsrS*, and *A. vinosum soxB*::Ω-Km was isolated and the concentration was determined as described in Prange et al. (2004). 250 ng of total RNA were used as template in RT-PCR analysis via the QuantiTect SYBR Green RT-PCR kit (Qiagen) and the iCycler iQ real-time detection system (Bio-Rad) according to the manufacturers' instructions. "No RT" control reactions were performed for each RNA sample. In case of DNA contamination, the RNA samples were digested with RNase-free DNase (Qiagen) and purified using RNeasy Mini Kit (Qiagen). Fragments of approximately 200 bp were amplified in all cases (*dsrA*: 215, *dsrE*: 217, *dsrC*: 196, dsrL: 186, *dsrR*: 181, *dsrS*: 172, *soxB*: 167, *soxX*: 163, *soxY*: 180 bp) following established protocols (Grimm et al., 2010b) and using primers listed by Grimm et al. (2010b) and in **Table 2**. RNA standards were generated as described in Fey et al. (2004). The samples were automatically quantified by the iCycler iQ software (Bio-Rad) based on the RNA standards. The absence of non-specific PCR products and primer–dimers that would otherwise contribute to the fluorescence signal was confirmed by melting curve analysis as described in Grimm et al. (2010b). The PCR products were furthermore analyzed by agarose gel electrophoresis. To guarantee comparability, the levels of *dsr* and *sox* gene expression were measured by absolute quantitative RT-PCR using gene-specific RNA standards in every run. It was assumed that the PCR efficiency did not vary in a single run between the samples and the *in vitro* transcribed RNA fragments, containing the target sequence that served as external standards. Variations in PCR efficiencies between different runs or different target genes were taken into account by quantifying the samples using the run-specific standard curve that allows for variations of reagents, primers, and sequence etc. The gene-specific RNA standards yielded calibration curves of high linearity in all cases (correlation coefficient >0.990).

Table 1 | Bacterial strains and plasmids.

Strains, primers, plasmids	Genotype, phenotype, or sequence	Source or reference
***ESCHERICHIA COLI* STRAINS**		
DH5α	F⁻Φ80d*lacZ*ΔM15Δ(*lacZYA-argF*)*U169 recA1 endA1 hsdR17* (r_K^- m_K^+) *supE44*λ⁻*thi-1 gyrA relA1*	Hanahan (1983)
S17-1	294 (*recA pro res mod*⁺) Tp^r Sm^r (pRP4-2-Tc::Mu-Km::Tn7)	Simon et al. (1983)
BL21(DE3)	F⁻*ompT hsdS*$_B$ (r_B^- m_B^-) *gal dcm met* (DE3)	Novagen
***ALLOCHROMATIUM VINOSUM* STRAINS**		
Rif50	Rif^r, spontaneous rifampicin-resistant mutant of *A. vinosum* DSM 180^T	Lübbe et al. (2006)
Δ*dsrS*	Rif^r, Δ*dsrS* (deletion: 645 bp of the *dsrS* gene)	This work
*soxB*ΩKm	Km^r, *soxB*::ΩKm in *A. vinosum* DSM 180^T	Hensen et al. (2006)
PLASMIDS		
pET-15b	Ap^r, His-Tag (N-terminal)	Novagen
pDsrS-N	Ap^r, *Nde*I–*Xho*I fragment of PCR-amplified *dsrS* in pET-15b	This work
pK18*mobsacB*	Km^r, Mob$^+$, *sacB*, *oriV*, *oriT*, *lacZ*α	Schäfer et al. (1994)
pPHU235	Tc^r, broad-host-range lacZ fusion vector	Hübner et al. (1991)
pPHU236	Tc^r, broad-host-range lacZ fusion vector	Hübner et al. (1991)
pK235	Km^r, Mob$^+$, *sacB*, *oriV*, *oriT*, *lacZ*α, *Eco*RI–*Sal*I fragment (promoterless *lacZ*) of pPHU235 in *Hin*dIII–*Eco*RI-digested pK18*mobsacB*	This work
pK236	Km^r, Mob$^+$, *sacB*, *oriV*, *oriT*, *lacZ*α, *Eco*RI–*Sal*I fragment (promoterless *lacZ*) of pPHU236 in *Hin*dIII–*Eco*RI of pK18*mobsacB*	This work
pK235–*soxB*	Km^r, Mob$^+$, *sacB*, *oriV*, *oriT*, *lacZ*α, *Pst*I–*Hin*dIII-PCR fragment (primers lacZp_soxB_for and lacZp_soxB_rev) of *soxB* promoter region in *Pst*I–*Hin*dIII of pK235	This work
pK235–*soxX*	Km^r, Mob$^+$, *sacB*, *oriV*, *oriT*, *lacZ*α, *Pst*I–*Hin*dIII-PCR fragment (primers lacZp_soxX_for and lacZp_soxX_rev) of *soxX* promoter region in *Pst*I–*Hin*dIII of pK235	This work
pK236–*soxY*	Km^r, Mob$^+$, *sacB*, *oriV*, *oriT*, *lacZ*α, *Pst*I–*Hin*dIII-PCR fragment (primers lacZp_soxY_for and lacZp_soxY_rev) of *soxY* promoter region in *Pst*I–*Hin*dIII of pK236	This work
pK18*mobsacB*ΔdsrS	Km^r, *Xba*I fragment of PCR-amplified genome region around *dsrS* with 645 bp deletion of *dsrS* sequence	This work
pBBR*dsr*PT–*dsrS*	Km^r, *Nhe*I–*Xma*JI fragment of PCR-amplified *dsrS* in *Nhe*I–*Xma*JI of pBBR*dsr*PT1	This work
pTS	Km^r, *Pst*I–*Hin*dIII fragment of PCR-amplified *lacZ* including rbs in *Pst*I–*Hin*dIII of pKdsrProm	Grimm et al. (2010b)
pTL	Km^r, *Pst*I–*Hin*dIII fragment of PCR-amplified *dsr* promoter region including the first 12 bp of *dsrA* in *Pst*I–*Hin*dIII of pK235	Grimm et al. (2010b)

CONSTRUCTION OF TRANSCRIPTIONAL AND TRANSLATIONAL REPORTER GENE FUSIONS

DNA fragments of 1074, 1046, and 733 bp encompassing the probable *soxB*, *soxX*, and *soxY* promoter regions, respectively, including the first 12 or 15 bp of the respective gene were amplified using primers that introduced *Pst*I and *Hin*dIII restriction sites. *A. vinosum* Rif50 chromosomal DNA served as a template. The fragments were introduced into plasmids pK235 or pK236 yielding plasmids pK235–*soxB,* pK235–*soxX*, and pK236–*soxY* (**Table 1**). Plasmids pK235 and pK236 were constructed by excising the promoterless *lacZ* gene with *Sal*I and *Eco*RI from the translational fusion vectors pPHU235 or pPHU236 (Hübner et al., 1991), respectively. The *Sal*I sites were filled in with the Klenow fragment of DNA polymerase. The fragments were then inserted into the 5670-bp *Eco*RI/*Hin*dIII fragment of pK18*mobsacB*.

Plasmids pK235–*soxB,* pK235–*soxX*, and pK236–*soxY* as well as the transcriptional gene fusion plasmid pTS (**Table 1**; Grimm et al., 2010b), containing a fusion of the *lacZ* gene to the *dsr* promoter $dsrA_p$ region without the Shine–Dalgarno sequence of *dsrA*, and the translational gene fusion plasmid pTL (**Table 1**; Grimm et al., 2010b), containing the $dsrA_p$ region including the first 12 bp of *dsrA* fused to the *lacZ* gene, were transferred into *A. vinosum* Rif50 by conjugation as described in Pattaragulwanit and Dahl (1995) and integrated into the genome via single-crossover. The plasmid carrying strains were grown on 12 mL modified Pfennig's medium containing 2 mM thiosulfate, 2 mM sulfide, 2 mM malate, 5 mM sulfite, or combinations thereof for 24 h under continuous illumination before β-galactosidase activity was tested as described in Grimm et al. (2010b). *A. vinosum* wild type did not exhibit any β-galactosidase activity.

SEQUENCE ANALYSIS

Promoter prediction for prokaryotic sequence was achieved with Neural Network Promoter Prediction[1] and BPROM[2]. The online version of the program REPuter[3] was used for detection of inverted or direct repeats in the nucleotide sequence upstream of *dsrA*. All amino acid sequences were obtained from GenBank. PSI-BLAST was used with default parameters to generate the protein sequence

[1]http://www.fruitfly.org/seq_tools/promoter.html

[2]http://www.softberry.com/berry.phtml

[3]http://bibiserv.techfak.uni-bielefeld.de/reputer

Table 2 | PCR primers.

PCR primers	Sequence	Source or reference
***dsrS:* CLONING IN PET-15B**		
DsrSNdef1	5′-TGTCCGGCATATGGACCTCAGTCACGAG-3′	This work
DsrSXhor3	5′-ATCGACGCCTCGAGCTAATCCCGGTCC-3′	This work
DELETION OF *dsrS*		
SXbaf1	5′-ATCTGTTGTCTAGATACAGCCATCTGCGC-3′	This work
srev1	5′-AGACCTCAGCGATTCGTCCATGATCCGGA-3′	This work
Sfor1	5′-TCCGGATCATGGACGAATCGCTGAGGTCT-3′	This work
sXbar1	5′-GCATCCAATCTAGATTGAGCACTGGCACG-3′	This work
COMPLEMENTATION		
TermDsrXbar1	5′-AGATCTGTCTAGAATCGTGCAACGCTCAGC-3′	This work
DsrSNhef1	5′-GCGTGTCGCTAGCATGGACCTCAGTCA-3′	This work
TRANSLATIONAL *sox* GENE FUSIONS		
lacZp_soxB_for	5′-ATCCTCCTGGGCATCGGTTAAAGCTTTTGTTC-3′	This work
lacZp_soxB_rev	5′-CAGCGAGGGTAGTGGTTCATGTCGACGATGGC-3′	This work
lacZp_soxX_for	5′-ACCTCTGTCGACTTGATGACGTAAGGCTCGAA-3′	This work
lacZp_soxX_rev	5′-CGAAATCTCCTCTCGATCATAAGCTTTGACGT-3′	This work
lacZp_soxY_for	5′-GCATAGGTCGACAATTCCTGCGCACCCATC-3′	This work
lacZp_soxY_rev	5′-TTTGCGTTTGGCTTCGCGAAGCTTTTCTTC-3′	This work
RT-PCR		
RNA–soxB-std-for	5′-TAATACGACTCACTATAGGGAGATCCATGACGCCGACGAA-3′	This work
RNA–soxB-std-rev	5′-CTGCTGCATATCACCGACAC-3′	This work
RNA–soxX-std-for	5′-TAATACGACTCACTATAGGGAATCGATCGCTATCCACCAC-3′	This work
RNA–soxX-std-rev	5′-CAGCGAGGGTAGTGGTTCAT-3′	This work
RNA–soxY-std-for	5′-TAATACGACTCACTATAGGGCGCAAAGACAAGAGAGGAGA-3′	This work
RNA–soxY-std-rev	5′-TGACTTCGTTGGTCTTGCTG-3′	This work
RNA–soxB-for	5′-GATGACGTAAGGCTCGAAGG-3′	This work
RNA–soxB-rev	5′-AGTTCACCTATGGCGACGAG-3′	This work
RNA–soxX-for	5′-GACCTTCCCGACGACCTC-3′	This work
RNA–soxX-rev	5′-GTGTGAAAGCTTGACGTTCAACGGCATGCG-3′	This work
RNA–soxY-for	5′-GGCGTCACTTCCATCAGTCT-3′	This work
RNA–soxY-rev	5′-GACGCTCTTGGCGTTCTTAT-3′	This work

family (Altschul et al., 1997). Putative helix-turn-helix motives were identified using GYM2.0 (Gao et al., 1999; Narasimhan et al., 2002) and Helix-turn-Helix Motif Prediction (Combet et al., 2000).

RESULTS

REGULATION OF *SOX* GENES IN *A. VINOSUM*

In *A. vinosum*, the *soxXAKL* genes (Hensen et al., 2006; Welte et al., 2009) form a transcriptional unit that may also include gene Alvin_2172 (formerly ORFb) located immediately downstream of *soxL* (**Figure 1**). Alvin_2172 encodes a conserved hypothetical protein predicted to be soluble and to reside in the cytoplasm. A typical Cys-X_2-Cys thioredoxin motif and a typical heme *c*-binding Cys-X_2-Cys-His binding motif are present. An inverted repeat with a potential for formation of a hairpin loop structure in the corresponding mRNA was found within the nucleotide sequence of the downstream gene Alvin_2173 (formerly ORFc) by Hensen et al. (2006) and proposed to function as a site for transcription termination. A second predicted transcriptional unit comprises the gene *soxB* and probably also includes Alvin_2166 (formerly ORFa). These genes are located upstream of *soxX* and are divergently transcribed. The product of Alvin_2166 is a putative multi-sensor histidine kinase. The corresponding putative response regulator is encoded by gene Alvin_2165. The genes *soxYZ* (Alvin_2111 and 2112) are not found in the vicinity of the other *sox* genes and are located in a third independent transcriptional unit (Hensen et al., 2006; **Figure 1**).

Transcriptional regulation of sox genes

When reconstituted *in vitro*, the *P. pantotrophus* Sox proteins do not only oxidize thiosulfate but also accept hydrogen sulfide, sulfur (or polysulfide), and also sulfite as substrates. In addition, it has been shown for *P. pantotrophus* and for the phototrophic alphaproteobacterial *Rhodovulum sulfidophilum* that the Sox system is not only essential for thiosulfate oxidation but is also strictly required for the oxidation of sulfide *in vivo* (Chandra and Friedrich, 1986; Wodara et al., 1994; Appia-Ayme et al., 2001). This prompted us to investigate expression of the *A. vinosum* genes *soxB*, *soxX*, and *soxY* during photoorganoheterotrophic growth with malate and photolithoautotrophic growth with thiosulfate, sulfide, or sulfite using quantitative RT-PCR with absolute standards. **Table 3** shows

a constitutive expression for all three genes during growth with malate in the absence of reduced sulfur compounds. When *A. vinosum* was grown in the presence of 2 mM thiosulfate as electron donor, the expression levels increased six and fourfold for *soxB* and *soxX*, respectively, and 23-fold for *soxY*. The presence of sulfide also induced the expression of the *sox* genes, albeit to a lesser extent. It can currently not be excluded that this is a secondary effect caused by the formation of thiosulfate from sulfide. It has been repeatedly reported that *A. vinosum* produces thiosulfate during growth with sulfide as electron donor (Steudel et al., 1990; Franz et al., 2009). Expression levels for all three studied *sox* genes were not increased by the presence of 5 mM sulfite as compared to growth on malate (**Table 3**).

Translational gene fusions

As the next step, we investigated expression of the three *sox*-genes also on the translational level by determining the specific β-galactosidase activity of Sox–LacZ fusion proteins (**Table 4**). All three Sox–LacZ fusion proteins showed a basal level activity during photoorganoheterotrophic growth with malate. When *A. vinosum* grew with 2 mM thiosulfate as an electron donor, specific β-galactosidase activity clearly increased and increasing thiosulfate concentrations led to even higher activities (**Table 5**). In contrast to the situation on the transcriptional level, sulfide did not induce significantly higher specific β-galactosidase activity of any of the Sox–LacZ fusion proteins. This effect might be caused by the different sensitivities of the assays. A formation of up to 0.15 mM thiosulfate has been documented when *A. vinosum* grows with 2 mM sulfide (Franz et al., 2009). While this rather low thiosulfate concentration may lead to an increase of transcription rates detectable by RT-PCR, the effect on the translational level may not cause increases of specific β-galactosidase activities significantly above the experimental error range. In coincidence with the RT-PCR results, the presence of 5 mM sulfite led to specific β-galactosidase activities comparable to those obtained during photoorganoheterotrophic growth, i.e., in contrast to thiosulfate sulfite does not induce *sox* gene expression in *A. vinosum*.

Proteins encoded by Alvin_2166 and Alvin_2165 as potential regulators of sox gene expression

The protein encoded by *A. vinosum* gene Alvin_2166 is homologous to multi-sensor histidine kinases from various proteobacteria. The protein is predicted to reside in the cytoplasm and shows a complex organization with several predicted conserved

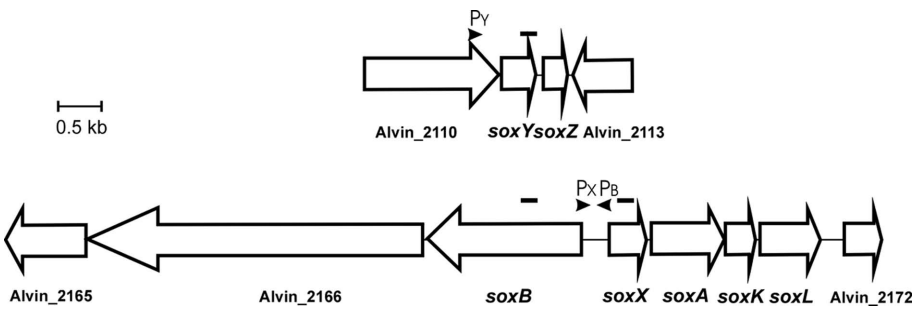

FIGURE 1 | Schematic overview of the two *sox* gene loci in *A. vinosum*. The location of potential promoters for *soxB, soxX,* and *soxY* is indicated. Amplicons generated for RT-PCR are indicated by black bars above the genes.

Table 3 | Expression levels of three *sox* genes under photoorganoheterotrophic (malate) and photolithoautotrophic (thiosulfate, sulfide, or sulfite) conditions determined by RT-PCR.

Electron donor	Copy number[a]		
	soxB	***soxX***	***soxY***
***ALLOCHROMATIUM VINOSUM* WILD TYPE**			
2 mM malate	$1.86 \times 10^7 \pm 1.20 \times 10^7$	$2.80 \times 10^7 \pm 1.16 \times 10^6$	$4.11 \times 10^7 \pm 2.00 \times 10^7$
2 mM thiosulfate	$1.15 \times 10^8 \pm 5.69 \times 10^6$	$1.08 \times 10^8 \pm 2.33 \times 10^7$	$9.39 \times 10^8 \pm 5.39 \times 10^7$
2 mM sulfide	$9.00 \times 10^7 \pm 2.26 \times 10^7$	$8.05 \times 10^7 \pm 1.88 \times 10^7$	$5.22 \times 10^8 \pm 8.34 \times 10^7$
5 mM sulfite	$1.81 \times 10^7 \pm 1.91 \times 10^6$	$1.68 \times 10^7 \pm 3.54 \times 10^6$	$5.17 \times 10^7 \pm 6.08 \times 10^6$
***A. VINOSUM soxB*::Ω-KM**			
2 mM malate	–	$4.12 \times 10^8 \pm 2.16 \times 10^8$	$3.63 \times 10^8 \pm 4.10 \times 10^7$
2 mM thiosulfate	–	$6.76 \times 10^8 \pm 2.40 \times 10^7$	$6.32 \times 10^8 \pm 7.99 \times 10^7$

The RNAs were isolated from A. vinosum wild type and the mutant soxB:: Ω*Km which carries an interposon causing a transcriptional and translational block in soxB. Samples of 250 ng RNA were used as template. Quantified external RNA fragments containing the target sequence served as standard. The results represent the means and standard deviations of two experiments.*

[a]*Numbers are given as copies per 250 ng RNA.*

domains specific for multi-sensor hybrid histidine kinases. At the N-terminus two PAS domains (cd00130) are located followed by a HisKA domain (cd00082), a HATPase_c domain (cd00075), and two carboxy-terminal REC domains (cd00156). Both PAS domains contain a Cys-X_2-Cys motif indicating a redox signal as a stimulus for the sensing domain of the putative histidine kinase. The protein encoded by Alvin_2165 shows homology to response regulators of two-component systems from various proteobacteria. It is also predicted to be a cytoplasmic protein and contains a conserved REC domain at the N-terminus and a GGDEF domain typical for di-guanylate cyclases at the C-terminus (cd01949; Chan et al., 2004). A helix-turn-helix motif is not predicted for Alvin_2165 indicating a role of cyclic di-GMP as a second messenger (Römling and Amikam, 2006) in the regulation of the *sox* genes in *A. vinosum*. Homologs of Alvin_2166 and Alvin_2165 are also present in two other sulfur oxidizers, namely *Halorhodospira halophila* SL1, a purple sulfur bacterium of the family Ectothiorhodospiraceae, and *Magnetococcus* sp. MC-1. In both organisms, however, the corresponding genes are not located in immediate vicinity of *sox* genes.

In order to find some experimental evidence for a role of the proteins encoded by Alvin_2166 and Alvin_2165 in *sox* gene regulation, transcription of *soxX* and sox*Y* was investigated in the *A. vinosum* mutant strain *soxB*::Ω-Km (Hensen et al., 2006). This strain carries an insertion of a polar Ω kanamycin resistance cassette (Frey and Krisch, 1985; Fellay et al., 1987) in *soxB* preventing the transcription of *soxB* and genes located downstream in the same transcriptional unit. **Table 3** shows the transcription rates of *soxX* and *soxY* in mutant *soxB*::Ω-Km as compared to those in the wild type. The expression levels of both genes were found to be significantly higher (about 10-fold increase in each case) in mutant *soxB*::Ω-Km than in the wild type during growth with malate in the absence of thiosulfate. The presence of 2 mM thiosulfate did not lead to increased expression levels of *soxY* and *soxX* in the mutant strain, i.e., the induction by thiosulfate observed for the wild type was lost in the mutant very probably due to the deleterious effect of the interposon on the formation of the Alvin_2166-encoded regulatory protein. This interpretation gains further support in case of *soxX* gene regulation by our finding that the basal level of expression was unaffected as compared to the wild type and induction of transcription by thiosulfate still observable in strain *A. vinosum* Δ*soxY* carrying an *in frame* deletion of the *soxY* gene (data not shown).

FURTHER INSIGHTS INTO REGULATION OF PURPLE BACTERIAL *dsr* GENES: ROLE OF DsrS

The only known gene region responsible for the oxidation of stored zero-valent sulfur is the *dsr* gene cluster (Dahl et al., 2008b; Grimm et al., 2008; Frigaard and Dahl, 2009; Sander and Dahl, 2009). In *A vinosum*, the first sulfur-oxidizing bacterium for which the *dsr* genes were described, this cluster encompasses 15 genes (*dsrABEFHCMKJLOPNRS*; Pott and Dahl, 1998; Dahl et al., 2005). The first two genes, *dsrAB*, encode a key enzyme of this pathway, the reverse-acting *dsr*. Comparison with the *dsr* sequences of other sulfur-oxidizing bacteria showed the genes *dsrABEFHCMKLJOPN* to be the core unit of the operon, present in all sulfur-oxidizing bacteria that form sulfur globules as an intermediate (Sander et al., 2006). While the proteins encoded by the core *dsr* genes have been the subject of a number of recent studies (Pott and Dahl, 1998; Dahl et al., 2005; Lübbe et al., 2006; Sander et al., 2006; Cort et al., 2008), hardly anything is known about *dsrS*, the last gene of the *A. vinosum dsr* operon.

Properties of DsrS and occurrence of the gene

The *dsrS* gene is predicted to encode a soluble cytoplasmic protein with a molecular mass of 41.1 kDa (Dahl et al., 2005). Neither conserved domains nor motifs are present in the sequence and significant similarities to proteins of known function are not apparent. Recombinant DsrS was purified from *E. coli* and its oligomerization state was investigated by gel filtration chromatography. DsrS eluted as a monomer and the sequence deduced mass of 43.3 kDa for the recombinant protein was confirmed (data not shown). UV–Vis spectra did not indicate the presence of any cofactors.

In fact, *A. vinosum* is so far the only organism in which *dsrS* is part of the *dsr* gene cluster. In other sulfur-oxidizing bacteria the gene is either absent [green sulfur bacetria (e.g. *Chlorobium tepidum* TLS, NC_002932, complete genome; *Chlorobium limicola* DSM 245, NC_010803, complete genome; *Chlorobaculum parvum* NCIB 8327, NC_011027, complete genome), *Halorhodospira halophila* SL1 (NC_008789, complete genome)] or located elsewhere in the genome [*Thiobacillus denitrificans* (NC_007404, complete genome), *Beggiatoa* sp. PS (NZ_ABBZ00000000, whole genome draft sequence), *Thioalkalivibrio* sp. HL-EbGR7 (NC_011901, complete genome), and endosymbionts Candidatus *Vesicomyosocius okutanii* HA (NC_009465, complete genome) and Candidatus *Ruthia magnifica* str. Cm (NC_008610, complete genome)]. Thus, the question arose whether the protein encoded by *dsrS* is at all

Table 4 | Expression of translational *sox* gene fusions in *A. vinosum*.

Electron donor	Specific β-galactosidase activity		
	soxB′–lacZ	*soxX′–lacZ*	*soxY′–lacZ*
2 mM malate	12.13 ± 1.34	15.67 ± 0.56	55.91 ± 13.37
2 mM thiosulfate	17.28 ± 3.15	25.14 ± 1.03	160.34 ± 27.03
2 mM sulfide	8.50 ± 2.33	13.37 ± 0.66	46.67 ± 26.67
2 mM sulfite	8.69 ± 3.40	11.25 ± 1.45	38.06 ± 14.29

The specific β-galactosidase activity is given as nmol o-nitrophenol min^{-1} (mg protein)$^{-1}$. The average protein content was 500 µg mL^{-1}. The results represent the means and standard deviation of three independent measurements.

Table 5 | Dependence on thiosulfate concentration of specific β-galactosidase activity of Sox–LacZ fusion proteins in *A. vinosum*.

Thiosulfate [mM]	Specific β-galactosidase activity		
	soxB′–lacZ	*soxX′–lacZ*	*soxY′–lacZ*
0.5	10.15 ± 0.81	20.02 ± 3.50	50.29 ± 8.18
2	17.28 ± 3.15	25.14 ± 1.03	160.34 ± 27.03
5	21.05 ± 4.32	80.24 ± 11.51	172.10 ± 9.17
10	39.52 ± 3.83	109.74 ± 10.54	216.35 ± 14.00
20	57.78 ± 3.44	135.08 ± 4.77	291.71 ± 17.32

Experimental details cf. **Table 4.**

involved in sulfur oxidation. We constructed and characterized an *A. vinosum* Δ*dsrS in frame* deletion mutant to answer this question and studied the effect of the gene deletion on transcription and translation of the *dsr* genes.

Construction, phenotypic characterization, and complementation of a Δ*dsrS A. vinosum in frame deletion strain*

To assess the importance of DsrS for sulfur oxidation we constructed an *A. vinosum* strain with *in frame* deletion of *dsrS*. In order to examine the phenotype of *A. vinosum* Δ*dsrS*, we cultivated the strain photolithoautotrophically in batch culture with 2 mM sulfide as electron source. As expected for a classical purple sulfur bacterium like *A. vinosum* (Brune, 1995), sulfide was immediately oxidized to zero-valent sulfur that was stored in periplasmic sulfur globules. During the oxidation of sulfide to sulfur of oxidation state zero, two different polysulfides are formed as intermediates by *A. vinosum* wild type (Prange et al., 2004). The exact chain length of the polysulfides formed is not known (Prange et al., 2004; Franz et al., 2009). The formation of both polysulfides was not affected in the Δ*dsrS* mutant (not shown). Neither the sulfide oxidation rate, the rate of sulfur globule formation nor the growth yield were affected by the deletion of *dsrS* (**Table 6**). When sulfide is depleted, *A. vinosum* further metabolizes stored sulfur to sulfate that is excreted into the medium. The Δ*dsrS* mutant was clearly still able to completely perform this pathway and formed sulfate as the end product, however, compared to the wild type it exhibited a specific sulfur oxidation rate that was significantly reduced by ~30% (**Table 6**). Complementation of the *A. vinosum* Δ*dsrS* strain with *dsrS in trans* under the control of the main *dsr* promoter $dsrA_p$ did not restore the wild type oxidation rate, but further reduced the sulfur oxidation rate to 45% of the wild type rate (**Table 6**).

In order to find an explanation for the observed phenotypes we performed comparative immunoblot analysis of *A. vinosum* wild type and Δ*dsrS* soluble cell fractions (**Figure 1**). These did not reveal any apparent influence of the lack of DsrS on the formation of the proteins DsrE and DsrL. These proteins are known to be essential for sulfur oxidation (Lübbe et al., 2006; Dahl et al., 2008b). Interestingly, the formation of DsrE and DsrL appeared to be disturbed in the Δ*dsrS* + *dsrS* complementation strain. Both of these proteins were hardly detectable in cells harvested while they were still oxidizing internal sulfur globules (**Figure 2**). In a later phase of sulfur oxidation, however, when sulfur globules had essentially vanished from the cells, both proteins were apparently no longer adversely affected. At that point, the same or even higher amounts of both proteins were detected in the Δ*dsrS* + *dsrS* strain as compared to the wild type or the Δ*dsrS* mutant (**Figure 2**). One likely explanation for these observations is that formation of DsrE and DsrL and possibly also other Dsr proteins is delayed in the complementation strain.

Table 6 | Characteristics of the *A. vinosum* Δ*dsrS* deletion mutant compared to the wild type and the complementation mutant.

Parameter	*A. vinosum* strain		
	Wild type	Δ*dsrS*	Δ*dsrS* + *dsrS*
Specific sulfide oxidation rate[a]	199.0 ± 18.2	210.4 ± 2.6	196.9 ± 9.9
Specific sulfur globule formation rate[a]	90.7 ± 0.6	91.6 ± 3.3	88.9 ± 9.1
Specific sulfur oxidation rate[a]	24.1 ± 0.3	17.5 ± 0.2	10.8 ± 0.9
Growth yield[b]	8.8 ± 0.9	8.9 ± 0.5	8.9 ± 0.5

The results represent the means and standard deviations of three independent growth experiments.
[a]Oxidation and formation rates are given as nmol min^{-1} (mg protein)$^{-1}$.
[b]The growth yield is given as g protein (mol sulfide)$^{-1}$.

Transcription of A. vinosum dsr genes is not affected by deletion of dsrS

We took a closer look at the transcript levels of several *dsr* genes via RT-PCR (**Figure 3**). In the wild type, the gene *dsrS* exhibited an enhanced expression under sulfur-oxidizing conditions, thus confirming the involvement of DsrS in sulfur oxidation. Interestingly, *dsrS* is transcribed at rates similar to those observed for the constitutively expressed gene *dsrC* (**Figure 3**). Furthermore, it has been previously observed that *dsrC* as well as *dsrS* are still transcribed in the *A. vinosum* interposon mutant 21D that carries a transcriptional and translational block in *dsrB* thus abolishing the expression of downstream genes transcribed from the *dsrA* promoter (Pott and Dahl, 1998; Grimm et al., 2010b). The high transcription levels of *dsrS* and the similarity to the transcription pattern of *dsrC*, for which a secondary promoter has already been postulated (Pott and Dahl, 1998), suggest a possible secondary internal promoter also for *dsrS*. Indeed, *in silico* analyses of the sequence upstream of *dsrS* using the online tools Neural Network Promoter Prediction and BPROM revealed potential promoter sequences in the region of *dsrNR* (**Figure 3**).

Effect of dsrS deletion on the transcriptional and post-transcriptional level

In an attempt to find an explanation for the reduced sulfur oxidation rate of the *A. vinosum* Δ*dsrS* strain we introduced *lacZ* reporter gene fusions into the Δ*dsrS* mutant strain and the wild

Table 7 | Expression of transcriptional and translational gene fusions.

A. vinosum strain[a]	Specific β-galactosidase activity[b]	
	Malate	Sulfide
WILD TYPE		
$dsrA_p$–*lacZ*	2.9 ± 0.7	9.1 ± 0.9
dsrA′–lacZ	42.6 ± 1.7	96.2 ± 27.1
Δ*dsrS*		
$dsrA_p$–*lacZ*	2.8 ± 0.3	8.8 ± 1.9
dsrA′–lacZ	26.1 ± 4.2	65.0 ± 2.1

[a]Photoorganoheterotrophically grown cultures, containing the transcriptional gene fusion ($dsrA_p$–lacZ) or the translational gene fusion (dsrA′–lacZ), were used to inoculate 12 mL of modified Pfennig's medium with 2 mM malate or sulfide. The β-galactosidase activity was measured 24 h after inoculation.
[b]The specific β-galactosidase activity is given as nmol o-nitrophenol min^{-1} (mg protein)$^{-1}$.
Under the given conditions 1 nmol/mL o-nitrophenol had an optical density at 420 nm of 0.0044. The protein content of each sample was determined by the Bradford method. The average protein content amounted to 500 μg mL^{-1}. The results represent the means and standard deviations of three independent biological replicates.

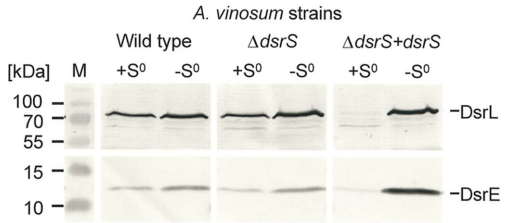

FIGURE 2 | Immunological detection of DsrE (14.6 kDa) and DsrL (71.4 kDa) in *dsrS* deletion (Δ*dsrS*) and complementation (Δ*dsrS* + *dsrS*) strains in comparison to *A. vinosum* wild type. Cells were grown in batch culture on 2 mM sulfide and harvested either at the maximum content of intracellularly stored sulfur (+S^0) or after the sulfur had been completely metabolized (–S^0). Sixty-eight microgram protein of the soluble fraction were used per lane. Both antisera were raised against oligopeptides comprising a highly immunogenic epitope deduced from the nucleotide sequence and their specific reaction with DsrE and DsrL overproduced in *E. coli* has been proven earlier (Dahl et al., 2005).

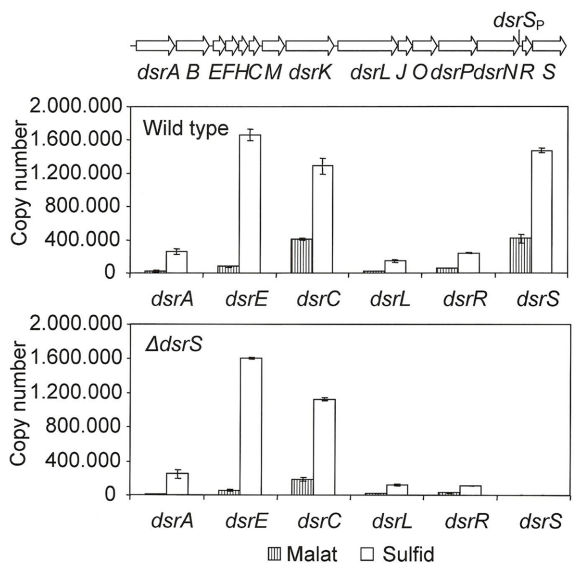

FIGURE 3 | Expression levels of six *dsr* genes under photoorganoheterotrophic (malate) and photolithoautotropic (sulfide) conditions determined by RT-PCR. The RNAs were isolated from *A. vinosum* wild type and the Δ*dsrS* mutant. Quantified external RNA fragments containing the target sequence served as standards. The location of a potential secondary promoter for *dsrS* as determined by BPROM and Neural Network Promoter Prediction is indicated.

type and examined the expression under photoorganoheterotrophic (malate) and photolithoautotrophic (CO_2 and sulfide) growth conditions. The transcription rate of the *dsrA* gene was measured by determining the specific β-galactosidase activities of the *lacZ* fusion to the main *dsr* promoter $dsrA_P$. A *dsrA′–lacZ* gene fusion, where both transcription and translation of the *lacZ* gene were dependent on *dsrA* gene expression, was used to determine the translation of the gene. The specific β-galactosidase activities were at a low basal level in malate-grown cells and increased approximately threefold under sulfur-oxidizing conditions (**Table 7**). In agreement with the RT-PCR results, the Δ*dsrS* mutant carrying the transcriptional fusion exhibited the same level of activities as the wild type. We deduce that DsrS has no effect on the transcription of *dsrA*. On the other hand, the Δ*dsrS* mutant carrying the translational fusion showed a ~35% reduction of β-galactosidase activities as compared to the wild type. The effect was independent of the growth conditions.

DISCUSSION

Here, we show that the *sox* genes which encode proteins essential for thiosulfate oxidation are constitutively expressed even in the absence of reduced sulfur compounds in the purple bacterium *A. vinosum*. A low basal expression has also been found for the *dsr* genes encoding the enzymes required for the oxidation of stored sulfur in the same organism under photoorganoheterotrophic growth conditions (Grimm et al., 2010b). Both, Dsr and Sox proteins are obviously constitutively formed to ensure a basal level, so that reduced sulfur compounds can be used as soon as they become available. This observations fits well with other lines of evidence that suggest a preferential utilization of reduced sulfur compounds over organic compounds as electron donors in *A. vinosum*, e.g., the reported repressive effect of thiosulfate on pyruvate utilization and the concomitant use of thiosulfate and pyruvate or acetate (Hurlbert and Lascelles, 1963; Hurlbert, 1968; Grimm et al., 2010b). Thiosulfate and possibly sulfide lead to an induction of *sox* gene transcription. Additional translational regulation was not apparent. Experiments with varying thiosulfate concentrations showed *sox* gene expression levels to be dependent on the strength of the inducing signal. Apparently, the expression can be modified according to demand.

Regulation of *soxXAKL* is probably performed by a two-component system encoded by Alvin_2166 and Alvin_2165 and consisting of a multi-sensor histidine kinase and a regulator with proposed di-guanylatecyclase activity. So far our experiments indicate a derepression of *soxXAKL* expression when the protein encoded by Alvin_2166 is not present in the cells. We base this conclusion on our finding that in the absence of thiosulfate transcript levels for *soxX* are lower in the wild type than in *A. vinosum soxB*::ΩKm carrying an interposon with an adverse effect also on Alvin_2166. The inductory effect of thiosulfate was lost in the mutant strain, i.e., the high transcript levels found in this strain were not further increased by the presence of the reduced sulfur compound. Sequence analyses indicate that Alvin_2166 has the potential to act as a redox sensor and the NADH/NAD^+ ratio which is directly coupled to the oxidation of thiosulfate via the photosynthetic electron transport chain might be a possible sensing signal. However, this hypothesis has to be substantiated in the future.

Apparently, regulation of *sox* genes in *A. vinosum* follows pathways fundamentally different from those described for the very few other organisms for which *sox* gene regulation has been studied. In *P. pantotrophus* the transcriptional ArsR family regulator SoxR has been shown to bind via a helix-turn-helix motif at two positions within the *sox* genes (Rother et al., 2005). Homology modeling of SigE and ORF1 in *Starkeya novella* provided evidence that SigE functions as a repressor binding via a helix-turn-helix motif at the promoter region while presence of reduced sulfur compounds led to binding of ORF1 to SigE and finally detachment of SigE from the DNA (Kappler et al., 2001; Bagchi and Ghosh, 2006). In *A. vinosum*

neither genes encoding homologs of SoxR nor genes encoding proteins resembling SigE or ORF1 appear to be present. When we take into account that homologs of Alvin_2165 and Alvin_2166 were found only in *H. halophila* SL1 and *Magnetococcus* MC-1 but closely related genes were not detected in the genomes of other sulfur-oxidizing prokaryotes harboring *sox* genes, *sox* gene regulation in *A. vinosum* appears to follow a quite unique mechanism.

In contrast to *soxXAKL*, expression of *soxYZ* is probably not regulated by Alvin_2166 and Alvin_2165. The copy numbers of *soxY* in *A. vinosum soxB*::Ω-Km indeed differ from the wild type ones in our RT-PCR experiments, but *soxY* shows the same expression pattern in a *soxX*::Ω-Km strain (data not shown). Therefore the changes in expression of *soxY* in *A. vinosum soxB*::ΩKm are unlikely due to the missing multi-sensor histidine kinase. In accordance with the fact that the three essential *sox* genes are located in three different transcription units (**Figure 1**) regulation of their expression seems to be quite complex and will require more attention in the future.

In the second part of this work we show that the *dsrS* encoded protein is relevant though not essential for the oxidation of sulfur stored in intracellular sulfur globules in the purple sulfur bacterium *A. vinosum*. We confirmed earlier sequence analyses by recombinant expression: the gene *dsrS* encodes a monomeric protein of the deduced 41.1-kDa molecular mass and does not contain cofactors. The gene is transcribed at a high level under photoorganoheterotrophic conditions in the absence of reduced sulfur compounds and the mRNA level further increases under sulfur-oxidizing conditions, indicating direct or indirect involvement of the encoded protein in the sulfur-oxidizing process. The transcript levels are similar to those observed for the constitutively and highly expressed gene *dsrC* for which a secondary promoter has been postulated. They are significantly higher than those for *dsrA* under photoorganoheterotrophic conditions in the absence of reduced sulfur compounds even though *dsrA* encodes a subunit of the key enzyme for intracellular sulfur oxidation. The presence of secondary promoters for *dsrC* and *dsrS* is in agreement with previous comparative analyses of *dsr* gene gene transcription in *A. vinosum* wild type and mutant 21D (Grimm et al., 2010b). Both, *dsrC* and *dsrS* were still expressed at a high level in the mutant strain. The mutant carries an insertion in *dsrB* of a kanamycin Ω interposon which abolishes transcription of any downstream genes in the same transcriptional unit unless secondary promoters are present. In addition, *in silico* analyses revealed potential promoter sequences in the regions upstream of *dsrC* and *dsrS* (Grimm et al., 2010b).

Characterization of a Δ*dsrS* mutant showed that DsrS is important though not essential for the oxidation of intracellular stored sulfur. Complementation *in trans* of the Δ*dsrS* strain with *dsrS* under control of the main *dsr* promoter $dsrA_p$ did not restore the sulfur oxidation rate to wild type levels even though comparable plasmids carrying a single *dsr* gene cloned immediately downstream of $dsrA_p$ have already been successfully used for complementation of *A. vinosum* mutants carrying deletions of the respective *dsr* gene. In all cases described so far, wild type oxidation rates were restored (Dahl et al., 2008b). The Δ*dsrS* + *dsrS* strain clearly behaved differently, indicating that the *dsrA* promoter may not be able to provide the cell with the necessary level of DsrS and pointing at the presence of a special secondary promoter for *dsrS*. When we consider that *dsrS* is not part of the *dsr* operon in other sulfur-oxidizing bacteria, it is not too surprising that *dsrS* is additionally regulated by a separate promoter in *A. vinosum*. This would explain why complementation of the *A. vinosum* Δ*dsrS* mutant with *dsrS* under control of the *dsrA* promoter did not cause the expected phenotype. The main *dsr* promoter $dsrA_p$ may not be the major factor in the expression of *dsrS*. In order to operate correctly, *dsrS* probably has to be under control of the correct regulating element(s). When we compared the transcription patterns of several *dsr* genes in the wild type with those in the Δ*dsrS* deletion mutant, major differences were not apparent, though the transcription of *dsrC* under organotrophic conditions appeared to be diminished in the Δ*dsrS* strain (**Figure 3**). In summary, the deletion of *dsrS* does not appear to have a major effect on the transcription of the *dsr* genes. This observation fits well with the results of the immunoblot analysis, as a perceptible reduction in the formation of DsrE and DsrL could not be observed.

Translational gene fusion experiments suggest a participation of DsrS in the post-transcriptional control of the *dsr* operon. The in frame deletion of *dsrS* lead to a reduced formation of DsrA′–LacZ and concomitantly to a reduced sulfur oxidation rate. In fact, a reduced production of DsrA protein is a straight forward explanation for the observed reduced sulfur oxidation rate of the ΔdsrS mutant. Apparently, less *dsrAB*-encoded sulfite reductase is formed when DsrS is lacking, than when it is not. DsrS could act either indirectly as part of a signal transducing reporter chain cascade or directly by stabilizing the ribosome–mRNA interaction and thus enhancing translation. Another possibility is that DsrS is involved in translational attenuation, i.e., induces a conformational change in the mRNA thereby permitting translational initiation. Interestingly, the entire Shine–Dalgarno sequence of *dsrA* is part of a possible stem-loop preventing ribosomal access.

Although we do not have enough direct evidence to clarify these possibilities at present, we showed that the region encompassing the *dsrA* ribosome binding site is required for the down-regulation of the accumulation of DsrA protein in the absence of DsrS. Additional studies are, however, necessary to elucidate the exact mechanism of the post-transcriptional-regulation of DsrA by DsrS and to explain the delayed formation of DsrE and DsrL in the complementation mutant.

CONCLUSION

Here we show, that the *sox* genes in *A. vinosum* are expressed on a low constitutive level even in the absence of reduced sulfur compounds. The extent of induction of *sox* gene transcription is dependent on the thiosulfate concentration. Additional translational regulation of the *A. vinosum sox* genes was not apparent. A two-component system consisting of a multi-sensor histidine kinase and a regulator with proposed di-guanylate cyclase activity probably exerts a regulatory effect on the *soxXAK* genes. In *A. vinosum* the expression of most *dsr* genes was also found to be at a low basal level in the absence of reduced sulfur compounds and to be enhanced in the presence of sulfide (Grimm et al., 2010b). In the present work, we demonstrate a participation of DsrS in the post-transcriptional control of the *dsr* operon. Previous work had suggested a participation in post-transcriptional control of the same operon also for DsrR, a protein

encoded immediately upstream of the *dsrS* gene (Grimm et al., 2010a). Apparently the regulation of the *dsr* operon and the function of DsrS are more intricate than previously expected. Further studies are clearly necessary to obtain a complete picture of the regulation of genes involved in sulfur oxidation in purple sulfur bacteria.

ACKNOWLEDGMENTS

This work was supported by grants Da 351/3-4, Da 351/3-5, and Da 351/4-3 from the Deutsche Forschungsgemeinschaft (DFG). We thank Bernd Masepohl for his helpful hints concerning gene fusions.

REFERENCES

Altschul, S. F., Madden, T. L., Schäffer, A. A., Zhang, J., Zhang, Z., Miller, W., and Lipman, D. J. (1997). Gapped BLAST and PSI-BLAST: a new generation of protein database search programs. *Nucleic Acids Res.* 25, 3389–3402.

Appia-Ayme, C., Little, P. J., Matsumoto, Y., Leech, A. P., and Berks, B. C. (2001). Cytochrome complex essential for photosynthetic oxidation of both thiosulfate and sulfide in *Rhodovulum sulfidophilum*. *J. Bacteriol.* 183, 6107–6118.

Bagchi, A., and Ghosh, T. C. (2006). Structural study of two proteins SigE and ORF1 to predict their roles in the biochemical oxidation of sulfur anions via the global sulfur oxidation operon (sox). *Comput. Biol. Chem.* 30, 227–232.

Brune, D. C. (1995). "Sulfur compounds as photosynthetic electron donors," in *Anoxygenic Photosynthetic Bacteria*, eds R. E. Blankenship, M. T. Madigan, and C. E. Bauer (Dordrecht: Kluwer Academic Publishers), 847–870.

Chan, C., Paul, R., Samoray, D., Amiot, N. C., Giese, B., Jenal, U., and Schirmer, T. (2004). Structural basis of activity and allosteric control of diguanylate cyclase. *Proc. Natl. Acad. Sci. U.S.A.* 101, 17084–17089.

Chandra, T. S., and Friedrich, C. G. (1986). Tn5-induced mutations affecting the sulfur-oxidizing ability (Sox) of *Thiosphaera pantotropha*. *J. Bacteriol.* 166, 446–452.

Combet, C., Blanchet, C., Geourjon, C., and Deleage, G. (2000). NPS@: network protein sequence analysis. *Trends Biochem. Sci.* 25, 147–150.

Cort, J. R., Selan, U. M., Schulte, A., Grimm, F., Kennedy, M. A., and Dahl, C. (2008). *Allochromatium vinosum* DsrC: solution-state NMR structure, redox properties and interaction with DsrEFH, a protein essential for purple sulfur bacterial sulfur oxidation. *J. Mol. Biol.* 382, 692–707.

Dahl, C. (2008). "Inorganic sulfur compounds as electron donors in purple sulfur bacteria," in *Sulfur in Phototrophic Organisms*, eds R. Hell, C. Dahl, D. B. Knaff, and T. Leustek (Dordrecht: Springer), 289–317.

Dahl, C., Engels, S., Pott-Sperling, A. S., Schulte, A., Sander, J., Lübbe, Y., Deuster, O., and Brune, D. C. (2005). Novel genes of the *dsr* gene cluster and evidence for close interaction of Dsr proteins during sulfur oxidation in the phototrophic sulfur bacterium *Allochromatium vinosum*. *J. Bacteriol.* 187, 1392–1404.

Dahl, C., Friedrich, C. G., and Kletzin, A. (2008a). "Sulfur oxidation in prokaryotes," in *Encyclopedia of Life Sciences (ELS)* (Chichester: John Wiley & Sons, Ltd.), doi: 10.1002/9780470015902.a0021155. Available at: http://www.els.net/

Dahl, C., Schulte, A., Stockdreher, Y., Hong, C., Grimm, F., Sander, J., Kim, R., Kim, S.-H., and Shin, D. H. (2008b). Structural and molecular genetic insight into a wide-spread bacterial sulfur oxidation pathway. *J. Mol. Biol.* 384, 1287–1300.

Fellay, R., Frey, J., and Krisch, H. M. (1987). Interposon mutagenesis of soil and water bacteria: a family of DNA fragments designed for in vivo insertional mutagenesis of Gram-negative bacteria. *Gene* 52, 147–154.

Fey, A., Eichler, S., Flavier, S., Christen, R., Höfle, M. G., and Guzmán, C. A. (2004). Establishment of a real-time PCR-based approach for accurate quantification of bacterial RNA targets in water, using *Salmonella* as a model organism. *Appl. Environ. Microbiol.* 70, 3618–3623.

Franz, B., Gehrke, T., Lichtenberg, H., Hormes, J., Dahl, C., and Prange, A. (2009). Unexpected extracellular and intracellular sulfur species during growth of *Allochromatium vinosum* with reduced sulfur compounds. *Microbiology* 155, 2766–2774.

Frey, J., and Krisch, H. M. (1985). Omega mutagenesis in Gram-negative bacteria: a selectable interposon which is strongly polar in a wide range of bacterial species. *Gene* 36, 143–150.

Frigaard, N.-U., and Dahl, C. (2009). Sulfur metabolism in phototrophic sulfur bacteria. *Adv. Microb. Physiol.* 54, 103–200.

Gao, Y., Mathee, K., Narasimhan, G., and Wang, X. (1999). "Motif detection in protein sequences," in *Proceedings of 6th International Symposium on String Processing and Information Retrieval*, Cancun, 63–72.

Grimm, F., Cort, J. R., and Dahl, C. (2010a). DsrR, a novel IscA-like protein lacking iron- and FeS-binding function involved in the regulation of sulfur oxidation in *Allochromatium vinosum*. *J. Bacteriol.* 192, 1652–1661.

Grimm, F., Dobler, N., and Dahl, C. (2010b). Regulation of *dsr* genes encoding proteins responsible for the oxidation of stored sulfur in *Allochromatium vinosum*. *Microbiology* 156, 764–773.

Grimm, F., Franz, B., and Dahl, C. (2008). "Thiosulfate and sulfur oxidation in purple sulfur bacteria," in *Microbial Sulfur Metabolism*, eds C. Dahl and C. G. Friedrich (Berlin: Springer), 101–116.

Hanahan, D. (1983). Studies on transformation of *Escherichia coli* with plasmids. *J. Mol. Biol.* 166, 557–580.

Hensen, D., Sperling, D., Trüper, H. G., Brune, D. C., and Dahl, C. (2006). Thiosulphate oxidation in the phototrophic sulphur bacterium *Allochromatium vinosum*. *Mol. Microbiol.* 62, 794–810.

Hübner, P., Willison, J. C., Vignais, P., and Bickle, T. A. (1991). Expression of regulatory *nif* genes in *Rhodobacter capsulatus*. *J. Bacteriol.* 173, 2993–2999.

Hurlbert, R. E. (1968). Effect of thiol-binding reagents on the metabolism of *Chromatium* D. *J. Bacteriol.* 95, 1706–1712.

Hurlbert, R. E., and Lascelles, J. (1963). Ribulose diphosphate carboxylase in Thiorhodaceae. *J. Gen. Microbiol.* 33, 445–458.

Kappler, U., Friedrich, C. G., Trüper, H. G., and Dahl, C. (2001). Evidence for two pathways of thiosulfate oxidation in *Starkeya novella* (formerly *Thiobacillus novellus*). *Arch. Microbiol.* 175, 102–111.

Lübbe, Y. J., Youn, H.-S., Timkovich, R., and Dahl, C. (2006). Siro(haem)amide in *Allochromatium vinosum* and relevance of DsrL and DsrN, a homolog of cobyrinic acid a,c diamide synthase for sulphur oxidation. *FEMS Microbiol. Lett.* 261, 194–202.

Narasimhan, G., Bu, C., Gao, Y., Wang, X., Xu, N., and Mathee, K. (2002). Mining for motifs in protein sequences. *J. Comput. Biol.* 9, 707–720.

Pattaragulwanit, K., and Dahl, C. (1995). Development of a genetic system for a purple sulfur bacterium: conjugative plasmid transfer in *Chromatium vinosum*. *Arch. Microbiol.* 164, 217–222.

Pott, A. S., and Dahl, C. (1998). Sirohaem-sulfite reductase and other proteins encoded in the dsr locus of *Chromatium vinosum* are involved in the oxidation of intracellular sulfur. *Microbiology* 144, 1881–1894.

Prange, A., Engelhardt, H., Trüper, H. G., and Dahl, C. (2004). The role of the sulfur globule proteins of *Allochromatium vinosum*: mutagenesis of the sulfur globule protein genes and expression studies by real-time RT PCR. *Arch. Microbiol.* 182, 165–174.

Römling, U., and Amikam, D. (2006). Cyclic di-GMP as a second messenger. *Curr. Opin. Microbiol.* 9, 218–228.

Rother, D., Orawski, G., Bardischewsky, F., and Friedrich, C. G. (2005). SoxRS-mediated regulation of chemotrophic sulfur oxidation in *Paracoccus pantotrophus*. *Microbiology* 151, 1707–1716.

Sander, J., and Dahl, C. (2009). "Metabolism of inorganic sulfur compounds in purple bacteria," in *Purple Bacteria*, eds C. N. Hunter, F. Daldal, M. C. Thurnauer, and J. T. Beatty (Dordrecht: Springer), 595–622.

Sander, J., Engels-Schwarzlose, S., and Dahl, C. (2006). Importance of the DsrMKJOP complex for sulfur oxidation in *Allochromatium vinosum* and phylogenetic analysis of related complexes in other prokaryotes. *Arch. Microbiol.* 186, 357–366.

Schäfer, A., Tauch, A., Jäger, W., Kalinowski, J., Thierbach, G., and Pühler, A. (1994). Small mobilizable multi-purpose cloning vectors derived from the *Escherichia coli* plasmids pK18 and pK19: selection of defined deletions in the chromosome of *Corynebacterium glutamicum*. *Gene* 145, 69–73.

Simon, R., Priefer, U., and Pühler, A. (1983). A broad host range mobilization system for in vivo genetic engineering: transposon mutagenesis in Gram negative bacteria. *Biotechnology* 1, 784–791.

Steudel, R., Holdt, G., Visscher, P. T., and van Gemerden, H. (1990). Search for polythionates in cultures of *Chromatium vinosum* after sulfide incubation. *Arch. Microbiol.* 155, 432–437.

Welte, C., Hafner, S., Krätzer, C., Quentmeier, A. T., Friedrich, C. G., and Dahl, C. (2009). Interaction between Sox proteins of two physiologically distinct bacteria and a new protein

involved in thiosulfate oxidation. *FEBS Lett.* 583, 1281–1286.

Wodara, C., Kostka, S., Egert, M., Kelly, D. P., and Friedrich, C. G. (1994). Identification and sequence analysis of the *soxB* gene essential for sulfur oxidation of *Paracoccus denitrificans* GB17. *J. Bacteriol.* 176, 6188–6191.

Zander, U., Faust, A., Klink, B. U., de Sanctis, D., Panjikar, S., Quentmeier, A., Bardischewsky, F., Friedrich, C. G., and Scheidig, A. J. (2010). Structural basis for the oxidation of protein-bound sulfur by the sulfur cycle molybdohemo-enzyme sulfane dehydrogenase SoxCD. *J. Biol. Chem.* 286, 8349–8360.

Conflict of Interest Statement: The authors declare that the research was conducted in the absence of any commercial or financial relationships that could be construed as a potential conflict of interest.

Received: 31 January 2011; accepted: 08 March 2011; published online: 22 March 2011.
Citation: Grimm F, Franz B and Dahl C (2011) Regulation of dissimilatory sulfur oxidation in the purple sulfur bacterium Allochromatium vinosum. Front. Microbio. ***2****:51. doi: 10.3389/fmicb.2011.00051*

This article was submitted to Frontiers in Microbial Physiology and Metabolism, a specialty of Frontiers in Microbiology.

frontiers in
MICROBIOLOGY

ORIGINAL RESEARCH ARTICLE
published: 24 May 2011
doi: 10.3389/fmicb.2011.00116

Mechanisms and evolution of oxidative sulfur metabolism in green sulfur bacteria

Lea H. Gregersen[1†], Donald A. Bryant[2] and Niels-Ulrik Frigaard[1]*

[1] *Department of Biology, University of Copenhagen, Helsingør, Denmark*
[2] *Department of Biochemistry and Molecular Biology, The Pennsylvania State University, University Park, PA, USA*

Edited by:
Martin G. Klotz, University of Louisville, USA

Reviewed by:
Ulrike Kappler, University of Queensland, Australia
Jan Kuever, Bremen Institute for Materials Testing, Germany

***Correspondence:**
Niels-Ulrik Frigaard, Section for Marine Biology, Department of Biology, University of Copenhagen, Strandpromenaden 5, DK-3000 Helsingør, Denmark.
e-mail: nuf@bio.ku.dk

†Present address:
Lea H. Gregersen, Max-Delbrück-Centrum für Molekulare Medizin, Berlin-Buch, Robert-Rössle-Strasse 10, D-13092 Berlin, Germany

Green sulfur bacteria (GSB) constitute a closely related group of photoautotrophic and thiotrophic bacteria with limited phenotypic variation. They typically oxidize sulfide and thiosulfate to sulfate with sulfur globules as an intermediate. Based on genome sequence information from 15 strains, the distribution and phylogeny of enzymes involved in their oxidative sulfur metabolism was investigated. At least one homolog of sulfide:quinone oxidoreductase (SQR) is present in all strains. In all sulfur-oxidizing GSB strains except the earliest diverging *Chloroherpeton thalassium*, the sulfide oxidation product is further oxidized to sulfite by the dissimilatory sulfite reductase (DSR) system. This system consists of components horizontally acquired partly from sulfide-oxidizing and partly from sulfate-reducing bacteria. Depending on the strain, the sulfite is probably oxidized to sulfate by one of two different mechanisms that have different evolutionary origins: adenosine-5′-phosphosulfate reductase or polysulfide reductase-like complex 3. Thiosulfate utilization by the SOX system in GSB has apparently been acquired horizontally from Proteobacteria. SoxCD does not occur in GSB, and its function in sulfate formation in other bacteria has been replaced by the DSR system in GSB. Sequence analyses suggested that the conserved *soxJXYZAKBW* gene cluster was horizontally acquired by *Chlorobium phaeovibrioides* DSM 265 from the *Chlorobaculum* lineage and that this acquisition was mediated by a mobile genetic element. Thus, the last common ancestor of currently known GSB was probably photoautotrophic, hydrogenotrophic, and contained SQR but not DSR or SOX. In addition, the predominance of the *Chlorobium–Chlorobaculum–Prosthecochloris* lineage among cultured GSB could be due to the horizontally acquired DSR and SOX systems. Finally, based upon structural, biochemical, and phylogenetic analyses, a uniform nomenclature is suggested for *sqr* genes in prokaryotes.

Keywords: horizontal gene transfer, metabolism evolution, green sulfur bacteria, purple sulfur bacteria, sulfide:quinone oxidoreductase, flavocytochrome *c*, SOX enzyme system, dissimilatory sulfite reductase

INTRODUCTION

Green sulfur bacteria (GSB; order Chlorobiales) are strictly anaerobic, photosynthetic bacteria that predominantly oxidize reduced sulfur compounds for photoautotrophic growth (Overmann, 2000, 2008; Garrity and Holt, 2001). They occur in anoxic, aquatic environments where light and sulfide coincide. They utilize predominantly sulfide, thiosulfate, biogenic and abiogenic sulfur globules, and H_2, as electron donors to support photoautotrophic growth (Brune, 1989; Frigaard and Dahl, 2009). One characterized GSB, *Chlorobium ferrooxidans*, utilizes Fe^{2+} as electron donor and does not grow on reduced sulfur compounds (Heising et al., 1999).

Based on isolated strains that have been characterized, GSB form a phylogenetically and physiologically coherent group (Imhoff, 2003, 2008). Following a recent proposal to reorganize the GSB nomenclature, the GSB currently comprise only four genera: *Chlorobium* (*Chl.*), *Chlorobaculum* (*Cba.*), *Prosthecochloris* (*Ptc.*), and *Chloroherpeton* (*Chp.*; Imhoff, 2003). The genus *Pelodictyon* (*Pld.*), previously used for some GSB, has been abandoned. Available SSU rRNA sequences from cultured GSB exhibit relatively little variation: there is at least 92% sequence identity among *Chlorobium*, *Chlorobaculum*, and *Prosthecochloris* and at least 88% sequence identity when *Chloroherpeton* is included. GSB constitute the only cultured members of the order Chlorobiales, and the phylum Chlorobi was proposed based on GSB (Garrity and Holt, 2001; Imhoff, 2008). Until *Ignavibacterium album* was isolated, the closest cultured relatives of the GSB were members of the *Bacteroidetes* (Iino et al., 2010). *I. album* is a non-phototrophic relative of GSB (about 82–83% SSU rRNA sequence identity with GSB; Iino et al., 2010), whose genome has recently been sequenced to reveal more about the physiology and evolution of this organism. Metagenomic sequence data derived from microbial mats of hot springs in Yellowstone National Park suggest that these mats harbor other uncharacterized relatives of GSB (Klatt et al., 2011; Liu et al., 2011). Preliminary analyses suggest that these organisms are photoheterotrophs that are physiologically distinct from well-studied Chlorobiales (Bryant et al., 2011).

The genome sequences of 15 strains of GSB are currently available (**Table 1**). Twelve of these genome sequences are publicly available[1], one other has been completed (*Ptc. bathyomarinum* Ty

[1]http://ncbi.nlm.nih.gov

Vent), and two are at the draft stage (*Ptc. phaeum* CIB 2401 and *Cba. limnaeum* DSM 1677; Bryant et al., 2011). Three of these strains were previously referred to as members of the *Chlorobium* (*Prosthecochloris* sp. BS1, *Ptc. phaeum* CIB 2401, and *Ptc. bathyomarinum* Ty Vent). However, phylogenetic sequence analyses of SSU rRNA and protein-encoding genes of these strains clearly show that they are more closely related to members of the genus *Prosthecochloris* than to members of the genera *Chlorobium* and *Chlorobaculum* (see below).

A defining feature of GSB as a group is their ability to oxidize inorganic sulfur compounds for photoautotrophic growth. The metabolic reactions involved in this dissimilatory sulfur metabolism are complex and have not yet been described in detail (**Figure 1**; Frigaard and Dahl, 2009). However, genome sequence information has provided significant insights into this metabolism, including which genes are likely to be involved and how they have evolved (Eisen et al., 2002; Chan et al., 2008; Frigaard and Bryant, 2008; Sakurai et al., 2010). Several enzymes from GSB have been identified using this information that have, or may have, a role in thiotrophic growth (e.g., Hanson and Tabita, 2001; Ogawa et al., 2008; Azai et al., 2009; Chan et al., 2009; Holkenbrink et al., 2011). Using genome sequence analysis, we have investigated the distribution of putative sulfur metabolism genes in all currently available genomes of GSB.

MATERIALS AND METHODS

SEQUENCE DATA AND ANALYSIS

Genome sequencing and annotation of GSB strains *Cba. limnaeum* DSM 1677, *Ptc. bathyomarinum* Ty Vent, and *Ptc. phaeum* CIB 2401 are currently being performed in our laboratories. Genome sequence information of PSB strains *Ectothiorhodospira* (*Ect.*) *haloalkaliphila* ATCC 51935, *Marichromatium* (*Mch.*) *purpuratum* DSM 1591, *Thiococcus* (*Tco.*) *pfennigii* 4520, *Thiocystis* (*Tcs.*) *violascens* DSM 198, *Thiodictyon* sp. Cad16, *Thioflavicoccus* (*Tfc.*) *mobilis* 8321, and *Thiorhodospira* (*Trs.*) *sibirica* ATCC 700588 was obtained from Joint Genome Institute, U.S. Department of Energy[2]. Genome sequence information from other bacteria was retrieved from GenBank[3]. Sequence analysis was performed primarily using tools available at

[2]http://www.jgi.doe.gov/

[3]http://www.ncbi.nlm.nih.gov/

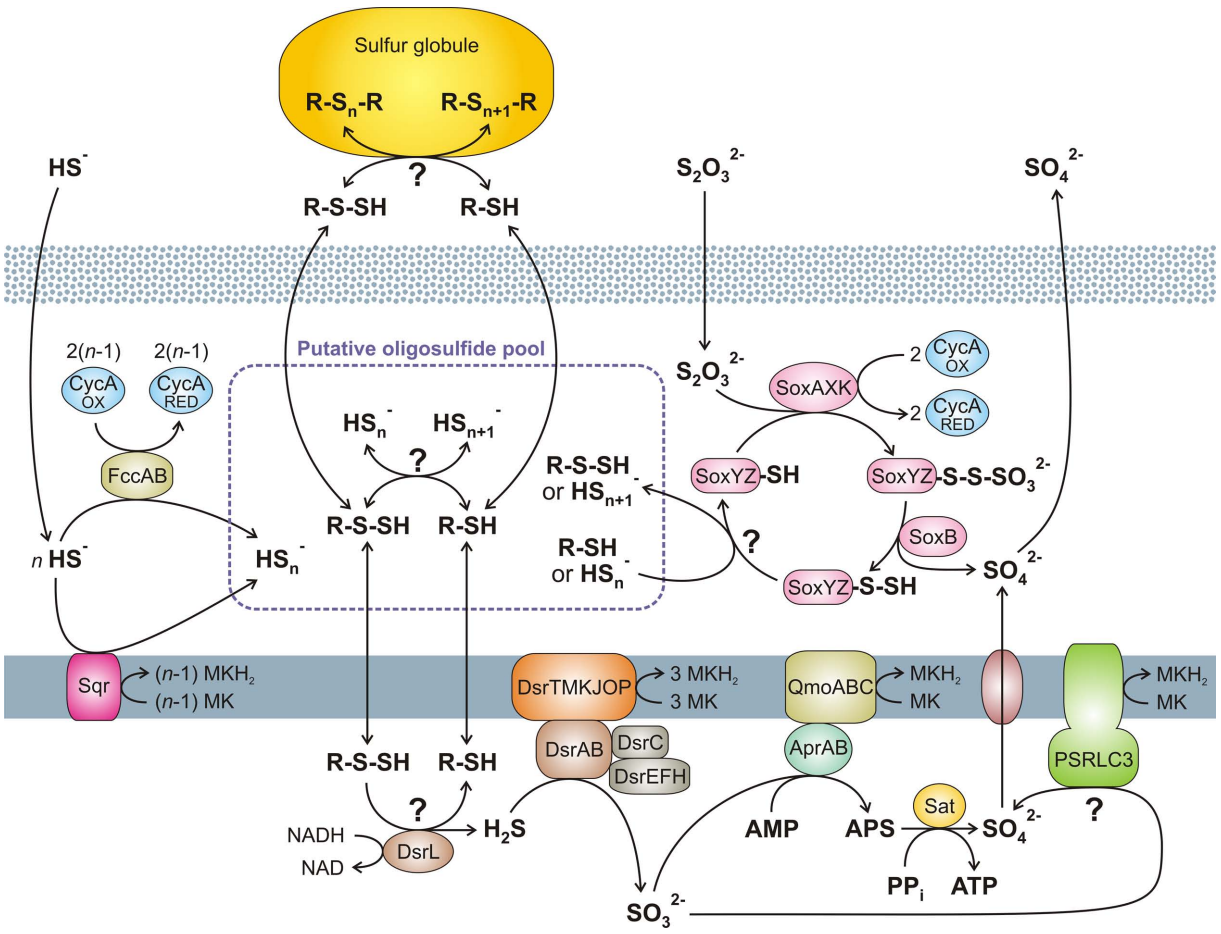

FIGURE 1 | Overview of the putative pathways of oxidative sulfur metabolism in GSB. All oxidative enzyme systems shown in the periplasm (SOX, SQR, and FCC systems) as well as extracellular sulfur globules contribute to a putative pool of oligosulfides (HS_n^- and possibly organic R-S_n-H). Complete oxidation of this pool to sulfate is dependent on the DSR system. No strain of GSB have all the reactions shown here. See text for further details. (Based on Eisen et al., 2002; Frigaard and Bryant, 2008; Frigaard and Dahl, 2009; Sakurai et al., 2010; Holkenbrink et al., 2011.) MK, menaquinone.

the National Center for Biotechnology Information[4] (NCBI) and at Integrated Microbial Genomes[5] (IMG). Analyses were performed locally primarily using the following software: MEGA 4 (sequence alignment and phylogenetics[6]; Tamura et al., 2007), Artemis 12.0 (sequence viewing and manipulation; Wellcome Trust Sanger Institute, Hinxton, UK[7]; Carver et al., 2008), FGENESB (sequence annotation; Softberry, Mount Kisco, NY, USA[8]), and ActivePerl 5.10 (ActiveState Software, Vancouver, BC, Canada[9]). Prediction of signal peptides was performed using SignalP[10]; Emanuelsson et al., 2007) and PRED-TAT[11]; Bagos et al., 2010). Promoter regions were predicted using FGENESB and BPROM[12]) and manually edited. The sequence logo of the *sox* promoter region was generated using WebLogo[13] version 2.8.2 (Crooks et al., 2004).

RESULTS

PHYLOGENY OF RIBOSOMAL RNA AND CORE METABOLIC FUNCTIONS

Analyses of the SSU rRNA gene and several cellular core proteins in the GSB strains with sequenced genomes revealed an overall congruent phylogeny (**Figures 2A,B**), which was in agreement with previous analyses performed on a smaller number of strains (Bryant et al., 2011). These analyses strongly supported the recent reclassification of GSB into four genera (Imhoff, 2003): *Chlorobium*, *Chlorobaculum*, *Prosthecochloris*, and *Chloroherpeton*. *Chloroherpeton* was consistently the earliest diverging genus within the Chlorobiales, *Prosthecochloris* was a sister clade to the *Chlorobium/Chlorobaculum* lineage, and *Chlorobium* and *Chlorobaculum* were the most closely related genera.

Phylogenetic analyses were made on selected enzymes functioning in several key metabolic processes in GSB. For example, analysis of PetB, the cytochrome *b* subunit of the Rieske–cytochrome *b* electron-transfer complex (PetB/CT0303; the locus tags for proteins from *Cba. tepidum* are provided to facilitate identification), showed that this enzyme is present in all strains and that its phylogeny is congruent, at least at the genus level (**Figure 2C**), with that of the SSU rRNA (**Figure 2A**) and with a phylogeny based on the concatenation of several proteins representing various house-keeping functions of these organisms (**Figure 2B**). Therefore, PetB was most likely present in the last common ancestor of the investigated GSB, and the *petB* gene probably has not undergone horizontal transfer (at least not between members of different genera). Identical analyses and conclusions were made for the following enzymes, which are present in the genomes of all sequenced strains of GSB: ATP-citrate lyase subunit 2 (AclA/CT1088), type I NADH dehydrogenase (concatenated NuoDHLMN/CT0769,CT0770,CT0774-CT0776), ferredoxin-NAD(P)$^+$ reductase (FNR/CT1512), RuBisCO-like protein (RLP/CT1772), and nitrogen fixation (concatenated NifAHDKENB/CT1529,CT1533,CT1536-CT1540; data not shown). (*Chp. thalassium* ATCC 35110 has two *nif* gene sets: one encoding [Mo–Fe]-nitrogenase and one encoding Fe-only nitrogenase; the latter was probably horizontally acquired.) Similar observations have previously been made with the Fenna–Matthews–Olson antenna protein (FMO/CT1499; Alexander et al., 2002; Imhoff, 2003) and magnesium chelatase large subunits (BchH/CT1957, BchS/CT1955, BchT/CT1295; Gomez Maqueo Chew et al., 2009). The same is true for the phylogeny of the HupSL [Ni–Fe]-hydrogenase (HupL/CT0777; data not shown), except that the *hupSL* genes have been lost in a few strains (**Table 1**).

Type I NADH dehydrogenase is the enzyme that normally couples oxidation of NADH to the reduction of menaquinone (or another isoprenoid quinone, depending on the organism) and thereby produces a transmembrane proton gradient (Yagi and Matsuno-Yagi, 2003; Sazanov and Hinchliffe, 2006; Efremov et al., 2010). The bacterial enzyme normally has 14 subunits, NuoABCDEFGHIJKLMN. With the exception of *Chp. thalassium*, all GSB have lost three subunits, NuoE, NuoF, and NuoG (Frigaard et al., 2003), which function in binding and oxidation of NADH (Yagi and Matsuno-Yagi, 2003; Sazanov and Hinchliffe, 2006; Efremov et al., 2010). Phylogenetic analysis suggests that the loss occurred after divergence of *Chloroherpeton* spp., because both *Chp. thalassium* and the earlier diverging *I. album* have all 14 subunits (data not shown). This loss could have important consequences for the electron-transfer function of this enzyme and is likely to represent a major physiological difference between *Chloroherpeton* spp. and other GSB, which could impact the oxidative sulfur metabolism.

In summary, phylogenetic analyses strongly support the division of the GSB into only four genera: *Chlorobium*, *Chlorobaculum*, *Prosthecochloris*, and *Chloroherpeton*. In addition, the observations support the notion that the last common ancestor of extant, cultured GSB was an anaerobic bacteriochlorophyll-containing photoautotroph capable of N_2 fixation, H_2 uptake, and CO_2 fixation by the reverse TCA cycle. Finally, these metabolic functions do not appear to have been exchanged by horizontal gene transfer in members of this clade. In contrast, many sulfur metabolism enzymes were apparently not present in the last common ancestor of extant GSB, and the genes encoding this metabolism have undergone extensive horizontal exchange with other bacterial phyla (see below).

SULFIDE:QUINONE OXIDOREDUCTASES

All characterized sulfide:quinone oxidoreductases (SQR) are single-subunit flavoproteins that are associated with the cytoplasmic membrane (Shahak and Hauska, 2008; Frigaard and Dahl, 2009). Based on the protein structure, a recently proposed classification identified six distinct types (numbered I through VI) of SQR homologs (Marcia et al., 2010). We propose a coherent genetic nomenclature that distinguishes among these SQR homologs in GSB and other organisms (**Table 1**; **Figure 3**). This nomenclature is necessary to identify clearly the multiple types of *sqr* genes often found in the same strain (Demerec et al., 1966).

We propose the gene designation *sqrA* for the type I SQR orthologs, which are typically found in Cyanobacteria, Proteobacteria, and Aquificaceae. This category includes the functionally well-characterized SQRs in *Oscillatoria limnetica* (AAF72962; Bronstein

[4]http://www.ncbi.nlm.nih.gov/
[5]http://img.jgi.doe.gov/
[6]http://www.megasoftware.net/
[7]http://www.sanger.ac.uk/
[8]http://linux1.softberry.com/
[9]http://www.activestate.com/
[10]http://www.cbs.dtu.dk/services/SignalP/
[11]http://www.compgen.org/tools/PRED-TAT/
[12]http://linux1.softberry.com
[13]http://weblogo.berkeley.edu/

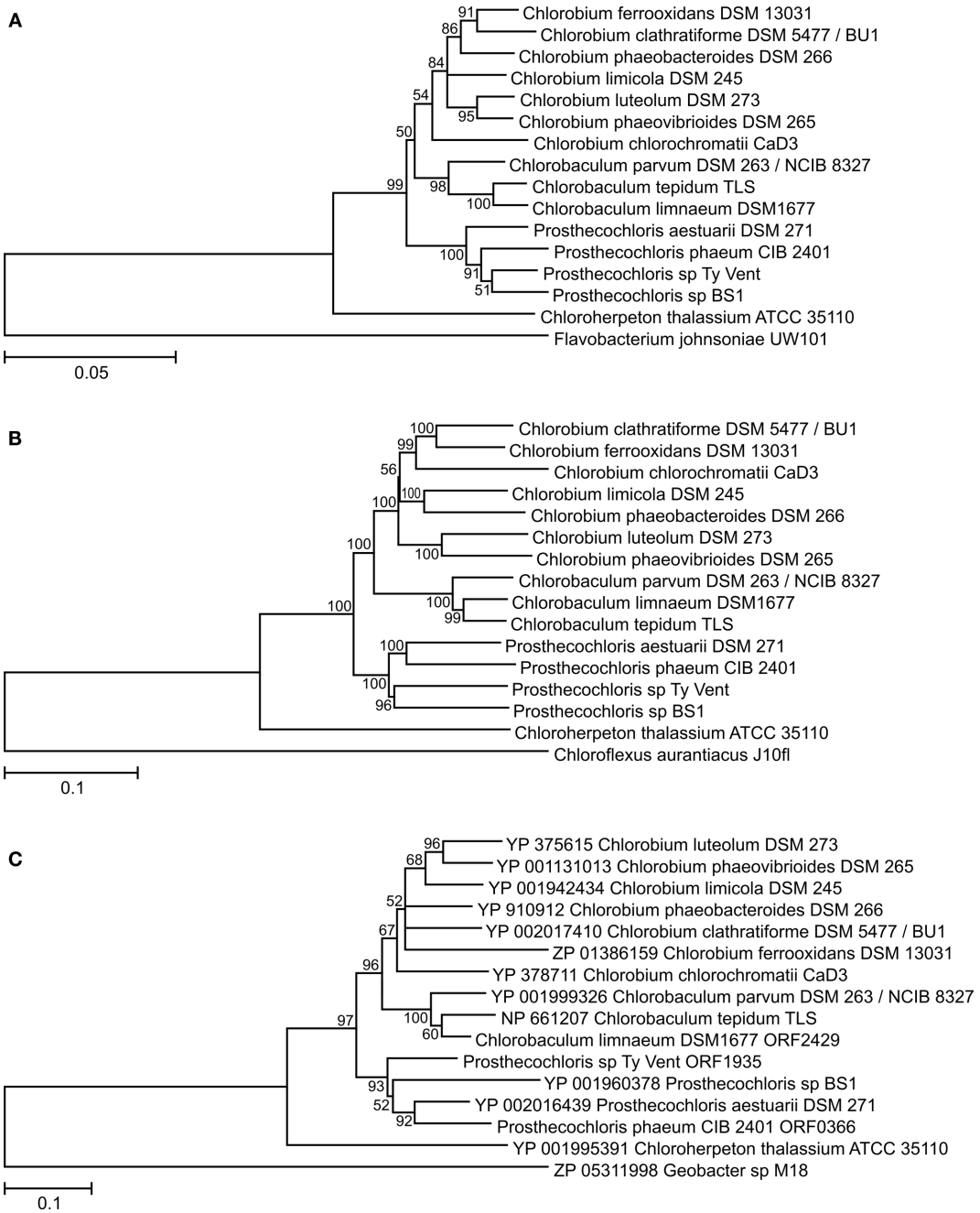

FIGURE 2 | Phylogenetic trees of ribosomal RNA and core metabolism enzymes of GSB. (A) SSU rRNA gene; rooted with *Flavobacterium johnsoniae*. **(B)** Concatenation of the following house-keeping proteins (with the protein name in *Cba. tepidum* TLS in parenthesis): RNA polymerase subunit beta (RpoB/CT0155), alanyl-tRNA synthetase (AlaS/CT0166), translation initiation factor IF-2 (InfB/CT0241), DNA gyrase subunit B (GyrB/CT2263), molecular chaperone DnaK (CT0643), F_0F_1 ATP synthase subunit α (AtpA/CT2033), preprotein translocase subunit SecY (CT2169), cell division protein FtsZ (CT0030), phospho-*N*-acetylmuramoyl-pentapeptide-transferase (MraY/CT0037), recombinase A (RecA/CT1930); rooted with *Chloroflexus aurantiacus* J-10-fl. **(C)** Cytochrome *b* subunit of the Rieske–cytochrome *b* electron-transfer complex (PetB/CT0303); rooted with *Geobacter* sp. M18. All trees are made using the neighbor-joining method and the Jukes–Cantor (nucleotides) or Jones–Taylor–Thornton (amino acids) substitution model. All positions containing alignment gaps and missing data were eliminated only in pairwise sequence comparisons. Bootstrap support of branches in percentage based on 1000 replications are shown; branches with bootstrap values less than 50% were collapsed.

et al., 2000), *Rhodobacter capsulatus* (CAA66112; Schütz et al., 1999), and *Aquifex aeolicus* (NP_214500; Nübel et al., 2000; Marcia et al., 2009). No GSB strain has a type I SQR (i.e., SqrA).

We propose the gene designation *sqrB* for the type II SQR orthologs, which include SQR homologs identified in eukaryotes such as the functionally characterized SQR in *Schizosaccharomyces*

Table 1 | Distribution of genes putatively involved in oxidative sulfur metabolism in the genomes of Chlorobi.

Strain	Accession number	Electron donor			Genotype [9]															
		S^{2-}	S^0	$S_2O_3^{2-}$	*sqrA*	*sqrB*	*sqrC* [10]	*sqrD*	*sqrE*	*sqrF*	*sqrX*	*fcc*	*soy*	*sox*	*dsr*	*apr*	*sat*	*qmo*	PSRLC3	*hup*
Cba. limnaeum DSM 1677^T [1]	n.a.	+	n.d.	+	–	–	+	+	–	+	–	+	–	+	+	+	+	+	–	+
Cba. parvum NCIB 8327^T (DSM 263^T) [2]	NC_011027	+	–	+	–	–	+	+	+	+	–	+	–	+	– [11]	–	–	–	–	+
Cba. tepidum TLS^T (ATCC 49652^T) [3]	NC_002932	+	+	+	–	–	+	+	+	+	–	+	–	+	+	+	+	+	–	– [12]
Chl. chlorochromatii CaD3	NC_007514	+	–	–	–	–	+	+	–	–	–	+	–	+	+	+	+	+	+	–
Chl. clathratiforme BU-1^T (DSM 5477^T) [4]	NC_011060	+	+	+	–	–	–	+	–	–	–	+	+	+	+	+	+	+	–	+
Chl. ferrooxidans DSM 13031^T	NZ_AASE00000000	–	–	–	–	–	–	+	–	+	–	–	–	–	–	–	–	–	–	+
Chl. limicola DSM 245^T	NC_010803	+	+	–	–	–	+	–	–	–	+	+	+	–	+	–	–	–	+	+
Chl. luteolum DSM 273^T [5]	NC_007512	+	+	–	–	–	+	+	–	+	+	–	–	–	+	–	–	–	+	+
Chl. phaeobacteroides DSM 266^T	NC_008639	+	+	–	–	–	–	–	–	–	+	+	+	–	+	–	–	–	+	+
Chl. phaeovibrioides DSM 265 [6]	NC_009337	+	+	+	–	–	+	+	–	–	+	+	–	+	+	–	–	–	+ [13]	–
Chp. thalassium ATCC 35110^T	NC_011026	+	? [14]	–	–	–	+	+	–	+	–	+	+	–	–	–	–	–	+	+
Prosthecochloris sp. BS1 [7]	NC_010831	+	n.d.	n.d.	–	–	+	–	–	–	+	+	–	–	+	+	+	+	–	+
Ptc. aestuarii SK-413^T (DSM 271^T)	NC_011059	+	+	–	–	–	+	–	–	–	+	+	+	–	+	–	–	–	+	+
Ptc. bathyomarinum Ty Vent	n.a.	+	n.d.	–	–	–	+	–	–	–	+	+	+	–	+	–	–	–	+	+
Ptc. phaeum CIB 2401 [8]	n.a.	+	n.d.	+	–	–	–	–	–	–	+	+	+	+	+	–	–	–	+	–
Ignavibacterium album DSM 19864^T	n.a.	n.d.	–	–	–	–	–	+	+	–	–	–	–	–	–	–	–	–	–	–

n.a., not available; n.d., not determined.

Previous name: [1]Chl. phaeobacteroides, [2]Chl. vibrioforme subsp. thiosulfatophilum, [3]Chl. tepidum, [4]Pld. phaeoclathratiforme, [5]Pld. luteolum, [6]Chl. vibrioforme subsp. thiosulfatophilum, [7]Chlorobium sp. BS1, [8]Pld. phaeum.

[9]The following abbreviations designate more than one gene: apr, aprBA; dsr, dsrNCABLUEFHTMKJOPVW; fcc, fccAB; hup, hupSL; PSRLC3, polysulfide reductase-like complex 3 (Frigaard and Bryant, 2008), sox, soxJXYZAKBW; soy, soyYZ; qmo, qmoABC.

[10]SQR activity has not yet been demonstrated for SqrC proteins.

[11]A truncated dsr gene cluster is present.

[12]A truncated hup gene cluster is present.

[13]The gene encoding the PsrA-like subunit has a frameshift mutation.

[14]Chp. thalassium is only capable of slow consumption of sulfur globules (Gibson et al., 1984).

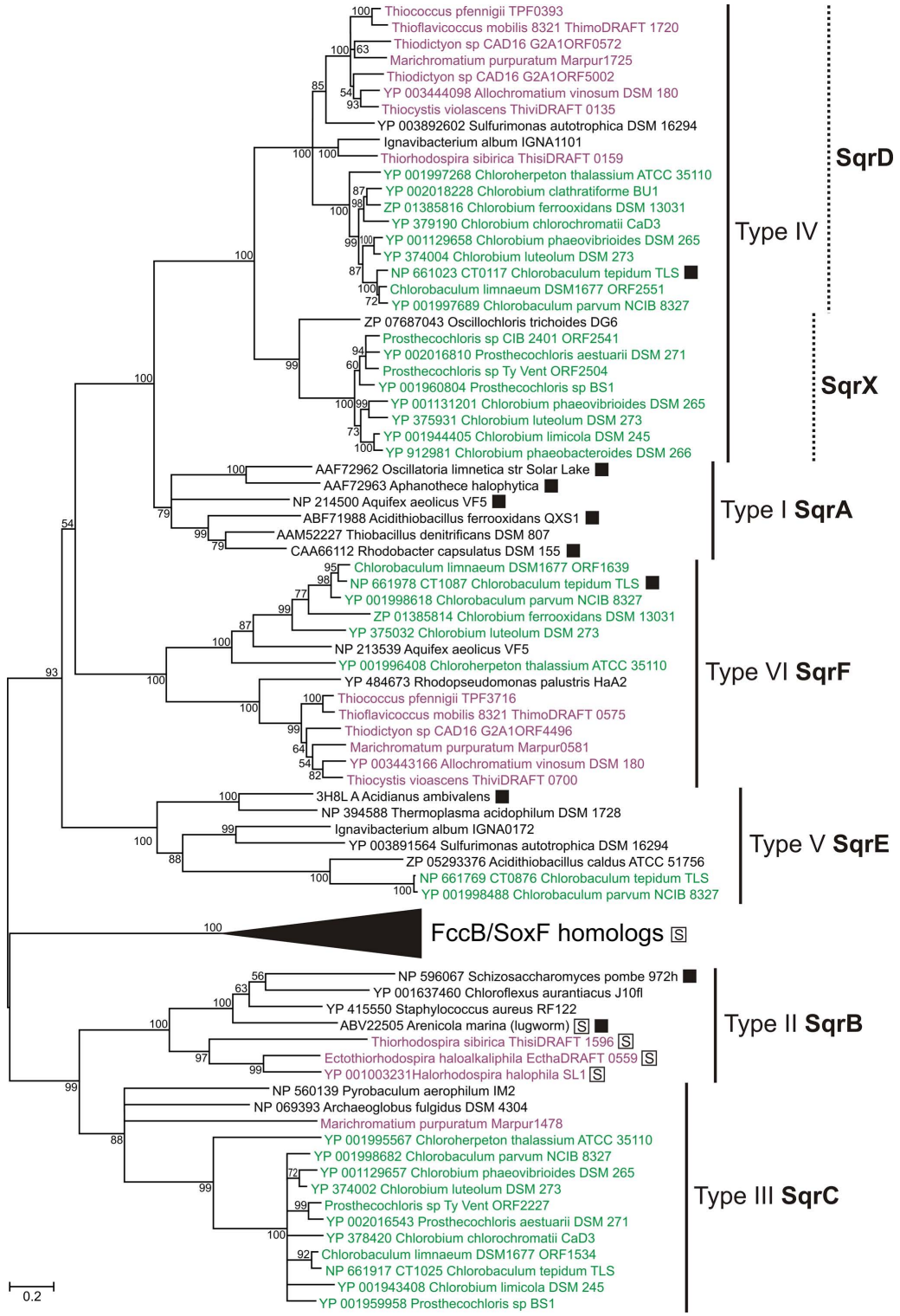

FIGURE 3 | Phylogenetic tree of sulfide:quinone oxidoreductase (SQR) homologs. Tree construction details were as in **Figure 2**, except that the tree is unrooted. The clade of FccB/SoxF homologs is expanded in **Figure 4A**. SQR activity has been demonstrated for proteins marked with a filled box. Proteins marked with a boxed "S" had a signal peptide. All proteins in the FccB/SoxF homologs clade (see **Figure 4A**) and proteins from PSB in the SqrB clade had a signal peptide for the twin-arginine translocon (data not shown). The only other sequence in the tree that encoded a signal peptide of any predictable type (Emanuelsson et al., 2007) was the eukaryotic SQR type II from the lugworm *Arenicola marina* (data not shown). Sequences from GSB are shown in green; sequences from PSB are shown in purple. See text for details.

pombe (NP_596067; Van de Weghe and Ow, 1999) and SQR homologs in the bacteria *Staphylococcus aureus* (YP_415550) and *Chloroflexus aurantiacus* (YP_001637460). No GSB strain has a type II SQR (i.e., SqrB).

We propose that the gene designation *sqrC* should be reserved for the group of SQR homologs that were assigned as type III by Marcia et al. (2010). These proteins are the only SQR homologs for which no representative has yet been shown to exhibit SQR activity. The sulfide oxidation activity of a *Cba. tepidum* mutant lacking a type III protein (CT1025/NP_661917) was not significantly lower than that of the wild type (Holkenbrink, 2010).

We propose the gene designation *sqrD* for type IV SQR, which includes the SQR that is responsible for most of the SQR activity in *Cba. tepidum* (CT0117/NP_661023; Chan et al., 2009; Holkenbrink et al., 2011). Orthologs of SqrD are also present in Proteobacteria and Actinobacteria. Phylogenetic analyses show that structure class IV splits into two paralogous clades, and we propose the designation *sqrX* for the second of these (see **Figure 3**). Examples of the SqrX family are present in about half of the sequenced GSB strains (e.g., YP_001944405 in *Chlorobium limicola* DSM 245) and thiotrophic Aquificaceae.

We propose the gene designation *sqrE* for type V SQR, which designates homologs of the functionally characterized SQR in the archaeon *Acidianus ambivalens* (3H8L; Brito et al., 2009). *Cba. tepidum* has an SqrE homolog (CT0876/NP_661769), although no SQR activity has been demonstrated for this protein (Chan et al., 2009).

We propose the gene designation *sqrF* for type VI SQR, which includes homologs of an SQR that has been functionally characterized in *Cba. tepidum* (CT1087/NP_661978; Chan et al., 2009). SqrF is important for growth of *Cba. tepidum* at high sulfide concentrations (≥4 mM). Orthologs of SqrF are also present in thiotrophic Proteobacteria and Aquificaceae.

In summary, no GSB strain characterized to date has SQR enzymes belonging to structure classes I (SqrA) or II (SqrB), and enzymes of structure class V (SqrE) were only found in two *Chlorobaculum* spp. (**Table 1**). All GSB have at least one SQR homolog of structure class IV (SqrD or SqrX) or structure class VI (SqrF; **Table 1**), which generally appear to be characteristic for thiotrophic bacteria and archaea (**Figure 3**; Marcia et al., 2010). Because the types of SQR (III, IV, and VI) in *Chp. thalassium* are the earliest diverging SQR sequences in GSB in their respective clades (**Figure 3**), these types of SQR may have been present in the last common ancestor of the GSB investigated here.

Similar to most GSB, all PSB of the *Chromatiaceae* investigated (*Alc. vinosum* DSM 180, *Mch. purpuratum* DSM 1591, *Tco. pfennigii* 4520, *Tcs. violascens* DSM 198, *Tfc. mobilis* 8321, and *Thiodictyon* sp. Cad16) have both SqrD and SqrF (**Figure 3**). In contrast and unlike other PSB and GSB, all PSB of the Ectothiorhodospiraceae investigated (*Ect. haloalkaliphila* ATCC 51935, *Hlr. halophila* SL1, and *Trs. sibirica* ATCC 700588) have SqrB (**Figure 3**). The only exception to this pattern is *Trs. sibirica*, which contains both SqrB and SqrD (**Figure 3**). It is striking that the type of SQR in all of these PSB is clearly correlated with the location of the sulfur globules produced by the organisms: SqrD-containing strains (i.e., all Chromatiaceae) produce intracellular sulfur globules and SqrB-containing strains (i.e., all *Ectothiorhodospiraceae*) produce extracellular sulfur globules. *Trs. sibirica* has both SqrB and SqrD, and this organism has been reported to produce both intracellular and extracellular sulfur globules (Bryantseva et al., 1999). In addition, only PSB that deposit intracellular sulfur globules (Chromatiaceae and *Trs. sibirica*) have homologs of the sulfur globule proteins SgpA and SgpB, which are absent from other PSB and from all GSB (data not shown). Described bacterial SQR sequences in general do not contain an N-terminal signal peptide (Shahak and Hauska, 2008; Marcia et al., 2010). Nevertheless, SqrA from *Rhodobacter capsulatus* and *Aquifex aeolicus*, which do not have an N-terminal signal peptide, are associated with the cytoplasmic membrane with the sulfide-binding site in the periplasm (Schütz et al., 1999; Marcia et al., 2009). It has been suggested that these proteins are translocated by an unknown mechanism that depends on a motif at the C-terminus of the SqrA polypeptide (Schütz et al., 1999). Surprisingly, all SqrB sequences of the *Ectothiorhodospiraceae* investigated here (*Ect. haloalkaliphila*, *Hlr. halophila*, and *Trs. sibirica*; **Figure 3**) had a signal peptide for the twin-arginine translocation (TAT; see Materials and Methods), which indicates that these proteins are translocated across the cytoplasmic membrane using the TAT pathway for proteins that require cytoplasmic assembly of a cofactor and folding prior to translocation. This implies that the active site of SqrB proteins also most likely resides in the periplasmic space. In conclusion, different types of SQR polypeptides are apparently targeted by different mechanisms. Furthermore, at least based on the nine PSB genomes analyzed here, the location of the deposited sulfur globules in PSB can be predicted by the type of the SQR that is present (SqrB or SqrD). This interpretation does not extend to GSB, because all GSB have type IV SQR (SqrD/SqrX) and not SqrB, and GSB produce only extracellular sulfur globules. The difference(s) responsible for SQR targeting and sulfur deposition between the PSB and GSB systems is currently not understood.

With respect to other phototrophic bacteria, purple non-sulfur bacteria and Cyanobacteria typically have SqrA and members of the *Chloroflexi* typically have SqrB.

FLAVOCYTOCHROME *C* AND SOXF HOMOLOGS

Flavocytochrome *c* in GSB and PSB consists of a large, sulfide-binding, flavoprotein subunit (FccB) and a small, *c*-type cytochrome subunit (FccA; Kusai and Yamanaka, 1973; Brune, 1989; Reinartz et al., 1998). Although the exact physiological function is still debated, the enzyme is located in the periplasm and appears to be involved in oxidative sulfur metabolism. In *Alc. vinosum* this complex is encoded by *fccAB* (Reinartz et al., 1998). The homologous genes in *Paracoccus pantotrophus* and other bacteria are denoted *soxEF* (Friedrich et al., 2008). Here, we denote the genes *fccAB* if they occur in phototrophic sulfur bacteria (i.e., GSB or PSB) and *soxEF* in all other organisms. Almost all GSB have *fccAB* genes encoding flavocytochrome *c* (**Table 1**). The *fccAB* genes do not cluster with *sox* genes in GSB, as is the case in *P. pantotrophus* and many other bacteria that contain *sox* genes (Friedrich et al., 2008). GSB that contain *soyYZ* genes may be considered to be an exception to this observation (**Table 1**). The *soyYZ* genes encode a putative, periplasmic SoyYZ complex that is paralogous to the SoxYZ complex, and SoyYZ may be involved in sulfur chemistry that does not involve either the SoxAX or SoxB proteins (Frigaard

and Bryant, 2008). When the *soyYZ* genes are present in a GSB strain, they always form the cluster *soyYZ-fccAB*, which strongly suggests that a functional link exists between FccAB and SoyYZ.

Some GSB encode an additional homolog of FccB/SoxF that we denote as SoxJ. Some authors have denoted this protein as SoxF (Ogawa et al., 2010) or SoxF2 (Verte et al., 2002). However, we prefer to denote this protein as SoxJ to distinguish it clearly from SoxF that is a subunit of the SoxEF/FccAB flavocytochrome *c* (see previous paragraph). The *soxJ* gene in GSB invariably occurs in a conserved cluster of *sox* genes (*soxJXYZAKBW*; see below) that notably does not include an *fccA/soxE* homolog. Monomeric SoxJ/CT1015 protein is readily isolated from *Cba. tepidum* and has been shown to enhance thiosulfate oxidation *in vitro* by a SOX enzyme system reconstituted from SoxAXK, SoxYZ, and SoxB isolated from *Cba. tepidum* (Ogawa et al., 2010). SoxF isolated from *P. pantotrophus* also stimulates thiosulfate oxidation by a reconstituted enzyme system of Sox proteins isolated from *P. pantotrophus* (Friedrich et al., 2008). Thus, based on genetic and biochemical evidence, SoxJ in GSB appears to enhance thiosulfate oxidation by the SOX system. FccB and SoxJ from GSB have high sequence similarity and do not form obvious, monophyletic groups in a phylogenetic analysis (**Figure 4A**); therefore, they are distinguished primarily on the basis of genetic context (see above). However, when combined, all FccB and SoxJ sequences from GSB form a monophyletic group (**Figure 4A**). This suggests that the horizontal transfer of an ancestral gene into the GSB lineage (probably as *fccAB*) only happened once and that SoxJ arose by duplication of FccB after this transfer to the GSB.

SOX ENZYME SYSTEM

Orthologs of some genes that encode the well-characterized, thiosulfate-oxidizing Sox enzyme system in *P. pantotrophus* (*soxXYZABCDEFGH*; Friedrich et al., 2005, 2008) were readily identified in seven of the GSB genomes (**Table 1**). All GSB capable of growth on thiosulfate contain *sox* genes. However, in agreement with previous observations (Eisen et al., 2002; Frigaard and Bryant, 2008), the *soxCD* genes that encode the essential SoxCD component of the reaction mechanism in *P. pantotrophus* were absent from all GSB genomes. The *sox* genes in GSB consistently occurred in a conserved cluster of eight genes, which were identical to the clusters originally identified in *Cba. thiosulfatiphilum* DSM 249 (Verté et al., 2002) and *Cba. tepidum* (Eisen et al., 2002). Because of their presence in this conserved cluster, two of the genes have been renamed *soxJ* (CT1015 in *Cba. tepidum* TLS; referred to as *soxF2* in *Cba. thiosulfatiphilum* DSM 249 by Verté et al., 2002) and *soxK* (CT1020 in *Cba. tepidum* TLS; referred to as orf6 in *Cba. thiosulfatiphilum* DSM 249 by Verté et al., 2002). SoxJ is a flavoprotein that is homologous to FccB/SoxF (described above). SoxK is a component of the trimeric SoxAXK complex isolated from *Cba. tepidum* and is essential for efficient thiosulfate oxidation when using Sox enzymes isolated from *Cba. tepidum* that are reconstituted *in vitro* (Ogawa et al., 2008). The presence of *soxK* in various bacteria is correlated with the occurrence of a SoxAX complex that comprises a monoheme SoxA and a monoheme SoxX; *P. pantotrophus* and many other bacteria have a diheme SoxA (Ogawa et al., 2008).

Among all *sox*-containing bacteria for which genome sequence data is currently available, the gene organization of the *sox* cluster in GSB (*soxJXYZAKBW*) is unique. Sequence analysis of the *sox* region in GSB suggested that there is only one promoter and that this promoter is located upstream of the *soxJ* gene (**Figure 5**). This observation suggests that the *soxJXYZAKBW* cluster probably is transcribed as a single mRNA. Consistent with this interpretation, transcription profiling shows that mRNA levels for all of the genes of this cluster are about 10-fold more abundant in cells growing on thiosulfate than on sulfide.

THIOSULFATE UTILIZATION MAY BE ENCODED BY A MOBILE GENETIC ELEMENT

A phylogenetic tree of concatenated Sox proteins from GSB is shown in **Figure 4B**. The eight proteins encoded by the *soxJXYZAKBW* cluster in GSB had largely congruent phylogeny (data not shown), which suggests that the cluster has been inherited intact in all GSB strains. The phylogeny of the Sox proteins within the *Chlorobium* and *Chlorobaculum* lineages (**Figure 4B**) was congruent with the cellular core phylogeny (**Figure 2**) with one exception: the *Chl. phaeovibrioides* DSM 265 Sox proteins grouped with the Sox proteins of the *Chlorobaculum* lineage (**Figure 4B**). This suggests that the *sox* cluster was horizontally transferred from a *Chlorobaculum* strain to an ancestor of *Chl. phaeovibrioides* DSM 265. It is also evident that the *sox* promoter region in *Chl. phaeovibrioides* DSM 265 is more similar to the *sox* promoter region in *Cba. parvum* DSM 263 than to the promoters in other GSB strains (**Figure 5**).

Figure 6 shows a comparison of syntenic regions of the genome in *Chl. phaeovibrioides* DSM 265 (sox^+) and the very closely related *Chl. luteolum* DSM 273 (sox^-). A global comparison of these two strains suggested that these were the two most similar GSB among the 15 sequenced strains (Bryant et al., 2011). **Figure 6** reveals that the *sox* genes in *Chl. phaeovibrioides* DSM 265 reside on an 11-kb island that is terminated by imperfect repeats (22–23 bp in length). Moreover, this island occurs in a region of the genome not otherwise related to sulfur metabolism. This 11-kb "*sox* island" harbors genes encoding a transposase, an integrase, and an RNA-directed DNA polymerase (reverse transcriptase), all of which are indicative of a mobile genetic element. The terminal imperfect inverted repeats suggest that the island was mobilized by the transposase. Integrase and reverse transcriptase usually do not occur on the same mobile element but the observation that the genes are located on a fragment flanked by inverted repeats suggests that they have the same origin. Reverse transcriptase occurs in a variety of mobile elements including retroviruses and bacterial retrons, suggesting that the mobile element could have been propagated via an RNA stage. No systems of this type, nor RNA or DNA viruses, have yet been characterized in GSB.

A 15-kb plasmid (accession number NC_002095) isolated from *Cba. thiosulfatiphilum* DSM 249 was reported to encode thiosulfate utilization when transformed into *Chl. limicola* DSM 245 (Méndez-Alvarez et al., 1994). However, this plasmid does not contain *sox* genes and it is not clear how this plasmid could encode thiosulfate utilization (Frigaard and Bryant, 2008).

DSR ENZYME SYSTEM

The dissimilatory sulfite reductase (DSR) system is essential for oxidation of sulfur globules in *Cba. tepidum* (Holkenbrink et al., 2011) and *Alc. vinosum* (Dahl et al., 2005). Most GSB strains contain *dsr* genes that occur as a single conserved gene cluster

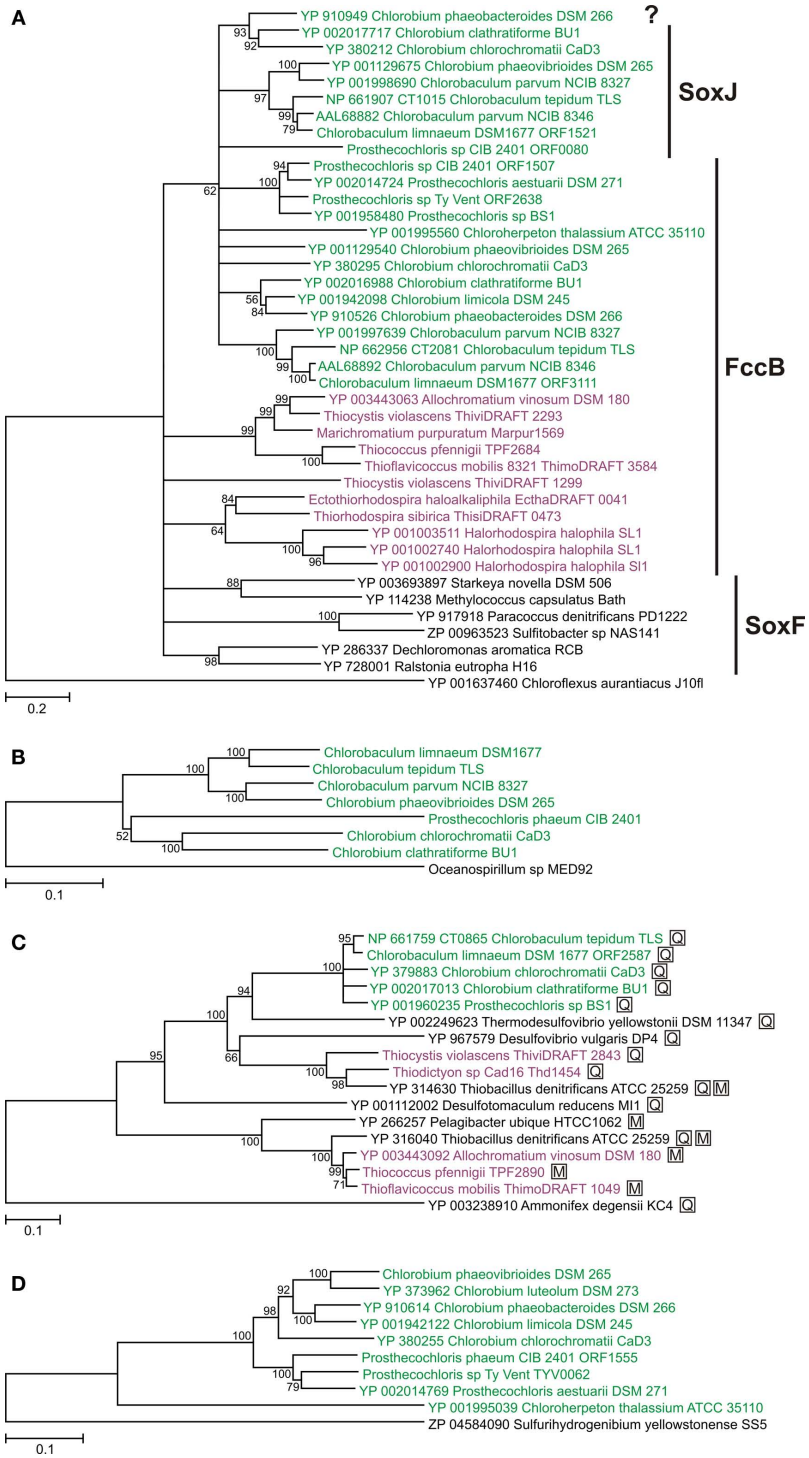

FIGURE 4 | Phylogenetic trees of oxidative sulfur metabolism enzymes. Tree construction details are as described for **Figure 2**. Sequences from GSB are shown in green; sequences from PSB are shown in purple. **(A)** FccB/SoxF/SoxJ homologs (the designation SoxJ is used if the gene is part of a *soxJXYZAKBW* cluster in GSB; the designation FccB is used if the gene is part of a *fccAB* cluster in GSB or PSB; the designation SoxF is used if the gene is part of a *soxEF* cluster in organisms other than GSB and PSB). The question mark indicates an unnamed protein. All proteins in the tree except the root had a signal peptide for the twin-arginine translocon (data not shown). The tree is rooted with *Cfx. aurantiacus* SqrB. **(B)** Concatenation of SoxXYZAKB proteins (CT1016–CT1021 in *Cba. tepidum*). The three is rooted with the same proteins from *Oceanospirillum* sp. MED92. **(C)** Adenosine-5′-phosphosulfate reductase alpha subunit (AprA). The three is rooted with a homologous protein from *Ammonifex degensii*. Proteins marked with a boxed "M" indicate that the organism has AprM; proteins marked with a boxed "Q" indicate that the organism has Qmo proteins. **(D)** Polysulfide reductase-like complex 3 (PSRLC3). The three is rooted with a homologous protein from *Sulfurihydrogenibium yellowstonense*. The PSRLC3 protein from *Chl. phaeovibrioides* DSM 265 used here was constructed by restoring a frameshift mutation in the gene (**Table 1**). See text for details.

dsrNCABLUEFHTMKJOPVW (**Table 1**). One exception is *Chl. ferrooxidans* DSM 13031, which lacks all *dsr* genes and most other genes related to oxidative sulfur metabolism (**Table 1**). This is consistent with the observation that this organism does not grow on reduced sulfur compounds (Heising et al., 1999). The only other strain that lacks all *dsr* genes is *Chp. thalassium* ATCC 35110, which has been reported to "slowly" consume sulfur globules (Gibson et al., 1984; see Discussion for further details). *Cba. parvum* DSM 263 has a single cluster of *dsr* genes (*dsrNCABLUTMKJOPVW*), which lacks the *dsrEFH* genes. This strain accumulates sulfur globules and does not produce sulfate when grown on sulfide (Kelly, 2008), which strongly suggests that the *dsrEFH* gene products are essential for a functional DSR system.

With respect to gene organization, the *dsr* gene cluster in *Cba. tepidum* is split and the *dsrCABL* genes are duplicated: *dsrNCABLUTMKJOPVW* (CT2251–CT2238) and *dsrCABLEFH* (CT0851–CT0857; Eisen et al., 2002). Although the current draft genome sequence of *Cba. limnaeum* DSM 1677 does not allow a definitive view of the gene organization, it appears that this organism also has all *dsr* genes, but that the *dsr* genes are split and duplicated in the same manner as in *Cba. tepidum*. Interestingly, the *dsr* gene cluster in *Cba. parvum* DSM 263 is identical to the longest cluster in *Cba. tepidum* (*dsrNCABLUTMKJOPVW*). Thus, the clustering of *dsr* genes is irregular in all investigated *Chlorobaculum* strains. One possible evolutionary scenario is that the canonical GSB *dsr* cluster (*dsrNCABLUEFHTMKJOPVW*) split into two clusters (*dsrNCABLUTMKJOPVW* and *dsrCABLEFH*) in a common ancestor of the investigated *Chlorobaculum* strains and that *Cba. parvum* DSM 263 subsequently lost the short cluster and thereby the ability to oxidize sulfur globules. *Cba. parvum* DSM 263 is naturally transformable and apparently has an active homologous recombination system that may have facilitated this loss (Ormerod, 1988).

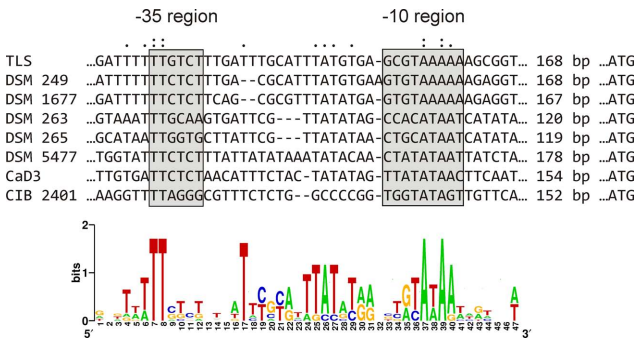

FIGURE 5 | Prediction of the promoter region of the *sox* gene cluster in GSB. The regions shown are upstream of the *soxJ* gene; the *soxJ* ATG start codon is indicated to the right.

ARE SOXCD AND DSR MUTUALLY EXCLUSIVE?

The SOX system in GSB only partially oxidizes thiosulfate (**Figure 1**), whereas the SOX system in *P. pantotrophus* and many other bacteria completely oxidizes thiosulfate to sulfate (Friedrich et al., 2008). This difference is dependent on the presence of SoxCD in *P. pantotrophus*, which is absent from GSB. Complete oxidation of sulfur compounds to sulfate in GSB requires the DSR system (**Figure 1**; Holkenbrink et al., 2011).

We surveyed 1429 publicly available genome sequences[14] for *sox* genes using BLASTP and known Sox protein sequences as queries. The retrieved sequences were then evaluated by sequence comparison, phylogenetic analysis, and gene clustering analyses to identify *bona fide* Sox proteins. We used the criterion that all Sox proteins of a given function must form a monophyletic clade, for which the clade was defined by a small number of query sequences.

The genomes were surveyed for SoxA/SoxB using BLASTP and the following query sequences (Meyer et al., 2007; Friedrich et al., 2008): YP_917913/YP_917914 (*Paracoccus denitrificans* PD1222), YP_144681/YP_144683 (*Thermus thermophilus* HB8), YP_487970/YP_487967 (*Rhodopseudomonas palustris* HaA2), YP_727992/YP_727989 (*Ralstonia eutropha* H16), NP_767651 (SoxA; *Bradyrhizobium japonicum* USDA 110), and NP_214237 (SoxB; *Aquifex aeolicus* VF5). The outgroup in phylogenetic

[14]http://www.ncbi.nlm.nih.gov/sutils/genom_table.cgi

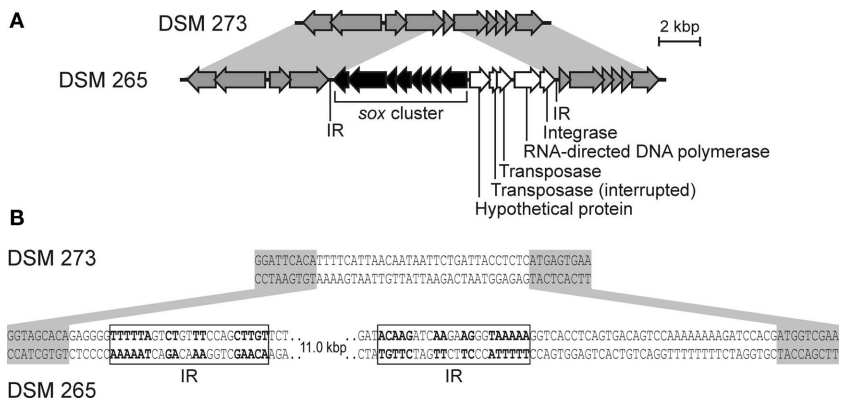

FIGURE 6 | The *sox* gene island in *Chl. phaeovibrioides* DSM 265. (A) Alignment of syntenic regions in *Chl. luteolum* DSM 273 and *Chl. phaeovibrioides* DSM 265. **(B)** Details of the *sox* gene island terminal sequences and insertion site. Genes marked in gray are not related to sulfur metabolism. Shades of gray indicate sequence similarity. IR, inverted repeat.

analyses of SoxA and SoxB was ZP_03609782 (*Campylobacter rectus* RM3267) and ZP_02950408 (*Clostridium butyricum* 5521), respectively. In total, 127 genomes were identified that contained both *soxA* and *soxB* (56 Alphaproteobacteria, 26 Betaproteobacteria, 15 Gammaproteobacteria, 8 Epsilonproteobacteria, 8 Aquificales, 5 Chlorobiaceae, 5 Thermaceae, 3 Deltaproteobacteria, and 1 *Magnetococcus* sp.). (*Magnetococcus* is member of the Proteobacteria whose subdivision affiliation is not resolved.) These genomes were then surveyed for SoxC/SoxD using BLASTP and the following query sequences (Friedrich et al., 2008): YP_917915/YP_917916 (*Paracoccus denitrificans* PD1222), YP_144677/YP_144676 (*Thermus thermophilus* HB8), YP_487966/YP_487965 (*Rhodopseudomonas palustris* HaA2), YP_727998/YP_841734/YP_727997/YP_841733 (*Ralstonia eutropha* H16), and NP_770156/NP_772761/NP_770157/NP_772760 (*Bradyrhizobium japonicum* USDA 110). Sequences that were more related to the homologous SorAB sulfite:cytochrome *c* oxidoreductase were eliminated. SorA/SorB queries used: AAF64400/AAF64401 (*Starkeya novella* DSM 506; Kappler et al., 2000) and YP_003892083/YP_003892084 (*Sulfurimonas autotrophica* DSM 16294). We found that most genomes (about 100 of the 127 genomes investigated) encoded SoxC and SoxD.

The DSR enzyme subunits DsrA and DsrB that function in sulfur oxidation (oxDsrAB) can be identified by sequence analysis, because these sequences form a monophyletic clade, which is clearly separated from the group of paralogous enzymes that function in sulfate reduction (redDsrAB; Loy et al., 2009). The 127 genomes that encoded SoxA and SoxB were surveyed for DsrA and DsrB using BLASTP and known DsrA and DsrB sequences as queries (Loy et al., 2009). The oxDsrA/oxDsrB queries used were NP_661746/NP_661747 (*Cba. tepidum* TLS), YP_003443222/YP_003443223 (*Alc. vinosum* DSM 180), and YP_866063/YP_866064 (*Magnetococcus* sp. MC-1). The redDsrA/redDsrB queries used were YP_967975/YP_967974 (*Desulfovibrio vulgaris* DP4), YP_001114514/YP_001114513 (*Desulfotomaculum reducens* MI-1), and NP_069259/NP_069260 (*Archaeoglobus fulgidus* DSM 4304). The obtained DsrA and DsrB sequences were easily identified and classified by sequence comparison and phylogenetic analysis. None of the 127 genomes that encoded SoxA and SoxB also encoded redDsrAB, which indicated that no sulfate-reducing bacterium has the SOX system. In contrast, oxDsrAB genes were present in 15 of the genomes that encoded SoxA and SoxB. None of these 15 genomes also encoded *soxCD*. Thus, this survey showed that SoxCD and DSR are mutually exclusive. Specifically, these 15 organisms were: five strains of GSB (**Table 1**), *Allochromatium vinosum* DSM 180, *Halorhodospira halophila* SL1, *Thioalkalivibrio* sp. HL-EbGR7, *Sideroxydans lithotrophicus* ES-1, *Thiobacillus denitrificans* ATCC 25259, *Beggiatoa* sp. PS, Candidatus *Vesicomyosocius okutanii* HA, Candidatus *Ruthia magnifica* str. Cm, *Magnetospirillum magnetotacticum* MS-1, and *Magnetococcus* sp. MC-1.

Interestingly, some SoxAB-encoding genomes encode neither SoxCD nor DsrAB (e.g., all of the eight strains of *Aquificales* examined including *Aquifex aeolicus* VF5 (Ghosh et al., 2009), *Hyphomonas neptunium* ATCC 15444, *Cupriavidus metallidurans* CH34, and *Ralstonia pickettii* 12D). These organisms must use an unknown mechanism to regenerate the SOX system.

OXIDATION OF SULFITE

Although GSB cannot grow on sulfite (Frigaard and Dahl, 2009), the DSR system presumably produces sulfite, which must be oxidized (**Figure 1**). None of the 16 genomes listed in **Table 1** encode homologs of the SorAB sulfite dehydrogenase (AAF64400/AAF64401) known from *Starkeya novella* (Kappler et al., 2000).

One-third of the analyzed GSB strains encode adenosine-5′-phosphosulfate (APS) reductase (APR; **Table 1**; **Figure 4C**; AprAB/CT0865-CT0864 in *Cba. tepidum* TLS). This APR probably functions in sulfite oxidation and may be coupled with ATP sulfurylase (Sat) and the membrane-bound QmoABC oxidoreductase as depicted in **Figure 1** (Frigaard and Dahl, 2009). These enzymes are encoded by a *sat-aprBA-qmoABC* gene cluster that is conserved in all GSB that have these genes (**Table 1**). None of the GSB investigated encodes the putative membrane-bound oxidoreductase AprM found in *Alc. vinosum* DSM 180 (Hipp et al., 1997). Deletion of the entire *sat-aprBA-qmoABC* gene cluster in *Cba. tepidum* TLS does not prevent the mutant strain from growth on sulfide and from producing sulfate (Holkenbrink, 2010). This observation suggests that even if APR functions in sulfite oxidation in GSB, it is not the only mechanism that oxidizes sulfite in *Cba. tepidum* TLS. One such possible mechanism is that sulfite reacts abiotically with oligosulfides to form thiosulfate, which subsequently is oxidized by the SOX system (Holkenbrink et al., 2011).

Polysulfide reductase-like complex 3 (PSRLC3) is a putative sulfite dehydrogenase that is found in some GSB (YP_910613 and YP_910614 in *Chl. phaeobacteroides* DSM 266; Frigaard and Bryant, 2008). In all *Chlorobium* strains (expect *Chl. limicola* DSM 245) the genes encoding PSRLC3 are located immediately upstream of the *dsr* gene cluster (Frigaard and Dahl, 2009; data not shown), consistent with a functional link between PSRLC3 and oxidative sulfur metabolism. Sequence analysis showed that all sulfur-oxidizing GSB have either APR or PSRLC3, except *Chl. chlorochromatii* CaD3 that has both enzymes (**Table 1**). Analysis of the PsrA-like subunit of PSRLC3 showed that the phylogeny (**Figure 4D**) is congruent, at least at the genus level, with that of cellular core genes (**Figure 2**). This suggests that PSRLC3 was present in the last common ancestor of the investigated GSB.

Like the GSB, PSB apparently do not use a single mechanism to oxidize sulfite. *Alc. vinosum* DSM 180 has APR that apparently is coupled with the putative membrane-bound oxidoreductase AprM (Hipp et al., 1997). Among the PSB examined here, three strains encode AprABM (*Alc. vinosum* DSM 180, *Tco. pfennigii* 4520, *Tfc. mobilis* 8321) and two strains encode AprAB-QmoAB (*Thiodictyon* sp. Cad16, *Tcs. violascens* DSM 198; **Figure 4C**). Sat, AprAB, and QmoAB were not found in any of the *Ectothiorhodospiraceae* (*Ect. haloalkaliphila* ATCC 51935, *Hlr. halophila* SL1, *Trs. sibirica* ATCC 700588) or *Mch. purpuratum* DSM 1591. SorAB and PSRLC3 have not yet been found in any PSB strain.

DISCUSSION

The congruent phylogenies of rRNA sequences and conserved house-keeping functions provide a solid foundation for understanding the evolution of the GSB lineage (**Figures 2A,B**). A selection of genes encoding physiological traits characteristic of GSB had overall congruent phylogenies with the rRNA and house-keeping functions, at least to the genus level (**Figure 2C**; and examples mentioned in Section "Results"). This suggests that these physiological functions were present in the last common ancestor of known extant GSB and

were passed on only by vertical descent. This includes elements of phototrophy, carbon fixation, nitrogen fixation, and hydrogen uptake (although a few strains have apparently lost their *hup* genes). Most of the genes encoding components of oxidative sulfur metabolism in GSB, on the other hand, have very different evolutionary histories.

The DSR system is not present in the earliest diverging GSB (*Chp. thalassium*) and appears to have been acquired by horizontal gene transfer, in part from other sulfide-oxidizing organisms and in part from sulfate-reducing organisms, after divergence of *Chloroherpeton* (Sander et al., 2006). It is not clear from the literature how, or whether, sulfide is oxidized to sulfate in *Chp. thalassium* (Gibson et al., 1984). The question arises because the DSR system is essential for this process in other GSB (Holkenbrink et al., 2011). It is also not clear how the sulfite produced by the DSR system is oxidized. A single sulfite oxidation mechanism present in all thiotrophic GSB or PSB has not been identified. Phylogenetic analyses suggest that the putative sulfite dehydrogenase PSRLC3 was present in the last common ancestor of the investigated GSB (**Figure 4D**). It is an attractive hypothesis that the APR system replaced the PSRLC3 in sulfite oxidation by horizontal gene transfer in a few GSB strains and that this acquisition was selected for due to increased energy conservation in the APR pathway as compared to the PSRLC3 pathway (**Figure 1**). A genetic transfer mechanism of the *sat-apr-qmo* genes has not been identified but a similar cluster of genes with high sequence similarity occurs in sulfate-reducing bacteria that typically co-occur with GSB in favorable habitats (Meyer and Kuever, 2007).

The SOX system for thiosulfate oxidation is widespread among very divergent organisms (Meyer et al., 2007). Formation of thiosulfate in the environment occurs under various conditions, such as by mixing of sulfide and O_2 (abiotic formation) and as a byproduct of sulfide oxidation in GSB and PSB (Holkenbrink et al., 2011). The SOX system is present only in some GSB strains and appears to have been acquired by horizontal gene transfer from members of the Proteobacteria (Meyer et al., 2007), and subsequently exchanged horizontally within the GSB lineage (**Figure 4B**). The SOX system in most organisms other than GSB and PSB includes the SoxCD complex, which together with other Sox components allows complete oxidation of one molecule of thiosulfate to two molecules of sulfate in the periplasm while producing reduced cytochrome *c*. However, SoxCD is not part of the SOX system in GSB and PSB, in which the DSR system completes the oxidation of the sulfane moiety of thiosulfate. The DSR-dependent mechanism presumably conserves more of the chemical energy available to the organism, because the reducing equivalents from the sulfane moiety are recovered as reduced isoprenoid quinones in the cytoplasmic membrane. In addition, chemical energy may be conserved by substrate-level phosphorylation by the APR system (**Figure 1**). If DSR-dependent thiosulfate oxidation indeed conserves more energy than SoxCD-dependent thiosulfate oxidation, this may explain why loss of *soxCD* genes has occurred in bacteria that contain both the SOX and DSR systems. Our genome sequence analyses showed that loss of the *soxCD* genes has occurred independently in unrelated DSR-containing organisms with divergent Sox systems, including GSB, PSB, the betaproteobacterium *Thiobacillus denitrificans* ATCC 25259, and the divergent proteobacterium *Magnetococcus* sp. MC-1.

The current collection of cultured GSB strains exhibits very limited physiological variation (Imhoff, 2003). Limited success and approaches to isolation of axenic cultures could explain part of this observation. However, many cases have been described where the GSB that are found in environmental studies of lakes and sediments (where one expects to find GSB), are similar to cultured strains (at least at the level of SSU rRNA sequence similarity, e.g., Koizumi et al., 2004; Manske et al., 2005; Alexander and Imhoff, 2006; Gregersen et al., 2009). Therefore, it is likely that these strains contain the DSR system. The DSR system provides GSB with an improved utilization of reduced sulfur compounds that is likely to be advantageous in sulfide-limited and energy-limited environments (Holkenbrink et al., 2011). Although the DSR system appears to allow GSB to prosper in certain environments, the DSR system may not be important to GSB-like organisms in environments with high sulfide concentrations or to organisms that participate in symbioses with microbes that reduce elemental sulfur. The former reason may in part explain why *Cba. parvum* has lost three essential genes (*dsrEFH*) and can no longer oxidize elemental sulfur (**Table 1**). GSB that can grow by oxidation of Fe^{2+} or H_2 as the sole electron donor also do not need DSR (Heising et al., 1999). *Chp. thalassium* is another GSB that thrives without DSR, although the ecophysiology of this organism is not yet described in detail (Gibson et al., 1984). It would be very interesting to know (i) if there are phototrophic relatives of GSB without DSR that are metabolically important community members; (ii) under which environmental conditions such GSB thrive; and (iii) the detailed metabolism and ecophysiology of such GSB. Cultivation-independent approaches (including metagenomics) and novel approaches to isolation of pure cultures may provide information on these issues.

CONCLUSION

The phylogenetic analyses presented here and elsewhere (Sander et al., 2006; Meyer and Kuever, 2007; Meyer et al., 2007; Frigaard and Bryant, 2008; Frigaard and Dahl, 2009; Loy et al., 2009) strongly suggest that the currently known and characterized GSB have obtained many of their oxidative sulfur metabolism genes by horizontal gene transfer from a variety of chemotrophic bacteria that either oxidize sulfur compounds or reduce sulfur compounds. In addition, certain steps in the oxidative sulfur metabolism in some GSB appear to have been replaced with pathways that we hypothesize improve conservation of chemical energy by introducing substrate-level phosphorylation reactions and increased transmembrane proton transfer (e.g., DSR replacing SoxCD in thiosulfate oxidation and APR putatively replacing PSRLC3 in sulfite oxidation). Although progress has been made in understanding the enzymes and pathways involved in oxidative sulfur metabolism in GSB, many essential aspects are still not understood. This includes the mechanisms for formation and consumption of sulfur globules, sulfite oxidation, and SQR-independent sulfide consumption. The rapidly increasing amount of genome sequence information for both GSB and PSB will surely improve our understanding of these processes.

ACKNOWLEDGMENTS

Niels-Ulrik Frigaard was supported by a grant from the Danish Natural Science Research Council (21-04-0463). Donald A. Bryant was supported by grants from the U.S. National Science Foundation (MCB-0523100), U.S. Department of Energy (DE-FG02-94ER20137) and NASA Exobiology (NNX09AM87G). Donald A. Bryant and Niels-Ulrik Frigaard thank the Joint Genome Institute for their assistance in generating draft genomes of some of the GSB and PSB discussed here.

REFERENCES

Alexander, B., Andersen, J. H., Cox, R. P., and Imhoff, J. F. (2002). Phylogeny of green sulfur bacteria on the basis of gene sequences of 16S rRNA and of the Fenna–Matthews–Olson protein. *Arch. Microbiol.* 178, 131–140.

Alexander, B., and Imhoff, J. F. (2006). Communities of green sulfur bacteria in marine and saline habitats analyzed by gene sequences of 16S rRNA and Fenna–Matthews–Olson protein. *Int. Microbiol.* 9, 259–266.

Azai, C., Tsukatani, Y., Harada, J., and Oh-Oka, H. (2009). Sulfur oxidation in mutants of the photosynthetic green sulfur bacterium *Chlorobium tepidum* devoid of cytochrome c-554 and SoxB. *Photosyn. Res.* 100, 57–65.

Bagos, P. G., Nikolaou, E. P., Liakopoulos, T. D., and Tsirigos, K. D. (2010). Combined prediction of Tat and Sec signal peptides with hidden Markov models. *Bioinformatics* 26, 2811–2817.

Brito, J. A., Sousa, F. L., Stelter, M., Bandeiras, T. M., Vonrhein, C., Teixeira, M., Pereira, M. M., and Archer, M. (2009). Structural and functional insights into sulfide:quinone oxidoreductase. *Biochemistry* 48, 5613–5622.

Bronstein, M., Schütz, M., Hauska, G., Padan, E., and Shahak, Y. (2000). Cyanobacterial sulfide-quinone reductase: cloning and heterologous expression. *J. Bacteriol.* 182, 3336–3344.

Brune, D. C. (1989). Sulfur oxidation by phototrophic bacteria. *Biochim. Biophys. Acta* 975, 189–221.

Bryant, D. A., Klatt, C. G., Frigaard, N.-U., Liu, Z., Li, T., Zhao, F., Garcia Costas, A. M., Overmann, J., and Ward, D. M. (2011). "Comparative and functional genomics of anoxygenic green bacteria from the taxa *Chlorobi, Chloroflexi,* and *Acidobacteria*," in *Advances in Photosynthesis and Respiration*, Vol. 33, *Functional Genomics and Evolution of Photosynthetic Systems*, eds R. L. Burnap and W. Vermaas (Dordrecht: Springer), in press.

Bryantseva, I. A., Gorlenko, V. M., Kompantseva, E. I., Imhoff, J. F., Süling, J., and Mityushina, L. (1999). *Thiorhodospira sibirica* gen. nov., sp. nov., a new alkaliphilic purple sulfur bacterium from a Siberian Soda lake. *Int. J. Syst. Bacteriol.* 49, 697–703.

Carver, T., Berriman, M., Tivey, A., Patel, C., Böhme, U., Barrell, B. G., Parkhill, J., and Rajandream, M. A. (2008). Artemis and ACT: viewing, annotating and comparing sequences stored in a relational database. *Bioinformatics* 24, 2672–2676.

Chan, L.-K., Morgan-Kiss, R., and Hanson, T. E. (2008). "Genetic and proteomic studies of sulfur oxidation in *Chlorobium tepidum* (syn. *Chlorobaculum tepidum*)," in *Sulfur Metabolism in Phototrophic Organisms*, R. Hell, C. Dahl, D. Knaff, and T. Leustek (New York: Springer), 363–379.

Chan, L. K., Morgan-Kiss, R. M., and Hanson, T. E. (2009). Functional analysis of three sulfide:quinone oxidoreductase homologs in *Chlorobaculum tepidum*. *J. Bacteriol.* 191, 1026–1034.

Crooks, G. E., Hon, G., Chandonia, J. M., and Brenner, S. E. (2004). WebLogo: a sequence logo generator. *Genome Res.* 14, 1188–1190.

Dahl, C., Engels, S., Pott-Sperling, A. S., Schulte, A., Sander, J., Lübbe, Y., Deuster, O., and Brune, D. C. (2005). Novel genes of the *dsr* gene cluster and evidence for close interaction of Dsr proteins during sulfur oxidation in the phototrophic sulfur bacterium *Allochromatium vinosum*. *J. Bacteriol.* 187, 1392–1404.

Demerec, M., Adelberg, E. A., Clark, A. J., and Hartman, P. E. (1966). A proposal for a uniform nomenclature in bacterial genetics. *Genetics* 54, 61–76.

Efremov, R. G., Baradaran, R., and Sazanov, L. A. (2010). The architecture of respiratory complex I. *Nature* 465, 441–445.

Eisen, J. A., Nelson, K. E., Paulsen, I. T., Heidelberg, J. F., Wu, M., Dodson, R. J., Deboy, R., Gwinn, M. L., Nelson, W. C., Haft, D. H., Hickey, E. K., Peterson, J. D., Durkin, A. S., Kolonay, J. L., Yang, F., Holt, I., Umayam, L. A., Mason, T., Brenner, M., Shea, T. P., Parksey, D., Nierman, W. C., Feldblyum, T. V., Hansen, C. L., Craven, M. B., Radune, D., Vamathevan, J., Khouri, H., White, O., Gruber, T. M., Ketchum, K. A., Venter, J. C., Tettelin, H., Bryant, D. A., and Fraser, C. M. (2002). The complete genome sequence of *Chlorobium tepidum* TLS, a photosynthetic, anaerobic, green-sulfur bacterium. *Proc. Natl. Acad. Sci. U.S.A.* 99, 9509–9514.

Emanuelsson, O., Brunak, S., von Heijne, G., and Nielsen, H. (2007). Locating proteins in the cell using TargetP, SignalP and related tools. *Nat. Protoc.* 2, 953–971.

Friedrich, C. G., Bardischewsky, F., Rother, D., Quentmeier, A., and Fischer, J. (2005). Prokaryotic sulfur oxidation. *Curr. Opin. Microbiol.* 8, 253–259.

Friedrich, C. G., Quentmeier, A., Bardischewsky, F., Rother, D., Orawski, G., Hellwig, P., and Fischer, J. (2008). "Redox control of chemotrophic sulfur oxidation in *Paracoccus pantotrophus*," in *Microbial Sulfur Metabolism*, eds C. Dahl and C. G. Friedrich, (Heidelberg: Springer), 139–150.

Frigaard, N.-U., and Bryant, D. A. (2008). "Genomics insights into the sulfur metabolism of phototrophic green sulfur bacteria," in *Advances in Photosynthesis and Respiration*, Vol. 27, eds R. Hell, C. Dahl, D. B. Knaff, and T. Leustek (Heidelberg: Springer), 337–355.

Frigaard, N.-U., and Dahl, C. (2009). "Sulfur metabolism in phototrophic sulfur bacteria," in *Advances in Microbial Physiology*, ed. R. K. Poole (London: Academic Press), 103–200.

Frigaard, N.-U., Gomez Maqueo Chew, A., Li, H., Maresca, J. A., and Bryant, D. A. (2003). *Chlorobium tepidum*: insights into the structure, physiology, and metabolism of a green sulfur bacterium derived from the complete genome sequence. *Photosyn. Res.* 78, 93–117.

Garrity, G. M., and Holt, J. G. (2001). "Phylum BXI. Chlorobi phy. nov.," in *Bergey's Manual of Systematic Bacteriology*, 2nd Edn., Vol. 1, eds D. R. Boone and R. W. Castenholz (New York, NY: Springer-Verlag), 601–623.

Ghosh, W., Mallick, S., and DasGupta, S. K. (2009). Origin of the Sox multienzyme complex system in ancient thermophilic bacteria and coevolution of its constituent proteins. *Res. Microbiol.* 160, 409–420.

Gibson, J., Pfennig, N., and Waterbury, J. B. (1984). *Chloroherpeton thalassium* gen. nov. et spec. nov., a nonfilamentous, flexing and gliding green sulfur bacterium. *Arch. Microbiol.* 138, 96–101.

Gomez Maqueo Chew, A., Frigaard, N.-U., and Bryant, D. A. (2009). Mutational analysis of three *bchH* paralogs in (bacterio-)chlorophyll biosynthesis in *Chlorobaculum tepidum*. *Photosyn. Res.* 101, 21–34.

Gregersen, L. H., Habicht, K. S., Peduzzi, S., Tonolla, M., Canfield, D. E., Miller, M., Cox, R. P., and Frigaard, N.-U. (2009). Dominance of a clonal green sulfur bacterial population in a stratified lake. *FEMS Microbiol. Ecol.* 70, 30–41.

Hanson, T. E., and Tabita, F. R. (2001). A ribulose-1,5-bisphosphate carboxylase/oxygenase (RubisCO)-like protein from *Chlorobium tepidum* that is involved with sulfur metabolism and the response to oxidative stress. *Proc. Natl. Acad. Sci. U.S.A.* 98, 4397–4402.

Heising, S., Richter, L., Ludwig, W., and Schink, B. (1999). *Chlorobium ferrooxidans* sp. nov., a phototrophic green sulfur bacterium that oxidizes ferrous iron in coculture with a "*Geospirillum*" sp. strain. *Arch Microbiol* 172, 116–124.

Hipp, W. M., Pott, A. S., Thum-Schmitz, N., Faath, I., Dahl, C., and Trüper, H.G. (1997). Towards the phylogeny of APS reductases and sirohaem sulfite reductases in sulfate-reducing and sulfur-oxidizing prokaryotes. *Microbiology* 143, 2891–2902.

Holkenbrink, C. (2010). *Thiotrophic sulfur metabolism in green sulfur bacteria.* Master's thesis, University of Copenhagen, Copenhagen, Denmark.

Holkenbrink, C., Ocón Barbas, S., Mellerup, A., Otaki, H., and Frigaard, N.-U. (2011). Sulfur globule oxidation in green sulfur bacteria is dependent on the dissimilatory sulfite reductase system. *Microbiology* 157, 1229–1239.

Iino, T., Mori, K., Uchino, Y., Nakagawa, T., Harayama, S., and Suzuki, K. (2010). *Ignavibacterium album* gen. nov., sp. nov., a moderately thermophilic anaerobic bacterium isolated from microbial mats at a terrestrial hot spring and proposal of *Ignavibacteria classis* nov., for a novel lineage at the periphery of green sulfur bacteria. *Int. J. Syst. Evol. Microbiol.* 60, 1376–1382.

Imhoff, J. F. (2003). Phylogenetic taxonomy of the family Chlorobiaceae on the basis of 16S rRNA and fmo (Fenna–Matthews–Olson protein) gene sequences. *Int. J. Syst. Evol. Microbiol.* 53, 941–951.

Imhoff, J. F. (2008). "Systematics of anoxygenic phototrophic bacteria," in *Sulfur Metabolism in Phototrophic Organisms*, eds R. Hell, C. Dahl, D. Knaff, and T. Leustek (Dordrecht: Springer), 269–287.

Kappler, U., Bennett, B., Rethmeier, J., Schwarz, G., Deutzmann, R., McEwan, A. G., and Dahl, C. (2000). Sulfite:cytochrome *c* oxidoreductase from *Thiobacillus novellus* – purification, characterization, and molecular biology of a heterodimeric member of the sulfite oxidase family. *J. Biol. Chem.* 275, 13202–13212.

Kelly, D. P. (2008). Stable sulfur isotope fractionation by the green bacterium *Chlorobaculum parvum* during photolithoautotrophic growth on sulfide. *Pol. J. Microbiol.* 57, 275–279.

Klatt, C. G., Wood, J. M., Rusch, D. B., Bateson, M. M., Heidelberg, J. F., Bryant, D. A., and Ward, D. W. (2011). Metagenomic analyses of phototrophic hot spring microbial mat communities. *ISME J.* (in press).

Koizumi, Y., Kojima, H., and Fukui, M. (2004). Dominant microbial composition and its vertical distribution in saline meromictic Lake Kaiike (Japan) as revealed by quantitative oligonucleotide probe membrane hybridization. *Appl. Environ. Microbiol.* 70, 4930–4940.

Kusai, K., and Yamanaka, T. (1973). The oxidation mechanisms of thiosulphate and sulphide in *Chlorobium thiosulphatophilum*: roles of cytochrome *c*-551 and cytochrome *c*-553. *Biochim. Biophys. Acta* 325, 304–314.

Liu, Z., Klatt, C. G., Wood, J., Rusch, D. B., Wittekindt, N., Tomsho, L., Schuster, S. C., Ward, D. M., and Bryant, D. A. (2011). Metatranscriptomic analyses of a hot spring microbial mat reveal temporal transcription differences

among oxygenic and anoxygenic phototrophs. *ISME J.* (in press).

Loy, A., Duller, S., Baranyi, C., Mussmann, M., Ott, J., Sharon, I., Béjà, O., Le Paslier, D., Dahl, C., and Wagner, M. (2009). Reverse dissimilatory sulfite reductase as phylogenetic marker for a subgroup of sulfur-oxidizing prokaryotes. *Environ. Microbiol.* 11, 289–299.

Manske, A. K., Glaeser, J., Kuypers, M. A. M., and Overmann, J. (2005). Physiology and phylogeny of green sulfur bacteria forming a monospecific phototrophic assemblage at a depth of 100 meters in the Black Sea. *Appl. Environ. Microbiol.* 71, 8049–8060.

Marcia, M., Ermler, U., Peng, G., and Michel, H. (2009). The structure of *Aquifex aeolicus* sulfide:quinone oxidoreductase, a basis to understand sulfide detoxification and respiration. *Proc. Natl. Acad. Sci. U.S.A.* 106, 9625–9630.

Marcia, M., Ermler, U., Peng, G., and Michel, H. (2010). A new structure-based classification of sulfide:quinone oxidoreductases. *Proteins* 78, 1073–1083.

Méndez-Alvarez, S., Pavón, V., Esteve, I., Guerrero, R., and Gaju, N. (1994). Transformation of *Chlorobium limicola* by a plasmid that confers the ability to utilize thiosulfate. *J. Bacteriol.* 176, 7395–7397.

Meyer, B., Imhoff, J. F., and Kuever, J. (2007). Molecular analysis of the distribution and phylogeny of the *soxB* gene among sulfur-oxidizing bacteria – evolution of the Sox sulfur oxidation enzyme system. *Environ. Microbiol.* 9, 2957–2977.

Meyer, B., and Kuever, J. (2007). Phylogeny of the alpha and beta subunits of the dissimilatory adenosine-5′-phosphosulfate (APS) reductase from sulfate-reducing prokaryotes – origin and evolution of the dissimilatory sulfate-reduction pathway. *Microbiology* 153, 2026–2044.

Nübel, T., Klughammer, C., Huber, R., Hauska, G., and Schütz, M. (2000). Sulfide:quinone oxidoreductase in membranes of the hyperthermophilic bacterium *Aquifex aeolicus* (VF5). *Arch. Microbiol.* 173, 233–244.

Ogawa, T., Furusawa, T., Nomura, R., Seo, D., Hosoya-Matsuda, N., Sakurai, H., and Inoue, K. (2008). SoxAX binding protein, a novel component of the thiosulfate oxidizing multienzyme system in the green sulfur bacterium *Chlorobium tepidum*. *J. Bacteriol.* 190, 6097–6110.

Ogawa, T., Furusawa, T., Shiga, M., Seo, D., Sakurai, H., and Inoue, K. (2010). Biochemical studies of a *soxF*-encoded monomeric flavoprotein purified from the green sulfur bacterium *Chlorobaculum tepidum* that stimulates in vitro thiosulfate oxidation. *Biosci. Biotechnol. Biochem.* 74, 771–780.

Ormerod, J. G. (1988). "Natural genetic transformation in *Chlorobium*," in *Green Photosynthetic Bacteria*, eds J. M. Olson, J. G. Ormerod, J. Amesz, E. Stackebrandt, and H. G. Trüper (New York: Plenum), 315–319.

Overmann, J. (2000). "The family Chlorobiaceae," in *The Prokaryotes: An Evolving Electronic Resource for the Microbiological Community*, 3rd Edn., release 3.1 (New York: Springer-Verlag). http://link.springer-ny.com/link/service/books/10125/

Overmann, J. (2008). "Ecology of phototrophic sulfur bacteria," in *Sulfur Metabolism in Phototrophic Organisms*, eds R. Hell, C. Dahl, D. B. Knaff, and T. Leustek (Dordrecht: Springer), 375–396.

Reinartz, M., Tschäpe, J., Brüser, T., Trüper, H. G., and Dahl, C. (1998). Sulfide oxidation in the phototrophic sulfur bacterium *Chromatium vinosum*. *Arch. Microbiol.* 170, 59–68.

Sakurai, J., Ogawa, T., Shiga, M., and Inoue, K. (2010). Inorganic sulfur oxidizing system in green sulfur bacteria. *Photosyn. Res.* 104, 163–176.

Sander, J., Engels-Schwarzlose, S., and Dahl, C. (2006). Importance of the DsrMKJOP complex for sulfur oxidation in *Allochromatium vinosum* and phylogenetic analysis of related complexes in other prokaryotes. *Arch. Microbiol.* 186, 357–366.

Sazanov, L. A., and Hinchliffe, P. (2006). Structure of the hydrophilic domain of respiratory complex I from *Thermus thermophilus*. *Science* 311, 1430–1436.

Schütz, M., Maldener, I., Griesbeck, C., and Hauska, G. (1999). Sulfide-quinone reductase from *Rhodobacter capsulatus*: requirement for growth, periplasmic localization, and extension of gene sequence analysis. *J. Bacteriol.* 181, 6516–6523.

Shahak, Y., and Hauska, G. (2008). "Sulfide oxidation from Cyanobacteria to humans: sulfide-quinone oxidoreductase (SQR)," in *Sulfur Metabolism in Phototrophic Organisms*, eds R. Hell, C. Dahl, D. B. Knaff, and T. Leustek (Dordrecht: Springer), 319–335.

Tamura, K., Dudley, J., Nei, M., and Kumar, S. (2007). MEGA4: molecular evolutionary genetics analysis (MEGA) software version 4.0. *Mol. Biol. Evol.* 24, 1596–1599.

Van de Weghe, J. G., and Ow, D. W. (1999). A fission yeast gene for mitochondrial sulfide oxidation. *J. Biol. Chem.* 274, 13250–13257.

Verté, F., Kostanjevecki, V., De Smet, L., Meyer, T. E., Cusanovich, M. A., and Van Beeumen, J. J. (2002). Identification of a thiosulfate utilization gene cluster from the green phototrophic bacterium *Chlorobium limicola*. *Biochemistry* 41, 2932–2945.

Yagi, T., and Matsuno-Yagi, A. (2003). The proton-translocating NADH-quinone oxidoreductase in the respiratory chain: the secret unlocked. *Biochemistry* 42, 2266–2274.

Conflict of Interest Statement: The authors declare that the research was conducted in the absence of any commercial or financial relationships that could be construed as a potential conflict of interest.

Received: 16 February 2011; accepted: 11 May 2011; published online: 24 May 2011. Citation: Gregersen LH, Bryant DA and Frigaard N-U (2011) Mechanisms and evolution of oxidative sulfur metabolism in green sulfur bacteria. Front. Microbio. 2:116. doi: 10.3389/fmicb.2011.00116
This article was submitted to Frontiers in Microbial Physiology and Metabolism, a specialty of Frontiers in Microbiology.

frontiers in
MICROBIOLOGY

ORIGINAL RESEARCH ARTICLE
published: 23 May 2011
doi: 10.3389/fmicb.2011.00112

Sulfite oxidation in *Chlorobaculum tepidum*

Jesse Rodriguez*[1†], *Jennifer Hiras*[2,3] *and Thomas E. Hanson*[1,2,3]

[1] *Department of Biological Sciences, University of Delaware, Newark, DE, USA*
[2] *School of Marine Science and Policy, University of Delaware Newark, DE, USA*
[3] *Delaware Biotechnology Institute, University of Delaware, Newark, DE, USA*

Edited by:
Martin G. Klotz, University of Louisville, USA

Reviewed by:
Judy D. Wall, University of Missouri, USA
Cornelius Friedrich, Dortmund University of Technology, Germany

***Correspondence:**
Thomas E. Hanson, Delaware Biotechnology Institute, University of Delaware, 127 DBI, 15 Innovation Way, Newark, DE 19711, USA.
e-mail: tehanson@udel.edu

[†]***Current address:***
Jesse Rodriguez, Post-Baccalaureate Research Education Program, University of Pennsylvania, Philadelphia, PA, USA.

The green sulfur bacterium *Chlorobaculum tepidum* is proposed to oxidize sulfide and elemental sulfur via sulfite as an obligate intermediate. The sulfite pool is predicted to be contained in the cytoplasm and be oxidized by the concerted action of ApsBA, which directly oxidizes sulfite, and QmoABC, which transfers electrons from ApsBA to the quinone pool. Like other green sulfur bacteria, *C. tepidum* was unable to use exogenously provided sulfite as the sole electron donor. However, exogenous sulfite significantly stimulated the growth yield of sulfide limited batch cultures. The growth of *C. tepidum* mutant strains, CT0867/*qmoB*::TnOGm and CT0868/*qmoC*::TnOGm, was not increased by sulfite. Furthermore, these strains accumulated sulfite and displayed a growth yield decrease when grown on sulfide as the sole electron donor. These results support an obligate, cytoplasmic sulfite intermediate as part of the canonical sulfur oxidation pathway in *C. tepidum* that requires the Qmo complex for oxidation.

Keywords: *Chlorobi*, sulfite, Qmo complex

INTRODUCTION

The *Chlorobi* are obligate phototrophic bacteria that utilize reduced sulfur compounds as electron donors to a photosynthetic electron transport chain that provides energy and reduced ferredoxin to drive carbon fixation, biosynthesis, and cell growth (Bryant and Frigaard, 2006; Overmann and Garcia-Pichel, 2006; Frigaard and Dahl, 2009). These organisms inhabit anoxic environments including sediments and euxinic waters. In these environments, they contribute to the oxidative branch of the sulfur cycle by converting reduced sulfur compounds to sulfate that can subsequently be utilized as an electron acceptor for the degradation of organic compounds by sulfate reducing bacteria. Relative to other phototrophic bacteria, the *Chlorobi* are generally adapted to lower light intensities and are often found as the deepest layer of phototrophic microbes in stratified sediments and waters (Overmann and Garcia-Pichel, 2006). Consequently, these organisms are often exposed to higher fluxes and concentrations of reduced sulfur compounds than more high light adapted phototrophs. Thus, deep in illuminated anoxic sediments and waters, the *Chlorobi* facilitate the tight coupling of sulfur and carbon cycling and likely serve to decrease fluxes of reduced sulfur compounds into overlying oxic ecosystems in much that has been observed for chemolithotrophic sulfur oxidizers in marine oxygen minimum zones (Lavik et al., 2009).

The *Chlorobi* have been intensively studied as models for the reductive TCA pathway of CO_2 fixation (Evans et al., 1966) and their highly ordered and efficient light harvesting antenna, the chlorosome (Oostergetel et al., 2010). There currently exist 11 complete and 1 draft genome sequences for members of this group (data from the DOE Joint Genome Institute[1]). Comparative genomic approaches (Frigaard and Dahl, 2009; Sakurai et al., 2010) have led to the identification of candidate genes encoding sulfur oxidizing activities. Genetic and biochemical analysis of the putative sulfur oxidation pathway outlined by these studies will lead to a detailed picture of the biochemistry of sulfur oxidation in the *Chlorobi*.

Sulfite (SO_3^{2-}) is predicted to be an obligate intermediate in sulfur oxidation by the *Chlorobi* (Frigaard and Dahl, 2009; Sakurai et al., 2010). In general, *Chlorobi* do not utilize sulfite as the sole electron donor for photosynthesis (Overmann and Garcia-Pichel, 2006). Current models predict that sulfite is generated in the cytoplasm and oxidized by a reversible adenylylphosphosulfate reductase activity (APS reductase, ApsBA) that conjugates AMP and sulfite to produce APS (**Figure 1**). The electrons liberated during this reaction are thought to be passed to the quinone pool by a quinone interacting membrane bound oxidoreductase (Qmo) complex, which was first described in the sulfate reducing bacterium *Desulfovibrio desulfuricans* (Pires et al., 2003). The APS is acted upon by a reversible ATP sulfurylase that releases sulfate as the terminal oxidation product with the production of one molecule of ATP. Sulfate is subsequently proposed to exit the cytoplasm by an unknown transporter system. This system is essentially reversal of the initial steps of dissimilatory sulfate reduction and homologous Qmo complexes are encoded by the genomes of some *Chlorobi*, nearly all sulfate reducing bacteria, and sulfate reducing archaea of the genus *Archaeoglobus* (**Figure 2**). In all organisms shown except for the Archaea, the Qmo complex genes are immediately downstream of the genes encoding ApsBA.

In the sulfate reducing bacterium *Desulfovibrio vulgaris*, a deletion mutant lacking the *qmoABC* genes was unable to grow with sulfate as the terminal electron acceptor while growth with either sulfite or thiosulfate was normal (Zane et al., 2010). This supports the idea that the QmoABC complex is a critical component for electron flow to the reduction of APS via ApsBA. The Qmo complex is of particular

[1]http://img.jgi.doe.gov

interest as it is homologous to the CoM–CoB heterodisulfide reductase found in the archaea (Hdr, **Table 1**). Hdr catalyzes the reductive regeneration of two major C_1-carrying cofactors in methanogenesis while conserving energy in the form of a proton gradient (Deppenmeier et al., 1999). Recently, this enzyme was proposed to contribute to energy conservation in hydrogenotrophic methanogens by an electron bifurcation mechanism (Thauer et al., 2008). This hypothesis has been supported by protein–protein interaction studies in *Methanococcus maripaludis* S2 demonstrating that the Hdr forms an apparent complex with formyl-methanofuran dehydrogenase that catalyzes the first step of methanogenesis, and the F420-non-reducing hydrogenase and formate dehydrogenase, both of which provide reducing equivalents for reduction of C_1 units to methane (Costa et al., 2010).

To test the proposed role of the Qmo complex in sulfite processing in *Chlorobaculum tepidum*, mutants in CT0867 (encoding the QmoB homolog, **Table 1**) and CT0868 (encoding QmoC, **Table 1**) were analyzed for defects in sulfite metabolism. The results clearly implicated the Qmo complex of *C. tepidum* in sulfite processing during growth.

MATERIALS AND METHODS

SEQUENCE ANALYSIS AND TREE CONSTRUCTION

Qmo subunit orthologs were identified using the tools of the Integrated Microbial Genomes database[2] using the sequences of *C. tepidum* ORFs CT0866-0868 to identify homologous sequences. To be included in the alignment as a putative Qmo complex, genes encoding the subunits had to be colocalized as a potential operon in the genome and be a bidirectional BLASTP best hit (i.e., the IMG definition of orthology) of the *C. tepidum* sequence. All sequence manipulations and calculations were performed in MEGA version 5, which is available for download at http://www.megasoftware.net (Tamura et al., 2007; Kumar et al., 2008). To produce the phylogenetic tree (**Figure 2**), Qmo subunit amino acid sequences were concatenated in the order noted in **Table 1** and subsequently aligned by Muscle. The alignment was then analyzed by maximum likelihood techniques, which identified the WAG model with a gamma rate distribution and fraction of invariant sites as the best descriptor of pairwise distances in the alignment. This model and parameters were used to construct and bootstrap a phylogenetic tree by maximum likelihood. The resulting tree was prepared for publication by coloring branches, formatting text, and re-sizing in CorelDraw version 11 without changing the relative branch lengths.

MICROBIAL STRAINS, GROWTH CONDITIONS, AND BIOMASS MEASUREMENTS

The wild type strain of *C. tepidum* used in this study is WT2321, the plating strain derived from the original isolate TLS1. Mutant strains CT0867/*qmoB*::TnOGm and CT0868/*qmoC*::TnOGm were produced by *in vitro* transposition mutagenesis and natural transformation of *C. tepidum* as previously described (Chan et al., 2008b). The base medium was Pf-7 with sulfide as the sole electron donor prepared as previously described (Chan et al., 2008b, 2009) with the exception that sodium thiosulfate was omitted. Sulfide concentrations in basal medium were typically 1–2 mM. Anoxic, neutralized stock solutions of sulfide and sulfite were used to adjust the concentrations of these electron donors to the concentrations noted in the figures and text after autoclaving. Starter cultures for all experiments were derived from glycerol stocks stored at −70°C and revived in Pf-7 with both sulfide and thiosulfate as electron donors at 42°C. Cultures of strains CT0867/*qmoB*::TnOGm and CT0868/*qmoC*::TnOGm were grown in the presence of 4 μg Gm ml^{-1}. Batch cultures for growth yield experiments were performed without antibiotic selection by inoculating cultures to a biomass concentration of ~4 μg protein ml^{-1} and incubated in 47°C water baths at a light intensity of ~20 μmol photons m^{-2} s^{-1} from full spectrum incandescent bulbs. Protein concentrations in cultures were measured by Bradford assay as previously described (Mukhopadhyay et al., 1999).

QUANTIFICATION OF SULFUR SPECIES

Sulfide and sulfite were quantified by bimane derivatization and reversed phase HPLC with fluorescence detection as previously described (Rethmeier et al., 1997). Standard curves were generated from dilution series of concentrated stock solutions diluted in Pf-7 medium base immediately before derivatization. Intracellular and extracellular concentrations of sulfite were separately quantified by capturing cells from 10 to 50 ml of culture on Whatman GF/F filters. A portion of the filtrate was directly added to a bimane derivatization reaction to quantify the extracellular pool. Cells immobilized on the filter were washed with a volume of sulfur free Pf-7 medium followed by three extractions of the filter with the same aliquot of bimane derivatization mix, which consisted of 9.4 mM monobromobimane (Sigma-Aldrich B4380), in 50% v/v acetonitrile:water + 50 mM HEPES + 5 mM EDTA, pH = 8.0. All filtrations and bimane extractions were carried out in a Coy anaerobic chamber using anaerobic solutions.

Chlorobaculum tepidum individual cell size in logarithmic growth was measured by fixing cells with formaldehyde (3.7% w/v final concentration) followed by phase contrast microscopy. Cell counts and samples for protein concentration were taken at the same time. Volume per cell was calculated from cell width (w) and length (l) by $V = \pi w^2 (l/4 - w/12)$ using the assumption that *C. tepidum* cells are rods composed of two half spheres connected by a cylinder (Sun and Liu, 2003). Based on protein concentration, cell concentration and volume per cell, a conversion factor for protein concentration to total cell volume in logarithmic phase cultures was developed. Intracellular sulfite concentrations were calculated as filter retained sulfite divided by the total cell volume determined from protein concentration measurements made at the same time the sample was taken for sulfite.

STATISTICS

Data presented are from the means of three independent cultures for each strain and condition. Student's t-tests assuming inequal variance between samples and a two-tailed distribution were performed in Microsoft Excel to assess the significance of differences between means. The resulting P-values are noted in the text where appropriate.

RESULTS

Qmo COMPLEX SEQUENCE RELATIONSHIPS

The sequences of putative Qmo complexes were identified in complete microbial genome sequences. The properties and annotations of the relevant sequences are outlined in **Table 1**.

[2]http://img.jgi.doe.gov

Table 1 | Qmo complex sequences used in phylogenetic tree construction, their annotation and properties.

	Qmo complex subunit ortholog annotations											
	QmoA				QmoB				QmoC			
	Heterodisulfide reductase subunit A				Heterodisulfide reductase, subunit A/hydrogenase, delta subunit, putative				Heterodisulfide reductase, transmembrane subunit, putative			
	4Fe–4S ferredoxin, iron–sulfur binding domain protein				Heterodisulfide reductase, subunit A and related polyferredoxins/Coenzyme F420-reducing hydrogenase, delta subunit				Heterodisulfide reductase, subunit E, putative			
Genome	**Locus tag**	**Length**	**SigP**	**TM**	**Locus tag**	**Length**	**SigP**	**TM**	**Locus tag**	**Length**	**SigP**	**TM**
CHLOROBIA												
Chlorobaculum tepidum TLS	CT0866	413	Yes	No	CT0867	750	No	No	CT0868	391	No	Yes
Chlorobium phaeobacteroides BS1	Cphamn1_1836	413	Yes	No	Cphamn1_1835	750	No	No	Cphamn1_1834	391	No	Yes
Chlorobium chlorochromatii CaD3	Cag_1584	412	Yes	No	Cag_1583	750	No	No	Cag_1582	392	No	Yes
Pelodictyon phaeoclathratiforme BU-1	Ppha_0037	413	Yes	No	Ppha_0036	750	No	No	Ppha_0035	393	No	Yes
DELTAPROTEOBACTERIA												
Desulfovibrio vulgaris Hildenborough	DVU0848	412	Yes	No	DVU0849	758	No	No	DVU0850	384	No	Yes
D. vulgaris DP4	Dvul_2135	412	Yes	No	Dvul_2134	758	No	No	Dvul_2133	384	No	Yes
D. vulgaris Miyazaki F	DvMF_2894	412	Yes	No	DvMF_2895	754	No	No	DvMF_2896	384	No	No
Desulfovibrio desulfuricans G20	Dde_1111	412	Yes	No	Dde_1112	756	No	No	Dde_1113	384	No	Yes
D. desulfuricans ATCC 27774	Ddes_2127	411	Yes	No	Ddes_2126	756	No	No	Ddes_2125	393	No	Yes
Desulfovibrio piger ATCC 29098	DESPIG_02771	411	Yes	No	DESPIG_02770	753	No	No	DESPIG_02769	394	No	Yes
Desulfovibrio magneticus RS-1	DMR_05410	413	Yes	No	DMR_05420	763	No	No	DMR_05430	399	No	Yes
Desulfomicrobium baculatum DSM 4028	Dbac_3199	413	Yes	No	Dbac_3200	763	No	No	Dbac_3201	408	No	Yes
Desulfohalobium retbaense DSM 5692	Dret_1965	411	Yes	No	Dret_1964	766	No	No	Dret_1963	407	No	Yes
Desulfurivibrio alkaliphilus AHT2	DaAHT2_1470	419	Yes	No	DaAHT2_1469	752	No	No	DaAHT2_1468	397	No	Yes
Desulfotalea psychrophila LSv54	DP1106	445	No	No	DP1107	753	No	No	DP1108	404	No	Yes
Desulfatibacillum alkenivorans AK-01	Dalk_1568	424	Yes	No	Dalk_1567	774	No	No	Dalk_1566	413	No	Yes
Desulfococcus oleovorans Hxd3	Dole_0999	423	Yes	No	Dole_1000	778	No	No	Dole_1001	398	No	Yes
Desulfobacterium autotrophicum HRM2	HRM2_04500	424	Yes	No	HRM2_04490	778	No	No	HRM2_04480	391	No	Yes
Syntrophobacter fumaroxidans MPOB	Sfum_1287	420	Yes	No	Sfum_1286	738	No	No	Sfum_1285	385	No	Yes
BETAPROTEOBACTERIA												
Thiobacillus denitrificans ATCC 25259	Tbd_1648	427	No	No	Tbd_1647	752	No	No	Tbd_1646	210	No	No
NITROSPIRA												
Thermodesulfovibrio yellowstonii	THEYE_A1831	415	No	No	THEYE_A1830	744	No	No	THEYE_A1829	382	No	No
ARCHAEOGLOBUS												
Archaeoglobus fulgidus DSM 4304	AF0663	404	No	No	AF0662	747	No	No	AF0661	379	No	Yes
Archaeoglobus profundus DSM 5631	Arcpr_1260	420	Yes	No	Arcpr_1259	740	No	No	Arcpr_1258	421	No	Yes

Length = amino acid residues in gene product, SigP = signal peptide prediction, TM = transmembrane helix prediction.

Putative Qmo complexes have a relatively restricted phylogenetic distribution being found only in multiple members of the *Deltaproteobacteria*, *Chlorobi,* and *Archaeoglobi* and isolated members of the *Betaproteobacteria* and *Nitrospira* phyla, although *Thermodesulfovibrio yellowstonii* is the sole complete genome sequence available from the *Nitrospira*. The common physiological thread that unites most of the organisms that contain putative Qmo complexes is the utilization of sulfur compounds as either the electron donor (*Chlorobi*, *Thiobacillus denitrificans*) or terminal electron acceptor (*Deltaproteobacteria*, *T. yellowstoneii*, *Archaeoglobi*) under anaerobic conditions.

Inspection of subunit length, signal peptide prediction and transmembrane helix prediction (**Table 1**) suggests that the topology and functional sites of the complex as proposed by Pires et al. (2003) are conserved across these groups (**Figure 1**). The Betaproteobacterium *T. denitrificans* is a notable exception, where the integral membrane subunit QmoC is severely truncated. Examination of the coding sequence suggests that this truncation is not a result of misannotation.

Phylogenetic analysis of concatenated Qmo complex subunit amino acid sequences produces a pattern of largely vertical descent of sequences within groups defined by 16S rRNA phylogeny (**Figure 2**). The exception to this is the strongly supported affiliation of the sequences from the Deltaproteobacterium *Syntrophobacter fumaroxidans* with the Betaproteobacterium *T. denitrificans*. This may be consistent with a directional transfer from sulfate reducing *Deltaproteobacteria* to *S. fumaroxidans* to *T. denitrificans*. However, the deeper branches of the phylogeny are not resolved, even when additional sequences, for example those of CoM–CoB heterodisulfide reductase complex subunits from methanogenic archaea, are added as outgroups.

The Qmo complex may have originated in the *Archaeoglobi* where paralogous genes encoding CoM–CoB heterodisulfide reductases that appear to encode functional products can be found in the same genome as those encoding the Qmo complex. In the Bacteria, the Qmo complex subunits are almost always closely associated with genes encoding the APS reductase, but these are found elsewhere in the *A. fulgidus* and *A. profundicola* genomes. The Qmo complex in *C. tepidum* is part of a large collection of genes colocalized on the genome that are implicated in the oxidation of reduced sulfur compounds. This region encodes one of the two copies of *dsrCABL* operon (encoding reverse dissimilatory sulfite reductase) that was recently shown to participate in sulfur globule oxidation in *C. tepidum* (Holkenbrink et al., 2011). In addition this region, sulfur island I (Chan et al., 2008a), contains *aprBA*, *sat* (encoding sulfate:adenylyl transferase), the QmoABC homolog encoding genes CT0866-0868 and one of three genes encoding homologs of sulfide:quinone oxidoreductase, CT0876 (Chan et al., 2009; Holkenbrink et al., 2011). The *C. tepidum* genome also contains a paralog of CT0866 (the QmoA homolog), CT1246, which resides in a potential operon (CT1245-1250) encoding homologs of hydrogenase and sulfur reductase subunits.

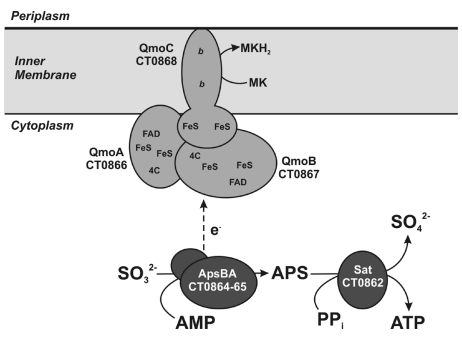

FIGURE 1 | A schematic of proposed functions for a sulfite oxidation metabolic module including the Qmo complex. The proteins are encoded by basepairs 819,144 to 828,176 of the *C. tepidum* genome (GenBank accession NC_002932.3). Assignments of putative cofactors in the *C. tepidum* Qmo complex are from Pires et al. (2003). FAD = FAD nucleotide binding site, FeS = putative 4Fe–4S cluster, *b* = heme *b*, 4C = conserved cysteine motif ($CXGXRDX_{6-8}CSX_2CC$), MK = menaquinone.

SULFITE STIMULATES THE GROWTH OF *C. TEPIDUM*

Genetic experiments have concretely implicated *qmo* genes in the reduction of sulfite by *D. vulgaris* (Zane et al., 2010). Therefore, we sought to quantify the effect of sulfite on the growth of *C. tepidum* as a pre-requisite to examining the physiological role of the putative Qmo complex in this sulfur oxidizing phototroph. In describing the isolation and characterization of the strain, Wahlund et al. (1991) found that adding 2 mM sulfite to medium with approximately 2.5 mM sulfide increased the growth yield of *C. tepidum* by 14%.

To confirm and extend this observation, varying amounts of sulfite were added to growth medium containing 4 mM sulfide and the protein concentration reached in stationary phase was determined (**Figure 3**). An increased sulfide concentration was employed based on prior work showing that *C. tepidum* can tolerate up to 8 mM sulfide without decreases in growth rate or yield (Chan et al., 2009). The increased sulfide concentration allows for a better estimate of growth yield on sulfide alone (i.e., the first point in **Figure 3**). Clearly, there is a positive correlation between added sulfite and increased biomass. The slope of a linear regression of this data ($r^2 = 0.86$, dashed line in **Figure 3**) indicates a yield of 4.3 g protein (mol sulfite)$^{-1}$. In this experiment, the yield from sulfide was 12.6 g protein (mol sulfide)$^{-1}$, which is consistent with previously published values for sulfide dependent growth yields (9–13 g protein (mol sulfide)$^{-1}$) (Mukhopadhyay et al., 1999; Chan et al., 2009). No growth was observed when cultures in medium with sulfite as the only electron donor. Thus, as is generally found for other *Chlorobi*, sulfite appears to not be utilized by *C. tepidum* as the sole electron donor.

MUTATION OF Qmo HOMOLOG ENCODING GENES LEADS TO A DEFECT IN SULFITE GROWTH STIMULATION

We previously reported that *C. tepidum* mutant strains carrying transposon insertions in the CT0867/*qmoB* or CT0868/*qmoC* genes had no strong phenotype relative to the wild type (Chan et al., 2008b). However, these experiments were carried out in medium with sulfide, thiosulfate or a mixture of both as the electron donor. Given the proposed role of the Qmo complex in sulfite oxidation and the data above that exogenous sulfite stimulates the growth of *C. tepidum*, these mutants were tested for their ability to benefit from the addition of 4 mM sulfite to

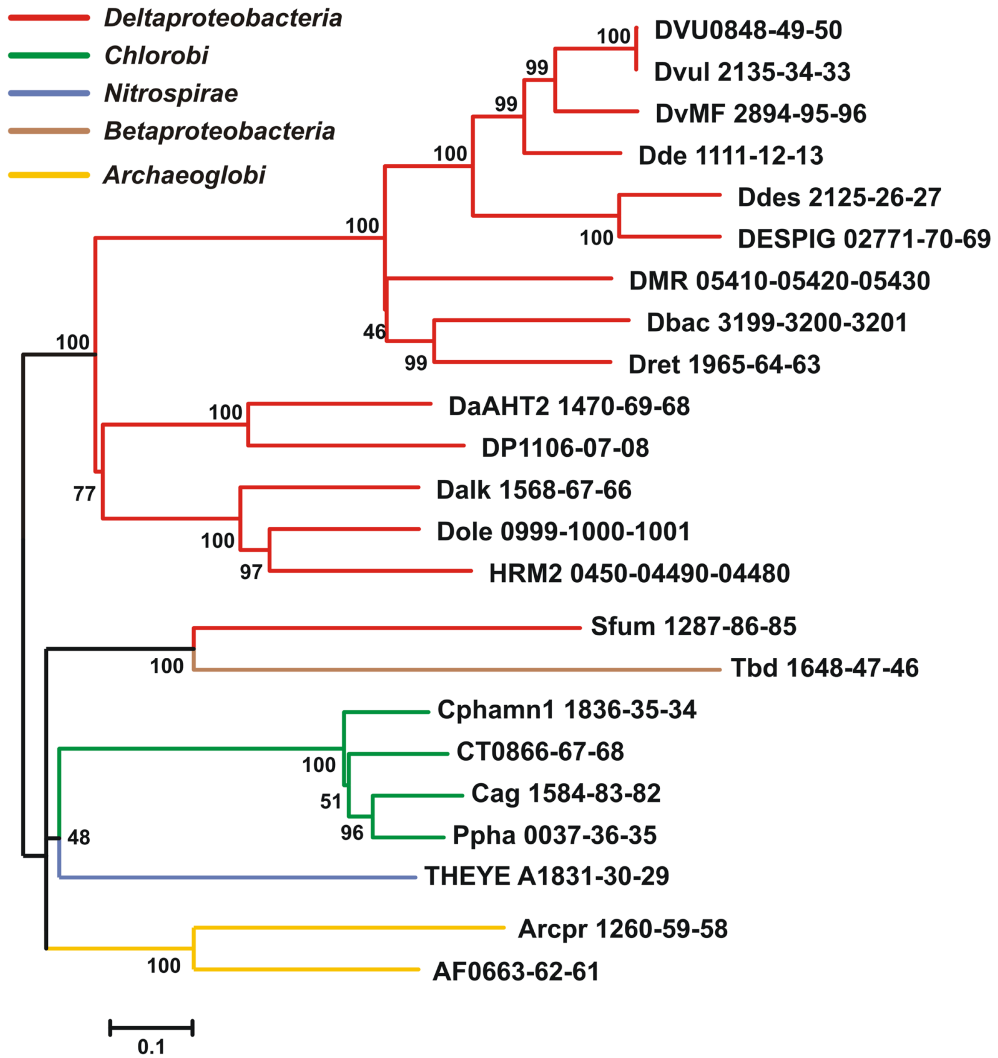

FIGURE 2 | Maximum likelihood phylogeny inferred from concatenated QmoABC amino acid sequences. The tree was constructed in MEGA5 using the WAG model of amino acid substitution with a gamma distribution = 1.8288 across five rate categories to account for differential substitution rates between sites and an invariable site frequency of 9.82%. A total of 1479 positions were included in the analysis and gaps handled by pairwise deletion. The scale bar represents 0.1 substitutions per site. Sequences are named according to the locus tags found in **Table 1** and colored to reflect their phylogenetic affiliation as determined by 16S rRNA sequencing using NCBI taxonomy terms.

medium containing 4 mM sulfide (**Figure 4**). As expected, the addition of 4 mM sulfite led to a 40% increase in the growth yield of the wild type ($P = 0.059$). In contrast, the growth yield of strain CT0867/*qmoB*::TnOGm was not increased by the addition of sulfite ($P = 0.430$). Strain CT0868/*qmoC*::TnOGm displayed an 18% increase in growth yield, but this was not statistically significant ($P = 0.204$). When comparing the growth of each mutant strain to the wild type with sulfide as the sole electron donor, a slight decrease in growth yield was detected: a significant 27% for the CT0867/*qmoB*::TnOGm ($P = 0.007$) and a non-significant 9% for the CT0868/*qmoC*::TnOGm strain ($P = 0.291$). The growth rates of the mutant and wild type strains in these experiments were not significantly different from one another with a mean doubling time of 2.0 ± 0.2 h, identical to the originally reported maximal growth rate (Wahlund et al., 1991).

MUTATION OF Qmo HOMOLOG ENCODING GENES RESULTS IN THE ACCUMULATION OF SULFITE

Given that the Qmo complex is predicted to be required for the oxidation of sulfite by *C. tepidum*, experiments were performed to determine if the mutant strains displayed any defects relative to sulfite metabolism under standard growth conditions (**Figure 5**). Under these conditions, sulfite should be a pathway intermediate that is predominantly confined to the cytoplasm (**Figure 1**). Strains were grown with sulfide + thiosulfate as electron donors and the internal and external pools of sulfite determined by bimane derivatization. Low levels of sulfite (<150 μM) were detected in the wild type under these growth conditions, with a 10:1 ratio of internal:external sulfite. In contrast, both mutant strains displayed large increases in both internal (13-fold average) and external (39-fold average) sulfite pools. In the case of the mutant strains,

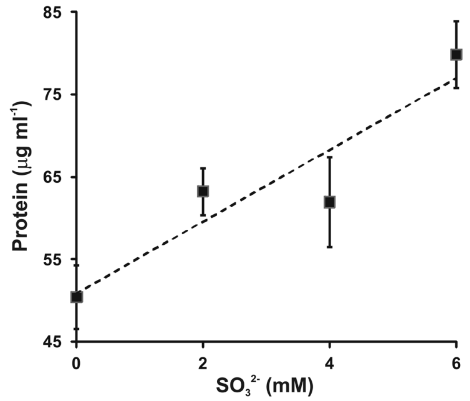

FIGURE 3 | Sulfite stimulation of *C. tepidum* growth. Sulfide limited (4 mM initial concentration) batch cultures were amended with the indicated concentrations of sulfite and the protein concentration determined in stationary phase. Data points are the means ± SE of three independent cultures for each concentration. The dashed line is a linear regression of the data that results in the equation [Protein] = 4.3[SO_3^{2-}] + 50.8.

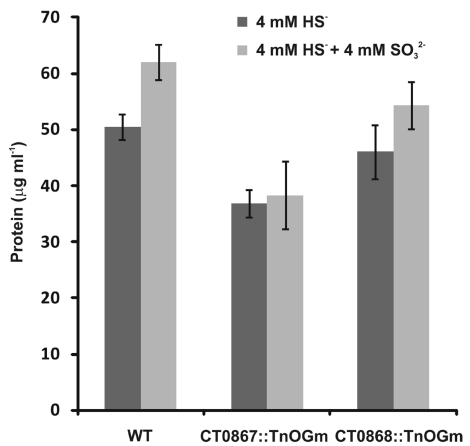

FIGURE 4 | A comparison of sulfite addition to wild type and mutant *C. tepidum* strains. Strains were grown in batch cultures containing sulfide-only (dark bars) or sulfide + sulfite (light bars) as electron donors for photosynthesis. The protein concentration was determined in stationary phase for three independent cultures for each condition and strain. The data are the means ± SE.

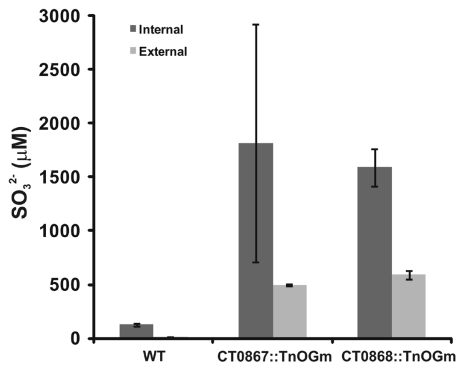

FIGURE 5 | A comparison of sulfite pools in wild type and mutant strains of *C. tepidum*. Cells were grown in medium containing sulfide + thiosulfate and harvested during logarithmic growth phase. The values presented are the means of three independent cultures ± SE. Measurement of internal (dark bars) and external (light bars) pools is described in Section "Quantification of Sulfur Species."

the internal:external ratio was decreased to 3.7- and 2.7-fold in the CT0867/*qmoB*::TnOGm and CT0868/*qmoC*::TnOGm strains, respectively.

DISCUSSION

The availability of the *C. tepidum* genome sequence (Eisen et al., 2002) has enabled the production of a detailed model for the oxidation of reduced sulfur compounds and electron transport (Frigaard and Dahl, 2009; Sakurai et al., 2010) that provide the energy for cell growth in this organism. Experimental data are now accumulating that will lead to the refinement of these models over time. The data outlined above provide experimental evidence that a putative Qmo complex in *C. tepidum* as part of a sulfite oxidation metabolic module (**Figure 1**).

If sulfite is an obligate intermediate in sulfide oxidation, one would expect a 25% decrease in growth yield if *C. tepidum* could not oxidize sulfite due to the loss of two out of eight electrons for the complete oxidation of sulfide to sulfate. The Qmo mutant strains displayed an average growth yield decrease of 18% with growth on sulfide as the sole electron donor, consistent with this prediction. Exogenously provided sulfite was found to stimulate the growth of *C. tepidum* with a yield of 4.3 g protein mol^{-1}, which is lower than the average yield value of 11 g protein mol^{-1} for sulfide from data in two independent studies (Mukhopadhyay et al., 1999; Chan et al., 2009) in addition to the value of 12.6 g protein mol^{-1} reported here (**Figure 3**). However, the growth stimulation was larger than 2.8 g protein mol^{-1} expected from the electron counting argument. The difference likely reflects the low redox potential of electrons from sulfite (−516 mV) relative to those derived from sulfide (−270 mV), which should lead to greater energy conservation and biomass production per mole of substrate oxidized for sulfite.

If the Qmo complex is indeed essential for sulfite oxidation, then one would expect that the mutant strains should no longer benefit from exogenous sulfite and this was observed. Sulfite produced during standard growth conditions was predominantly found intracellularly, which is consistent with other studies that do not observe significant sulfite concentrations culture supernatants (Chan et al., 2008b; Holkenbrink et al., 2011). This is consistent with the proposal that sulfite is a cytoplasmic intermediate in the sulfur oxidation pathway (Frigaard and Dahl, 2009; Sakurai et al., 2010). This is further supported by the dramatic increases in intracellular sulfite in the mutant strains grown under standard conditions. Together these results suggest there is a transport requirement to deliver exogenous sulfite to AprBA in the cytoplasm. The fact that sulfite does not support the growth of *C. tepidum* as a sole substrate may indicate a co-solute requirement for sulfite transport or that co-substrates are required to maintain expression of AprBA to facilitate sulfite oxidation.

In general, the CT0867/*qmoB*::TnOGm mutant strain showed a more severe growth yield and sulfite accumulation defect than the CT0868/*qmoC*::TnOGm strain. This may occur for several reasons. First and most likely, the transposon insertion in CT0867 is likely

polar on CT0868 and may effectively behave as a double *qmoB*/*qmoC* mutant. Less likely, but still possible, is that QmoB may be absolutely required to accept electrons from ApsBA while QmoC may be at least partially dispensable for transferring these electrons to the quinone pool. More precise genetic experiments to specifically ablate the heme *b* sites on QmoC will be valuable to address this question as will protein–protein interaction studies. By analogy to the sulfate reducing Qmo complex (Pires et al., 2003; Zane et al., 2010), the function of the *C. tepidum* Qmo complex is to transfer electrons from the APS reductase to the quinone pool (**Figure 1**), which should require at least transient contact between these two complexes. Studies on Hdr proteins homologous to Qmo subunits highlight this point. In methanogenic archaea, HdrA proteins were His-tagged and affinity purified from cell lysates, which allowed the identification of multi-protein interactions with other important enzymes in the methanogenic pathway (Costa et al., 2010). Soluble Hdr subunits have also co-purified with a methyl viologen reducing hydrogenase in *Archaeoglobus fulgidus* (Mander et al., 2004). As His-tagging of *C. tepidum* proteins by genetic methods has already been demonstrated with a sulfide:quinone oxidoreductase encoded by CT1087 (Chan et al., 2009), this should be a productive path forward to define the interactions of the *C. tepidum* Qmo complex with other enzymes. This may show that both Qmo- and Hdr-complexes serve as key organizing points of electron transfer in extremely physiologically diverse bacteria and archaea.

ACKNOWLEDGMENTS

This work was supported by an NSF CAREER award to Thomas E. Hanson (MCB-0447649), Jesse Rodriguez was supported in part by the University of Delaware McNair Scholars and the EPSCoR REU programs (EPS-0814251). Jennifer Hiras was supported in part by a Preston C. Townsend fellowship.

REFERENCES

Bryant, D. A., and Frigaard, N. U. (2006). Prokaryotic photosynthesis and phototrophy illuminated. *Trends Microbiol.* 14, 488–496.

Chan, L. K., Morgan-Kiss, R. M., and Hanson, T. E. (2008a). "Sulfur oxidation in *Chlorobium tepidum* (syn. *Chlorobaculum tepidum*): genetic and proteomic analyses," in *Microbial Sulfur Metabolism*, eds C. Dahl and C. G. Friedrich (Berlin: Springer-Verlag), 117–126.

Chan, L. K., Weber, T. S., Morgan-Kiss, R. M., and Hanson, T. E. (2008b). A genomic region required for phototrophic thiosulfate oxidation in the green sulfur bacterium *Chlorobium tepidum* (syn. *Chlorobaculum tepidum*). *Microbiology* 154, 818–829.

Chan, L. K., Morgan-Kiss, R. M., and Hanson, T. E. (2009). Functional analysis of three sulfide:quinone oxidoreductase homologs in *Chlorobaculum tepidum*. *J. Bacteriol.* 191, 1026–1034.

Costa, K. C., Wong, P. M., Wang, T., Lie, T. J., Dodsworth, J. A., Swanson, I., Burn, J. A., Hackett, M., and Leigh, J. A. (2010). Protein complexing in a methanogen suggests electron bifurcation and electron delivery from formate to heterodisulfide reductase. *Proc. Natl. Acad. Sci. U.S.A.* 107, 11050–11055.

Deppenmeier, U., Lienard, T., and Gottschalk, G. (1999). Novel reactions involved in energy conservation by methanogenic archaea. *FEBS Lett.* 457, 291–297.

Eisen, J. A., Nelson, K. E., Paulsen, I. T., Heidelberg, J. F., Wu, M., Dodson, R. J., Deboy, R., Gwinn, M. L., Nelson, W. C., Haft, D. H., Hickey, E. K., Peterson, J. D., Durkin, A. S., Kolonay, J. L., Yang, F., Holt, I., Umayam, L. A., Mason, T., Brenner, M., Shea, T. P., Parksey, D., Nierman, W. C., Feldblyum, T. V., Hansen, C. L., Craven, M. B., Radune, D., Vamathevan, J., Khouri, H., White, O., Gruber, T. M., Ketchum, K. A., Venter, J. C., Tettelin, H., Bryant, D. A., and Fraser, C. M. (2002). The complete genome sequence of *Chlorobium tepidum* TLS, a photosynthetic, anaerobic, green-sulfur bacterium. *Proc. Natl. Acad. Sci. U.S.A.* 99, 9509–9514.

Evans, M. C. W., Buchanan, B. B., and Arnon, D. I. (1966). A new ferredoxin-dependent carbon reduction cycle in a photosynthetic bacterium. *Proc. Natl. Acad. Sci. U.S.A.* 55, 928–934.

Frigaard, N. U., and Dahl, C. (2009). Sulfur metabolism in phototrophic sulfur bacteria. *Adv. Microb. Physiol.* 54, 103–200.

Holkenbrink, C., Ocon Barbas, S., Mellerup, A., Otaki, H., and Frigaard, N. U. (2011). Sulfur globule oxidation in green sulfur bacteria is dependent on the dissimilatory sulfite reductase system. *Microbiology*. doi: 10.1099/mic.0.044669-0. [Epub ahead of print].

Kumar, S., Nei, M., Dudley, J., and Tamura, K. (2008). MEGA: A biologist-centric software for evolutionary analysis of DNA and protein sequences. *Brief. Bioinform.* 9, 299–306.

Lavik, G., Stuhrmann, T., Bruchert, V., Van der Plas, A., Mohrholz, V., Lam, P., Mussmann, M., Fuchs, B. M., Amann, R., Lass, U., and Kuypers, M. M. (2009). Detoxification of sulphidic african shelf waters by blooming chemolithotrophs. *Nature* 457, 581–854.

Mander, G. J., Pierik, A. J., Huber, H., and Hedderich, R. (2004). Two distinct heterodisulfide reductase-like enzymes in the sulfate-reducing archaeon *Archaeoglobus profundus*. *Eur. J. Biochem.* 271, 1106–1116.

Mukhopadhyay, B., Johnson, E. F., and Ascano, M. Jr. (1999). Conditions for vigorous growth on sulfide and reactor-scale cultivation protocols for the thermophilic green sulfur bacterium *Chlorobium tepidum*. *Appl. Environ. Microbiol.* 65, 301–306.

Oostergetel, G. T., van Amerongen, H., and Boekema, E. J. (2010). The chlorosome: a prototype for efficient light harvesting in photosynthesis. *Photosyn. Res.* 104, 245–255.

Overmann, J., and Garcia-Pichel, F. (2006). "The phototrophic way of life," In *The Prokaryotes*, 3rd Edn, eds M. Dworkin, S. Falkow, E. Rosenberg, K.-H. Schleifer, and E. Stackebrandt (New York: Springer), 32–85.

Pires, R. H., Lourenco, A. I., Morais, F., Teixeira, M., Xavier, A. V., Saraiva, L. M., and Pereira, I. A. (2003). A novel membrane-bound respiratory complex from *Desulfovibrio desulfuricans* ATCC 27774. *Biochim. Biophys. Acta* 1605, 67–82.

Rethmeier, J., Rabenstein, A., Langer, M., and Fischer, U. (1997). Detection of traces of oxidized and reduced sulfur compounds in small samples by combination of different high-performance liquid chromatography methods. *J. Chromatogr. A* 760, 295–302.

Sakurai, H., Ogawa, T., Shiga, M., and Inoue, K. (2010). Inorganic sulfur oxidizing system in green sulfur bacteria. *Photosyn. Res.* 104, 163–176.

Sun, J., and Liu, D. (2003). Geometric models for calculating cell biovolume and surface area for phytoplankton. *J. Plankton Res.* 25, 1131–1146.

Tamura, K., Dudley, J., Nei, M., and Kumar, S. (2007). MEGA4: Molecular evolutionary genetics analysis (mega) software version 4.0. *Mol. Biol. Evol.* 24, 1596–1599.

Thauer, R. K., Kaster, A. K., Seedorf, H., Buckel, W., and Hedderich, R. (2008). Methanogenic archaea: ecologically relevant differences in energy conservation. *Nat. Rev. Microbiol.* 6, 579–591.

Wahlund, T. M., Woese, C. R., Castenholz, R. W., and Madigan, M. T. (1991). A thermophilic green sulfur bacterium from New Zealand hot springs, *Chlorobium tepidum* Sp–Nov. *Arch. Microbiol.* 156, 81–90.

Zane, G. M., Yen, H. C., and Wall, J. D. (2010). Effect of the deletion of *qmoABC* and the promoter-distal gene encoding a hypothetical protein on sulfate reduction in *Desulfovibrio vulgaris* Hildenborough. *Appl. Environ. Microbiol.* 76, 5500–5509.

Conflict of Interest Statement: The authors declare that the research was conducted in the absence of any commercial or financial relationships that could be construed as a potential conflict of interest.

Received: 17 January 2011; accepted: 09 May 2011; published online: 23 May 2011.
*Citation: Rodriguez J, Hiras J and Hanson TE (2011) Sulfite oxidation in Chlorobaculum tepidum. Front. Microbio. **2**:112. doi: 10.3389/fmicb.2011.00112*
This article was submitted to Frontiers in Microbial Physiology and Metabolism, a specialty of Frontiers in Microbiology.

frontiers in
MICROBIOLOGY

REVIEW ARTICLE
published: 12 August 2011
doi: 10.3389/fmicb.2011.00172

Bacterial catabolism of dimethylsulfoniopropionate (DMSP)

Chris R. Reisch[1], Mary Ann Moran[2] and William B. Whitman[1]*

[1] *Department of Microbiology, University of Georgia, Athens, GA, USA*
[2] *Department of Marine Sciences, University of Georgia, Athens, GA, USA*

Edited by:
Thomas E. Hanson, University of Delaware, USA

Reviewed by:
Andrew W. B. Johnston, University of East Anglia, UK
Rich Boden, University of Warwick, UK

***Correspondence:**
William B. Whitman, Department of Microbiology, University of Georgia, Athens, GA 30602, USA.
e-mail: whitman@uga.edu

Dimethylsulfoniopropionate (DMSP) is a metabolite produced primarily by marine phytoplankton and is the main precursor to the climatically important gas dimethylsulfide (DMS). DMS is released upon bacterial catabolism of DMSP, but it is not the only possible fate of DMSP sulfur. An alternative demethylation/demethiolation pathway results in the eventual release of methanethiol, a highly reactive volatile sulfur compound that contributes little to the atmospheric sulfur flux. The activity of these pathways control the natural flux of sulfur released to the atmosphere. Although these biochemical pathways and the factors that regulate them are of great interest, they are poorly understood. Only recently have some of the genes and pathways responsible for DMSP catabolism been elucidated. Thus far, six different enzymes have been identified that catalyze the cleavage of DMSP, resulting in the release of DMS. In addition, five of these enzymes appear to produce acrylate, while one produces 3-hydroxypropionate. In contrast, only one enzyme, designated DmdA, has been identified that catalyzes the demethylation reaction producing methylmercaptopropionate (MMPA). The metabolism of MMPA is performed by a series of three coenzyme-A mediated reactions catalyzed by DmdB, DmdC, and DmdD. Interestingly, *Candidatus Pelagibacter ubique*, a member of the SAR11 clade of *Alphaproteobacteria* that is highly abundant in marine surface waters, possessed functional DmdA, DmdB, and DmdC enzymes. Microbially mediated transformations of both DMS and methanethiol are also possible, although many of the biochemical and molecular genetic details are still unknown. This review will focus on the recent discoveries in the biochemical pathways that mineralize and assimilate DMSP carbon and sulfur, as well as the areas for which a comprehensive understanding is still lacking.

Keywords: roseobacters, dimethylsulfoniopropionate, *Pelagibacter ubique* (SAR11), methyl mercaptopropionate, acetate, acrylate, dimethylsulfide, methanethiol

INTRODUCTION

Dimethylsulfoniopropionate (DMSP) is ubiquitous in marine surface waters, ranging in concentration from less than 1 nM in the open oceans to several micromolar in phytoplankton blooms (Van Duyl et al., 1998). The primary sources of DMSP in marine surface waters are micro and macro-algae (Yoch, 2002), although some halophytic plants also produce DMSP (Otte et al., 2004). DMSP is released from phytoplankton upon cellular lysis caused by zooplankton grazing (Wolfe and Steinke, 1997), senescence (Stefels and Van Boeckel, 1993), and viral infection (Hill et al., 1998). DMSP is produced by marine phytoplankton where it has been shown to possess a variety of functions, although its osmotic potential to regulate cell volume is the most widely recognized (Kirst, 1990). In some organisms it may function as an antioxidant (Sunda et al., 2002), predator deterrent (Wolfe and Steinke, 1997), and cryoprotectant (Karsten et al., 1996). These functions are common properties of other well-studied organic osmolytes (Yancey, 2005), thus DMSP may have different roles in different organisms. Consistent with its function as an organic osmolyte, DMSP accumulates to very high and osmotically significant concentrations in some marine phytoplankton, ranging from 0.1 to 1 M (reviewed in Stefels, 2000; Yoch, 2002).

The importance of DMSP lies not only in its availability as a source of reduced sulfur and carbon for marine microbes, but also because DMSP is the precursor for the climatically active gas dimethylsulfide (DMS; Lovelock et al., 1972). DMS is the primary natural source of sulfur to the atmosphere, where it is oxidized to sulfate, sulfur dioxide, methanesulfonic acid, and other products that act as cloud condensation nuclei (Hatakeyama et al., 1982). Although the total flux of DMS is less than half that of anthropogenic sulfur dioxide emissions, the longer residence time of DMS oxidation products in the atmosphere and the global distribution of DMS release result in a greater contribution of DMS to the atmospheric sulfur burden (Chin and Jacob, 1996). The relationship between solar radiation and DMS concentration is known as the CLAW hypothesis, an acronym from the first letter of the author's surnames (Charlson et al., 1987), which states that increased levels of solar radiation and the resulting higher temperatures encourage growth of DMSP-producing marine phytoplankton and increased total DMSP production. The resulting increase

in the amount of DMS released into the atmosphere then causes an increase in the abundance of cloud condensation nuclei, which then causes a decrease in solar radiation, slower growth of marine phytoplankton, and decreased DMSP production. These coupled processes then form a negative feedback loop. James Lovelock, an author on the original CLAW hypothesis, later proposed the "anti-CLAW" hypothesis, which described a positive feedback between global temperature and DMS production. Increasing global temperatures and resulting surface water temperatures may cause increased stratification of the oceans. Stratification would then decrease the flux of nutrients from deeper waters to the surface, resulting in decreased phytoplankton growth, thereby decreasing DMSP and DMS production (Lovelock, 2006).

In support of the CLAW hypothesis, strong correlations between DMS concentration and the dose of solar radiation have been reported (Vallina and Simo, 2007). However, the factors governing the production and atmospheric release of DMS are complicated. Marine bacteria were only identified as the primary mediators of DMSP catabolism after the publication of the CLAW hypothesis. It was also discovered that marine bacteria consume DMSP through an alternative pathway that does not produce DMS. Instead, it produces the more highly reactive volatile sulfur species methanethiol (MeSH) that contributes little to the atmospheric sulfur flux (Kiene and Taylor, 1988b; Taylor and Gilchrist, 1991). This phenomenon led to the proposal of a "bacterial switch," in which marine bacteria shift between producing more or less DMS and MeSH (Simo, 2001). The gene responsible for the initial demethylation of DMSP leading to MeSH production, whose expression and activity contribute to control for the bacterial switch, was identified in 2006 (Howard et al., 2006). This was first of several genes identified that encode enzymes that directly consume DMSP, the details of which are discussed below. Many of these studies were performed in cultured representatives of the well-studied roseobacters, a phylogenetically coherent clade of clade of *Alphaproteobacteria* that are mostly marine in origin (Buchan et al., 2005; Wagner-Dobler and Biebl, 2006).

BACKGROUND

Studies involving the enzymatic reactions of important sulfur transformations have been ongoing for years. Despite this, there are large gaps in our understanding of the specific transformations of DMSP and its degradation products. While a number of enzymes were previously purified and characterized as discussed below, the genes were not identified at the time. The lack of identified genes was unfortunate as the explosion in metagenomic and metatranscriptomic data provided an opportunity to further our understanding of their distribution and expression in the environment. However, in the last few years the identification of gene products responsible for the direct transformations of DMSP through the cleavage or demethylation pathways, as well as down-stream metabolic pathways, have made such studies possible (Howard et al., 2008; Raina et al., 2010; Varaljay et al., 2010; Vila-Costa et al., 2010; Reisch et al., 2011).

DMSP SYNTHESIS

Three pathways have been described for the biosynthesis of DMSP: in the beach sunflower [*Wollastonia biflora* (L.) DC; Rhodes et al., 1997], the smooth cordgrass (*Spartina alterniflora* Loisel; Kocsis and Hanson, 2000), and sea lettuce (*Ulva lactuca* L.; Gage and Rhodes, 1997). However, the genes that encode most of the enzymes are not known. Each of these pathways share methionine as the starting compound but differ in the subsequent steps. Thus, the sulfur from DMSP and methionine share the same origin. Most evidence suggests that this sulfur is assimilated from sulfate using the adenosine 5′-phosphosulfate/3′-phosphoadenosine 5′-phosphosulfate (APS/PAPS) system that produces sulfite (Stefels, 2000). Sulfite is then reduced to sulfide in a reaction catalyzed by sulfite reductase and requiring six electrons. Sulfide is incorporated into cysteine, the precursor of methionine biosynthesis.

ENVIRONMENTAL FATE OF DMSP

There are three separate fates of DMSP sulfur: (1) production of volatile species and evolution to the atmosphere, (2) assimilation by marine microorganisms, (3) oxidation followed by release or re-assimilation. These three fates were demonstrated in a study using a ^{35}S DMSP tracer to track the partitioning of DMSP sulfur to various products in oceanic and coastal seawater (Kiene and Linn, 2000). About 15% of added DMSP was taken up by bacterial cells but not further metabolized even after 24 h of incubation, suggesting an intracellular accumulation of DMSP. This phenomenon was also observed in studies of chemostat-grown *Ruegeria pomeroyi,* a model organism for the roseobacter clade of marine *Alphaproteobacterium* (Reisch et al., 2008). In the Kiene and Linn (2000) study most of the DMSP was incorporated into protein or transformed to dissolved non-volatile products (DNVS). The DNVS was probably formed by oxidation to DMSO and sulfate. There was also a large difference in the amount of DMSP routed through the demethylation pathway and partitioned as protein or DNVS between coastal and open ocean waters. In coastal samples, 60% of DMSP was assimilated. In ocean samples, only 16% was assimilated, and the remainder was found as DNVS. The reason for this difference is thought to be related to the sulfur demand of the cells from different marine environments. Cells within the coastal samples are likely to have higher growth rates and therefore an increased sulfur demand, causing more sulfur to be assimilated, and less oxidized. In both coastal and oceanic samples, only a small portion of the total DMSP, an average of 10%, was routed through the DMSP-cleavage pathway and DMS production.

PHYTOPLANKTON CLEAVAGE

Marine phytoplankton are the primary synthesizers of DMSP, while marine bacteria are the primary degraders. However, field studies have suggested that dinoflagellates may contribute significantly to the release of DMS in phytoplankton blooms (Steinke et al., 2002), and some marine phytoplankton also have the capacity to degrade DMSP through the cleavage pathway. Four out of five cultured strains of the dinoflagellate *Symbiodinium microadriaticum* possessed DMSP lyase activity, although the rates varied significantly between strains (Yost and Mitchelmore, 2009). In addition, while DMSP production in coccolithophores is ubiquitous, DMSP lyase activity is not. A study of 10 strains of coccolithophores found that only those closely related to *Emiliania huxleyi* (Lohm.) Hay and Mohler and *Gephyrocapsa oceanica*

Kamptner were capable of DMS production (Franklin et al., 2010). *E. huxleyi* is a well-studied model organism that is highly abundant in marine surface waters where it is often, but not always, numerically dominant. The distribution of DMSP lyase activity across the phylogenetic range of the coccolithophores is not yet known, complicating our understanding of the coccolithophore contribution to DMS production (Franklin et al., 2010). Studies of *E. huxleyi* showed that significant amounts of DMS are only produced upon cell damage. This evidence suggests that the DMSP lyase is physically separated from the cell's cytoplasm, where intracellular DMSP is stored and may act as a signaling molecule (Wolfe and Steinke, 1996).

Dimethylsulfoniopropionate lyase enzymes have been purified from the green macroalgae [*Ulva curvata* (Kütz.) De Toni; De Souza and Yoch, 1995a] and the red macroalgae (*Polysiphonia paniculata* Montagne; Nishiguchi and Goff, 1995). The identities of genes encoding these enzymes remain unknown, and it is not known whether or not the two enzymes are related.

While marine bacteria are the primary mediators of DMSP degradation, there is evidence that phytoplankton may be responsible for a large part of the DMSP-cleavage reaction and DMS release in the ocean. A number of modeling studies have recently attributed increased importance to the phytoplankton contribution to DMS production (Toole and Siegel, 2004; Toole et al., 2006, 2008). One study found that the solar radiation-induced release of DMS from phytoplankton cells was necessary to produce realistic DMS predictions and reproduce the summer DMS accumulation found in surface waters (Vallina et al., 2008). Models that omit DMS release from phytoplankton underestimate the surface-to-air flux by 25%, indicating a significant phytoplankton contribution to the DMSP-cleavage pathway (Van Den Berg et al., 1996).

BACTERIAL CLEAVAGE

Dimethylsulfoniopropionate in marine waters undergoes a non-enzymatic hydrolysis that releases DMS and acrylate. In the absence of biotic processes, the half-life of DMSP in seawater is about 8 years, a rate of hydrolysis that is far too low to account for the observed turnover of DMSP in natural waters (Dacey and Blough, 1987). This realization and the identification of DMS-producing bacteria suggested that bacteria were the primary mediators of DMSP degradation. A bacterial DMSP lyase (E.C. 4.4.1.3) was first purified and characterized in 1995 from a marine isolate, *Alcaligenes faecalis* M3A (De Souza and Yoch, 1995b). The enzyme had a K_m for DMSP of 1.41 mM and a V_{max} of 402 μmol min^{-1} mg of $protein^{-1}$. However, the protein-encoding gene was not identified until about 15 years later.

DMSP-CLEAVAGE ENZYME DddY

A recent re-examination of *A. facecalis* M3A identified the gene responsible for encoding the DMSP lyase (Curson et al., 2011). This protein, designated DddY, possessed no known functional domains, and unlike the other DMSP-cleavage enzymes identified was located in the bacterial periplasmic space, as originally found in 1995 (De Souza and Yoch, 1995b). The *dddY* gene was located on the chromosome near genes that conferred the ability to metabolize acrylate, much like the pathway discussed below from *Halomonas* HTNK1. Interestingly, this gene was not present in the global ocean survey (GOS) marine metagenomic database (Rusch et al., 2007), which suggests that it does not play a major role in DMSP processing in marine surface waters. However, it may be abundant in anoxic areas of marine sediment, where it may have some ecological significance (Curson et al., 2011).

DMSP-CLEAVAGE ENZYME DddD

Most early predictions regarding the pathways of DMSP catabolism assumed that the DMSP-cleavage pathway would split DMSP into DMS and acrylate. Identification of genes catalyzing the cleavage reaction have mostly proven these early hypotheses correct, with the exception of the first cleavage enzyme identified, DddD. This enzyme turned out to produce 3-hydroxypropionate instead of acrylate (Todd et al., 2007, 2009b). The gene was identified in a bacterial isolate cultured from the rhizosphere of the salt marsh grass *Spartina anglica* C.E.Hubb. Based upon 16S rRNA gene sequencing, the bacterium was closely related to a member of the genus *Marinomonas,* and was designated strain MWYL1. A *dddD* mutation in this organism completely abolished DMS production. However, in *R. pomeroyi*, *dddD* does not appear to encode a major pathway of DMSP-cleavage. Inactivation of the *dddD* gene in *R. pomeroyi* had no effect on DMSP metabolism under the conditions tested, but this organism contains three additional DMSP-cleavage enzymes, as discussed below (Todd et al., 2010). The *dddD* gene possessed similarity to acyl-CoA transferases, which was unexpected for a lyase. Because of this annotation, the enzyme was originally hypothesized to catalyze the formation of a DMSP-coenzyme-A-thioester, which would spontaneously hydrolyze to DMS and 3-hydroxypropionyl-CoA. Although the DddD enzyme has not been purified and characterized biochemically, the activity of the recombinant *dddD* from *Halomonas* HTNK1 was investigated (Todd et al., 2009b). When *dddD* alone was expressed and the culture was provided with [1-^{13}C] or [1-^{14}C] DMSP, only 3-hydroxypropionate was detected after overnight incubation. The authors conclude that 3-hydroxypropionate, not a DMSP-CoA thioester as initially proposed, was the product of the DddD catalyzed reaction. However, these experiments used millimolar concentrations of DMSP, and it is unlikely that an equimolar buildup of a coenzyme-A thioester would occur. Thus, the actual product of DddD may be a coenzyme-A thioester, such as acryloyl-CoA or 3-hydroxypropionyl-CoA, which *E. coli* then metabolizes releasing 3-hydroxypropionate. The authors note that, for unknown reasons, cell extracts with DddD possess no activity, thus precluding *in vitro* biochemical characterization.

DMSP-CLEAVAGE ENZYME DddL

Identification of the first gene encoding an authentic DMSP lyase was reported in 2008 and designated *dddL* (Curson et al., 2008). The gene was identified by expression of a cosmid library of the *Sulfitobacter* sp. EE-36 genome in the *Rhizobium leguminosarum* strain J391. This strain was used for expression because it was an *Alphaproteobacterium*, like *Sulfitobacter* sp. EE-36, making expression of recombinant proteins more likely. The clone that possessed *dddL* was able to produce low levels of DMS and consequently a *dddL* deletion mutant in *Sulfitobacter* EE-36 was unable to produce DMS from DMSP. The amino acid sequence of DddL lacked similarity to any proteins of known function, and homologous

genes in both the cultured and metagenomic databases were rare. However, two strains of *Rhodobacter sphaeroides*, a well-studied organism not previously known to consume DMSP, possessed *dddL*, while a third strain did not. Accordingly, the two strains with *dddL* produced DMS from DMSP but not the third. Although DddL was not purified and characterized *in vitro*, recombinant *E. coli* expressing DddL released large amounts of acrylate into the medium when provided DMSP, suggesting that DddL was a DMSP lyase.

DMSP-CLEAVAGE ENZYME DddP

In 2009 a third enzyme, designated DddP, was identified using a cosmid library from *Roseovarius nubinhibens* ISM (Todd et al., 2009a). Mutation of the *dddP* gene in both *R. nubinhibens* and *R. pomeroyi* significantly decreased but did not abolish the production of DMS from DMSP, suggesting that these organisms possessed a second DMSP-cleaving enzyme (Todd et al., 2009a, 2010). Upon purification and characterization of the enzyme, ^{13}C, and ^{14}C-DMSP isotope studies showed that the enzyme was a true DMSP lyase, releasing DMS, and acrylate (Kirkwood et al., 2010). The gene was originally annotated as an M24 metallopeptidase, but the subsequent characterization showed that the DddP was neither a metalloenzyme nor a peptidase. This observation was unusual, but not unprecedented. Creatinase from *Paracoccus* sp. WB1 was also annotated as a metallopeptidase but also did not contain metals (Wang et al., 2006). The enzyme had a K_m of 13.8 mM and V_{max} of 0.3 μmol min^{-1} mg of protein^{-1} with DMSP as the substrate. Compared to the kinetic values described above for DddY, both the affinity and maximum rate of catalysis are low. Low affinities for DMSP were previously reported for a DMSP-cleavage enzyme (De Souza and Yoch, 1995b) and the DMSP demethylase discussed below. Unfortunately, substrate specificity of the enzyme was not examined, and given the low V_{max} it is possible that DMSP is not the only physiological substrate. Thus, the enzyme may have a broad substrate specificity and catalyze multiple reactions in the cell. While the enzymes specificity may have physiological implications, it would nonetheless catalyze the DMSP-cleavage reaction. Close homologs to the *dddP* gene were found in several roseobacters and, surprisingly, in a few fungal species. It was confirmed that fungal species with the *dddP* gene produced DMS, while those without the gene were not, suggesting that horizontal gene transfer was responsible for this unusual gene distribution (Todd et al., 2009a).

DMSP-CLEAVAGE ENZYME DddQ

The fourth enzyme identified was encoded by a gene designated *dddQ* (Todd et al., 2010). As stated above, the *dddP* gene knockout in *Roseovarius nubinhibens* did not abolish the production of DMS. Therefore, the cosmid library was searched for a second gene capable of conferring DMSP-cleavage activity. Two adjacent genes in the middle of a 10 gene cluster were identified. When cloned and expressed in *E. coli*, each gene conferred the ability to produce DMS from DMSP, and they were designated *dddQ*. Assays with cell extracts from the recombinant *E. coli* with [1-^{13}C] and [1-^{14}C] DMSP showed that the three carbon moiety produced in the reaction was acrylate. A few roseobacters possessed *dddQ* homologs, including *R. pomeroyi*. Unlike *R. nubinhibens*, which has two adjacent copies, *R. pomeroyi* possesses only one copy. *R. pomeroyi* with a mutation in the *dddQ* gene was still capable of DMS production, though the rate was diminished by 95%, which is consistent with the presence of additional DMSP-cleavage enzymes.

DMSP-CLEAVAGE ENZYME DddW

The sixth enzyme identified that catalyzes DMSP-cleavage was encoded by a gene designated *dddW* (Todd et al., 2011). This gene was identified in *R. pomeroyi*, where microarray experiments showed that the gene was significantly induced in the presence of DMSP. Cloning and expressing the gene in *E. coli* conferred the ability to form DMS from DMSP. Cell-free extracts possessed activity that cleaved DMSP into acrylate and DMS. This gene possessed no sequence similarity to genes with known function, but the polypeptide sequence possessed a predicted cupin-binding fold, like that of DddP and DddQ.

DISTRIBUTION OF DMSP-CLEAVAGE ENZYMES

The distribution and abundance of the DMSP-catabolizing genes in the metagenomic database have recently been reported (Howard et al., 2008; Raina et al., 2010; Moran et al., 2012). While numbers alone are unlikely to fully decipher the ecological role or significance of DMSP catabolism in the environment, they do reveal which genes are likely to be important on a global scale. As discussed below, the DMSP demethylase gene, *dmdA*, is the most abundant gene found in the GOS that acts directly on DMSP. Of the DMSP-cleavage enzymes identified thus far, *dddP* is by far the most abundant, found in 6% of bacteria examined in the GOS (Moran et al., 2012). This abundance is due to the genes presence in many roseobacters, as well as *Candidatus Puniceispirillum marinum*, the cultured representative of the SAR116 clade of *Alphaproteobacteria*. The abundance is consistent with the ribotype abundance identified in the GOS, where the SAR116 cluster represented 2.7% and the roseobacters 2.6% of sequences (Biers et al., 2009). In contrast, the SAR11 clade of the *Alphaproteobacteria* constitutes 31% of sequenced ribotypes in the GOS (Biers et al., 2009), which is consistent with the *dmdA* abundance of 27% (Moran et al., 2012).

The diversity of the DMSP-cleavage enzymes identified thus far is surprising. While there are numerous examples of non-homologous isofunctional enzymes (Omelchenko et al., 2010), six examples in closely related bacteria is unusual. This diversity suggests that there may be more, yet-unidentified enzymes catalyzing the cleavage reaction. For example, *dddW*, the most recently identified DMSP lyase gene, has only one highly similar homolog in the entire genomic database (Todd et al., 2011). This gene was identified in the well-studied bacterium *R. pomeroyi*, and it is likely that if other bacteria were screened with similar depth, by either whole-genome transcriptional analysis or whole-genome cloning, more cleavage enzymes would be found. The contribution of these low-abundance DMSP-cleavage enzymes to the flux of DMSP in the environment is probably minimal on an individual basis. But if there are in fact more of these novel DMSP lyases harbored by less understood bacteria, they may contribute significantly to the total flux.

DMSP DEMETHYLATION

The gene catalyzing the initial demethylation of DMSP was identified in 2006 in *R. pomeroyi* using a transposon mutant library. The

gene, designated *dmdA*, was originally annotated as a glycine cleavage T-protein (GcvT), one of four proteins in the glycine degradation system (Okamuraikeda et al., 1982). Like GcvT, DmdA requires tetrahydrofolate (THF) to accept the methyl group from DMSP. DmdA from both *Candidatus P. ubique* and *R. pomeroyi* were purified and characterized, and both possessed similar kinetic properties (Reisch et al., 2008). The enzymes had low affinities for DMSP, with K_ms of 13.2 and 5.4 mM for the enzymes from *Candidatus P. ubique* and *R. pomeroyi*, respectively. During growth on DMSP, *R. pomeroyi* cultures maintained an intracellular concentration of DMSP of ~70 mM, which would allow for near maximal activity of DmdA *in vivo*. Such a high concentration of DMSP is osmotically significant and suggests that *R. pomeroyi* accumulates DMSP as an organic osmolyte. It is notable that the enzyme had a strict substrate specificity, indicating that the enzyme evolved to function with DMSP and was not a promiscuous enzyme that catalyzed multiple reactions.

Subsequent analysis of *dmdA* in marine metagenomic data showed that this gene is particularly abundant in ocean surface waters, with estimates placing the number of cells that possess this gene ranged at 27% (Moran et al., 2012). One reason for this high abundance was confirmed recently. In laboratory experiments the SAR11 clade bacterium *Candidatus P. ubique* required an exogenous source of reduced sulfur, such as DMSP or methionine, to reach high cell density in culture (Tripp et al., 2008). Despite very high concentrations of sulfate in most of the surface ocean, *Candidatus P. ubique* is incapable of utilizing this potential sulfur source as it does not possess the genes required for assimilatory sulfate reduction (Tripp et al., 2008). Instead, the bacterium uses only reduced sources of sulfur, and they are even selective in their use of reduced species. For instance, cysteine did not increase growth yields to the same extent as DMSP and methionine. Presumably, the inability to assimilate oxidized sulfur compounds results from the energetic costs associated with sulfate reduction. For these extreme oligotrophs, electron donors may be very scarce.

FIRST DEMETHYLATION CARBON

There are two products of the DMSP demethylation reaction catalyzed by DmdA, MMPA, and 5-methyl-THF, which carries the methyl group removed from DMSP (**Figure 1**). The fate of 5-methyl-THF has not been directly studied, but the possibilities are numerous as it is a major donor of single carbon units in bacterial cells (**Figure 2**). Many organisms oxidize 5-methyl-THF to 5,10-methylene-THF by 5,10-methylene-THF reductase (MetF, 1.5.1.20) and subsequently to 5-formyl-THF by methylene-THF

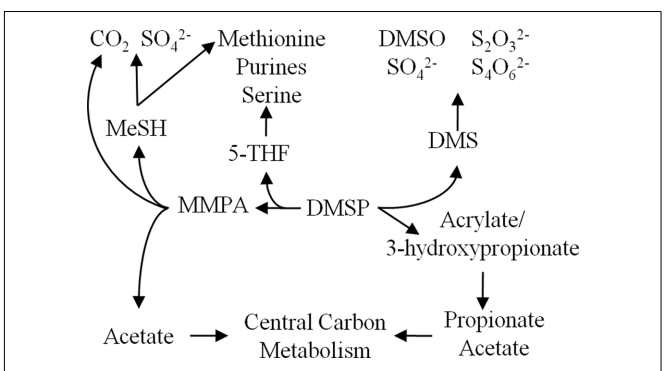

FIGURE 1 | Overview of DMSP catabolic pathways in marine bacteria and the fates of carbon and sulfur.

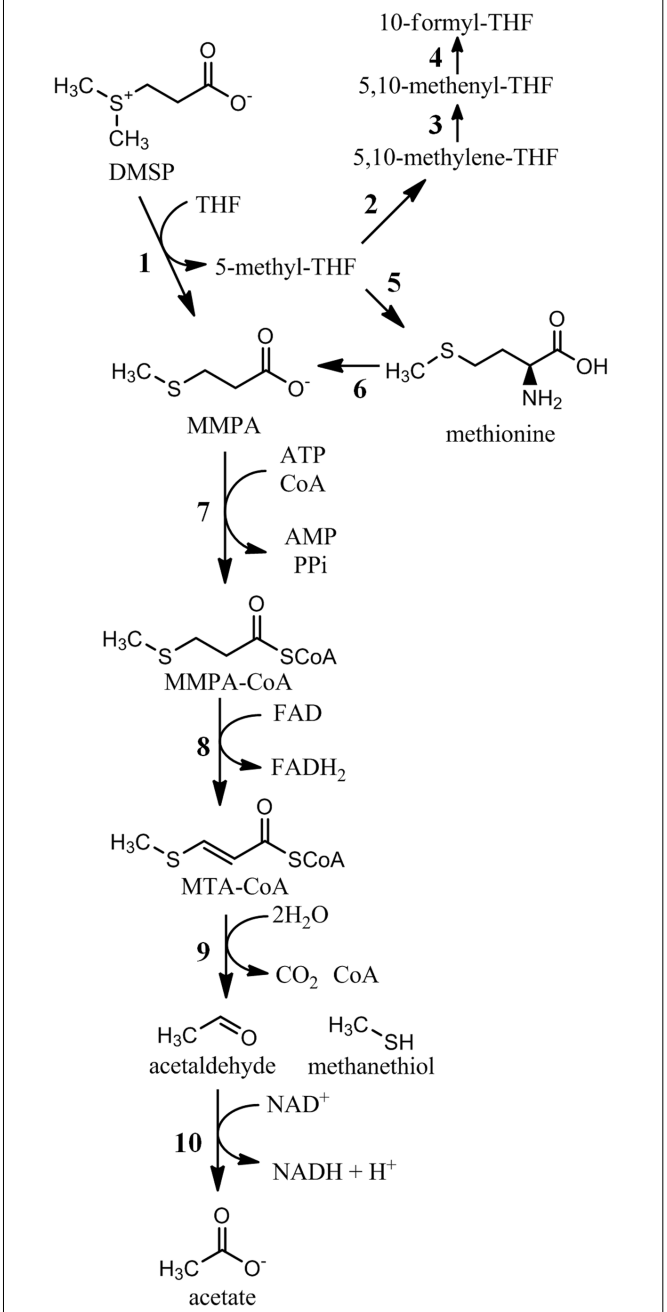

FIGURE 2 | Biochemical pathways of DMSP demethylation. 1, DMSP demethylase (DmdA); 2, 5,10-methylene-THF reductase (MetF, E.C. 1.5.1.20); 3, methylene-THF dehydrogenase (FolD, E.C. 1.5.1.5); 4, methenyl-THF-cyclohydrolase (E.C. 3.5.4.9); 5, methionine synthase (MetH, E.C. 2.1.1.13); 6, methionine salvage pathway (multiple enzymes); 7, MMPA-CoA ligase (DmdB); 8, MMPA-CoA dehydrogenase (DmdC); 9, methylthioacryloyl-CoA hydratase (DmdD); 10, acetaldehyde dehydrogenase (E.C. 1.2.1.10).

dehydrogenase (FolD, 1.5.1.5). 5-methyl-THF is also the methyl donor for methionine and *S*-adenosyl-methionine synthesis, while 5-formyl-THF is the source of two carbon atoms in purine nucleoside biosynthesis. 5,10-methylene-THF serves as a carbon donor for the conversion of glycine to serine, a reaction that is also part of the serine assimilation pathway for C-1 assimilation.

MMPA DEMETHIOLATION

Most MMPA produced during DMSP degradation is further processed through a demethiolation pathway that releases the volatile sulfur compound MeSH (**Figure 3**). This transformation was long thought be the result of a cleavage or a reductive cleavage reaction, producing the three carbon intermediate propionate or acrylate (Kiene and Taylor, 1988b; Taylor and Gilchrist, 1991). However, an alternative hypothesis suggested that MMPA may be catabolized in a fatty acid β-oxidation-like pathway (Taylor and Visscher, 1996; Bentley and Chasteen, 2004). Recently, it was confirmed that the latter pathway is present in *R. pomeroyi* and required for MeSH production (Reisch et al., 2011). In this pathway, a series of three coenzyme-A mediated reactions catalyze the demethiolation of MMPA. First, a MMPA-CoA thioester is formed in an ATP-dependent reaction catalyzed by an enzyme designated as DmdB, encoded by a gene originally annotated as a medium chain fatty-acid-CoA ligase. Next, the MMPA moiety of MMPA-CoA is dehydrogenated between its α and β carbons, creating a double bond, transferring two electrons to FAD, and forming methylthioacryloyl-CoA (MTA-CoA). The third step, which mediates the actual demethiolation, is a unique reaction catalyzed by a crotonase-type enzyme. Hydration of MTA-CoA leads to its decomposition into MeSH, acetaldehyde, CO_2, and free CoA. Like *dmdA*, the genes that encode *dmdB* and *dmdC* are abundant in the marine metagenomic database. In contrast, *dmdD* is rare, although an *Ruegeria lacuscaerulensis*, which did not possess *dmdD*, was also capable of the DmdD-catalyzed reaction, suggesting a non-orthologous gene had replaced *dmdD* in at least some bacteria. Unlike *dmdA* though, the MMPA-CoA pathway was shown to be present in a wide variety of bacteria, including many that are not associated with DMSP catabolism.

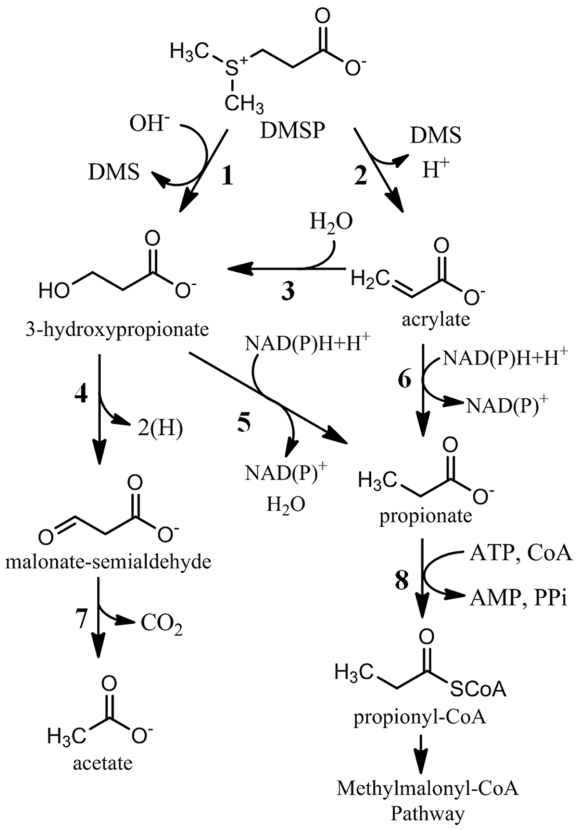

FIGURE 3 | Dimethylsulfoniopropionate cleavage pathways leading to central carbon metabolism. Reactions 5 and 6 may be coenzyme-A mediated and would therefore bypass reaction 8. 1, DMSP-cleavage enzyme (DddD); 2, DMSP lyase (DddL, DddP, DddQ, DddY, DddW, E.C. 4.4.1.3); 3, acrylate hydratase; 4, 3-hydroxypropionate dehydrogenase; 5, 3-hydroxypropionate reductase; 6, acrylate reductase (1.3.99.3); 7, malonate semialdehyde dehydrogenase/decarboxylase (E.C. 1.2.1.18); 8, propionate-CoA ligase (PrpE, E.C. 6.2.1.17).

METHIONINE AS A SOURCE OF MMPA

The distribution of the key genes of the MMPA-CoA pathway (*dmdB* and *dmdC*) is much broader than that of *dmdA*. Moreover, recombinant proteins from many terrestrial bacteria possess these activities and whole cells of several distantly related bacteria release MeSH from MMPA (Reisch et al., 2011). Conservation of this pathway amongst such a diverse group of bacteria suggests physiological importance but raises the question of how cells that are incapable of demethylating DMSP obtain MMPA.

A possible source of MMPA may be the methionine salvage pathway, which is found in many types of organisms and has a primary function of recycling the reduced thiomethyl moiety from methionine (reviewed in Albers, 2009). The condensation of methionine and ATP results in production of the one-carbon donor *S*-adenosyl-methionine (SAM). In polyamine synthesis, the aminopropyl group of decarboxylated SAM is transferred to putrescine, yielding spermine, and methylthioadenosine (MTA). MTA, which contains the methylthio moiety of methionine, is the start of the methionine salvage pathway. After several steps there is a branch point where an aci-reductone dioxygenase can catalyze one of two reactions, depending upon the presence of either Fe^{2+} or Ni^{2+}. When bound to Fe^{2+}, the enzyme catalyzes the production of formate and 4-methylthio-2-oxobutyrate, which can be aminated to methionine in a single step (Heilbronn et al., 1999). However, when bound to Ni^{2+}, the enzyme produces MMPA, carbon monoxide, and formate in an "off-pathway" reaction (Dai et al., 1999). The physiological significance of this off-pathway transformation is unknown and it has not been demonstrated that it is an alternative source of MMPA.

MeSH ASSIMILATION

The product of MMPA degradation, MeSH, is a source of cellular sulfur for marine bacteria. A report in 1999 examined the fate of DMSP sulfur in pure cultures of several marine *Alphaproteobacteria* (Gonzalez et al., 1999). Using ^{35}S-labeled DMSP, this work showed that nearly all the sulfur from DMSP was converted into TCA-insoluble material, most of which was protein. Interestingly,

the percentage of ^{35}S that was found in TCA-insoluble material decreased significantly as the concentration of DMSP increased. The authors hypothesized that once the bacterial sulfur demand was fulfilled; most DMSP was routed through the cleavage pathway and released as DMS. A more extensive study describing the fate of the sulfur and methyl carbons of DMSP was performed using both pure cultures and natural populations in marine surface waters (Kiene et al., 1999). These experiments also showed that much of the DMSP-derived sulfur was found in TCA-insoluble material. Pure cultures of an organism incapable of producing MeSH from DMSP were nonetheless capable of assimilating sulfur from ^{35}S-MeSH, which is consistent with the widespread distribution of the MMPA-CoA pathway. Furthermore, with [^{3}H-methyl] MeSH, the methyl group was incorporated into the methyl group of methionine. Similar trends and rates of assimilation were observed when using ^{35}S- and ^{3}H-MeSH, suggesting that both the S and methyl groups are directly incorporated into methionine, possibly by the enzyme cystathionine γ-synthetase (Kanzaki et al., 1987; Kiene et al., 1999). This hypothesis is supported by the observation that two inhibitors of the enzyme, vinylglycine and propargylglycine, caused a significant decrease in the incorporation of ^{35}S into TCA-insoluble material.

While the direct incorporation of MeSH into sulfur-containing amino acids is likely, it is also possible that the sulfur and methyl moieties are incorporated independently. The initial demethylation of DMSP transfers one methyl group to tetrahydrofolate, producing 5-methyl-tetrahydrofolate (Reisch et al., 2008). The traditional route of methionine biosynthesis through methionine synthase transfers a methyl group from 5-methyl-THF to homocysteine. Therefore, organisms rapidly consuming DMSP will likely have an abundance of 5-methyl-THF that can be used in methylating reactions, including methionine synthesis. It is also likely that different organisms possess different metabolic capabilities, leaving open the possibility that both the direct incorporation of MeSH and the separate incorporation of C and S are possible in different organisms. Biochemical confirmation of these hypothesized pathways and elucidation of the genes catalyzing these reactions will allow for further investigation of the cellular assimilation of MeSH.

MeSH OXIDATION

While one major fate of MeSH in marine surface waters is the incorporation into sulfur-containing amino acids, much of the MeSH is completely oxidized (**Figure 4**). This MeSH oxidation pathway is expected to be initiated by a MeSH-oxidase (E.C. 1.8.3.4), which produces formaldehyde, hydrogen sulfide, and hydrogen peroxide. This enzyme has been purified from *Thiobacillus thioparus* (Gould and Kanagawa, 1992), *Hyphomicrobium* EG (Suylen et al., 1987), and *Rhodococcus rhodochrous* (Kim et al., 2000), but the gene encoding this enzyme has not been reported. None of the enzymes require exogenous cofactors, but the reported molecular weights are different, making it unclear as to whether these enzymes are related. Given the high turnover reported for MeSH in marine surface waters (Kiene, 1996; Kiene et al., 1999) and for cultured marine bacteria (Gonzalez et al., 1999), identification of this enzyme would be a significant step in understanding of the fate of MeSH in marine systems.

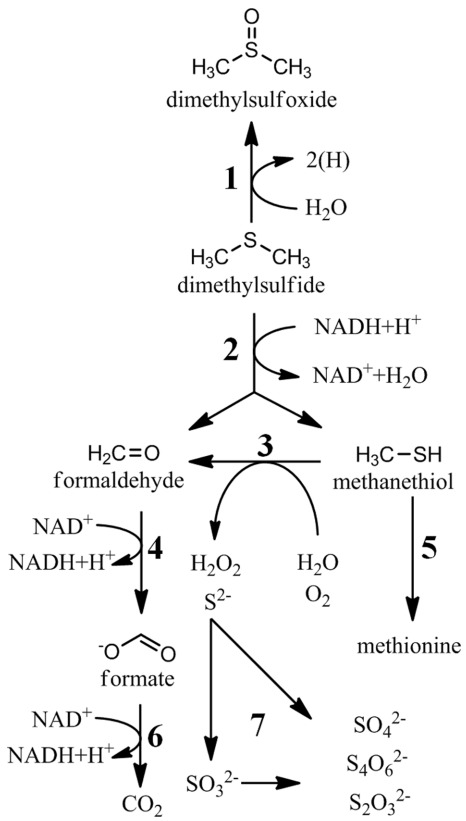

FIGURE 4 | Bioconversions of dimethylsulfide and methanethiol. 1, DMS dehydrogenase; 2, DMS monooxygenase; 3, methanethiol oxidase (E.C. 1.8.3.4); 4, formaldehyde oxidation (various enzymes); 5, cystathionine γ-synthetase (E.C. 2.5.1.48); 6, formate dehydrogenase (E.C. 1.2.1.2); 7, sulfide oxidation (many enzymes).

DMS CONSUMPTION

The fate of DMS in marine surface waters is of great interest due to its contribution to cloud condensation nuclei in the atmosphere. Due to biotic and abiotic consumption of DMS in the ocean mixed layer, only 2–10% of the DMS produced is released to the atmosphere (Kiene and Bates, 1990; Archer et al., 2002; Zubkov et al., 2002). The biological degradation of DMS in seawater has long been recognized, but these transformations are still poorly understood. Unlike MeSH, very little sulfur from DMS is assimilated into cells in natural populations, suggesting that only specialized methylotrophs are capable of its assimilation (Vila-Costa et al., 2006). Nonetheless, numerous bacteria have been isolated by their ability to grow on DMS, although many were not isolated from marine sources (reviewed in Schafer et al., 2010). The biological fates of DMS are oxidation to DMSO, sulfate, thiosulfate, and tetrathionate (De Zwart et al., 1997; Vila-Costa et al., 2006; Del Valle et al., 2007; Boden et al., 2010; **Figures 1** and **4**). In marine surface water, most data indicates that DMSO and sulfate are the primary products of DMS oxidation (Kiene and Linn, 2000; Vila-Costa et al., 2006; Del Valle et al., 2007). However, it is unknown if these studies attempted to quantify thiosulfate and tetrathionate concentrations, as they were not generally believed to be products

of DMS degradation. Another possibility is that much of the flux is routed through thiosulfate or tetrathionate, which are then rapidly consumed to produce sulfate.

A dimethylsulfide dehydrogenase that catalyzes the oxidation of DMS to DMSO was identified in *Rhodovulum sulfidophilum*, a purple non-sulfur member of the *Alphaproteobacteria* (Mcdevitt et al., 2002). The protein belonged to the DMSO reductase family of molybdoproteins, and showed high similarity to nitrate reductase. Few highly similar homologs are found in the genomic or metagenomic databases, thus the ecological significance of this reaction is unclear. However, the biological production of DMSO from DMS in marine surface has been demonstrated, so other DMSO dehydrogenase reactions must occur (Del Valle et al., 2007).

A DMS monooxygenase, which oxidizes DMS to MeSH and formaldehyde, was characterized from *Hyphomicrobium sulfonivorans*, an *Alphaproteobacterium* belonging to the order *Rhizobiales* that was originally isolated from garden soil (Boden et al., 2011). Homologs to the gene encoding the monooxygenase gene were abundant in the genomic database, but the organisms harboring the genes were mostly terrestrial in origin. Only one member of the roseobacters possessed close homologs, *Citreicella sp.* SE45. Likewise, GOS metagenomic database contained only a few homologs. Thus, it is unlikely that this DMS monooxygenase plays a significant role in marine surface waters. Nevertheless it is possible that an unrelated enzyme catalyzes a similar reaction in the marine systems.

A member of the *Gammaproteobacteria, Methylophaga thiooxydans* possessed a novel pathway of DMS oxidation that produced tetrathionate with thiosulfate as an intermediate (Boden et al., 2010). In the environment, tetrathionate would probably be rapidly oxidized because it is rich in electrons. The genes involved in the production of tetrathionate through this pathway and, therefore, its distribution and abundance in the environment are unknown. Similarly, *Methylophaga sulfidovorans* was able to transform DMS into thiosulfate (De Zwart et al., 1997). Biochemical and molecular specifics of this conversion were not reported, and it is unclear if this is a common fate of DMS in marine systems.

SULFUR OXIDATION

A major fate of DMSP-derived sulfur in environmental studies is the complete oxidation to sulfate (Kiene and Linn, 2000), but there is remarkably little information on the enzymes and pathways utilized by bacteria that inhabit marine surface waters. Overall, there is a large diversity of bacterial sulfur oxidation systems (reviewed in Ghosh and Dam, 2009), but many of these systems were identified in extremophilic microbes or phototrophic bacteria that are unlikely to inhabit marine surface waters where most DMSP cycling occurs. Thus, the distribution of these sulfur oxidation systems in marine surface waters remains unclear.

It is assumed that most, if not all, of the sulfur transformed into sulfate is routed through the demethylation/demethiolation pathway of DMSP degradation. Since the sulfur moiety from the demethiolation pathway is in the form MeSH, complete oxidation of the sulfur and carbon would yield 14 electrons. If methanethiol oxidase initiates the oxidation of MeSH in marine bacteria, the sulfur moiety is transformed to sulfide. Two enzymes are known that oxidize sulfide to elemental sulfur; flavocytochrome c-sulfide dehydrogenase and sulfide: quinone reductase (Dolata et al., 1993; Schutz et al., 1997). The oxidation of elemental sulfur is not well understood and different mechanisms exist in different bacteria. Some meso-acidophilic bacteria were shown to use a reduced thiol, such as glutathione, to activate elemental sulfur in a reaction that yields glutathione persulfide, which was then oxidized to sulfite (Rohwerder and Sand, 2003). The green sulfur bacteria possess a reverse-acting dissimilatory sulfite reduction pathway that also oxidizes a persulfide to yield sulfite (Pott and Dahl, 1998). Other bacteria use the Kelly–Friedrich pathway, discussed below, to oxidize elemental sulfur to sulfate (Mukhopadhyaya et al., 2000).

The oxidation of sulfite to sulfate may proceed through at least two mechanisms. One possibility is that a sulfite dehydrogenase (E.C. 1.8.2.1) directly oxidizes sulfite while transferring two electrons to a cytochrome (Kappler, 2011). The second mechanism uses an AMP-dependent pathway that has reverse activities of APS reductase (E.C. 1.8.99.2) and ATP sulfhydrolase (E.C. 2.7.7.4), resulting in the production of ATP (reviewed in Kappler and Dahl, 2001). Interestingly, *Candidatus P. ubique* possesses gene homologs for the AMP-dependent pathway, but does not possess genes enabling oxidation of inorganic sulfur to sulfite (Kuever and Meyer, 2007). Thus, the sulfite may be derived from the sulfur of DMSP, but the pathways producing sulfite are unknown.

In the *Alphaproteobacteria*, it is likely that sulfide oxidation proceeds through the well-studied Kelly–Friedrich pathway (Lu et al., 1985; Friedrich et al., 2001). This system completely oxidizes sulfide to sulfate without the formation of sulfite. Interestingly, the *Alphaproteobacterium Starkeya novella* possesses a both the sulfite dehydrogenase described above as well as parts of the Kelly–Friedrich pathway (Kappler et al., 2001). The Kelly–Friedrich pathway is widely distributed in the marine roseobacters, as 23 of the 32 sequenced genomes have the *sox* genes that encode for this pathway (Newton et al., 2010). Those roseobacters that possess the Kelly–Friedrich pathway are able to gain energy from the oxidation of sulfide derived from MeSH or possibly DMS degradation. However, a number of roseobacters that possess DMSP degradation genes do not possess the *sox* genes. In these bacteria the fate of the DMSP derived sulfur is unclear. It is possible that some of these roseobacters that have been cultured and sequenced, but not physiologically characterized, may possess sulfur oxidation pathways similar to those discussed above, whose molecular characteristics are still unknown.

Oxidation of thiosulfate, produced in inorganic sulfur oxidation or DMS consumption, proceeds through a pathway in which tetrathionate is formed. Despite extensive investigations, the molecular specifics of this pathway are mostly unknown, and the biochemical specifics may differ between groups of bacteria (Ghosh and Dam, 2009). A thiosulfate dehydrogenase first forms tetrathionate from two molecules of thiosulfate. A hydrolase then releases sulfite from tetrathionate, before being oxidized to sulfate by one of the mechanisms discussed above.

DOUBLE DEMETHYLATION OF DMSP

One possible fate of DMSP that has remained largely unstudied involves a second demethylation of DMSP and the conversion of MMPA to mercaptopropionate (MPA). The production of MPA from DMSP was first reported in 1988 in anoxic surface sediments

(Kiene and Taylor, 1988a), but the importance of MPA in aerobic surface waters remains unclear. An aerobic bacterium showed a stoichiometric production of MPA from DMSP or MMPA (Visscher and Taylor, 1994), suggesting it may be a dead-end product of limited physiological significance. Other reports have indicated that pure cultures of anaerobic bacteria metabolized MPA to H_2S and acrylate (Taylor and Visscher, 1996). Methane production from MMPA has also been demonstrated in a limited number of strains of the strictly anaerobic methanogens of the genus *Methanosarcina*, where it was hypothesized that a transmethylation of coenzyme-M from MMPA was the likely mechanism (Vandermaarel et al., 1995). The biological implications of this reaction may be significant in anoxic areas, but most evidence suggests that double demethylation is not a major fate of DMSP in marine surface waters. However, until progress is made in understanding the biochemical reactions and gene products catalyzing these reactions, the possibility of a major role cannot be ruled out.

ACRYLATE AND 3-HYDROXYPROPIONATE ASSIMILATION

In addition to the uncertainty in the initial steps of DMSP metabolism, the fate of the three carbon moiety of DMSP is not well understood. As detailed above, five of the DMSP-cleavage enzymes identified thus far likely result in the production of acrylate, while the other results in 3-hydroxypropionate (**Figure 3**). In *Halomonas* HTNK1, acrylate is believed to be metabolized to 3-hydroxypropionate, indicating that DMSP and acrylate degradation share a common intermediate (Todd et al., 2009b). 3-hydroxypropionate is further metabolized by an alcohol dehydrogenase, encoded by *dddA,* which produces an intermediate hypothesized to be malonate semialdehyde (**Figure 3**). The gene product of *dddC,* which encodes for an enzyme annotated as a methylmalonate-semialdehyde dehydrogenase, may transform malonate-semialdehyde to acetyl-CoA (Stines-Chaumeil et al., 2006; Todd et al., 2009b). In *E. coli* expressing *dddC* and provided [1-^{14}C] DMSP, the ^{14}C is released as carbon dioxide, presumably by decarboxylation of malonate-semialdehyde. The distribution of this first pathway identified for bacterial DMSP-cleavage and its ecological significance remain unclear, as homologs for *dddA* and *dddC* in the metagenomic databases are rare.

Another possibility is that acrylate is assimilated as a three carbon moiety in a pathway similar to that of propionate. In the methylmalonyl-CoA pathway, propionyl-CoA is carboxylated to the four carbon intermediate methylmalonyl-CoA, which is then re-arranged to the TCA cycle intermediate succinyl-CoA (Flavin and Ochoa, 1957). The genes for this pathway are widespread throughout members of roseobacter clade. The transformation of acrylate to propionyl-CoA could occur through at least two different mechanisms. One possibility is the direct reduction of acrylate or acryl-CoA to propionate or propionyl-CoA, respectively. The CoA-dependent reduction of acrylate to propionate was observed in the Crenarchaeota and in *Clostridium propionicum* (Hetzel et al., 2003; Teufel et al., 2009). Given the distant taxonomic relationship between these prokaryotes and Proteobacteria, it is difficult to identify an ortholog in the roseobacter genomes solely on sequence similarity. An alternative route for forming propionyl-CoA would involve an initial hydration of acrylate or acryloyl-CoA to 3-hydroxypropionate or 3-hydroxypropionyl-CoA, as discussed above for *Halomonas* HTNK1. A reduction to propionate or propionyl-CoA is then possible. A trifunctional enzyme that catalyzes the complete conversion of 3-hydroxypropionate to propionyl-CoA was identified in *Chloroflexus atlanticus* (Alber and Fuchs, 2002). Again, the distant taxonomic relationship between *Chloroflexus* and Proteobacteria make it difficult to identify this enzyme in bacteria in marine surface waters.

ACETATE ASSIMILATION

As described above, DMSP catabolism frequently yields acetate. The simplest form of acetate assimilation, the glyoxylate shunt, is absent from most roseobacters but present in the cultured representatives of the SAR11 clade. The glyoxylate shunt requires only two enzymes, isocitrate lyase (E.C. 4.1.3.1) and malate synthase (E.C. 2.3.3.9) in addition to the enzymes of the TCA cycle. The glyoxylate shunt bypasses the two decarboxylation steps of the TCA cyle, resulting in the net assimilation of acetate. The pathway for acetate assimilation in isocitrate lyase-negative organisms has been the subject of investigation for decades, but recently a complete pathway was described and designated the ethylmalonyl-CoA pathway (Erb et al., 2007). All of the enzymes in the pathway were subsequently identified (Erb et al., 2009), and homologous genes for most of the proteins in this pathway are present in *R. pomeroyi* and other roseobacters. However, further investigations are needed to confirm the physiological significance of this pathway for the assimilation of DMSP.

CONCLUSION

Several major discoveries regarding the molecular biology and enzymology of DMSP metabolism have occurred during the last several years. These discoveries have enabled the use of molecular approaches to dissect DMSP biogeochemistry and interrogate the environmental significance of DMSP transformations. While these breakthroughs have significantly enhanced our understanding of DMSP and sulfur transformation in the environment, many of the microbial sulfur transformations remain "black boxes." Elucidation of the carbon and sulfur transformations within these black boxes on both the molecular and biochemical level is critical to our understanding of the marine microbial food web and global sulfur cycle.

ACKNOWLEDGMENTS

Financial support was provided by a dissertation completion grant from the University of Georgia, the National Science Foundation (MCB-07021258 and OCE-0724017), and the Gordon and Betty Moore Foundation.

REFERENCES

Alber, B. E., and Fuchs, G. (2002). Propionyl-coenzyme A synthase from *Chloroflexus aurantiacus*, a key enzyme of the 3-hydroxypropionate cycle for autotrophic CO2 fixation. *J. Biol. Chem.* 277, 12137–12143.

Albers, E. (2009). Metabolic characteristics and importance of the universal methionine salvage pathway recycling methionine from 5′-methylthioadenosine. *IUBMB Life* 61, 1132–1142.

Archer, S. D., Gilbert, F. J., Nightingale, P. D., Zubkov, M. V., Taylor, A. H., Smith, G. C., and Burkill, P. H. (2002). Transformation of dimethylsulphoniopropionate to dimethyl sulphide during summer in the North Sea with an examination of key processes via a modelling approach. *Deep Sea Res.* 49, 3067–3101.

Bentley, R., and Chasteen, T. G. (2004). Environmental VOSCs–formation and degradation of dimethyl sulfide, methanethiol and related materials. *Chemosphere* 55, 291–317.

Biers, E. J., Sun, S. L., and Howard, E. C. (2009). Prokaryotic genomes and diversity in surface ocean waters: interrogating the global ocean sampling metagenome. *Appl. Environ. Microbiol.* 75, 2221–2229.

Boden, R., Borodina, E., Wood, A. P., Kelly, D. P., Murrell, J. C., and Schafer, H. (2011). Purification and characterization of dimethylsulfide monooxygenase from *Hyphomicrobium sulfonivorans*. *J. Bacteriol.* 193, 1250–1258.

Boden, R., Kelly, D. P., Murrell, J. C., and Schafer, H. (2010). Oxidation of dimethylsulfide to tetrathionate by *Methylophaga thiooxidans* sp. nov.: a new link in the sulfur cycle. *Environ. Microbiol.* 12, 2688–2699.

Buchan, A., Gonzalez, J. M., and Moran, M. A. (2005). Overview of the marine *Roseobacter* lineage. *Appl. Environ. Microbiol.* 71, 5665–5677.

Charlson, R. J., Lovelock, J. E., Andreae, M. O., and Warren, S. G. (1987). Oceanic phytoplankton, atmospheric sulfur, cloud albedo and climate. *Nature* 326, 655–661.

Chin, M., and Jacob, D. J. (1996). Anthropogenic and natural contributions to tropospheric sulfate: a global model analysis. *J. Geophys. Res.* 101, 18691–18699.

Curson, A. R., Sullivan, M. J., Todd, J. D., and Johnston, A. W. (2011). DddY, a periplasmic dimethylsulfoniopropionate lyase found in taxonomically diverse species of Proteobacteria. *ISME J.* 5, 1191–1200.

Curson, A. R. J., Rogers, R., Todd, J. D., Brearley, C. A., and Johnston, A. W. B. (2008). Molecular genetic analysis of a dimethylsulfoniopropionate lyase that liberates the climate-changing gas dimethylsulfide in several marine alpha-proteobacteria and *Rhodobacter sphaeroides*. *Environ. Microbiol.* 10, 1099–1099.

Dacey, J. W. H., and Blough, N. V. (1987). Hydroxide decomposition of dimethylsulfoniopropionate to form dimethylsulfide. *Geophys. Res. Lett.* 14, 1246–1249.

Dai, Y., Wensink, P. C., and Abeles, R. H. (1999). One protein, two enzymes. *J. Biol. Chem.* 274, 1193–1195.

De Souza, M. P., and Yoch, D. C. (1995a). Comparative physiology of dimethyl sulfide production by dimethylsulfoniopropionate lyase in *Pseudomonas doudoroffii* and *Alcaligenes* sp. strain M3A. *Appl. Environ. Microbiol.* 61, 3986–3991.

De Souza, M. P., and Yoch, D. C. (1995b). Purification and characterization of dimethylsulfoniopropionate lyase from an *Alcaligenes*-like dimethyl sulfide-producing marine isolate. *Appl. Environ. Microbiol.* 61, 21–26.

De Zwart, J., Sluis, J., and Kuenen, J. G. (1997). Competition for dimethyl sulfide and hydrogen sulfide by *Methylophaga sulfidovorans* and *Thiobacillus thioparus* T5 in continuous cultures. *Appl. Environ. Microbiol.* 63, 3318–3322.

Del Valle, D. A., Kieber, D. J., and Kiene, R. P. (2007). Depth-dependent fate of biologically-consumed dimethylsulfide in the Sargasso Sea. *Mar. Chem.* 103, 197–208.

Dolata, M. M., Vanbeeumen, J. J., Ambler, R. P., Meyer, T. E., and Cusanovich, M. A. (1993). Nucleotide-sequence of the heme subunit of flavocytochrome c from the purple phototrophic bacterium, chromatium-vinosum – a 2.6-kilobase pair dna fragment contains 2 multiheme cytochromes, a flavoprotein, and a homolog of human ankyrin. *J. Biol. Chem.* 268, 14426–14431.

Erb, T. J., Berg, I. A., Brecht, V., Muller, M., Fuchs, G., and Alber, B. E. (2007). Synthesis of C-5-dicarboxylic acids from C-2-units involving crotonyl-CoA carboxylase/reductase: the ethylmalonyl-CoA pathway. *Proc. Natl. Acad. Sci. U.S.A.* 104, 10631–10636.

Erb, T. J., Fuchs, G., and Alber, B. E. (2009). (2S)-Methylsuccinyl-CoA dehydrogenase closes the ethylmalonyl-CoA pathway for acetyl-CoA assimilation. *Mol. Microbiol.* 73, 992–1008.

Flavin, M., and Ochoa, S. (1957). Metabolism of propionic acid in animal tissues. 1. Enzymatic conversion of propionate to succinate. *J. Biol. Chem.* 229, 965–979.

Franklin, D. J., Steinke, M., Young, J., Probert, I., and Malin, G. (2010). Dimethylsulphoniopropionate (DMSP), DMSP-lyase activity (DLA) and dimethylsulphide (DMS) in 10 species of coccolithophore. *Mar. Ecol. Prog. Ser.* 410, 13–23.

Friedrich, C. G., Rother, D., Bardischewsky, F., Quentmeier, A., and Fischer, J. (2001). Oxidation of reduced inorganic sulfur compounds by bacteria: emergence of a common mechanism? *Appl. Environ. Microbiol.* 67, 2873–2882.

Gage, D. A., and Rhodes, D. (1997). A new route for synthesis of dimethylsulphoniopropionate in marine algae. *Nature* 387, 891.

Ghosh, W., and Dam, B. (2009). Biochemistry and molecular biology of lithotrophic sulfur oxidation by taxonomically and ecologically diverse bacteria and archaea. *FEMS Microbiol. Rev.* 33, 999–1043.

Gonzalez, J. M., Kiene, R. P., and Moran, M. A. (1999). Transformation of sulfur compounds by an abundant lineage of marine bacteria in the alpha-subclass of the class Proteobacteria. *Appl. Environ. Microbiol.* 65, 3810–3819.

Gould, W. D., and Kanagawa, T. (1992). Purification and properties of methyl mercaptan oxidase from *Thiobacillus thioparus* TK-m. *J. Gen. Microbiol.* 138, 217–221.

Hatakeyama, S., Okuda, M., and Akimoto, H. (1982). Formation of sulfur-dioxide and methanesulfonic-acid in the photo-oxidation of dimethyl sulfide in the air. *Geophys. Res. Lett.* 9, 583–586.

Heilbronn, J., Wilson, J., and Berger, B. J. (1999). Tyrosine aminotransferase catalyzes the final step of methionine recycling in Klebsiella pneumoniae. *J. Bacteriol.* 181, 1739–1747.

Hetzel, M., Brock, M., Selmer, T., Pierik, A. J., Golding, B. T., and Buckel, W. (2003). Acryloyl-CoA reductase from *Clostridium propionicum*. An enzyme complex of propionyl-CoA dehydrogenase and electron-transferring flavoprotein. *Eur. J. Biochem.* 270, 902–910.

Hill, R. W., White, B. A., Cottrell, M. T., and Dacey, J. W. H. (1998). Virus-mediated total release of dimethylsulfoniopropionate from marine phytoplankton: a potential climate process. *Aquat. Microb. Ecol.* 14, 1–6.

Howard, E. C., Henriksen, J. R., Buchan, A., Reisch, C. R., Burgmann, H., Welsh, R., Ye, W., Gonzalez, J. M., Mace, K., Joye, S. B., Kiene, R. P., Whitman, W. B., and Moran, M. A. (2006). Bacterial taxa that limit sulfur flux from the ocean. *Science* 314, 649–652.

Howard, E. C., Sun, S. L., Biers, E. J., and Moran, M. A. (2008). Abundant and diverse bacteria involved in DMSP degradation in marine surface waters. *Environ. Microbiol.* 10, 2397–2410.

Kanzaki, H., Kobayashi, M., Nagasawa, T., and Yamada, H. (1987). Purification and characterization of cystathionine gamma-synthase type-II from *Bacillus sphaericus*. *Eur. J. Biochem.* 163, 105–112.

Kappler, U. (2011). Bacterial sulfite-oxidizing enzymes. *Biochim. Biophys. Acta* 1807, 1–10.

Kappler, U., and Dahl, C. (2001). Enzymology and molecular biology of prokaryotic sulfite oxidation. *FEMS Microbiol. Lett.* 203, 1–9.

Kappler, U., Friedrich, C. G., Truper, H. G., and Dahl, C. (2001). Evidence for two pathways of thiosulfate oxidation in *Starkeya novella* (formerly *Thiobacillus novellus*). *Arch. Microbiol.* 175, 102–111.

Karsten, U., Kuck, K., Vogt, C., and Kirst, G.O. (1996). "Dimethylsulphoniopropionate production in phototrophic organisms and its physiological function as a cryoprotectant," in *Biological and Environmental Chemistry of DMSP and Related Sulfonium Compounds*, eds R. P. Kiene, P. T. Visscher, M. D. Keller, and G. O. Kirst (New York: Plenum Press), 143–153.

Kiene, R. P. (1996). Production of methanethiol from dimethylsulfoniopropionate in marine surface waters. *Mar. Chem.* 54, 69–83.

Kiene, R. P., and Bates, T. S. (1990). Biological removal of dimethyl sulfide from sea-water. *Nature* 345, 702–705.

Kiene, R. P., and Linn, L. J. (2000). The fate of dissolved dimethylsulfoniopropionate (DMSP) in seawater: tracer studies using S-35-DMSP. *Geochim. Cosmochim. Acta* 64, 2797–2810.

Kiene, R. P., Linn, L. J., Gonzalez, J., Moran, M. A., and Bruton, J. A. (1999). Dimethylsulfoniopropionate and methanethiol are important precursors of methionine and protein-sulfur in marine bacterioplankton. *Appl. Environ. Microbiol.* 65, 4549–4558.

Kiene, R. P., and Taylor, B. F. (1988a). Biotransformations of organosulfur compounds in sediments via 3-mercaptopropionate. *Nature* 332, 148–150.

Kiene, R. P., and Taylor, B. F. (1988b). Demethylation of dimethylsulfoniopropionate and production of thiols in anoxic marine sediments. *Appl. Environ. Microbiol.* 54, 2208–2212.

Kim, S. J., Shin, H. J., Kim, Y. C., Lee, D. S., and Yang, J. W. (2000). Isolation and purification of methyl mercaptan oxidase from *Rhodococcus rhodochrous* for mercaptan detection. *Bioprocess Biosyst. Eng.* 5, 465–468.

Kirkwood, M., Le Brun, N. E., Todd, J. D., and Johnston, A. W. B. (2010). The dddP gene of *Roseovarius nubinhibens* encodes a novel lyase that cleaves dimethylsulfoniopropionate into acrylate plus dimethyl sulfide. *Microbiology* 156, 1900–1906.

Kirst, G. O. (1990). Salinity tolerance of eukaryotic marine algae. *Annu. Rev. Plant Physiol.* 41, 21–53.

Kocsis, M. G., and Hanson, A. D. (2000). Biochemical evidence for two novel enzymes in the biosynthesis of 3-dimethylsulfoniopropionate in *Spartina alterniflora*. *Plant Physiol.* 123, 1153–1161.

Kuever, J., and Meyer, B. (2007). Phylogeny of the alpha and beta subunits of the dissimilatory adenosine-5′-phosphosulfate (APS) reductase from sulfate-reducing prokaryotes – origin and evolution of the dissimilatory sulfate-reduction pathway. *Microbiology* 153, 2026–2044.

Lovelock, J. (2006). *The Revenge of Gaia: Earth's Climate in Crisis and the Fate of Humanity*. New York: Basic Books.

Lovelock, J. E., Maggs, R. J., and Rasmussen, R. A. (1972). Atmospheric dimethyl sulfide and natural sulfur cycle. *Nature* 237, 452–453.

Lu, W. P., Swoboda, B. E. P., and Kelly, D. P. (1985). Properties of the thiosulfate-oxidizing multi-enzyme system from *Thiobacillus versutus*. *Biochim. Biophys. Acta* 828, 116–122.

Mcdevitt, C. A., Hugenholtz, P., Hanson, G. R., and Mcewan, A. G. (2002). Molecular analysis of dimethyl sulphide dehydrogenase from *Rhodovulum sulfidophilum*: its place in the dimethyl sulphoxide reductase family of microbial molybdopterin-containing enzymes. *Mol. Microbiol.* 44, 1575–1587.

Moran, M. A., Reisch, C. R., Kiene, R. P., and Whitman, W. B. (2012). Genomic insights into bacterial DMSP transformations. *Annu. Rev. Mar. Sci.* 4. doi: 10.1146/annurev-marine-120710-100827

Mukhopadhyaya, P. N., Deb, C., Lahiri, C., and Roy, P. (2000). A soxA gene, encoding a diheme cytochrome c, and a sox locus, essential for sulfur oxidation in a new sulfur lithotrophic bacterium. *J. Bacteriol.* 182, 4278–4287.

Newton, R. J., Griffin, L. E., Bowles, K. M., Meile, C., Gifford, S., Givens, C. E., Howard, E. C., King, E., Oakley, C. A., Reisch, C. R., Rinta-Kanto, J. M., Sharma, S., Sun, S. L., Varaljay, V., Vila-Costa, M., Westrich, J. R., and Moran, M. A. (2010). Genome characteristics of a generalist marine bacterial lineage. *ISME J.* 4, 784–798.

Nishiguchi, M. K., and Goff, L. J. (1995). Isolation, purification, and characterization of DMSP lyase [dimethylpropiothetin dethiomethylase (4.4.1.3)] from the red alga *Polysiphonia paniculata*. *J. Phycol.* 31, 567–574.

Okamuraikeda, K., Fujiwara, K., and Motokawa, Y. (1982). Purification and characterization of chicken liver T-protein, a component of the glycine cleavage system. *J. Biol. Chem.* 257, 135–139.

Omelchenko, M. V., Galperin, M. Y., Wolf, Y. I., and Koonin, E. V. (2010). Non-homologous isofunctional enzymes: A systematic analysis of alternative solutions in enzyme evolution. *Biol. Direct* 5, 1–20.

Otte, M. L., Wilson, G., Morris, J. T., and Moran, B. M. (2004). Dimethylsulphoniopropionate (DMSP) and related compounds in higher plants. *J. Exp. Bot.* 55, 1919–1925.

Pott, A. S., and Dahl, C. (1998). Sirohaem sulfite reductase and other proteins encoded by genes at the dsr locus of *Chromatium vinosum* are involved in the oxidation of intracellular sulfur. *Microbiology* 144, 1881–1894.

Raina, J. B., Dinsdale, E. A., Willis, B. L., and Bourne, D. G. (2010). Do the organic sulfur compounds DMSP and DMS drive coral microbial associations? *Trends Microbiol.* 18, 101–108.

Reisch, C. R., Moran, M. A., and Whitman, W. B. (2008). Dimethylsulfoniopropionate-dependent demethylase (DmdA) from *Pelagibacter ubique* and *Silicibacter pomeroyi*. *J. Bacteriol.* 190, 8018–8024.

Reisch, C. R., Stoudemayer, M. J., Varaljay, V. A., Amster, I. J., Moran, M. A., and Whitman, W. B. (2011). Novel pathway for assimilation of dimethylsulphoniopropionate widespread in marine bacteria. *Nature* 473, 208–211.

Rhodes, D., Gage, D. A., Cooper, A., and Hanson, A. D. (1997). S-Methylmethionine conversion to dimethylsulfoniopropionate: evidence for an unusual transamination reaction. *Plant Physiol.* 115, 1541–1548.

Rohwerder, T., and Sand, W. (2003). The sulfane sulfur of persulfides is the actual substrate of the sulfur-oxidizing enzymes from *Acidithiobacillus* and *Acidiphilium* spp. *Microbiology* 149, 1699–1709.

Rusch, D. B., Halpern, A. L., Sutton, G., Heidelberg, K. B., Williamson, S., Yooseph, S., Wu, D. Y., Eisen, J. A., Hoffman, J. M., Remington, K., Beeson, K., Tran, B., Smith, H., Baden-Tillson, H., Stewart, C., Thorpe, J., Freeman, J., Andrews-Pfannkoch, C., Venter, J. E., Li, K., Kravitz, S., Heidelberg, J. F., Utterback, T., Rogers, Y. H., Falcon, L. I., Souza, V., Bonilla-Rosso, G., Eguiarte, L. E., Karl, D. M., Sathyendranath, S., Platt, T., Bermingham, E., Gallardo, V., Tamayo-Castillo, G., Ferrari, M. R., Strausberg, R. L., Nealson, K., Friedman, R., Frazier, M., and Venter, J. C. (2007). The sorcerer ii global ocean sampling expedition: Northwest Atlantic through eastern tropical pacific. *PLoS Biol.* 5, e77. doi: 10.1371/journal.pbio.0050077

Schafer, H., Myronova, N., and Boden, R. (2010). Microbial degradation of dimethylsulphide and related C-1-sulphur compounds: organisms and pathways controlling fluxes of sulphur in the biosphere. *J. Exp. Bot.* 61, 315–334.

Schutz, M., Shahak, Y., Padan, E., and Hauska, G. (1997). Sulfide-quinone reductase from Rhodobacter capsulatus – purification, cloning, and expression. *J. Biol. Chem.* 272, 9890–9894.

Simo, R. (2001). Production of atmospheric sulfur by oceanic plankton: biogeochemical, ecological and evolutionary links. *Trends Ecol. Evol. (Amst.)* 16, 287–294.

Stefels, J. (2000). Physiological aspects of the production and conversion of DMSP in marine algae and higher plants. *J. Sea Res.* 43, 183–197.

Stefels, J., and Van Boeckel, W. (1993). Production of DMS from dissolved DMSP in axenic cultures of the marine phytoplankton species *Phaeocystis* sp. *Mar. Ecol. Prog. Ser.* 97, 11–18.

Steinke, M., Malin, G., Archer, S. D., Burkill, P. H., and Liss, P. S. (2002). DMS production in a coccolithophorid bloom: evidence for the importance of dinoflagellate DMSP lyases. *Aquat. Microb. Ecol.* 26, 259–270.

Stines-Chaumeil, C., Talfournier, F., and Branlant, G. (2006). Mechanistic characterization of the MSDH (methylmalonate semialdehyde dehydrogenase) from *Bacillus subtilis*. *Biochem. J.* 395, 107–115.

Sunda, W., Kieber, D. J., Kiene, R. P., and Huntsman, S. (2002). An antioxidant function for DMSP and DMS in marine algae. *Nature* 418, 317–320.

Suylen, G. M. H., Large, P. J., Vandijken, J. P., and Kuenen, J. G. (1987). Methyl mercaptan oxidase, a key enzyme in the metabolism of methylated sulfur-compounds by *Hyphomicrobium* EG. *J. Gen. Microbiol.* 133, 2989–2997.

Taylor, B. F., and Gilchrist, D. C. (1991). New routes for aerobic biodegradation of dimethylsulfoniopropionate. *Appl. Environ. Microbiol.* 57, 3581–3584.

Taylor, B. F., and Visscher, P. T. (1996). "Metabolic pathways involved in DMSP degradation," in *Biological and Environmental Chemistry of DMSP and Related Sulfonium Compounds*, eds R. P. Kiene, P. T. Visscher, M. D. Keller, and G. O. Kirst (New York: Plenum Press), 265–276.

Teufel, R., Kung, J. W., Kockelkorn, D., Alber, B. E., and Fuchs, G. (2009). 3-hydroxypropionyl-coenzyme A dehydratase and acryloyl-coenzyme A reductase, enzymes of the autotrophic 3-hydroxypropionate/4-hydroxybutyrate cycle in the Sulfolobales. *J. Bacteriol.* 191, 4572–4581.

Todd, J. D., Curson, A. R., Dupont, C. L., Nicholson, P., and Johnston, A. W. (2009a). The dddP gene, encoding a novel enzyme that converts dimethylsulfoniopropionate into dimethyl sulfide, is widespread in ocean metagenomes and marine bacteria and also occurs in some ascomycete fungi. *Environ. Microbiol.* 11, 1376–1385.

Todd, J. D., Curson, A. R., Nikolaidou-Katsaraidou, N., Brearley, C. A., Watmough, N. J., Chan, Y., Page, P. C., Sun, L., and Johnston, A. W. (2009b). Molecular dissection of bacterial acrylate catabolism – unexpected links with dimethylsulfoniopropionate catabolism and dimethyl sulfide production. *Environ. Microbiol.* 12, 327–343.

Todd, J. D., Curson, A. R., Kirkwood, M., Sullivan, M. J., Green, R. T., and Johnston, A. W. (2010). DddQ, a novel, cupin-containing, dimethylsulfoniopropionate lyase in marine roseobacters and in uncultured marine bacteria. *Environ. Microbiol.* 13, 427–438.

Todd, J. D., Kirkwood, M., Newton-Payne, S., and Johnston, A. W. (2011). DddW, a third DMSP lyase in a model *Roseobacter marine* bacterium, *Ruegeria pomeroyi* DSS-3. *ISME J.* doi:10.1038/ismej.2011.79

Todd, J. D., Rogers, R., Li, Y. G., Wexler, M., Bond, P. L., Sun, L., Curson, A. R., Malin, G., Steinke, M., and Johnston, A. W. (2007). Structural and regulatory genes required to make the gas dimethyl sulfide in bacteria. *Science* 315, 666–669.

Toole, D. A., and Siegel, D. A. (2004). Light-driven cycling of dimethylsulfide (DMS) in the Sargasso Sea: closing the loop. *Geophys. Res. Lett.* 31, 1–4.

Toole, D. A., Siegel, D. A., and Doney, S. C. (2008). A light-driven, one-dimensional dimethylsulfide biogeochemical cycling model for the Sargasso Sea. *J. Geophys. Res.* 113, 1–20.

Toole, D. A., Slezak, D., Kiene, R. P., Kieber, D. J., and Siegel, D. A. (2006). Effects of solar radiation on dimethylsulfide cycling in the western Atlantic Ocean. *Deep Sea Res.* 53, 136–153.

Tripp, H. J., Kitner, J. B., Schwalbach, M. S., Dacey, J. W. H., Wilhelm, L. J., and Giovannoni, S. J. (2008). SAR11 marine bacteria require exogenous reduced sulphur for growth. *Nature* 452, 741–744.

Vallina, S. M., and Simo, R. (2007). Strong relationship between DMS and the solar radiation dose over the global surface ocean. *Science* 315, 506–508.

Vallina, S. M., Simo, R., Anderson, T. R., Gabric, A., Cropp, R., and Pacheco, J. M. (2008). A dynamic model of oceanic sulfur (DMOS) applied to the Sargasso Sea: simulating the dimethylsulfide (DMS) summer paradox. *J. Geophys. Res.* 113, 1–23.

Van Den Berg, A. J., Turner, S. M., Vanduyl, F. C., and Ruardij, P. (1996). Model structure and analysis of dimethylsulphide (DMS) production in the southern North Sea, considering phytoplankton dimethylsulphoniopropionate-(DMSP) lyase and eutrophication effects. *Mar. Ecol. Prog. Ser.* 145, 233–244.

Van Duyl, F. C., Gieskes, W. W. C., Kop, A. J., and Lewis, W. E. (1998). Biological control of short-term variations in the concentration of DMSP and DMS during a *Phaeocystis* spring bloom. *J. Sea Res.* 40, 221–231.

Vandermaarel, M. J. E. C., Jansen, M., and Hansen, T. A. (1995). Methanogenic conversion of 3-S-methylmercaptopropionate to 3-mercaptopropionate. *Appl. Environ. Microbiol.* 61, 48–51.

Varaljay, V. A., Howard, E. C., Sun, S., and Moran, M. A. (2010). Deep sequencing of a dimethylsulfoniopropionate-degrading gene (dmdA) by using PCR primer pairs designed on the basis of marine metagenomic data. *Appl. Environ. Microbiol.* 76, 609–617.

Vila-Costa, M., Del Valle, D. A., Gonzalez, J. M., Slezak, D., Kiene, R. P., Sanchez, O., and Simo, R. (2006). Phylogenetic identification and metabolism of marine dimethylsulfide-consuming bacteria. *Environ. Microbiol.* 8, 2189–2200.

Vila-Costa, M., Rinta-Kanto, J. M., Sun, S., Sharma, S., Poretsky, R., and Moran, M. A. (2010). Transcriptomic analysis of a marine bacterial community enriched with dimethylsulfoniopropionate. *ISME J.* 4, 1410–1420.

Visscher, P. T., and Taylor, B. F. (1994). Demethylation of dimethylsulfoniopropionate to 3-mercaptopropionate by an aerobic marine bacterium. *Appl. Environ. Microbiol.* 60, 4617–4619.

Wagner-Dobler, I., and Biebl, H. (2006). Environmental biology of the marine *Roseobacter* lineage. *Annu. Rev. Microbiol.* 60, 255–280.

Wang, Y. Y., Ma, X. H., Zhao, W. F., Jia, X. M., Kai, L., and Xu, X. H. (2006). Study on the creatinase from *Paracoccus* sp strain WB1. *Process Biochem.* 41, 2072–2077.

Wolfe, G. V., and Steinke, M. (1996). Grazing-activated production of dimethyl sulfide (DMS) by two clones of *Emiliania huxleyi*. *Limnol. Oceanogr.* 41, 1151–1160.

Wolfe, G. V., and Steinke, M. (1997). Grazing-activated chemical defence in a unicellular marine alga. *Nature* 387, 894–897.

Yancey, P. H. (2005). Organic osmolytes as compatible, metabolic and counteracting cytoprotectants in high osmolarity and other stresses. *J. Exp. Biol.* 208, 2819–2830.

Yoch, D. C. (2002). Dimethylsulfoniopropionate: its sources, role in the marine food web, and biological degradation to dimethylsulfide. *Appl. Environ. Microbiol.* 68, 5804–5815.

Yost, D. M., and Mitchelmore, C. L. (2009). Dimethylsulfoniopropionate (DMSP) lyase activity in different strains of the symbiotic alga *Symbiodinium microadriaticum*. *Mar. Ecol. Prog. Ser.* 386, 61–70.

Zubkov, M. V., Fuchs, B. M., Archer, S. D., Kiene, R. P., Amann, R., and Burkill, P. H. (2002). Rapid turnover of dissolved DMS and DMSP by defined bacterioplankton communities in the stratified euphotic zone of the North Sea. *Deep Sea Res.* 49, 3017–3038.

Conflict of Interest Statement: The authors declare that the research was conducted in the absence of any commercial or financial relationships that could be construed as a potential conflict of interest.

Received: 29 April 2011; accepted: 28 July 2011; published online: 12 August 2011.
Citation: Reisch CR, Moran MA and Whitman WB (2011) Bacterial catabolism of dimethylsulfoniopropionate (DMSP). Front. Microbio. ***2****:172. doi: 10.3389/fmicb.2011.00172*
This article was submitted to Frontiers in Microbial Physiology and Metabolism, a specialty of Frontiers in Microbiology.

frontiers in
MICROBIOLOGY

ORIGINAL RESEARCH ARTICLE
published: 25 March 2011
doi: 10.3389/fmicb.2011.00055

Structured multiple endosymbiosis of bacteria and archaea in a ciliate from marine sulfidic sediments: a survival mechanism in low oxygen, sulfidic sediments?

Virginia P. Edgcomb[1]*, Edward R. Leadbetter[2], William Bourland[3], David Beaudoin[4] and Joan M. Bernhard[1]

[1] *Geology and Geophysics Department, Woods Hole Oceanographic Institution, Woods Hole, MA, USA*
[2] *Marine Chemistry and Geochemistry Department, Woods Hole Oceanographic Institution, Woods Hole, MA, USA*
[3] *Department of Sciences, Boise State University, Boise, ID, USA*
[4] *Biology Department, Woods Hole Oceanographic Institution, Woods Hole, MA, USA*

Edited by:
Martin G. Klotz, University of Louisville, USA

Reviewed by:
Thorsten Stoeck, University of Kaiserslautern, Germany
O. Roger Anderson, Lamont–Doherty Earth Observatory of Columbia University, USA

****Correspondence:***
Virginia P. Edgcomb, Geology and Geophysics Department, Woods Hole Oceanographic Institution, Woods Hole, MA 02543-1050, USA.
e-mail: vedgcomb@whoi.edu

Marine micro-oxic to sulfidic environments are sites of intensive biogeochemical cycling and elemental sequestration, where prokaryotes are major driving forces mediating carbon, nitrogen, sulfur, phosphorus, and metal cycles, important from both biogeochemical and evolutionary perspectives. Associations between single-celled eukaryotes and bacteria and/or archaea are common in such habitats. Here we describe a ciliate common in the micro-oxic to anoxic, typically sulfidic, sediments of Santa Barbara Basin (CA, USA). The ciliate is 95% similar to *Parduzcia orbis* (18S rRNA). Transmission electron micrographs reveal clusters of at least three different endobiont types organized within membrane-bound sub-cellular regions. Catalyzed reporter deposition–fluorescent in situ hybridization and 16S rRNA clone libraries confirm the symbionts include up to two sulfate reducers (Desulfobulbaceae, Desulfobacteraceae), a methanogen (Methanobacteriales), and possibly a Bacteroidete (*Cytophaga*) and a Type I methanotroph, suggesting synergistic metabolisms in this environment. This case study is discussed in terms of implications to biogeochemistry, and benthic ecology.

Keywords: ciliate, anoxia, symbiosis, TEM, SSU rRNA, FISH

INTRODUCTION

Anoxic habitats are common, including certain marine and freshwater sediments and water columns, water-logged soils, sewage, the gastro-intestinal tracts of animals, the carcasses of dead mammals on the sea-floor, and the interiors of some suspended organic aggregates. Many of these habitats not only lack oxygen, but have considerable, and sometimes physiologically significant (e.g., Bagarinao, 1992) concentrations of hydrogen sulfide, which inhibits aerobic respiration. The abundant bacteria and archaea found in anoxic and potentially sulfidic environments are grazed upon by anaerobic protists (Fenchel and Finlay, 1990). Through grazing on prokaryotic and other eukaryotic prey, protists modify or re-mineralize organic matter, and regenerate nutrients (Taylor, 1982; Jumars et al., 1989; Sherr and Sherr, 2002). Protist grazing in marine environments also can affect the quantity, activity and physiological state of their prey, and hence, through these direct and indirect effects, may help determine the metabolic potential of prey communities (Madsen et al., 1991; Sherr and Sherr, 2002; Frias-Lopez et al., 2009). Anaerobic protists, including many groups of eukaryotes that lack mitochondria, such as anaerobic ciliates, were first documented by Fenchel et al. (1977). Many anaerobic eukaryotes, including the anaerobic ciliates are currently considered to be secondarily amitochondriate, and more recently adapted to an anaerobic lifestyle (see discussion by Embley and Finlay, 1994). Fenchel et al. (1977) first showed that several ciliate genera, including *Caenomorpha, Metopus, Parablepharisma, Plagiopyla, Saprodinium*, and *Sonderia* lack mitochondria and cytochrome oxidase. Like many other anaerobic eukaryotes however, they have specialized redox organelles called hydrogenosomes (possibly of mitochondrial origin, see Müller, 1988 and recent discussion in Barbera et al., 2010). Hydrogenosomes carry out an H_2-evolving fermentation thought to play an integral role in the symbiosis between anaerobic ciliates and certain bacteria and archaea including methanogens (commonly members of Methanobacteriales and Methanomicrobiales; Embley and Finlay, 1994).

Endosymbiotic associations are common within protists (for recent review see Nowack and Melkonin, 2010). The acquisition of endosymbionts has been proposed to represent a general evolutionary strategy in protists to acquire novel biochemical functions (Nowack and Melkonin, 2010) and, in the case of micro-oxic (up to 0.1 ml/L; Bernhard and Sen Gupta, 1999) or anoxic, and potentially sulfidic marine environments, symbiosis may represent a strategy for exploiting these otherwise inhospitable habitats. Examples of symbiotic relationships between bacteria, archaea, and eukaryotes in deep-sea oxygen-depleted marine environments have been well documented for some groups, starting with the discovery of associations between metazoa and bacteria at hydrothermal vents (Cavanaugh et al., 1981; Cavanaugh, 1994), cold seeps (Barry et al., 1996), and the edges of silled basins (e.g., Distel and Felbeck, 1988). Chemosynthetic autotrophy supports many of these associations and often involves the oxidation of hydrogen sulfide or methane by endosymbiotic bacteria within the animal hosts.

The symbionts of some marine ciliates have been described phylogenetically, including some from oxygenated habitats (Amman et al., 1991; Springer et al., 1993; Beier et al., 2002; Vannini et al., 2004) and some from anoxic habitats (Embley et al., 1992; Embley and Finlay, 1994). Much information about ciliate endosymbionts has come from morphological and functional approaches (e.g., Fenchel and Finlay, 1991b; Fenchel and Bernard, 1993; and for review see Görtz, 2002). Multiple endosymbionts have been described in individuals of certain ciliate species. For example, in the parasitic ciliate *Ichthyophthirius multifiliis*, a common pathogen of freshwater fish, 16S rRNA gene sequencing and fluorescent *in situ* hybridization (FISH) demonstrated that three classes of bacteria were present, including Alphaproteobacteria (Rickettsiales), Sphingobacteria (in the cytoplasm), and *Flavobacterium columnare* (associated with cilia; Sun et al., 2009). In another freshwater ciliate, *Cyclidium porcatum,* an internal structure is present that consists of hydrogenosomes interspersed with methanogens and unidentified bacteria. This association is stable and persistent, indicative of an anaerobic symbiotic consortium of three functional partners (Esteban et al., 1993).

Methanogens are common endosymbionts in free-living anaerobic ciliates (e.g., Fenchel and Finlay, 1991a; van Hoek et al., 2000). In the anaerobic free-living ciliates *Metopus contortus, M. striatus, M. palaeformis, Trimyema* sp., and *C. porcatum*, methanogens from three different genera were identified on the basis of rRNA gene sequencing and microscopy (Embley and Finlay, 1993, 1994). These authors determined that such endosymbioses have formed repeatedly and independently, and that most likely, some were recent events. There have been different levels of association observed between hydrogenosomes in anaerobic ciliates and their endosymbiotic methanogens (Embley and Finlay, 1994). The endosymbiotic methanogens may use the H_2 produced by hydrogenosomes to reduce CO_2 and generate energy (Van Bruggen et al., 1983; Jones et al., 1987), and in the process may release dissolved organics utilizable by the host (Fenchel and Finlay, 1991a). Some ciliates clearly benefit from this association because the growth rate of these ciliates is much lower if their methanogens are inhibited (Fenchel and Finlay, 1991b; Finlay and Fenchel, 1992).

Ciliates are perhaps the most studied protist group in terms of taxonomy. A unifying feature of ciliates is that they all contain two types of nuclei, a germ or micronucleus and a polyploid somatic macronucleus, the latter of which is most actively transcribed (Raikov, 1985). The karyorelictid ciliates have been hypothesized to be primitive within the phylum Ciliophora because of their simple form of nuclear dualism whereby the macronuclei are nearly diploid and do not divide once they differentiate from a micronucleus (Corliss, 1979; Hirt et al., 1995). Here we describe a karyorelictid ciliate and its bacterial and archaeal associates recovered from the oxygen-depleted sediments of Santa Barbara Basin, CA, USA.

MATERIALS AND METHODS

SAMPLE COLLECTION

The Santa Barbara Basin, which is located off California (USA), has a maximum depth of ~600 m and sill depth of ~475 m. The samples used for this study were collected using a Soutar box corer or an MC800 multicorer from sea-floor sediments (580–592 m depth) collected between September 2007 and June 2009 using the RV *Robert Gordon Sproul.* Initial examination of sediments revealed a relatively abundant brown ciliate. Samples bearing the targeted ciliate were collected along a north-south trending transect along 120°02′W, from 34°17.6′N to 34°13.0′N. Our samples were collected from box cores that exhibited a surface covering of sulfide-oxidizing bacteria (either *Thioploca* or *Beggiatoa*, both of which require sulfide and little or no oxygen; e.g., McHatton et al., 1996). Surface ~0–2 cm sediments were transferred to 100–250 ml high-density polyethylene (HDPE) bottles, completely filled with bottom water, and stored at ~7°C. Sample bottles were kept tightly closed until aliquots were removed for ciliate harvest. Once a bottle was opened, the redox chemistry changed sufficiently so that within about a week most of the target ciliates died. We did not amend bottles with substrates or food. This approach has been used successfully by Bernhard for many studies (e.g., Bernhard et al., 2000, 2006; Edgcomb et al., 2010).

For specimen counts, aliquots of archived quantitative surface 1-cm^3 samples were counted for ciliate abundances. Quantitative samples were taken from boxcores using 60-cc syringe cores. Concurrent with sediment sampling, oxygen concentrations were obtained for bottom waters using the microwinkler method (Browenkow and Cline, 1969).

LIGHT MICROSCOPY

For light microscope observation, cells were observed under the dissecting microscope in ice-chilled Petri dishes containing sample water and sediment. Cells were selected using micropipettes. Live ciliates were studied at magnifications of 40–1000× with brightfield, phase contrast, and differential interference contrast (DIC) using a Zeiss Axioskop 2 plus microscope. A minimum of 50 living target ciliates were observed and photographed. Cells lysed within minutes of illumination under a cover glass making *in vivo* observations quite difficult. Consistent with the experience of others studying marine karyorelictids, we had great difficulty with fixation and silver impregnation of these ciliates (Foissner and Dragesco, 1996; Dragesco, 1999; Foissner and Al-Rasheid, 1999). We employed the techniques described by Foissner and Dragesco (1996) and Foissner and Al-Rasheid (1999), including many of our own modifications, without success. Consequently protargol impregnations were of suboptimal quality. Although some temporary preparations done according to the method of Foissner and Dragesco (1996) were adequate for determining general morphologic features, many details were often obscured by densely impregnating cortical granules. Microphotographs and measurements of fixed cells were made using a Zeiss AxioCam and Axiovision imaging software or a Flex digital camera and Spot imaging software (Diagnostic Instruments Inc., Sterling Heights, MI, USA). Microphotographs of uncompressed cells were used for *in vivo* measurements. Terminology is according to Dragesco (1999), Foissner and Xu (2007), and Lynn (2008). Classification is according to Lynn (2008).

TRANSMISSION ELECTRON MICROSCOPY

Aboard the ship, aliquots of bulk sediments were fixed in 3% glutaraldehyde (final concentration) buffered with 0.1 M Na-cacodylate (pH 7.2), from which specimens were isolated from the coarse residue after sieving with buffer over a 63-μm screen. Specimens were processed for transmission electron microscopy (TEM) following

our standard procedures (Bernhard et al., 2000). Sections from approximately 10 individuals were examined with a Zeiss 10CA transmission electron microscope.

DNA EXTRACTION, PCR AMPLIFICATION, AND PHYLOGENETIC ANALYSIS

Single cells of the brown-pigmented ciliate were picked from sediments using a dissecting microscope. In order to greatly minimize contamination, cells were rinsed three times in sterile seawater (0.2 μm filtered) before being placed into 2.0 ml microfuge tubes and frozen at −20°C for DNA extraction. Surface sterilization with antibiotic such as streptomycin was not possible because these ciliates lysed within ~10 min of being removed from their bottles for hand picking. Exposure to an antibiotic solution as per methods of Vannini et al. (2004) caused immediate lysis of this ciliate. Individuals were divided into two groups: single individuals/PCR tube for direct PCR amplification or pools of ~25–50 individuals for DNA extraction. DNA was extracted from pooled samples using the DNAeasy kit (Qiagen, USA) following the manufacturer's recommendations.

Bacteria-, eukarya-, and archaea-specific primers were tested for positive PCR amplification. Bacterial primers were Bact8F (Amman et al., 1995) paired with U1492R (Longnecker and Reysenbach, 2001). Archaeal primers were ARC4F (Jolivet et al., 2003) paired with 1492R (Lane, 1991), followed by ARC21F (DeLong, 1992) paired with ARC915R (Stahl and Amann, 1991). Eukaryotic primers were 82F (Dawson and Pace, 2002), 360F (Medlin et al., 1988), and 528F (Elwood et al., 1985) paired with U1492R. PCR amplification conditions for the bacterial and eukaryotic primer pairs were: 95°C for 5 min, followed by 40 cycles of 95°C for 1 min, 45°C for 1 min, 72°C for 1.5 min, and a final cycle of 72°C for 7 min. For archaea, a nested amplification was used with SpeedSTAR HS DNA Polymerase (TaKaRa) as described by the manufacturer: 98°C for 2 min followed by 30 cycles of 98°C for 5 s, 55°C for 15 s, and 72°C for 20 s, and a final cycle of 72°C for 2 min. This was followed by another round of 98°C for 2 min followed by 30 cycles of 98°C for 5 s, 58°C for 15 s, and 72°C for 20 s with a final cycle of 72°C for 2 min. We also amplified one of the key genes of sulfate reduction, *dsrAB* using the primer mixes DSR1F and DSR4R according to the protocols in Loy et al. (2004). Cycling conditions were: 95°C for 5 min followed by 35 cycles of 94°C for 40 s, 48°C for 40 s, and 72°C for 90 s with a final 72°C incubation for 7 min.

Amplified DNA was checked for quality by agarose gel electrophoresis, bands of the expected sizes were gel purified using the Zymoclean Gel DNA Recovery Kit (Zymo Research) and positive reactions were cloned into the vector pCR4-TOPO using the TOPO TA Cloning Kit (Invitrogen) following the manufacturer's instructions. Plasmid DNA from 16 clones (12 clones for *dsrAB* gene sequences) per primer pair was prepared using a MWG Biotech RoboPrep2500, and inserts were sequenced bi-directionally using the universal M13F and M13R primers and an Applied Biosystems 3730XL capillary sequencer at the Keck Facility at the Josephine Bay Paul Center at the Marine Biological Laboratory (MBL), Woods Hole, MA, USA. Processing of sequence data used PHRED and PHRAP (Ewing and Green, 1998; Ewing et al., 1998) and a pipeline script. The sequences were checked for chimeras using the Bellerophon Chimera Check and the Check_Chimera utilities (Ribosomal Database Project; Cole et al., 2003).

For phylogenetic analyses, we aligned the clone sequences from archaeal and bacterial amplifications to 16S rRNA sequences available in the ARB package (Ludwig et al., 2004; http://www.arb-home.de). The rRNA alignment was corrected manually according to secondary structure information. Only unambiguously aligned positions (961 bp for the host ciliate alignment, 844 for the archaeal data set, and 982 for the bacterial data set) were used to construct phylogenetic trees. To these alignments, we added the closest relatives of our original sequences retrieved from GenBank using BLASTn. Alignments were subjected to Bayesian and Maximum Likelihood inference using RAxML (Stamatakis et al., 2008) and MrBayes (Ronquist and Huelsenbeck, 2003). All phylogenetic analyses were performed on the CIPRES portal (Miller et al., 2009) under the GTR + Gamma model using 1000 bootstrap replicates and estimation of the proportion of invariable sites. Bayesian analyses consisted of two independent runs with 4×10^6 generations. Trees were sampled every 1000 generations with 25% discarded as burn-in. Topologies of ML and Bayesian trees were compared and the tree with the best likelihood was chosen for presentation.

CATALYZED REPORTER DEPOSITION–FLUORESCENT *IN SITU* HYBRIDIZATION

Catalyzed reporter deposition (CARD)–FISH was performed with only minor modifications to the methods of Pernthaler et al. (2002). A minimum of 80 cells were hand picked and rinsed in sterile seawater and fixed in Bouin's solution for 2 h (Stoeck et al., 2003), then rinsed three times with 5 ml sterile phosphate buffered saline (PBS) by filtration onto a 0.2-μm pore size, 25 mm Isopore GTTP filter (Millipore, USA). Air-drying caused the cells to collapse and release their contents, and so in most cases we did not permit the filters to dry completely before overlaying them with 37°C 0.2% (w/v) Metaphor agarose and drying at 50°C. To inactivate endogenous peroxidases, filter sections were incubated in 10 ml of 0.01 M HCl for 10 min at room temperature. Filters were washed in 50 ml 1× PBS, then in 50 ml of distilled, deionized water (ddH_20). The host and endobiont cells were permeabilized by incubating the individual filter pieces in 2.0 ml Eppendorf microfuge tubes for 60 min at 37°C in a lysozyme solution (0.05 M EDTA, pH 8.0; 0.1 M Tris HCl, pH 8.0; 10 mg/ml lysozyme). The filters were washed in 1× PBS for 2 min, followed by treatment for 20 min in a solution of proteinase K (50 μl of 1064 U/μl in 10 ml Tris EDTA buffer) at room temperature. Proteinase K was inactivated in a solution of 0.01 M HCL for 20 min at room temperature, and filters were washed in 50 ml 1× PBS for 1 min and then 50 ml ddH_20 for 2 min, followed by 50 ml of absolute ethanol (96%) and air-dried or partially air-dried prior to embedding in Metaphor agarose. For visualization of archaeal endobionts, we tested 0.5–5.0 U of pseudomurein endoisopeptidase (PeiW) per filter according to the methods of Nakamura et al. (2006). Hybridization buffer and probe were mixed 300:1 in 2.0 ml Eppendorf tubes (probe at 50 ng/μl). For 50 ml of hybridization buffer we mixed 3.6 ml 5 M NaCl, 0.4 ml 1 M Tris HCl and ddH_20 depending on formamide concentration for each probe used (see **Table 1**). The remainder of the CARD–FISH procedure followed the protocol of Edgcomb et al. (2010). The Alexa488-labeled probes used include EUB338 I-III (Daims et al., 2001), NON338 (Wallner et al., 1993), Arch915 (Stahl and Amann, 1991), Alf968 (Neef, 1997), Gam42a (Manz et al., 1992) and Gam42a competitor (Yeates et al.,

Table 1 | Percent formamide concentrations and concentration of NaCl used in wash buffers for probes used in this study.

Probe	Specificity	% FA	Concentration NaCl in wash buffer in mol
EUB338-I-III	Most bacteria	35	0.080
NON 338	Background control	35	0.080
ARCH915	Most archaea	35	0.080
GAM42a	Most gamma-proteobacteria	35	0.080
GAM42a competitor		35	0.080
BET42a	Most beta-proteobacteria	35	0.080
BET42a competitor		35	0.080
DELTA495 a, b, and c	Most delta-proteobacteria	35	0.080
cDELTA495 a, b, and c		35	0.080
DSBAC357	Desulfobacteraceae and Syntrophobacteraceae	35	0.080
DSB706	Desulfobulbaceae and	45	0.040
DSS658	Desulfobacteraceae	60	0.014
ALF968	Most alpha-proteobacteria	35	0.080
EPS549	Most epsilon-proteobacteria	55	0.020

2003), BET42a (Manz et al., 1992) and BET42a competitor (Yeates et al., 2003), DELTA495a, b, and c and the corresponding competitor probes for each, cDELTA495a, b, and c (Lucker et al., 2007), EPS549 (Lin et al., 2006), DSBAC357 (Lucker et al., 2007), DSB706 (Loy et al., 2002), DSB658 (Manz et al., 1998), and EPS549 (Lin et al., 2006). Formamide and NaCl concentrations used in wash buffers are noted in **Table 1**. CARD–FISH images were taken on a Zeiss Axioplan 2 microscope equipped with a Zeiss AxioCam camera. Confocal microscope images were taken with an Olympus Fluoview 300 Laser Scanning Confocal Microscope equipped with an Argon laser for FITC/Alexa488.

RESULTS

OXYGEN CONCENTRATIONS AND CELL COUNTS OF BROWN-PIGMENTED CILIATE

Dissolved oxygen concentrations in bottom waters overlying sediments used for recovery of the brown-pigmented ciliate analyzed for CARD–FISH ranged from 0.2 to 0.5 μM. Concentrations <1 μM are typical for these sites (Bernhard et al., 2000, 2003). It should be noted that bottom-water oxygen and sulfide concentrations vary considerably in Santa Barbara Basin depending on timing of flushing events (e.g., Reimers et al., 1990, 1996; Kuwabara et al., 1999; Bernhard et al., 2003).

Concentrations of the brown-pigmented ciliate ranged from an average of 19.1 cells/cm^3 when bottom waters were 10.8 μM O_2 to 71.6 cells/cm^3 when bottom waters were 0.1 μM O_2 (**Table 2**), indicating a clear preference for low oxygen sedimentary environments.

Table 2 | Average counts of the Geleiid karyorelictean ciliate from different sites in Santa Barbara Basin with varying bottom-water oxygen concentrations.

Santa Barbara basin site	Water depth (m)	Bottom water ([0_2] μM)	Average no./cm^3 sediment
1	590	0.1	71.6
2	550	0.9	65.9
3	525	4.3	38.0
4	510	5.6	17.6
5	500	10.8	19.1

Three replicate 1-ml sediment samples were counted per site, from three separate bottles.

LIGHT MICROSCOPY DESCRIPTION OF HOST CILIATE

The size of the host ciliate *in vivo* was ~280–365 × 120–150 μm ($n = 20$). The body shape is obpyriform, roughly elliptical in cross-section and slightly laterally compressed. The anterior part forms a broad leftward-curving neck, terminating in a bluntly rounded rostrum. The anterior is lanceolate in more strongly contracted individuals (**Figures 1A,B**). The posterior is bluntly tapered. This ciliate moves slowly, is sluggishly contractile, writhing through detritus, and does not swim. The cell shape is broadly ovate after fixation, ~325 μm × 250 μm. The buccal overture is subapical. The overhanging rostrum forms a raised lip around the anterior margin of the buccal cavity (**Figure 1C**). The nuclear apparatus is located centrally, obscured by cortical granules *in vivo*, and consists of two adjacent but unattached spherical macronuclear nodules ~20–25 μm across in impregnated specimens. A single ~ 8 μm diameter spherical micronucleus is present between but not attached to the macronuclei. The macronuclei contain ~20 densely impregnating nucleoli ~3–7 μm across after protargol (**Figure 2B**, inset). There was no evidence of a contractile vacuole. The cortex is flexible.

A disorganized concentration of ~0.6 μm diameter brownish-pink pigment granules is located within each kinety with two rows of more loosely spaced granules between kineties (**Figures 1E** and **2D,E**). Cortical granules and larger cytoplasmic pigmentocysts give the cells a deep brownish-pink color under DIC and phase contrast illumination (**Figures 1A–C,E**). Wavy fibrillar structures, likely contracted myonemes, are located between kineties (**Figure 1D**) and the cytoplasm contains numerous shiny brownish-pink pigmentocysts, ~3–5 μm in diameter (**Figure 1C**). Food vacuoles were observed rarely, occasionally containing pennate diatoms (**Figure 2C**). The somatic infraciliature is comprised of ~40–50 meridional kineties, ~9 μm apart in impregnated specimens, and consisting of ciliated dikinetids. Kineties originate anteriorly at a short preoral suture, and converge at the posterior pole (**Figures 2B,D,E**). There are occasional incomplete somatic kineties but no true postoral kineties (**Figures 2D,E**). There is no postoral suture. The somatic cilia are ~13 μm long. Kinety 1 and kinety *n* diverge at the posterior end of the buccal overture to pass right and left of it, respectively (**Figure 2E**). The elliptical, cup-shaped oral apparatus is subapical, and extends ~20–25% of the cell length. An aggregation of pigmentocysts is present at the center of the cytostome *in vivo* and in protargol impregnated specimens

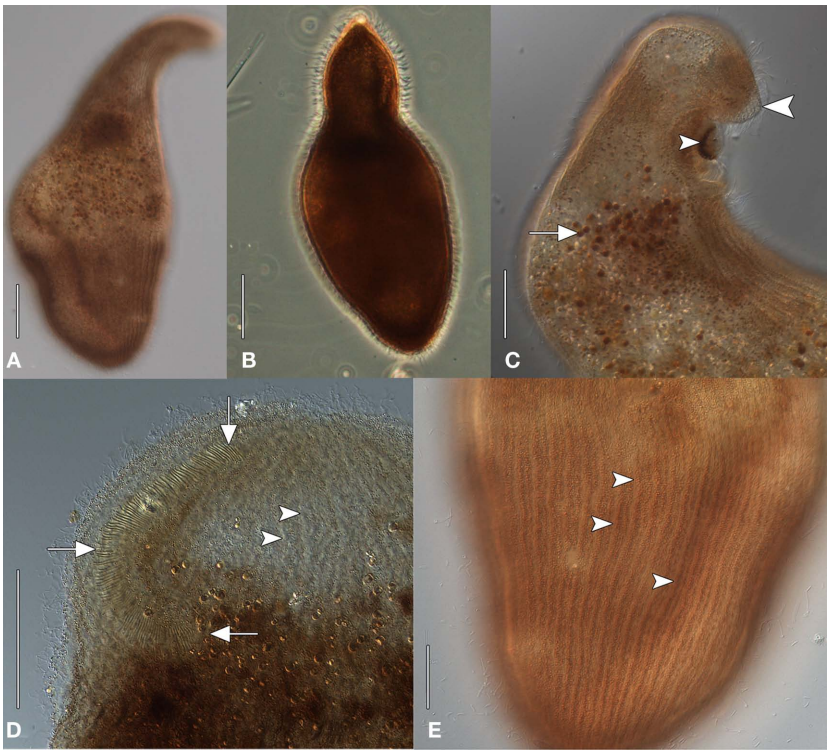

FIGURE 1 | Geleiid karyorelictean ciliate recovered from sulfidic sediments, *in vivo* [(A, C–D), differential interference contrast, DIC; (B) phase contrast]. **(A)** Cell shape, dorsal view. **(B)** Strongly contracted cell with more acutely tapered anterior end. **(C)** Anterior end, lateral view. A mass of pigmentocysts is located at the cytostome (small arrowhead). The blunt rostrum forms a lip that overhangs the anterior margin of buccal overture (large arrowhead). Pigmentocysts are scattered throughout the cytoplasm (arrow). **(D)** Detail of anterior end, ventral view. The right paroral polykinety (arrows) extends for a short distance onto the left side of the buccal overture. Arrowheads mark probable longitudinal interkinetidal myonemes. **(E)** Detail of cortex, ventral view. Densely packed cortical pigment granules are located within somatic kineties (arrowheads). Scale bars: **(A–D)** = 50 μm, **(E)** = 25 μm.

(**Figures 1C** and **2A,D,F**). The right paroral polykinety is ~12 μm wide, and consists of ~100 densely spaced files of basal bodies. The paroral polykinety occupies the entire right margin of the buccal overture, curving around it posteriorly onto the left margin for a short distance (**Figures 1D** and **2F**). Paroral polykinety cilia are longer, ~17–20 μm, and finer than somatic cilia (**Figure 2E**). A densely impregnating line of granules medial to the right oral polykinety probably represents a "paraoral intrabuccal kinety" described in *Parduczia* and other Geleiides (Dragesco, 1999, Figure 180 in that text). Better-quality silver impregnations are necessary for a complete characterization of the oral infraciliature and statistically meaningful morphometric data.

TRANSMISSION ELECTRON MICROSCOPY

Transmission electron microscopy analysis revealed a consistent dorso-centrally located region of double membrane-bound vesicles arranged in a kidney bean-shape (shape description based on FISH images only), each containing numerous prokaryotic cells (**Figure 3A**). Cells inside the membrane-bound structures exhibiting satisfactory preservation usually showed a consistent distribution within each vesicle (**Figures 3A–C**). A minimum of three morphotypes of endobionts were observed, which may or may not each represent unique species. One prominent electron-dense rod-shaped endobiont often lined the inner surface of the membrane-bound vesicle. This rod ranged in size from ~2 to 7 μm in length and ~1 to 2 μm in diameter (**Figures 3B,C**). Many of these showed internal membranes typical of Type I methanotrophs (Garrity et al., 2005; **Figures 3C,D**). A second morphotype was represented by smaller rod-shaped cells (~0.5–1.0 μm diameter and ~1–2 μm in length), many with apparent internal granules reminiscent of some sulfate-reducing bacteria within the Desulfobacteraceae and Desulfobulbaceae (Widdel and Bak, 1992; **Figures 3B,C**). The third morphotype is a curved rod approximately 1–3 μm in length, and ~0.2–0.5 μm in diameter (**Figure 3E**). Outside of each membrane-bound vesicle in the kidney bean-shaped cluster of vesicles in the host ciliate, there are pear-shaped double membrane-bound objects reminiscent of hydrogenosomes (**Figures 3B,C**). We observed these to be typically nestled between the vesicles and in contact with the membrane of at least one vesicle.

The nuclei were consistent in appearance with observations made by light microscopy (**Figure 3F**). It should also be noted that other membrane-bound vesicles containing what appears to be a single prokaryote morphotype were consistently located along the host cell periphery (**Figure 3G**). Epibiotic organisms were not observed with either light microscopy or TEM.

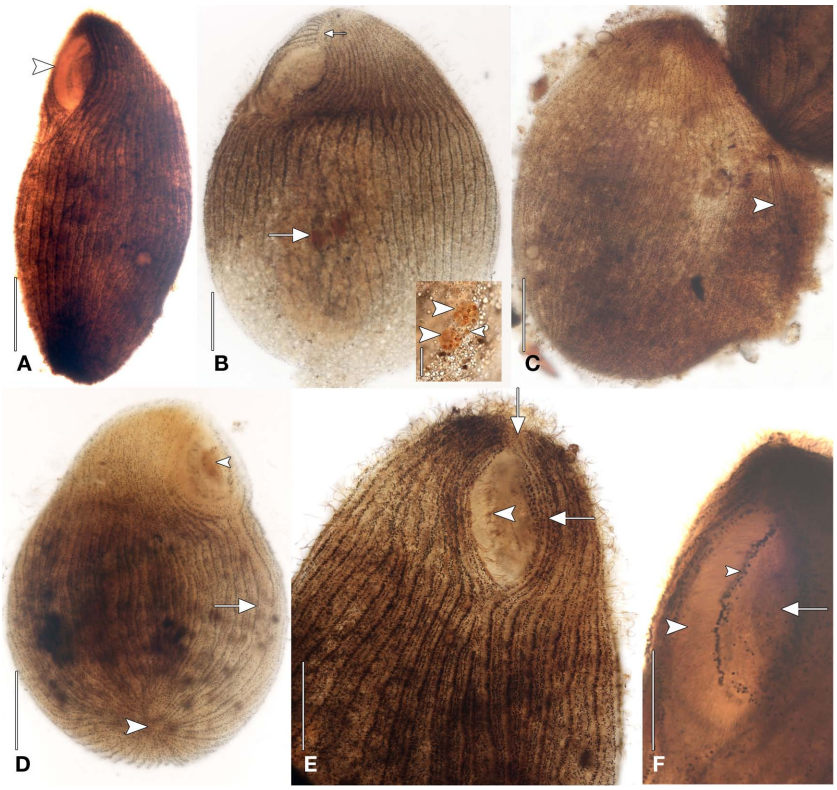

FIGURE 2 | Geleiid karyorelictean ciliate recovered from sulfidic sediments after protargol. (A) Left anterolateral view showing position of cytostome (arrowhead). **(B)** Left anterolateral view of infraciliature. Right and left somatic kineties originate at short preoral suture (small arrow). The nuclear apparatus consisting of two macronuclear nodules and a single nearby micronucleus is located centrally (large arrow). Inset, detail of nuclear apparatus. The macronuclear nodules (large arrowheads) contain densely impregnating nucleoli. The single micronucleus is located between the macronuclei (small arrowhead). **(C)** Dorsal view of infraciliature. The cytoplasm, containing an ingested diatom (arrowhead), has ruptured through the cortex. **(D)** Posteroventral view of infraciliature. Somatic kineties converge at the posterior pole (large arrowhead). Some somatic kineties are incomplete (arrow). A mass of impregnated pigmentocysts is seen at the cytostome (small arrowhead). **(E)** Anteroventral view. Long, fine cilia arise from the right paroral polykinety (arrowhead). Kinety *n* probably becomes the first adoral kinety and continues into the preoral suture (arrows). **(F)** Left anteroventral view. A line of granules marks the course of a paroral intrabuccal kinety. Scale bars: **(A–E)** = 50 μm, Inset **(B,F)**= 25 μm.

PCR, SEQUENCING, AND PHYLOGENETIC ANALYSES

The eukaryotic primer sets 82F/U1492R, 528F/U1492R, and 360F/U1492R all provided positive amplication. BLASTn analysis of the small subunit ribosomal RNA (SSU rRNA) gene indicated that this sequence was most closely related to *P. orbis* (sequences are 95% similar). A phylogenetic analysis including all major groups of ciliates confirmed the affiliation with *P. orbis* within the Karyorelictea with 100% bootstrap support under maximum likelihood and a Bayesian posterior probability of 1.0 (**Figure 4**). Tree topologies under Bayesian and maximum likelihood analyses were congruent.

Positive PCR amplification was obtained with bacterial primers, and we cloned and sequenced 12 clones. The results of phylogenetic analyses indicate the presence of two types of sulfate-reducing bacteria, one affiliating with the Desulfobacteraceae with 100% bootstrap support under maximum likelihood, and one affiliating with the Desulfobulbaceae with 97% bootstrap support under maximum likelihood (**Figure 5**). A positive PCR amplification was also obtained with the nested archaeal primer sets ARC4F/1492R and ARC21F/ARC915R. Phylogenetic analysis indicates this sequence is most closely related to members of the Methanobacteria with 100% bootstrap support under maximum likelihood (**Figure 6**). Successful amplification was also achieved using primers to one of the functional genes of sulfate reduction *dsrAB*. Seven of the 12 *dsrAB* clones we sequenced BLASTed as "uncultured sulfate-reducing bacterium dsr A/B" (EF065041). Two of the *dsrAB* clones were then sequenced with internal primers DSR1F1 and DSR1R1 (Bahr et al., 2005) resulting in nearly full-length sequences of 1964 bp. These two sequences were 99.6% identical. The sequence belonging to the closest cultured relative was a sequence from a Desulfobacteraceae. SSU rRNA gene (for the ciliate and the endobionts) and *dsrAB* sequences have been deposited in GenBank under the accession numbers JF327423-JF327426 and JF439663-JF439664.

CATALYZED REPORTER DEPOSITION–FLUORESCENT *IN SITU* HYBRIDIZATION

Fixation did not always permit the visualization of original vesicle orientation/content structure, as cells that were agar-overlaid after drying collapsed and the cell membrane was often compromised. Permeabilization of intact host ciliates was challenging, as treatment with lysozyme, proteinase K,

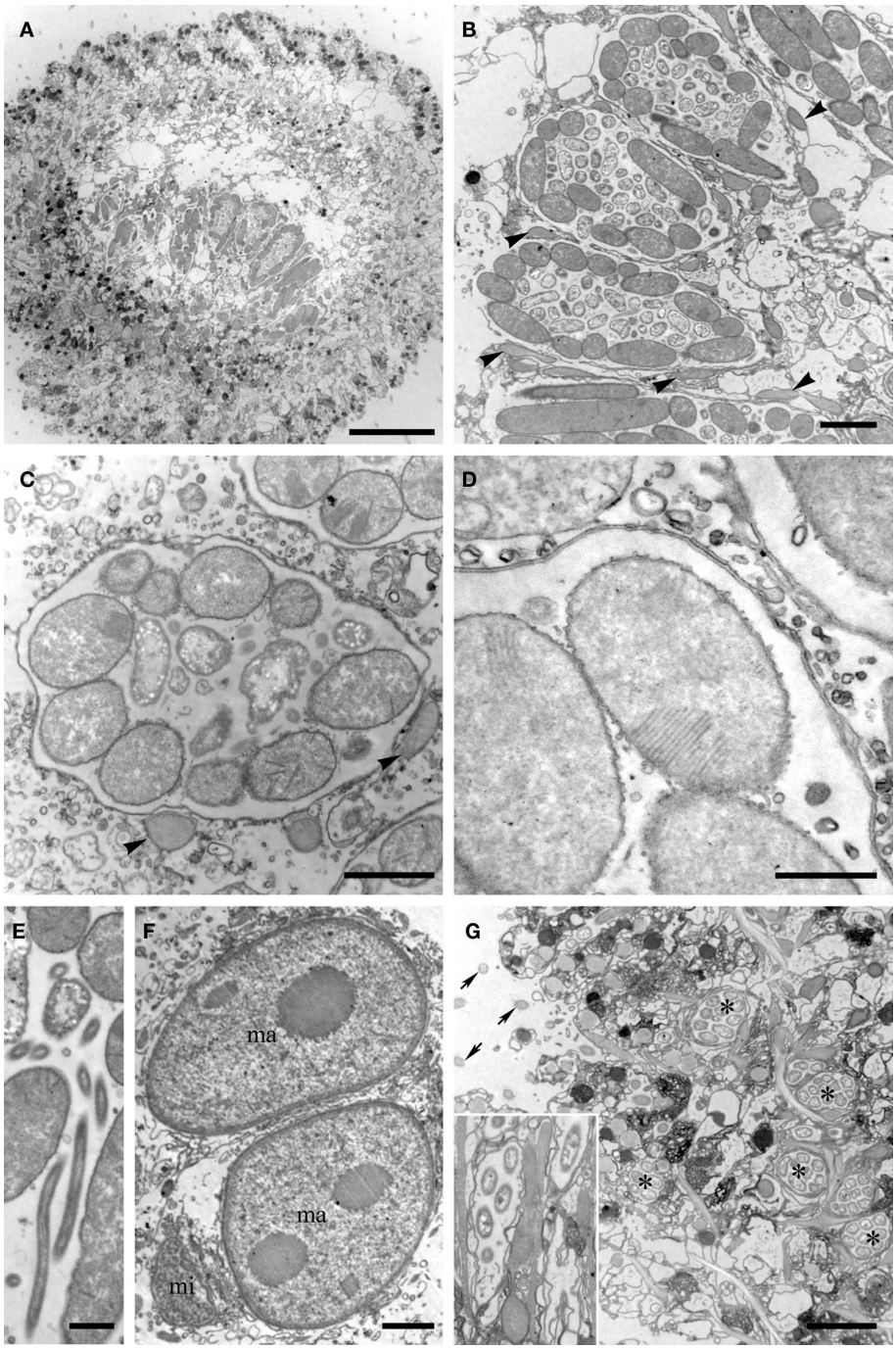

FIGURE 3 | Transmission electron micrographs of the Santa Barbara Geleiid karyorelictean ciliate. (A) View of cross-section through ciliate showing portion of the kidney-shaped membrane-bound vesicle region. **(B)** Cross-section view through three double membrane-bound vesicles. Note the structured orientations of the long rod-shaped endobionts vs. shorter forms. Arrowheads = putative hydrogenosomes. **(C)** Close up of endobionts in a vesicle, showing vesicle double membrane. Note stacked membranes in many of the endobionts. Arrowheads = putative hydrogenosomes. **(D)** Close up showing stacked membranes in endobiont and double membrane of vesicle. **(E)** Close up of suspected *Cytophaga*. **(F)** View of two macronuclei (ma) and micronucleus (mi). **(G)** Ciliate periphery showing additional vesicles (*) with single endobiont morphotype. Arrows = Cilia. Inset shows close up including rod-shaped endobiont. Scale bars: **(A)** = 10 μm; **(B,F,G)** = 2 μm; **(C–E)** = 0.5 μm.

or PeiW often caused lysis, but visualization of CARD–FISH probe hybridization to the endobionts was not successful without these treatments. Both positive (general eubacterial probe) and negative (no probe and NON probe) control filters were included to be sure that permeabilization was sufficient in any individual experiment to interpret a negative result correctly.

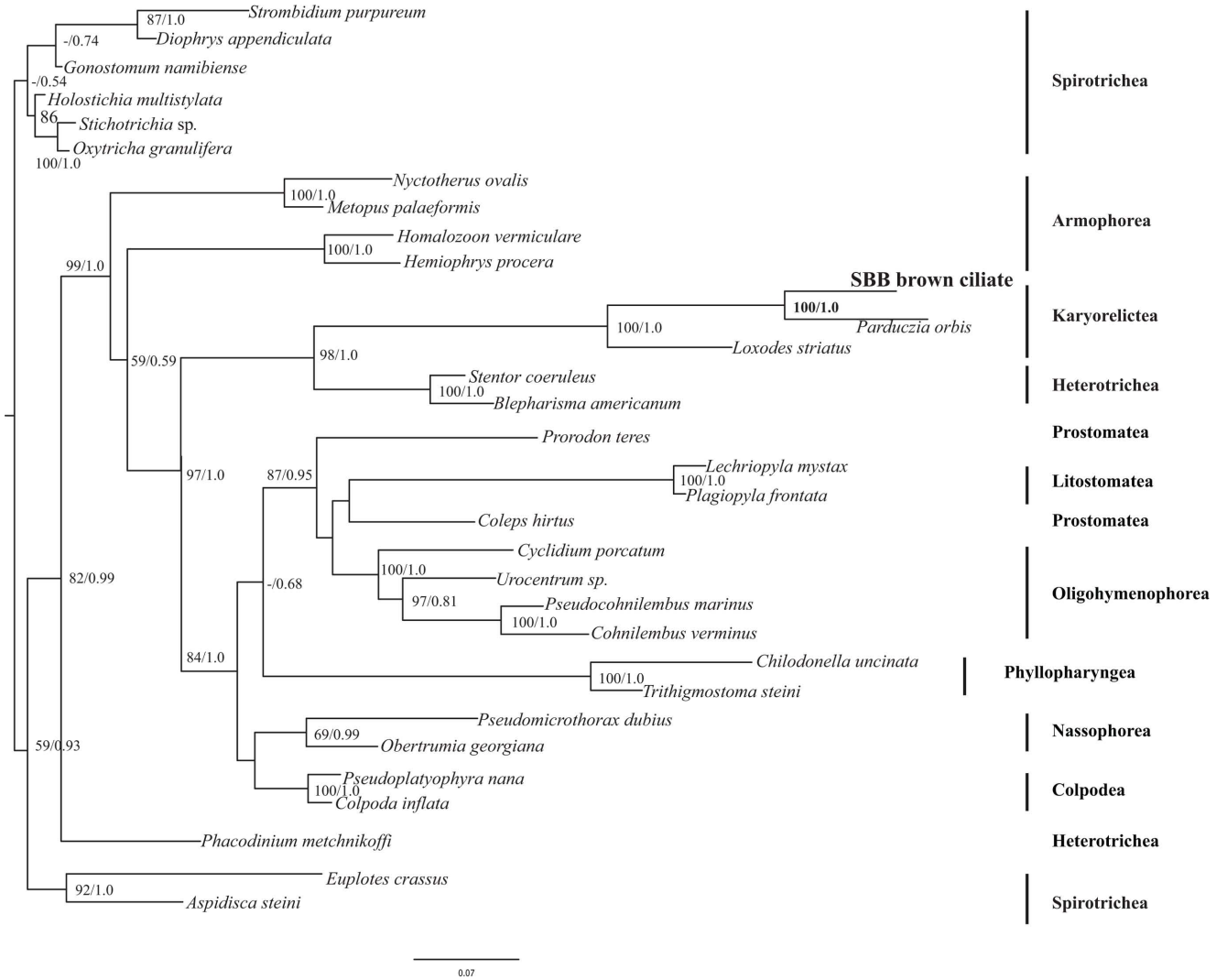

FIGURE 4 | Phylogenetic analysis of 18S rRNA gene from the Santa Barbara Basin Geleiid karyorelictean ciliate. Tree is based on an alignment of 961 nucleotides. Bootstrapping and determination of the best estimate of the ML tree topology for this data set was conducted with the Rapid Bootstrapping algorithm of RAxML version 7.0 under the GTR + Gamma model. Maximum likelihood and Bayesian analyses were run on the CIPRES portal (www.phylo.org). Numbers at nodes present maximum likelihood bootstrap support above 50% and Bayesian posterior probabilities above 0.5, respectively.

DAPI staining was included in all experiments, and this consistently revealed a ~30- to 50-μm diameter and ~200- to 250-μm long kidney bean-shaped area within the ciliate endoplasm where a dense region of endobiont cells was located (**Figure 7A** insert, **Figures 7E,G**). A representative image of the NON probe hybridization is shown in **Figure 7B**. The general eubacterial probe produces strong hybridization signal in this same region, showing clearly the ~10- to 12-μm long vesicles containing the endobionts (**Figures 7C,D**). Hybridization signal with the gammaproteobacterial probe was positive, with signal also coming from the central region of the double membrane-bound vesicles (**Figure 7F**). Hybridization with the general sulfate-reducing bacteria (SRB) probe also was detected in the region of the densely-packed vesicles (**Figure 7H**), and also could be seen in the periphery of the cell (data not shown). The probe specific to the Desulfobacteraceae produced strong signal from within the cluster of membrane-bound vesicles (**Figure 7I**) and laser scanning confocal microscopy shows these positive signals to be coming from cells no larger than ~1–1.5 μm (**Figure 7J**), consistent with the size and morphology of some of the cells located on the interior of the vesicle-bound consortium as described above. Signal from the second group-specific SRB probe to the Desulfobulbaceae was generally more sparsely distributed within the region of the densely-packed vesicles (**Figure 7K**). Positive signal emanated from the region of the vesicles with the general archaeal probe, showing ~5 μm long cells (**Figures 7L,M**). Coenzyme F420-based blue-green autofluorescence typical of many methanogens was also observed (**Figure 7N**). The host

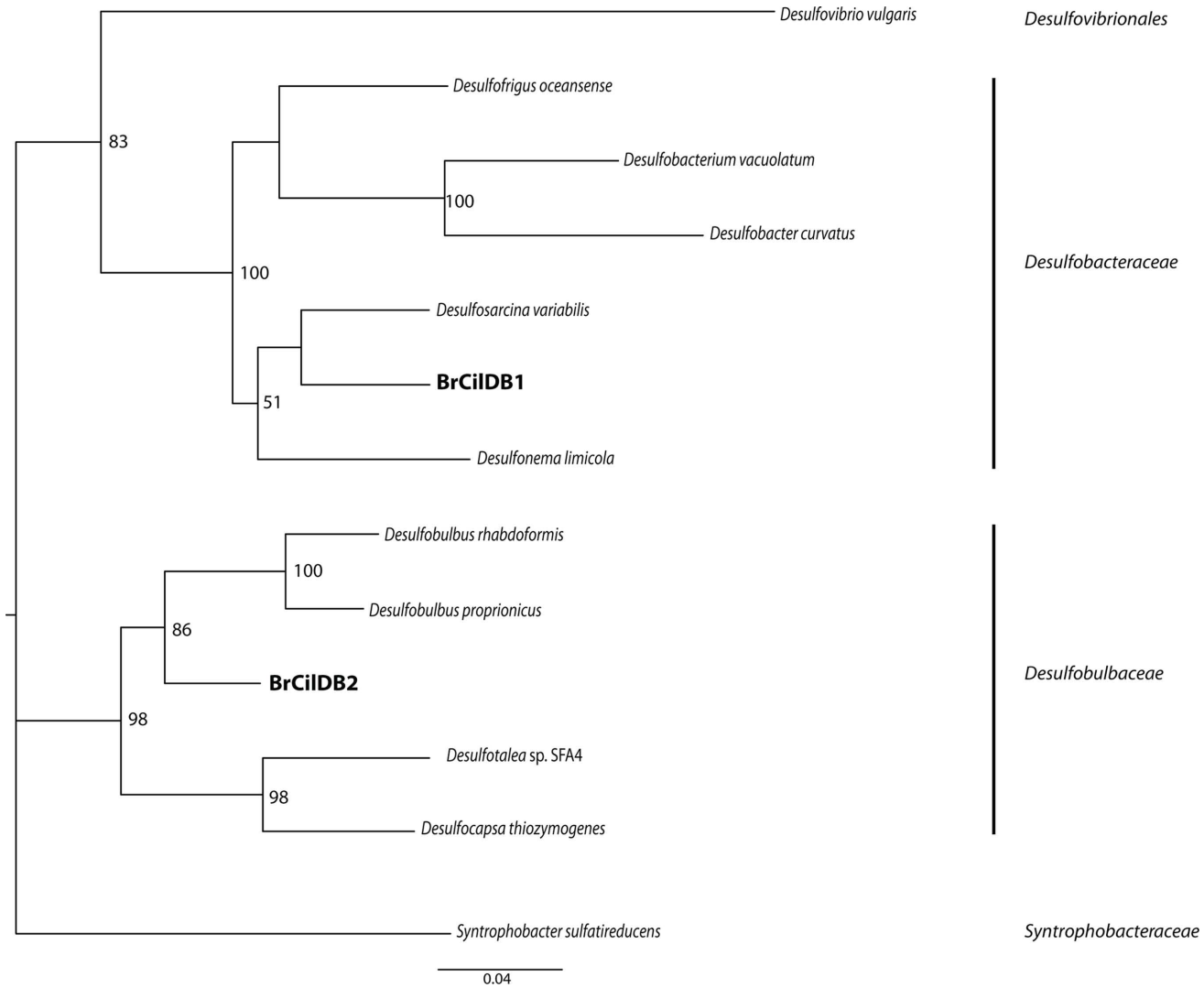

FIGURE 5 | Phylogenetic analysis of 16S rRNA gene sequences from bacterial endobionts of the Santa Barbara Basin Geleiid karyorelictean ciliate. Tree is based on an alignment of 982 nucleotides. Bootstrapping and determination of the best estimate of the ML tree topology for this data set was conducted with the Rapid Bootstrapping algorithm of RAxML version 7.0 under the GTR + Gamma model, run on the CIPRES portal (www.phylo.org). Numbers at nodes present maximum likelihood bootstrap support values above 50%.

nucleus was usually (but not always) visible with DAPI, depending on the cell's orientation and degree of flattening (**Figure 7G**). Hybridizations with the alpha-, beta-, and epsilon-proteobacterial probes were all negative (data not shown).

DISCUSSION

Abundance data indicate that this conspicuous ciliate species is prevalent in micro-oxic to anoxic and sulfidic Santa Barbara Basin sediments, yet is rare in adjacent well oxygenated sediments. During periodic oxygenation events in the basin, we presume that the ciliate migrates deeper into the sediments to avoid oxygen exposure. The vertical migration of benthic Santa Barbara Basin benthos in response to changing environmental conditions was documented by Bernhard et al. (2003).

Phylogenetic analysis of the SSU rRNA gene from this brown-pigmented ciliate confirms that it is a karyorelictid, as implied by light microscopy, and together with BLASTn analysis, that the most closely related organism in public databases is another karyorelictid, *P. orbis* (95% sequence similarity), a member of the Geleiidae. Morphological observations suggest a close relationship to *Parduczia* or *Avelia*. It has oral pigmentocysts like *Avelia* sp. (**Figures 2E,F**), however unlike *Avelia* sp., and more like *Parduczia* sp., this ciliate has a subapical position of the oral apparatus, and a beak or rostrum at the anterior end. Setting this ciliate apart from other members of Geleiidae are (1) the markedly smaller size (~10–20% that of other geleiids) and (2) the amphoriform/obpyriform, rather than a very slender, filiform shape (**Figure 8**). As noted, due to difficulties

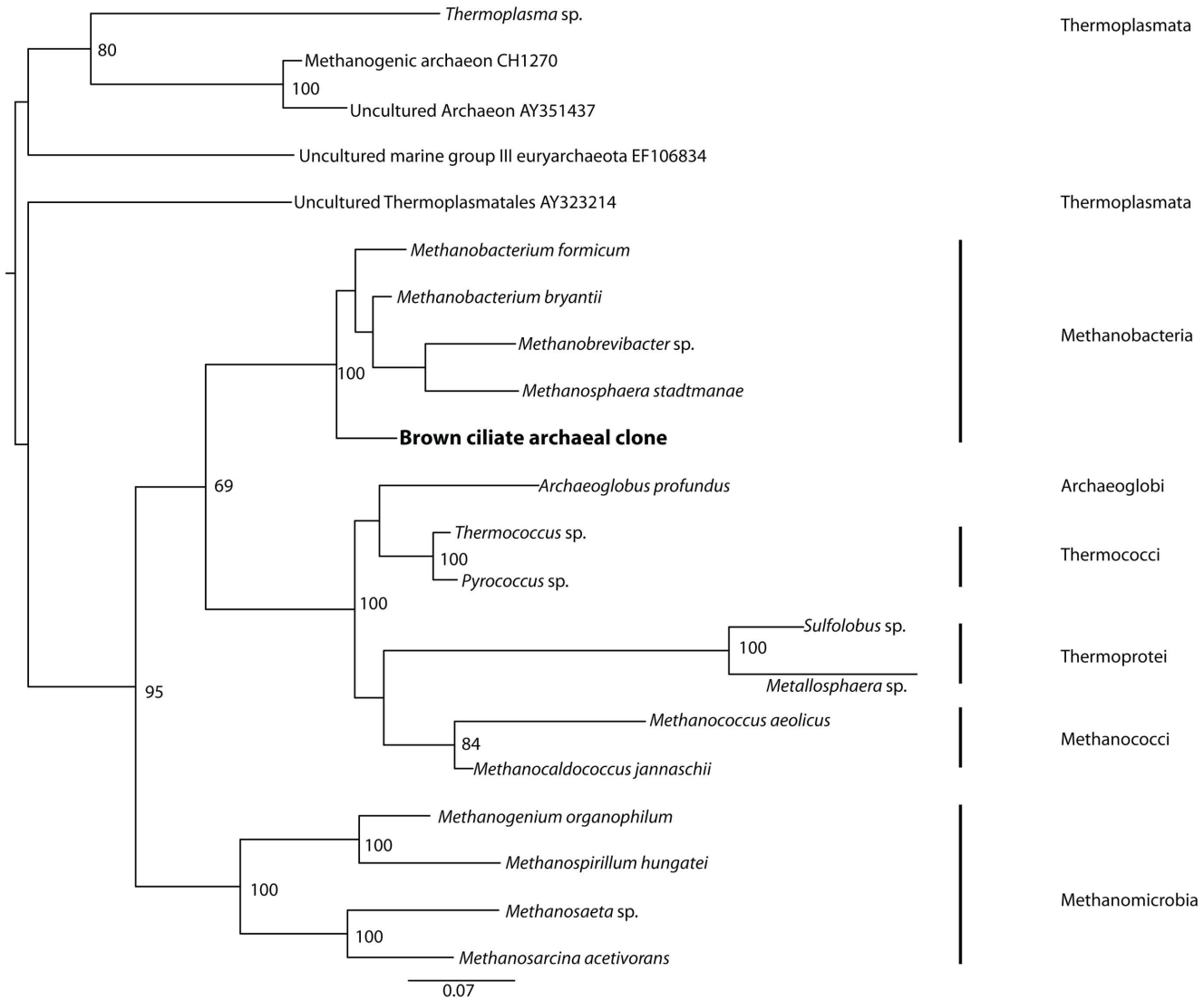

FIGURE 6 | Phylogenetic analysis of 16S rRNA gene sequences from archaeal endobionts of the Santa Barbara Basin Geleiid karyorelictean ciliate. Tree is based on an alignment of 844 nucleotides. Bootstrapping and determination of the best estimate of the ML tree topology for this data set was conducted with the Rapid Bootstrapping algorithm of RAxML version 7.0 under the GTR + Gamma model, run on the CIPRES portal (www.phylo.org). Numbers at nodes present maximum likelihood bootstrap support values above 50%.

encountered during fixation and silver impregnation, there are not yet sufficient taxonomic details to formally describe this as a new species (or genus).

Most protist taxa observed in the micro-oxic and sulfidic sediments of Santa Barbara Basin harbor bacterial epibionts and/or endobionts (e.g., Bernhard et al., 2000, 2006), so it is not a surprise that this brown-pigmented, *Parduczia*-like ciliate also harbors endobionts. Within this Geleiid karyorelictean ciliate the internal double membrane-bound vesicles containing endobionts were consistently observed in the same dorso-central region of cells in every specimen examined. These structures were persistent in ciliates maintained in sample bottles containing sediments and bottom water in our cold room for more than 6 months after collection. The consistent observation of a highly specific ultrastructural affinity between this karyorelictid and its bacterial and archaeal endobionts, as well as the phylogenetic identity of some of the endobionts, leads us to infer symbiotic relationships that are likely mutualistic.

Phylogenetic and CARD–FISH analyses indicate that the endobionts include at least one archaeon within the Methanobacteria, and two types of sulfate-respiring bacteria. This ensemble of endobionts is surrounded by a double membrane, which may suggest a secondary endosymbiosis series of events. CARD–FISH and cellular ultrastructure also suggest the possibility of a methane-oxidizing gammaproteobacterium in the consortium. Although demonstrating metabolic exchange between the host and endobionts

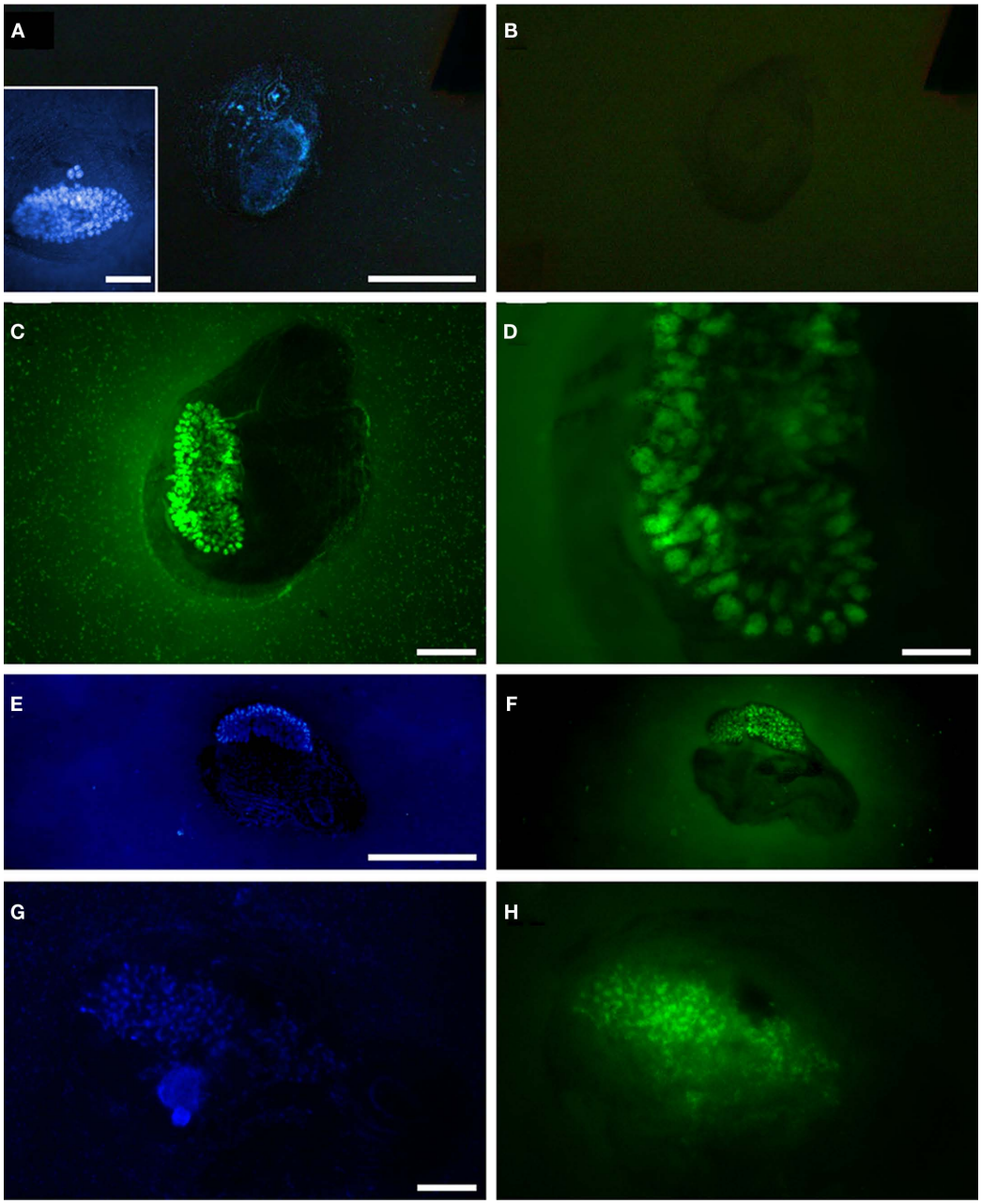

FIGURE 7 | Catalyzed reporter deposition–fluorescent *in situ* hybridization analyses of Santa Barbara Geleiid karyorelictean ciliate. (A,B) DAPI and Alexa488-NON338 (negative control) images, insert presents DAPI of cell showing host nuclei, **(C,D)** Alexa488-EUB338I-III (general eubacteria) probe, **(E,F)** DAPI and Alexa488-GAM42a (gammaproteobacteria) probe, **(G,H)** DAPI and Alexa488-DELTA495a, b, and c (general deltaproteobacteria) probe, (Continued)

was outside the scope of this project, there are four reasons to allow inferences about the putative roles and metabolic interactions of these varied microbes. These factors include (1) the array of morphotypes observed in our TEM analyses, (2) probable physiotypes deduced from positive FISH hybridization results, (3) the positive recovery of one of the key genes of sulfate reduction, and (4) phylogenetic analysis of bacterial and archaeal small subunit ribosomal RNA genes.

Examples of these potential physiological contributions include sulfate reduction, methane oxidation, methanogenesis, and hydrogen and acetate generation (**Figure 9**). Evidence for the presence of two types of sulfate reducers comes from the recovery of one SSU rRNA gene signature affiliated with the Desulfobulbaceae, and another affiliated with the Desulfobacteraceae, as well as positive CARD–FISH hybridization to cells within the membrane-bound vesicles using probes to these two different groups

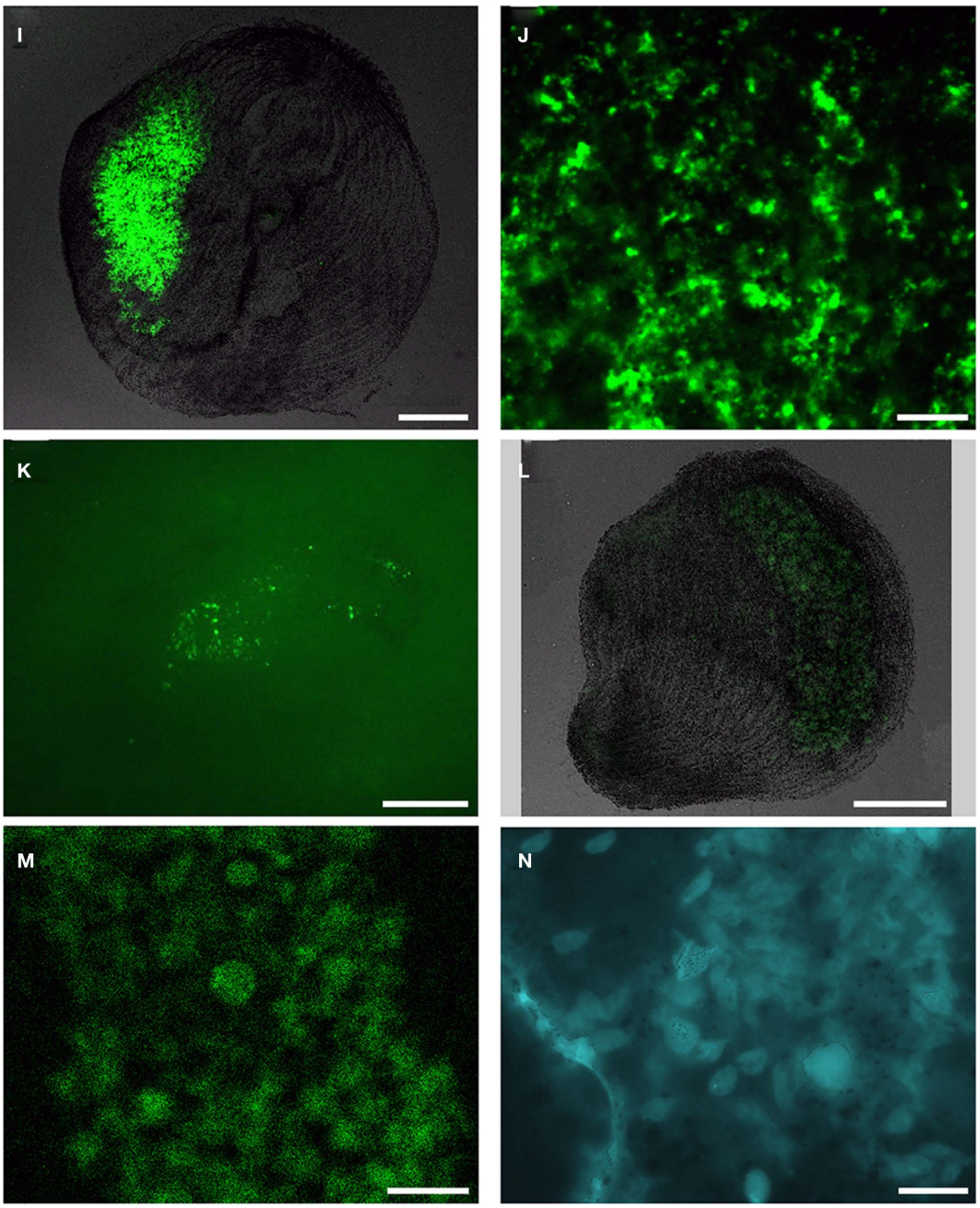

FIGURE 7 | (Continued) Catalyzed reporter deposition–fluorescent *in situ* hybridization analyses of Santa Barbara Geleiid karyorelictean ciliate. (I,J) Alexa488-DSBAC357 (Desulfobacteraceae) probe, **(K)** Alexa488-DSS658 (Desulfobulbaceae) probe, **(L,M)** Alexa488-ARCH915 (general archaea) probe, **(N)** autofluorescence in region of membrane-bound vesicles. Scale bars: **(A–C,E–I,L)**, inset **(A)** = 50 μm, **(D,K,N)** = 20 μm; **(J,M)** = 10 μm.

of sulfate-reducing bacteria. As noted, we also recovered sequences affiliating most closely with the *dsrAB* gene from an uncultured sulfate-reducing bacterium. This gene is one of the key genes involved in sulfate reduction (Wagner et al., 1998; Klein et al., 2001). Evidence for the presence of a methanogen comes from the recovery of an archaeal SSU rRNA gene sequence affiliating with the Methanobacteria, positive CARD–FISH hybridization with a general archaeal probe, and from the presence of autofluorescence typical of most methanogens within the kidney bean-shaped area inside the host ciliate. Evidence for the presence of a gammaproteobacterial methanotroph is not as strong. We surmised the presence of this organism within the internal vesicle-associated consortia on the basis of positive CARD–FISH hybridization within the described region of membrane-bound vesicles using a probe specific to gammaproteobacteria, and cell ultrastructure reminiscent of Type I methanotrophs based on internal membrane structure.

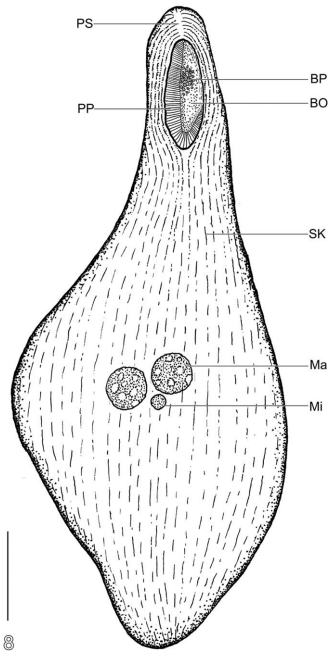

FIGURE 8 | Semi-schematic body plan of Santa Barabara Geleiid karyorelictean ciliate. BO, buccal overture; BP, buccal pigmentocysts; Ma, macronuclear nodule; Mi, micronucleus; PP, right paroral polykinety; PS, preoral suture; SK, somatic kinety. Scale bar = 50 μm.

We did not recover a SSU rRNA gene sequence of a gammaproteobacteria, but we attribute this to the relatively low sequencing effort in this study (only 12 clones). Confirming the presence of a methanotroph with deeper sequencing, as well as demonstrating the metabolic activities associated with sulfate reduction and methanogenesis via other avenues of investigation are areas of future research in our laboratories.

Elucidating the benefits of putative symbioses such as these for both the host and endobionts is not always straightforward. Although food vacuoles were only occasionally observed with light microscopy, this ciliate likely grazes on bacteria present in the sediments, and the fermentation of this food may produce a range of low molecular weight metabolites (including lactate and pyruvate and nitrogen compounds). Any lactate available from ciliate fermentation processes could be used for the growth of the sulfate-reducing bacteria (**Figure 9**). Although not directly demonstrated, the small double membrane-bound objects nestled along the outside of each vesicle are likely to be hydrogenosomes, as previously surmised. This is a logical explanation considering that many anaerobic ciliates described to date contain hydrogenosomes (Embley et al., 1995; Fenchel and Finlay, 1995). Hydrogenosomes could utilize available pyruvate resulting from the host fermentation processes as a carbon source, and would release molecular hydrogen and acetate (**Figure 9**). Both products, plus any available pyruvate, could be utilized as an electron donor and carbon source for growth and sulfate reduction by the sulfate-reducing bacteria. Methanogens, which

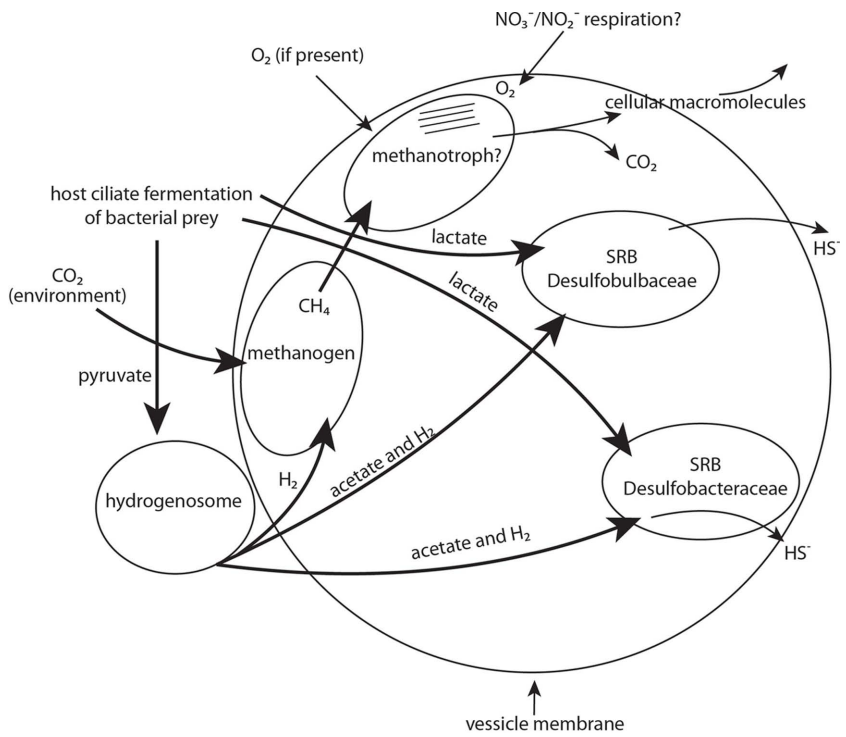

FIGURE 9 | Schematic representation of proposed diverse endobiont and host cell metabolisms and their potential interactions. Major physiotypes include sulfate respiration, methanogenesis, methanotrophy, and hydrogenosome activity. Other activities might include nitrate and nitrite respiration. Bold arrows indicate carbon source/electron donor.

are common endobionts of anaerobic ciliates (e.g., Finlay and Fenchel, 1989, and see recent synopsis by Hackstein, 2011) likely utilize some of the hydrogen produced by the hydrogenosomes along with CO_2 diffused either from the ciliate's metabolism or from the environment to produce methane (**Figure 9**). This methane could possibly be oxidized anaerobically via the coupling of this oxidation with the reduction of sulfate by sulfate-reducing bacteria (e.g., Hinrichs et al., 1999; Boetius et al., 2000; Orphan et al., 2001) but this coupling is usually between a sulfate-reducing bacterium and an archaeon.

Alternatively, we consider the possibility that enough oxygen may be present for aerobic methane oxidation by the bacterial methanotroph. Oxygen could be delivered via diffusion into the ciliate at periodic intervals when the ciliate migrates to micro-oxic zones, or via a mechanism similar to the recently described process of nitrite-driven anaerobic methane oxidation (Ettwig et al., 2010). Ettwig et al. (2010) report an anaerobic denitrifying bacterium that bypasses the denitrification intermediate nitrous oxide by the conversion of two nitric oxide molecules to dinitrogen and oxygen, which is used to oxidize methane by an unknown mechanism. Since this ciliate inhabits anoxic to micro-oxic sediments, it is likely that any methane oxidizer present must be able to conduct this process anaerobically. However, if the host ciliate were to migrate to sediments where limited oxygen is present, this gammaproteobacterium might switch to aerobic oxidation of methane since this is energetically more favorable (Caldwell et al., 2008). A methanotroph would likely evolve CO_2 and cellular materials (e.g., polysaccharides, lipids, and proteins). It should be noted that even aerobic metabolism of *Escherichia coli* can function at unusually low oxygen concentrations (Stolper et al., 2010). An avenue for future investigation will be to obtain a small subunit ribosomal RNA signature from a gammaproteobacterium and to perhaps trace the movement of isotopically labeled compounds through this consortium. Although we obtained a SSU rRNA sequence from the *Cytophaga/Flexibacter* group, and a thin (~0.2 μm by 1–3 μm) curved endobiont was observed with TEM within the membrane-bound vesicles, we did not perform FISH analyses to confirm that the observed curved cell morphology is a member of that group. Members of this group are often decomposers of polysaccharides (Dworkin et al., 1999).

CONCLUSION

In sum, the endobionts of this ciliate likely benefit by obtaining a constant supply of nutrients via the host digestive processes. They also live in a protected environment, and are delivered by the ciliate to the appropriate redox gradient in the sediments for their cellular metabolisms. The benefits to the host are less clear, although the endobionts through their respective metabolisms likely provide the host with a wide range of conveniently internalized nutrients. The TEM images of the membrane-bound vesicles containing endobionts are consistent with speculations about their function: the highly organized arrangement of different endobiont morphologies within the vesicles was found consistently in this region of the cell, and was not reminiscent of food vacuoles. The prokaryote cells inside these vesicles appear morphologically intact, unlike those typical of food vacuoles. We cannot rule out the possibility however that under certain circumstances, the ciliate host may turn to these functional consortia of endobionts as a food source. This ciliate is host to a complex consortium of prokaryotic endobionts that may function to elegantly and intricately meld the sulfur cycle with cycling of carbon and nitrogen. We look forward to learning more about the metabolic interactions between these endobionts and to elucidating additional protist – prokaryote symbioses from such habitats. These avenues of investigation will expand our knowledge of the diversity of life on our planet and of the potential impacts of these microbial populations on major biogeochemical cycles.

ACKNOWLEDGMENTS

We thank the captain and crew of the RV *Robert Gordon Sproul* and Richard Sperduto who helped with sampling, Louis Kerr for TEM sectioning, Dagmar Woebkin for helpful discussions about CARD–FISH methods, Barbara MacGregor for help with deltaproteobacterial probes, Hilary Morrison and Rich Fox at MBL for the use of their pipeline script, David Patterson for assistance with initial ciliate identification and photo-documentation, and Margot Wilstermann and Marius Karolinski for performing counts of ciliates in our quantitative samples. We also thank Colleen Cavanaugh, Tom Fenchel, and Andreas Teske for helpful discussions about the endobionts. This research was supported by grants from NSF (MCB-0604084 to Virginia P. Edgcomb and Joan M. Bernhard and MCB-0702491 to Joan M. Bernhard, Virginia P. Edgcomb, and K. L. Casciotti).

REFERENCES

Amman, R., Springer, N., Ludwig, W., Görtz, H.-D., and Schleifer, K.-H. (1991). Identification in situ and phylogeny of uncultured bacterial endosymbionts. *Nature* 351, 161–164.

Amman, R. I., Ludwig, W., and Schleifer, K.-H. (1995). Phylogenetic identification and in situ detection of individual microbial cells without cultivation. *Microbiol. Rev.* 59, 143–169.

Bagarinao, T. (1992). Sulfide as an environmental factor and toxicant – tolerance and adaptations in aquatic organisms. *Aquat. Toxicol.* 24, 21–62.

Bahr, M., Crump, B. C., Klepac-Ceraj, V., Teske, A., Sogin, M. L., and Hobbie, J. E. (2005). Molecular characterization of sulfate-reducing bacteria in a New England salt marsh. *Environ. Microbiol.* 7, 1175–1185.

Barbera, M. J., Ruiz-Trillo, I., Tufts, J. Y. A., Bery, A., Silberman, J. D., and Roger, A. J. (2010). *Sawyeria marylandensis* (Heterolobosea) has a hydrogenosome with novel metabolic properties. *Eukaryot. Cell* 9, 1913–1924.

Barry, J. P., Greene, H. G., Orange, D. L., Baxter, C. H., Robinson, B. H., Kochevar, R. E., Nybakken, J. W., Reed, D. L., and McHugh, C. M. (1996). Biologic and geologic characteristics of cold seeps in Monterey Bay, California. *Deep Sea Res.* 43, 1739–1762.

Beier, C. L., Horn, M., Michel, R., Schweikert, M., Görtz, H.-D., and Wagner, M. (2002). The genus *Caedibacter* comprises endosymbionts of *Paramecium* spp. related to the Rickettsiales (Alphaproteobacteria) and to *Francisella tularensis* (Gammaproteobacteria). *Appl. Environ. Microbiol.* 68, 6043–6050.

Bernhard, J. M., Buck, K. R., Farmer, M. A., and Bowser, S. S. (2000). The Santa Barbara Basin is a symbiosis oasis. *Nature* 403, 77–80.

Bernhard, J. M., Habura, A., and Bowser, S. S. (2006). An endobiont-bearing allogromiid from the Santa Barbara Basin: implications for the early diversitfication of foraminifera. *J. Geophys. Res.* 111, G03002.

Bernhard, J. M., and Sen Gupta, B. K. (1999). "Foraminifera of oxygen-depleted environments," in *Modern Foraminifera*, ed. B. K. Sen Gupta (Dordrecht: Kluwer Academic Publishers), 201–216.

Bernhard, J. M., Visscher, P. T., and Bowser, S. S. (2003). Submillimeter life positions of bacteria, protists, and metazoans in laminated sediments of the Santa Barbara Basin. *Limnol. Oceanogr.* 45, 813–828.

Boetius, A., Ravenschlag, K., Shubert, C. J., Rickert, D., Widdel, F., Gieseke, A., Amann, R., Jørgensen, B.B., Witte, U., and Pfannkuche, O. (2000). Microscopic identification of a microbial consortium apparently mediating anaerobic methane oxidation above marine gas hydrates. *Nature* 407, 623–626.

Browenkow, W. W., and Cline, J. D. (1969). Colorimetric determination

of dissolved oxygen at low concentrations. *Limnol. Oceanogr.* 14, 450–454.

Caldwell, S. L., Laidler, J. R., Brewer, E. A., Eberly, J. O., Sandborgh, S. C., and Colwell, F. S. (2008). Anaerobic oxidation of methane: mechanisms, bioenergetics, and the ecology of associated microorganisms. *Environ. Sci. Technol.* 42, 6791–6799.

Cavanaugh, C. M. (1994). Microbial symbiosis: patterns of diversity in the marine environment. *Am. Zool.* 34, 79–89.

Cavanaugh, C. M., Gardiner, S. L., Jones, M. L., Jannasch, H. W., and Waterbury, J. B. (1981). Prokaryotic cells in the hydrothermal vent tube worm *Riftia pachyptila* Jones: possible chemoautotrophic symbionts. *Science* 213, 340–341.

Cole, J. R., Chai, B., Marsh, T. L., Farris, R. J., Wang, Q., Kulam, S. A., Chandra, S., McGarrell, D. M., Schmidt, T. M., Garrity, G. M., and Tiedje, J. M. (2003). The Ribosomal Database Project (RDP-II): previewing a new autoaligner that allows regular updates and the new prokaryotic taxonomy. *Nucleic Acids Res.* 31, 442–443.

Corliss, J. O. (1979). *The Ciliated Protozoa*, 2nd Edn. Oxford: Pergamon Press.

Daims, H., Ramsing, N. B., Schleifer, K.-H., and Wagner, M. (2001). Cultivation-independent, semiautomatic determination of absolute bacterial cell numbers in environmental samples by fluorescence in situ hybridization. *Appl. Environ. Microbiol.* 67, 5810–5818.

Dawson, S. C., and Pace, N. R. (2002). Novel kingdom-level eukaryotic diversity in anoxic environments. *Proc. Natl. Acad. Sci. U.S.A.* 99, 8324–8329.

DeLong, E. F. (1992). Archaea in coastal marine environments. *Proc. Natl. Acad. Sci. U.S.A.* 89, 5685–5689.

Distel, D. L., and Felbeck, H. (1988). Pathways of inorganic carbon fixation in the endosymbiont-bearing lucinid clam *Lucinoma aequizonata*. I. Purification and characterization of endosymbiotic bacteria. *J. Exp. Zool.* 247, 1–10.

Dragesco, J. (1999). Revision des Geléiides (Ciliophora, Karyorelictea). *Stapfia* 66, 1–91.

Dworkin, M., Falkow, S., Rosenberg, E., Schleifer, K.-H., and Stackebrandt, E. (eds). (1999). *The Prokaryotes: A Handbook on the Biology of Bacteria*, 3rd Edn. Singapore: Springer.

Edgcomb, V., Breglia, S. A., Yubuki, N., Beaudoin, D., Patterson, D. J., Leander, B. S., and Bernhard, J. M. (2010). Identity of epibiotic bacteria on symbiontid euglenozoans in O2-depleted marine sediments: evidence for symbiont and host co-evolution. *ISME J.* 5, 1–13.

Elwood, H. J., Olsen, G. J., and Sogin, M. L. (1985). The small-subunit ribosomal RNA gene sequences from the hypotrichous ciliates *Oxytricha nova* and *Stylonychia pustulata*. *Mol. Biol. Evol.* 2, 399–410.

Embley, T. M., and Finlay, B. J. (1993). Systematic and morphological diversity of endosymbiotic methanogens in anaerobic ciliates. *Antonie Van Leeuwenhoek* 64, 261–271.

Embley, T. M., and Finlay, B. J. (1994). The use of small subunit rRNA sequences to unravel the relationships between anaerobic ciliates and their methanogen endosymbionts. *Microbiology* 140, 225–235.

Embley, T. M., Finlay, B. J., Dyal, P., Hirt, R. P., Wilkinson, M., and Williams, A. G. (1995). Multiple origins of anaerobic ciliates with hydrogenosomes within the radiation of aerobic ciliates. *Proc. R. Soc. Lond. B Biol. Sci.* 262, 87–93.

Embley, T. M., Finlay, B. J., Thomas, R. H., and Dyal, P. L. (1992). The use of rRNA sequences and fluorescent probes to investigate the phylogenetic positions of the anaerobic ciliate *Metopus palaeformis* and its archaeobacterial endosymbiont. *J. Gen. Microiol.* 138, 1479–1487.

Esteban, G., Guhl, B., Clarke, K., Embley, T., and Finlay, B. (1993). *Cyclidium porcatum* n. sp.: a free-living anaerobic scuticociliate containing a stable complex of hydrogenosomes, eubacteria and archaeobacteria. *Eur. J. Protistol.* 29, 262–270.

Ettwig, K. F., Butler, M. K., Le Paslier, D., Pelletier, E., Mangenot, S., Kuypers, M. M., Schreiber, F., Dutih, B. E., Zedelius, J., de Beer, D., Gloerich, J., Wessels, H. J., van Alen, T., Luesken, F., Wu, M. L., van de Pas-Schoonen, K. T., Op den Camp, H. J., Janssen-Megens, E. M., Francoijs, K. J., Stunnenberg, H., Weissenbach, J., Jetten, M. S., and Strous, M. (2010). Nitrite-driven anaerobic methane oxidation by oxygenic bacteria. *Nature* 464, 543–548.

Ewing, B., and Green, P. (1998). Base-calling of automated sequencer traces using phred. II. Error probabilities. *Genome Res.* 8, 186–194.

Ewing, B., Hillier, L., Wendl, M. C., and Green, P. (1998). Base-calling of automated sequencer traces using phred. I. Accuracy assessment. *Genome Res.* 8, 175–185.

Fenchel, T., and Bernard, C. (1993). Endosymbiotic purple non-sulphur bacteria in an anaerobic ciliated protozoon. *FEMS Microbiol. Lett.* 110, 21–25.

Fenchel, T., and Finlay, B. J. (1990). Anaerobic free-living protozoa: growth efficiencies and the structure of anaerobic communities. *FEMS Microbiol. Ecol.* 74, 269–276.

Fenchel, T., and Finlay, B. J. (1991a). The biology of free-living anaerobic ciliates. *Eur. J. Protistol.* 26, 201–215.

Fenchel, T., and Finlay, B. J. (1991b). Endosymbiotic methanogenic bacteria in anaerobic ciliates: significance for the growth efficiency of the host. *J. Protozool.* 38, 18–22.

Fenchel, T., and Finlay, B. J. (1995). *Ecology and Evolution in Anoxic Worlds*. Oxford: Oxford University Press.

Fenchel, T., Perry, T., and Thane, A. (1977). Anaerobiosis and symbiosis with bacteria in free-living ciliates. *J. Protozool.* 24, 154–163.

Finlay, B. J., and Fenchel, T. (1989). Hydrogenosomes in some anaerobic protozoa resemble mitochondria. *FEMS Microbiol. Ecol.* 65, 311–314.

Finlay, B. J., and Fenchel, T. (1992). Methanogens and other bacteria as symbionts of free-living anaerobic ciliates. *Symbiosis* 14, 375–390.

Foissner, W., and Al-Rasheid, K. A. S. (1999). Updating the Tracheleocercids (Ciliophora, Karyorelictea). VI. A detailed description of *Sultanophrys arabica* nov. gen., nov. spec. (Sultanophryidae nov. fam.). *Eur. J. Protistol.* 35, 146–160.

Foissner, W., and Dragesco, J. (1996). Updating the Trachelocercids (Ciliophora, Karyorelictea). I. A detailed description of the infraciliature of *Trachelolophos giga* N.G., N. sp. and *T. filum* (Dragesco and Dragesco-Kernelis, 1986) N. Comb. *J. Eukaryot. Microbiol.* 43, 12–25.

Foissner, W., and Xu, K. (2007). Monograph of the Spathidiida (Ciliophora, Haptoria). Vol. I: Protospathidiidae, Arcuospathidiidae, Apertospathulidae. *Monogr. Biol.* 81, 1–485.

Frias-Lopez, J., Thompson, A., Waldbauer, J., and Chisholm, S. W. (2009). Use of stable isotope-labelled cells to identify active grazers of picocyanobacteria in ocean surface waters. *Environ. Microbiol.* 11, 512–525.

Garrity, G. M., Brenner, D. J., Krieg, N. R., and Staley, J. R. (eds). (2005). *Bergey's Manual of Systematic Bacteriology, Vol. 2: The Proteobacteria*. Baltimore, MD: Williams and Wilkins.

Görtz, H.-D. (2002). "Symbiotic associations between ciliates and prokaryotes," in *The Prokaryotes: an Evolving Electronic Resource for the Microbiological Community*, 3rd Edn. Available at http://141.150.157.117:8080/prokPUB/chaprender/jsp/showchap.jsp?chapnum=355

Hackstein, J. H. P. (2011). Anaerobic ciliates and their methanogenic endosymbionts. *Microbiol. Monogr.* 19, 12–23.

Hinrichs, K. U., Hayes, J. M., Sylva, S. P., Brewster, P. G., and DeLong, E. F. (1999). Methane-consuming archaebacteria in marine sediments. *Nature* 398, 802–805.

Hirt, R. P., Dyal, P. L., Wilkinson, M., Finlay, B. J., Roberts, D. M., and Embley, T. M. (1995). Phylogenetic relationships among Karyorelictids and Heterotrichs inferred from small subunit rRNA sequences: resolution at the base of the ciliate tree. *Mol. Phylogenet. Evol.* 4, 77–87.

Jolivet, E., L'Haridon, S., Corre, E., Forterre, P., and Prieur, D. (2003). *Thermococcus gammatolerans* sp. nov., a hyperthermophilic archaeon from a deep-sea hydrothermal vent that resists ionizing radiation. *Int. J. Syst. Evol. Microbiol.* 53, 847–851.

Jones, W. J., Nagle, D. P., and Whitman, W. B. (1987). Methanogens and the diversity of archaebacteria. *Microbiol. Rev.* 51, 135–177.

Jumars, P. A., Penry, D. L., Baross, J. A., Perry, M. J., and Frost, B. W. (1989). Closing the the microbial loop: dissolved carbon pathway to heterotrophic bacteria from incomplete ingestion, digestion and absorption in animals. *Deep Sea Res.* 36, 483–495.

Klein, M., Friedrich, M., Roger, A. J., Fishbain, S., Hugenholtz, P., Abicht, A., Blackall, L. L., Stahl, D. A., and Wagner, M. (2001). Multiple lateral transfer events of dissimilatory sulfite-reductase genes between major lineages of bacteria. *J. Bacteriol.* 183, 6028–6034.

Kuwabara, J. S., van Geen, A., McCorkle, D. C., and Bernhard, J. M. (1999). Dissolved sulfide distributions in the water column and sediment pore waters of the Santa Barbara basin. *Geochim. Cosmochim. Acta* 63, 2199–2209.

Lane, D. J. (1991). "16S/23S rRNA sequencing," in *Nucleic Acid Techniques in Bacterial Systematics*, eds E. Stackebrandt and M. Goodfellow (New York: Wiley), 115–148.

Lin, X., Wakeham, S. G., Putnam, I. F., Astor, Y. M., Scranton, M. I., Chistoserdov, A. Y., and Taylor, G. T. (2006). Comparison of vertical distributions of prokaryotic assemblages in the anoxic Cariaco Basin and Black Sea by use of fluorescence in situ hybridization. *Appl. Environ. Microbiol.* 72, 2679–2690.

Longnecker, K., and Reysenbach, A. L. (2001). Expansion of the geographic distribution of a novel lineage of epsilon-Proteobacteria to a hydrothermal vent site on the Southern East Pacific Rise. *FEMS Microbiol. Ecol.* 35, 287–293.

Loy, A., Kusel, K., Lehner, A., Drake, H. L., and Wagner, M. (2004). Microarray and functional gene analysis of sulfate-reducing prokaryotes in low sulfate, acidic fens reveal co-occurrence of

recognized genera and novel lineages. *Appl. Environ. Microbiol.* 70, 6998–7009.

Loy, A., Lehner, A., Lee, N., Adamczyk, J., Meier, H., Ernst, J., Schleifer, K. H., and Wagner, M. (2002). Oligonucleotide microarray for 16S rRNA gene-based detection of all recognized lineages of sulfate-reducing prokaryotes in the environment. *Appl. Environ. Microbiol.* 68, 5064–5081.

Lucker, S., Steger, D., Kjeldsen, K. U., MacGregor, B. J., Wagner, M., and Loy, A. (2007). Improved 16S rRNA-targeted probe set for analysis of sulfate-reducing bacteria by fluorescence in situ hybridization. *J. Microbiol. Methods* 69, 523–528.

Ludwig, W., Strunk, O., Westram, R., Richter, L., Meier, H., Yadhukumar, Buchner, A., Lai, T., Steppi, S., Jobb, G., Förster, W., Brettske, I., Gerber, S., Ginhart, A. W., Gross, O., Grumann, S., Hermann, S., Jost, R., König, A., Liss, T., Lüssmann, R., May, M., Nonhoff, B., Reichel, B., Strehlow, R., Stamatakis, A., Stuckmann, N., Vilbig, A., Lenke, M., Ludwig, T., Bode, A., and Schleifer, K. H. (2004). ARB: a software environment for sequence data. *Nucleic Acids Res.* 32, 1363–1371.

Lynn, D. H. (2008). *The Ciliated Protozoa: Characterization, Classification and Guide to the Literature.* Dordrecht: Springer.

Madsen, E. L., Sinclair, J. L., and Ghiorse, W. C. (1991). In situ biodegradation: microbiological patterns in a contaminated aquifer. *Science* 252, 830–833.

Manz, W., Amann, R., Ludwig, W., Wagner, M., and Schleifer, K.-H. (1992). Phylogenetic oligodeoxynucleotide probes for the major subclasses of proteobacteria – problems and solutions. *Syst. Appl. Microbiol.* 15, 539–600.

Manz, W., Eisenbrecher, M., Neu, T. R., and Szewzyk, U. (1998). Abundance and spatial organization of Gram-negative sulfate-reducing bacteria in activated sludge investigated by in situ probing with specific 16S rRNA targeted oligonucleotides. *FEMS Microbiol. Ecol.* 25, 43–61.

McHatton, S. C., Barry, J. P., Jannasch, H. W., and Nelson, D. C. (1996). High nitrate concentrations in vacuolate, autotrophic marine *Beggiatoa* spp. *Appl. Environ. Microbiol.* 62, 954–958.

Medlin, L., Elwood, H. J., Stickel, S., and Sogin, M. L. (1988). The characterization of enzymatically amplified eukaryotic 16S-like rRNA-coding regions. *Gene* 71, 491–499.

Miller, M. A., Holder, M. T., Vos, R., Midford, P. E., Liebowitz, T., Chan, L., Hoover, P., and Warnow, T. (2009). *The CIPRES Portals.* Available at: http://www.webcitation.org/5imQUeQa

Müller, M. (1988). Energy metabolism of protozoa without mitochondria. *Annu. Rev. Microbiol.* 42, 465–488.

Nakamura, K., Terada, T., Sekiguchi, Y., Shinzato, N., Meng, X.-Y., Enoki, M., and Kamagata, Y. (2006). Application of pseudomurein endoisopeptidase to fluorescence in situ hybridization of methanogens within the family Methanobacteriaceae. *Appl. Environ. Microbiol.* 72, 6907–6913.

Neef, A. (1997). *Anwendung der in situ-Einzelzell-Identifizierung von Bakterien zur Populationsanalyse in komplexen mikrobiellen Biozonose.* Munchen: TU.

Nowack, E. C., and Melkonin, M. (2010). Endosymbiotic associations within protists. *Philos. Trans. R. Soc. Lond. B Biol. Sci.* 365, 699–712.

Orphan, V. J., Hinrichs, K. U., Ussler, I. W., Paull, C. K., Taylor, L. T., Sylva, S. P., Hayes, J. M., and Delong, E. F. (2001). Comparative analysis of methane-oxidizing archaea and sulfate-reducing bacteria in anoxic marine sediments. *Appl. Environ. Microbiol.* 67, 1922–1934.

Pernthaler, A., Pernthaler, J., and Amann, R. (2002). Fluorescence in situ hybridization and catalyzed reporter deposition for the identification of marine bacteria, *Appl. Environ. Microbiol.* 68, 3094–3101.

Raikov, I. B. (1985). Primitive never-dividing macronuclei of some lower ciliates. *Int. Rev. Cytol.* 95, 267–325.

Reimers, C. E., Lange, C. B., Tabak, M. and Bernhard, J. M. (1990). Seasonal spillover and varve formation in the Santa Barbara Basin, California. *Limnol. Oceanogr.* 35, 1577–1585.

Reimers, C. E., Ruttenberg, K. C., Canfield, D. E., Christiansen, M. B., and Martin, J. B. (1996). Porewater pH and authigenic phases formed in the uppermost sediments of the Santa Barbara Basin. *Geochim. Cosmochim. Acta* 60, 4037–4057.

Ronquist, F., and Huelsenbeck, J. P. (2003). MrBayes 3: Bayesian phylogenetic inference under mixed models. *Bioinformatics* 19, 1572–1574.

Sherr, E. B., and Sherr, B. F. (2002). Significance of predation by protists in aquatic microbial food webs. *Antonie Van Leeuwenhoek* 81, 293–308.

Springer, N., Ludwig, W., Amman, R., Schmidt, H. J., Görtz, H.-D., and Schleifer, K.-H. (1993). Occurrence of fragmented 16S rRNA in an obligate bacterial endosymbiont of *Paramecium caudatum. Proc. Natl. Acad. Sci. U.S.A.* 90, 9892–9895.

Stahl, D. A., and Amann, R. (eds). (1991). *Development and Application of Nucleic Acid Probes in Bacterial Systematics.* Chichester: Wiley & Sons Ltd.

Stamatakis, A., Hoover, P., and Rougemont, J. (2008). A rapid bootstrap algorithm for the RAxML Web servers. *Syst. Biol.* 57, 758–771.

Stoeck, T., Fowle, W. H., and Epstein, S. S. (2003). Methodology of protistan discovery: from rRNA detection to quality scanning electron microscope images. *Appl. Environ. Microbiol.* 69, 6856–6863.

Stolper, D. A., Revsbech, N. P., and Canfield, D. E. (2010). Aerobic growth at nanomolar oxygen concentrations. *Proc. Natl. Acad. Sci. U.S.A.* 107, 18755–18760.

Sun, H. Y., Noe, J., Barber, J., Coyne, R. S., Cassidy-Hanley, D., Clark, T. G., Findly, R. C., and Dickerson, H. W. (2009). Endosymbiotic bacteria in the parasitic ciliate *Ichthyophthirius multifillis. Appl. Environ. Microbiol.* 75, 7445–7452.

Taylor, G. T. (1982). The role of pelagic heterotrophic protozoa in nutrient cycling: a review. *Ann. Inst. Oceanogr. (Suppl.), Paris* 58, 227–241.

Van Bruggen, J. J. A., Stumm, C. K., and Vogels, G. D. (1983). Symbiosis of methanogenic bacteria and sapropelic protozoa. *Arch. Microbiol.* 136, 89–96.

van Hoek, A. H., van Alen, T. A., Sprakel, V. S., Leunissen, J. A., Brigge, T., Vogels, G. D., and Hackstein, J. H. (2000). Multiple acquisition of methanogenic archaeal symbionts by anaerobic ciliates. *Mol. Biol. Evol.* 17, 251–258.

Vannini, C., Rosati, G., Verni, F., and Petroni, G. (2004). Identification of the bacterial endosymbionts of the marine ciliate *Euplotes magnicirratus* (Ciliophora, Hypotrichia) and proposal of '*Candidatus* Dovosia euplotis'. *Int. J. Syst. Evol. Microbiol.* 54, 1151–1156.

Wagner, M., Roger, A. J., Flax, J. L., Brusseau, G. A., and Stahl, D. A. (1998). Phylogeny of dissimilatory sulfite reductases supports an early origin of sulfate reduction. *J. Bacteriol.* 180, 2975–2982.

Wallner, G., Amman, R. I., and Beisker, W. (1993). Optimizing fluorescent in situ hybridization with rRNA-targeted oligonucleotide probes for flow cytometric identification of microorganisms. *Cytometry* 14, 136–143.

Widdel, F., and Bak, F. (eds). (1992). *Gram-Negative Mesophilic Sulfate-Reducing Bacteria.* New York, NY: Springer-Verlag.

Yeates, C., Saunders, A. M., Crocetti, G. R., and Blackall, L. L. (2003). Limitations of the widely used GAM42a and BET42a probes targeting bacteria in the Gammaproteobacteria radiation. *Microbiology* 149, 1239–1247.

Conflict of Interest Statement: The authors declare that the research was conducted in the absence of any commercial or financial relationships that could be construed as a potential conflict of interest.

Received: 27 January 2011; paper pending published: 14 February 2011; accepted: 10 March 2011; published online: 25 March 2011.

*Citation: Edgcomb VP, Leadbetter ER, Bourland W, Beaudoin D and Bernhard JM (2011) Structured multiple endosymbiosis of bacteria and archaea in a ciliate from marine sulfidic sediments: a survival mechanism in low oxygen, sulfidic sediments? Front. Microbio. **2**:55. doi: 10.3389/fmicb.2011.00055*

This article was submitted to Frontiers in Microbial Physiology and Metabolism, a specialty of Frontiers in Microbiology.

frontiers in
MICROBIOLOGY

REVIEW ARTICLE
published: 05 July 2011
doi: 10.3389/fmicb.2011.00146

Close interspecies interactions between prokaryotes from sulfureous environments

Johannes Müller*† *and Jörg Overmann*†

Bereich Mikrobiologie, Department Biologie I, Ludwig-Maximilians-Universität München, Planegg-Martinsried, Germany

Edited by:
Thomas E. Hanson, University of Delaware, USA

Reviewed by:
Jennifer Macalady, Pennsylvania State University, USA
James T. Hollibaugh, University of Georgia, USA

****Correspondence:***
Jörg Overmann, Leibniz-Institut, Deutsche Sammlung von Mikroorganismen und Zellkulturen, Inhoffenstraße 7B, 38124 Braunschweig, Germany.
e-mail: joerg.overmann@dsmz.de
† ***Present address:***
Johannes Müller and Jörg Overmann, Leibniz-Institut, Deutsche Sammlung von Mikroorganismen und Zellkulturen Braunschweig and Technical University of Braunschweig, Inhoffenstraße 7B, 38124 Braunschweig, Germany.

Green sulfur bacteria are obligate photolithoautotrophs that require highly reducing conditions for growth and can utilize only a very limited number of carbon substrates. These bacteria thus inhabit a very narrow ecologic niche. However, several green sulfur bacteria have overcome the limits of immobility by entering into a symbiosis with motile *Betaproteobacteria* in a type of multicellular association termed phototrophic consortia. One of these consortia, "*Chlorochromatium aggregatum*," has recently been established as the first culturable model system to elucidate the molecular basis of this symbiotic interaction. It consists of 12–20 green sulfur bacteria epibionts surrounding a central, chemoheterotrophic betaproteobacterium in a highly ordered fashion. Recent genomic, transcriptomic, and proteomic studies of "*C. aggregatum*" and its epibiont provide insights into the molecular basis and the origin of the stable association between the two very distantly related bacteria. While numerous genes of central metabolic pathways are upregulated during the specific symbiosis and hence involved in the interaction, only a limited number of unique putative symbiosis genes have been detected in the epibiont. Green sulfur bacteria therefore are preadapted to a symbiotic lifestyle. The metabolic coupling between the bacterial partners appears to involve amino acids and highly specific ultrastructures at the contact sites between the cells. Similarly, the interaction in the equally well studied archaeal consortia consisting of *Nanoarchaeum equitans* and its host *Ignicoccus hospitalis* is based on the transfer of amino acids while lacking the highly specialized contact sites observed in phototrophic consortia.

Keywords: *Chlorochromatium aggregatum*, phototrophic consortia, symbiosis, green sulfur bacteria, *Ignicoccus hospitalis*, *Nanoarchaeum equitans*

INTRODUCTION

In their natural environment, planktonic bacteria reach total cell numbers of 10^6 ml^{-1}, whereas in sediments and soils, 10^9 and 10^{11} bacterial cells·cm^{-3}, respectively, have been observed (Fægri et al., 1977; Whitman et al., 1998). Assuming a homogenous distribution, distances between bacterial cells in these environments would amount to 112 μm for planktonic, 10 μm for sediment environments and about 1 μm for soil bacteria (Overmann, 2001b). Taking into account the estimated number of bacterial species in soil that range from 500,000 (Dykhuizen, 1998) to 8.3×10^6 (Gans et al., 2005), the closest neighbors of each cell statistically should represent different species. A spatially close association of different bacterial species can result in metabolic complementation or other synergisms. In this context, the most extensively studied example is the conversion of cellulose to methane and carbon dioxide in anoxic habitats. The degradation is only possible by a close cooperation of at least four different groups of bacteria that encompass primary and secondary fermenting bacteria as well as two types of methanogens. Along this anaerobic food chain, end products of one group are exploited by the members downstream the flow of electrons. Although the bacteria involved in the first steps of cellulose degradation do not obligately depend on the accompanying bacteria for provision of growth substrates, they profit energetically from the rapid consumption of their excretion products. This renders their metabolism energetically more favorable or makes some reactions even possible (Bryant, 1979; Zehnder et al., 1982; McInerney, 1986; Schink, 1992). Recent studies of syntrophic communities in Lake Constance profundal sediments yielded new and unexpected results. The dominant sugar-degrading bacteria were not the typical fermenting bacteria that dominate in anaerobic sludge systems or the rumen environment. They rather represented syntrophic bacteria most closely related to the genus *Bacillus* that could only be grown anaerobically and in coculture with the hydrogen-using methanogen *Methanospirillum hungatei* (Müller et al., 2008). For efficient syntrophic substrate oxidation, close physical contact of the partner organisms is indispensable. Monocultures of *Pelotomaculum thermopropionicum* strain SI and *Methanothermobacter thermautotrophicus* show dispersed growth of the cells. In contrast, cocultures of the two strains formed tight aggregates when grown on propionate, for which the allowed distance for syntrophic propionate oxidation was estimated to be approximately 2 μm (Ishii et al., 2005). Interestingly, the H_2-consuming partner in syntrophic relationships can be replaced by an H_2-purging culture vessel, allowing *Syntrophothermus lipocalidus* to grow on butyrate and *Aminobacterium colombiense* on alanine in

pure culture (Adams et al., 2006). Thus, the syntrophic associations investigated to date are typically based on efficient H_2-removal as obligate basis for their interdependence. Additional types of bacterial interactions have been described more recently. Cultures of *Pseudomonas aeruginosa* were shown to only grow on chitin if in coculture with a chitin degrading bacterium like *Aeromonas hydrophila*. In addition to simply growing on the degradation products produced by the exoenzymes of the partner, *P. aeruginosa* induced release of acetate in *A. hydrophila* by inhibiting its aconitase employing pyocyanin. The resulting incomplete oxidation of chitin to acetate by *A. hydrophila* is then exploited by *P. aeruginosa* for its own growth (Jagmann et al., 2010).

Although these well-characterized associations certainly are of major ecological relevance in their respective environments, they were typically obtained using standard defined growth media. As a result, presently available laboratory model systems were selected based on their ability to grow readily and – under at least some experimental conditions – on their own in pure culture. Obviously, this cultivation strategy counterselects against bacterial associations of obligately or at least tight interdependence. While the significant advances in the development of cultivation-independent techniques permit a partial analysis of so-far-uncultured associations (Orphan et al., 2001; Blumenberg et al., 2004; Pernthaler et al., 2008), laboratory grown model systems are still indispensable for in-depth studies of gene expression and metabolism. One model system of prokaryotic associations that meanwhile can be grown indefinitely in laboratory culture is the phototrophic consortium "*Chlorochromatium aggregatum*." This consortium represents the most highly developed bacteria–bacteria symbiosis known to date. In parallel, the archaea–archaea association between *Ignicoccus hospitalis* and *Nanoarchaeum equitans* has emerged as a second laboratory model over the past years (Huber et al., 2003). A comparison between the two model systems that represent two different domains of life provides first insights into the general principles of tight interactions in the prokaryotic world.

CHARACTERIZATION OF PHOTOTROPHIC CONSORTIA AND ESTABLISHING "*CHLOROCHROMATIUM AGGREGATUM*" AS A MODEL SYSTEM FOR CLOSE BACTERIAL INTERACTIONS

Phototrophic consortia were already discovered in 1906 (Lauterborn, 1906) and invariably encompass green or brown-colored bacteria as epibionts that surround a central bacterium in a highly ordered fashion. Several decades later, electron microscopic analyses documented the presence of chlorosomes in the epibiont cells and led to the conclusion that the phototrophic epibionts belong to the green sulfur bacteria (Caldwell and Tiedje, 1975). This was confirmed by the application of fluorescence *in situ* hybridization employing a highly specific oligonucleotide probe against green sulfur bacterial 16S rRNA (Tuschak et al., 1999). The other partner bacterium of the symbiosis remained much less investigated than its epibionts. First, it had even been overlooked due to its low contrast in the light microscope. Over 90 years later, the central bacterium was identified as a *Betaproteobacterium* (Fröstl and Overmann, 2000) that exhibits a rod-shaped morphology with tapered ends (Overmann et al., 1998). Electron microscopy revealed the cells to be monopolarly monotrichously flagellated (Glaeser and Overmann, 2003b). Within the *Betaproteobacteria* the central bacterium represents a so far isolated phylogenetic lineage belonging to the family of the *Comamonadaceae*. The closest relatives are *Rhodoferax* spp., *Polaromonas vacuolata* and *Variovorax paradoxus* (Kanzler et al., 2005).

Based solely on their morphology, 10 different phototrophic consortia can be distinguished to date (Overmann, 2001a; Overmann and Schubert, 2002). The majority of the morphotypes are motile, motility being conferred by the central colorless bacterium. The 13–69 epibiont cells are either green or brown-colored representatives of the green sulfur bacteria. The smaller consortia like "*Chlorochromatium aggregatum*" (harboring green epibionts) and "*Pelochromatium roseum*" (brown epibionts), are barrel shaped and consist of 12–20 epibiont cells (Overmann et al., 1998). Rather globular in shape and consisting of ≥40 epibionts are the significantly larger consortia "*Chlorochromatium magnum*" (green epibionts; Fröstl and Overmann, 2000), "*Pelochromatium latum*" (brown epibionts; Glaeser and Overmann, 2004) and "*Pelochromatium roseo-viride*" (Gorlenko and Kusnezow, 1972). The latter consortium is the only one harboring two types of epibionts, with brown cells forming an inner layer and green ones an outer layer. "*Chloroplana vacuolata*" and "*Cylindrogloea bactifera*" can be distinguished from the other consortia by their immotility and different cell arrangement. "*Chloroplana vacuolata*" consists of rows of green sulfur bacteria alternating with colorless bacteria forming a flat sheath (Dubinina and Kuznetsov, 1976), with both species containing gas vacuoles. In "*Cylindrogloea bactifera*," a slime layer containing green sulfur bacteria is surrounding filamentous, colorless bacteria (Perfiliev, 1914; Skuja, 1956). Since they consist of two different types of bacteria, the names of consortia are without standing in nomenclature (Trüper and Pfennig, 1971) and, accordingly, are given here in quotation marks.

When 16S rRNA gene sequences of green sulfur bacteria from phototrophic consortia were investigated from a total of 14 different lakes in Europe and North America (Glaeser and Overmann, 2004), a total of 19 different types of epibionts could be detected. Of those, only two types occurred on both, the European and North American continents. Although morphologically identical consortia from one lake always contained just a single epibiont phylotype, morphologically indistinguishable consortia from different lakes frequently harbored phylogenetically different epibionts. Phylogenetic analyses demonstrated that the epibiont sequences do not constitute a monophyletic group within the radiation of green sulfur bacteria. Therefore, it was concluded that the ability to form symbiotic interactions was gained independently by different ancestors of epibionts or, alternatively, was present in the common ancestor of the green sulfur bacteria. In parallel, the phylogeny of central bacteria of phototrophic consortia was investigated. This analysis exploited a rare tandem *rrn* operon arrangement in these bacteria that involves an unusual short interoperon spacer of 195 bp (Pfannes et al., 2007). *Betaproteobacteria* with this genomic feature were exclusively encountered in chemocline environments and form a novel, distinct and highly diverse subcluster within the subphylum. Within this cluster, the sequences of central bacteria of phototrophic consortia were found to be polyphyletic. Thus, like in their green sulfur bacterial counterparts, the ability to become a central bacterium may have evolved independently in

several lineages of betaproteobacteria, or was already present in a common ancestor of the different central bacteria. In the barrel-shaped types of consortia, the green sulfur bacterial epibionts have overcome their immotility. However, the existence of two different types of non-motile consortia indicates that motility is not the only advantage gained by green sulfur bacteria that form these interspecies association with heterotrophic bacteria. As described below (see Evidence for Metabolic Coupling), the exchange of metabolites seems to play a major role in the symbiotic interaction, and might therefore be the key selective factor of symbiosis in immotile phototrophic consortia.

At present, "*Chlorochromatium aggregatum*" is the only phototrophic consortium that can be successfully cultivated in the laboratory (Fröstl and Overmann, 1998). From the stable enrichment culture it was possible to isolate the epibiont of the consortium in pure culture using deep agar dilution series supplemented with optimized growth media (Vogl et al., 2006). On the basis of 16S rRNA sequence comparisons, the strain is distantly related to other known green sulfur bacteria (≤94.6% sequence homology) and therefore represents a novel species within the genus *Chlorobium*, *Chlorobium chlorochromatii* strain CaD. However, physiological and molecular analyses of the novel isolate did not reveal any major differences to already described strains of the phylum *Chlorobi*. Thus, *C. chlorochromatii* CaD is obligately anaerobic and photolithoautotrophic, and photoassimilates acetate and peptone in the presence of sulfide and hydrogen carbonate (Vogl et al., 2006). As a difference to its free-living counterparts the epibiont contains only a low cellular concentration of carotenoids and cannot synthesize chlorobactene. A similar anomaly had also been observed in the brown epibionts of the phototrophic consortium "*Pelochromatium roseum*" that do not seem to form isorenieratene (Glaeser et al., 2002; Glaeser and Overmann, 2003a). In contrast to the epibiont of "*Chlorochromatium aggregatum*," all efforts to cultivate the central bacterium in the absence of its epibionts have failed so far.

PREADAPTATION OF GREEN SULFUR BACTERIA TO SYMBIOSIS

Green sulfur bacteria (Family *Chlorobiaceae*) constitute a phylogenetically distinct lineage within the phylum *Chlorobi* of the domain *Bacteria* (Overmann, 2001a). Recently, the chemotrophic *Ignavibacterium album* gen. nov. sp. nov., was described (Iino et al., 2010), this novel isolate represents a deeply branching phylogenetic lineage and hence a new class within the phylum *Chlorobi*, whereas all green sulfur bacteria *sensu stricto* that are known to date represent strictly anaerobic photolithoautotrophs. Since a considerable number of different 16S rRNA gene sequence types of green sulfur bacteria engaged in a symbiotic association with the central *Betaproteobacteria* (see section Characterization of Phototrophic Consortia and Establishing "*Chlorochromatium aggregatum*" as a Model System for Close Bacterial Interactions), green sulfur bacteria may be specifically preadapted to symbiosis and the advent of symbiotic green sulfur bacterial epibionts during evolution may have involved only limited genomic changes. Indeed, several of the physiological characteristics of green sulfur bacteria are regarded as preadaptive traits for interactions with other prokaryotes.

One feature of green sulfur bacteria which provides interaction with other prokaryotes is their carbon metabolism. Green sulfur bacteria autotrophically assimilate CO_2 through the reductive tricarboxylic acid cycle. One instantaneous product of photosynthetic fixation of CO_2 is 2-oxoglutarate, and 2-oxo acids represent typical excretion products of photosynthesizing cells (Sirevag and Ormerod, 1970). In natural environments, *Chlorobium limicola* excretes photosynthetically fixed carbon (Czeczuga and Gradzki, 1973) and thus constitutes a potential electron donor for associated bacteria. Excretion of organic carbon compounds has also been demonstrated for *C. chlorochromatii* strain CaD, the epibiont of the phototrophic consortium "*Chlorochromatium aggregatum*" (Pfannes, 2007). *Vice versa*, green sulfur bacteria can also take advantage of organic carbon compounds produced by other, for example, fermenting, bacteria. During phototrophic growth, they are capable of assimilating pyruvate as well as acetate and propionate through reductive carboxylation in the presence of CO_2 (pyruvate:ferredoxin oxidoreductase; Uyeda and Rabinowitz, 1971) or HCO_3^- (phosphoenolpyruvate carboxylase; Chollet et al., 1996). The assimilation of organic carbon compounds reduces the amount of electrons required per unit cellular carbon synthesized. This capability thus enhances photosynthetic growth yield and results in a competitive advantage for green sulfur bacteria.

In their natural environment, green sulfur bacteria are limited to habitats where light reaches anoxic bottom waters such as in thermally stratified or meromictic lakes. Here, cells encounter conditions favorable for growth exclusively in a rather narrow (typically cm to dm thick) zone of overlap between light and sulfide. Compared to other phototrophs, green sulfur bacteria are extremely low-light adapted and capable of exploiting minute light quantum fluxes by their extraordinarily large photosynthetic antenna complexes, the chlorosomes. In contrast to other photosynthetic antenna complexes, the bacteriochlorophyll *c, d,* or *e* molecules in chlorosomes are not attached to a protein scaffold but rather form paracrystalline, tight aggregates (Griebenow and Holzwarth, 1989; Blankenship et al., 1995). Until recently, the heterogeneity of pigments complicated the identification of the structural composition of chlorosomes. When a *Chlorobaculum tepidum* triple mutant that almost exclusively harbors BChl *d* was constructed, a *syn-anti* stacking of monomers and self-assembly of bacteriochlorophylls into tubular elements could be demonstrated within the chlorosomes (Ganapathy et al., 2009).

Since they minimize the energetically costly protein synthesis, chlorosomes represent the most effective light harvesting system known. Up to 215,000 ± 80,000 bacteriochlorophyll molecules (in *Chlorobaculum tepidum*; Montano et al., 2003) can constitute a single chlorosome, that is anchored to 5–10 reaction centers in the cytoplasmic membrane (Amesz, 1991). This ratio of chlorophyll to reaction center is orders of magnitudes higher compared with other photosynthetic antenna structures. In the phycobilisomes of cyanobacteria the ratio is 220:1 (Clement-Metral et al., 1985), 100–140:1 in light harvesting complex II of anoxygenic phototrophic proteobacteria (Van Grondelle et al., 1983) and 28:1 in the light harvesting complex I (Melkozernov et al., 2006). The

enormous size of the photosynthetic antenna of green sulfur bacteria enables them to colonize extreme low-light habitats up to depths of 100 m in the Black Sea (Overmann et al., 1992; Marschall et al., 2010) or below layers of other phototrophic organisms like purple sulfur bacteria (Pfennig, 1978). Commensurate with their adaptation to extreme light limitation, green sulfur bacteria also exhibit a significantly reduced maintenance energy requirement compared to other bacteria (Veldhuis and van Gemerden, 1986; Overmann et al., 1992). *Chlorobium* phylotype BS-1 isolated from the Black Sea maintained a constant level of cellular ATP over 52 days, if exposed to low-light intensities of 0.01 mmol quanta m^{-2} s^{-1} (Marschall et al., 2010). The high efficiency of green sulfur bacteria allows them to colonize habitats in which other photosynthetic bacteria are unable to grow. A chemotrophic bacterium that associates with green sulfur bacteria and is capable of exploiting part of their fixed carbon thus would gain a selective advantage during evolution.

SELECTIVE ADVANTAGE OF CONSORTIA FORMATION

Free-living representatives of green sulfur bacteria are immotile and only species able to produce gas vacuoles can regulate their vertical position. However, changes in buoyant density mediated by gas vesicle production occur only over time periods of several days (Overmann et al., 1991). Due to the motility that is conferred by the flagellated central bacterium, the consortium can orientate itself much faster in light and sulfide gradients and reaches locations with optimal conditions for photosynthesis in a shorter period of time. In fact, "*C. aggregatum*" has been found to vary its position rapidly across the chemocline in two Tasmanian lakes (Croome and Tyler, 1984). A scotophobic response, that is swimming away from darkness toward light, has been demonstrated for intact consortia in the laboratory (Fröstl and Overmann, 1998; Glaeser and Overmann, 2003a) and leads to a rapid accumulation of consortia in (dim)light. In addition, laboratory cultures as well as natural populations of phototrophic consortia exhibit a strong chemotaxis toward sulfide (Fröstl and Overmann, 1998; Glaeser and Overmann, 2003b).

In contrast to light, the spatial distribution of sulfide does not necessarily occur in a strictly vertical gradient in the natural habitat. In analogy to the presence of point sources of organic carbon substrates (Azam and Malfatti, 2007) that attract chemotrophic aquatic bacteria in zones extending tens to hundred micrometer around the sources (Krembs et al., 1998), organic particles sinking into anoxic water layers may develop into hot spots of sulfate reduction. Due to the motility of phototrophic consortia, the otherwise immotile green sulfur bacteria epibionts would gain rapid access and thus a highly competitive advantage over their free-living relatives especially in laterally inhomogeneous environments. If photosynthetically fixed carbon is indeed transferred to the central bacterium, however, the net balance of the increased availability of sulfide and the loss of electrons to the central bacterial partner must still be positive for the green sulfur bacterium.

The tight packing of epibiont cells in the phototrophic consortium raises the question whether dissolved compounds can actually diffuse into the consortium and reach the central bacterium or if the epibionts represent a diffusion barrier around the central bacterium. This question was addressed by adding carboxyfluorescein diacetate succinimidyl ester (CFDA-SE) to intact consortia and following fluorescence in epibionts and central bacteria over time (Bayer, 2007). CFDA-SE enters cells by diffusion and, after cleavage by intracellular esterase enzymes, confers fluorescence to the bacterial cell. Central bacteria were already detectable after 2 min of exposure (**Figure 1A**), whereas epibionts in the same sample could only be detected after 12 min of incubation with CFDA-SE and developed only weak fluorescence (**Figure 2**). The fluorescence activity of the central rod remained strong throughout the experiment which is indicative of a higher esterase activity than in the epibiont. Since the central bacterium is presumably heterotrophic, it is likely to express esterases such as lipases at a higher number or intracellular concentration. These results indicate that, even in intact phototrophic consortia, diffusion of small water-soluble molecules toward the central bacterium is not significantly impeded by the surrounding layer of epibionts. Therefore, sensing of sulfide by the central bacterium itself, eliciting the sulfide chemotactic response observed for the consortia is feasible. However, in analogy to the proposal that heterotrophic bacteria colonizing the heterocysts of cyanobacteria may shield them from high ambient O_2 concentrations (Paerl and Kellar, 1978), one could speculate that the consumption of sulfide by the epibionts might decrease the concentration of sulfide reaching the central bacterium. Thus, if sensing of sulfide is carried out by the central bacterium, the photosynthetic activity of the epibiont could have a regulatory function regarding the chemotaxis of the consortium toward sulfide.

The orientation of the consortium toward light and sulfide is of special interest since probably neither of these attractants is used in the metabolism of the motile central

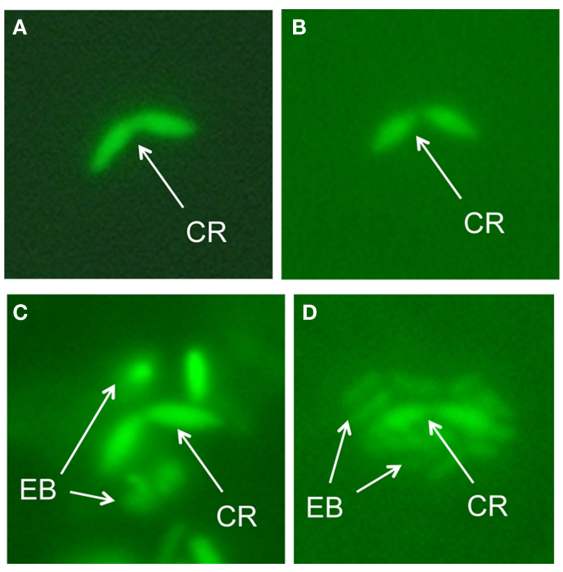

FIGURE 1 | CFDA-SE stained phototrophic consortia. CR, central rod; EB, epibiont. **(A,B)** 2 **(A)** and 5 min **(B)** of staining; only the central bacterium is visible. **(C)** 12 min of staining; epibionts become visible. **(D)** 15-min staining; whole consortium stained.

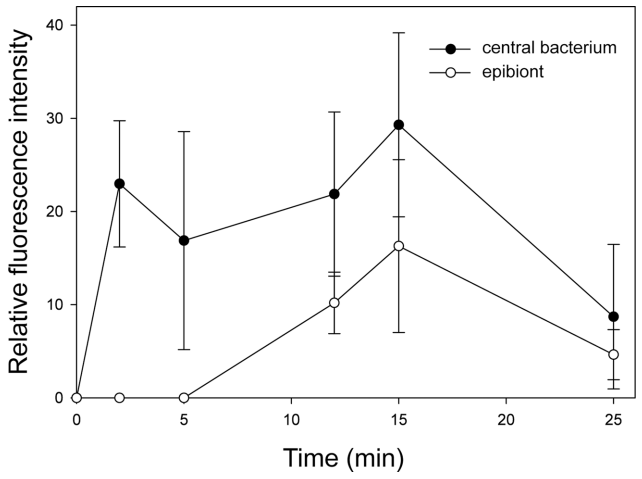

FIGURE 2 | Time course of fluorescence intensities of CFDA-SE stained central bacteria and epibiont cells.

bacterium. From the perspective of the epibiont, relying on a non-photosynthetic partner for transportation would pose the risk of being carried into dark, and/or sulfide-free unfavorable deeper water layers. Consortia formation thus would either require the expression of a suitable chemotactic response (i.e., toward sulfide) and of a suitable photosensor in the central bacterium or effective means of interspecific communication. Acquisition of these traits must have been a critical stage and happened early during the coevolution of the bacterial partners in phototrophic consortia.

In recent ultrastructural studies of the central bacterium of "*C. aggregatum*," conspicuous 35-nm-thick and up to 1-μm-long zipper-like crystalline structures were found that resemble the chemotaxis receptor Tsr of *Escherichia coli* (Wanner et al., 2008). In a comparative ultrastructural study of 13 distantly related organisms harboring chemoreceptor arrays from all seven major signaling domain classes, receptors were found to possess an universal structure which has presumably been conserved over long evolutionary distances (Briegel et al., 2009). The prominent ultrastructure discovered in the central bacterium exhibits several similarities to the chemoreceptors reported and provides a first indication that a chemotaxis receptor is present in the central bacterium.

One characteristic feature of green sulfur bacteria that provides a basis for interaction with other bacteria is the extracellular deposition of sulfur globules (zero valence sulfur), the initial product of sulfide oxidation during anoxygenic photosynthesis. This sulfur is further oxidized to sulfate only after depletion of sulfide. The extracellular deposition renders the sulfur available to other bacteria such as, for example, sulfur reducers. Therefore, it had initially been proposed that the central bacterium of phototrophic consortia is a sulfate- or sulfur-reducing bacterium. In that case, extracellular sulfur produced by the green sulfur bacteria could be utilized by the central bacterium to establish a close sulfur cycle within the phototrophic consortium (Pfennig, 1980). Such a sulfur cycle has been established in defined syntrophic cocultures of *Chlorobium phaeovibrioides* and *Desulfuromonas acetoxidans*. In these cocultures, acetate is oxidized by *Desulfuromonas acetoxidans* with sulfur as electron acceptor, which leads to a recycling of the sulfide that can then be used again for anoxygenic photosynthesis by *Chl. phaeovibrioides*. Only minute amounts of sulfide (10 μM) are required to keep this sulfur cycle running (Warthmann et al., 1992). Similarly, sulfate reducers are able to grow syntrophically with green sulfur bacteria with only low equilibrium concentrations of sulfide (Biebl and Pfennig, 1978). In addition, such interactions may also encompass transfer of organic carbon compounds between the partners. In mixed cultures of *Desulfovibrio desulfuricans* or *D. gigas* with *Chlorobium limicola* strain 9330, ethanol is oxidized to acetate with sulfate as electron acceptor and the acetate formed is incorporated by *Chl. limicola* such that ethanol is completely converted to cell material.

However, the hypothesis of a sulfur cycling within phototrophic consortia became less likely by the discovery that the central bacterium belongs to the *Betaproteobacteria*, whereas only the *Deltaproteobacteria* or *Firmicutes* encompass typical sulfur- or sulfate-reducers (Fröstl and Overmann, 2000). As shown above, the exchange of sulfur compounds has been established across a physiologically and phylogenetically diverse range of prokaryotes. But those symbiotic interactions were not accompanied by consortia formation. It is thereby concluded, that sulfur cycling does not appear to be sufficiently selective to explain the advent of phototrophic consortia during evolution.

MOLECULAR BASIS OF THE SYMBIOTIC INTERACTION IN PHOTOTROPHIC CONSORTIA

FEATURES OF THE EPIBIONT GENOME THAT RELATE TO SYMBIOSIS

In order to make a first assessment of the imprint of symbiotic lifestyle on the genome of the epibiont, the genome features of *C. chlorochromatii* CaD can be compared to those of *Nanoarchaeum equitans* and *Ignicoccus hospitalis* in the archaeal consortia.

Nanoarchaeum equitans is the representative of a new archaeal phylum *Nanoarchaeota* and most likely represents a parasitic epibiont of *Ignicoccus*. The *N. equitans* genome comprises only 491 kb and encodes 552 genes, rendering it the smallest genome for an exosymbiont known to date (Waters et al., 2003). Genome reduction includes almost all genes required for the *de novo* biosynthesis of amino acids, nucleotides, cofactors, and lipids as well as many known pathways for carbon assimilation. Commensurate with this findings, the *Nanoarchaeum equitans* epibiont appears to acquire its lipids from its host (Waters et al., 2003). Yet, the *N. equitans* genome harbors only few pseudogenes or regions of non-coding DNA compared with genomes of obligate bacterial symbionts that undergo reductive evolution, and thus is genomically significantly more stable than other obligate parasites. This has been interpreted as evidence for a very ancient relationship between *N. equitans* and *Ignicoccus* (Brochier et al., 2005). The recent bioinformatic analysis also suggest that *N. equitans* represents a derived, fast-evolving euryarchaeal lineage rather than the representative of a deep-branching basal phylum (Brochier et al., 2005). With a size of 1.30 Mbp and 1494 predicted open reading frames (ORFs), the genome of *I. hospitalis* shows a pronounced

genome reduction that has been attributed to the reduced metabolic complexity of its anaerobic and autotrophic lifestyle and an highly efficient adaptation to the low energy yield of its metabolism (Podar et al., 2008).

Similar to *I. hospitalis*, the genome size of *Pelagibacter ubique* (1.31 Mbp and 1354 ORFs) so far marks the lower limit of free-living organisms. It exhibits hallmarks of genome streamlining such as the lack of pseudogenes, introns, transposons, extrachromosomal elements, only few paralogs, and the shortest intergenic spacers yet observed for any cell (Giovannoni et al., 2005). This likely reduces the costs of cellular replication (Mira et al., 2001). As a second feature, the genome of *P. ubique* has a G:C content of 29.7% that may decrease its cellular requirements for fixed nitrogen (Dufresne et al., 2005).

By comparison, a much larger genome size of 2.57 Mbp has been determined for *C. chlorochromatii* CaD. This size represents the average value of the 11 other publicly available genomes of green sulfur bacteria (**Table 1**). Thus, a reduction in genome size that is characteristic for bacterial endosymbionts (Andersson and Kurland, 1998; Moran et al., 2002, 2008) and for the archaeal consortium (Podar et al., 2008) did not occur during the evolution of the epibiont of "*C. aggregatum*." This suggests (i) a shorter period of coevolution of the two partner bacteria in phototrophic consortia, (ii) a significantly slower rate of evolution of their genomes, or (iii) that the genome of *C. chlorochromatii* is not undergoing a streamlining process as observed in other symbiotic associations. The latter suggestion would indicate a lack of selective advantage for "*Chl. aggregatum*" from genome streamlining.

Wet-lab and *in silico* analyses of the epibiont genome revealed the presence of several putative symbiosis genes. An initial combination of suppression subtractive hybridization with bioinformatics approaches identified four ORFs as candidates. Two of the ORFs (Cag0614 and 0616) exhibit similarities to putative filamentous hemagglutinins that harbor RGD (arginine–glycine–aspartate) tripeptides. In pathogenic bacteria, hemagglutinins with these motifs are involved in the attachment to mammalian cells (Vogl et al., 2008). Most notably, a comparative study of 580 sequenced prokaryotic genomes revealed that Cag 0614 and 0616 represent the largest genes detected in prokaryotes so far. In fact, Cag 0616 is only surpassed in length by the exons of the human titin gene (Reva and Tümmler, 2008). The two other genes detected (Cag1919 and 1920) resembles repeats in toxin (RTX)-like proteins and hemolysins, respectively. All four genes have in common that they are unique in *C. chlorochromatii* CaD and that certain domains of their inferred products are only known from bacterial virulence factors. If the four genes were not misassigned, they are potentially involved in the symbiotic interaction between the two partner bacteria in phototrophic consortia.

To identify additional symbiosis genes, *in silico* subtractive hybridization between the genome sequence of *C. chlorochromatii* CaD and the other 11 sequences of green sulfur bacterial genomes was performed. This yielded 186 ORFs unique to the epibiont (Wenter et al., 2010), 99 of which encode for hypothetical proteins of yet unknown function. Although this provides a large number of putative symbiosis genes, the numbers are rather low compared to the unique and unknown ORFs in the other green sulfur bacteria (**Table 1**). Even if it is assumed that all of these unknown genes encode for proteins involved in symbiosis, this number is still rather small compared to the 1387 genes encoding niche-specific functions in enterohemorrhagic *E. coli* O157:H7 (Perna et al., 2001). Low numbers of niche-specific genes have been reported for *Salmonella enterica* or *Bacillus anthracis* and have been interpreted as indication for preadaptation of the non-pathogenic ancestor. This supports the hypothesis of a preadaptation of green sulfur bacteria to symbiosis. From a broader perspective, the discovery of putative symbiosis genes in the epibiont genome that resemble typical bacterial virulence factors suggest that modules thought to be limited to bacterial pathogens are employed in a much wider biological context.

THE REGULATORY RESPONSE EVOKED BY SYMBIOSIS INVOLVES GENES OF THE NITROGEN METABOLISM

When the proteome of *C. chlorochromatii* CaD in the free-living state was compared to that of the symbiotic state by 2-D differential gel electrophoresis (2-D DIGE), it became apparent that symbiosis-specific regulation involves genes of central metabolic pathways rather than symbiosis-specific genes (Wenter et al., 2010). In the soluble proteome, 54 proteins were expressed exclusively in consortia. Among them were a considerable number of proteins involved in amino acid metabolism. These included glutamate synthase, 2-isopropylmalate synthase, and the nitrogen regulatory protein P-II. The latter showed the highest overall upregulation that amounted to a 189-fold increase in transcript abundance as determined by subsequent RT-qPCR. It is thereby concluded that the amino acid requirement in the consortium is higher than in the epibiont in pure culture.

Parallel investigations of the membrane proteome revealed that a branched chain amino acid ABC-transporter binding protein was expressed only in the associated state of the epibiont. Interestingly, the expression of the ABC-transporter binding protein could also be induced in the free-living state by addition of sterile filtered supernatant of the consortia culture, but not with peptone or branched chain amino acids themselves. This is an evidence for a signal exchange between the two symbiotic partners mediated through the surrounding medium.

The results of the proteome analysis were supplemented by transcriptomic studies of the epibiont in the associated and the free-living state (Wenter et al., 2010). Of the 328 differentially expressed genes, 19 genes were found to be up-regulated and are involved in amino acid synthesis while six genes of the amino acid pathways were down-regulated. The conclusion that nitrogen metabolism of the epibiont is stimulated in the symbiotic state is commensurate with the simultaneous up-regulation of the *nifH*, *nifE*, and *nifB* genes and with the prominent expression of the P-II nitrogen regulatory protein.

The results of the proteome analyses indicates that (i) a signal exchange occurs between the central bacterium and the epibiont that controls the expression of symbiosis relevant genes and (ii)

Table 1 | Comparison of green sulfur bacterial genomes against each other.

Green sulfur bacterium	Genome size (Mbp)	ORFs-in genome	Unique ORFs	Genome (%)	Unknown unique ORFs	G + C (%)
Chlorobium chlorochromatii CaD3	2.57	2002	186	9.3	99	44.3
Chlorobaculum parvum NCIB 8327	2.29	2078	139	6.7	81	55.8
Chlorobaculum tepidum TLS	2.15	2252	396	17.6	366	56.5
Chlorobium ferrooxidans DSM 13031	2.54	2158	181	8.4	84	50.1
Chlorobium limicola DSM 245	2.76	2522	204	8.1	149	51.3
Chlorobium phaeobacteroides BS1	2.74	2559	331	12.3	211	48.9
Chlorobium phaeobacteroides DSM 266	3.13	2743	266	9.7	164	48.4
Chlorobium phaeovibrioides DSM 265	1.97	1773	56	3.2	33	53.0
Chloroherpeton thalassium ATCC 35110	3.29	2731	971	35.6	396	45.0
Pelodictyon phaeoclathratiforme BU-1	3.02	2911	550	18.9	394	48.1
Chlorobium luteolum DSM 273	2.36	2083	100	4.8	49	57.3
Prosthecochloris aestuarii SK413, DSM 271	2.58	2402	409	17.0	215	50.1
Average	2.61	2351.2	315.8	12.6	186.8	50.1.

In silico subtractive hybridization was conducted with the Phylogenetic Profiler available at the DOE Joint genome Institute website (http://img.jgi.doe.gov).

metabolic coupling between *C. chlorochromatii* and the central *Betaproteobacterium* may involve amino acids. Metabolic coupling has also been detected in the two-membered microbial consortium consisting of *Anabaena* sp. strain SSM-00 and *Rhizobium* sp. strain WH2K. Between the two species, nanoscale secondary ion mass spectrometry (nanoSIMS) analyses indicated an exchange of metabolites containing ^{13}C and ^{15}N fixed by the heterocysts of the filamentous cyanobacteria to the attached epibiont cells (Behrens et al., 2008).

EVIDENCE FOR METABOLIC COUPLING

The proteomic and transcriptomic evidence described in the preceding paragraphs point toward an exchange of metabolites between the two symbiotic partners of "*C. aggregatum*." Meanwhile, more direct evidence for a transfer of carbon between the bacterial partners of phototrophic consortia has been obtained. In a series of labeling experiments with ^{14}C, a rapid exchange of labeled carbon from the epibiont to the central bacterium was observed (Johannes Müller and Jörg Overmann, unpublished observations). External addition of several amino acids as well as 2-oxoglutarate to the growth medium inhibited this carbon exchange. Together with the observed excretion of photosynthetically fixed carbon by *C. chlorochromatii* CaD, these results suggest a transfer of newly synthesized small molecular weight organic matter to the central bacterium. Such a transfer may provide the central bacterium with a selective advantage in illuminated sulfidic environments where degradation of organic matter proceeds mainly through the anaerobic food chain and involves competition of chemoheterotrophs for organic carbon compounds. By transferring amino acids, the epibiont may not only support growth of the central bacterium with respect to carbon, but also to nitrogen and even sulfur.

To date it has remained unclear whether the association in phototrophic consortia also offers an additional advantage for the green sulfur bacterial epibiont apart from the gain of motility and the resulting potential increase in sulfide supply. Extensive substrate utilization assays with *C. chlorochromatii* CaD revealed that only the addition of acetate and peptone stimulated the growth of the epibiont of "*C. aggregatum*" (Vogl et al., 2006). It remains to be tested whether transfer of organic carbon in this form occurs in the opposite direction from the central bacterium to the epibiont.

Stable isotope signatures (^{13}C) of *I. hospitalis* and *N. equitans* were analyzed to investigate a possible carbon transfer between the two archaeal partners. Labeling patterns of *Ignicoccus* amino acids grown in the coculture as well as in pure culture were compared to those in the *Nanoarchaeum* amino acids. Therefore, amino acids were separated by chromatography and incorporation of ^{13}C at specific carbon positions was identified by NMR spectroscopy. The labeling patterns from all three cultures were exactly identical. In addition, genes involved in the *de novo* biosynthesis of amino acids are missing in the *Nanoarchaeum* genome. Based on this combined evidence, it was concluded that amino acids are transferred from the *I. hospitalis* host to the *N. equitans* cells (Jahn et al., 2008). In addition, cellular macromolecules seem to be exchanged between the partners in the archaeal consortia. In the latter, LC–MS analyses of membrane lipids in their intact polar forms showed very similar chemical patterns in both organisms with archaeol and caldarchaeol constituting the main core lipids. Furthermore, stable isotope labeling (^{13}C) yielded nearly identical results for the hydrocarbons derived from *N. equitans* and *I. hospitalis*. Those results, combined with a lack of genes for lipid biosynthesis in the genome of *N. equitans* led to the conclusion that lipids in the archaeal consortium are synthesized in *I. hospitalis* and transported to its partner organism (Jahn et al., 2004).

Amino acids also seem to be of central importance for other symbioses. The deep sea tube worm *Riftia pachyptila* is dependent on arginine supplied by its bacterial endosymbionts (Minic and Hervé, 2003), whereas in legume-root nodules, amino acids are used as both an ammonium and a carbon shuttle (Lodwig et al., 2003). Interestingly, *Rhizobia* become symbiotic auxotrophs for branched chain amino acids after infecting the host plant due to a downregulation of the respective biosynthetic

pathways, making them dependent on the supply by the plant (Prell et al., 2009).

MECHANISMS OF METABOLITE EXCHANGE

The very structure of the phototrophic consortium in itself facilitates the putative transfer of compounds from one partner to the other since the direct cell–cell contact prevents a diffusion of compounds over larger distance and hence minimizes transfer time. Theoretically, the metabolic coupling of the two partners of the consortium "*C. aggregatum*" may be based on an unspecific excretion of substrates by the epibiont followed by the uptake via the central bacterium, or involve specific molecular structures and mechanisms of substrate exchange. Several observations indicate that the latter is the case in "*C. aggregatum.*"

The ultrastructure of the contact sites in "*C. aggregatum*" and in the archaeal consortia have been studied in detail using different electron microscopy approaches (Junglas et al., 2008; Wanner et al., 2008). In free-living epibionts, as well as in all other known green sulfur bacteria, chlorosomes are distributed evenly among the inner face of the cytoplasmic membrane. However, in the associated state, chlorosomes are absent in the green sulfur bacterial epibionts at the site of attachment to the central bacterium. Replacing the antenna structures, a 17 nm-thick layered structure of yet unknown function has been discovered (Vogl et al., 2006; Wanner et al., 2008). Interestingly, treatment of the epibionts with the extracellular cross-linkers DTSSP and BS_3 revealed the branched chain amino acid ABC-transporter binding protein (compare The Regulatory Response Evoked by Symbiosis Involves Genes of the Nitrogen Metabolism) to be cross-linking with other proteins, indicating that it is localized at the cell surface or in the periplasm (Wenter et al., 2010).

In contrast to the epibionts of the phototrophic consortium "*Chlorochromatium aggregatum*" that maintain a permanent cell–cell contact to the central bacterium, *Nanoarchaeum equitans* has been observed in different states of attachment to *Ignicoccus hospitalis*. The surface structures of the two organisms may either be in direct contact or, alternatively, in close vicinity to each other. In the latter case, fibers bridging the gap between the cells are clearly visible. In "*C. aggregatum*," connections between the two partner bacteria stretching out from the central bacterium are more prominent than in the archaeal consortium. Periplasmic tubules (PT) are formed by the outer membrane and are in linear contact with the epibionts (**Figure 3A**). The PT are distributed over the entire cell surface (**Figure 3B**) and reach 200 nm in length at the poles of the central bacterium.

It had been speculated that the periplasmic tubules represent connections of a shared periplasmic space (Wanner et al., 2008). However, this could not be confirmed by fluorescence recovery after photobleaching (FRAP)-analyses (Johannes Müller and Jörg Overmann, unpublished observations). After staining of the consortia with calcein acetoxymethylester (calcein AM), only the epibionts but not the central bacterium could be detected by fluorescence microscopy (**Figure 4A**). Obviously, the central bacterium (arrows in **Figure 4A**) is lacking an esterase specific for cleaving calcein AM. This result in itself already contradicts the hypothesis of a combined periplasm because the highly fluorescent dye calcein should have diffused after its formation from the epibiont cells into the central bacterium. Furthermore, after subsequent bleaching of one of the epibiont cells (arrowheads in **Figures 4B,C**) using confocal microscopy, a recovery of fluorescence could not be detected in the bleached cell, which excludes the possibility of free diffusion between the epibiont cells through the interconnecting pili (**Figures 4B,C**).

A similar experiment has been conducted with the filamentous cyanobacterium *Anabaena cylindrica* which is considered to be a truly multicellular prokaryote. Single calcein stained cells within an *Anabaena* filament fully recovered calcein fluorescence 12 s after bleaching. This effect was ascribed to intercellular channels allowing free diffusion of molecules from cytoplasm to cytoplasm (Mullineaux et al., 2008). Such a rather unspecific transfer is unlikely to occur across the contact site of the phototrophic consortium "*C. aggregatum*" where it must be much more substrate-specific.

CONCLUSIONS

While the different types of symbioses and syntrophic associations discussed in the preceding sections all provide an energetic advantage to one or both partners, only few of these associations reached the level of organizational complexity of the highly structured, permanent consortia. Thus, a permanent cell–cell contact is not mandatory in the case of syntrophic cultures in which depletion of substrates can lead to disaggregation of the associations (Peduzzi et al., 2003). The highly developed and obligate interaction in phototrophic consortia is likely to be related to the pronounced energy limitation in the low-light habitats and to the efficient and regulated exchange of metabolites. Phototrophic

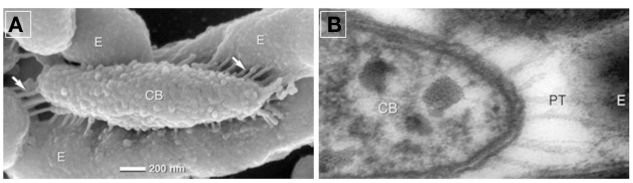

FIGURE 3 | (A) Scanning electron photomicrographs of a partially disaggregated consortium, E, epibiont, CB, central bacterium, arrows pointing toward periplasmic tubules (PT). **(B)** Transmission electron photomicrographs of ultra-thin sections showing elongated PT at the tip of the central bacterium. Modified after Wanner et al. (2008).

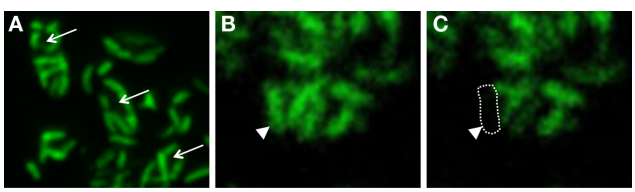

FIGURE 4 | "*Chlorochromatium aggregatum*" consortia after calcein AM staining. (A) Arrows pointing toward unstained central bacteria. **(B,C)** Consortium before and after photo-bleaching; arrows pointing toward bleached epibiont cell.

consortia harboring other prokaryotes than green sulfur bacteria have not been found so far, emphasizing the role of preadaptation of the green sulfur bacterial partner for the development of the symbiosis that was augmented by the gain of specific functions such as genes similar to virulence genes, periplasmic tubules for cell–cell contact or the intracellular sorting of chlorosomes in the epibionts. The gain of motility by the epibiont seems to constitute a selective advantage that led to the coevolution with a motile betaproteobacterium. The recent completion of the central bacterial genome sequence for "*C. aggregatum*" should help to determine whether and which additional preadaptations of the betaproteobacterium were essential for establishing this symbiosis.

ACKNOWLEDGMENTS

We thank Anne Bayer for supplying material for **Figures 1** and **2** and Andreas Binder, Genetics, Department Biology I, University of Munich, for help with confocal laser scanning microscopy. This work was supported by a grant of the Deutsche Forschungsgemeinschaft to Jörg Overmann (grant DFG OV20/10-2).

REFERENCES

Adams, C. J., Redmond, M. C., and Valentine, D. L. (2006). Pure-culture growth of fermentative bacteria, facilitated by H_2 removal: bioenergetics and H_2 production. *Appl. Environ. Microbiol.* 72, 1079–1085.

Amesz, J. (1991)."Green photosynthetic bacteria and heliobacteria," in *Variations in Autotrophic Life*, eds J. M. Shively and L. L. Barton (London: Academic Press), 99–119.

Andersson, S. G. E., and Kurland, C. G. (1998). Ancient and recent horizontal transfer events: the origins of mitochondria. *APMIS* Suppl. 106, 5–14.

Azam, F., and Malfatti, F. (2007). Microbial structuring of marine ecosystems. *Nat. Rev. Microbiol.* 5, 782–791.

Bayer, A. I. (2007). *Neue Ansätze zur Analyse der bakteriellen Interaktionen in phototrophen Konsortien*. Diploma Thesis, University of Munich 180p.

Behrens, S., Lösekann, T., Pett-Ridge, J., Weber, P. K., Ng, W. O., Stevenson, B. S., Hutcheon, I. D., Relman, D. A., and Spormann, A. M. (2008). Linking microbial phylogeny to metabolic activity at the single-cell level by using enhanced element labeling-catalyzed reporter deposition fluorescence in situ hybridization (EL-FISH) and NanoSIMS. *Appl. Environ. Microbiol.* 74, 3143–3150.

Biebl, H., and Pfennig, N. (1978). Growth yields of green sulfur bacteria in mixed cultures with sulfur and sulfate reducing bacteria. *Arch. Microbiol.* 117, 9–16.

Blankenship, R. E., Madigan, M. T., and Bauer, C. E. (eds). (1995). *Anoxygenic Photosynthetic Bacteria* (New York, NY: Springer), 1368.

Blumenberg, M., Seifert, R., Reitner, J., Pape, T., and Michaelis, W. (2004). Membrane lipid patterns typify distinct anaerobic methanotrophic consortia. *Proc. Natl. Acad. Sci. U.S.A.* 101, 11111–11116.

Briegel, A., Ortega, D. R., Tocheva, E. I., Wuichet, K., Zhuo, L., Songye, C., Müller, A., Iancu, C. V., Murphy, G. E., Dobro, M. J., Zhulin, I. B., and Jensen, G. J. (2009). Universal architecture of bacterial chemoreceptor arrays. *Proc. Natl. Acad. Sci. U.S.A.* 106, 17181–17186.

Brochier, C., Gribaldo, S., Zivanovic, Y., Confalonieri, F., and Forterre, P. (2005). Nanoarchaea: representatives of a novel archaeal phylum or a fast-evolving euryarchaeal lineage related to Thermococcales? *Genome Biol.* 6, R42.

Bryant, M. P. (1979). Microbial methane production-theoretical aspects. *J. Anim. Sci.* 48, 193–201.

Caldwell, D. E., and Tiedje, J. M. (1975). A morphological study of anaerobic bacteria from the hypolimnia of two Michigan lakes. *Can. J. Microbiol.* 21, 362–376.

Chollet, R., Vidal, J., and O'Leary, M. H. (1996). Phosphoenolpyruvate carboxylase: a ubiquitous, highly regulated enzyme in plants. *Annu. Rev. Plant. Physiol. Plant. Mol. Biol.* 47, 273–298.

Clement-Metral, J. D., Gantt, E., and Redlinger, T. (1985). A photosystem II-phycobilisome preparation from the red alga, *Porphyridium cruentum*: oxygen evolution, ultrastructure, and polypeptide resolution. *Arch. Biochem. Biophys.* 238, 10–17.

Croome, R. L., and Tyler, P. A. (1984). The microanatomy and ecology of "Chlorochromatium aggregatum" in two meromictic lakes in Tasmania. *J. Gen. Microbiol.* 130, 2717–2723.

Czeczuga, B., and Gradzki, F. (1973). Relationship between extracellular and cellular production in the sulphuric green bactreium *Chlorobium limicola* Nads. (Chlorobacteriaceae) as compared to primary production of phytoplankton. *Hydrobiologia* 42, 85–95.

Dubinina, G. A., and Kuznetsov, S. I. (1976). The ecological and morphological characteristica of microorganisms in Lesnaya Lamba (Karelia). *Int. Rev. Hydrobiol.* 61, 1–19.

Dufresne, A., Garczarek, L., and Partensky, F. (2005). Accelerated evolution associated with genome reduction in a free-living prokaryote. *Genome Biol.* 6, R14.

Dykhuizen, D. E. (1998). Santa Rosalia revisited: Why are there so many species of bacteria? Antonie van Leeuwenhoek. *Int. J. Gen. Mol. Microbiol.* 73, 25–33.

Fægri, A., Torsvik, V. L., and GoksÖyr, J. (1977). Bacterial and fungal activities in soil: separation of bacteria and fungi by a rapid fractionated centrifugation technique. *Soil Biol. Biochem.* 9, 105–112.

Fröstl, J. M., and Overmann, J. (1998). Physiology and tactic response of the phototrophic consortium "*Chlorochromatium aggregatum*." *Arch. Microbiol.* 169, 129–135.

Fröstl, J. M., and Overmann, J. (2000). Phylogenetic affiliation of the bacteria that constitute phototrophic consortia. *Arch. Microbiol.* 174, 50–58.

Ganapathy, S., Oostergetel, G. T., Wawrzyniak, P. K., Reus, M., Gomez Maqueo Chew, A., Buda, F., Boekema, E. J., Bryant, D. A., Holzwarth, A. R., and de Groot, H. J. (2009). Alternating syn-anti bacteriochlorophylls form concentric helical nanotubes in chlorosomes. *Proc. Nat. Acad. Sci. U.S.A.* 106, 8525–8530.

Gans, J., Wolinsky, M., and Dunbar, J. (2005). Microbiology: computational improvements reveal great bacterial diversity and high toxicity in soil. *Science* 309, 1387–1390.

Giovannoni, S. J., Tripp, H. J., Givan, S., Podar, M., Vergin, K. L., Baptista, D., Bibbs, L., Eads, J., Richardson, T. H., Noordewier, M., Rappé, M. S., Short, J. M., Carrington, J. C., and Mathur, E. J. (2005). Genetics: genome streamlining in a cosmopolitan oceanic bacterium. *Science* 309, 1242–1245.

Glaeser, J., Baneras, L., Rütters, H., and Overmann, J. (2002). Novel bacteriochlorophyll *e* structures and species-specific variability of pigment composition in green sulfur bacteria. *Arch. Microbiol.* 177, 475–485.

Glaeser, J., and Overmann, J. (2003a). Characterization and *in situ* carbon metabolism of phototrophic consortia. *Appl. Environ. Microbiol.* 69, 3739–3750.

Glaeser, J., and Overmann, J. (2003b). The significance of organic carbon compounds for *in situ* metabolism and chemotaxis of phototrophic consortia. *Environ. Microbiol.* 5, 1053–1063.

Glaeser, J., and Overmann, J. (2004). Biogeography, evolution, and diversity of epibionts in phototrophic consortia. *Appl. Environ. Microbiol.* 70, 4821–4830.

Gorlenko, W. M., and Kusnezow, S. I. (1972). Über die photosynthetisierenden bakterien des kononjer-sees. *Arch. Hydrobiol.* 70, 1–13.

Griebenow, K., and Holzwarth, A. R. (1989). Pigment organization and energy transfer in green bacteria 1. Isolation of native chlorosomes free of bound bacteriochlorophyll *a* from *Chloroflexus aurantiacus* by gel-electrophoretic filtration. *Biochim. Biophys. Acta* 973, 235–240.

Huber, H., Hohn, M. J., Stetter, K. O., and Rachel, R. (2003). The phylum Nanoarchaeota: present knowledge and future perspectives of a unique form of life. *Res. Microbiol.* 154, 165–171.

Iino, T., Mori, K., Uchino, Y., Nakagawa, T., Harayama, S., and Suzuki, K. I. (2010). *Ignavibacterium album* gen. nov., sp. nov., a moderately thermophilic anaerobic bacterium isolated from microbial mats at a terrestrial hot spring and proposal of Ignavibacteria classis nov., for a novel lineage at the periphery of green sulfur bacteria. *Int. J. Sys. Evol. Microbiol.* 60, 1376–1382.

Ishii, S., Kosaka, T., Hori, K., Hotta, Y., and Watanabe, K. (2005). Coaggregation facilitates interspecies hydrogen transfer between *Pelotomaculum thermopropionicum* and *Methanothermobacter thermautotrophicus*. *Appl. Environ. Microbiol.* 71, 7838–7845.

Jagmann, N., Brachvogel, H. P., and Philipp, B. (2010). Parasitic growth of *Pseudomonas aeruginosa* in co-culture with the chitinolytic bacterium *Aeromonas hydrophila*. *Environ. Microbiol.* 12, 1787–1802.

Jahn, U., Gallenberger, M., Paper, W., Junglas, B., Eisenreich, W., Stetter, K. O., Rachel, R., and Huber, H. (2008). *Nanoarchaeum equitans* and *Ignicoccus hospitalis*: new insights into a unique, intimate association of two archaea. *J. Bacteriol.* 190, 1743–1750.

Jahn, U., Summons, R., Sturt, H., Grosjean, E., and Huber, H. (2004). Composition of the lipids of *Nanoarchaeum equitans* and their origin from its host *Ignicoccus* sp. strain KIN4/I. *Arch. Microbiol.* 182, 404–413.

Junglas, B., Briegel, A., Burghardt, T., Walther, P., Wirth, R., Huber, H., and Rachel, R. (2008). *Ignicoccus hospitalis* and *Nanoarchaeum equitans*: ultrastructure, cell-cell interaction, and 3D reconstruction from serial sections of freeze-substituted cells and by electron cryotomography. *Arch. Microbiol.* 190, 395–408.

Kanzler, B. E. M., Pfannes, K. R., Vogl, K., and Overmann, J. (2005). Molecular characterization of the non-photosynthetic partner bacterium in the consortium "*Chlorochromatium aggregatum*." *Appl. Environ. Microbiol.* 71, 7434–7441.

Krembs, C., Juhl, A. R., Long, R. A., and Azam, F. (1998). Nanoscale patchiness of bacteria in lake water studied with the spatial information preservation method. *Limnol. Oceanogr.* 43, 307–314.

Lauterborn, R. (1906). Zur Kenntnis der sapropelischen flora. *Allg. Bot. Z.* 12, 196–197.

Lodwig, E. M., Hosie, A. H. F., Bourdès, A., Findlay, K., Allaway, D., Karunakaran, R., Downie, J. A., and Poole, P. S. (2003). Amino-acid cycling drives nitrogen fixation in the legume-*Rhizobium* symbiosis. *Nature* 422, 722–726.

Marschall, E., Jogler, M., Henssge, U., and Overmann, J. (2010). Large-scale distribution and activity patterns of an extremely low-light-adapted population of green sulfur bacteria in the Black Sea. *Environ. Microbiol.* 12, 1348–1362.

McInerney, M. J. (1986). Transient and persistent associations among prokaryotes. *Bacteria Nat.* 2, 293–338.

Melkozernov, A. N., Barber, J., and Blankenship, R. E. (2006). Light harvesting in photosystem I supercomplexes. *Biochemistry* 45, 331–345.

Minic, Z., and Hervé, G. (2003). Arginine metabolism in the deep sea tube worm *Riftia pachyptila* and its bacterial endosymbiont. *J. Biol. Chem.* 278, 40527–40533.

Mira, A., Ochman, H., and Moran, N. A. (2001). Deletional bias and the evolution of bacterial genomes. *Trends Genet.* 17, 589–596.

Montano, G. A., Bowen, B. P., LaBelle, J. T., Woodbury, N. W., Pizziconi, V. B., and Blankenship, R. E. (2003). Characterization of *Chlorobium tepidum* chlorosomes: a calculation of bacteriochlorophyll *c* per chlorosome and oligomer modeling. *Biophys. J.* 85, 2560–2565.

Moran, N. A., McCutcheon, J. P., and Nakabachi, A. (2008). Genomics and evolution of heritable bacterial symbionts. *Annu. Rev. Genet.* 42, 165–190.

Moran, P. J., Cheng, Y., Cassell, J. L., and Thompson, G. A. (2002). Gene expression profiling of *Arabidopsis thaliana* in compatible plant-aphid interactions. *Arch. Insect Biochem. Physiol.* 51, 182–203.

Müller, N., Griffin, B. M., Stingl, U., and Schink, B. (2008). Dominant sugar utilizers in sediment of Lake Constance depend on syntrophic cooperation with methanogenic partner organisms. *Environ. Microbiol.* 10, 1501–1511.

Mullineaux, C. W., Mariscal, V., Nenninger, A., Khanum, H., Herrero, A., Flores, E., and Adams, D. G. (2008). Mechanism of intercellular molecular exchange in heterocyst-forming cyanobacteria. *EMBO J.* 27, 1299–1308.

Orphan, V. J., House, C. H., Hinrichs, K. U., McKeegan, K. D., and DeLong, E. F. (2001). Methane-consuming archaea revealed by directly coupled isotopic and phylogenetic analysis. *Science* 293, 484–487.

Overmann, J. (2001a). "Green sulfur bacteria," in *Bergey´s Manual of Systematic Bacteriology,* 2nd Edn. Vol. 1, eds D. R. Boone and R. W. Castenholz (Baltimore: Williams and Wilkins), 601–630.

Overmann, J. (2001b)."Phototrophic consortia: a tight cooperation between non-related eubacteria," in *Symbiosis: Mechanisms and Model Systems,* ed. J. Seckbach (Dordrecht: Kluwer Academic Publishers), 239–255.

Overmann, J., Cypionka, H., and Pfennig, N. (1992). An extremely low-light-adapted phototrophic sulfur bacterium from the Black Sea. *Limnol. Oceanogr.* 37, 150–155.

Overmann, J., Lehmann, S., and Pfenning, N. (1991). Gas vesicle formation and buoyancy regulation in *Pelodictyon phaeoclathratiforme* (Green sulfur bacteria). *Arch. Microbiol.* 157, 29–37.

Overmann, J., and Schubert, K. (2002). Phototrophic consortia: model systems for symbiotic interrelations between prokaryotes. *Arch. Microbiol.* 177, 201–208.

Overmann, J., Tuschak, C., Sass, H., and Fröstl, J. (1998). The ecological niche of the consortium "*Pelochromatium roseum.*" *Arch. Microbiol.* 169, 120–128.

Paerl, H. W., and Kellar, P. E. (1978). Significance of bacterial (Cyanophyceae) *Anabaena* associations with respect to N_2 fixation in freshwater. *J. Phycol.* 14, 254–260.

Peduzzi, S., Tonolla, M., and Hahn, D. (2003). Isolation and characterization of aggregate-forming sulfate-reducing and purple sulfur bacteria from the chemocline of meromictic Lake Cadagno, Switzerland. *FEMS Microbiol. Ecol.* 45, 29–37.

Perfiliev, B. V. (1914). On the theory of symbiosis of '*Chlorochromatium aggregatum*' Lauterb. (*Chloronium mirabile Buder*) and *Cylindrogloea bacterifera* nov. gen., nov. spec. (in Russian). *Mikrobiol. Petrogr.* 1, 222–225.

Perna, N. T., Plunkett, G., Burland, V., Mau, B., Glasner, J. D., Rose, D. J., Mayhew, G. F., Evans, P. S., Gregor, J., Kirkpatrick, H. A., Pósfai, G., Hackett, J., Klink, S., Boutin, A., Shao, Y., Miller, L., Grotbeck, E. J., Davis, N. W., Lim, A., Dimalanta, E. T., Potamousis, K. D., Apodaca, J., Anantharaman, T. S., Lin, J., Yen, G., Schwartz, D. C., Welch, R. A., and Blattner, F. R. (2001). Genome sequence of enterohaemorrhagic *Escherichia coli* O157:H7. *Nature* 409, 529–533.

Pernthaler, A., Dekas, A. E., Brown, C. T., Goffredi, S. K., Embaye, T., and Orphan, V. J. (2008). Diverse syntrophic partnerships from deep-sea methane vents revealed by direct cell capture and metagenomics. *Proc. Natl. Acad. Sci. U.S.A.* 105, 7052–7057.

Pfannes, K. R. (2007). *Characterization of the Symbiotic Bacterial Partners in Phototrophic Consortia.* Dissertation, University of Munich, 180p.

Pfannes, K. R., Vogl, K., and Overmann, J. (2007). Heterotrophic symbionts of phototrophic consortia: members of a novel diverse cluster of Betaproteobacteria characterized by a tandem rrn operon structure. *Environ. Microbiol.* 9, 2782–2794.

Pfennig, N. (1978). "General physiology and ecology of photosynthetic bacteria", in *The Photosynthetic Bacteria,* eds R. K. Clayton and W. R.Sistrom (New York, NY: Plenum Press), 3–18.

Pfennig, N. (1980). "Syntrophic mixed cultures and symbiotic consortia with phototrophic bacteria: a review," in *Anaerobes and Anaerobic Infections*, eds G. Gottschalk and P. N. Werner (Stuttgart, NY: Fischer), 127–131.

Podar, M., Anderson, I., Makarova, K. S., Elkins, J. G., Ivanova, N., Wall, M. A., Lykidis, A., Mavromatis, K., Sun, H., Hudson, M. E., Chen, W., Deciu, C., Hutchison, D., Eads, J. R., Anderson, A., Fernandes, F., Szeto, E., Lapidus, A., Kyrpides, N. C., Saier, M. H., Richardson, P. M., Rachel, R., Huber, H., Eisen, J. A., Koonin, E. V., Keller, M., and Stetter, K. O. (2008). A genomic analysis of the archaeal system *Ignicoccus hospitalis-Nanoarchaeum equitans. Genome Biol.* 9, R158.

Prell, J., White, J. P., Bourdes, A., Bunnewell, S., Bongaerts, R. J., and Poole, P. S. (2009). Legumes regulate Rhizobium bacteroid development and persistence by the supply of branched-chain amino acids. *Proc. Natl. Acad. Sci. U.S.A.* 106, 12477–12482.

Reva, O., and Tümmler, B. (2008). Think big – Giant genes in bacteria. *Environ. Microbiol.* 10, 768–777.

Schink, B. (1992). "Syntrophism among prokaryotes," in *The Prokaryotes,* 2nd edn. eds A. Balows, H. G. Trüper, M. Dworkin, W. Harder, and K.-H. Schleifer (New York, NY: Springer Verlag), 276–299.

Sirevag, R., and Ormerod, J. G. (1970). Carbon dioxide fixation in green sulphur bacteria. *Biochem. J.* 120, 399–408.

Skuja, H. (1956). Taxonomische und biologische Studien über das Phytoplankton schwedischer Binnengewässer. *Nova. Acta. Reg. Soc. Sci. Upsal. Ser 4* 16, 1–404.

Trüper, H. G., and Pfennig, N. (1971). Family of phototrophic green sulfur bacteria: *Chlorobiaceae Copeland*, the correct family name; rejection of *Chlorobacterium Lauterborn*; and the taxonomic situation of the consortium-forming species. *Int. J. Syst. Bacteriol.* 21, 8–10.

Tuschak, C., Glaeser, J., and Overmann, J. (1999). Specific detection of green sulfur bacteria by *in situ* hybridization with a fluorescently labeled oligonucleotide probe. *Arch. Microbiol.* 171, 265–272.

Uyeda, K., and Rabinowitz, J. C. (1971). Pyruvate-ferredoxin oxidoreductase. IV. Studies on the reaction mechanism. *J. Biol. Chem.* 246, 3120–3125.

Van Grondelle, R., Hunter, C. N., Bakker, J. G. C., and Kramer, H. J. M. (1983). Size and structure of antenna complexes of photosynthetic bacteria as studied by singlet-singlet quenching of the bacteriochlorophyll fluorescence yield. *Biochim. Biophys. Acta.* 723, 30–36.

Veldhuis, M. J. W., and van Gemerden, H. (1986). Competition between purple and brown phototrophic bacteria in stratified lakes: sulfide, acetate, and light as limiting factors. *FEMS Microbiol. Lett.* 38, 31–38.

Vogl, K., Glaeser, J., Pfannes, K. R., Wanner, G., and Overmann, J. (2006). *Chlorobium chlorochromatii* sp. nov., a symbiotic green sulfur bacterium isolated from the phototrophic consortium "*Chlorochromatium aggregatum*." *Arch. Microbiol.* 185, 363–372.

Vogl, K., Wenter, R., Dressen, M., Schlickenrieder, M., Ploscher, M., Eichacker, L., and Overmann, J. (2008). Identification and analysis of four candidate symbiosis genes from '*Chlorochromatium aggregatum*', a highly developed bacterial symbiosis. *Environ. Microbiol.* 10, 2842–2856.

Wanner, G., Vogl, K., and Overmann, J. (2008). Ultrastructural characterization of the prokaryotic symbiosis in "*Chlorochromatium aggregatum*." *J. Bacteriol.* 190, 3721–3730.

Warthmann, R., Cypionka, H., and Pfennig, N. (1992). Photoproduction of H_2 from acetate by syntrophic cocultures of green sulfur bacteria and sulfur-reducing bacteria. *Arch. Microbiol.* 157, 343–348.

Waters, E., Hohn, M. J., Ahel, I., Graham, D. E., Adams, M. D., Barnstead, M., Beeson, K. Y., Bibbs, L., Bolanos, R., Keller, M., Kretz, K., Lin, X., Mathur, E., Ni, J., Podar, M., Richardson, T., Sutton, G. G., Simon, M., Soll, D., Stetter, K. O., Short, J. M., and Noordewier, M. (2003). The genome of *Nanoarchaeum equitans*: insights into early archaeal evolution and derived parasitism. *Proc. Natl. Acad. Sci. U.S.A.* 100, 12984–12988.

Wenter, R., Hütz, K., Dibbern, D., Li, T., Reisinger, V., Ploscher, M., Eichacker, L., Eddie, B., Hanson, T., Bryant, D. A., and Overmann, J. (2010). Expression-based identification of genetic determinants of the bacterial symbiosis '*Chlorochromatium aggregatum*'. *Environ. Microbiol.* 12, 2259–2276.

Whitman, W. B., Coleman, D. C., and Wiebe, W. J. (1998). Prokaryotes: the unseen majority. *Proc. Natl. Acad. Sci. U.S.A.* 95, 6578–6583.

Zehnder, A. J. B., Ingvorsen, K., and Marti, T. (1982). "Microbiology of methane bacteria," in *Anaerobic Digestion*, eds D. E. Hughes, D. A. Stafford, B. I. Wheatley, W. Baader, G. Lettinga, E. J. Nyns, W. Verstraete, and R. L. Wentworth (Amsterdam: Elsevier Biomedical Press), 45–68.

Conflict of Interest Statement: The authors declare that the research was conducted in the absence of any commercial or financial relationships that could be construed as a potential conflict of interest.

Received: 24 February 2011; paper pending published: 26 April 2011; accepted: 20 June 2011; published online: 05 July 2011. Citation: Müller J and Overmann J (2011) Close interspecies interactions between prokaryotes from sulfureous environments. Front. Microbio. ***2****:146. doi: 10.3389/fmicb.2011.00146*
This article was submitted to Frontiers in Microbial Physiology and Metabolism, a specialty of Frontiers in Microbiology.

frontiers in
MICROBIOLOGY

ORIGINAL RESEARCH ARTICLE
published: 20 June 2011
doi: 10.3389/fmicb.2011.00134

Metatranscriptomic analysis of sulfur oxidation genes in the endosymbiont of *Solemya velum*

Frank J. Stewart[1]*, Oleg Dmytrenko[2], Edward F. DeLong[3] and Colleen M. Cavanaugh[2]

[1] *School of Biology, Georgia Institute of Technology, Atlanta, GA, USA*
[2] *Department of Organismic and Evolutionary Biology, Harvard University, Cambridge, MA, USA*
[3] *Department of Civil and Environmental Engineering, Massachusetts Institute of Technology, Cambridge, MA, USA*

Edited by:
Donald A. Bryant, The Pennsylvania State University, USA

Reviewed by:
Donald A. Bryant, The Pennsylvania State University, USA
Christiane Dahl, Rheinische Friedrich-Wilhelms-Universität Bonn, Germany

***Correspondence:**
Frank J. Stewart, School of Biology, Georgia Institute of Technology, Ford ES&T Building, Room 1242, 311 Ferst Drive, Atlanta, GA 30332, USA.
e-mail: frank.stewart@biology.gatech.edu

Thioautotrophic endosymbionts in the Domain Bacteria mediate key sulfur transformations in marine reducing environments. However, the molecular pathways underlying symbiont metabolism and the extent to which these pathways are expressed *in situ* are poorly characterized for almost all symbioses. This is largely due to the difficulty of culturing symbionts apart from their hosts. Here, we use pyrosequencing of community RNA transcripts (i.e., the metatranscriptome) to characterize enzymes of dissimilatory sulfur metabolism in the model symbiosis between the coastal bivalve *Solemya velum* and its intracellular thioautotrophic symbionts. High-throughput sequencing of total RNA from the symbiont-containing gill of a single host individual generated 1.6 million sequence reads (500 Mbp). Of these, 43,735 matched Bacteria protein-coding genes in BLASTX searches of the NCBI database. The taxonomic identities of the matched genes indicated relatedness to diverse species of sulfur-oxidizing Gammaproteobacteria, including other thioautotrophic symbionts and the purple sulfur bacterium *Allochromatium vinosum*. Manual querying of these data identified 28 genes from diverse pathways of sulfur energy metabolism, including the dissimilatory sulfite reductase (Dsr) pathway for sulfur oxidation to sulfite, the APS pathway for sulfite oxidation, and the Sox pathway for thiosulfate oxidation. In total, reads matching sulfur energy metabolism genes represented 7% of the Bacteria mRNA pool. Together, these data highlight the dominance of thioautotrophy in the context of symbiont community metabolism, identify the likely pathways mediating sulfur oxidation, and illustrate the utility of metatranscriptome sequencing for characterizing community gene transcription of uncultured symbionts.

Keywords: chemosynthesis, endosymbiosis, sulfide, thiosulfate, gene expression

INTRODUCTION

Symbioses between thioautotrophic bacteria and invertebrates perform important steps in the marine sulfur cycle. In these associations, bacteria living intra- or extra-cellularly with a eukaryotic host oxidize reduced sulfur compounds as an energy source for autotrophic CO_2 fixation, providing a substantial source of fixed carbon for the host (Cavanaugh et al., 2006; Dubilier et al., 2008). Such symbioses have been described in 7 host phyla, from ciliates to giant tubeworms (Stewart et al., 2005), and are routinely discovered in new species as marine environments become better explored (Losekann et al., 2008; Fujiwara et al., 2010; Rodrigues et al., 2010). In reducing habitats (e.g., anaerobic sediments, hydrothermal vents, hydrocarbon seeps), these symbioses may dominate the biomass, playing critical roles in local primary production and sulfur transformations (Sievert et al., 2007).

Despite their ubiquity and ecological importance, thioautotrophic symbioses are poorly described molecularly. Characterization of the genes and proteins mediating symbiont metabolism has been hindered by the inability (as of yet) to culture most symbionts outside their hosts. Genomic and metagenomic sequencing has helped reverse this trend, clarifying the genetic basis for diverse biochemical transformations in a handful of thioautotrophic symbioses (Woyke et al., 2006; Newton et al., 2007; Grzymski et al., 2008; Robidart et al., 2008). For example, a comparative genomics approach has been used to characterize the probable sulfur oxidation pathways in two endosymbionts of deep-sea vent clams (family Vesicomyidae; (Harada et al., 2009). However, DNA sequences do not reflect the actual metabolic activity of microorganisms. In contrast, methods that measure gene transcription (transcriptomics) and translation (proteomics) can provide more direct descriptions of symbiont function and metabolism, particularly if administered under *in situ* conditions (Markert et al., 2007; Harada et al., 2009; Wilmes and Bond, 2009).

Notably, technical advancements in RNA amplification and parallel pyrosequencing have made it possible to obtain hundreds of thousands of sequences from the microbial community RNA pool, i.e., the metatranscriptome. Such methods enable inferences of the relative metabolic activity of hundreds of diverse metabolic pathways using transcript abundance as a proxy for gene expression (Frias-Lopez et al., 2008; Stewart et al., 2011b). While metatranscriptomics has been increasingly used to study community metabolism in free-living microorganisms

of the open ocean (Poretsky et al., 2009; Hewson et al., 2010; Stewart et al., 2011a), transcriptomic analysis of marine symbioses has been restricted to only a few taxa, and has focused primarily on host gene expression (Nyholm et al., 2008; Bettencourt et al., 2010). Here, we use pyrosequencing to analyze the *in situ* metatranscriptome of a model thiotrophic symbiont, the bacterial endosymbiont of the coastal bivalve *Solemya velum*, focusing specifically on transcripts encoding proteins of dissimilatory sulfur metabolism.

Studies of the protobranch *S. velum* and its endosymbiont were some of the first to describe the physiology and ecology of thioautotrophic symbioses (see review in Stewart and Cavanaugh, 2006). *S. velum* lives in shallow, sulfur-rich sediments along the Atlantic Coast (Florida to Canada), obtaining the bulk of its nutrition (>97% of host carbon) from a dense population of autotrophic bacteria living within specialized cells of the host gills (Cavanaugh, 1983; Krueger et al., 1992). Early molecular evidence (16S rRNA gene sequence) suggested that the symbiont population consists of a single, unique bacterial phylotype within the Gammaproteobacteria (Eisen et al., 1992). Sulfur-based autotrophy in the symbiont population was initially demonstrated through physiological and molecular studies showing (1) the activity and corresponding gene sequence for ribulose 1,5-bisphosphate carboxylase–oxygenase (RubisCO), the primary CO_2-fixing enzyme of the Calvin cycle, in host gills (Cavanaugh, 1983; Schwedock et al., 2004), (2) an increase in symbiont CO_2 fixation and oxygen consumption in response to sulfide and thiosulfate addition (Cavanaugh, 1983; Anderson et al., 1987), and (3) the activity of two enzymes in the APS pathway mediating sulfite oxidation, APS reductase, and ATP sulfurylase (Chen et al., 1987). While these data confirm that *S. velum* symbionts can oxidize reduced sulfur for energy, the full biochemical pathway through which this occurs, and the extent to which this pathway is expressed, remains uncharacterized.

Here, pyrosequencing of the symbiont-enriched RNA fraction from *S. velum* sampled from the environment revealed a strong representation by genes of dissimilatory sulfur metabolism in the total transcript pool. These results underscore the importance of thioautotrophy in the symbiosis, identify the likely pathways by which sulfur oxidation occurs, and illustrate the utility of metatranscriptome sequencing for characterizing symbiont community metabolism across thousands of genes.

MATERIALS AND METHODS

SAMPLE COLLECTION

Individuals of *S. velum* were collected at low tide from Bluff Hill Cove, Point Judith Pond, Rhode Island (RI; 41.380°N, −71.502°W) on 5 December 2009. Bluff Hill Cove is connected to the ocean by a narrow inlet and bordered by extensive mud flats that support a stable and abundant population of *S. velum*. At the time of collection the average sediment temperature was 8°C. Individuals were dissected in the field upon collection, with symbiont-containing gill tissue placed immediately into RNAlater® and stored frozen until RNA extraction.

SYMBIONT RNA EXTRACTION AND ENRICHMENT

Symbiont-containing gill tissue of a single host individual was lysed using a FastPrep FP120 tissue homogenizer (Savant) with 770–1180 μm glass beads. Total gill RNA (symbiont + host) was extracted with a chloroform–ethanol method using miRNeasy Mini Kit (Qiagen) according to the protocol for purification of total RNA, including small RNA, from animal cells. An aliquot of total RNA was then enriched for symbiont RNA using the MICROBEnrich™ kit (Ambion) according to the manufacturer's instructions. The kit employs capture oligonucleotides and subtractive hybridization to selectively remove eukaryotic polyadenylated mRNAs, enriching for non-polyadenylated prokaryotic RNA. This kit is also designed to remove eukaryotic 18S and 28S rRNA. However, because capture oligonucleotides for rRNA removal are optimized for use with mammalian 18S/28S sequences (Ambion internal documentation), the removal efficiency of bivalve host rRNA was anticipated to be low.

RNA AMPLIFICATION AND cDNA SYNTHESIS

Symbiont-enriched RNA was linearly amplified and converted to cDNA as described in Frias-Lopez et al. (2008), Shi et al. (2009). Briefly, using the MessageAmp™ II-Bacteria kit (Ambion), total RNA was polyadenylated, converted to double-stranded cDNA via reverse transcription, and then transcribed *in vitro* to produce large quantities (tens of micrograms) of single-stranded antisense RNA. Amplified RNA was then converted to double-stranded cDNA using the SuperScript® III First-Strand Synthesis System (Invitrogen) with priming via random hexamers for first-strand synthesis, and the SuperScript™ Double-Stranded cDNA synthesis kit (Invitrogen) for second-strand synthesis. cDNA was then purified with the QIAquick PCR purification kit (Qiagen), digested with *Bpm*I to remove poly(A) tails, and used directly for pyrosequencing.

SEQUENCING

Purified cDNA was used for the generation of single-stranded DNA libraries and emulsion PCR via standard protocols (454 Life Sciences, Roche). Amplified library fragments were sequenced via a single full plate run on a Roche Genome Sequencer FLX instrument using Titanium series chemistry. Sequencing yields are shown in **Table 1**.

Table 1 | Metatranscriptome read statistics.

Total reads	1,591,449
Mean length (bp)	316
Mean GC%	50.1
Non-rRNA reads[1]	203,641
Protein-coding reads[2]	70,427
Bacteria (%)	62.1
Eukarya (%)	37.3
Other (%)	0.6

[1] *Reads not matching ribosomal RNA genes.*

[2] *Reads with significant matches (bit score > 50) to protein-coding genes in NCBI-nr; designation as Bacteria or Eukarya according to NCBI annotations of top BLASTX matches; "other" = Archaeal (0.08%), viral (0.03%), or unclassified (0.48%) genes.*

DATA ANALYSIS

Duplicate sequence reads (reads with 100% nucleotide similarity and identical length), which may arise as artifacts of the pyrosequencing method, were identified as in Stewart et al. (2010) using the program CD-HIT (Li and Godzik, 2006) and removed from the dataset. Non-duplicate reads matching ribosomal RNA genes were identified by BLASTN searches against a custom database of prokaryotic and eukaryotic small and large subunit rRNA nucleotide sequences (5S, 16S, 18S, 23S, 28S rRNA, compiled from microbial genomes and sequences in the ARB SILVA databases, and including the published 16S rRNA gene sequence of the *S. velum* symbiont, http://www.arb-silva.de) and removed from the analysis. Protein-coding gene sequences were identified among the remaining non-duplicate, non-rRNA reads by BLASTX searches against the NCBI non-redundant protein database (NCBI-nr, as of May 2010). The top reference gene(s) matching each read above a bit score cutoff of 50 was used to designate each protein-coding read. For reads having multiple top matches with equal bit score, each matching reference gene was designated a top hit, with its representation scaled proportionate to the number of genes sharing an equal bit score. Read counts per gene were tabulated and normalized as a proportion of the total number of protein-coding reads (or protein-coding reads from the Domain Bacteria) in each sample. The taxonomic identity of protein-coding genes was inferred from the annotation affiliated with each gene, and tabulated according to the NCBI taxonomy using the program MEGAN (Huson et al., 2007).

Detailed analysis of all functional gene categories in the dataset is beyond the scope of this paper, and is the topic of a separate study (Dmytrenko et al., in preparation). Here, we focus only on transcripts matching genes of dissimilatory sulfur metabolism, as detected via BLASTX against all protein-coding genes in NCBI-nr. BLASTX results were manually queried to infer the relative abundance of genes encoding proteins of the primary pathways of dissimilatory sulfur metabolism, including: the dissimilatory sulfite reductase (DsrABCEFHMKLJOPNRS) pathway catalyzing sulfur oxidation to sulfite; the sulfur oxidation (SoxABCDEFGHRSVWXYZ) pathway responsible for thiosulfate oxidation; the APS pathway mediating the conversion of sulfite to sulfate via an APS intermediate, via the enzymes adenosine-5′-phosphosulfate (APS) reductase (AprAB), APS reductase membrane anchor (AprM), quinone-interacting membrane-bound oxidoreductase (QmoABC), and sulfate adenylyltransferase (SAT); and the sulfide oxidation step involving flavocytochrome *c* sulfide dehydrogenase (FccAB) and sulfide–quinone reductase (Sqr), which initiate electron flow from sulfide to the transport chain. When specified, sequence read counts per gene were normalized based on a best approximate gene length (estimated based on full-length open reading frames from sequenced genomes).

SEQUENCE DATA

All transcript sequences generated in this study have been deposited in the Community Cyberinfrastructure for Advanced Microbial Ecology Research and Analysis (CAMERA) Portal for access by the broader scientific community.

RESULTS

READ STATISTICS

Pyrosequencing generated ∼1.6 million sequence reads (∼500 Mbp) from the symbiont-enriched gill metatranscriptome (**Table 1**). Reads matching ribosomal RNA represented 87% of the dataset. Of 284,553 ribosomal reads with top matches to the prokaryotic (Bacteria or Archaea) small subunit rRNA (16S rRNA) gene, 278,192 (98%) matched the published *S. velum* symbiont 16S rRNA sequence at 97% nucleotide identity or greater, with 233,904 (82%) matching at ≥ 99% identity. These results suggest a genetically homogenous microbial population within the *S. velum* gill. However, this pattern does not rule out the co-occurrence of distinct symbiont lineages (strains) within the same host or of non-symbiont microorganisms associated with the gill surface. Our dataset therefore reflects a "meta" transcriptome representing the transcriptional activity of the entire gill-associated microbial community.

TAXONOMIC IDENTITIES OF PROTEIN-CODING READS

Removal of ribosomal RNA reads from the dataset left a total of 203,641 non-rRNA sequences, of which 70,427 (34.7%) matched protein-coding genes in the NCBI-nr database (above bit score 50). Of these, 62.1% matched genes from Bacteria and 37.3% matched genes from Eukarya, with the remainder matching taxonomically unclassified or Archaeal/viral genes (**Table 1**). The relative abundance of Bacteria reads suggests that the symbiont-enrichment protocol used here (see Methods), while not 100% efficient, likely did increase the proportion of symbiont mRNA in the total transcript pool. The proportion of total mRNA in the metatranscriptome could likely have been further enriched by implementing sample-specific methods to remove symbiont and host rRNA reads, e.g., subtractive hybridization with taxon-specific probes (Stewart et al., 2010).

The annotations of NCBI-nr genes can be used to infer the taxonomic relatedness of symbiont and host sequences to reference organisms. Approximately 80% of all protein-coding transcripts from Bacteria matched genes of Gammaproteobacteria as their closest sequence relative (BLASTX searches of NCBI-nr). Among the Gammaproteobacterial reads, nearly half matched species of the Order Chromatiales (**Figure 1**), with the freshwater purple sulfur bacterium *Allochromatium vinosum* DSM 180 constituting over 17% of the Bacteria protein-coding reads (>10% of the total protein-coding reads; **Figures 1–3**). Other highly represented Gammaproteobacteria included the haloalkaliphilic, sulfur-oxidizing species *Thioalkalivibrio* sp. HL-EbGR7 (Chromatiales) and the sulfur-oxidizing symbionts of marine invertebrates, notably *Endoriftia persephone*, the endosymbiont of the hydrothermal vent tubeworm *Riftia pachyptila* (**Figure 2**). The non-Bacteria protein-coding reads in the dataset matched eukaryotes from diverse phyla, suggesting a lack of close relatives to *S. velum* in the database (**Figure 2**).

SULFUR OXIDATION GENES

BLASTX results revealed a dominant role for transcripts matching genes of dissimilatory sulfur oxidation pathways in the symbiont metatranscriptome. The putative functions of proteins encoded

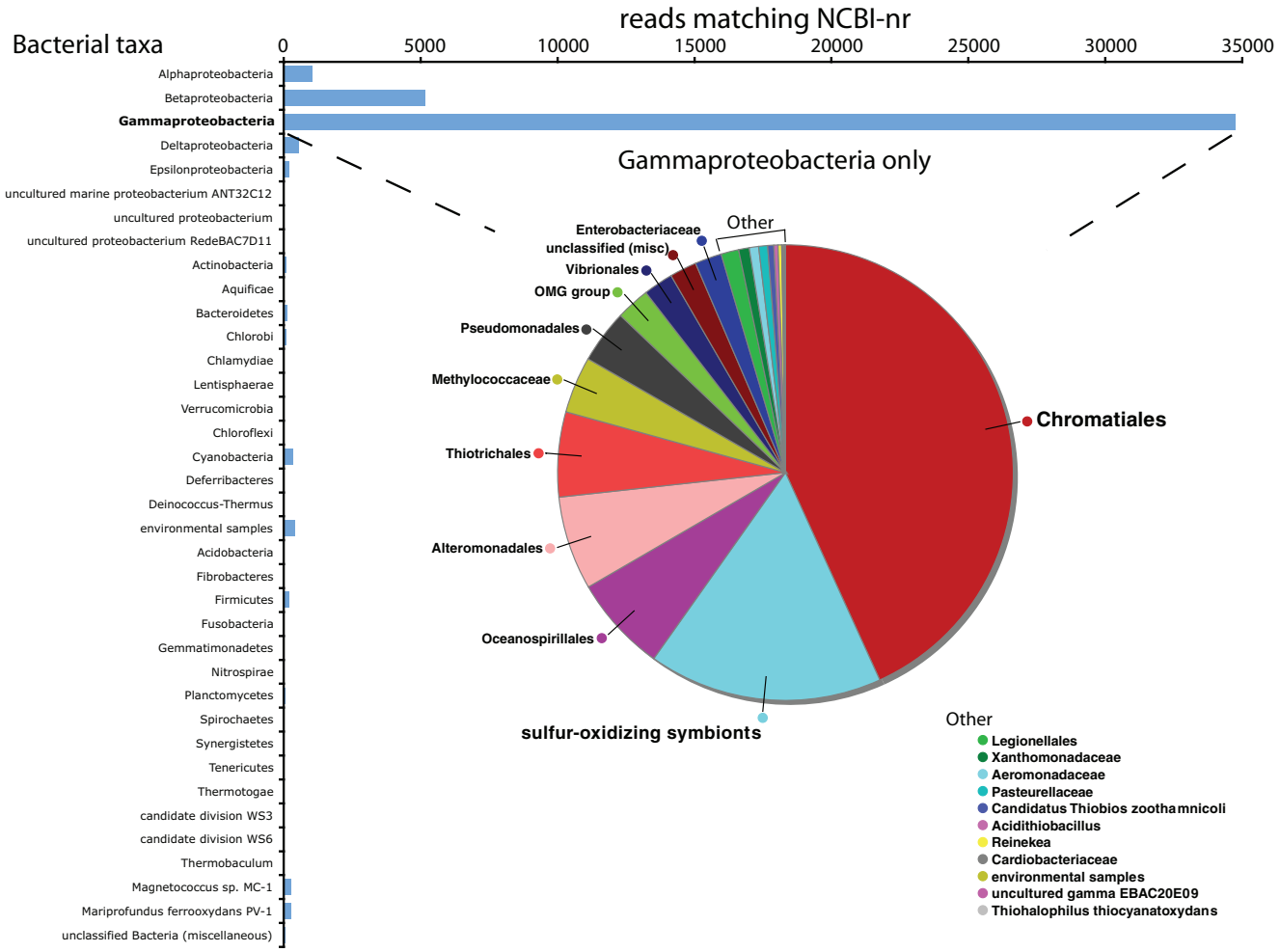

FIGURE 1 | Taxonomic breakdown of all identified protein-coding transcripts assigned to the Domain Bacteria. Inset pie chart shows breakdown within the Gammaproteobacteria, which represented 79.4% of all protein-coding transcripts from the Domain Bacteria.

by these transcripts is inferred here based on the well characterized pathways from model sulfur-oxidizing bacteria, notably the Dsr pathway of the purple sulfur bacterium *A. vinosum* and the Sox pathway of the Alphaproteobacterium *Paracoccus pantotrophus* (for detailed descriptions of these pathways, see (Friedrich et al., 2001, 2005; Dahl et al., 2005; Frigaard and Dahl, 2009; Ghosh and Dam, 2009).

Our analysis revealed 2888 transcript sequences matching a total of 28 genes from the primary sulfur oxidation pathways (**Figure 4**). Of these, 65% (1886 reads) matched 14 genes encoding proteins of the Dsr pathway, including the dissimilatory sulfite reductase enzyme (DsrAB), the DsrAB-interacting flavoprotein DsrL, the transmembrane electron transport complex DsrKMJOP, and the putative sulfur relay molecules DsrEFH and DsrC, with the latter constituting the single most abundant sulfur gene in the transcriptome when read counts were corrected for variation in gene length (circles, **Figure 4A**).

Seven genes of the Sox system were detected, including five genes encoding the core proteins of the thiosulfate oxidation cycle: the SoxAX complex responsible for the fusion of thiosulfate to the carrier complex, the carrier complex SoxYZ, and SoxB, a putative thiol esterase mediating the hydrolytic release of sulfate from sulfur-bound SoxYZ (**Figure 4B**). Two additional *sox* genes, *soxH*, encoding a beta lactamase domain-containing protein, and *soxW*, encoding a periplasmic thioredoxin, were detected at low abundance. In *P. pantotrophus*, neither *soxH* or *soxW* appears necessary for autotrophic growth on thiosulfate (Rother et al., 2001; Bardischewsky et al., 2006).

Several additional sulfur energy metabolism genes were well represented in the transcriptome (**Figure 4**). These included four genes of the APS pathway for sulfite oxidation to sulfate: *aprAB* and *aprM*, encoding APS reductase (adenylylsulfate reductase) and the APS reductase membrane anchor, respectively, and SAT, encoding ATP sulfurylase (sulfate adenylyltransferase). Together, these four genes were represented by 672 sequences (23% of the reads matching sulfur genes). Finally, the analysis detected transcripts encoding two primary enzymes for sulfide oxidation: the membrane-bound sulfide–quinone reductase (Sqr), mediating

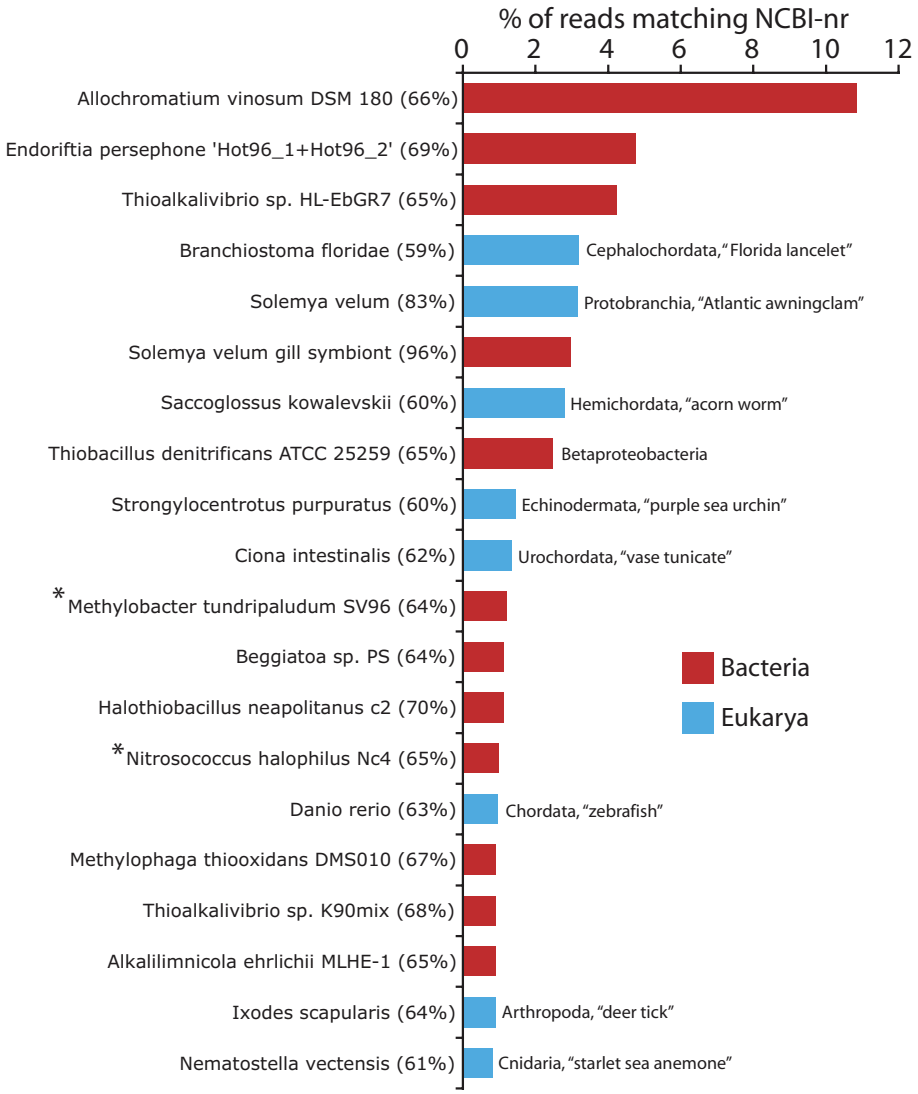

FIGURE 2 | Top 20 taxa from the Domains Bacteria and Eukarya identified as best matches to protein-coding transcripts. All Bacteria taxa (red bars) belong to the Gammaproteobacteria and are putatively capable of chemolithotrophic growth on reduced sulfur compounds, unless otherwise marked (∗ = no evidence of sulfur-based chemolithotrophy). Eukarya (blue bars) are labeled according to phylum or subphylum designation. Numbers in parentheses are the amino acid identities averaged across all sequence reads matching a given taxon as a top BLASTX hit (above bit score 50). Identities reflect only the high-scoring segment pair (HSP) region for each BLAST result; gaps were not included in identity calculations.

electron transport to quinone, and flavocytochrome *c* sulfide dehydrogenase (FccAB), mediating transport to a *c*-type cytochrome (Dahl and Friedrich, 2008).

DISCUSSION

This study provides the first molecular evidence that diverse genes of sulfur energy metabolism are present and actively transcribed in the *S. velum* symbiont population under *in situ* conditions. The metatranscriptome contained Bacteria transcripts encoding genes of several primary sulfur oxidation pathways, including the reverse dissimilatory sulfite reductase (Dsr) complex for sulfur oxidation to sulfite, the adenosine-5′-phosphate (APS) reductase pathway for sulfite oxidation, and the sulfur oxidation (Sox) pathway mediating thiosulfate oxidation. In total, the sulfur oxidation genes identified here ($n = 28$; **Figure 4**) represented 6.6% of the Bacteria protein-coding reads in the dataset (1 in 15 sequences). Several genes encoding enzymes for sulfide and thiosulfate oxidation, including the *dsr* genes and SAT (ATP sulfurylase), were among the top most abundant reference genes (i.e., unique accession numbers) detected in the study (**Figure 3**). Many of these were most closely related to homologs from known sulfur-oxidizing Gammaproteobacteria (**Figures 1–3**), in particular *A. vinosum* and *Endoriftia persephone*, the symbiont of the tubeworm *Riftia pachyptila*, consistent with the phylogenetic placement of the *Solemya* symbiont within this group (Eisen et al., 1992; Distel, 1998). Strikingly, a single reference gene, the previously characterized *cbbL* gene encoding the large subunit of the CO_2 fixation enzyme RubisCO (ribulose 1,5-bisphosphate

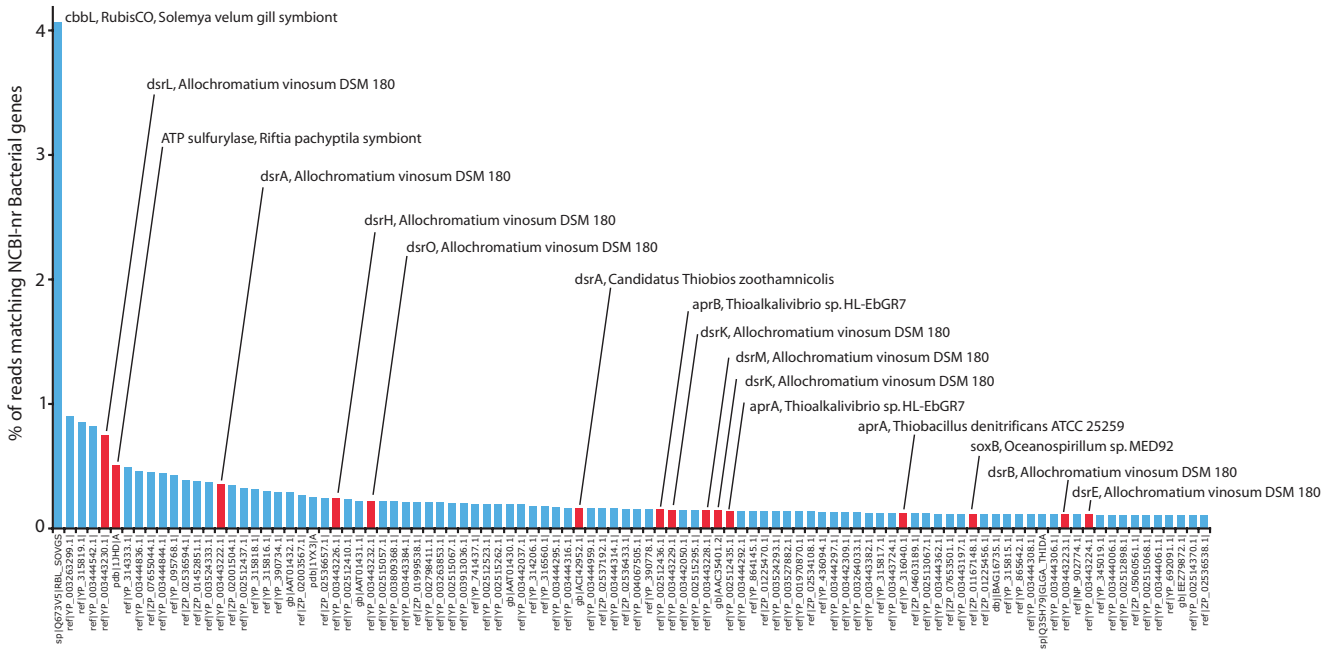

FIGURE 3 | Top 100 most abundant reference genes (unique accession numbers) in the Domain Bacteria detected in the metatranscriptome, as a percentage of the total sequence reads matching Bacteria genes in the NCBI-nr database (accession numbers at bottom). Red bars indicate genes involved in sulfur-based energy metabolism.

carboxylase–oxygenase) of the *S. velum* symbiont, accounted for over 4% of all protein-coding reads (**Figure 3**). The high abundance of transcripts for enzymes of sulfur compound oxidation and carbon fixation suggests that thioautotrophy dominated symbiont community metabolism at the time of collection in early winter.

Genes of the reverse Dsr pathway were among the most highly expressed in the symbiont metatranscriptome (**Figures 3** and **4**). In sulfate-reducing Bacteria and Archaea, dissimilatory sulfite reductase (DsrAB) mediates sulfite reduction to sulfide (Klein et al., 2001; Wagner et al., 2005). DsrAB homologs have been isolated from a wide variety of sulfur-oxidizing taxa (Loy et al., 2009), in which the enzymes are thought to operate in the oxidative direction in conjunction with a diverse set of accessory proteins, including the transmembrane complex DsrMKJOP, the sulfur shuttle molecules DsrEFH and DsrC, and the cytoplasmic flavoprotein DsrL (Dahl et al., 2005; Ghosh and Dam, 2009), all of which were detected in the *Solemya* symbiont transcriptome (**Figure 4**). It has been suggested that sulfide for oxidation by the DsrAB complex is released via the reduction of a polysulfur carrier molecule, as catalyzed by the NADH: (acceptor) oxidoreductase activity of DsrL (Dahl et al., 2005), which has been shown to be critical for sulfur oxidation in *A. vinosum* (Lubbe et al., 2006). In this species, the carrier molecule may be an organic perthiol involved with bringing stored elemental sulfur (sulfur globules) from the periplasm to the cytoplasm (Frigaard and Dahl, 2009). Stored sulfur globules in *A. vinosum* are produced during growth on sulfide by enzymes including FccAB and Sqr or via the activity of the Sox pathway during growth on thiosulfate (Frigaard and Dahl, 2009; Ghosh and Dam, 2009). Interestingly, the deposition of sulfur storage globules, while common in other thioautotrophic symbionts (e.g., *Endoriftia persephone*), has not been observed in *Solemya*, suggesting a potentially rapid turnover of elemental sulfur compounds by an active Dsr system. While the exact roles of Dsr enzymes remain to be confirmed in the *Solemya* symbiont, our data indicate a prominent role for sulfur oxidation to sulfite in this symbiosis.

Consistent with this finding, transcripts encoding the APS pathway for sulfite oxidation were abundant in the dataset. Use of the APS pathway by *Solemya* symbionts was established previously by enzyme assays showing the activity of APS reductase (AprAB) and ATP sulfurylase (SAT; Chen et al., 1987). Together, these enzymes catalyze the AMP-dependent oxidation of sulfite to APS and the subsequent ATP-generating conversion of APS to sulfate (**Figure 4**). Here, AprAB and SAT-encoding transcripts represented a combined 1.5% of all protein-coding Bacteria reads. Additionally, transcripts encoding the transmembrane anchor AprM were detected at low abundance. In other Bacteria taxa, electron transport from the cytoplasmic APS reductase to the membrane quinol/quinone pool is mediated via interactions with either AprM, which is more common in Gammaproteobacterial sulfur-oxidizers (e.g., *A. vinosum*), or the functionally associated membrane-bound redox complex QmoABC, common in green sulfur bacteria of the Order Chlorobiales (Meyer and Kuever, 2007). Here, detection of *aprM* but not *qmoABC* transcripts is consistent with the placement of the *Solemya* symbiont among the Gammaproteobacteria. Together, these data suggest a functional sulfite oxidation complex in this symbiosis.

The detection of transcripts matching genes of the Sox pathway also confirmed an active role for thiosulfate oxidation in

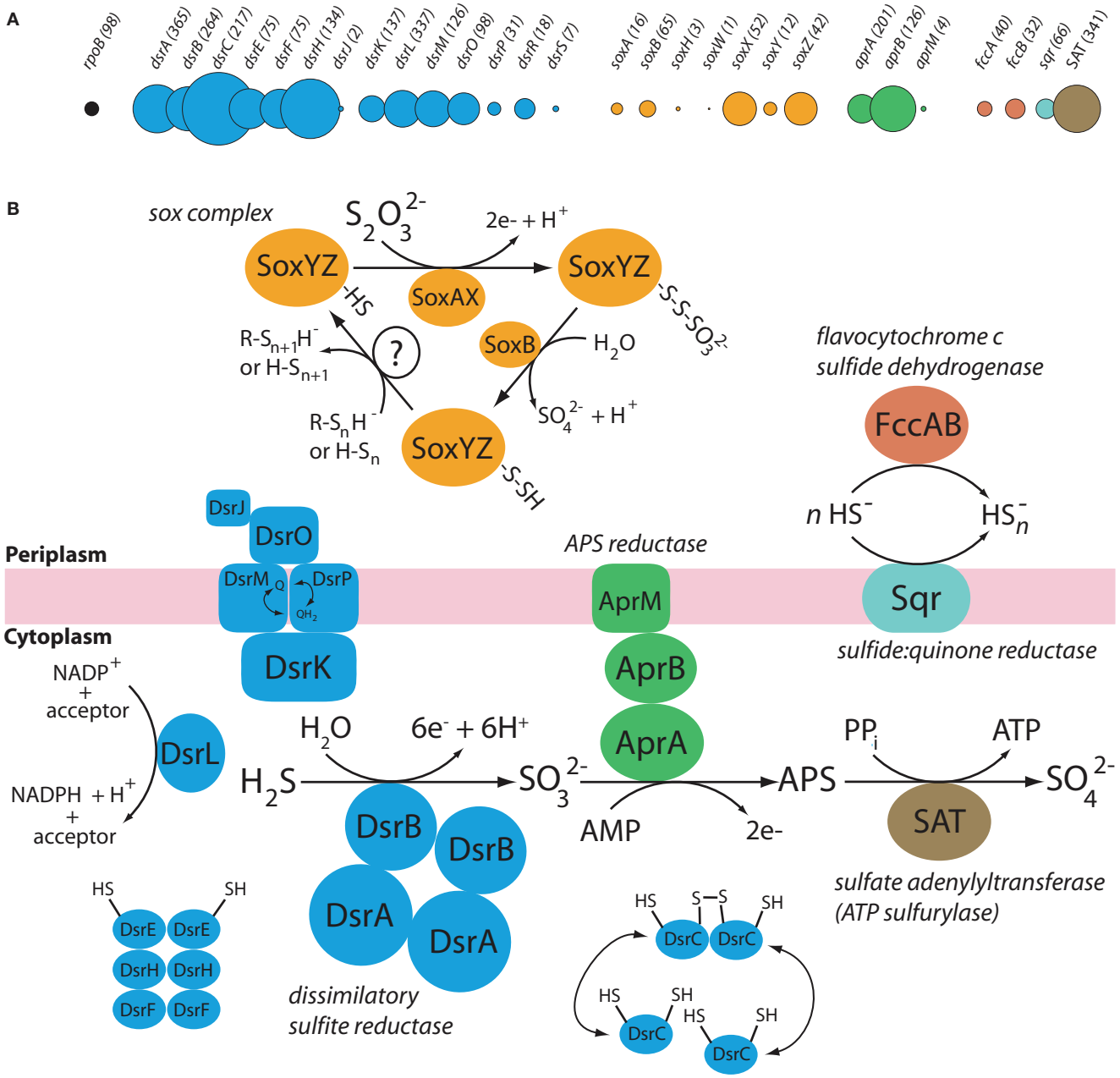

FIGURE 4 | Relative abundance of transcripts encoding key enzymes of sulfur energy metabolism in the *Solemya velum* symbiont metatranscriptome. (A) Abundances of transcripts with top matches (BLASTX) to dissimilatory sulfur metabolism genes, shown relative to the abundance of transcripts matching RNA polymerase subunit B (*rpoB*), which typically occurs in a single copy per Bacteria genome. Numbers = read counts per gene. Circle area = read counts per gene normalized to the approximate gene length (in kilobases) inferred from published genomes. Sequences matching the same gene from different organisms have been pooled, in contrast to the data in **Figure 3**. **(B)** Putative metabolic function of corresponding enzymes, according to Dahl et al. (2005) and Frigaard and Dahl (2009). *dsr* = dissimilatory sulfite reductase gene cluster, *sox* = sulfur oxidation gene cluster; *aprAB* = adenosine-5′-phosphosulfate (APS) reductase; *aprM*, APS reductase membrane anchor; *fccAB*, flavocytochrome *c* sulfide dehydrogenase; SQR, sulfide–quinone reductase; SAT, sulfate adenylyltransferase.

S. velum symbionts. The Sox (sulfur oxidation) pathway mediates the oxidation of thiosulfate to sulfate in a variety of both non-photosynthetic and photosynthetic sulfur-oxidizing bacteria (Frigaard and Dahl, 2009; Ghosh and Dam, 2009; Sakurai et al., 2010). The pathway has been extensively studied in the Alphaproteobacterium *Paracoccus pantotrophus*, in which 15 genes soxRSVWXYZABCDEFGH comprise the *sox* operon (Friedrich et al., 2001, 2005; Rother et al., 2001). Of these, seven genes (*soxABCDXYZ*) encode the core periplasmic sox proteins, SoxB, SoxXA, SoxYZ, and SoxCD, with SoxYZ acting as the primary

carrier molecule at every step in the pathway (Friedrich et al., 2001; **Figure 4**). Analysis of the *S. velum* symbiont metatranscriptome revealed transcripts matching two peripheral sox genes (*soxHW*) at low abundance and five of the seven core sox genes (*soxABXYZ*) at higher abundances (**Figure 4**). Transcripts encoding the sulfur dehydrogenase SoxCD were not detected in our analysis, consistent with the absence of these genes from the genomes of a variety of green and purple sulfur bacteria, including *A. vinosum* and the endosymbionts of deep-sea clams and tubeworms (Frigaard and Dahl, 2009; Harada et al., 2009). Alternatively, it is possible that soxC and *soxD* are present in the symbiont genome, but were not transcribed (above the level of detection) at the time of collection. In organisms lacking *soxCD*, the sulfur atom of the sulfane intermediate (SoxYZ-S-SH, **Figure 4**) is transferred to other acceptor substrates (RS_nH^- and $^-HS_n^-$ in **Figure 4**) and eventually into sulfur storage globules, or enters other sulfur oxidation pathways (Sauve et al., 2007; Frigaard and Dahl, 2009). The deposition of elemental sulfur globules has not yet been demonstrated for *S. velum*. However, the potential for globule storage under varying concentrations of thiosulfate or sulfide has not yet been exhaustively explored.

IMPLICATIONS

Our metatranscriptome data indicates the use of diverse pathways for both sulfide and thiosulfate oxidation by *S. velum* symbionts under environmental conditions, consistent with prior experiments showing that both substrates stimulate symbiont carbon fixation (Cavanaugh, 1983; Scott and Cavanaugh, 2007). The utilization of multiple sulfur oxidation pathways is not unusual among thioautotrophic bacteria and is likely related to substrate availability (Ghosh and Dam, 2009). For the endosymbionts of deep-sea clams, which share a complement of sulfur oxidation genes similar to that in *S. velum* symbionts (Kuwahara et al., 2007; Newton et al., 2007), it has been argued that the ability to oxidize both thiosulfate (Sox system) and sulfide (Dsr, Sqr/Fcc) is linked to the relative abundance of these compounds in the clam microhabitat (basaltic cracks and fissures in zones of diffuse-flow venting; Harada et al., 2009). In contrast, the endosymbiont of the tubeworm *Riftia pachyptila* putatively lacks the Sox pathway (Markert et al., 2007; Robidart et al., 2008), which may reflect an adaptation to a greater reliance on sulfide in the zones surrounding black smokers where this symbiosis occurs (Nelson and Fisher, 1995; Harada et al., 2009).

For *S. velum*, the relative abundance of reduced sulfur species available for symbiont oxidation has not been directly characterized. The host bivalve lives in coastal muds, positioning itself at the convergence of a Y-shaped burrow (Levinton, 1977) where it can access anoxic water from lower in the sediment. This water is likely enriched in sulfide but may also contain thiosulfate, perhaps resulting from chemical sulfide oxidation during burrow ventilation (Howarth et al., 1983; Elsgaard and Jorgensen, 1992). Alternatively, thiosulfate may also be available via sulfide oxidation by host mitochondria, as has been demonstrated in the Pacific congener *S. reidi* (Obrien and Vetter, 1990). Though both sulfide and thiosulfate can fuel symbiont autotrophy, sulfide has a much stronger effect (sevenfold) on carbon fixation rates in *S. velum* symbionts (Scott and Cavanaugh, 2007), suggesting that the symbiosis is adapted to use sulfide most efficiently.

Our transcriptome data, showing the relative abundance of transcripts in the Dsr and Sqr/Fcc pathways (**Figure 4**), potentially indicates a dominant role for sulfide metabolism in the *S. velum* symbiosis. However, transcript abundance may not be tightly coupled to protein abundance or enzyme activity (Taniguchi et al., 2010) and should be interpreted as a proxy for metabolic activity without supporting biochemical data. In other endosymbioses, namely those involving deep-sea hydrothermal vent clams, diverse sulfur pathways (Sox, Dsr, APS) have been shown to be constitutively expressed under variable environmental conditions (e.g., oxygen concentration; (Harada et al., 2009). However, compared to gene expression in the relatively stable environment of the deep sea, expression of *S. velum* symbiont genes, and the relative reliance on diverse reduced sulfur sources, may be more stochastic given the potential for diel and seasonal variation in the coastal environment.

Metatranscriptomics can now provide a comprehensive molecular framework for interpreting physiochemical measurements of metabolism in uncultured symbionts. Such analyses can be easily integrated into studies exploring the links between sulfur availability, environmental conditions, and symbiont gene expression. Our study confirms that genes of sulfur energy metabolism are a dominant component of the transcriptionally active symbiont gene pool in *S. velum*. Future experiments will help determine the extent to which genes of thioautotrophy co-vary with other metabolic pathways in the transcriptome (Dmytrenko et al., in preparation) and with the biochemical transformations of sulfur mediated by this model symbiosis.

ACKNOWLEDGMENTS

We thank Rachel Barry for preparing cDNA samples for pyrosequencing. Generous support for this study came from the Gordon and Betty Moore Foundation (EFD) and the National Science Foundation (CMC, OCE-0453901).

REFERENCES

Anderson, A. E., Childress, J. J., and Favuzzi, J. A. (1987). Net uptake of CO_2 driven by sulfide and thiosulfate oxidation in the bacterial symbiont containing clam *Solemya reidi*. *J. Exp. Biol.* 133, 1–31.

Bardischewsky, F., Fischer, J., Holler, B., and Friedrich, C. G. (2006). SoxV transfers electrons to the periplasm of *Paracoccus pantotrophus* – an essential reaction for chemotrophic sulfur oxidation. *Microbiology* 152, 465–472.

Bettencourt, R., Pinheiro, M., Egas, C., Gomes, P., Afonso, M., Shank, T., and Santos, R. S. (2010). High-throughput sequencing and analysis of the gill tissue transcriptome from the deep-sea hydrothermal vent mussel *Bathymodiolus azoricus*. *BMC Genomics* 11, 559. doi: 10.1186/1471-2164-11-559

Cavanaugh, C. M. (1983). Symbiotic chemoautotrophic bacteria in marine invertebrates from sulfide rich habitats. *Nature* 302, 58–61.

Cavanaugh, C. M., McKiness, Z. P., Newton, I. L. G., and Stewart, F. J. (2006). "Marine chemosynthetic symbioses," in *The Prokaryotes*, 3rd Edn, eds M. Dworkin, E. Rosenberg, K. H. Schleifer, and E. Stackebrandt (New York: Springer).

Chen, C., Rabourdin, B., and Hammen, C. S. (1987). The effect of hydrogen sulfide on the metabolism of *Solemya velum* and enzymes of sulfide oxidation in gill tissue. *Comp. Biochem. Physiol.* 88, 949–952.

Dahl, C., Engels, S., Pott-Sperling, A. S., Schulte, A., Sander, J., Lubbe, Y., Deuster, O., and Brune, D. C. (2005). Novel genes of the dsr gene cluster and evidence for close interaction of Dsr proteins during sulfur oxidation in the phototrophic sulfur bacterium *Allochromatium vinosum*. *J. Bacteriol.* 187, 1392–1404.

Dahl, C., and Friedrich, C. G. (2008). *Microbial Sulfur Metabolism*. Berlin: Springer-Verlag.

Distel, D. L. (1998). Evolution of chemoautotrophic endosymbioses in bivalves – Bivalve-bacteria chemosymbioses are phylogenetically diverse but morphologically similar. *Bioscience* 48, 277–286.

Dubilier, N., Bergin, C., and Lott, C. (2008). Symbiotic diversity in marine animals: the art of harnessing chemosynthesis. *Nat. Rev. Microbiol.* 6, 725–740.

Eisen, J. A., Smith, S. W., and Cavanaugh, C. M. (1992). Phylogenetic relationships of chemoautotrophic bacterial symbionts of *Solemya velum* say (Mollusca, Bivalvia) determined by 16S ribosomal RNA gene sequence analysis. *J. Bacteriol.* 174, 3416–3421.

Elsgaard, L., and Jorgensen, B. B. (1992). Anoxic transformations of radiolabeled hydrogen sulfide in marine and fresh water sediments. *Geochim. Cosmochim. Acta* 56, 2425–2435.

Frias-Lopez, J., Shi, Y., Tyson, G. W., Coleman, M. L., Schuster, S. C., Chisholm, S. W., and DeLong, E. F. (2008). Microbial community gene expression in ocean surface waters. *Proc. Natl. Acad. Sci. U.S.A.* 105, 3805–3810.

Friedrich, C. G., Bardischewsky, F., Rother, D., Quentmeier, A., and Fischer, J. (2005). Prokaryotic sulfur oxidation. *Curr. Opin. Microbiol.* 8, 253–259.

Friedrich, C. G., Rother, D., Bardischewsky, F., Quentmeier, A., and Fischer, J. (2001). Oxidation of reduced inorganic sulfur compounds by bacteria: emergence of a common mechanism? *Appl. Environ. Microbiol.* 67, 2873–2882.

Frigaard, N. U., and Dahl, C. (2009). Sulfur metabolism in phototrophic sulfur bacteria. *Adv. Microb. Physiol.* 54, 103–200.

Fujiwara, Y., Kawato, M., Noda, C., Kinoshita, G., Yamanaka, T., Fujita, Y., Uematsu, K., and Miyazaki, J. I. (2010). Extracellular and mixotrophic symbiosis in the whale-fall mussel *Adipicola pacifica*: a trend in evolution from extra- to intracellular symbiosis. *PLoS ONE* 5, e11808. doi: 10.1371/journal.pone.0011808

Ghosh, W., and Dam, B. (2009). Biochemistry and molecular biology of lithotrophic sulfur oxidation by taxonomically and ecologically diverse bacteria and archaea. *FEMS Microbiol. Rev.* 33, 999–1043.

Grzymski, J. J., Murray, A. E., Campbell, B. J., Kaplarevic, M., Gao, G. R., Lee, C., Daniel, R., Ghadiri, A., Feldman, R. A., and Cary, S. C. (2008). Metagenome analysis of an extreme microbial symbiosis reveals eurythermal adaptation and metabolic flexibility. *Proc. Natl. Acad. Sci. U.S.A.* 105, 17516–17521.

Harada, M., Yoshida, T., Kuwahara, H., Shimamura, S., Takaki, Y., Kato, C., Miwa, T., Miyake, H., and Maruyama, T. (2009). Expression of genes for sulfur oxidation in the intracellular chemoautotrophic symbiont of the deep-sea bivalve *Calyptogena okutanii*. *Extremophiles* 13, 895–903.

Hewson, I., Poretsky, R. S., Tripp, H. J., Montoya, J. P., and Zehr, J. P. (2010). Spatial patterns and light-driven variation of microbial population gene expression in surface waters of the oligotrophic open ocean. *Environ. Microbiol.* 12, 1940–1956.

Howarth, R. W., Giblin, A., Gale, J., Peterson, B. J., and Luther, G. W. (1983). Reduced sulfur compounds in the pore waters of a New England salt marsh. *Ecol. Bull.* 35, 135–152.

Huson, D. H., Auch, A. F., Qi, J., and Schuster, S. C. (2007). MEGAN analysis of metagenomic data. *Genome Res.* 17, 377–386.

Klein, M., Friedrich, M., Roger, A. J., Hugenholtz, P., Fishbain, S., Abicht, H., Blackall, L. L., Stahl, D. A., and Wagner, M. (2001). Multiple lateral transfers of dissimilatory sulfite reductase genes between major lineages of sulfate-reducing prokaryotes. *J. Bacteriol.* 183, 6028–6035.

Krueger, D. M., Gallager, S. M., and Cavanaugh, C. M. (1992). Suspension feeding on phytoplankton by *Solemya velum*, a symbiont-containing clam. *Mar. Ecol. Prog. Ser.* 86, 145–151.

Kuwahara, H., Yoshida, T., Takaki, Y., Shimamura, S., Nishi, S., Harada, M., Matsuyama, K., Takishita, K., Kawato, M., Uematsu, K., Fujiwara, Y., Sato, Y., Kato, C., Kitagawa, M., Kato, I., and Maruyama, T. (2007). Reduced genome of the thioautotrophic intracellular symbiont in a deep-sea clam, *Calyptogena okutanii*. *Curr. Biol.* 17, 881–886.

Levinton, J. (1977). "Ecology of shallow water – deposit-feeding communities, Quissett Harbor, Massachusetts," in *Ecology of Marine Benthos*, ed. B. C. Coull (Columbia, SC: University of South Carolina Press).

Li, W. Z., and Godzik, A. (2006). Cd-hit: a fast program for clustering and comparing large sets of protein or nucleotide sequences. *Bioinformatics* 22, 1658–1659.

Losekann, T., Robador, A., Niemann, H., Knittel, K., Boetius, A., and Dubilier, N. (2008). Endosymbioses between bacteria and deep-sea siboglinid tubeworms from an Arctic Cold Seep (Haakon Mosby Mud Volcano, Barents Sea). *Environ. Microbiol.* 10, 3237–3254.

Loy, A., Duller, S., Baranyi, C., Mussmann, M., Ott, J., Sharon, I., Beja, O., Le Paslier, D., Dahl, C., and Wagner, M. (2009). Reverse dissimilatory sulfite reductase as phylogenetic marker for a subgroup of sulfur-oxidizing prokaryotes. *Environ. Microbiol.* 11, 289–299.

Lubbe, Y. J., Youn, H. S., Timkovich, R., and Dahl, C. (2006). Siro(haem)amide in *Allochromatium vinosum* and relevance of DsrL and DsrN, a homolog of cobyrinic acid a,c-diamide synthase, for sulphur oxidation. *FEMS Microbiol. Lett.* 261, 194–202.

Markert, S., Arndt, C., Felbeck, H., Becher, D., Sievert, S. M., Hugler, M., Albrecht, D., Robidart, J., Bench, S., Feldman, R. A., Hecker, M., and Schweder, T. (2007). Physiological proteomics of the uncultured endosymbiont of *Riftia pachyptila*. *Science* 315, 247–250.

Nelson, D. C., and Fisher, C. R. (1995). "Chemoautotrophic and methanotrophic endosymbiotic bacteria at deep-sea vents and seeps," in *The Microbiology of Deep-Sea Hydrothermal Vents*, ed. D. M. Karl (CRC Press).

Newton, I. L. G., Woyke, T., Auchtung, T. A., Dilly, G. F., Dutton, R. J., Fisher, M. C., Fontanez, K. M., Lau, E., Stewart, F. J., Richardson, P. M., Barry, K. W., Saunders, E., Detter, J. C., Wu, D., Eisen, J. A., and Cavanaugh, C. M. (2007). The *Calyptogena magnifica* chemoautotrophic symbiont genome. *Science* 315, 998–1000.

Nyholm, S. V., Robidart, J., and Girguis, P. R. (2008). Coupling metabolite flux to transcriptomics: insights into the molecular mechanisms underlying primary productivity by the hydrothermal vent tubeworm *Ridgeia piscesae*. *Biol. Bull.* 214, 255–265.

Obrien, J., and Vetter, R. D. (1990). Production of thiosulfate during sulfide oxidation by mitochondria of the symbiont-containing bivalve *Solemya reidi*. *J. Exp. Biol.* 149, 133–148.

Poretsky, R. S., Hewson, I., Sun, S. L., Allen, A. E., Zehr, J. P., and Moran, M. A. (2009). Comparative day/night metatranscriptomic analysis of microbial communities in the North Pacific subtropical gyre. *Environ. Microbiol.* 11, 1358–1375.

Robidart, J. C., Bench, S. R., Feldman, R. A., Novoradovsky, A., Podell, S. B., Gaasterland, T., Allen, E. E., and Felbeck, H. (2008). Metabolic versatility of the *Riftia pachyptila* endosymbiont revealed through metagenomics. *Environ. Microbiol.* 10, 727–737.

Rodrigues, C. F., Webster, G., Cunha, M. R., Duperron, S., and Weightman, A. J. (2010). Chemosynthetic bacteria found in bivalve species from mud volcanoes of the Gulf of Cadiz. *FEMS Microbiol. Ecol.* 73, 486–499.

Rother, D., Henrich, H. J., Quentmeier, A., Bardischewsky, F., and Friedrich, C. G. (2001). Novel genes of the sox gene cluster, mutagenesis of the flavoprotein SoxF, and evidence for a general sulfur-oxidizing system in *Paracoccus pantotrophus* GB17. *J. Bacteriol.* 183, 4499–4508.

Sakurai, H., Ogawa, T., Shiga, M., and Inoue, K. (2010). Inorganic sulfur oxidizing system in green sulfur bacteria. *Photosyn. Res.* 104, 163–176.

Sauve, V., Bruno, S., Berks, B. C., and Hemmings, A. M. (2007). The SoxYZ complex carries sulfur cycle intermediates on a peptide swinging arm. *J. Biol. Chem.* 282, 23194–23204.

Schwedock, J., Harmer, T. L., Scott, K. M., Hektor, H. J., Seitz, A. P., Fontana, M. C., Distel, D. L., and Cavanaugh, C. M. (2004). Characterization and expression of genes from the RubisCO gene cluster of the chemoautotrophic symbiont of *Solemya velum*: cbbLSQO. *Arch. Microbiol.* 182, 18–29.

Scott, K. M., and Cavanaugh, C. M. (2007). CO_2 uptake and fixation by endosymbiotic chemoautotrophs from the bivalve *Solemya velum*. *Appl. Environ. Microbiol.* 73, 1174–1179.

Shi, Y. M., Tyson, G. W., and DeLong, E. F. (2009). Metatranscriptomics reveals unique microbial small RNAs in the ocean's water column. *Nature* 459, 266–269.

Sievert, S. M., Kiene, R. P., and Schulz-Vogt, H. N. (2007). The sulfur cycle. *Oceanography* 20, 117–123.

Stewart, F. J., and Cavanaugh, C. M. (2006). Bacterial endosymbioses in *Solemya* (Mollusca: Bivalvia): model systems for studies of symbiont-host adaptation. *Antonie Van Leeuwenhoek* 90, 343–360.

Stewart, F. J., Newton, I. L. G., and Cavanaugh, C. M. (2005). Chemosynthetic endosymbioses: adaptations to oxic-anoxic interfaces. *Trends Microbiol.* 13, 439–448.

Stewart, F. J., Ottesen, E. A., and DeLong, E. F. (2010). Development and quantitative analyses of a universal rRNA-subtraction protocol for microbial metatranscriptomics. *ISME J.* 4, 896–907.

Stewart, F. J., Sharma, A. K., Bryant, J. A., Eppley, J. M., and Delong, E. F. (2011a). Community transcriptomics reveals universal patterns of protein sequence conservation in natural microbial communities. 12, R26.

Stewart, F. J., Ulloa, O., and DeLong, E. F. (2011b). Microbial metatranscriptomics in a permanent marine oxygen minimum zone. *Environ. Microbiol.* (in press). doi: 10.1111/j.1462-2920.2010.02400x

Taniguchi, Y., Choi, P. J., Li, G. W., Chen, H. Y., Babu, M., Hearn, J., Emili, A., and Xie, X. S. (2010). Quantifying *E. coli* proteome and transcriptome with single molecule sensitivity in single cells. *Science* 329, 533–538.

Wagner, M., Loy, A., Klein, M., Lee, N., Ramsing, N. B., Stahl, D. A., and Friedrich, M. W. (2005). Functional marker genes for identification of sulfate-reducing prokaryotes. *Environ. Microbiol.* 397, 469–489.

Wilmes, P., and Bond, P. L. (2009). Microbial community proteomics: elucidating the catalysts and metabolic mechanisms that drive the Earth's biogeochemical cycles. *Curr. Opin. Microbiol.* 12, 310–317.

Woyke, T., Teeling, H., Ivanova, N. N., Huntemann, M., Richter, M., Gloeckner, F. O., Boffelli, D., Anderson, I. J., Barry, K. W., Shapiro, H. J., Szeto, E., Kyrpides, N. C., Mussmann, M., Amann, R., Bergin, C., Ruehland, C., Rubin, E. M., and Dubilier, N. (2006). Symbiosis insights through metagenomic analysis of a microbial consortium. *Nature* 443, 950–955.

Conflict of Interest Statement: This research was conducted in the absence of any commercial or financial relationships that could be construed as a potential conflict of interest.

Received: 16 May 2011; paper pending published: 03 June 2011; accepted: 09 June 2011; published online: 20 June 2011.
*Citation: Stewart FJ, Dmytrenko O, DeLong EF and Cavanaugh CM (2011) Metatranscriptomic analysis of sulfur oxidation genes in the endosymbiont of Solemya velum. Front. Microbio. **2**:134. doi: 10.3389/fmicb.2011.00134*
This article was submitted to Frontiers in Microbial Physiology and Metabolism, a specialty of Frontiers in Microbiology.

frontiers in
MICROBIOLOGY

REVIEW ARTICLE
published: 21 March 2011
doi: 10.3389/fmicb.2011.00044

The microbial sulfur cycle at extremely haloalkaline conditions of soda lakes

Dimitry Y. Sorokin[1,2]*, J. Gijs Kuenen[2] and Gerard Muyzer[2]

[1] *Winogradsky Institute of Microbiology, Russian Academy of Sciences, Moscow, Russia*
[2] *Department of Biotechnology, Delft University of Technology, Delft, Netherlands*

Edited by:
Martin G. Klotz, University of Louisville, USA

Reviewed by:
Aharon Oren, The Hebrew University of Jerusalem, Israel
Yanhe Ma, Institute of Microbiology Chinese Academy of Sciences, China

***Correspondence:**
Dimitry Y. Sorokin, Winogradsky Institute of Microbiology, Russian Academy of Sciences, Prospect 60-let Octyabrya 7/2, 117312 Moscow, Russia
e-mail: soroc@inmi.host.ru; d.sorokin tudelft.nl

Soda lakes represent a unique ecosystem with extremely high pH (up to 11) and salinity (up to saturation) due to the presence of high concentrations of sodium carbonate in brines. Despite these double extreme conditions, most of the lakes are highly productive and contain a fully functional microbial system. The microbial sulfur cycle is among the most active in soda lakes. One of the explanations for that is high-energy efficiency of dissimilatory conversions of inorganic sulfur compounds, both oxidative and reductive, sufficient to cope with costly life at double extreme conditions. The oxidative part of the sulfur cycle is driven by chemolithoautotrophic haloalkaliphilic sulfur-oxidizing bacteria (SOB), which are unique for soda lakes. The haloalkaliphilic SOB are present in the surface sediment layer of various soda lakes at high numbers of up to 10^6 viable cells/cm^3. The culturable forms are so far represented by four novel genera within the *Gammaproteobacteria*, including the genera *Thioalkalivibrio*, *Thioalkalimicrobium*, *Thioalkalispira*, and *Thioalkalibacter*. The latter two were only found occasionally and each includes a single species, while the former two are widely distributed in various soda lakes over the world. The genus *Thioalkalivibrio* is the most physiologically diverse and covers the whole spectrum of salt/pH conditions present in soda lakes. Most importantly, the dominant subgroup of this genus is able to grow in saturated soda brines containing 4 M total Na^+ – a so far unique property for any known aerobic chemolithoautotroph. Furthermore, some species can use thiocyanate as a sole energy source and three out of nine species can grow anaerobically with nitrogen oxides as electron acceptor. The reductive part of the sulfur cycle is active in the anoxic layers of the sediments of soda lakes. The *in situ* measurements of sulfate reduction rates and laboratory experiments with sediment slurries using sulfate, thiosulfate, or elemental sulfur as electron acceptors demonstrated relatively high sulfate reduction rates only hampered by salt-saturated conditions. However, the highest rates of sulfidogenesis were observed not with sulfate, but with elemental sulfur followed by thiosulfate. Formate, but not hydrogen, was the most efficient electron donor with all three sulfur electron acceptors, while acetate was only utilized as an electron donor under sulfur-reducing conditions. The native sulfidogenic populations of soda lakes showed a typical obligately alkaliphilic pH response, which corresponded well to the *in situ* pH conditions. Microbiological analysis indicated a domination of three groups of haloalkaliphilic autotrophic sulfate-reducing bacteria belonging to the order *Desulfovibrionales* (genera *Desulfonatronovibrio*, *Desulfonatronum*, and *Desulfonatronospira*) with a clear tendency to grow by thiosulfate disproportionation in the absence of external electron donor even at salt-saturating conditions. Few novel representatives of the order *Desulfobacterales* capable of heterotrophic growth with volatile fatty acids and alcohols at high pH and moderate salinity have also been found, while acetate oxidation was a function of a specialized group of haloalkaliphilic sulfur-reducing bacteria, which belong to the phylum *Chrysiogenetes*.

Keywords: sulfur-oxidizing bacteria, sulfidogenesis, sulfate-reducing bacteria, sulfur reduction, thiosulfate reduction, soda lakes

INTRODUCTION

Sulfur is an important element for life. Apart of its structural importance as a component of various proteins, a complex sulfur cycle exists in the biosphere based on the ability of sulfur atom to change its valence from −2 (sulfide) to +6 (sulfate). Most of the sulfur redox reactions are not spontaneous at ambient conditions and, therefore, are catalyzed by prokaryotes capable of exploiting various inorganic sulfur compounds in their energy-transformation ("-generating") metabolism, either as electron donors (lithotrophic sulfur-oxidizing prokaryotes, anoxygenic phototrophic bacteria) or as electron acceptors (sulfidogenic prokaryotes). The biological sulfur cycle is an integral part of the whole biogeochemical cycle and connected to many other main element cycles, such as carbon (CO_2 fixation, oxidation of organic compounds, formation

of organo-sulfur compounds), nitrogen (thiodenitrification), and metal (formation of metal sulfides) cycles. Due to its significance, the microbial sulfur cycle is very well investigated, both in the oxidative and reductive branches. Most of the knowledge, however, was obtained from habitats that are very acidic (e.g., acid mine drainage) or at neutral pH (e.g., marine and fresh waters). Until recently, practically nothing was known about the possibility of dissimilatory sulfur transformations at extremely high pH. This review summarizes 15 years of research on the microbial sulfur cycle in naturally occurring habitats with a stable high pH and a high salinity called "soda lakes."

SODA LAKES AS A UNIQUE HABITAT

Soda lakes form a specific type of salt lakes where sodium carbonate/bicarbonate is among the dominant salts. Soda lakes are located in areas with dry climate conditions that facilitate salt accumulation in depressions by evaporative concentration. The earliest scientific record on the natron-depositing salt lakes (Wadi an Natrun, Egypt) already appeared in 1898 (Schweinfurth and Lewin, 1898). The genesis of soda lakes is based on the leaching of sodium-rich rocks by high CO_2-containing ground waters concomitant with low Ca and Mg background (Eugster, 1970). The presence of sodium carbonate at high concentrations (soluble alkalinity) creates a uniquely stable, natural alkaline habitat, buffered from the acidifying influence of atmospheric CO_2 with pH values of brines usually above 9.5, and salt concentrations varying within a broad range, depending on the local conditions. Sodium is the dominant cation in the brines of soda lakes, while chloride and sulfate are, apart from carbonate/bicarbonate, the dominant anions. So, soda lakes seem to be the only natural environment with appropriate conditions for the stable development of obligately alkaliphilic, salt-tolerant microorganisms, which usually grow optimally at a pH around 10 and need at least 0.1 M Na^+ for growth. Most studied examples of typical soda lakes are located in Kenya and Tanzania (Bogoria, Magadi, Natron), in Egypt (Wadi Natrun), and California (Mono Lake). Another area abundant in saline alkaline lakes is Central Asia, where the Transbaikal dry steppe stretches from south Siberia to north-east China. Here the lakes are much smaller, more shallow, and with a relatively unstable water regimen and a freezing winter period causing frequent and substantial fluctuations of the water salinity and temperature.

Our studies were mostly focused on Siberian soda lakes, although sulfur-oxidizing bacteria (SOB) were also actively investigated in samples from Kenyan and American soda lakes. The main characteristics of the lakes studied are given in **Table 1**.

The unusually high pH imposes several chemical changes important for the microbial sulfur cycling. First of all, sulfide is present entirely in the ionic form as HS^-, which, in contrast to H_2S, cannot freely cross the membrane and therefore, is not as toxic as H_2S. Accordingly, alkaliphilic SOB and sulfidogens can tolerate much higher substrate/product concentrations than their neutrophilic counterparts. Next, sulfide can react chemically with insoluble sulfur forming soluble polysulfides that are stable at high pH. At aerobic conditions polysulfide is rapidly oxidized to thiosulfate, while at anaerobic conditions it is stable, and hence can accumulate to high concentrations representing a true substrate for sulfur-reducing prokaryotes. High alkalinity would be favorable for SOB, because of a buffering effect of the sulfuric acid produced during sulfur oxidation in the periplasm. On the other hand, domination of carbonate over bicarbonate at pH values close to 10 and above is unfavorable for CO_2 fixation, setting a limitation for the growth of autotrophic alkaliphiles at extremely high pH.

SULFUR-OXIDIZING BACTERIA IN SODA LAKES

DISTRIBUTION AND DIVERSITY

The first pure cultures of SOB able to grow at pH 10 were isolated from the low salt soda lake Hadyn in Tuva (Russia). Strains AL2 and AL3 became the type strains of type species for the two different genera of haloalkaliphilic SOB, *Thioalkalivibrio*, and *Thioalkalimicrobium,* respectively, commonly found in soda lakes all over the world (Sorokin et al., 2000). Subsequent investigation of the samples from different geographic locations (**Table 1**) resulted in the isolation of more than 100 strains of obligately alkaliphilic chemolithoautrophic SOB. This revealed a previously unrecognized fact that SOB can thrive in extremely high pH/salt habitats (Sorokin and Kuenen, 2005; Sorokin et al., 2006). Apart from that, soda lakes yielded numerous strains of heterotrophic haloalkaliphiles identified as *Halomonas* spp., capable of sulfide and thiosulfate oxidation to sulfur and tetrathionate, respectively, without obvious energy gain (Sorokin, 2003; this group is out of the scope of this review).

Table 1 | Main characteristics of soda lakes studied.

Area	Examples	Total salts, g l^{-1}	pH	Total carbonate alkalinity (M)
Kenya	Magadi, Bogoria, Crater lake, Elmenteita	20–220	9.5–11.0	0.12–1.16
Wadi Natrun (Egypt)	Rozita, Beida, Gaar, Fazda, Zugm, Hamra, Umm-Risha, Khadra	200–380	9.5–10.3	0.11–0.75
California	Mono lake, Searles lake, Owens lake	90–220	9.7	0.5–1.0
Washington State	Soap lake	20–140	9.9	No data
Transbaikal Steppe (Russia)	Hilganta, Hadyn, Ulan-Nor, Gorbunka	5–40	9.5–10.2	0.02–0.11
Kulunda Steppe (Altai, Russia)	Tanatar lake system, Bitter lake system, Cock soda lake	20–380	9.3–10.6	0.02–5.2
North-eastern Mongolia	Hotontyn, Shar-Burdiin, Dzun-Uldziit, Baga-Nur	5–360	9.2–10.5	0.02–1.20

Combining enrichment and serial dilution procedures demonstrated a relatively high density of viable SOB in the surface sediments of various soda lakes (10^3–10^8 cells/cm^3) capable of chemolithoautotrophic growth at pH 10 and salt concentrations from 0.2 to 4 M total Na^+ in the form of carbonates. These bacteria apparently took advantage of the extremely high buffering capacity of the soda media thereby reaching high biomass density which, in the case of neutrophilic SOB, would only have been possible under pH-controlled conditions.

The soda lake SOB isolates formed four distinct phylogenetic groups within the *Gammaproteobacteria* and were described as four new genera *Thioalkalimicrobium, Thioalkalivibrio* (Sorokin et al., 2001a, 2002a, 2007a), *Thioalkalispira* (Sorokin et al., 2002b), and *Thioalkalibacter* (Banciu et al., 2008; **Figure 1**). The first three genera include exclusively obligately alkaliphilic salt-tolerant organisms, except for a single facultatively alkaliphilic *Thioalkalivibrio halophilus*. The genus *Thioalkalibacter* includes a single species, *Thb. halophilus*, which is a facultatively alkaliphilic halophile. In general, the *Thioalkalimicrobium* group dominated enrichment cultures from the low-saline Asian soda lakes. It also could be enriched from the more saline soda lakes, but only from fresh samples. The genus *Thioalkalivibrio* dominated in enrichments from hypersaline soda lakes and from aged samples, and was always dominant when the enrichment medium contained >1.5 M total Na^+. Therefore, the most important selective force influencing survival of alkaliphilic SOB in soda lakes appeared to be the salt concentration. The genus *Thioalkalivibrio* is apparently the most widely distributed SOB type in soda lakes. Among its more than 100 isolates, several large geographical populations each containing about 20 isolates could be distinguished (Foti et al., 2006). Extremely salt-tolerant isolates from the Kulunda Steppe and Mongolia are clustered together and also resemble strains from Mono Lake and Soap Lake, while most of the Wadi Natrun isolates are clustering with *Tv. halophilus*. Such clustering correlates with the anionic composition of the brines (see below).

The only other culturable evidences on haloalkaliphilic SOB came from the dry soda lake Texcoco in Mexico (Granada et al., 2009), although none of the isolates were characterized.

The presence of the SOB related to the genus *Thioalkalivibrio* detected in 16S rRNA gene-based libraries has been reported over the past 10 years in various saline habitats, including marine (AB189351, AB286100), hypersaline mats (DQ103664; Sørensen et al., 2005), and soda lakes (Humayoun et al., 2003; Mesbah et al., 2007). Marine clones, however, had only 90–95% sequence similarity to the species of *Thioalkalivibrio*, and, therefore, might belong to another SOB genus. Use of a specific functional marker for the key enzyme of the Calvin cycle (RuBisCO gene *cbb*) to detect autotrophic members of the soda lake microbial communities showed the common presence of the *Thioalkalivibrio*-related sequences in hypersaline soda lakes and clones related to the *Thioalkalimicrobium–Thiomicrospira* cluster (Giri et al., 2004; Kovaleva et al., 2011).

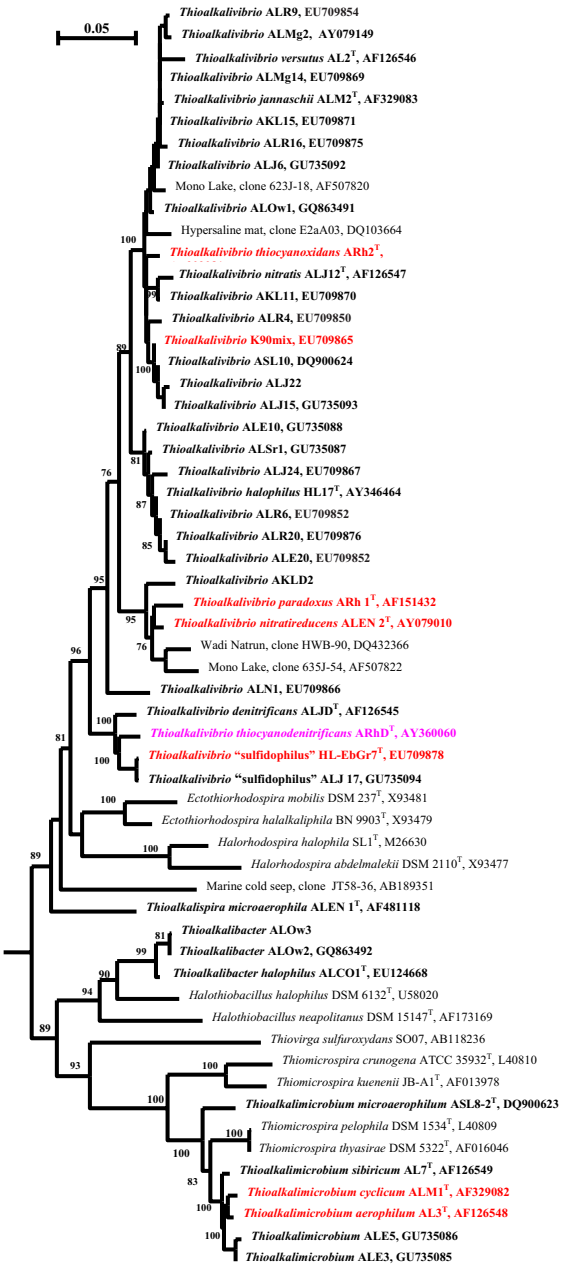

FIGURE 1 | Phylogenetic position of haloalkaliphilic SOB from soda lakes (in bold) within the *Gammaproteobacteria* based on 16S rRNA sequence analysis. The strain abbreviations are as follows: AL, strains from Transbaikal region (Russia); AKL, strains from Kulunda Steppe (Altai, Russia); ALMg, strains from north-eastern Mongolia; ALJ, strains from Kenya; ALE, strains from Wadi Natrun in Egypt; ASL, strain from Soap Lake (USA); ASLr, strain from Searles Lake (USA); ALOw, strains from Owens lake (California); ALN1, extremely haloalkaliphilic nitrate-reducing strain from Wadi Natrun; ALR, strains from a lab-scale sulfide-oxidizing bioreactor; HL-EbGr7, a strain from a full-scale sulfide-oxidizing bioreactor. In red are the strains with sequenced genome and in pink are strains which genome sequencing is in progress. Numbers at the nodes indicate the percentage of bootstrap values for the clade of this group in 1000 replications (the values for maximum-likelihood method are given in parentheses). Only values above 70% are shown. Bar, 5 substitutions per 100 nucleotides (nt).

BASIC PHYSIOLOGY OF HALOALKALIPHILIC SOB

The comparative properties of soda lake SOB are summarized in **Table 2**. In their basic physiology, the soda lake SOB represent typical chemolithoautotrophic thiotrophs using the Calvin cycle for

Table 2 | Basic properties of haloalkaliphilic SOB from soda lakes.

Property	*Thioalkalimicrobium* spp.	*Thioalkalispira microaerophila*	*Thioalkalivibrio* spp.	*Thioalkalibacter halophilus*
Number of validated species*	4	1	9	1
Close relative	*Thiomicrospira pelophila*	No	*Ectothiorhodospira*	*Halothiobacillus*
Cell morphology	Rods and spirilla	Spirilla	Rods, vibrios, spirilla, and cocci	Rods
Sulfur compounds oxidized	HS^-, S_n^{2-}, $S_2O_3^{2-}$	HS^-, S_n^{2-}, $S_2O_3^{2-}$	HS^-, S_n^{2-}, $S_2O_3^{2-}$, S_8, SO_3^{2-}, $S_4O_6^{2-}$, SCN^-	HS^-, S_n^{2-}, $S_2O_3^{2-}$
Electron acceptors	O_2	O_2 microaerophile	O_2, NO_3^-, NO_2^-, N_2O	O_2
pH optimum	9.5–10.0	10.0	10.0–10.2	8.5
Upper salt limit	1.5 M Na^+	1.4 M Na^+	4.3 M Na^+	3.5 M Na^+
Maximal specific growth rate	0.33 h^{-1}	0.08 h^{-1}	0.25 h^{-1}	0.22 h^{-1}
Maximal growth yield with $S_2O_3^{2-}$	3.5 mg protein $mmol^{-1}$	5.8 mg protein $mmol^{-1}$	6.5 mg protein $mmol^{-1}$	3.5 mg protein $mmol^{-1}$
Rate of HS^- oxidation	Extremely high	Low	Low	High
Dominant compatible solute	Ectoine	nd	Glycine betaine	Ectoine
Yellow membrane pigment	–	+	+	–
*nif*H	–	+	–	–
Distribution	Asia, Africa, North America	Egypt	Asia, Africa, North America	Asia, North America

**Up to date.*

Table 3 | Influence of anion composition of the medium on accumulation of compatible solutes by facultatively alkaliphilic extremely salt-tolerant SOB from hypersaline alkaline lakes.

Parameter	*Tv. halophilus*		*Tb. halophilus*	
	Na-carbonate	NaCl	Na-carbonate	NaCl
Osmotic pressure (osm kg^{-1})	5.0	9.3	nd	nd
Ectoine, % of dry weight	–	–	5.2	13.5
Glycine betaine, % of dry weight	12.4	19.8	1.3	0.9
Total compatible solute content, % of dry weight	12.4	19.8	6.5	14.4

Thioalkalivibrio halophilus was grown at 4 M total Na^+, Thioalkalibacter halophilus – at 3 M total Na^+, both at pH 10.

inorganic carbon fixation (Tourova et al., 2006, 2007) and growing best with thiosulfate (batch) and sulfide (substrate-limited chemostat). The main difference with their neutrophilic counterparts is not in sulfur metabolism (except for less sulfide toxicity and polysulfide stability at high pH), but in the possibility to realize the lithoautotrophic phenotype in general at extremely high pH and salinity. The potential for this kind of metabolism was not known before. So, the main characteristic of the soda lake SOB is their preference for a sodium carbonate-based environment with optimal growth at pH around 10. The most robust data for the growth/activity pH response were obtained in pH-controlled continuous cultures (Sorokin et al., 2003a; Banciu et al., 2004a). The growth pH maximum reached in this experimental set up was 10.5 for both genera, whilst metabolic activity remained active up to pH 11. Our explanation is that the growth, i.e., CO_2 fixation, was limited by inorganic carbon availability (domination of unavailable carbonate over available bicarbonate), whereas sulfur metabolism could still proceed at he higher pH values. The situation is somewhat analogous to that of the xerophytic plants inhabiting cold wetlands – there is enough water present, but it is not possible to take it up, because it is too cold.

Direct comparison of the growth, c.q. activity of *Thioalkalimicrobium aerophilum* with its close phylogenetic relatives, *Thiomicrospira pelophila* and *Thiomicrospira crunogena*, showed that the three species correspond to three different pH-anion types which may be common also for other physiological groups: the neutrophilic "NaCl type" (marine *Tms. crunogena*), the alkalitolerant "$NaHCO_3$ type" (littoral *Tms. pelophila*) and the alkaliphilic "Na_2CO_3 type" (soda lake *Tm. aerophilum*; **Figure 2**). The first two types cannot tolerate the presence of carbonate and pH 10, which are specific optimal conditions for the soda lake organisms. Further work with two facultatively alkaliphilic and extremely salt-tolerant SOB, *Thioalkalivibrio halophilus* (Banciu et al., 2004b). and *Thioalkalibacter halophilus* (Banciu et al., 2008)

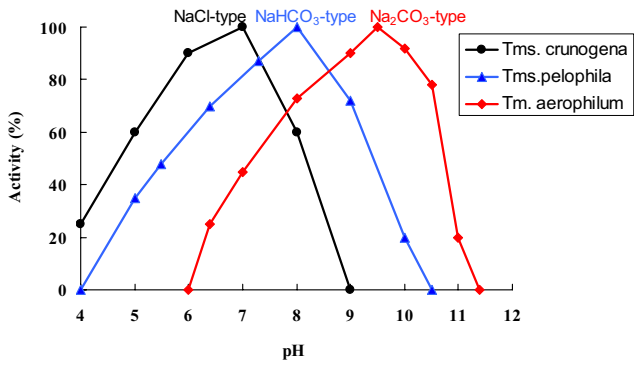

FIGURE 2 | Illustration of the three different anion-pH types of closely related SOB species from saline habitats. *Thiomicrospira crunogena* is a deep-see marine halophile, *Thiomicrospira pelophila* – a bicarbonate-loving alkalitolerant type from an littoral marine habitat, which may have temporal pH increase due to the phototrophic activity, and *Thioalkalimicrobium aerophilum* is a typical carbonate-loving type from a soda lake. 100% rates were 0.8, 2.2, and 3.8 μmol O_2 (mg protein min)$^{-1}$ for *Tm. crunogena*, *Tm. Pelophila*, and *Tm aerophilum*, respectively.

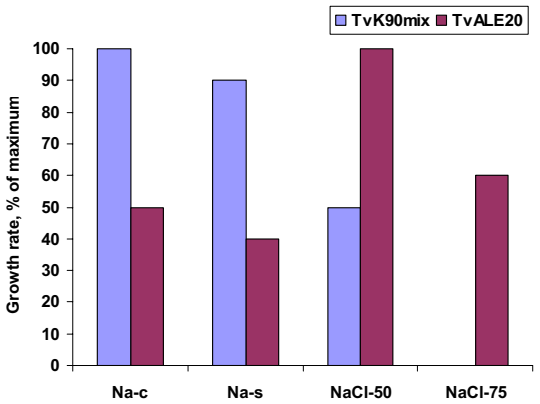

FIGURE 3 | Illustration of the concept of *natrono*phily among the extremely salt-tolerant soda lake SOB, showing the influence of counter-anion of sodium on growth of two different types of extremely salt-tolerant *Thialkalivibrio* isolates. The strains were grown at 4 M total Na^+ and pH 10. Sodium carbonate and sodium sulfate represent weak electrolytes in contrast to the strong electrolyte NaCl. *Thioalkalivibrio* K90mix represent a typical *natrono*phile from soda lakes in the Kulunda Steppe, while *Thioalkalivibrio* ALE20 represents a *haloalkali*phile from hypersaline alkaline lakes of Wadi Natrun. Na-c, medium with 90% carbonates/10% Cl^- Na-s, medium with 90% sulfate/10% carbonates; NaCl50, medium with 50% Cl^-/50% carbonate; NaCl75, medium with 75% Cl^-/25% carbonate.

allowed us to identify a previously ignored biological difference between *halo*philes (NaCl-loving) and *natrono*philes (soda-loving) organisms and bring forward the concept of *natrono*phily (**Table 3**). The essence of the latter is that the preference of soda lake microbes for soda might be at least partially explained by its weak electrolytic properties as compared to the strongly electrolytic NaCl. A direct measurement of osmotic parameters of two media used in our experiments with the mentioned SOB species, both containing in total 4 M Na^+ at pH 10, but one based on NaCl and another – on sodium carbonate buffer, showed two times higher values for the former, which is also obvious from conductivity measurements. This means that the osmotic burden in saturated soda brines (as well as in sodium sulfate brines) is two times less than in NaCl brines. Therefore, the *natrono*philes would need two times less specific compatible solutes concentration than the organisms living in NaCl brines. Compatible solutes (or osmolytes) in most of the bacteria are small organic molecules accumulating at high salt to protect the cytoplasm from desiccation (Roeßler and Müller, 2001; Roberts, 2005). The experimental results obtained for the two facultatively alkaliphilic halophilic SOB species grown in NaCl-dominate and in soda-dominated brines confirmed this conclusion (**Figure 3**). So, from one hand, life at extremely high pH demands extra energy for pH homeostasis, but, on the other hand this is balanced by much less cost of compatible solute synthesis than in neutraphilic halophiles. Such a tendency can also be seen in comparison of the growth dynamic of a typical obligate *natrono*philic SOB *Thioalkalivibrio* K90mix from hypersaline soda lakes in Siberia and a *haloalkali*philic *Thioalkalivibrio* ALE20 from hypersaline alkaline lakes in Wadi Natrun. The former definitely preferred to grow in week electrolytes and was inhibited by NaCl above 2 M, while the latter grew optimally in presence of at least 2 M NaCl (**Figure 4**). Moreover, *Thioalkalivibrio* K90mix has another extraordinary difference from halophiles. It can still grow well at pH 10 when 90% of sodium carbonate is replaced by potassium carbonate (i.e., 3.6 M K^+/0.4 M Na^+ as carbonates), while halophilic SOB from chloride-sulfate lakes could not grow already at 50% replacement (Sorokin, 2008). Obviously, the microorganisms from true soda lakes with preference for sodium carbonates cannot be called (as is usually done in the literature) *haloalkali*philes, but, must be called *natrono*philes. We also have evidence of the specific requirement for sodium cations for sulfide- and TMPD-dependent respiratory activity of the isolated membrane vesicles from *Thioalkalivibrio* strains pointing to the involvement of sodium-based elements in the bioenergetic machinery of natronophilic chemolithoautotrophs (Grischuk et al., 2003).

SPECIFIC METABOLIC PROPERTIES OF MEMBERS OF THE GENUS THIOALKALIVIBRIO

Thiodenitrification at extremely high pH

Anoxic enrichments from soda lake sediments with thiosulfate or sulfide as electron donor and nitrate as electron acceptor were positive only at a relatively low salinity (0.5–1.5 M total Na^+), but the enrichment culture did not normally yield complete denitrifiers. Instead, partial denitrifiers only reducing nitrate to nitrite with formation of copious sulfur were dominating. One of the enrichment cultures from Wadi Natrun, however, resulted in the complete denitrification of nitrate to nitrogen gas with only intermediate nitrite production. A stable co-culture of two facultatively anaerobic haloalkaliphilic SOB was selected from this enrichment consisting of a nitrate to nitrite reducing and nitrite/N_2O-reducing members (Sorokin et al., 2003b). They represented two different species of the genus *Thioalkalivibrio*, *Tv. Nitratireducens*, and *Tv. denitrificans*, respectively. The type strain of the latter has originally been obtained from the enrichment with N_2O as electron acceptor (Sorokin et al., 2001b). In pure culture, *Tv. nitratireducens* could grow anaerobically

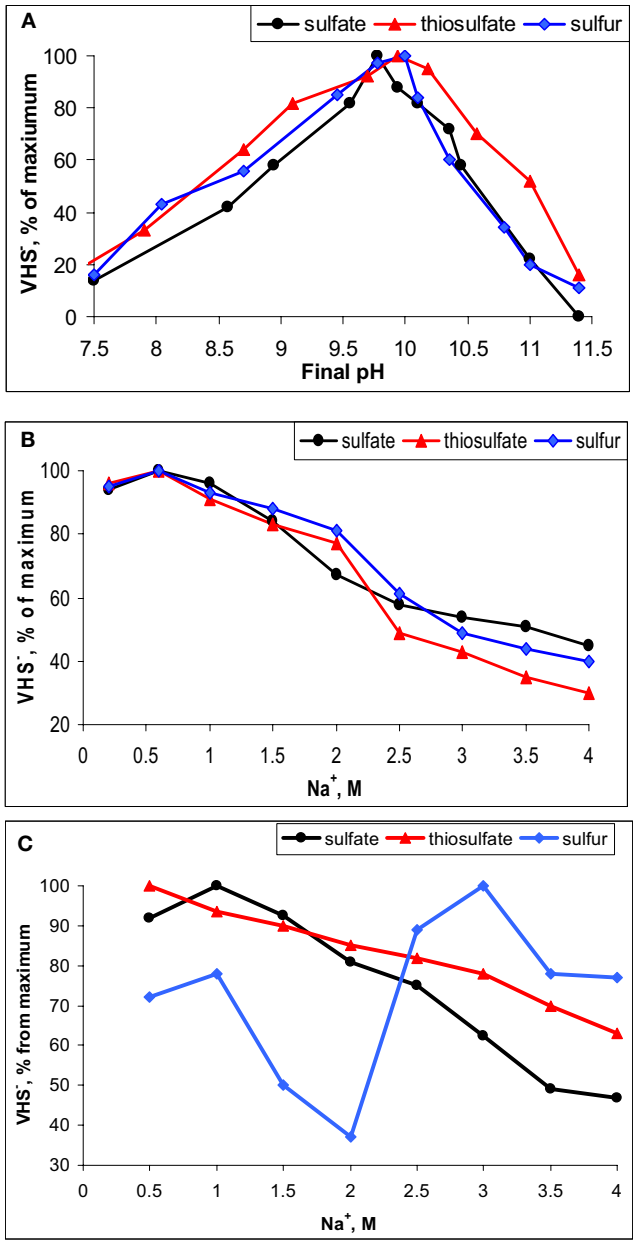

FIGURE 4 | Examples of pH (A) and salt (B,C) on the rate of sulfidogenesis (VHS^-) in benthic microbial communities of soda lakes. (A,B), moderately saline lake Tanatar-5; **(C)**, hypersaline lake Tanatar-1 (both in Kulunda Steppe, Altai, Russia). Electron donor – formate.

by nitrate-reduction to nitrite (Sorokin et al., 2003c), while the second organism, *Tv. denitrificans*, lacking NAR, was capable of further reducing nitrite to N_2 via N_2O (Sorokin et al., 2001b):

$8\ NO_3^- + 2\ S_2O_3^{2-} + 2\ H_2O$ >>>	$8\ NO_2^- + 4\ SO_4^{2-} + 4\ H^+$	*Tv. nitratireducens*
$8\ NO_2^- + 3\ S_2O_3^{2-} + 2\ H^+$ >>>	$4\ N_2 + 6\ SO_4^{2-} + H_2O$	*Tv. denitrificans*
$8\ NO_3^- + 5\ S_2O_3^{2-} + H_2O$	**$4\ N_2 + 10\ SO_4^{2-} + 2\ H^+$**	**Tandem result**

This consortium represented the first example of microbial thiodenitrification at extremely high pH. Moreover, in a chemostat at pH 10 *Tv. denitrificans* grew well with N_2O and polysulfide – a form of autotrophic denitrification unique to alkaliphiles. Apparently, all the denitrifying reductases in these SOB must be adapted to pH 10 or higher, since they are located in the periplasmic space. Indeed, the *in vitro* assays showed that Nir and Nos activity had a pH optimum above 10, while Nar is less alkalitolerant with an optimum at pH 9.5.

Thiocyanate oxidation at extremely high pH

Thiocyanate ($N{\equiv}C{-}S^-$) is a one-carbon sulfur compound which is much more difficult to utilize as energy source for SOB as compared to other inorganic sulfur species. Only a few neutrophilic *Thiobacillus* species can use it as an energy source after a primary degradation to sulfide, ammonia and CO_2, for which two basic pathways have been proposed, either through the C≡N or the C–S bond hydrolytic cleavage, respectively (Kelly and Baker, 1990):

$N{\equiv}C{-}S^- + H_2O \longrightarrow O{=}C{=}S + NH_3$ "*COS pathway*"

$N{\equiv}C{-}S^- + H_2O \longrightarrow C{\equiv}N{-}O^- + H_2S$ "*cyanate pathway*"

The existence of the "COS pathway" has recently been proven for the neutrophilic SOB *Thiobacillus thioparus* and halophilic *Thiohalophilus thiocyanatoxidans*, and the enzyme responsible for the primary degradation of the nitrile bond of thiocyanate was characterized as a specific type of Cobalt-containing nitrile hydratase (Katayama et al., 1998; Bezsudnova et al., 2007). On the other hand, no direct proof of the "cyanate pathway" had been offered until recently.

Aerobic enrichment cultures in medium containing thiocyanate at pH 10 and moderate salinity from various soda lake sediments resulted in the isolation of several strains of haloalkaliphilic, obligately autotrophic SOB growing on thiocyanate as energy and nitrogen source (Sorokin et al., 2001c). The isolates fell into two distinct lineages within the genus *Thioalkalivibrio* and were described as *Tv. thiocyanoxidans* and *Tv. paradoxus* (Sorokin et al., 2002c). At denitrifying conditions another novel species was obtained and described as *Tv. thiocyanodenitrificans*, which is capable of anaerobic growth with thiocyanate as *e*-donor and nitrate as *e*-acceptor at pH 10 (Sorokin et al., 2004a). The aerobic species accumulated large amounts of cyanate in the medium during thiocyanate utilization, which was the first direct confirmation of the involvement of the "cyanate pathway" in the primary thiocyanate degradation in pure bacterial cultures. Interestingly, the cyanase activity (whose presence had been implicated previously as the only confirmation of the "cyanate" pathway in thiobacilli; Youatt, 1954) was completely blocked during growth of the alkaliphilic SOB on thiocyanate. Another peculiar property of the degradation system in alkaliphiles emerged during a detailed study of the mechanism of thiocyanate degradation. The result of a biochemical investigation indicated that the primary degradation reaction resulting in cyanate formation is not hydrolysis (as is the case in the COS pathway), but, rather, a direct oxidation of the sulfane atom to the stage of elemental sulfur according to the following scheme (unpublished results):

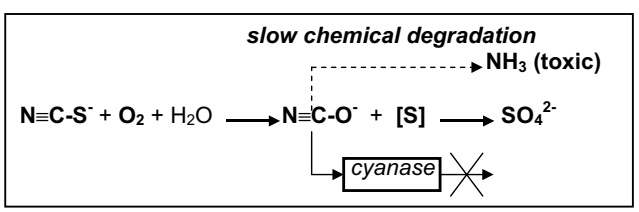

At present, the responsible enzyme has been purified and the gene has been sequenced. The protein has no significant homology to any oxido-reductases in the database. The genomes of all three representatives of the SCN-oxidizing alkaliphilic SOB are in the process of genome sequencing, which must help to better understand their thiocyanate metabolism.

GENOME INFORMATION FROM TWO STRAINS OF THE GENUS THIOALKALIVIBRIO

The complete genome sequencing of two *Thioalkalivibrio* representatives has just been finished and annotated by the Joint Genome Institute. The low salt-tolerant isolate from a full-scale Thiopaq bioreactor in the Netherlands (see also last section), *Thioalkalivibrio* "*sulfidophilus*" HL-EbGr7, belongs to the *Thioalkalivibrio denitrificans* cluster, and the extremely natronophilic strain *Thioalkalivibrio* spp. K90mix obtained from a mixed sample of sediments from different Siberian hypersaline soda lakes is a typical representative of the core group of the genus (see **Figure 1**). The first is microaerophilic and prefers sulfide as the substrate, the latter grows best at fully aerobic conditions with thiosulfate. According to the genome information, the sulfur oxidation pathways in these two SOB strains are different. The *Tv.* "*sulfidophilus*" pathway is a combination of the partial "Sox pathway" (lacking *sox*CD) for oxidation of the sulfane atom of thiosulfate and the reversed sulfate reduction pathway for the oxidation of zero-valent sulfur atom to sulfate, similar to what has been recognized in green and purple anaerobic SOB *Chlorobium* (Sakurai et al., 2010) and *Allochromatium* (Sander and Dahl, 2009). Sulfide oxidation is apparently proceeding through the flavocytochrome *c* (Fcc) sulfide dehydrogenase (Muyzer et al., 2011). A partial "Sox pathway" also operates in *Thioalkalivibrio* K90mix. However, the genes coding for the reversed Dsr cluster are absent and there is no obvious candidate to fulfill the central function of oxidation of zero-valent sulfur atom to sulfite. On the other hand, there are two possibilities for sulfite oxidation. The *aps* and *sor*A genes, present in the chromosome, are coding for the AMP-dependent (APS reductase) and independent sulfite dehydrogenases, respectively. Further work is needed to fully understand the sulfur oxidation mechanism in these SOB species.

SULFIDOGENESIS IN SODA LAKES

ACTIVITY OF SULFIDOGENESIS IN SODA LAKE SEDIMENTS

Usually, the top sediments in soda lakes have a dark color and a high content of acid labile sulfides ($HS^- + FeS$) indicating active sulfidogenesis. For example, in the sediment pore brines of Kulunda soda lakes we detected up to 5 mM free sulfide. A limited number of direct *in situ* measurements of sulfate reduction rates with $^{35}SO_4^{2-}$ (Gorlenko et al., 1999; Sorokin et al., 2004b; Kulp et al., 2006) and sulfate reduction potential in sediment slurries (Kulp et al., 2007) indicated the presence of active sulfate-reducing bacteria (SRB) populations in various soda lakes with rates comparable to those observed in coastal marine sediments. More detailed recent studies conducted with sediments of Kulunda Steppe soda lakes confirmed active sulfate reduction, but also demonstrated that the most active sulfidogenesis was with elemental sulfur as electron acceptor, followed by thiosulfate, while sulfate was less active (Sorokin et al., 2010a). Sulfidogenesis was stimulated by addition of electron donors of which formate was the most efficient. Hydrogen did not lead to increased sulfide production with any of the inorganic sulfur acceptors, whilst acetate only stimulated sulfur reduction. Furthermore, native benthic sulfidogenic populations in Kulunda soda lakes clearly exhibited an obligately alkaliphilic pH response with optimal activity at pH 9–10 (**Figure 4A**), while a salinity above 2 M of total Na^+ significantly inhibited the activity of sulfate reduction. The same result has also been well documented for hypersaline chloride–sulfate lakes at neutral pH (Brandt et al., 2001; Sørensen et al., 2004). However, thiosulfate and, especially sulfur reduction, in hypersaline soda lakes, such as Bitter-1 and Tanatar-1 in Kulunda Steppe, were much less sensitive to high salt concentrations (**Figures 4B,C**).

MOLECULAR ANALYSIS OF DIVERSITY OF SRB IN SODA LAKES

16S rRNA gene-based molecular analysis of the soda lake prokaryotic communities only rarely detected typical SRB from the *Deltaproteobacteria*. Particularly, sequences affiliated with the previously described genus *Desulfonatronum* from soda lakes (Pikuta et al., 1998, 2003; Zhilina et al., 2005) were found in Mono Lake (Scholten et al., 2005), Wadi Natrun lakes (Mesbah et al., 2007), and in Kulunda Steppe lakes (Foti et al., 2008). More specific analysis using the functional marker *dsr*AB, encoding an essential enzyme in the sulfate reduction pathway, demonstrated the presence of SRB sequences belonging to the orders *Desulfovibrionales* and *Desulfobacterales* in Siberian soda lakes (Foti *et al.*, 2007). In the *Desulfovibrionales*, the sequences were affiliated with the genera *Desulfonatronum* and *Desulfonatronovibrio* (Zhilina et al., 1997), previously found in soda lakes, while the detection of *dsr*AB clones within the order *Desulfobacterales* indicated the presence of yet unknown heterotrophic SRB in soda lakes.

CULTURE-DEPENDENT ANALYSIS OF SULFIDOGENS FROM SODA LAKES

Lithotrophic SRB

Until recently, only a few SRB's have been cultured from soda lakes. They belong to two genera of the family of the haloalkaliphilic *Desulfovibrionales*, i.e., *Desulfonatronovibrio* (a single species), and *Desulfonatronum* (three species). The former is obligate lithotroph, utilizing only H_2 and formate, while the three species of the genus *Desulfonatronum* also oxidize EtOH and lactate to acetate in addition to H_2 and formate. Both are moderately alkaliphilic with a pH optimum of 9–9.5 and moderately salt-tolerance with the upper limit of 1.5 M total Na^+ for *Desulfonatronum* and 2.0 M for *Desulfonatronovibrio*. The finding of these SRB was a significant discovery, because it was assumed that SRB could not grow under these conditions. However, the question remained, whether there are other SRB in soda lakes, which would be able to grow at much higher salinity occurring in hypersaline soda lakes and whether they would utilize other substrates.

Our enrichment attempts using soda media with 3–4 M Na^+ at pH 10 and sulfate as the electron acceptor were negative. However, when sulfate was replaced by sulfite or thiosulfate, positive sulfidogenic enrichments were obtained from the Kulunda Steppe and Wadi Natrun either with formate as electron donor or even without any additional electron donors. The latter was totally unexpected, but soon it became clear, that autotrophic growth by sulfite/thiosulfate disproportionation is a common trait among haloalkaliphilic SRB. Despite a very low energy yield (see comparison below), it allowed the SRB to outcompete the acetogens, which were otherwise more successful at extremely natronophilic conditions.

$$S_2O_3^{2-} + OH^- >>> HS^- + SO_4^{2-} (\Delta G^{o'} = -22\,kJ/mol)\ disproportionation$$

$$4SO_3^{2-} + H^+ >>> HS^- + 3SO_4^{2-} (\Delta G^{o'} = -58\,kJ/mol)\ disproportionation$$

$$SO_4^{2-} + 4H_2 + H^+ >>> HS^- + 4H_2O (\Delta G^{o'} = -152\,kJ/mol)\ sulfate\ reduction$$

The disproportionation enrichments resulted in the isolation of several extremely natronophilic SRB strains growing optimally at 1.5–2 M total Na^+ (and up to 4 M Na^+) and pH 10 either by sulfite/thiosulfate disproportionation autotrophically or by "normal" dissimilatory sulfate reduction with H_2, formate and lactate as e-donors. The group was described as a new genus *Desulfonatronospira* within the family *Desulfohalobiaceae* with *Desulfonatronospira thiodismutans* as the type species (**Figure 5**; Sorokin et al., 2008). 16% (w/w) glycine betaine was detected in the cells of *Desulfonatronospira thiodismutans* grown at 3 M total Na^+ accumulated as a compatible solute. The cost of such an "investment" is enormous (Oren, 1999) and, yet, the energy metabolism of this organism is apparently sufficient, although the growth rate is extremely low. The genome of the type strain is currently sequenced by the Joint Genome Institute and its analysis must shed some light on the molecular mechanism of adaptation to extreme natronophilic conditions.

The SRB isolates from Kulunda soda lake sediments, which were enriched at moderate salinity (0.6–2.0 M Na^+), pH 10 and sulfate as the electron acceptor (**Table 4**), could only be enriched and further separated from acetogens by using formate as the electron donor and sulfate as the electron acceptor or at disproportionating conditions.. The multiple lithotrophic SRB's isolated from soda lake sediments (**Table 4**) fell into the two known *Desulfovibrionales* genera, *Desulfonatronum*, and *Desulfonatronovibrio*. However, none of them were closely related (less than 97% of 16S rRNA gene sequence similarity) to the described species (**Figure 5**). This demonstrated a high diversity of these two lithotrophic haloalkaliphilic SRB genera in soda lakes and corresponded well to the results of culture-independent studies. All isolates were obligate alkaliphiles with a pH optimum around 9.5–10. The upper salt limit was 2 M total Na^+ for the *Desulfonatronum* isolates and 3 M total Na^+ for the *Desulfonatronovibrio*. However, all of them grew optimally at low salt (around 0.5 M). **Figure 6** shows the comparative salt/pH profiles for the three groups of lithotrophic soda lake SRB. The most common and ecologically important physiological trait of these SRB was the capacity to grow litho(auto)trophically by thiosulfate disproportionation. It must be mentioned, that, despite the observed high potential (activity) of resting cells for sulfur reduction, none of the SRB isolates were able to use elemental sulfur as an *e*-acceptor for growth. Production of sulfide in the presence of elemental sulfur at high pH would lead to the formation of polysulfide and, apparently this compound is much more toxic to alkaliphilic SRB than sulfide.

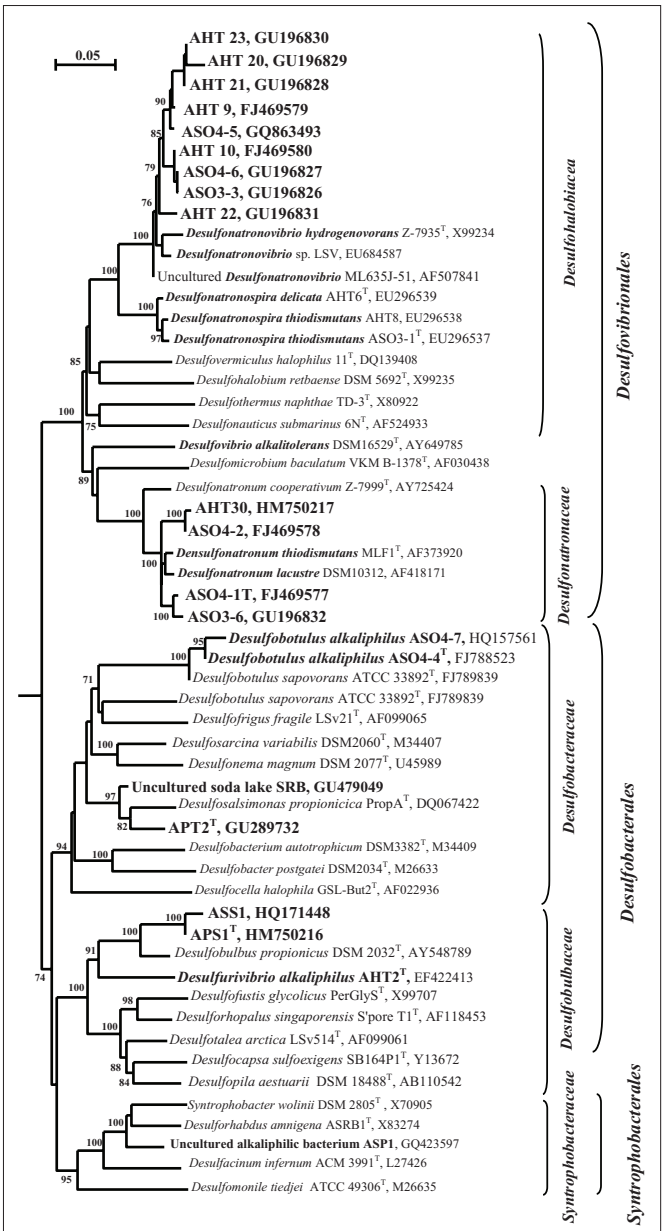

FIGURE 5 | 16S rRNA-based phylogeny of haloalkaliphilic SRB from soda lakes within the *Deltaproteobacteria* (sequences are in bold). Numbers at the nodes indicate the percentage of bootstrap values for the clade of this group in 1000 replications (the values for maximum-likelihood method are given in parentheses). Only values above 70% are shown. Bar, 5 substitution per 100 nt. *E. coli* was used as an outgroup.

Heterotrophic SRB

As was mentioned above, the molecular studies indicated the presence of members of the order *Desulfobacterales* in soda lakes. Most of them, in contrast to *Desulfovibrionales*, can utilize volatile fatty acids (VFA) as electron donor and carbon source. Our enrichments at pH 10 with sediments from Kulunda Steppe soda lakes resulted in positive sulfidogenic cultures with propionate, butyrate, and benzoate, but only at the lowest salinity used (0.6 M total Na^+). From the seven positive enrichments, five pure cultures and two syntrophic associations were eventually obtained. Their basic properties are presented in **Table 5**. Four pure cultures belonged to three different clusters within the order *Desulfobacterales* which corresponds to the results of *dsr* detection (Foti et al., 2007), while the SRB member

Table 4 | Novel lithotrophic SRB isolates from soda lakes (type strains are in bold).

Strain number	Source		Enrichment conditions (pH 10)			Key properties					Affiliation
	Lake	Area	*e*-donor/ C source	*e*-acceptor	Total Na^+ (M)	Autotrophy	Dismutation	pH range (optimum)	Maximal salt-tolerance M Na^+	μ_{max} h^{-1}	
ASO4-1	Tanatar-1	Kulunda Steppe (Altai, Russia)	Formate/ acetate	Sulfate	0.6	2 Strains	+	8.0–10.5 (9.3–10.0)	1.3–2.3	0.042–0.055	*Desulfonatronum*
ASO4-2	Picturesque		Pyruvate	Sulfate							
ASO3-6	Cock soda		EtOH*	Sulfite							
AHT30	Mixed sample		Formate/ acetate	Sulfate							
AHT9	Tanatar-5	Kulunda Steppe	Formate/ acetate	Thiosulfate	0.6	4 Strains	+	8.5–10.5 (9.5–10.0)	2.0–3.0	0.035–0.040	*Desulfonatronovibrio*
AHT10	Bitter-1		Formate/ acetate	Thiosulfate	2.0						
ASO4-6	Cock soda		Formate/ acetate	Sulfate	0.6						
ASO3-2	Tanatar-5		EtOH*	Thiosulfate	0.6						
ASO3-3	Bitter-1		Formate/ acetate	Sulfite	0.6						
AHT20	Tanatar-5		Thiosulfate/ acetate	Thiosulfate	0.6						
AHT21	Cock Soda		Thiosulfate/ acetate	Thiosulfate	0.6						
AHT22	Tanatar-5		Thiosulfate/ acetate	Thiosulfate	0.6						
AHT23	Bitter-1		Thiosulfate/ acetate	Thiosulfate	0.6						
AHT33	Tanatar-5		Thiosulfate/ acetate	Thiosulfate	0.6						
ASO4-5	Owens	California	Formate/ acetate	Sulfate	2.0						
ASO3-1	Mixed sediment	Kulunda Steppe	Sulfite	Sulfite	4.0	+	+	8.5–10.6 (9.5–10.0)	3.5–4.0	0.020	*Desulfonatronospira*
AHT8			Formate/ acetate	Thiosulfate	3.0						
AHT26			Thiosulfate/ acetate	Thiosulfate	4.0						
AHT6	Wadi Natrun	Egypt	Thiosulfate/ acetate	Thiosulfate	3.0						

**Subsequent isolation of pure cultures was possible after replacement of EtOH by formate.*

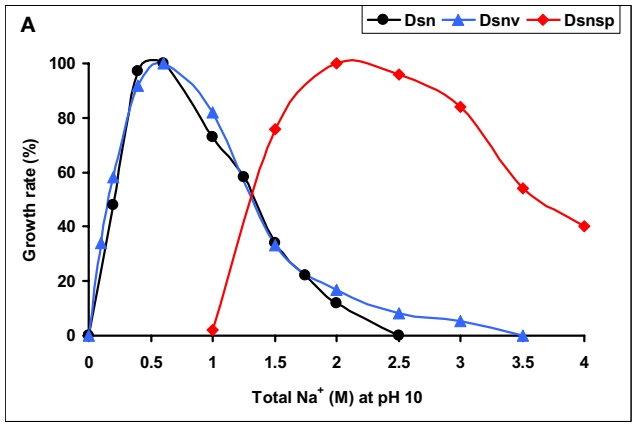

FIGURE 6 | Salt [(A), at pH 10] and pH [(B), at optimum salinity] profiles for growth in three subgroups of lithotrophic SRB from soda lakes. Dsn, *Desulfonatronum* isolates, Dsnv, *Desulfonatronovibrio* isolates, Dsnsp, *Desulfonatronospira thiodismutans*. 100% growth rates were 0.05, 0.04, and 0.02 h^{-1} for Dsn, Dsnv, and Dsnp, respectively.

of the syntrophic propionate-utilizing culture was a member of the order *Synthrophobacterales* (**Figure 5**). The SRB member of the benzoate-utilizing association was isolated under autotrophic conditions with H_2 and sulfate and identified as a member of the genus *Desulfonatronum*. This situation was similar to that of the acetate-utilizing syntrophic culture from soda lakes, which yielded *Desulfonatronum cooperativum* (Zhilina et al., 2005). The organism responsible for benzoate oxidation was identified by sequence analysis as a novel representative of the class *Clostridia* (89% sequence similarity to *Natranaerobius* spp.; unpublished results).

From the pure cultures of heterotrophic SRB currently only two similar strains selected with butyrate/BuOH and sulfate are validly described as a new species of the genus *Desulfobotulus, Dsb. alkaliphilus* (Sorokin et al., 2010b). They oxidize a range of linear VFA incompletely to acetate. Another pair of incomplete oxidizers selected with propionate and sulfate represents a novel haloalkaliphilic member of the genus *Desulfobulbus*. Finally, strain APT2, a novel member of the family *Desulfobacteraceae,* is a first cultured example of haloalkaliphilic SRB completely oxidizing VFA to CO_2. However, it cannot utilize external acetate as energy source, which is similar to its nearest phylogenetic relative, halophilic *Desulfosalsimonas propionicica* (Kjeldsen et al., 2010). None of the SRB isolates, listed in **Table 5** can grow litho(auto)trophically with H_2 or formate or by disproportionation of sulfite/thiosulfate, in contrast to the haloalkaliphilic members of the order *Desulfovibrionales*.

Gram-positive SRB in soda lakes

The 16S rRNA-based approach showed the presence in Mono Lake of two novel clusters of *Clostridiales* related to *Desulfotomaculum* (Scholten et al., 2005), although no *dsr* sequences belonging to the Gram-positive SRB have been found yet in soda lakes. Our attempt to enrich and isolate endospore-forming SRB from soda lakes in Kulunda Steppe using pasteurized sediments were not successful. Instead, a binary sulfidogenic culture consisting of two endospore-forming haloalkaliphilic clostridia has been selected with pyruvate as the

Table 5 | Properties of heterotrophic SRB from soda lakes in Kulunda Steppe enriched and isolated at pH 10 and 0.6 M total Na^+.

Strain number	Enrichment conditions			Key properties					Affiliation
	e-donor/ C source	*e*-acceptor	*e*-donor/ C source	*e*-acceptor	c/i*	pH optimum	Upper salt limit (M Na^+)	μ_{max} (h^{-1})	
ASO4-4 ASO4-7	Butyrate BuOH	Sulfate Sulfate	C4–C9 VFA, BuOH	Sulfate, $S_2O_3^{2-}$ sulfite	i	10.0	1.75	0.03	*Desulfobotulus alkaliphilus*
APT2	Propionate	$S_2O_3^{2-}$	C3–C8 VFA,	Sulfate, $S_2O_3^{2-}$ sulfite	c	10.0	1.5	0.019	*Desulfobacteraceae*
APS1 ASS1	Propionate Succinate >> propionate	Sulfate	Propionate, PrOH, BuOH	Sulfate, sulfite	i	9.4–9.5	1.75	0.020	*"Desulfobulbus alkaliphilus"*
ASP1-syntr	Propionate	Sulfate	Propionate, PrOH	Sulfate	nd	9.5	1.5	nd	*Synthrophobacteraceae*

**c, complete oxidizers; i, incomplete oxidizers; nd, not determined.*

e-donor/C source and thiosulfate as the *e*-acceptor. Both could grow with thiosulfate, but only one (related to *Natronovirga*) reduced thiosulfate partially to sulfite and sulfide, while the second member, described as a novel genus and species *Desulfitispora alkaliphila*, was able to grow with sulfite as an *e*-acceptor. So, it may be considered as a "crippled" SRB lacking a pathway for sulfate activation. Interestingly, when grown together, the growth rate and final biomass yield of the consortium with thiosulfate was higher, than for *Desulfitispora* alone, indicating a positive cooperation (Sorokin and Muyzer, 2010a).

Dissimilatory sulfur-reducing bacteria in soda lakes

As was already mentioned above, sulfur reduction was the most active sulfidogenic process in soda lake sediments. Two interesting results were that (1) acetate was apparently utilized as the *e*-donor only when sulfur acted as the *e*-acceptor and (2) that in hypersaline soda lakes the activity of lithotrophic sulfur reduction (H_2- and formate-dependent) was not inhibited and, in some cases, even stimulated, at saturated salt conditions, in contrast to sulfate/thiosulfate reduction. Also assuming that alkaliphilic SRB were unable to use elemental sulfur as an *e*-acceptor, it became clear, that there must be specialized dissimilatory sulfur-reducing microbes in soda lakes different from SRB.

Enrichments with either acetate or propionate as *e*-donors and sulfur as *e*-acceptor at moderate salinity from the Kulunda soda lake sediments showed relatively fast growth with copious polysulfide formation and high dominance of a single spiral-shaped morphotype. Two pure cultures obtained from the enrichments shared some common phenotypic traits (**Table 6**) and were described as a novel genus and species *Desulfurispira natronophila*, a member of the phylum *Chrysiogenetes* (Sorokin and Muyzer, 2010b). The most important property of these bacteria was fast growth with and complete oxidation of acetate and propionate, which was lacking when sulfur had been replaced by sulfate. Another important property was the relatively high salt-tolerance (despite the original selection at low salt) of 3 M Na^+ at pH 10 for sulfur reduction with acetate. The final amount of reduced sulfur (sulfide/sulfane of polysulfide) in these sulfidogenic alkaliphiles was several times higher that in the SRB cultures, reaching 80 mM. The most obvious question, why sulfur reduction, but not sulfate reduction was active under soda lake conditions, may, at least partially, be answered by the (beneficial) stability of the true electron acceptor (which is not insoluble sulfur itself, but soluble polysulfide) at high pH and by proton formation during the reaction. Both contribute to a favorable change of the available reaction energy in comparison to standard neutral conditions. According to our calculations, those changes make sulfur reduction with acetate [$\Delta G' = (-50)–(-70)$ kJ/mol acetate] more favorable than sulfate reduction ($\Delta G^{0'} = -47$ kJ/mol acetate; Sorokin et al., 2010a).

Table 6 | Phenotypic comparison of *Desulfurispira natronophila* from soda lake isolates with related bacteria from the phylum *Chrysiogenetes*.

Characteristic	*Desulfurispira natronophila*		*Desulfurispirillum alkaliphilum*	*Chrysiogenes arsenatis*
	AHT11^T	**AHT19**		
Cell morphology	Spirillum with bipolar flagellum			Vibrio, single polar flagellum
Autotrophic growth	–	–	–	–
ELECTRON DONORS				
H_2	+	–	+	–
Formate	+	–	–	–
Acetate, pyruvate, lactate, malate, succinate, fumarate	+	+	+	+
Propionate	+	+	+	–
Citrate	–	–	+	–
Glycerol	+	–	–	–
ELECTRON ACCEPTORS				
O_2	–	–	–	–
Sulfur (polysulfide)	+	+	+	–
NO^{3-}, NO^{2-} (to NH_3)	–	–	+	+
N_2O	–	–	–	–
AsO_4^{3-}	+	+	–	+
SeO_4^{2-}, Fe^{3+}, $S_2O_3^{2-}$,	–	–	–	–
Oxidation of HS^- with nitrate	–	–	+	nd
pH range (optimum)	8.5–10.9 (**10.2**)	8.2–10.5 (**9.8**)	8.0–10.2 (9.0)	Neutrophilic
Salt range (M Na^+)	0.2–**3.0**	0.2–**3.0**	0.1–2.5	Na-independent
Habitat	**Soda lakes**		Bioreactor	Gold mine

The most essential properties are highlighted in bold.

Further exploration of potential of dissimilatory sulfur reduction in soda lakes at extremely high salt and pH 10 (saturated soda brines) gave unexpected microbiological results. With H_2, formate, and acetate as the electron donors three extremely natronophilic bacterial strains identical in morphology and very close to each other phylogenetically were enriched and isolated from hypersaline soda lakes in the Kulunda Steppe and from Wadi Natrun (**Table 7**). They had 96–97% 16S rRNA gene sequence similarity to *Natroniella acetigena* – a heterotrophic homoacetogenic natronophile from soda lake Magadi (Zhilina et al., 1995). In contrast to the type species, the novel isolates were obligate sulfur respirers and not capable of acetogenic growth with organic compounds, but, instead, could grow lithoautotrophically with formate and hydrogen. One of the isolates was even able to utilize acetate as an *e*-donor, which is supposed to be a final metabolic product in this genus.

Even more unexpected results came from enrichments under the same conditions but with C_4–C_6 VFA as the *e*-donors. In all of them the dominant morphotype was represented by irregular coccid cells that looked flat – a typical characteristic of the haloarchaea. The isolation of a pure culture, was possible only when the VFA were replaced by formate. The isolated strain grew by sulfur respiration utilizing only H_2, formate, and pyruvate as the *e*-donors in pure culture. It could gradually be adapted for aerobic heterotrophic growth with C_2–C_8 VFA through microoxic conditions and in the presence of oxygen the biomass acquired the typical red pigmentation of haloarchaea. Phylogenetic analysis put this isolate into the cluster of natronarchaea with an uncharacterized isolate from Little Lake Magadi in Kenya (Jones et al., 1998) and the members of recently described genus *Natronolimnobius* (Itoh et al., 2007) as closest relatives. As far as we know, none of the so far described members of the order *Halobacteriales* have the type of metabolism as possessed by strain AHT32, which makes it truly unique.

These two examples of extremely natronophilic obligatory sulfur-respiring prokaryotes from hypersaline soda lakes with unexpected phylogenetic affiliation to completely different metabolic groups are important for the general understanding of mechanisms of adaptation of prokaryotic life to extreme salinity. If one accepts the hypothesis of A. Oren about the existence of a direct relation between the ability of prokaryotes to grow at high salt and their efficiency of catabolism (Oren, 1999, 2011), an attempt can be made to rationally explain different cases of the extreme natronophilism observed in sulfur cycle prokaryotes from hypersaline soda lakes (**Figure 8**). The essence of concept is that there may be two different ways of adaptation to cope with such extreme conditions. One is based on a very efficient energy metabolism, such as in the aerobic SOB of the genus *Thioalkalivibrio*, providing a possibility to generate sufficient energy required for the synthesis of high concentrations of organic compatible solutes. In that case the metabolic specialization is primary to the secondary adaptation to high salt. In the second strategy it is opposite, i.e., existing structural adaptation to high salt is primary to the low energy-yielding metabolic specialization. The second strategy is represented by the two examples of extremely natronophilic sulfur respirers – the bacterium *Natroniella* "*sulfidigena*" and the archaeon *Natronolimnobius* AHT32. Both have in common the energy-inexpensive ("cheap") osmotic strategy based on the import of K^+, giving them an advantage over the competitors with an "organic" osmotic strategy in exploiting the low energy catabolic reactions at extremely high salt. Of course, this is only part of the story, there must be other factors involved in such "fitness." For example, several strains of the genus *Thioalkalivibrio* and all members of the genus *Thioalkalimicrobium* can not grow at extreme salinity, having the same type of energy metabolism as the extremely salt-tolerant representatives of the genus *Thioalkalivibrio*. Another exception – *Desulfonatronospira* with an organic compatible solute strategy, growing chemolithoautotrophically in saturated soda brines (albeit very slowly) using energy-poor catabolic reactions (disproportionation). Comparative analysis of genomes from low and high salt-tolerant *Thioalkalivibrio* strains might shed a light on those additional properties.

Table 7 | Properties of extremely natronophilic, obligately sulfur-reducing isolates from hypersaline soda lakes in comparison with their closest phylogenetic relatives.

Property	*Natroniella* "sulfidigena" (3 strains)	*Natroniella acetigena*	*Natronolimnobius* strain AHT32	*Natronolimnobius innermongolicus*
Taxonomy	Bacteria, *Halanaerobiales*		Euryarchaeota, *Halobacteriales*	
Acetogenesis	–	EtOH, lactate, pyruvate, PrOH	–	–
Anaerobic growth with sulfur as *e*-acceptor	+	–	+	–*
Aerobic growth	–	–	C_2–C_8 VFA, yeast extract	C_6-sugars, propionate, citrate, lactate, malate, pyruvate, fumarate
Use of H_2 and formate as *e*-donors	+	–	+	–
Acetate as *e*-donor	+ (In one strain)	–	+	+
Autotrophy	+	–	+**	–
pH optimum	9.8–10.0	10.0	10.0	9.5
Minimal salt requirement (M Na^+)	1.5–2.0	1.7	2.5	1.7
Habitat	Hypersaline soda lakes			

The most essential properties are highlighted in bold.
**Sulfide was produced aerobically; **needs to be confirmed.*

A generalized scheme showing various sulfidogenic processes and microbes involved, which have been found so far in soda lakes, is given in **Figure 7**. The main factor influencing the soda lake SRB responsible for sulfate reduction and thiosulfate reduction/disproportionation is salinity. Sulfur reduction is a function of specialized groups, whose most important properties include the potential to utilize acetate as the *e*-donor and to grow in saturated soda brines.

APPLICATION OF HALOALKALIPHILIC SOB

Full-scale bioreactors (Thiopaq reactors, Paques B.V., The Netherlands) offer an attractive alternative to chemical processes for efficient H_2S removal from gases. Briefly, H_2S is stripped from the gas phase into alkaline solution at pH 9. Since the gases also contain CO_2, the resulting spent liquid is essentially sulfide solution in sodium bicarbonate, which is then transferred to a second reactor containing haloalkaliphilic SOB. The reactor is operating at extreme oxygen-limited conditions and very low redox potential to limit the oxidation of sulfide to elemental sulfur (Janssen et al., 2009). At such conditions both aerobic and anaerobic part of the microbial sulfur cycle can coexist. Recent analysis of the microbial communities in several of these reactors using DGGE and cultivation approach showed that the dominant population was represented by a single microaerophilic sulfide-specialized haloalkaliphilic SOB species belonging to the genus *Thioalkalivibrio* (*Tv.* "*sulfidophilus*"). Several other alkaliphilic and alkalitolerant SOB species belonging to the genera *Thioalkalivibrio, Thioalkalimicrobium*, and *Thiomicrospira* (*Tm. pelophila* group) could be isolated from the reactors as well, but they represented minor populations. Although molecular analysis did not detect any significant presence of the anaerobic sulfur cycle bacteria, alkalitolerant SRB, and sulfur-reducing bacteria could be enriched from the reactor biomass. The SRB belonged to *Desulfonatronum* spp. and *Desulfovibrio alkalitolerans* (Abildgaard et al., 2006), whilst the sulfur reducers were represented by a novel genus and species *Desulfurispirillum alkaliphilum* related to *Desulfurispira natronophila* from soda lakes (Sorokin et al., 2007b).

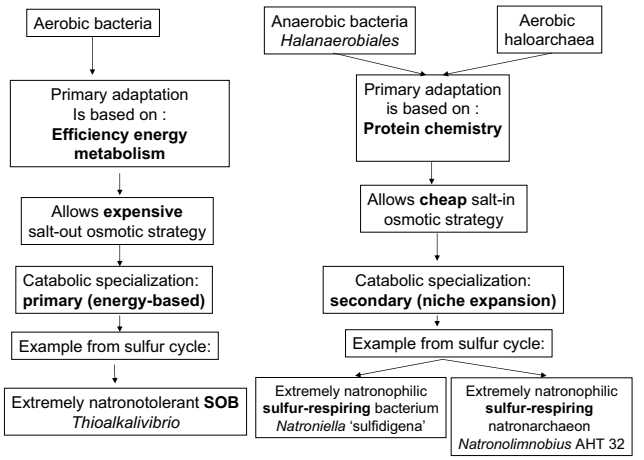

FIGURE 7 | Possible adaptation scenario of prokaryotes to functioning in saturated soda brines: case of sulfur cycling.

GENERAL CONCLUSIONS

Fifteen years of research on the microbial sulfur cycle in extremely alkaline and saline (soda) lakes showed that the cycle is complete and active at native pH up to salt-saturating conditions. The major (cultured) players include four different groups of aerobic and denitrifying chemolithoautotrophic SOB within the *Gammaproteobacteria*, two major groups of SRB within the *Deltaproteobacteria* and three different groups of sulfur-reducing prokaryotes. The culture-independent molecular approach also indicated the presence of several groups of

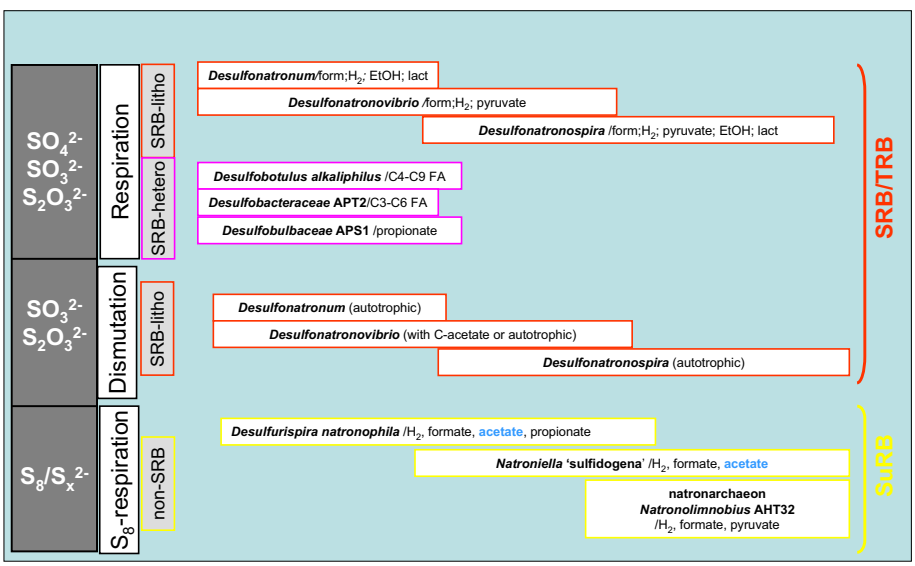

FIGURE 8 | A generalized microbial sulfidogenic system detected in soda lakes at pH 9.5–11.

SOB and SRB, which so far lack cultured representatives. The inherent properties of these sulfur-catabolizing prokaryotes from soda lakes are their obligate alkaliphily and preference for sodium carbonate as salt over sodium chloride. Being a weak electrolyte, sodium carbonate brines impose two times less osmotic pressure than strongly electrolytic NaCl brines with the same sodium content and, thus, are beneficial for the soda lake organisms, most of which are rather *natrono*(soda)philic than *halo*(sodium chloride)alkaliphilic. Nevertheless, even sodium carbonates at saturating concentrations, as present in hypersaline soda lakes, impose severe limitations on possible sulfur cycle catabolic reactions. In particular, only a few SOB and a single SRB have been found capable of growing in saturated soda brines. On the other hand, sulfur-reducing extreme natronophiles, possessing an "inorganic" osmotic strategy, may drive sulfidogenesis at soda-saturated conditions with simple electron donors, such as H_2, formate, and acetate. In fact, it may be speculated that two types of sulfur cycling exist at the soda lake sediment interface depending primarily on salinity (**Figure 9**). At low-to-moderate salinity the "long" sulfur cycle is possible with complete oxidation of sulfide/thiosulfate to sulfate by moderately natronophilic SOB and sulfate/thiosulfate reduction by natronophilic SRB. In saturated soda brines only a limited number of players can operate, such as the extremely natronotolerant SOB *Thioalkalivibrio* and the extremely natronophilic sulfur reducers, such as very specialized representatives of the *Halanaerobiales* and of the natronoarchaea. Also assuming less oxygen availability, the "short" sulfur cycle is most probable at salt-saturating conditions, with a specific reduced sulfur compound stable at high pH, i.e., polysulfide, as the central intermediate. In this cycle, sulfide is incompletely oxidized to elemental sulfur that in turn, chemically reacts with sulfide to form polysulfide. Polysulfide is a true substrate for sulfur reducers, but can also easily be converted to thiosulfate abiotically.

Future research in this field will obviously benefit from focused work on the bioenergetics of natronophiles with different metabolism and from whole genome analysis to understand the adaptation mechanisms to extreme natron-alkaline conditions. Recently, a metagenomic project on Kulunda Steppe soda lakes has been approved in the Community Sequencing Program of the Joint Genome Institute of the US Department of Energy, which should further advance research in this direction.

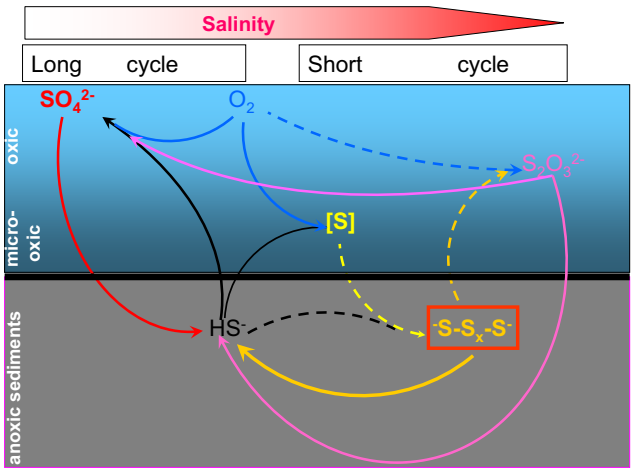

FIGURE 9 | Proposed scheme of microbial sulfur cycling in soda lakes. Dashed lines indicate abiotic reactions and solid lines show microbial conversions. The horizontal color gradient shows increase in salinity from left to right.

ACKNOWLEDGMENTS

This work was supported by RFBR grant 10-04-00152 to Dimitry Y. Sorokin and by the Dutch Foundations NWO and STW over the previous years of research. We are grateful to our colleagues Brian Jones, William Grant, George Zavarzin, Vladimir Gorlenko, and Holly Pinkart for providing samples from soda lakes in Kenya and the USA.

REFERENCES

Abildgaard, L., Nielsen, M. B., Kjeldsen, K. U., and Ingvorsen, K. (2006). *Desulfovibrio alkalitolerans* sp. nov., a novel alkalitolerant, sulfate-reducing bacterium isolated from district heating water. *Int. J. Syst. Evol. Microbiol.* 56, 1019–1024.

Banciu, H., Sorokin, D. Y., Kleerebezem, R., Muyzer, G., Galinski, E. A., and Kuenen, J. G. (2004a). Influence of sodium on the growth of haloalkaliphilic sulfur-oxidizing bacterium *Thioalkalivibrio versutus* strain ALJ 15 in continuous culture. *Extremophiles* 8, 185–192.

Banciu, H., Sorokin, D. Y., Galinski, E. A., Muyzer, G., Kleerebezem, R., and Kuenen, J. G. (2004b). *Thialkavibrio halophilus* sp. nov., a novel obligately chemolithoautotrophic facultatively alkaliphilic and extremely salt-tolerant sulfur-oxidizing bacterium from a hypersaline alkaline lake. *Extremophiles* 8, 325–334.

Banciu, H., Sorokin, D. Y., Tourova, T. P., Galinski, E. A., Muntyan, M. S., Kuenen, J. G., and Muyzer, G. (2008). Influence of salts and pH on growth and activity of a novel facultatively alkaliphilic, extremely salt-tolerant, obligately chemolithoautotrophic sufur-oxidizing gammaproteobacterium *Thioalkalibacter halophilus* gen. nov., sp. nov. from south-western Siberian soda lakes. *Extremophiles* 12, 391–404.

Bezsudnova, E. Y., Sorokin, D. Y., Tichonova, T. V., and Popov, V. O. (2007). System of primary thiocyanate degradation in a novel halophilic sulfur-oxidizing bacterium *Thiohalophilus thiocyanoxidans*. *Biochim. Biophys. Acta* 1774, 1563–1570.

Brandt, K. K., Vester, F., Jensen, A. N., and Ingvorsen, K. (2001). Sulfate reduction dynamics and enumeration of sulfate-reducing bacteria in hypersaline sediments of the Great Salt Lake (Utah, USA). *Microb. Ecol.* 41, 1–11.

Eugster, H. P. (1970). Chemistry and origins of the brines of Lake Magadi. *Mineral. Soc. Am. Spec. Publ.* 3, 215–235.

Foti, M., Ma, S., Sorokin, D. Y., Rademaker, J. L. W., Kuenen, J. G., and Muyzer, G. (2006). Genetic diversity and biogeography of haloalkaliphilic sulfur-oxidizing bacteria belonging to the genus *Thioalkalivibrio*. *FEMS Microbiol. Ecol.* 56, 95–101.

Foti, M., Sorokin, D. Y., Lomans, B., Mussman, M., Zakharova, E. E., Pimenov, N. V., Kuenen, J. G., and Muyzer, G. (2007). Diversity, activity and abundance of sulfate-reducing bacteria in saline and hypersaline soda lakes. *Appl. Environ. Microbiol.* 73, 2093–2100.

Foti, M., Sorokin, D. Y., Zakharova, E. E., Pimenov, N. V., Kuenen, J. G., and Muyzer, G. (2008). Bacterial diversity and activity along a salinity gradient in soda lakes of the Kulunda Steppe (Altai, Russia). *Extremophiles* 12, 133–145.

Giri, B. J., Bano, N., and Hollibaugh, J. T. (2004). Distribution of RuBisCO genotypes along a redox gradient in Mono Lake, California. *Appl. Environ. Microbiol.* 70, 3443–3448.

Gorlenko, V. M., Namsaraev, B. B., Kulyrova, A. V., Zavarzina, D. G., and Zhilina, T. N. (1999). Activity of sulfate-reducing bacteria in the sediments of the soda lakes in south-east Transbaikal area. *Microbiology* 68, 580–586.

Granada, C., Revah, S., and Le Borgne, S. (2009). Diversity of culturable bacteria in an alkaliphilic sulfur-oxidizing microbial consortium. *Adv. Mat. Res.* 71–73, 137–140.

Grischuk, Y. V., Muntyan, M. S., Popova, I. V., and Sorokin, D. Y. (2003). Ion transport coupled to terminal oxidase functioning in the extremely alkaliphilic halotolerant bacterium *Thioalkalivibrio*. *Biochemistry* 68, 385–390.

Humayoun, S. B., Bano, N., and Hollibaugh, J. T. (2003). Depth distribution of microbial diversity in Mono Lake, a meromictic soda lake

in California. *Appl. Environ. Microbiol.* 69, 1030–1042.

Itoh, T., Yamaguchi, T., Zhou, P., and Takashina, T. (2007). *Natronolimnobius baerhuensis* gen. nov., sp. nov. and *Natronolimnobius innermongolicus* sp. nov., novel haloalkaliphilic archaea isolated from soda lakes in Inner Mongolia, China. *Extremophiles* 9, 111–116.

Janssen, A. J. H., Lens, P., Stams, A. J. M., Plugge, C. M., Sorokin, D. Y., Muyzer, G., Dijkman, H., van Zessen, E., Luimes, P., and Buisman, C. J. N. (2009). Application of bacteria involved in the biological sulfur cycle for paper mill effluent purification. *Sci. Total Environ.* 407, 1333–1343.

Jones, B. E., Grant, W. D., Duckworth, A. W., and Owenson, G. G. (1998). Microbial diversity of soda lakes. *Extremophiles* 2, 191–200.

Katayama, Y., Matsushita, Y., Kaneko, M., Kondo, M., Mizuno, T., and Nyunoya, H. (1998). Cloning of genes coding for the subunits of thiocyanate hydrolase of *Thiobacillus thioparus* THI 115 and their evolutionary relationships to nitrile hydratase. *J. Bacteriol.* 180, 2583–2589.

Kelly, D. P., and Baker, S. C. (1990). The organosulfur cycle: aerobic and anaerobic processes leading to turnover of C1-sulfur compounds. *FEMS Microbiol. Rev.* 87, 241–246.

Kjeldsen, K. U., Jakobsen, T. F., Glastrup, J., and Ingvorsen, K. (2010). *Desulfosalsimonas propionicica* gen. nov. sp. nov., a novel halophilic sulfate-reducing member of the family Desulfobacteraceae isolated from sediment of Great Salt Lake (Utah). *Int. J. Syst. Evol. Microbiol.* 60, 1060–1065.

Kovaleva, O. L., Tourova, T. P., Muyzer, G., Kolganova, T. V., and Sorokin, D. Y. (2011). Diversity of RuBisCO and ATP citrate lyase genes in soda lake sediments. *FEMS Microbiol. Ecol.* 35, 37–47.

Kulp, T. R., Han, S., Saltikov, C. V., Lanoil, B. D., Zargar, K., and Oremland, R. S. (2007). Effects of imposed salinity gradients on dissimilatory arsenate reduction, sulfate reduction, and other microbial processes in sediments from two California soda lakes. *Appl. Environ. Microbiol.* 73, 5130–5137.

Kulp, T. R., Hoeft, S. E., Miller, L. G., Saltikov, C., Murphy, J. N., Han, S., Lanoil, B., and Oremland, R. S. (2006). Dissimilatory arsenate and sulfate reduction in sediments of two hypersaline, arsenic-rich soda lakes: Mono and Searles Lakes, California. *Appl. Environ. Microbiol.* 72, 6514–6526.

Mesbah, N. M., Abou-El-Ela, S. H., and Wiegel, J. (2007). Novel and unexpected prokaryote diversity in water and sediments of the alkaline hypersaline lakes of the Wadi An Natrun, Egypt. *Microb. Ecol.* 54, 598–617.

Muyzer, G., Sorokin, D. Y., Mavromatis, K., Lapidus, A., Clum, A., Ivanova, N., Pati, A., d'Haeseleer, P., Woyke, T., and Kyrpides, N. C. (2011). Complete genome sequence of *Thioalkalivibrio* "sulfidophilus" HL-EbGr7. *Stand. Genomic Sci.* 4, doi:10.4056/sigs.1483693

Oren, A. (1999). Bioenergetic aspects of halophilism. *Microbiol. Mol. Biol. Rev.* 63, 34–348.

Oren, A. (2011). Thermodynamic limits to microbial life at high salt concentrations. *Environ. Microbiol.* doi: 10.1111/j.1462-2920.2010.02365.x. [Epub ahead of print].

Pikuta, E. V., Hoover, R. B., Bej, A. K., Marsic, D., Whitman, W. B., Cleland, D., and Krader, P. (2003). *Desulfonatronum thiodismutans* sp. nov., a novel alkaliphilic, sulfate-reducing bacterium capable of lithoautotrophic growth. *Int. J. Syst. Evol. Microbiol.* 53, 1327–1332.

Pikuta, E. V., Zhilina, T. N., Zavarzin, G. A., Kostrikina, N. A., Osipov, G. A., and Rainey, F. A. (1998). *Desulfonatronum lacustre* gen. nov., sp. nov.: a new alkaliphilic sulfate-reducing bacterium utilizing ethanol. *Microbiology* 67, 105–113.

Roberts, M. F. (2005). Organic compatible solutes of halotolerant and halophilic microorganisms. *Saline Syst.* 1, 5.

Roeßler, M., and Müller, V. (2001). Osmoadaptation in bacteria and archaea: common principles and differences. *Environ. Microbiol.* 3, 743–754.

Sakurai, H., Ogawa, T., Shiga, M., and Inoue, K. (2010). Inorganic sulfur-oxidizing system in green sulfur bacteria. *Photosyn. Res.* 104, 163–176.

Sander, J., and Dahl, C. (2009). "Metabolism of inorganic sulfur compounds in purple bacteria," in *The Purple Sulfur Bacteria*, eds N. Hunter, F. Daldal, M. C. Thurnauer, and J. T. Beatty (Dordrecht: Springer Science + Business Media B.V.), 595–692.

Scholten, J. C. M., Joye, S. B., Hollibaugh, J. T., and Murrell, J. C. (2005). Molecular analysis of the sulfate reducing and archaeal community in a meromictic soda lake (Mono Lake, California) by targeting 16S rRNA, mcrA, apsA, and dsrAB genes. *Microb. Ecol.* 50, 29–39.

Schweinfurth, G., and Lewin, L. (1898). Beiträge zur Topographie und Geochemie des ägyptischen Natron-Thals. *Z. Gesamte Erdk.* 33, 1–25.

Sørensen, K. B., Canfield, D. E., and Oren, A. (2004). Salinity responses of benthic microbial communities in a solar saltern (Eilat, Israel). *Appl. Environ. Microbiol.* 70, 1608–1616.

Sørensen, K. B., Canfield, D. E., Teske, A. P., and Oren, A. (2005). Community composition of a hypersaline endoevaporitic microbial mat. *Appl. Environ. Microbiol.* 71, 7352–7365.

Sorokin, D. Y. (2003). Oxidation of inorganic sulfur compounds by obligately organotrophic bacteria. *Microbiology* 72, 725–739.

Sorokin, D. Y. (2008). "Diversity of halophilic sulfur-oxidizing bacteria in hypersaline habitats," in *Microbial Sulfur Metabolism, Proceedings of the International Symposium on Microbial Sulfur Metabolism*, 29.06.2006 to 02.07.2006, eds C. Dahl and C. G. Friedrich (Münster: Springer-Berlin), 225–237.

Sorokin, D. Y., Banciu, H., Robertson, L. A., and Kuenen, J. G. (2006). "Haloalkaliphilic sulfur-oxidizing bacteria," in *The Prokaryotes: A Handbook on the Biology of Bacteria*, 3rd Edn, Vol. 2, eds M. Dworkin, S. Falkow, E. Rosenberg, K.-H. Schleifer, and E. Stackebrandt (New York: Springer-Verlag), 969–984.

Sorokin, D. Y., Banciu, H., van Loosdrecht, M., and Kuenen, J. G. (2003a). Growth physiology and competitive interaction of obligately chemolithoautotrophic, haloalkaliphilic, sulfur-oxidizing bacteria from soda lakes. *Extremophiles* 7, 195–203.

Sorokin, D. Y., Antipov, A. N., and Kuenen, J. G. (2003b). Complete denitrification in coculture of obligately chemolithoautotrophic haloalkaliphilic sulfur-oxidizing bacteria from a hypersaline soda lake. *Arch. Microbiol.* 180, 127–133.

Sorokin, D. Y., Tourova, T. P., Sjollema, K. A., and Kuenen, G. J. (2003c). *Thioalkalivibrio nitratireducens* sp. nov., a nitrate-reducing member of an autotrophic denitrifying consortium from a soda lake. *Int. J. Syst. Evol. Microbiol.* 53, 1779–1783.

Sorokin, D. Y., Foti, M., Tindall, B. J., and Muyzer, G. (2007a). *Desulfurispirillum alkaliphilum* gen. nov. sp. nov., a novel obligately anaerobic sulfur- and dissimilatory nitrate-reducing bacterium from a full-scale sulfide-removing bioreactor. *Extremophiles* 11, 363–370.

Sorokin, D. Y., Foti, M., Pinkart, H. C., and Muyzer, G. (2007b). Sulfur-oxidizing bacteria in Soap Lake (Washington, USA), a meromictic, haloalkaline lake with an unprecedented high sulfide content. *Appl. Environ. Microbiol.* 73, 451–455.

Sorokin, D. Y., Gorlenko, V. M., Tourova, T. P., Kolganova, T. V., Tsapin, A. I., Nealson, K. H., and Kuenen, J. G. (2002a). *Thioalkalimicrobium cyclicum* sp. nov. and Thioalkalivibrio jannaschii sp. nov., new species of alkaliphilic, obligately chemolithoautotrophic sulfur-oxidizing bacteria from a hypersaline alkaline Mono Lake (California). *Int. J. Syst. Evol. Microbiol.* 52, 913–920.

Sorokin, D. Y., Tourova, T. P., Kolganova, T. V., Sjollema, K. A., and Kuenen, J. G. (2002b). *Thioalkalispira microaerophila* gen. nov., sp. nov., a novel lithoautotrophic, sulfur-oxidizing bacterium from a soda lake. *Int. J. Syst. Evol. Microbiol.* 52, 2175–2182.

Sorokin, D. Y., Tourova, T. P., Lysenko, A. M., Mityushina, L. L., and Kuenen, J. G. (2002c). *Thioalkalivibrio thiocyanooxidans* sp. nov. and *Thioalkalivibrio paradoxus* sp. nov., novel alkaliphilic, obligately autotrophic, sulfur-oxidizing bacteria from the soda lakes able to grow with thiocyanate. *Int. J. Syst. Evol. Microbiol.* 52, 657–664.

Sorokin, D. Y., and Kuenen, J. G. (2005). Haloalkaliphilic sulfur-oxidizing bacteria in soda lakes. *FEMS Microbiol. Rev.* 29, 685–702.

Sorokin, D. Y., Lysenko, A. M., Mityushina, L. L., Tourova, T. P., Jones, B. E., Rainey, F. A., Robertson, L. A., and Kuenen, J. G. (2001a). *Thioalkalimicrobium aerophilum* gen. nov., sp. nov. and *Thioalkalimicrobium sibericum* sp. nov., and *Thioalkalivibrio versutus* gen. nov., sp. nov., *Thioalkalivibrio nitratis* sp. nov. and *Thioalkalivibrio denitrificans* sp. nov., novel obligately alkaliphilic and obligately chemolithoautotrophic sulfur-oxidizing bacteria from soda lakes *Int. J. Syst. Evol. Microbiol.* 51, 565–580.

Sorokin, D. Y., Kuenen, J. G., and Jetten, M. (2001b). Denitrification at extremely alkaline conditions in obligately autotrophic alkaliphilic sulfur-oxidizing bacterium *Thioalkalivibrio denitrificans*. *Arch. Microbiol.* 175, 94–101.

Sorokin, D. Y., Tourova, T. P., Lysenko, A. M., and Kuenen, J. G. (2001c). Microbial thiocyanate utilization under highly alkaline conditions. *Appl. Environ. Microbiol.* 67, 528–538.

Sorokin, D. Y., and Muyzer, G. (2010a). Haloalkaliphilic spore-forming sulfidogens from soda lake sediments and description of *Desulfitispora alkaliphila* gen. nov., sp. nov. *Extremophiles* 14, 313–320.

Sorokin, D. Y., and Muyzer, G. (2010b). *Desulfurispira natronophila* gen. nov. sp. nov.: an obligately anaerobic dissimilatory sulfur-reducing bacterium from soda lakes. *Extremophiles* 14, 349–355.

Sorokin, D. Y., Robertson, L. A., and Kuenen, J. G. (2000). Isolation and characterization of obligately chemolithoautotrophic alkaliphilic

sulfur-oxidizing bacteria. *Ant. V. Leeuwenhoek* 77, 251–260.

Sorokin, D. Y., Rusanov, I. I., Pimenov, N. V., Tourova, T. P., Abbas, B., and Muyzer, G. (2010a). Sulfidogenesis at extremely haloalkaline conditions in soda lakes of Kulunda Steppe (Altai, Russia). *FEMS Microbiol. Ecol.* 73, 278–290.

Sorokin, D. Y., Detkova, E. N., and Muyzer, G. (2010b). Propionate and butyrate dependent bacterial sulfate reduction at extremely haloalkaline conditions and description of *Desulfobotulus alkaliphilus* sp. nov. *Extremophiles* 14, 71–77.

Sorokin, D. Y., Tourova, T. P., Antipov, A. N., Muyzer, G., and Kuenen, J. G. (2004a). Anaerobic growth of the haloalkaliphilic denitrifying sulphur-oxidising bacterium *Thialkalivibrio thiocyanodenitrificans* sp. nov. with thiocyanate. *Microbiology* 150, 2435–2442.

Sorokin, D. Y., Gorlenko, V. M., Namsaraev, B. B., Namsaraev, Z. B., Lysenko, A. M., Eshinimaev, B. T., Khmelenina, V. N., Trotsenko, Y. A., and Kuenen, J. G. (2004b). Prokaryotic communities of the north-eastern Mongolian soda lakes. *Hydrobiologia* 522, 235–248.

Sorokin, D. Y., Tourova, T. P., Henstra, A. M., Stams, A. J. M., Galinski, E. A., and Muyzer, G. (2008). Sulfidogenesis at extremely haloalkaline conditions by *Desulfonatronospira thiodismutans* gen. nov., sp. nov., and *Desulfonatronospira delicata* sp. nov. – a novel lineage of *Deltaproteobacteria* from hypersaline soda lakes. *Microbiology* 154, 1444–1453.

Tourova, T. P., Spiridonova, E. M., Berg, I. A., Kuznetsov, B. B., and Sorokin, D. Y. (2006). Occurrence, phylogeny and evolution of ribulose-1,5-bisphosphate carboxylase/oxygenase genes in obligately chemolithoautotrophic sulfur-oxidizing bacteria of the genera *Thiomicrospira and Thioalkalimicrobium. Microbiology* 152, 2159–2169.

Tourova, T. P., Spiridonova, E. M., Berg, I. A., Slobodova, N. V., Boulygina, E. S., and Sorokin, D. Y. (2007). Phylogeny and evolution of the family Ectothiorhodospiraceae based on comparison of 16S rRNA, *cbb*L and *nif*H gene sequences. *Int. J. Syst. Evol. Microbiol.* 57, 2387–2398.

Youatt, J. B. (1954). Studies on the metabolism of *Thiobacillus thiocyanooxidans. J. Gen. Microbiol.* 11, 139–149.

Zhilina, T. N., Zavarzin, G. A., Detkova, E. N., and Rainey, F. A. (1995). *Natroniella acetigena* gen. nov. sp. nov., an extremely haloalkaliphilic, homoacetic bacterium: a new member of Haloanaerobiales. *Curr. Microbiol.* 32, 320–326.

Zhilina, T. N., Zavarzin, G. A., Rainey, F. A., Pikuta, E. N., Osipov, G. A., and Kostrikina, N. A. (1997). *Desulfonatronovibrio hydrogenovorans* gen. nov., sp. nov., an alkaliphilic, sulfate-reducing bacterium. *Int. J. Syst. Bacteriol.* 47, 144–149.

Zhilina, T. N., Zavarzina, D. G., Kuever, J., Lysenko, A. M., and Zavarzin, G. A. (2005). *Desulfonatronum cooperativum* sp. nov., a novel hydrogenotrophic, alkaliphilic, sulfate-reducing bacterium, from a syntrophic culture growing on acetate. *Int. J. Syst. Evol. Microbiol.* 55, 1001–1006.

Conflict of Interest Statement: The authors declare that the research was conducted in the absence of any commercial or financial relationships that could be construed as a potential conflict of interest.

Received: 30 January 2011; paper pending published: 22 February 2011; accepted: 25 February 2011; published online: 21 March 2011.

Citation: Sorokin DY, Kuenen JG and Muyzer G (2011) The microbial sulfur cycle at extremely haloalkaline conditions of soda lakes. Front. Microbio. ***2****:44. doi: 10.3389/fmicb.2011.00044*

This article was submitted to Frontiers in Microbial Physiology and Metabolism, a specialty of Frontiers in Microbiology.

frontiers in
MICROBIOLOGY

ORIGINAL RESEARCH ARTICLE
published: 13 June 2011
doi: 10.3389/fmicb.2011.00130

Microbial communities and chemosynthesis in Yellowstone Lake sublacustrine hydrothermal vent waters

Tingting Yang[1], Shawn Lyons[1], Carmen Aguilar[2], Russell Cuhel[2] and Andreas Teske[1]*

[1] *Department of Marine Sciences, University of North Carolina at Chapel Hill, Chapel Hill, NC, USA*
[2] *Great Lakes WATER Institute, University of Wisconsin – Milwaukee, Milwaukee, WI, USA*

Edited by:
Thomas E. Hanson, University of Delaware, USA

Reviewed by:
Marina Kalyuzhnaya, University of Washington, USA
Matthew Schrenk, East Carolina University, USA

***Correspondence:**
Andreas Teske, Department of Marine Sciences, University of North Carolina at Chapel Hill, 351 Chapman Hall, CB 3300, Chapel Hill, NC 27599, USA.
e-mail: teske@email.unc.edu

Five sublacustrine thermal spring locations from 1 to 109 m water depth in Yellowstone Lake were surveyed by 16S ribosomal RNA gene sequencing in relation to their chemical composition and dark CO_2 fixation rates. They harbor distinct chemosynthetic bacterial communities, depending on temperature (16–110˚C) and electron donor supply (H_2S <1 to >100 μM; NH_3 <0.5 to >10 μM). Members of the *Aquificales*, most closely affiliated with the genus *Sulfurihydrogenibium*, are the most frequently recovered bacterial 16S rRNA gene phylotypes in the hottest samples; the detection of these thermophilic sulfur-oxidizing autotrophs coincided with maximal dark CO_2 fixation rates reaching near 9 μM C h^{-1} at temperatures of 50–60˚C. Vents at lower temperatures yielded mostly phylotypes related to the mesophilic gammaproteobacterial sulfur oxidizer *Thiovirga*. In contrast, cool vent water with low chemosynthetic activity yielded predominantly phylotypes related to freshwater Actinobacterial clusters with a cosmopolitan distribution.

Keywords: Yellowstone, hydrothermal vents, chemosynthesis, *Sulfurihydrogenibium*, *Thiovirga*, sublacustrine springs

INTRODUCTION

In-depth geophysical and geochemical exploration and lake floor mapping of Yellowstone Lake, the largest Alpine Lake in the United States, has revealed numerous sublacustrine hot vents and hydrothermal features in geothermally active areas on the lake bottom (Klump et al., 1988, 1995; Remsen et al., 1990; Morgan et al., 2003a,b). Direct observations by SCUBA and ROV have revealed a wide range of hydrothermal features, including large hydrothermal chimneys; gas fumaroles; seepage of hot, shimmering water; and sulfur-oxidizing microbial mats growing around hot water seeps and vents (Remsen et al., 2002). Examination of an ancient vent chimney revealed internal conduit structures with metal sulfide precipitates, indicating long-term hydrothermal activity (Cuhel et al., 2004).

In contrast to the well-studied photosynthetic and chemosynthetic aerial hot spring communities of Yellowstone Park terrestrial habitats (Ward et al., 1998; Spear et al., 2005), systematic analyses of these Yellowstone Lake hydrothermal microbial communities are in their early stages, but have already demonstrated the potential for autotrophic, thermophilic chemosynthetic microbial communities. For example, the vents at Steamboat Point and Mary Bay at the northern edge of the lake, and deep-water vents off Stevenson island in the center of the lake, harbor chemosynthetic bacteria that assimilate dissolved inorganic carbon (DIC) in the dark at rates typically 0.08–0.5 μM C h^{-1}, with maxima at approximately 0.75 μM C h^{-1} (Cuhel et al., 2002). Thus, chemosynthetic rates often exceed the photosynthetic rate at the lake surface, approximately 0.25 μM C h^{-1} (Cuhel et al., 2002). Microbial biodiversity in Yellowstone Lake thermal springs is largely unexplored. The isolation of the thermophilic sulfate-reducing bacterium *Thermodesulfovibrio yellowstonii*, a deeply branching bacterial lineage from Yellowstone Lake thermal vents, implies untapped potential for further discoveries (Henry et al., 1994).

Here, we present results of a preliminary 16S rRNA gene clone library survey of the bacterial communities in five different thermal vent locations in Yellowstone Lake with distinct chemical signatures and distinct temperature-dependent chemosynthetic rates. The 16S rRNA gene clone libraries indicate the existence of distinct chemosynthetic bacterial communities, dominated either by Gammaproteobacteria affiliated with the mesophilic sulfur-oxidizing genus *Thiovirga*, or by phylotypes most closely related to cultured species and strains of the extremely thermophilic Aquificales.

MATERIALS AND METHODS

SAMPLING AND DNA EXTRACTION

Hydrothermal vent waters were collected in July 2003 from five locations (**Table 1**) in Yellowstone Lake for microbial community analysis by 16S rRNA gene sequencing (**Table 1**). The first two samples come from the Mary Bay area near the northeastern shore of the lake, one of the hydrothermally most active areas of Yellowstone Lake, with high heat flux and numerous hydrothermal vents (Morgan et al., 2003b): Mary Bay West 12 is a surface water sample taken above a nearshore bubbling warm fumarole in shallow water (1 m), and Mary Bay Canyon 28 represents warm deep water (52 m) below the sill of an underwater canyon in Mary Bay. The third and hottest water sample, Stevenson Island 72, comes from a deep trench east of Stevenson Island in the central portion of the lake, where small, well-developed hydrothermal vents coalesce along northwest-trending deep fissures that reach maximally 133 m depth, the deepest point in the lake (Morgan et al., 2003b). The fourth sample, West Thumb Canyon 129, represents hot vent

water from a sublacustrine explosion crater in the western part of West Thumb basin, in the westernmost part of the lake (Morgan et al., 2003b). The fifth sample from the West Thumb Basin, West Thumb 98, represents a cooler, low activity water sample from the West Thumb area. *In situ* temperatures measured by ROV, and chemistry of the syringe-sampled waters are shown in **Table 1**.

Water was collected into 2-L polycarbonate piston-style syringe samplers mounted on a tethered ROV (Eastern Oceanics, Inc.) using an articulated arm outfitted with a thermistor probe at the end to measure the temperature of the water as it was collected (Aguilar et al., 2002). Using a checkvalve system, each piston sample was rinsed with 300–500 mL of vent sample prior to filling. The ROV is fully operator-controlled with thrusters that allow for lake floor reconnaissance and positioning for sampling, and included live video for vent identification and guided sampling (Lovalvo et al., 2010); it is deployed from RV Cutthroat, the Yellowstone Lake research vessel owned and operated by the National Park Service. Vent water samples were retrieved from the ROV collection syringes and put into smaller, all-plastic syringes through a three-way valve without exposure to air. Subsamples of 150–310 mL volume (**Table 1**) were used for filtration and cell capture on 0.22 μm polycarbonate filters. The filters were frozen at −80°C until DNA isolation in the laboratory in Chapel Hill, by phenol/chloroform extraction (Teske et al., 1996). Near-complete 16S rRNA genes were PCR-amplified with bacterial primers 8F (5′-AGRGTTTGATCCTGGCTCAG-3′)

Table 1 | Yellowstone Lake vent samples: summary of chemistry, dark C fixation, and 16S rRNA gene sequence data.

Sampling location and sample code	Mary Bay West 12 MBW	Mary Bay Canyon 28 V03-13P	Stevenson Island 72 V03-28P	West Thumb Canyon 129 V03-46P	West Thumb 98 V03-36P	Yellowstone Lake station LW-02
Sample volume and date	310 mL 7-16-03	190 mL 7-18-03	303 mL 7-22-03	150 mL 7-29-03	303 mL 7-25-03	N/A 7-1-03
Water depth (m)	1	47.9	109.3	52.4	21.7	0
Temperature (°C)	19	49	110	77	16	Ambient
DOC (mg/l)	1.77	1.89	n.d.	n.d.	1.45	n.d.
H_2S (μM)	2.2	119.3	59.5	17.2	0.7	0
SO_3^{2-} (μM)	1.3	4.5	5.3	8.4	3.7	0
$S_2O_3^{2-}$ (μM)	0.1	1.4	19.9	1.52	0.5	0
SO_4^{2-} (μM)	104	122	93	187	86	83
NH_4^+ (μM)	1.5	12.7	11.0	8.8	0.0	0.7
$NO_3^- + NO_2^-$ (μM)	0.1	0.2	0.9	1.0	0.0	0.0
SRP (μM)	0.21	1.84	0.68	2.51	0.59	0.32
SiO_2 (μM)	192	325	197	1865	159	178
Cl^- (μM)	146	210	132	1971	156	125
Summary of dark CO_2 fixation rates (μM C h^{-1})	1.08, 15°C 6.46, 15°C with S	1.7 at 15°C 8.6 at 60°C no. S stimulation	<0.01, 15°C 0.4 at 50°C 0.67 at 60°C	Near 0.1 at 50 and 60°C 0.83–1.66, with S, 60°C	Near 0.003 with S, 50°C <0.003 otherwise	0.003
No. of bacterial 16S rRNA gene sequences	44	23	37	54	38	
Aquificales	–	2	16	13	–	
Gammaproteobacteria	21	5	1	–	1	
Betaproteobacteria	8	3	6	10	13	
Alphaproteobacteria	1	1	–	–	–	
Deltaproteobacteria	–	7	–	–	–	
Epsilonproteobacteria	–	1	–	–	–	
Actinobacteria	6	–	7	10	16	
Planctomycetales	–	–	4	–	2	
CFB phylum	2	1	–	3	–	
Chloroflexi	2	–	–	6	1	
Acidobacteria	–	3	–	–	–	
Cyanobacteria	2	–	1	–	3	
Thermodesulfovibrio	–	–	–	7	–	
Verrucomicrobium	1	–	2	–	2	
OP10	1	–	–	–	–	
Chlorobia	–	–	–	2	–	
Thermodesulfobacteria	–	–	–	3	–	

and 1492R (5′-CGGCTACCTTGTTACGACTT-3′); these primers were successful in recovering extremely diverse bacterial communities, including members of novel phyla (Teske et al., 2002). PCR products were cloned using the TOPO XL PCR cloning kit (Invitrogen Corporation, Carlsbad, CA, USA) following the manufacturers instructions, and sequenced at the sequencing center of the University of North Carolina with primers M13F (5′-GTAAAACGACGGCCAG-3′) and M13R (5′-CAGGAAACAGCTATGAC-3′).

CHEMICAL ANALYSIS AND DARK C FIXATION RATE MEASUREMENTS

Analytical equipment was transported to Yellowstone National Park and set up as a field laboratory at the National Park Service Lake Station. Freshly collected samples for stable analytes were filtered through 0.2-μm filters (Supor-200, Pall Corp.) and aliquoted for the different analyses. Dissolved compounds were measured by flow injection analysis (silicate, nitrate, nitrite), ion chromatography (chloride, sulfate), and spectrophotometry (ammonium, phosphate) according to standard methods (APHA, 1992).

All labile species were analyzed on site within 1 day of collection and analytical preparation. Rubber-free all polypropylene (PP) syringes with three-way valves were used to collect water from the 2-L ROV-mounted piston syringe samplers without introducing headspace. The ROV's screw drive was used to squeeze the water into receiving syringes to maximally retain dissolved gases. Total DIC was analyzed by the Teflon-membrane flow injection method of Hall and Aller (1992), in which the sipper tube was inserted through the three-way valve and the syringe plunger used to prevent formation of headspace during injection. For deep samples from Stevenson Island, unavoidable degassing effects were reduced by shaking the syringe thoroughly just before sipping, as the method measures all forms of CO_2 including dissolved gas. Reduced sulfur compounds (hydrogen sulfide, thiosulfate, sulfite) were quantified by a scaled-up modification of the microbore high-performance liquid chromatographic (HPLC) method of Vairavamurthy and Mopper (1990), using dithiobis-nitropyridine (DTNP) derivatization. Samples were collected in PP syringes and after rinsing, exactly 10 mL were squeezed through 0.2 μm nylon syringe filters (Whatman Acrodisc) into acid-washed 20 mL liquid scintillation vials (LSV). Using a positive displacement repeating pipette, the DTNP reagent was added, the vial capped with a cone-seal cap, and mixed vigorously before storing in a cooler with ice. After return to the laboratory, the precipitated unreacted DTNP was removed with another syringe and nylon filter during injection into the 100-μL HPLC sample loop. Each analysis required 45 min in a dual mobile phase gradient separation on a 250-mm C18 5 μm HS reversed phase column (Alltech Assoc.) so as many as 30 samples could be analyzed daily.

Light and dark CO_2 incorporation rates were determined by measuring the biological conversion of acid-labile ^{14}C-bicarbonate into acid-stable organic ^{14}C, as described previously (Cuhel et al., 2002). Briefly, suitable aliquots of fresh vent water or lake samples, usually 180 mL, were dispensed with minimal mixing into an acid-washed PP beaker. Enough high specific activity ^{14}C-bicarbonate (56 mCi mmol^{-1}, MP Biomedical) was added to give about 2×10^6 DPM mL^{-1}. The sample was drawn into a positive displacement 50 mL repeating pipette tip, and 10 mL aliquots were gently added to acid-washed 20 mL LSV in custom machined aluminum incubator blocks. Additions (thiosulfate, inhibitors, other stimulants, etc.) had been previously loaded into the appropriate vials at 1:100 to 1:1000× dilution from concentrated stocks. Temperature was controlled by a water bath circulator through the large 64-place block for 15°C incubations with triplicates and many treatments. Photosynthesis was measured identically, except that the projector lamp light source (ELH, 4 × 300 W) was turned on and incubations spanned only 3 h.

Elevated temperature incubation (controls, +thiosulfate in duplicate only) was accomplished in electrically heated aluminum dry block incubators. In these, 10 mL of sample were heated from ambient to 80°C in about 11 min during a ∼12 h incubation, minimizing artifacts of transient temperature increases in the upper mesophilic range. All vials were capped with cone-seal caps to reduce loss of volatile species, while the atmospheric oxygen contained in 12 mL of headspace guaranteed aerobic conditions for the measurements (>4 mM dissolved oxygen equivalents). Anaerobic chemosynthesis assays were beyond the capabilities of the field laboratory. For practical reasons, most incubations were initiated in late evening after field sampling and sample processing, and terminated prior to the next morning's ROV expedition, usually 10–14 h of incubation. Each measurement was terminated by injection of 0.25 mL 2 N H_2SO_4 followed by >12 h shaking (100 RPM) to remove unmetabolized ^{14}C, addition of liquid scintillation cocktail (Hydrofluor; National Diagnostics), and storage until counting. Duplicate 10 mL aliquots for background ^{14}C contamination were shot into acid-containing LSV immediately after dispensing block samples; in 2003 these typically yielded <500 DPM from the 2×10^7 DPM added initially. The time course measurements for Mary Bay 12 were accomplished in 250 mL tissue culture flasks with additions of supplements and ^{14}C-bicarbonate as above but in the larger volume of sample. The flasks were placed on the large aluminum blocks set for 15°C and covered with foil. At zero time and at each successive time point, 10 mL were pipetted into an LSV containing the sulfuric acid and treated as above.

PHYLOGENETIC ANALYSIS AND SEQUENCE QUALITY CONTROL

Forward and reverse reads were assembled and aligned in ARB (Ludwig et al., 2004). PCR primer regions were excluded from the alignment underlying phylogenetic inference. Phylogenies were inferred using neighbor-joining analysis of Jukes–Cantor distance matrix; primer regions were excluded. For bootstrap analysis, the alignments were exported in paup format, and tree topologies were checked with 1000 distance neighbor-joining bootstrap replicates in PAUP 4.0 (Swofford, 2000). By comparing phylogenetic trees based separately on the first and the second halves of the alignments, chimeric sequences were identified and removed from the dataset; indicators for chimeras included inconsistent topologies in multiple trees based on the different 16S rRNA gene subsections, combined with low or lacking bootstrap support, and sequence removal improving the bootstrap support for the branch harboring the problem sequence (Hugenholtz and Huber, 2003). The sequences have GenBank accession numbers HM446045 to HM4461154 (**Table 2**).

Table 2 | List of clone names, Genbank accession numbers, phylogenetic affiliation, and sample of origin.

Clone	GenBank accession number	Phylum	Sampling sites
MB28_023	HM446067	Acidobacteria	Mary Bay 28
MB28_029	HM446068	Acidobacteria	Mary Bay 28
MB28_030	HM446070	Acidobacteria	Mary Bay 28
MB12_019	HM446046	Actinobacteria	Mary Bay 12
MB12_023	HM446049	Actinobacteria	Mary Bay 12
MB12_066	HM446052	Actinobacteria	Mary Bay 12
MB12_071	HM446053	Actinobacteria	Mary Bay 12
SI72_007	HM446084	Actinobacteria	Stevenson Island 72
SI72_016	HM446086	Actinobacteria	Stevenson Island 72
SI72_057	HM446094	Actinobacteria	Stevenson Island 72
SI72_059	HM446095	Actinobacteria	Stevenson Island 72
SI72_069	HM446096	Actinobacteria	Stevenson Island 72
SI72_071	HM446097	Actinobacteria	Stevenson Island 72
WT98_026	HM446105	Actinobacteria	West Thumb 98
WT98_035	HM446107	Actinobacteria	West Thumb 98
WT98_048	HM446110	Actinobacteria	West Thumb 98
WT98_049	HM446111	Actinobacteria	West Thumb 98
WT98_055	HM446112	Actinobacteria	West Thumb 98
WT98_067	HM446115	Actinobacteria	West Thumb 98
WT98_074	HM446118	Actinobacteria	West Thumb 98
WT98_075	HM446119	Actinobacteria	West Thumb 98
WT98_079	HM446120	Actinobacteria	West Thumb 98
WT98_092	HM446122	Actinobacteria	West Thumb 98
WT98_094	HM446123	Actinobacteria	West Thumb 98
WT129_012	HM446128	Actinobacteria	West Thumb 129
WT129_027	HM446133	Actinobacteria	West Thumb 129
WT129_041	HM446135	Actinobacteria	West Thumb 129
WT129_044	HM446137	Actinobacteria	West Thumb 129
WT129_070	HM446146	Actinobacteria	West Thumb 129
WT129_075	HM446148	Actinobacteria	West Thumb 129
WT129_081	HM446151	Actinobacteria	West Thumb 129
MB12_089	HM446063	Alphaproteobacteria	Mary Bay 12
MB28_002	HM446076	Alphaproteobacteria	Mary Bay 28
MB28_013	HM446069	Aquificales	Mary Bay 28
MB28_032	HM446071	Aquificales	Mary Bay 28
SI72_008	HM446085	Aquificales	Stevenson Island 72
SI72_055	HM446092	Aquificales	Stevenson Island 72
WT129_036	HM446134	Aquificales	West Thumb 129
WT129_042	HM446136	Aquificales	West Thumb 129
WT129_051	HM446138	Aquificales	West Thumb 129
WT129_071	HM446147	Aquificales	West Thumb 129
WT129_076	HM446149	Aquificales	West Thumb 129
WT129_092	HM446154	Aquificales	West Thumb 129
MB12_009	HM446045	Bacteroidetes	Mary Bay 12
MB12_053	HM446051	Bacteroidetes	Mary Bay 12
MB28_005	HM446066	Bacteroidetes	Mary Bay 28
WT129_019	HM446130	Bacteroidetes	West Thumb 129
WT129_025	HM446132	Bacteroidetes	West Thumb 129
WT129_063	HM446144	Bacteroidetes	West Thumb 129
MB12_003	HM446057	Betaproteobacteria	Mary Bay 12
MB12_010	HM446058	Betaproteobacteria	Mary Bay 12
MB12_043	HM446060	Betaproteobacteria	Mary Bay 12

(*Continued*)

Table 2 | Continued

Clone	GenBank accession number	Phylum	Sampling sites
MB12_060	HM446061	Betaproteobacteria	Mary Bay 12
MB12_075	HM446062	Betaproteobacteria	Mary Bay 12
MB12_106	HM446064	Betaproteobacteria	Mary Bay 12
MB12_113	HM446065	Betaproteobacteria	Mary Bay 12
MB28_022	HM446072	Betaproteobacteria	Mary Bay 28
MB28_028	HM446082	Betaproteobacteria	Mary Bay 28
SI72_039	HM446089	Betaproteobacteria	Stevenson Island 72
SI72_082	HM446098	Betaproteobacteria	Stevenson Island 72
SI72_096	HM446099	Betaproteobacteria	Stevenson Island 72
WT98_014	HM446103	Betaproteobacteria	West Thumb 98
WT98_032	HM446106	Betaproteobacteria	West Thumb 98
WT98_058	HM446113	Betaproteobacteria	West Thumb 98
WT98_060	HM446114	Betaproteobacteria	West Thumb 98
WT98_071	HM446116	Betaproteobacteria	West Thumb 98
WT98_080	HM446121	Betaproteobacteria	West Thumb 98
WT129_001	HM446124	Betaproteobacteria	West Thumb 129
WT129_006	HM446126	Betaproteobacteria	West Thumb 129
WT129016	HM446129	Betaproteobacteria	West Thumb 129
WT129_024	HM446131	Betaproteobacteria	West Thumb 129
WT129_062	HM446143	Betaproteobacteria	West Thumb 129
WT129_088	HM446153	Betaproteobacteria	West Thumb 129
MB12_021	HM446047	Chloroflexi	Mary Bay 12
MB12_022	HM446048	Chloroflexi	Mary Bay 12
WT98_073	HM446117	Chloroflexi	West Thumb 98
WT129_005	HM446125	Chlorobia	West Thumb 129
WT129_056	HM446139	Chlorobia	West Thumb 129
WT129_059	HM446142	Chloroflexi/Thermomicrobium	West Thumb 129
WT129_064	HM446145	Chloroflexi	West Thumb 129
WT129_084	HM446152	Chloroflexi	West Thumb 129
MB12_042	HM446050	Cyanobacteria	Mary Bay 12
MB12_088	HM446055	Cyanobacteria	Mary Bay 12
SI72_036	HM446088	Cyanobacteria	Stevenson Island 72
WT98_013	HM446102	Cyanobacteria	West Thumb 98
MB28_034	HM446073	Deltaproteobacteria	Mary Bay 28
MB28_001	HM446077	Deltaproteobacteria	Mary Bay 28
MB28_011	HM446079	Deltaproteobacteria	Mary Bay 28
MB28_016	HM446080	Deltaproteobacteria	Mary Bay 28
MB28_031	HM446083	Epsilonproteobacteria	Mary Bay 28
MB12_039	HM446059	Gammaproteobacteria	Mary Bay 12
MB28_025	HM446074	Gammaproteobacteria	Mary Bay 28
MB28_003	HM446075	Gammaproteobacteria	Mary Bay 28
MB28_010	HM446078	Gammaproteobacteria	Mary Bay 28
MB28_027	HM446081	Gammaproteobacteria	Mary Bay 28
SI72_048	HM446091	Gammaproteobacteria	Stevenson Island 72
WT98_041	HM446109	Gammaproteobacteria	West Thumb 98
WT98_019	HM446104	Actinobacteria/Microthrix	West Thumb 98
MB12_107	HM446056	OP10	Mary Bay 12
SI72_029	HM446087	Planctomycetes	Stevenson Island 72
SI72_041	HM446090	Verrucomicrobia	Stevenson Island 72
SI72_056	HM446093	Planctomycetes	Stevenson Island 72
WT98_005	HM446100	Planctomycetes	West Thumb 98

(*Continued*)

Table 2 | Continued

Clone	GenBank accession number	Phylum	Sampling sites
WT129_010	HM446127	Thermodesulfobacteria	West Thumb 129
WT129_057	HM446140	Thermodesulfovibrio-related	West Thumb 129
WT129_058	HM446141	Thermodesulfovibrio-related	West Thumb 129
WT129_078	HM446150	Thermodesulfovibrio-related	West Thumb 129
MB12_076	HM446054	Verrucomicrobia	Mary Bay 12
WT98_006	HM446101	Verrucomicrobia	West Thumb 98
WT98_037	HM446108	Verrucomicrobia	West Thumb 98

PRINCIPAL COMPONENT ANALYSIS

The 16S rRNA gene clone libraries were examined for statistical correlations to each other by principal component analysis, based on the number of shared vs separate phylotypes (operational taxonomic units, OTUs) between different clone libraries, and weighted for abundance. The analysis was performed online at the Unifrac website (http://128.138.212.43/unifrac/index.psp; Lozupone et al., 2006). OTU definition was based on more than 3% 16S rRNA sequence difference over a shared alignment length of approx. 500 nucleotides (*E. coli* positions 28–537).

RESULTS

CHEMICAL COMPOSITION OF HYDROTHERMAL VENT WATERS

The chemical composition of the five water samples from sublacustrine Yellowstone Lake vents was distinct for every sample; reduced sulfur ($HS^-/S^=$ or H_2S), ammonia (NH_4^+ or NH_3) and DIC ($HCO_3^-/CO_3^=$ or CO_2) are of particular significance to chemolithotrophic metabolism. Sulfide and different oxidation states of sulfur (sulfite, thiosulfate) occurred in all water samples, but especially in the warmest samples Mary Bay Canyon 28, Stevenson Island 72, and West Thumb 129 (**Table 1**). A non-hydrothermal surface lake water reference sample from the Northwest shore, near the Lake Village laboratory, contained only the most oxidized sulfur species, sulfate, at detectable concentrations. DIC concentrations were highest in the same three samples, Mary Bay Canyon 28, Stevenson Island 71, and West Thumb 129; also, ammonia was most abundant in these three warmest vents (**Table 1**). The mixture of microbial electron donors (reduced sulfur and nitrogen species) and the elevated DIC concentration are compatible with high chemosynthetic activity (**Table 1**). While these chemical species likely indicate deeply sourced components of the vent fluid, a diagenetic source of sulfide, DIC, and ammonia, from decomposition of buried biomass is also possible.

In contrast, chloride is an unequivocal conservative marker for geothermal fluid because it has no diagenetic source. Silicate enrichment may also be a signal, though dissolution of diatom frustules can lead to enrichment in surficial sediments near vent orifices. Mary Bay Canyon 28 and West Thumb 129 showed chloride and silicate enrichment by factors 2 and >10 relative to lake water (**Table 1**), and were likely to have deep geothermal fluid sources; this interpretation is supported by previous porewater analyses from hydrothermally active sediments of Mary Bay and West Thumb that had yielded very high chloride concentrations, near 4–9 mM at 30 cm sediment depth (Aguilar et al., 2002). Thus, the localized high concentrations of ammonia, DIC, and sulfide at these two vents at least in part represented deeply sourced chemical species. Interestingly, the deep and hot Stevenson Island 72 sample showed no selective chloride or silicate enrichment that unequivocally distinguishes deep geothermal fluid sources. The high concentrations of sulfide, DIC, and ammonia may arise through transport in subsurface conduits as gases in the steam phase rather than as dissolved ionic species.

The samples Mary Bay West 12 and West Thumb 98 showed the lowest sulfide, DIC, ammonia, and nitrate concentrations, and no conservative marker signature (chloride, silicate) of deeply sourced geothermal fluids; the shallow West Thumb 98 sample showed no chemical enrichment of any parameter besides sulfite (**Table 1**). Dissolved organic carbon (DOC) was poorly related to physical–chemical variables and likely derived from lake water admixture at vent orifices.

Nitrate, an important substrate for anaerobic respiration, was virtually absent in Yellowstone Lake waters. During the 2003 season, 133 water samples, including 69 from hydrothermal vents, were analyzed for nitrate. Only 13 samples, 10 of these in the Stevenson Island domain, had nitrate concentrations above 0.5 μM; none exceeded 2 μM.

CHEMOSYNTHETIC ACTIVITY

The vent water samples showed distinct, temperature-dependent patterns of dark CO_2 fixation (**Figure 1**). The addition of the bacterial protein synthesis inhibitor chloramphenicol reduced chemosynthetic activity, whereas the eukaryotic protein synthesis inhibitor cycloheximide did not affect chemosynthesis rates (data not shown). Biomass nutrient elements N and P were sufficient to support chemosynthesis at the level of electron donors available in these measurements.

Of all dark CO_2 fixation measurements at cool temperatures (15°C), Mary Bay Canyon 28 showed the highest activity near 1.7 $\mu M\,C\,h^{-1}$ (**Figure 1**), even higher than the persistently active shallow bubbler at Mary Bay 12 (1.08 $\mu M\,C\,h^{-1}$). Addition of 5 mM thiosulfate did not stimulate dark CO_2 fixation rates at Mary Bay Canyon 28, but was extremely stimulatory over the 12- to 14-h incubation period at Mary Bay 12 (6.46 $\mu M\,h^{-1}$) in a manner indicative of population growth. The conspicuous difference in thiosulfate stimulation at 15°C rates between Mary Bay 12 and 28 could be influenced by their different setting: Mary Bay West 12 vent fluids emerge into shallow, well-mixed open water, subject to immediate dilution, whereas Mary Bay West 28 vent fluids remain confined within a deep, narrow canyon. The highest chemosynthetic rates in unamended samples (around 8.6 $\mu M\,C\,h^{-1}$) were

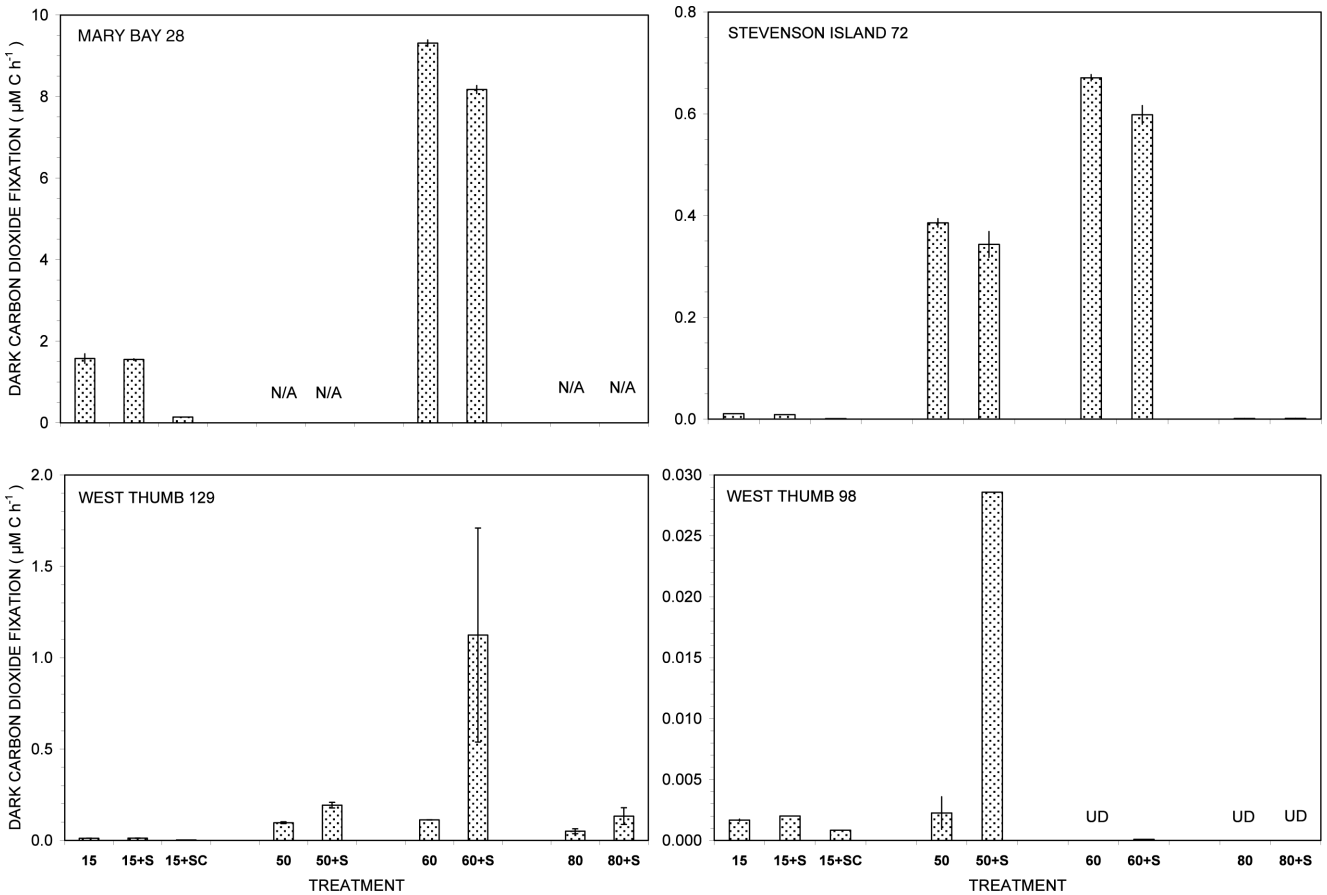

FIGURE 1 | Dark carbon dioxide fixation by Yellowstone Lake hydrothermal vent samples measured in triplicate (15˚C) or duplicate incubations (50, 60, and 80˚C) with (+S) or without addition of 5 mM thiosulfate. Biological fixation controls with added S + 20 µg/mL chloramphenicol (SC) were tested at 15˚C only. UD, undetectable (<0.0005 µM C h^{-1}); N/A, not available.

commonly found in the thermophilic range at 60˚C, at Mary Bay Canyon 28 (**Figure 1**); high temperature rates are not available for Mary Bay West 12.

Thiosulfate stimulation was only evident in the West Thumb samples (**Figure 1**). In West Thumb Canyon 129, stimulation was unequivocal (>10×) at 50˚C but was associated with very high replicate error for 60˚C incubations. Because the replicates for almost all other incubations agreed to a few percent, it is likely that the West Thumb 129 sample contained bacteria either clumped or attached to particles with patchy distribution. The positive dark fixation results at 50 and/or 60˚C in Mary Bay, West Thumb 129, and Stevenson Island 72 strongly implicate chemosynthetic activity by thermophilic autotrophs in these samples. Chemosynthetic activity in the mesophilic range at 15˚C was low at West Thumb 129 and Stevenson Island 72 (below 0.02 µM C h^{-1}), indicating mesophilic autotrophs in reduced numbers or activity compared to the Mary Bay samples. West Thumb 129 was the only sample that showed low but detectable chemosynthetic activity at 80˚C, indicating the existence of hyperthermophiles.

The West Thumb 98 sample showed very low dark CO_2 fixation rates close to the detection limit and the lake water background, generally below 0.002 µM C h^{-1} for all temperatures; a low but detectable rate near 0.028 µM C h^{-1} was obtained for thiosulfate-amended water at 50˚C (**Figure 1**).

The distinct temperature effects on chemosynthetic activity suggest the existence of two groups of chemosynthetic microorganisms: chemosynthetic mesophiles in the two Mary Bay Samples, and thermophiles in the Mary Bay Canyon 28, West Thumb Canyon 129, and Stevenson Island 72 samples. The Mary Bay Canyon 28 sample likely contained both types of chemosynthetic communities. The nearly inactive West Thumb 98 sample should contain few detectable chemoautotrophs, although seed populations might be present that account for low-level thermophilic sulfur stimulation.

These inferences are consistent with the results of previous sampling surveys. During a previous 3-year sampling period of 1997, 1998, and 1999, Mary Bay water samples showed the highest sulfide concentrations (max. 0.7–0.8 mM), the highest DIC concentrations (max. 16–17 mM), and also the highest dark CO_2 fixation rates (max. 0.3–0.6 µM C h^{-1}) at mesophilic temperatures, in comparison to significantly lower concentrations and rates found in Stevenson Island and West Thumb water samples (Cuhel et al., 2002). Thus, previous studies also suggest the

existence of mesophilic, chemosynthetic microbial communities in Mary Bay.

PHOTOSYNTHETIC ACTIVITY

Photosynthesis-irradiance curves for surface samples from the three domains of Mary Bay, Stevenson Island, and West Thumb demonstrated light-saturable photosynthetic CO_2 fixation (**Figure 2**). Light stimulated photosynthetic rates to 200 μmol PAR photons m^{-2} s^{-1}, about 10% of full sunlight, above which rates remained constant at 0.14 ± 0.01 μM C h^{-1}. Because this discussion concerns volumetric carbon fixation, the data were not normalized for varying algal biomass as chlorophyll *a* and are presented in the same units as chemosynthesis for direct comparison.

MICROBIAL COMMUNITY COMPOSITION

Consistent with the working hypotheses based on temperature-sensitive chemosynthetic rates, the clone libraries from the five sampling locations show distinct microbial community compositions (**Table 1**). The clone libraries from the two samples with the highest temperatures, West Thumb Canyon 129 and Stevenson Island 72, consistently cluster together in Principal Component analysis based on shared 16S rRNA phylotypes (**Figure 3**). The clone libraries for the other sites did not show any correlations, a

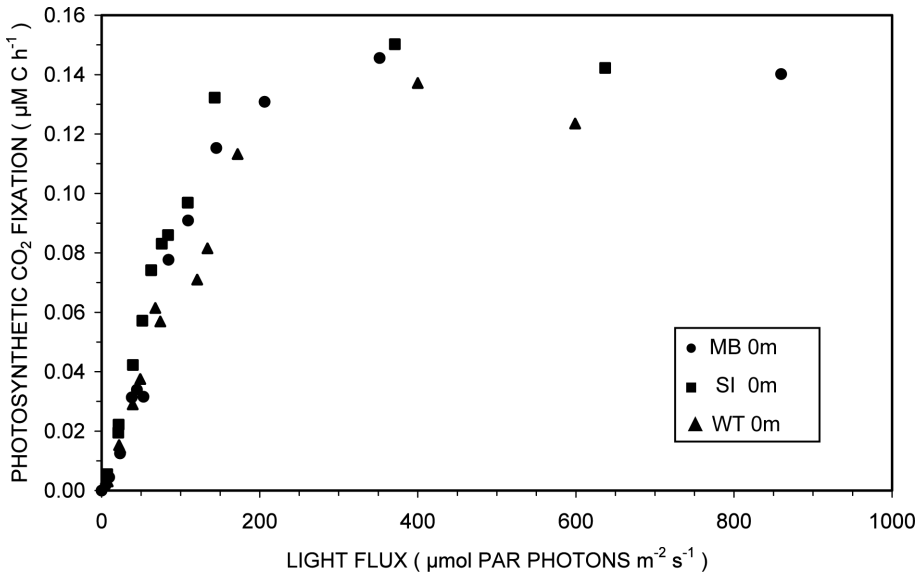

FIGURE 2 | Photosynthesis-irradiance relationships at 15°C for surface waters overlying hydrothermal vent fields in Mary Bay (●), Stevenson Island (■), and West Thumb (▲).

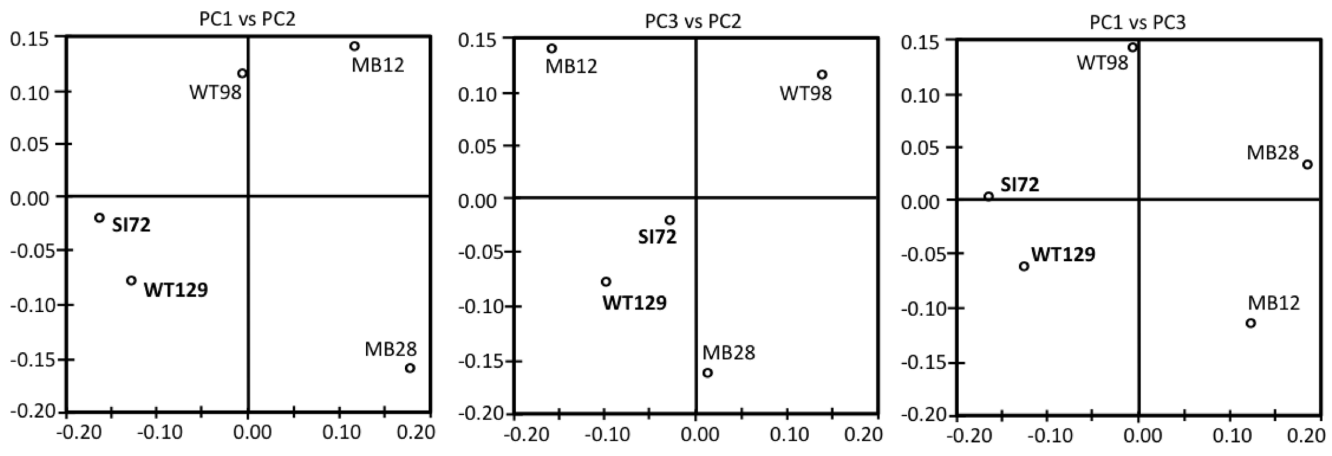

FIGURE 3 | Principal component analysis plots showing the clustering of 16S rRNA clone libraries based on shared OTUs, weighted for abundance. Each axis indicates the fraction of the variance in the data that the axis accounts for. The first and the second Principal Component explain most of the data ($P1 = 41.4$, $P2 = 30$, $P3 = 17.8\%$).

possible consequence of data set size but also evident from deeply divergent microbial community composition (**Table 1**).

The Mary Bay West 12 sample, from an active bubbling vent near the lake shore, was dominated by gammaproteobacterial phylotypes related to the mesophilic sulfur oxidizer *Thiovirga sulfuroxydans*; this bacterium has an optimal growth temperature of 30–34˚C (total growth range 15–42˚C), and grows as an obligate chemolithoautotroph by oxidizing sulfur, sulfide, and thiosulfate aerobically; its 16S rRNA gene sequence forms a monophyletic lineage with very similar (at least 97% similarity) phylotypes from sulfidic and geothermal waters (Ito et al., 2005). The Mary Bay West 12 sample also yielded clones related to a betaproteobacterial cluster from diverse freshwater environments that included the freshwater bacteria *Variovorax* and *Rhodoferax* (**Table 1**; **Figure 4**). This betaproteobacterial cluster is generally found in freshwater environments, and has a cosmopolitan distribution (Zwart et al., 2002). The Mary Bay Canyon 28 sample harbored *Thiovirga*-related clones as well, but its bacterial community appeared to be differently structured and consisted at least in part of clones related to anaerobic bacteria (**Table 1**); no PCA clustering of the two Mary Bay samples was observed (**Figure 3**). Several clones were affiliated with anaerobic *Deltaproteobacteria* that usually occur in aquatic sediments but not in the water column; these include sulfate-reducing bacteria of the Desulfobacteraceae, with the butyrate oxidizer *Desulfatirhabdium butyrativorans* as the closest match (Balk et al., 2008); the heterotrophic halorespiring bacterium *Anaeromyxobacter dehalogenans* (Sanford et al., 2002); and uncultured bacteria from the sediment of an eutrophic lake. No other water sample yielded deltaproteobacterial clones. Also, Mary Bay West 28 contained close relatives of the anaerobic, nitrate-reducing and sulfur-oxidizing autotrophic bacterium *Thiobacillus denitrificans* within the Betaproteobacteria, and of the facultatively anaerobic, microaerophilic, or nitrate-reducing sulfur oxidizer *Sulfuricurvum kujiense* within the Epsilonproteobacteria (Kodama and Watanabe, 2004; **Figure 4**). This distinct microbial community signature corresponded to a different setting. Mary Bay 12 was a bubbler in shallow open water at low temperature (15˚C) and high mixing rate, which never exceeded 20˚C and was near freezing for 6 months of the year. In contrast, the hot Mary Bay Canyon 28 sample (49˚C at sampling), the most confined of all the sample locations, came from the bottom of a canyon-like crater at ca. 56 m depth, with nearby sediments hot enough to melt a core liner. With a sill depth of 20 m, these steep-walled hydrothermal explosion craters are characteristic for Mary Bay (Morgan et al.,

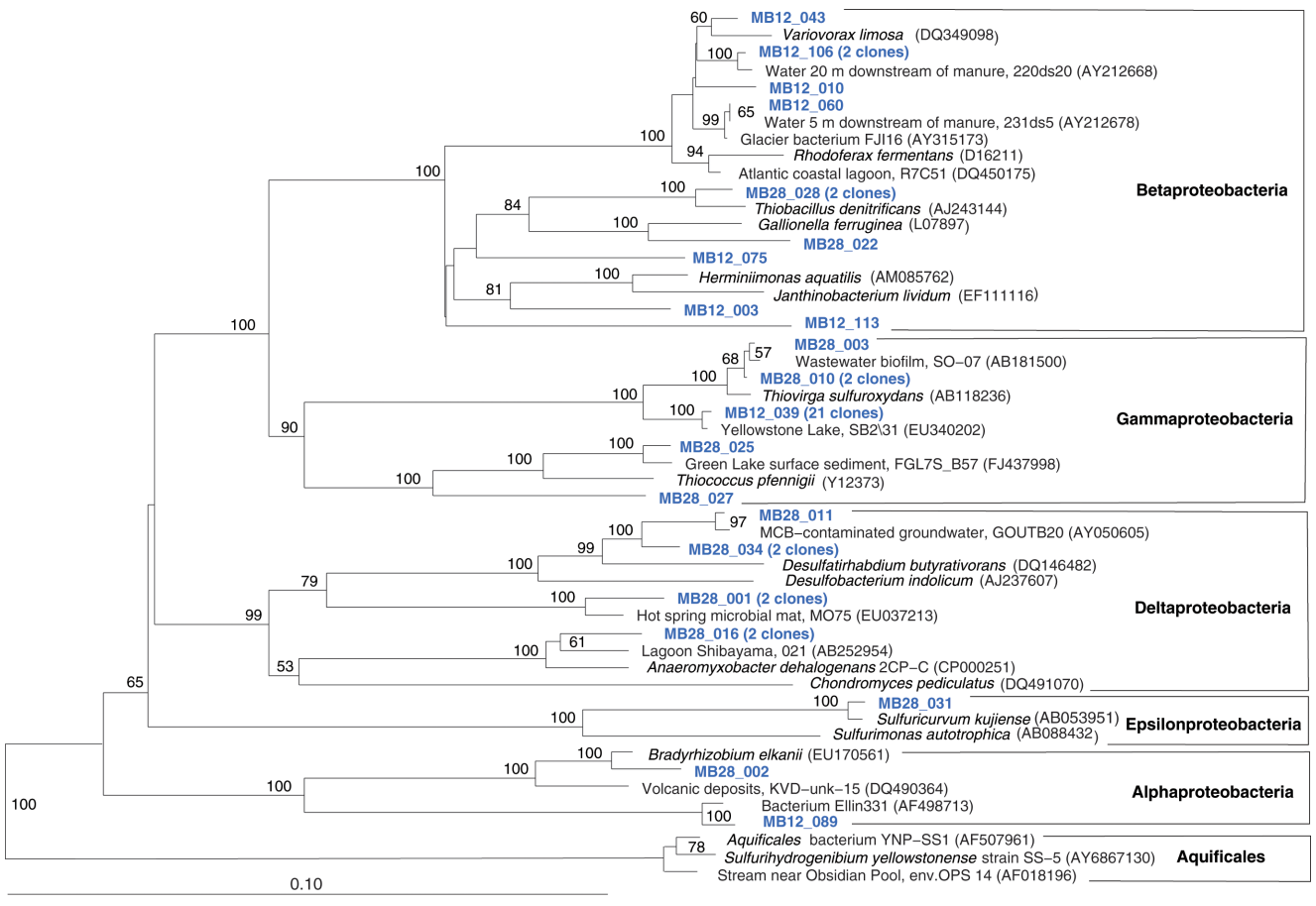

FIGURE 4 | Phylogeny of Mary Bay West 12 and Mary Bay Canyon 28 proteobacterial clones, based on *E. coli* 16S rRNA gene nucleotide positions 723–1491.

2003b) and provide more geochemically favorable conditions for anaerobic, especially heterotrophic bacterial growth. The conspicuous sequence signature of obligately or facultatively anaerobic bacteria may indicate deep-growing populations from hydrothermal sediments at the bottom of the crater that undergo upward advection and suspension within into the deep-water layers of this enclosed basin.

In addition, Mary Bay Canyon 28 harbored a clone most closely related to the autotrophic iron-oxidizing bacterium *Gallionella ferruginea*, and two clones of the thermophilic, chemosynthetic phylum Aquificales, specifically the hydrogen- and sulfur-oxidizing genus *Sulfurihydrogenibium* (**Figure 4**). Thus, Mary Bay Canyon 28 contains an unusually multifaceted microbial community, consisting of mesophilic and thermophilic chemosynthetic bacteria within the Beta-, Gamma-, and Epsilonproteobacteria and the Aquificales (consistent with high chemosynthetic rates at both temperature regimes), as well as nitrate- and sulfate-reducing anaerobes.

The microbial community of the deep, hot Stevenson Island 72 sample was distinct from those of both Mary Bay samples. Almost half of the cloned 16S rRNA gene sequences grouped with the *Aquificales* (**Table 1**) and are most closely related to clones from other Yellowstone Park locations (**Figure 5**) and the cultured strain *Sulfurihydrogenibium* spp. YO3AOP1 from Obsidian Pool in Yellowstone National Park (Reysenbach et al., 2009). These populations were likely from the vent throat or orifice near deep lake water; the thermistor on the sampling arm of the ROV gave 110˚C, indicating source fluid temperatures possibly above 125˚C. The temperature optimum of cultured *Sulfurihydrogenibium* strains and species is between 65 and 70˚C; depending on the species, growth is possible between 40 and 78˚C (Nakagawa et al., 2005). The species most closely related to the Yellowstone Lake clones, *Sulfurihydrogenibium yellowstonense* strain SS-5, has a growth temperature range of 55–78˚C, 5–8˚C more tolerant of high temperatures than other described species (Nakagawa et al., 2005); it uses sulfur and thiosulfate but not hydrogen as electron donors, and is obligately aerobic; it assimilates organic carbon compounds for biosynthetic purposes, but is unable to use them as energy sources (Nakagawa et al., 2005). Other phylum-level bacterial groups in the Stevenson Island sample included *Betaproteobacteria*, *Actinobacteria*, *Planctomycetales*, and *Verrucomicrobia*, plus a single *Thiovirga*-related gammaproteobacterial clone (**Table 1**).

The microbial communities of the Stevenson Island 72 and West Thumb Canyon 129 resembled each other, as confirmed by clustering in PCA analysis (**Figure 3**). West Thumb Canyon 129 had the next-highest temperature (77˚C) after the Stevenson Island sample; both samples shared abundant *Aquificales* clones specifically related to the cultured species of the genus *Sulfurihydrogenibium*, and to *Sulfurihydrogenibium*-related clones from different locations within Yellowstone National Park (**Figure 6**). The abundance of *Sulfurihydrogenibium* clones is consistent with the high sulfur-stimulated chemosynthetic rates at 60˚C, and the lower but still substantial rates at 50˚C in these two samples (**Figure 1**). Since chemosynthesis rates and sulfur stimulation persisted at 80˚C at West Thumb Canyon 129 (**Figure 1**), it is possible that this sample contained high-temperature-adapted strains of *Sulfurihydrogenibium*, or different types of thermophiles and hyperthermophiles that remain to be found. Next to the Aquificales, the most frequently recovered clones represent *Betaproteobacteria* and *Actinobacteria*, which occur in the West Thumb Canyon 129, Stevenson Island 72, Mary Bay West 12, and (to a lesser extent, only Betaproteobacteria) the Mary Bay Canyon 28 samples (**Table 1**).

The West Thumb Canyon 129 sample also contained, in similar abundance, phylotypes of the *Chloroflexi* and the *Thermodesulfovibrio* lineages; the latter was not found in other clone libraries (**Table 1**), potentially a result of terrestrial spring influx limited to the West Thumb region. Within the *Thermodesulfovibrio* lineage, the phylotypes from West Thumb Canyon 129 were most closely related to the autotrophic, hydrogen-oxidizing, iron-reducing bacterium *Geothermobacterium ferrireducens* (**Figure 6**) previously isolated from hot spring sediments in Yellowstone National Park (Kashefi et al., 2002). The West Thumb area harbors a suitable biogeochemical niche for this bacterium: iron-manganese oxide crusts were found on the hydrothermally active lake bottom, and the upper sediment layers contain porewater concentrations of 20–40 μM dissolved, reduced iron (Aguilar et al., 2002).

The fifth sample, a relatively cool West Thumb 98 sample with low chemosynthetic activity, yielded no Aquificales or other chemosynthetic bacterial populations, but predominantly members of the *Actinobacteria* (**Figure 7**) and the *Betaproteobacteria* (**Figure 8**), the bacterial community components that occur to some extent in all Yellowstone Lake water samples (**Table 1**). The actinobacterial clones in this and other Yellowstone Lake samples are members of uncultured Actinobacterial freshwater lineages with a cosmopolitan distribution, the acI and acIV clusters (Warnecke et al., 2004). In subsequent sequencing surveys of freshwater lakes, 16S rRNA genes of these clusters were found very frequently and in high diversity. The clades were further subdivided into clades AI to AVII for the acI linage (Newton et al., 2007) and clades acIV-A to acIV-E for the acIV lineage (Warnecke et al., 2004; Holmfeldt et al., 2009); this nomenclature is followed in phylogenetic trees in this study. Actinobacterial acI or acIV clades were found in almost every water sample, Mary Bay 12 (**Figure 9**), Stevenson Island 72 (**Figure 5**), West Thumb Canyon 129 (**Figure 6**), and West Thumb 98 (**Figure 7**), and most likely represent the admixture of Yellowstone Lake water and its indigenous microbial community to the thermal water samples. Since acI and acIV strains have not been cultured yet, a physiological rationale for the occurrence of these bacteria in Yellowstone Lake water is hard to infer. Interestingly, comparative quantifications of the acI clade in high mountains lakes have identified UV irradiation as a potential factor selecting for acI actinobacteria (Warnecke et al., 2005).

DISCUSSION

HYDROGEN- AND SULFUR-BASED CHEMOSYNTHESIS

The results from the Yellowstone Lake hydrothermal vents form an interesting contrast to previous results from multiple aerial hot springs in Yellowstone National Park (Spear et al., 2005). By combining chemical analysis of spring waters for electron donors including sulfide and hydrogen, thermodynamic modeling of energy yields from the aerobic oxidation of these electron

donors, and extensive 16S rRNA gene sequencing, aerobic hydrogen oxidation was identified as the favored energy source in Yellowstone hot springs, consistent with 16S rRNA gene clone libraries dominated by hydrogenotrophic genera of the Aquificales, such as *Hydrogenothermus*, *Hydrogenobacter*, and *Hydrogenobaculum* (Spear et al., 2005). Close relatives of mesophilic sulfur-oxidizing bacteria (*Thiovirga* spp.) occur in some locations, for example in the Mary Bay sampling sites, and most likely contribute to dark CO_2 fixation rates measured at cool temperatures. Consistent with these results, previous studies have shown that dark CO_2 fixation rates at Mary Bay locations are strongly stimulated by thiosulfate enrichment (Cuhel et al., 2002). In contrast, clone library results from the hot Stevenson Island and West Thumb Canyon vents, show that mesophilic sulfur oxidizers such as *Thiovirga* spp. are not detected in these habitats, or occur only as a minority. Here, the spectrum of clones changes toward phylotypes that are most closely related to thermophilic and hyperthermophilic chemolithoautotrophs of the genus *Sulfurihydrogenibium* that use

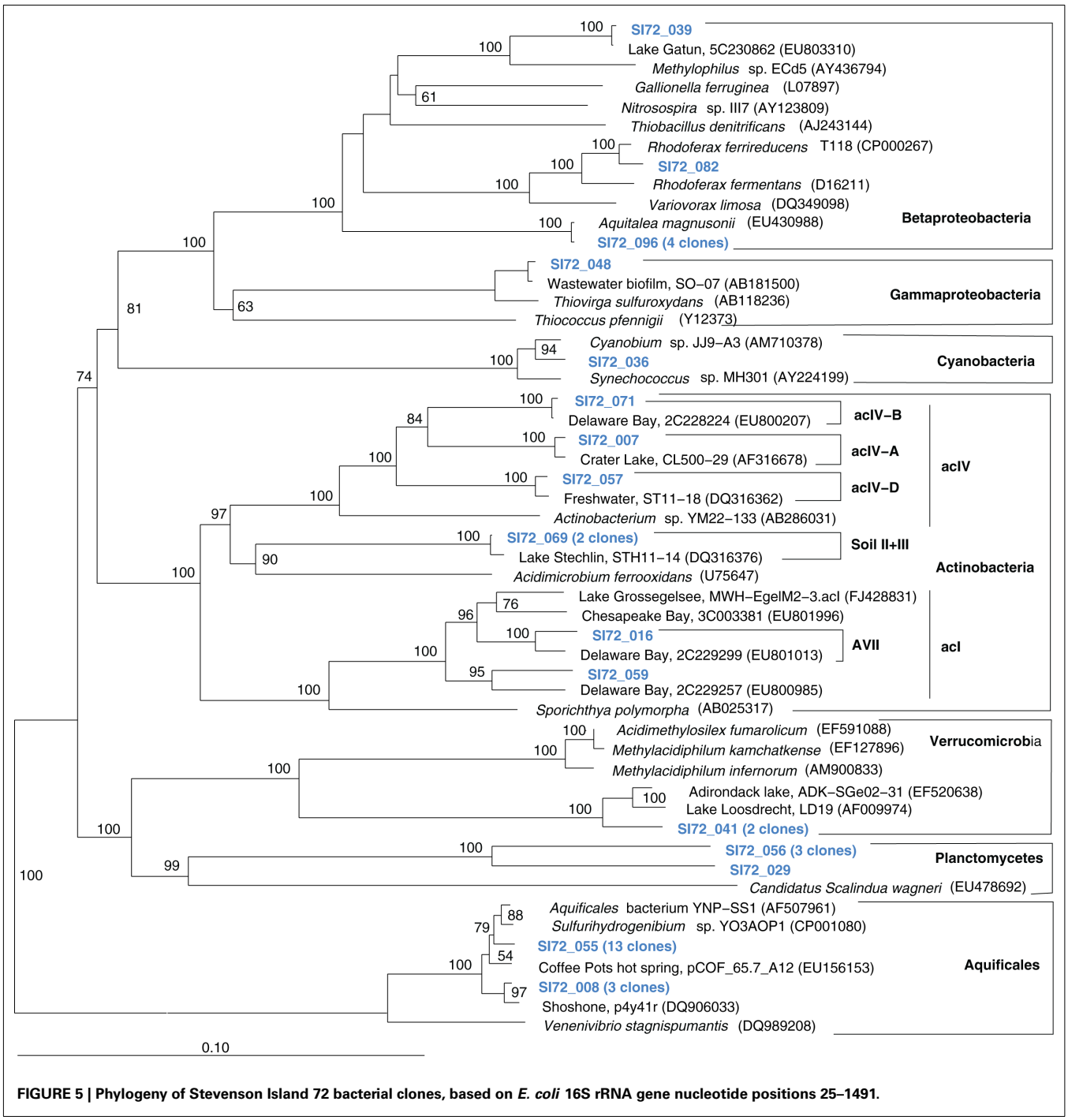

FIGURE 5 | Phylogeny of Stevenson Island 72 bacterial clones, based on *E. coli* 16S rRNA gene nucleotide positions 25–1491.

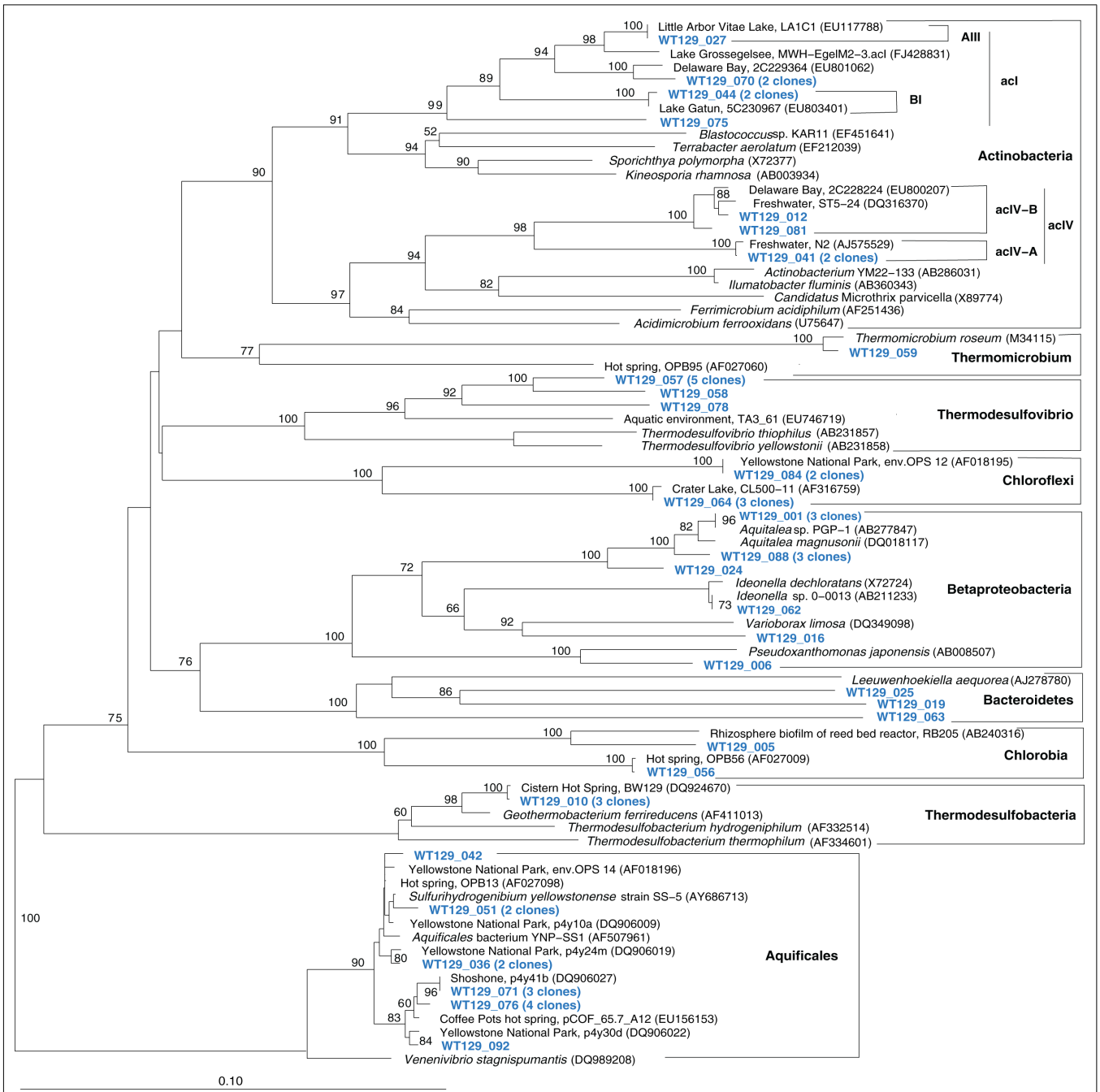

FIGURE 6 | Phylogeny of West Thumb Canyon 129 bacterial clones, based on *E. coli* gene nucleotide positions 25–573.

sulfur and hydrogen as electron donors. As a caveat, *S. yellowstonense,* the closest relative to the Yellowstone Lake clones in this dataset, oxidizes sulfur and thiosulfate, but not hydrogen.

Since chemolithoautotrophic microorganisms may use one or several different electron donors, including reduced sulfur compounds such as H_2S, $S_2O_3^=$, $SO_3^=$, polythionates, Fe(II), Mn(II), NH_3, or H_2, our results have obvious limitations. Here, thiosulfate ($S_2O_3^=$) was chosen as model reduced sulfur stimulant of chemosynthesis because it does not as easily react with other substrates as might have happened with H_2S as a supplement. Since thiosulfate was rarely found in quantity even when H_2S was abundant (**Table 1**), it was most likely utilized rapidly upon (a)biotic production from sulfide. Thiosulfate-stimulated autotrophic CO_2 fixation implicated the presence of bacteria capable of using it, and possibly other reduced sulfur compounds, as electron donors. A lack of thiosulfate stimulation would imply either electron donor saturation, or the absence of thiosulfate-oxidizing bacteria. Interestingly, thermophilic dark CO_2 fixation

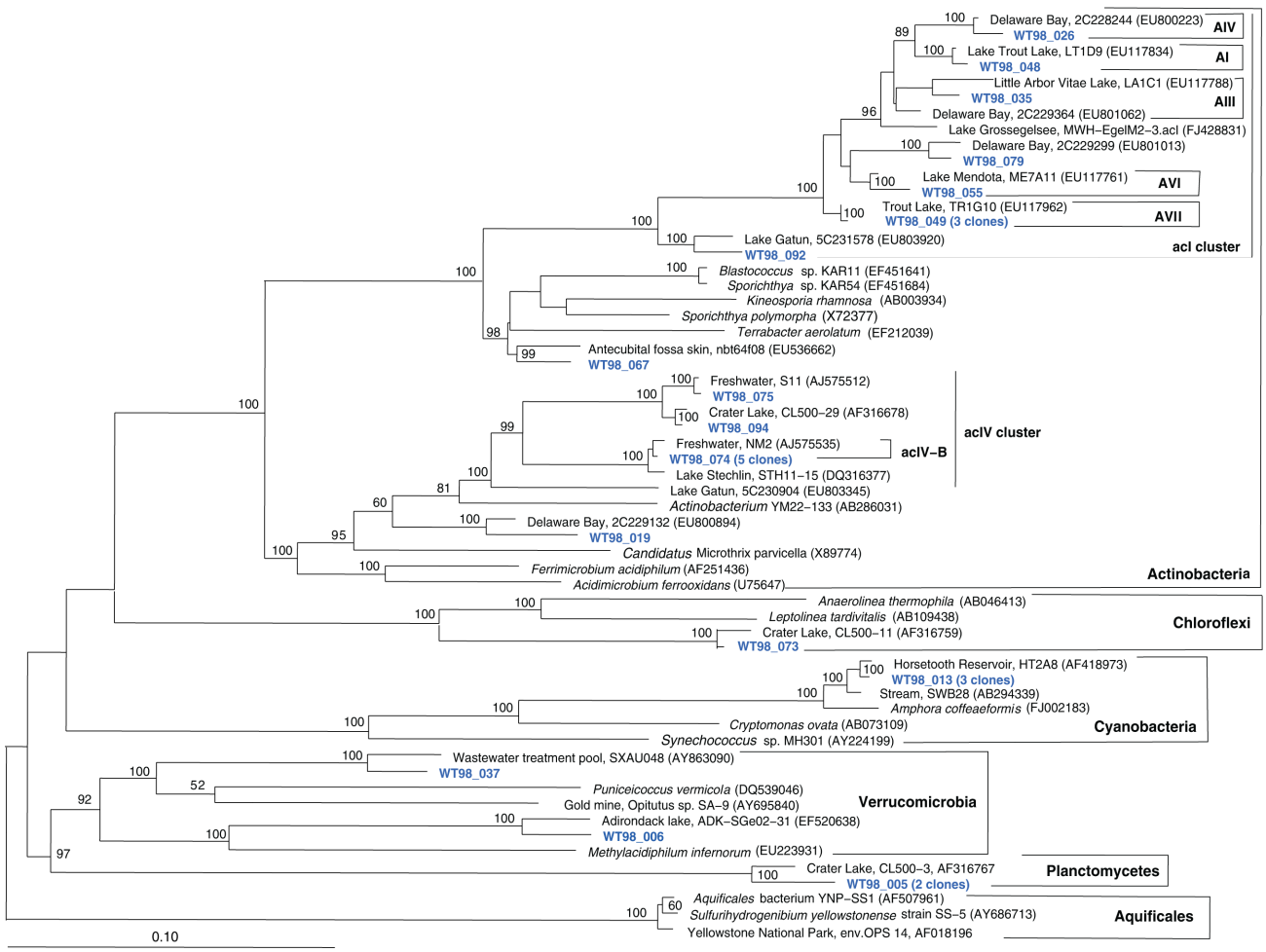

FIGURE 7 | Phylogeny of West Thumb 98 bacteria except Proteobacteria, based on *E. coli* 16S rRNA gene nucleotide positions 25–1491.

rates at Mary Bay Cayon 28 and Stevenson Island 72 were reduced by ca. 10% after thiosulfate addition (**Figure 1**); reactions of the added thiosulfate (or its disproportionation products) with other electron donors such as Fe(II), might reduce their availability, and thus reduce the autotrophic contribution of non-sulfur lithotrophs.

NITRATE REDUCTION AND METAL REDUCTION

The chemosynthesis rates in this study were measured aerobically, assuming that chemosynthetic microbial communities venting into a well-oxygenated oligotrophic lake would respire with oxygen. The prevalence of 16S rRNA gene sequences related to aerobic chemosynthetic bacteria (*Thiovirga*, Aquificales) supports this assumption. Niches certainly exist for anaerobic, nitrate- and metal-reducing chemosynthesis in Lake Yellowstone, for example anaerobic vent fluid, sediments or hydrothermal mineral deposits. Very low oxygen solubility at high temperature, and the presence of reducing compounds including Fe(II) and H_2S, might facilitate anoxic conditions in vent source waters and possibly during channelized flow toward the lake-bottom orifice. As a result, phylotypes related to anaerobic chemosynthetic bacteria, such as the nitrate-reducing sulfur oxidizers *Thiobacillus denitrificans* and *Sulfuricurvum kujiense*, or the iron-reducing hydrogenotroph *Geothermobacterium ferrireducens*, were detected as well. Because 16S rRNA genes related to nitrate-reducing sulfur oxidizers were detected in Mary Bay 28, this deep, stratified canyon represents a likely habitat where nitrate-respiring vent or sediment populations accumulate to sufficient densities to be detected in clone libraries; such microbial nitrate sinks could compound the functional absence of nitrate (usually $<0.2\,\mu M$) in any of the lake and vent water habitats sampled. Authigenic iron and manganese oxide crusts on the lake bottom, and bottom sediments with 20–50 μM porewater concentrations of Fe(II) (Aguilar et al., 2002) could provide a niche for hyperthermophilic iron-reducing hydrogenotrophs such as *Geothermobacterium ferrireducens*. Hydrothermal sediment cores show porewater chemical profiles consistent with sulfide oxidation and sulfate production, ammonia oxidation, and DIC consumption,

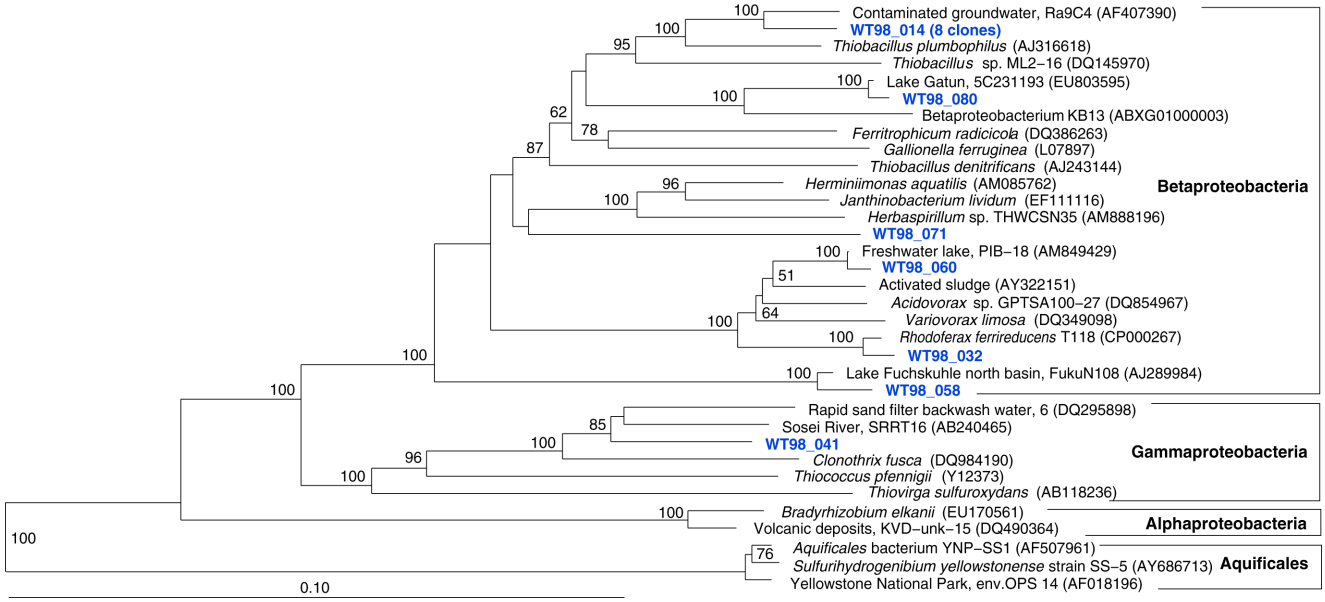

FIGURE 8 | Phylogeny of West Thumb 98 proteobacterial clones, based on *E. coli* 16S rRNA gene nucleotide positions 25–1491.

from 30 cm depth toward the sediment surface (Aguilar et al., 2002). To summarize, anaerobic chemosynthesis remains to be systematically investigated by quantitative microbial sampling and measurements of anaerobic respiration rates.

NEW DISCOVERIES AT WEST THUMB

In previous studies of Yellowstone Lake water column and vent fluids, samples could be grouped by geochemical and chemosynthetic characteristics into functional domains (Cuhel et al., 2002): West Thumb was characterized by low concentrations of electron donors, and high levels of chloride and silicate; Stevenson Island and Mary Bay sites were characterized by high electron donor and low chloride concentrations; Sedge Bay showed reducing gases in fumarole-dominated emanations in combination with low chloride (Konkol et al., 2010); and South Arm served as a control area outside of caldera influence. The latter two are not presented here. In pre-2002 surveys, West Thumb vents rarely exceeded 0.02 μM C h^{-1} in chemosynthesis and did not display thiosulfate stimulation, while different Mary Bay sites and to a more sporadic extent Stevenson Island vents frequently reached 10 times that value (Cuhel et al., 2002) and were often stimulated by thiosulfate addition. The present work adds the chemosynthetically active site West Thumb Canyon 129, the result of more sophisticated ROV-based sampling and continuous search for new vent fields. While the very low rates of chemosynthesis at ambient temperature (ca. 15˚C) in the West Thumb Canyon 129 samples are consistent with past results in the wider West Thumb area (Cuhel et al., 2002), the persistent and apparently reduced sulfur-stimulated dark CO_2 fixation at 50–80˚C in the West Thumb Canyon 129 vent fluids may indicate hitherto undiscovered communities that function deeply enough in the vent conduits to both completely consume electron donors and to cool to unresponsive conditions after collection by previous sampling technologies.

CAVEATS ON LINKING VENT FLUID CHEMISTRY, CHEMOSYNTHESIS RATES AND COMMUNITY STRUCTURE

In this study, linkages between the 16S rRNA sequence data and the chemosynthetic rates are indirect: the chemosynthetic bacteria whose activity is measured in the rates may appear in the clone libraries, but do not constitute them – the clone libraries contain other bacteria as well, and are subject to the methodological problems of DNA extraction, PCR and cloning bias. Vice versa, the dark CO_2 fixation rates as measured (aerobic and thiosulfate-stimulated rates) provide a window on the overall chemosynthetic potential, but cannot be equated with it. Other chemosynthetic bacteria that require different testing conditions might be present, for example the phylotypes related to nitrate- and iron-reducing bacteria. Chemosynthesis rates and 16S rRNA sequence data could be linked more effectively by cultivation, quantification, and dark CO_2 fixation rate measurements of key species, such as the Yellowstone Lake strains of *Thiovirga* and *Sulfurihydrogenibium.*

Chemosynthetic activity is not only determined by the presence or absence of inorganic electron donors, but also by the residence time of vent fluids, a function of admixture of sediment porewater or lake water. Although vent flow rates were not quantified in this study, efflux of water from vent orifices into the cold Yellowstone Lake water column was often clearly visible, and suggested that the residence time of vent fluids recovered by the sipper system might range from minutes to hours in the vicinity of the vent orifice. These turbulent mixtures of hot, reducing vent fluids and cold, oxygenated, oligotrophic Lake water would select for mesophilic, neutrophilic, and chemolithoautotrophic sulfide and hydrogen oxidizers with fast specific growth rates, exemplified

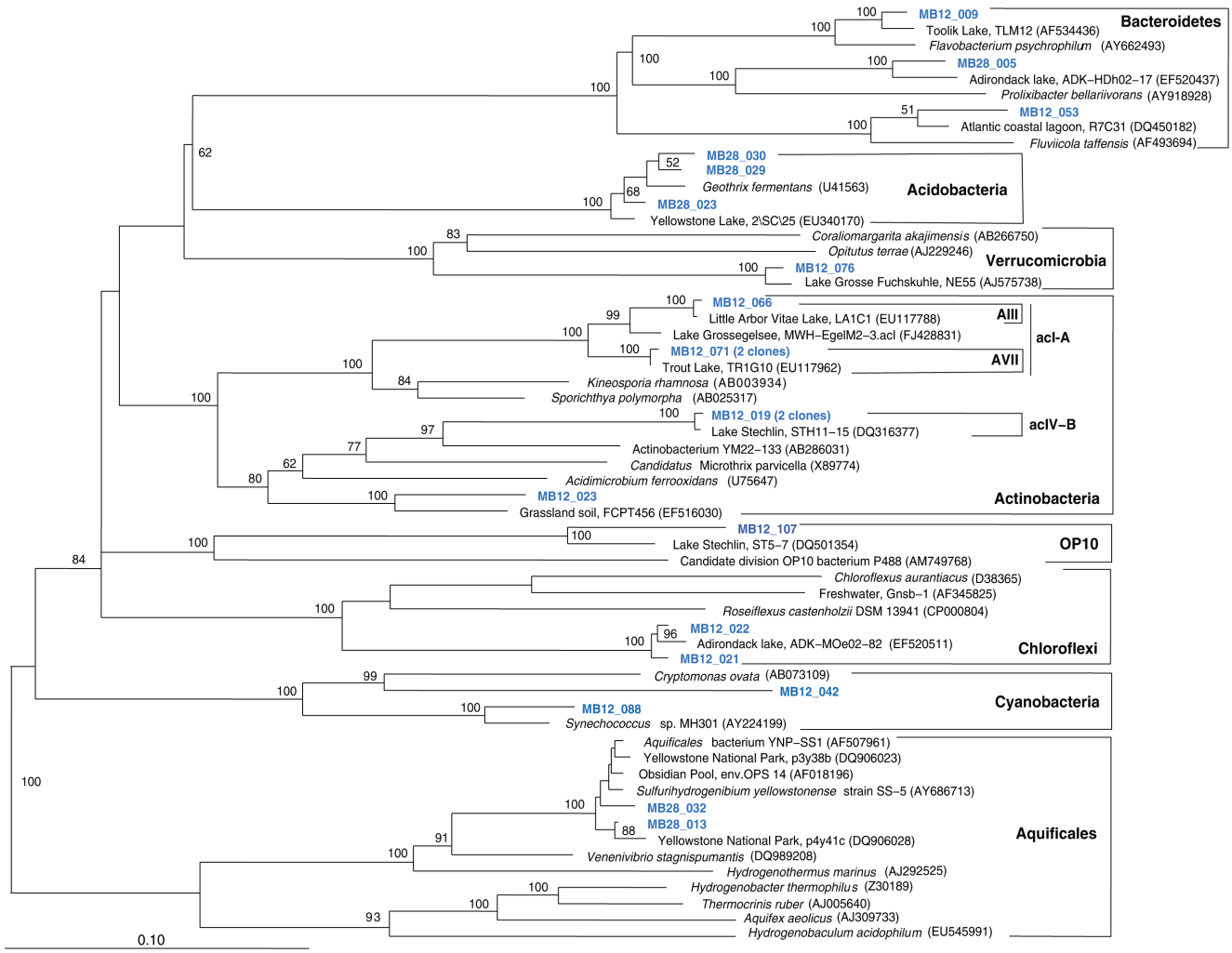

FIGURE 9 | Phylogeny of Mary Bay West 12 and Mary Bay Canyon 28 bacterial clones, except Proteobacteria, based on *E. coli* 16S rRNA gene nucleotide positions 723–1491.

by the genera *Thiovirga* (Ito et al., 2005), as detected here, and by *Thiomicrospira* (Jannasch et al., 1985; Brinkhoff et al., 1999). Within the very hot and chemically distinctive fluids, clones are more likely to reflect locally active populations than in bulk lake water. Here, high chemosynthesis rates may stimulate growth of heterotrophic consumers, who – depending on growth rate and abundance relative to the *in situ* chemosynthetic community – might escape phylogenetic detection. In vents with low content of reduced minerals, bacterial populations growing in the throat of the conduit may have consumed electron donors prior to sampling, yielding phylotypes in apparent absence of their energy source. Thus, the expected correlations between community structure and chemosynthetic rates will always be impacted by hydrothermal fluid concentration, temperature, fluid flow, and mixing rates; controlling for these variables over time requires long-term *in situ* chemical, physical, and microbiological monitoring efforts similar to those at deep-sea hydrothermal vents (Huber et al., 2002; Page et al., 2008).

CHEMOSYNTHETIC CONTRIBUTION TO YELLOWSTONE LAKE PRODUCTIVITY

The contribution of microbial chemosynthesis to overall biological productivity of Yellowstone Lake is hard to quantify, due to a lack of spatially integrated data for dark CO_2 fixation. Yet, chemosynthetic rate measurements at different sites in Yellowstone Lake since 1994 have consistently shown that maximum volume-based dark CO_2 fixation rates of hydrothermal water samples, mostly from Mary Bay, are at least in the same order of magnitude (0.15–0.75 $\mu M\, C\, h^{-1}$) as volume-based maximum photosynthesis rates at the lake surface (**Figure 2**; Aguilar et al., 2002). Further, chemosynthesis rates at specific sites can be significantly higher, such as the Mary Bay samples surveyed in 2003, and increase further with added reduced S. Some sections of the lake, for example the Mary Bay domain with its exceptionally high geothermal heatflow and abundance of active vents (Morgan et al., 2003b), are likely to have a substantial chemosynthetic contribution to total biomass production. This assumption is supported

by observations of localized biological oases supported by Yellowstone Lake vents, for example extensive microbial mats covering sediments and macrophytes in Sedge Bay (Remsen et al., 2002; Konkol et al., 2010), or a warm DIC-rich vent in the West Thumb region that sustained an aquatic moss colony inhabited by crustaceans, segmented worms and flatworms (Lovalvo et al., 2010).

This study has shown that sublacustrine vents of Yellowstone Lake provide fascinating and novel opportunities to explore microbial community structure and function of chemosynthetically supported aquatic ecosystems. The combination of biogeochemical ecophysiology and phylogenetic analysis enables a deeper understanding of extremophilic microbiology in Yellowstone Lake hydrothermal vent habitats.

ACKNOWLEDGMENTS

We gratefully acknowledge the National Science Foundation Research Experience for Undergraduates (REU, OCE 0097622), Life in Extreme Environments (LExEn, NSF-EAR 0085515), and Environmental Geochemistry and Biogeochemistry (EGB, NSF-EAR 9708501) programs awarded to Cuhel, Aguilar and Maki (Marquette University), and the Great Lakes WATER Institute at the University of Wisconsin – Milwaukee for supporting annual Yellowstone Lake expeditions and sampling opportunities. We truly appreciate David Lovalvo for extraordinarily skilled ROV operations. We are indebted to National Park Service leaders John Varley, John Lounsbury, and especially Todd Koel and the Fisheries and Aquatic Sciences Program and personnel YNP, WY for sampling access and accommodation of the project. Appreciation is extended to the 2003 REU undergraduates Jamie Becker, Erin Howard, and Lynn Killberg for their contribution to the extensive chemical analyses. Andreas Teske and Shawn Lyons were supported by the NASA Astrobiology Institute "Environmental Genomes." Tingting Yang was supported by NSF grant No. 0727175.

REFERENCES

Aguilar, C., Cuhel, R. L., and Klump, J. V. (2002). "Porewater and hydrothermal vent water input into Yellowstone Lake, Wyoming," in *Yellowstone Lake: Hotbed of Chaos or Reservoir of Resilience? Proceedings of the 6th Biennial Scientific Conference on the Greater Yellowstone Ecosystem*, eds R. J. Anderson and D. Harmon (Yellowstone National Park, WY: Yellowstone Center for Resources and George Wright Society), 1–18.

APHA. (1992). *Standard Methods for the Examination of Water and Wastewater*, 18th Edn. Washington, DC: American Public Health Association.

Balk, M., Altinbas, M., W. Rijpstra, I. C., Sinninghe Damste, J. S., and Stams, A. J. M. (2008). *Desulfatirhabdium butyrativorans* gen. nov., sp. nov., a butyrate-oxidizing, sulfate-reducing bacterium isolated from an anaerobic bioreactor. *Int. J. Syst. Evol. Microbiol.* 58, 110–115.

Brinkhoff, T., Muyzer, G., Wirsen, C. O., and Küver, J. (1999). *Thiomicrospira chilensis* sp. nov, a mesophilic obligately chemolithoautotrophic sulfur-oxidizing bacterium isolated from a *Thioploca* mat. *Int. J. Syst. Bacteriol.* 49, 875–879.

Cuhel, R. L., Aguilar, C., Anderson, P. D., Maki, J. S., Paddock, R. W., Remsen, C. C., Klump, J. V., and Lovalvo, D. (2002). "Underwater domains in Yellowstone Lake: hydrothermal geochemistry and bacterial chemosynthesis," in *Yellowstone Lake: Hotbed of Chaos or Reservoir of Resilience? Proceedings of the 6th Biennial Scientific Conference on the Greater Yellowstone Ecosystem*, eds R. J. Anderson and D. Harmon (Yellowstone National Park, WY: Yellowstone Center for Resources and George Wright Society), 27–53.

Cuhel, R. L., Aguilar, C., Remsen, C. C., Maki, J. S., Lovalvo, D., Klump, J. V., and Paddock, R. W. (2004). The bridge bay spires: collection and preparation of a scientific specimen and museum piece. *Yellowstone Sci.* 12, 35–40.

Hall, P. O. J., and Aller, R. C. (1992). Rapid, small-volume, flow injection analysis for CO_2 and NH_4^+ in marine, and freshwaters. *Limnol. Oceanogr.* 37, 1113–1119.

Henry, E. A., Devereux, R., Maki, J. S., Gilmour, C. C., Woese, C. R., Mandelco, L., Schauder, R., Remsen, C. C., and Mitchell, R. (1994). Characterization of a new thermophilic sulfate-reducing bacterium *Thermodesulfovibrio yellowstonii*, gen. nov. and sp. nov.: its phylogenetic relationship to *Thermodesulfobacterium commune* and their origins deep within the bacterial domain. *Arch. Microbiol.* 161, 62–69.

Holmfeldt, K., Dziallas, C., Titelman, J., Pohlmann, K., Grossart, H.-P., and Riemann, L. (2009). Diversity and abundance of freshwater *Actinobacteria* along environmental gradients in the brackish northern Baltic Sea. *Environ. Microbiol.* 11, 2042–2054.

Huber, J. A., Butterfield, D. A., and Baross, J. A. (2002). Temporal changes in archaeal diversity and chemistry in a mid-ocean ridge subseafloor habitat. *Appl. Environ. Microbiol.* 68, 1585–1594.

Hugenholtz, P., and Huber, T. (2003). Chimeric 16S rDNA sequences of diverse origin are accumulating in the public databases. *Int. J. Syst. Evol. Microbiol.* 53, 289–293.

Ito, T., Sugita, K., Yumoto, I., Nodasaka, Y., and Okabe, S. (2005). *Thiovirga sulfuroxydans* gen. nov., sp. nov., a chemolithoautotrophic sulfur-oxidizing bacterium isolated from a microaerobic waste-water biofilm. *Int. J. Syst. Evol. Microbiol.* 55, 1059–1064.

Jannasch, H. W., Wirsen, C. O., Nelson, D. C., and Robertson, L. A. (1985). *Thiomicrospira crunogena* sp. nov., a colorless, sulfur-oxidizing bacterium from a deep-sea hydrothermal vent. *Int. J. Syst. Bacteriol.* 35, 422–424.

Kashefi, K., Holmes, D. E., Reysenbach, A.-L., and Lovley, D. R. (2002). Use of Fe(III) as an electron acceptor to recover previously uncultured hyperthermophiles: isolation and characterization of *Geothermobacterium ferrireducens* gen. nov., sp. nov. *Appl. Environ. Microbiol.* 68, 1735–1742.

Klump, J. V., Remsen, C. C., and Kaster, J. L. (1988). "The presence and potential impact of geothermal activity on the chemistry and biology of Yellowstone Lake, Wyoming," in *NOAA Symposium Series for Undersea Research*, Vol. 6 (Rockville, MD: NOAA, Oceanic and Atmospheric Research, Office of Undersea Research), 81–97.

Klump, J. V., Remsen, C. C., Lovalvo, D., Anderson, P. D., Cuhel, R. L., Kaplinski, M., Kaster, J. L., Maki, J. S., and Paddock, R. W. (1995). 20,000 Leagues under Yellowstone Lake: strangeness and beauty in the hidden deeps. *Yellowstone Sci.* 3, 10–14.

Kodama, Y., and Watanabe, K. (2004). *Sulfuricurvum kujiense* gen. nov. sp. nov., a facultatively anaerobic, chemolithoautotrophic sulfur-oxidizing bacterium isolated from an underground crude-oil storage cavity. *Int. J. Syst. Evol. Microbiol.* 54, 2297–2300.

Konkol, N. R., Bruckner, J. C., Aguilar, C., Lovalvo, D., and Maki, J. S. (2010). Dominance of epithytic filamentous *Thiothrix* spp. on an aquatic macrophyte in a hydrothermal vent flume in Sedge Bay, Yellowstone Lake, Wyoming. *Microb. Ecol.* 60, 528–538.

Lovalvo, D., Clingelpeel, S. R., McGinnis, S., Macur, R. E., Varley, J. D., Inskeep, W. P., Glime, J., Nealson, K., and McDermott, T. R. (2010). A geothermal-linked biological oasis in Yellowstone Lake, Yellowstone National Park, Wyoming. *Geobiology* 8, 327–336.

Lozupone, C., Hamady, M., and Knight, R. (2006). UniFrac – an online tool for comparing microbial community diversity in a phylogenetic context. *BMC Bioinformatics* 7, 371. doi: 10.1186/1471-2105-7-371

Ludwig, W., Strunk, O., Westram, R., Richter, L., Meier, H., Yadhu, K., Buchner, A., Lai, T., Steppi, S., Jobb, G., Förster, W., Brettske, I., Gerber, S., Ginhart, A. W., Gross, O., Grumann, S., Hermann, S., Jost, R., König, A., Liss, T., Lüßmann, R., May, M., Nonhoff, B., Reichel, B., Strehlow, R., Stamatakis, A., Stuckmann, N., Vilbig, A., Lenke, M., Ludwig, T., Bode, A., and Schleifer K.-H. (2004). ARB: a software environment for sequence data. *Nucleic Acids Res.* 32, 1363–1371.

Morgan, L. A., Shanks, P., Lovalvo, D., Pierce, K., Lee, G., Webring, M., Stephenson, W., Johnson, S., Finn, C., Schulze, B., and Harlan, S. (2003a). The floor of Yellowstone Lake is anything but quiet. *Yellowstone Sci.* 11, 15–30.

Morgan, L. A., Shanks, W. C. III, Lovalvo, D. A., Johnson, S. Y., Stephenson, W. J., Pierce, K. L., Harlan, S. S., Finn, C. A., Lee, G., Webring, M., Schulze, B., Dühn, J., Sweeney, R., and Balistrieri, L. (2003b). Exploration and discovery in Yellowstone Lake: results from high-resolution sonar imaging, seismic reflection profiling, and submersible studies. *J. Volcanol. Geoth. Res.* 122, 221–242.

Nakagawa, S., Shtaih, Z., Banta, A., Beveridge, T. J., Sako, Y., and Reysenbach, A.-L. (2005). *Sulfurihydrogenibium yellowstonense* sp. nov., an extremely thermophilic, facultatively heterotrophic, sulfur-oxidizing bacterium from Yellowstone National Park, and emended descriptions of the genus *Sulfurihydrogenibium*, *Sulfurihydrogenibium subterraneum* and *Sulfurihydrogenibium azorense*. *Int. J. Syst. Evol. Microbiol.* 55, 2263–2268.

Newton, R. J., Jones, S. E., Helmus, M. R., and McMahon, K. D. (2007). Phylogenetic ecology of the freshwater *Actinobacteria* acI lineage. *Appl. Environ. Microbiol.* 73, 7169–7176.

Page, A., Tivey, M. K., Stakes, D., and Reysenbach, A.-L. (2008). Temporal and spatial archaeal colonization of hydrothermal vent deposits. *Environ. Microbiol.* 10, 874–884.

Remsen, C. C., Klump, J. V., Kaster, J. L., Paddock, R. W., and Anderson, P. D. (1990). Hydrothermal springs and gas fumaroles in Yellowstone Lake, Yellowstone National Park, Wyoming. *Natl. Geogr. Res.* 6, 509–515.

Remsen, C. C., Maki, J. S., Klump, J. V., Aguilar, C., Anderson, P. D., Buchholz, L., Cuhel, R. L., Lovalvo, D., Paddock, R. W., Waples, J., Bruckner, J. C., and Schroeder, C. M. (2002). "Sublacustrine geothermal activity in Yellowstone Lake: studies past and present," in *Yellowstone Lake: Hotbed of Chaos or Reservoir of Resilience? Proceedings of the 6th Biennial Scientific Conference on the Greater Yellowstone Ecosystem*, eds R. J. Anderson and D. Harmon (Yellowstone National Park, WY: Yellowstone Center for Resources and George Wright Society), 192–212.

Reysenbach, A.-L., Hamamura, N., Podar, M., Griffiths, E., Ferreira, S., Hochstein, R., Heidelberg, J., Johnson, J., Mead, D., Pohorille, A., Sarmiento, M., Schweighofer, K., Seshadri, R., and Voytek, M. A. (2009). Complete and draft genome sequences of six members of the *Aquificales*. *J. Bacteriol.* 191, 1992–1993.

Sanford, A. R., Cole, J. R., and Tiedje, J. M. (2002). Characterization and description of *Anaeromyxobacter dehalogenans* gen. nov, sp. nov., an aryl-halorespiring facultative anaerobic myxobacterium. *Appl. Environ. Microbiol.* 68, 893–900.

Spear, J. R., Walker, J. J., McCollom, T. M., and Pace, N. R. (2005). Hydrogen and bioenergetics in the Yellowstone geothermal ecosystem. *Proc. Natl. Acad. Sci. U.S.A.* 102, 2555–2560.

Swofford, D. L. (2000). PAUP*. *Phylogenetic Analysis Using Parsimony (and Other Methods)*, Version 4. Sunderland, MA: Sinauer Associates.

Teske, A., Hinrichs, K.-U., Edgcomb, V., de Vera Gomez, A., Kysela, D., Sylva, S. P., Sogin, M. L., and Jannasch, H. W. (2002). Microbial diversity in hydrothermal sediments in the Guaymas Basin: evidence for anaerobic methanotrophic communities. *Appl. Environ. Microbiol.* 68, 1994–2007.

Teske, A., Wawer, C., Muyzer, G., and Ramsing, N. B. (1996). Distribution of sulfate-reducing bacteria in a stratified fjord (Mariager Fjord, Denmark) as evaluated by most-probable-number counts and denaturing gradient gel electrophoresis of PCR-amplified ribosomal DNA fragments. *Appl. Environ. Microbiol.* 62, 1405–1415.

Vairavamurthy, A., and Mopper, K. (1990). Determination of sulfite and thiosulfate in aqueous samples including anoxic seawater by liquid chromatography after derivatization with 2,2′-dithiobis (5-nitropyridine). *Environ. Sci. Technol.* 24, 333–337.

Ward, D. M., Ferris, M. J., Nold, S. C., and Bateson, M. M. (1998). A natural view of microbial biodiversity within hot spring cyanobacterial mat communities. *Microbiol. Mol. Biol. Rev.* 62, 1353–1370.

Warnecke, F., Amann, R., and Pernthaler, J. (2004). Actinobacterial 16S rRNA genes from freshwater habitats cluster in four distinct lineages. *Environ. Microbiol.* 6, 242–253.

Warnecke, F., Sommaruga, R., Sekar, R., Hofer, J. S., and Pernthaler, J. (2005). Abundances, identity, and growth state of actinobacteria in mountain lakes of different UV transparency. *Appl. Environ. Microbiol.* 71, 5551–5559.

Zwart, G., Crump, B., Kamst-van Agterveld, M. P., Hagen, F., and Han, S.-K. (2002). Typical freshwater water: an analysis of available 15S rRNA gene sequences from plankton of lakes and rivers. *Aquat. Microb. Ecol.* 28, 141–155.

Conflict of Interest Statement: The authors declare that the research was conducted in the absence of any commercial or financial relationships that could be construed as a potential conflict of interest.

Received: 03 February 2011; accepted: 26 May 2011; published online: 13 June 2011.

*Citation: Yang T, Lyons S, Aguilar C, Cuhel R and Teske A (2011) Microbial communities and chemosynthesis in Yellowstone Lake sublacustrine hydrothermal vent waters. Front. Microbio. **2**:130. doi: 10.3389/fmicb.2011.00130*

This article was submitted to Frontiers in Microbial Physiology and Metabolism, a specialty of Frontiers in Microbiology.

frontiers in
MICROBIOLOGY

ORIGINAL RESEARCH ARTICLE
published: 09 April 2011
doi: 10.3389/fmicb.2011.00062

Thermodynamics and kinetics of sulfide oxidation by oxygen: a look at inorganically controlled reactions and biologically mediated processes in the environment

George W. Luther III[1]*, Alyssa J. Findlay[1], Daniel J. MacDonald[1], Shannon M. Owings[1], Thomas E. Hanson[1], Roxanne A. Beinart[2] and Peter R. Girguis[2]

[1] *School of Marine Science and Policy, College of Earth, Ocean and Environment, University of Delaware, Lewes, DE, USA*
[2] *Department of Organismic and Evolutionary Biology, Harvard University, Cambridge, MA, USA*

Edited by:
Martin G. Klotz, University of Louisville, USA

Reviewed by:
Marc Strous, Max Planck Institute for Marine Microbiology, Germany
Donald A. Bryant, The Pennsylvania State University, USA

****Correspondence:***
George W. Luther III, School of Marine Science and Policy, College of Earth, Ocean and Environment, University of Delaware, 700 Pilottown Road, Lewes, DE 19958, USA.
e-mail: luther@udel.edu

The thermodynamics for the first electron transfer step for sulfide and oxygen indicates that the reaction is unfavorable as unstable superoxide and bisulfide radical ions would need to be produced. However, a two-electron transfer is favorable as stable S(0) and peroxide would be formed, but the partially filled orbitals in oxygen that accept electrons prevent rapid kinetics. Abiotic sulfide oxidation kinetics improve when reduced iron and/or manganese are oxidized by oxygen to form oxidized metals which in turn oxidize sulfide. Biological sulfur oxidation relies on enzymes that have evolved to overcome these kinetic constraints to affect rapid sulfide oxidation. Here we review the available thermodynamic and kinetic data for H_2S and HS• as well as O_2, reactive oxygen species, nitrate, nitrite, and NO_x species. We also present new kinetic data for abiotic sulfide oxidation with oxygen in trace metal clean solutions that constrain abiotic rates of sulfide oxidation in metal free solution and agree with the kinetic and thermodynamic calculations. Moreover, we present experimental data that give insight on rates of chemolithotrophic and photolithotrophic sulfide oxidation in the environment. We demonstrate that both anaerobic photolithotrophic and aerobic chemolithotrophic sulfide oxidation rates are three or more orders of magnitude higher than abiotic rates suggesting that in most environments biotic sulfide oxidation rates will far exceed abiotic rates due to the thermodynamic and kinetic constraints discussed in the first section of the paper. Such data reshape our thinking about the biotic and abiotic contributions to sulfide oxidation in the environment.

Keywords: sulfide, oxidation, abiotic, biotic, *Chlorobaculum tepidum*, chemolithotrophy, photolithotrophy

INTRODUCTION

The oxidation of hydrogen sulfide is arguably one of the most important processes in the environment as the oceans have been suboxic or anoxic and euxinic (i.e., sulfidic) for long spans of geologic time (Canfield and Raiswell, 1999; Turchyn and Schrag, 2006). These are the oceans in which eukaryotes evolved and sulfur metabolism may have helped shape initial symbiotic events leading to the eukaryotic lineage (Overmann and van Gemerden, 2000; Theissen et al., 2003; Mentel and Martin, 2008). Modern analogs of these euxinic environments can be found in anoxic marine basins like the deep Black Sea (Wakeham et al., 2007), near the Cariaco Trench (Lin et al., 2008), and highly sulfidic marine sediments like those in the Santa Barbara Basin that have been characterized as symbiosis oases (Bernhard et al., 2000). Other oceanic regions experience periodic anoxia and sulfidic water columns due to the disturbance of sulfide laden sediments underlying areas of high primary productivity, like the upwelling zones off the coasts of Chile (Canfield et al., 2010) and Namibia (Bruchert et al., 2003). In addition, hydrothermal vents are a key source of H_2S to the ocean and for vent associated ecosystems supported by sulfide driven chemolithotrophic primary production (Jannasch and Wirsen, 1979).

The sulfide produced in modern systems is released to overlying waters where it can be a toxin for aerobic organisms (Eghbal et al., 2004; Julian et al., 2005). At many sites where sulfide emanates, various microbes form microbial mats (Jorgensen, 1994; Baumgartner et al., 2006), and these organisms as well as macrofauna carrying microbial have the capability of oxidizing sulfide using chemical oxidants such as O_2 and NO_3^- (Jorgensen and Gallardo, 1999; Girguis et al., 2000) while using the energy released to survive and grow. In the deep sea sulfide oxidation using oxygen as oxidant forms the basis for symbiotic associations, most notably the association between the Vestimentiferan tubeworm *Riftia pachyptila* with its sulfide-oxidizing gamma proteobacterial community found in the trophosome, a specialized organ (Wilmot and Vetter, 1990; Arndt et al., 2001). In shallower environments, phototrophic anaerobic microbes use sunlight to affect the oxidation of sulfide via the enzyme systems sulfide:quinone oxidoreductase (SQR; e.g., Theissen et al., 2003) or flavocytochrome *c* (FCC, also known as flavocytochrome *c* sulfide dehydrogenase; Reinartz et al., 1998).

In addition to biologically mediated sulfide oxidation, oxidized metal compounds such as Fe(III) and Mn(III, IV) phases are efficient chemical oxidants for sulfide (Poulton et al., 2004; Yücel et al., 2010). In sediments and at the interface zones of sulfide and

oxygen in anoxic basins, dissolved Mn and Fe are present and help to overcome the kinetic barrier to sulfide oxidation with oxygen as Mn(II) and Fe(II) can be oxidized abiotically or by microbial activity (Trouwborst et al., 2006; Clement et al., 2009). Here the oxidation of Fe(II) and Mn(II) to Fe(III) and Mn(III, IV) chemical species permit the oxidation of sulfide, which is a trace metal catalyzed process as Fe(II) and Mn(II) are regenerated (Konovalov et al., 2003; Ma et al., 2006; Yakushev et al., 2009).

While the importance of microbial biochemistry to sulfide oxidation in many systems is recognized (e.g., Lavik et al., 2009), this paper seeks to provide a concise demonstration of the underlying chemical principles for this observation. In this paper, we summarize the thermodynamics of one and two-electron transfers in sulfide oxidation showing that one-electron transfers are unfavorable whereas two-electron transfers are favorable. However, two-electron transfers have a kinetic barrier for the direct reaction of sulfide and oxygen, which is a paramagnetic species, or of sulfide with nitrate. To demonstrate this point clearly, we compare abiotic rates of sulfide oxidation with O_2 under trace metal clean conditions as well as with biotic rates for the anaerobic photolithotroph, *Chlorobaculum tepidum*, and aerobic chemolithotrophic bacterial symbionts from Lau Basin and free-living microbial communities from the Juan de Fuca Ridge. These data reveal that microbes enhance sulfide oxidation by three or more orders of magnitude and indicate that chemolithotrophic organisms are able to overcome the kinetic barrier for the reaction of sulfide with oxygen. By comparison with existing literature data, we demonstrate that biological sulfide oxidation rates will exceed trace metal catalyzed abiotic sulfide oxidation rates under many conditions.

MATERIALS AND METHODS

ABIOTIC REACTIONS

All abiotic sulfide oxidation experiments were performed in a class 100 clean bench to prevent metal contamination. Plastic falcon tubes and other materials were cleaned of trace metal contamination by performing the following procedure. First the plastic materials are cleaned with a detergent in deionized (DI) water; then for a day each in three consecutive acid baths of (1) 10% trace metal clean HCl acid followed by DI water rinsing; (2) another 10% trace metal clean HCl acid followed by DI water rinsing; (3) 1% ultra pure HCl acid followed by DI water rinsing. After the last step, the plasticware is used for reaction or stored in plastic freezer bags until needed. Pipette tips were left to soak in 10% trace metal clean HCl until needed and were rinsed with DI water before they were used.

The sulfide reactions with oxygen were performed in trace metal clean base, ~15 mM NaOH. The trace metal clean base was prepared by adding NaOH to air saturated DI water and then 0.01 M $MgCl_2 \cdot 6H_2O$ was added to precipitate any oxidized Fe and other trace metal contaminants. The solution is then centrifuged and decanted into an acid washed bottle. The pH of the resulting solution is about 12. A stock solution of sulfide was made by dissolving solid $Na_2S \cdot 9H_2O$ in trace metal clean base to give a concentration of 24 mg mL^{-1} (0.01 M). The solid $Na_2S \cdot 9H_2O$ was first rinsed with DI water and dried with a kimwipe before it was weighed and dissolved. An aliquot of a $Na_2S \cdot 9H_2O$ solution is then added to the oxygen saturated (~250 μM) base solution so that the total sulfide in the solution is 50 or 100 μM. The loss of HS^- is monitored over time by UV–Vis spectrophotometry using the 230-nm peak (Ellis and Golding, 1959). When an aliquot is taken for analysis, it is discarded and not returned to the reaction vessel. The vessel is shaken to insure air saturation after each aliquot is removed.

BIOTIC REACTIONS

Chlorobaculum tepidum is a phototrophic, anoxygenic sulfide-oxidizing bacterium. Electrochemical methods were employed in order to measure the rate of sulfide loss in the presence of these bacteria under different light intensities.

Culture growth

Wild type *C. tepidum* (strain TLS 1, Wahlund et al., 1991) were grown at 42°C under 20 μmol photons m^{-2} s^{-1} provided by a full spectrum 60 W incandescent bulb for 3 days in Pf-7 medium containing 2.71 mM sulfide. Cultures were started by transferring 1 mL of a previously grown culture into a 100-mL septum vial containing anoxic media, which was then pressurized with argon gas to 10 psi. The vial was stored in the dark for 45 min, then transferred to a water bath for growth under the conditions specified above. After 3 days, 50 mL of cells were centrifuged at 3000 rpm for 45 min and rinsed in anoxic HEPES buffer (0.1 M, pH 7.4) to remove salts from the cells. After three rinses, the cells were stored in 5 mL anoxic HEPES buffer in a sealed 20 mL septum vial. Conditions were kept anoxic by using a glove bag purged with ultra high purity argon gas for transferring the cells. To determine the number of cells in the culture, 90 μL of cells were fixed with 10 μL of paraformaldehyde and diluted 1000-fold in 9 mL HEPES and 1 mL Triton X-100. Five milliliter of this solution were filtered through a 0.20-μm polycarbonate filter, and biomass was found through direct counts done by fluorescence microscopy using 4′,6-diamidino-2-phenylindole (DAPI) stain and a UV light (Cottrell and Kirchman, 2003). Concentrations were calculated from the average of 10 fields of view with a 250-s exposure time. The concentration of cells after the final rinse was 3.3×10^9 cells $mL^{-1} \pm 0.4 \times 10^9$ cells mL^{-1}.

ANALYTICAL METHODS

Voltammetry with solid state electrodes was used to monitor sulfide loss, and the details of the method are described in Brendel and Luther (1995) and Luther et al. (2008). Briefly, a typical three-electrode cell for the placement of electrodes with ports for stirring, the introduction of materials, and the purging with argon was used to measure sulfide loss *in situ* and in the absence of oxygen. The cell consists of a 100-μm gold amalgam (Au–Hg) working electrode, a platinum counter electrode, and a Ag/AgCl reference electrode, used in conjunction with a DLK-60 electrochemical analyzer [Analytical Instrument Systems (AIS), Inc.]. AIS software was used to run the equipment, and data were analyzed using a program written in Python. Peak heights were converted to concentrations using the method of standard additions in HEPES buffer with no cells. Cyclic voltammetric scans were run from −0.1 to −1.8 V and back to −0.1 V at a scan rate of 2 V s^{-1}. Two conditioning steps preceded each scan: one at −0.9 V for 5 s, which served as an electrochemical cleaning step to prevent sulfide from plating onto the electrode, and another at −0.1 V for 2 s (Eq. 1). Under these experimental conditions, sulfide reacts at the Au–Hg

electrode to form a HgS surface via the following equations and the peak for the removal of sulfide from the HgS surface near −0.7 V from Eq. 2 is used for analysis:

$$HS^- + Hg \rightarrow HgS + 2e^- \quad (1)$$

$$HgS + H^+ + 2e^- \rightarrow HS^- + Hg \quad (2)$$

The solution was stirred with a mechanical stirrer prior to each scan. The detection limit for sulfide using this method is about 0.2 μM.

Stock solutions of HEPES and sulfide were made from salts dissolved in DI water that was purged in a pressure equalizing dropping funnel for 45 min with ultra high purity argon gas prior to use. The sulfide solution was prepared as above by first rinsing the solid $Na_2S•9H_2O$ with DI water and drying it with kimwipes before being weighed and dissolved in degassed DI water.

EXPERIMENTAL PROCEDURE FOR PHOTOTROPHIC SULFIDE OXIDATION

Experiments were run in sterile, anoxic HEPES buffer (0.1 M, pH 7.4) at 44°C. Temperature was held constant using a water jacketed electrochemical cell mated to a thermostatically controlled water bath, and an argon purge was used to keep oxygen from entering the cell. Once anoxic conditions were established, an appropriate volume of cells was added to the cell and were diluted to the desired concentration. The number of cells used varied between experiments, and ranged from 3.0×10^8 to 1.4×10^{10}. Replicate experiments were conducted with different cultures to determine sulfide oxidation rate reproducibility. After a short period was allowed for the cells and solution to reach thermal equilibrium, up to 100 μM sulfide was added. The electrochemical cell was then capped to eliminate headspace and minimize volatile sulfide loss. Electrochemical measurements were taken every 9 s throughout the course of the experiment. Light was provided by a full spectrum 60 W incandescent bulb and the intensity was measured using a LI-COR Biosciences LI-1400 data logger light meter inside the electrochemical cell and ambient light was measured to be 5 μmol photons m^{-2} s^{-1}. For dark conditions (0 μmol photons m^{-2} s^{-1}) the electrochemical cell was covered, and measurements with the light meter ensured that no light was infiltrating the cell. For each set of conditions, experiments were also run without cells in order to establish sulfide loss due to abiotic factors with voltammetric measurements taken every 30 s for an hour. Rates were calculated from the linear range of a plot of sulfide concentration (μM) versus time for each experiment.

DETERMINING RATES OF CHEMOLITHOTROPHIC SULFIDE OXIDATION BY SYMBIONTS

All experiments were conducted on board the R/V Thomas G. Thompson during an expedition in June and July 2009 at Lau Basin. *Ifremeria nautilei* (Bouchet and Warén, 1991; Windoffer and Giere, 1997) snails were collected by the ROV JASON from the ABE vent field (20 45.794323°S, 176 11.466148°W) during dive J2-423 from a depth of 2152 m. Snails were brought to the surface in a thermally insulated container (Mickel and Childress, 1982). After arrival on board ship, the snails most responsive to touch were immediately placed into titanium flow-through, high-pressure respirometer aquaria (as in Henry et al., 2008), where they were maintained in 0.2 micron filter-sterilized flowing seawater for approximately 24 h at 15°C and 27.5 Mpa prior to experimentation.

To simulate the seawater chemistry found *in situ*, the 0.2-micron filter-sterilized seawater was pumped into an acrylic gas equilibration column and bubbled with carbon dioxide, hydrogen sulfide, oxygen, and nitrogen to achieve the desired dissolved gas concentrations (Girguis and Childress, 2006). Seawater from the equilibration column was delivered to the three aquaria by high-pressure pumps (American Lewa, Inc. Holliston, MA, USA). High-pressure aquaria were maintained in our climate-controlled laboratory, while aquaria pressures were maintained at 27.5 Mpa via diaphragm back pressure valves (StraVal, Inc.). Vessel effluents were directed through a computer-controlled stream-selection valve that diverted one stream to the analytical instrumentation every 30 min so that either the initial water or a chamber with live animals could be analyzed for chemical components. The analytical system consisted of a membrane-inlet quadrupole mass spectrometer to determine all dissolved gas concentrations, an inline oxygen optode (Golden Scientific Inc.), and an inline pH electrode (Radiometer Inc.). In addition to the mass spectrometric analyses, hydrogen sulfide concentrations were determined by a quantitative colorimetric assay (Cline, 1969). For this study, a voltammetric flow cell was also added to the inline analytical instrumentation (Luther et al., 2002) so that hydrogen sulfide, polysulfides, thiosulfate, and oxygen could be determined. All carbon dioxide and hydrogen sulfide measurements were confirmed and calibrated using discrete samples analyzed back using a Hewlett-Packard 5890 Series II gas chromatograph (as in Childress et al., 1991).

For these experiments, *I. nautilei* were placed in the respirometer aquaria and were maintained in conditions typical of those *in situ*, namely total dissolved inorganic carbon (i.e., ΣCO_2) = 5.5 to 6 mM, total dissolved sulfide (i.e., ΣH_2S) from 312 to 650 μM, dissolved O_2 from 110 to 180 μM, and dissolved NO_3 = 40–50 μM, pH = 6.1 to 6.6, temperature = 15–30°C, pressure = 27.5 Mpa, flow rate = 15 mL min^{-1}. *I. nautilei* were maintained in these conditions until "autotrophy," during which they exhibited a net uptake of dissolved inorganic carbon, oxygen, and sulfide, as well as net elimination of proton equivalents. All dissolved substrate concentrations, as well as pH and temperature, were held at these "typical" conditions for the duration of the experiment. At the end of each experiment, snails were promptly removed, weighed on a motion-compensated shipboard balance, dissected, and frozen in liquid nitrogen for other analyses. Once removed, "free-living" microbes remained in the chambers and the aquaria were re-pressurized so experiments with only microbes could be performed.

DETERMINING RATES OF CHEMOLITHOTROPHIC SULFIDE OXIDATION BY FREE-LIVING ASSEMBLAGES

All experiments were conducted on board the *R/V Atlantis* during an expedition in August 2008 to the Juan de Fuca ridge. Active solid sulfide samples were collected by the *DSV Alvin* using a sampling scoop, and were brought to the surface in a thermally insulated container (Mickel and Childress, 1982). After arrival on board ship, sulfide samples were immediately placed into titanium flow-through, high-pressure respirometer aquaria (as in Henry et al., 2008), where they were maintained in 0.2 μm filter-sterilized flowing seawater for approximately 24 h at 15°C and 27.5 Mpa prior to experimentation.

In situ seawater chemistry was simulated as described above. We incubated the sulfide samples at the following conditions: 5 mM inorganic carbon, 650 μM hydrogen sulfide, 110 μM oxygen, pH 5.0, temperature of 30°C, and pressure of 27.5 Mpa (ca. 4000 psi). All fluids were directed through a computer-controlled stream-selection valve that diverted one stream to the analytical instrumentation every 30 min as described above. All dissolved substrate concentrations, as well as pH and temperature, were held at the aforementioned conditions for the duration of the experiment. At the end of each experiment, sulfide samples were promptly removed, weighed on a motion-compensated shipboard balance, dissected, and frozen in liquid nitrogen for other analyses.

RESULTS AND DISCUSSION

THERMODYNAMICS OF SULFIDE OXIDATION

The thermodynamic equations and calculations for the reactions of sulfide with various oxidants have been demonstrated in Luther (2010), who used the thermodynamic data (at 25°C and 1 atm) tabulated by Maloy (1985), Stumm and Morgan (1996) and Stanbury (1989). Briefly a reduction half reaction and an oxidation half reaction are combined to provide a ΔG or Δlog K, which indicates the favorability of a given reaction over pH. For example the one-electron transfer reaction (Eq. 3) of O_2 with HS^- leads to two thermodynamically unfavorable products (superoxide ion and bisulfide radical).

$$O_{2(aq)} + HS^- \rightarrow O^-_{2(aq)} + HS\bullet \quad (3)$$

The thermodynamic functions for the reduction half reactions are Eqs 4 and 5. The function pεis the log K for the half reaction at a given pH; pε° is the log K value at the standard state for all reactants and products. The complete reaction for Eq. 3 is the sum of Eq. 4 minus Eq. 5. An extensive list of half reactions are given in Luther (2010).

$$O_{2(aq)} + e^- \rightarrow O^-_{2(aq)} \quad p\varepsilon = p\varepsilon^\circ = -2.72 \quad (4)$$

$$HS\bullet + H^+ + e^- \rightarrow H_2S \quad p\varepsilon = p\varepsilon^\circ - pH = 25.21 - pH \quad (5)$$

Similarly, the two-electron transfer reaction of O_2 with H_2S leads to stable products (Eq. 6).

$$O_{2(aq)} + H_2S \rightarrow S^0 + H_2O_2 \quad (6)$$

The thermodynamic functions for the reduction half reactions describing Eq. 6 are given in Eqs 7 and 8. Equation 6 is an accurate representation for the energy driving chemolithotrophy by an aerobic sulfide oxidizer using O_2 as the terminal electron acceptor.

$$1/2O_{2(aq)} + H^+ + e^- \rightarrow \tfrac{1}{2}\, H_2O_2 \quad p\varepsilon = p\varepsilon^\circ - pH = 13.18 - pH \quad (7)$$

$$1/2S + H^+ + e^- \rightarrow \tfrac{1}{2}\, H_2S \quad p\varepsilon = p\varepsilon^\circ - pH = 2.44 - pH \quad (8)$$

Figure 1 shows plots over pH for one and two-electron transfer reactions for the reaction of sulfide with oxygen, reactive oxygen species and oxidized nitrogen species. In some instances there is no pH dependence for a given reaction, but in most instances there is a significant pH dependence. **Figure 1A** describes the thermodynamics of sulfide oxidation in one-electron transfers of oxygen in four steps from O_2 to O_2^- to H_2O_2 to OH• to produce H_2O. Only OH• can lead to formation of HS•. Even the oxidation of sulfide by O_3 and $^1O_2$ are unfavorable. However, the two-electron transfer reactions (e.g., Eq. 6) for O_2 to H_2O_2, H_2O_2 to H_2O, $^1O_2$ to H_2O_2, and O_3 to O_2 and H_2O are thermodynamically favorable over all pH.

Figures 1C,D are the data for the one-electron and two-electron transfer reactions of oxidized nitrogen species with sulfide. Again one-electron transfer reactions are not thermodynamically favorable over all pH as HS• results whereas two-electron transfer reactions are favorable. The one-electron thermodynamic calculations show that the oxidation of sulfide by other oxidants has similar problems as O_2. Also, the reaction of sulfide at near neutral or basic pH has a kinetic constraint as nitrate and nitrite are anions as is HS^-; thus, two negative species repel each other as they come near each other in the transition state.

A major problem for the reaction of O_2 with any reactant that can donate a pair of electrons is the partial occupancy of the highest occupied π antibonding orbitals, which are similar in energy (**Figure 2**). A direct two-electron transfer is not possible and a one-electron transfer requires the unpairing of electrons in a donor such as sulfide. Thus, there is a kinetic constraint on O_2 reactivity and this constraint needs to be overcome as it is in chemolithotrophic sulfide-oxidizing microbes. On the other hand, these kinetic constraints allow sulfide to persist for long enough periods in oxic and nitrate dominated environments thereby defining niches that can be exploited by sulfide-oxidizing microbes.

Figure 3 shows the ΔG for three reaction sequences. First, the one-electron transfer sequential reactions of O_2 with H_2S to form O_2^- and HS• and of O_2^- with HS• to form H_2O_2 and S(0) (blue). In this case, the first step is thermodynamically unfavorable. A second reaction possibility is the reaction of O_2 with H_2S to form O_2^- and HS• followed by the reaction of another O_2 with HS• to form O_2^- and S(0). Again, the first step is thermodynamically unfavorable. The direct two-electron transfer reaction of O_2 with H_2S described in Eq. 6 (red) is favorable.

ABIOTIC REACTION OF SULFIDE WITH OXYGEN

A concrete demonstration of kinetic limitations on the direct oxidation of sulfide by O_2 can be found by examining the reaction of bisulfide ion (HS^-) with excess O_2 in basic solutions. Over the pH range 8–12, Millero et al. (1987) showed that the kinetics of oxidation do not change at constant temperature (T) and ionic strength (I) where HS^- is the dominant sulfide species. **Figure 4** shows a plot for the abiotic oxidation of sulfide in air saturated solutions at a pH of 12 and 25°C using trace metal clean base solution. The slope of the ln (sulfide) versus time shows pseudo first order behavior and yields the pseudo first order rate constant, *k*. For three replicates, *k* is 7.12×10^{-3} day^{-1} ($\pm 1.96 \times 10^{-4}$). The half-life is 55 ± 1 day and the loss of sulfide is 0.91 μM day^{-1}.

We compare our data with those of Millero et al. (1987). In their work, they found the rate expression

$$-d[H_2S]/dt = k_2[H_2S][O_2] \quad (9)$$

where k_2 is the second order rate constant (M^{-1} h^{-1}) and has the following form for pH = 4–8.

$$\log k_2 = 10.5 + 0.16\ pH - (3 \times 10^3)\ T^{-1} + 0.49\ I^{1/2} \quad (10)$$

From our concentration and rate data as in **Figure 4** and using Eq. (9), we calculate using initial rate theory a k_2 of 6.99 M^{-1} h^{-1} or log k_2 of 0.845 assuming first order behavior for HS^- and O_2. Our

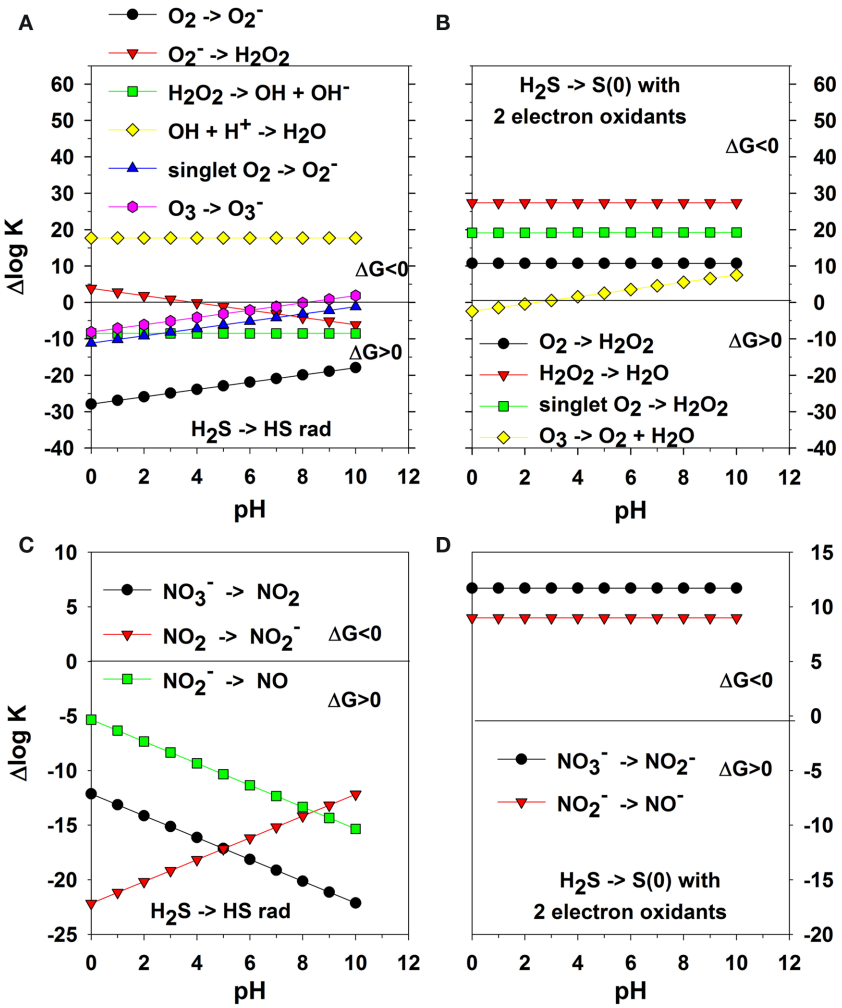

FIGURE 1 | One-electron transfer reactions of H_2S with oxygen species; the + Δlog K on the *y*-axis indicates a favorable complete reaction and – Δlog K indicates an unfavorable reaction as $\Delta G^o = -RT\ lnK = -2.303\ RT\ log\ K$. HS^- reactions are not included but are similar in reactivity (note pK of H_2S ~7 and depends on salinity and temperature). **(A)** one-electron transfer reactions of oxygen species coupled with Eq. 5. **(B)** two-electron transfer reactions of oxygen species coupled with Eq. 8. **(C)** one-electron transfer reactions of oxidized nitrogen species coupled with Eq. 5. **(D)** two-electron transfer reactions of oxidized nitrogen species coupled with Eq. 8.

k_2 value is significantly smaller than that found by Millero et al. (1987). Because Millero et al. (1987) found a faster half-life of about 1–2 days for reactions at pH values similar to ours, we conclude that trace metal clean conditions hinder the oxidation of sulfide with O_2. In their work, their plexi glass reaction vessel was rinsed with acid prior to (re)use whereas each experiment here was performed in a separate trace metal clean plastic tube. The trace metal clean condition shows clearly that the reaction of O_2 and sulfide is not a favorable reaction.

In subsequent work, Vazquez et al. (1989) showed that the addition of trace metals in particular Fe(II) to the reaction vessel increased the rate of oxidation such that the half-life is on the order of minutes. Vazquez et al. (1989) showed that the rate doubled at the concentrations of Mn(II)found in the Black Sea, but increased 20-fold at the Fe(II) concentrations found at the Black Sea interface. The metal data indicate that the reaction of sulfide with oxygen is truly slow. As indicated by the thermodynamics, one-electron reactions are unfavorable whereas two-electron reactions are favorable, but have a kinetic problem due to the spin pairing problem with O_2 (**Figure 2**). Ma et al. (2006) showed that a catalytic Fe, O_2, H_2S cycle occurs at the oxic – anoxic interface, and this cycle results in sulfide oxidation to elemental sulfur.

SULFIDE OXIDATION KINETICS OF ANAEROBIC PHOTOLITHOTROPHIC BACTERIA

Figure 5 shows representative data for sulfide oxidation in the presence and absence of *C. tepidum* under laboratory light of 5 μmol photons $m^{-2}\ s^{-1}$. The rate of sulfide oxidation in the absence of cells is negligible as O_2 or other dissolved oxidants are not present; thus, Eq. 9 is not operative. Any minor sulfide loss is due to volatilization. The loss of sulfide over time with *C. tepidum* (3.3×10^9 cells mL^{-1})

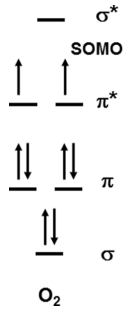

FIGURE 2 | The molecular orbital diagram for O_2 showing the partially filled orbitals that accept electrons.

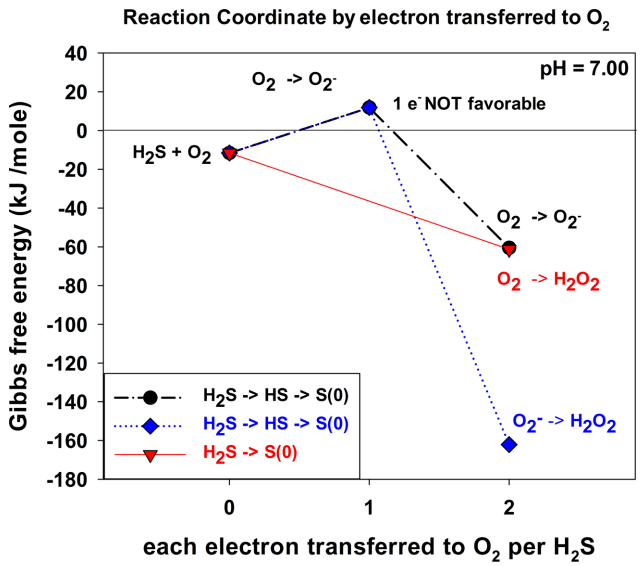

FIGURE 3 | Thermodynamics of stepwise oxidation reactions for O_2 oxidation with H_2S for both one and two-electron transfer reactions. At zero electrons transferred, ΔG° is the sum of the standard state ΔG° values before a reaction occurs.

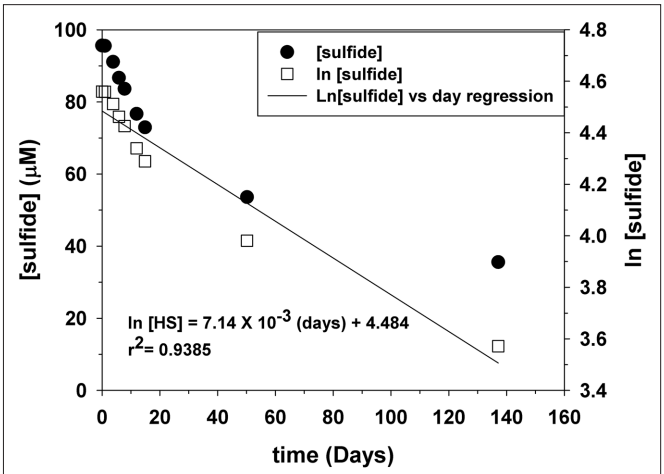

FIGURE 4 | Representative plot for the kinetics of sulfide oxidation in air saturated water under trace metal clean conditions. The ln of the sulfide concentration versus time shows pseudo first order behavior.

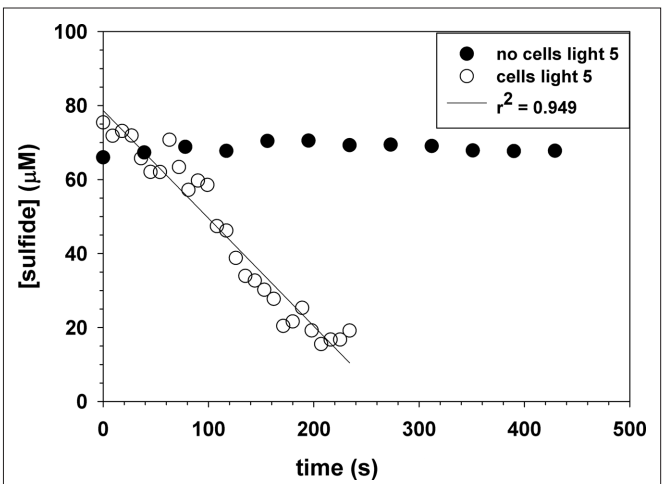

FIGURE 5 | Representative plot for the photo oxidation of sulfide in the presence of *C. tepidum* cells during stationary growth phase with 5 μmol photons m^{-2} s^{-1} of light intensity. The control with no cells shows no sulfide loss.

and light is linear with $r^2 = 0.949$ versus a first order plot for the ln (sulfide) versus time giving $r^2 = 0.930$. The linear plot of sulfide with time indicates that the reaction is zeroth order in sulfide and that sulfide oxidation depends on light as the external stimulus and not the concentration of sulfide as a reactant. The rate law for a zeroth order reaction is given as

$$-d[H_2S]/dt = k \quad (11)$$

which on integration gives

$$kt = [H_2S]_i - [H_2S] \quad (12)$$

where $[H_2S]_i$ is the initial sulfide concentration. In our experiments, the value of k may include constants for the intensity of light and the number of cells.

This zeroth order kinetic pattern has been shown for Fe(II) oxidation in hot springs when cyanobacteria produce O_2, which then reacts with Fe(II) and removes it as Fe(III) solid phases (Trouwborst et al., 2007). The Fe(II) oxidation is external to the cyanobacterial cells whereas sulfide oxidation with *C. tepidum* occurs internally. Genetic experiments have shown that SQR is required for *C. tepidum* to grow with sulfide as the electron donor (Chan et al., 2009). SQR's are flavin containing enzymes that pass two-electrons from sulfide via the flavin cofactor to the quinone pool. The quinone pool ultimately is reoxidized by the activity of the photosynthetic reaction center. This model predicts the observed light dependence of sulfide oxidation as observed by the electrochemical experiments here.

In the presence of cells in stationary growth phase, the sulfide oxidation rate is 26,200 ± 1200 μM day^{-1} at 44°C and a pH = 7.4. The data in **Figures 4 and 5** can be compared to give relative rates for abiotic oxidation under trace metal clean conditions to biotic oxidation with *C. tepidum* cells of 0.91: 26,200. If we assume that the abiotic rate

doubles for every 10°C increase, then the ratio becomes 1: 7,200 at 25°C. **Figure 6** shows the variation of sulfide oxidation rate versus cell counts when independent cultures of *C. tepidum* were in exponential phase growth. The average sulfide oxidation rate is 6,500 ± 2900 μM day^{-1} $(10^9$ cells$)^{-1}$ at 44°C and a pH = 7.4. The rate of sulfide loss varies only eightfold over the two orders of magnitude range in cell count. Replicates rates for the same cell count and culture have a SD of 300 μM day^{-1} normalized to cell count. These data suggest that under most conditions, phototrophic sulfide oxidizers are not limited by the abiotic oxidation rate of sulfide under anoxic conditions. Furthermore, these data allow one to conclude that in anoxic systems dominated by anoxygenic phototrophs, biological sulfide oxidation rates will exceed abiotic oxidation by several orders of magnitude as no oxygen is present to oxidize sulfide. While the cell concentrations used here may seem high, in the New Zealand mats where *C. tepidum* was isolated and in other microbial mat systems, cell densities of 10^8–10^9 g^{-1} of sediment are not uncommon (Wahlund et al., 1991).

SULFIDE OXIDATION KINETICS OF AEROBIC CHEMOLITHOTROPHIC SYMBIONTS AND FREE-LIVING ASSEMBLAGES

As chemolithotrophic symbionts cannot be cultured in the lab, we relied on shipboard high-pressure incubations with freshly collected samples to make inferences about the nature and capacity for sulfide oxidation. **Table 1** shows data for the chemolithotrophic oxidation of sulfide by chemolithotrophic symbionts of the vent snail *I. nautilei* in high-pressure incubation chambers (geochemical conditions are described in the Materials and Methods). These incubations were conducted in the presence of sulfide (H_2S), and there is substantial uptake of H_2S. Notably, the effluent from these vessels after exposure to *I. nautilei* showed substantial enrichment in polysulfide S(−2) and S(0) (Rozan et al., 2000) The sulfide oxidation rate from these data is 27.83 ± 1.89 μM min^{-1} (40,100 μM day^{-1}) compared to the calculated abiotic rate of 0.0304 μM min^{-1} (43.8 μM day^{-1}) for these conditions using Eqs 9 and 10. Previous studies (Girguis and Childress, 2006) have also shown that the majority of sulfide oxidation is attributable to the symbiont. However, it is apparent that non-symbiotic animals, e.g., *Urechis* sp. worms, also have a native sulfide oxidation capacity though at substantially lower rates (Girguis et al., 2002). The data presented here are the first to characterize the different species of soluble oxidized sulfur compounds produced by intact symbioses, and future studies should aim to better characterize this response in other symbioses, as well as non-symbiotic animals.

Moreover, **Table 2** also shows data for the chemolithotrophic oxidation of sulfide by free-living chemolithotrophic microbes in high-pressure incubation chambers (geochemical conditions are described in the Materials and Methods). The actual sulfide oxidation rate is 34.6 μM min^{-1} (49,800 μM day^{-1}) compared to the calculated abiotic rate of 0.0105 μM min^{-1} (15.1 μM day^{-1}) Eqs 9 and 10.

These data clearly illustrate that biologically mediated oxidation of H_2S by O_2 occurs rapidly, and indicates that chemolithotrophic microbes have found an efficient way to perform a two-electron transfer as in **Figure 1B** while overcoming any kinetic constraints based on the electron orbital diagram in **Figure 2**. These chemolithotrophic rates are over 10^4 times that of the abiotic rate from Eqs 9 and 10 (**Table 3**). It is important to note that these data cannot resolve the relative contributions of sulfide oxidation by the mineralogical assemblage versus the biological community, but iron (oxy)hydroxide phases have rates on par with the trace metal catalyzed reactions (Vazquez et al., 1989). Again, these data provide a first glimpse at rates of sulfide oxidation by free-living microbes associated with sulfides, and future experiments should be aimed at differentiating the relative contributions of biotic and abiotic sulfide oxidation, as well as the relative differences in oxidation by different microbial communities (e.g., diffuse flow communities versus high temperature communities) and mineralogical assemblages.

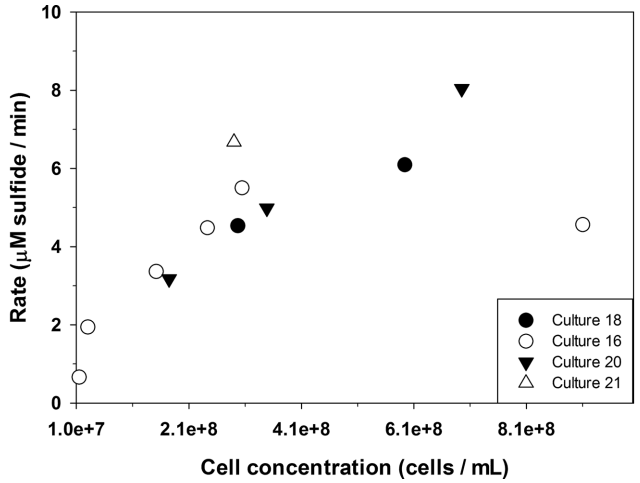

FIGURE 6 | The relationship between the rate of sulfide loss and varying *C. tepidum* cell counts from independent cultures in exponential phase growth with 5 μmol photons m^{-2} s^{-1} of light intensity.

Table 1 | Dissolved data for the chemolithotrophic oxidation of H_2S with O_2 using *I. nautilei* in high-pressure incubation chambers.

Organisms initial time (h)	Incurrent sulfide (μM)	Excurrent H_2S (μM)	Excurrent S(0) (μM)	H_2S uptake rate (μM min^{-1})
I. nautilei 12.43	312.5	20.69	25.04	26.3
I. nautilei 14.43	280.5	24.39	24.41	30.0
I. nautilei 16.93	271.6	22.03	20.91	27.3

The H_2S data indicate the substantial loss of sulfide on exiting the reaction chamber, and the S(0) data indicate an oxidized product as polysulfide. Sulfide uptake and oxidation rate calculations are based on the mass of the animals in the chamber.

Table 2 | Data for the chemolithotrophic oxidation of H_2S with O_2 in high-pressure incubation chambers by free-living microbial communities (40 mL volume) recovered from hydrothermal diffuse flows.

Organisms initial time (h)	Incurrent H_2S (μM)	Excurrent H_2S (μM)	H_2S uptake rate (μM min^{-1}; *N* = number of scans)
Free-living community, 12	154.7	21.2	33.3
Free-living community, 22	137.2	16.9	30.3
Free-living community, 36	184.5	23.7	40.2

The H_2S data indicate the substantial loss of sulfide on exiting the reaction chamber.

Table 3 | Comparative rates for the oxidation of sulfide under abiotic and biotic conditions.

	Sulfide oxidation relative rate (μM day^{-1})
SULFIDE OXIDATION WITH O_2	
Trace metal clean (this work)	1
Millero et al. (1987)	43.8
Vazquez et al. (1989) – 8 μM Mn(II)	87.6
Vazquez et al. (1989) – 0.3 μM Fe(II)	832
I. nautilei with chemolithotrophic microbes	40,100
Chemolithotrophic microbes alone	49,800
SULFIDE OXIDATION WITHOUT O_2	
C. tepidum (stationary phase)	7,200
C. tepidum (exponential phase)	1,625

The first six entries oxygen is the oxidant. The last two entries are for the anaerobic photolithotroph. The relative rates are corrected to a temperature of 25°C as the C. tepidum experiments were performed at 44–45°C.

CONCLUSION

The goal for this work was to integrate theoretical chemical considerations with newly collected data to provide a concise rationale for why biological sulfide oxidation rates far exceed abiotic sulfide oxidation rates under both aerobic and anaerobic conditions. Direct comparison of the rates from our experiments with those from previous work (**Table 3**) indicate that chemolithotrophic sulfide oxidizers using O_2 as the oxidant display sulfide oxidation rates over three orders of magnitude greater than the newly established abiotic oxidation rate of bisulfide. This new rate was determined in strict trace metal clean conditions and suggests that prior estimates of the direct reactivity of HS^- with O_2 are too high, and that biologically mediated sulfide oxidation may be responsible for the majority of oxidation observed in the field. The data from photolithotrophic organisms further indicates that biological processes in anaerobic environments are also likely to exceed abiotic rates of sulfide oxidation in aerobic environments, even when the presence of metal oxidants is considered. The implication of these findings is that flux of sulfide from anaerobic environments will largely be determined by the population size and activity of microbial communities in anaerobic–aerobic transition zones rather than by chemical oxidants alone. This implication is consistent with many other observations and is explained by the thermodynamic and kinetic constraints of 1 versus 2-electron transfer reactions from HS^- to O_2.

ACKNOWLEDGMENTS

This work was supported by grants from the National Science Foundation to Thomas E. Hanson and George W. Luther III (MCB-0919682; OCE-0732439) and to Peter R. Girguis (OCE-0732369) and a grant from NASA to Peter R. Girguis (NASA-ASTEP NNX07AV51G). We thank the crews of the ROV JASON II and the R/V Thomas G. Thompson for their expertise and help.

REFERENCES

Arndt, C., Gaill, F., and H. Felbeck. (2001). Anaerobic sulfur metabolism in thiotrophic symbioses. *J. Exp. Biol.* 204, 741–750.

Baumgartner, L. K., Reid, R. P., Dupraz, C., Decho, A. W., Buckley, D. H., Spear, J. R., Przekop, K. M., and Visscher, P. T. (2006). Sulfate reducing bacteria in microbial mats: changing paradigms, new discoveries. *Sediment. Geol.* 185, 131–145.

Bernhard, J. M., Buck, K. R., Farmer, M. A., and Bowser, S. S. (2000). The Santa Barbara Basin is a symbiosis oasis. *Nature* 403, 77–80.

Bouchet, P., and Warén, A. (1991). *Ifremeria nautilei*, a new gastropod from hydrothermal vents, probably associated with symbiotic bacteria. *Comptes Rendus De L'Academie Des Sciences Series III-Sciences De La Vie* 312, 495–501.

Brendel, P., and Luther, G. W. (1995). Development of a gold amalgam voltammetric microelectrode for the determination of dissolved Fe, Mn, O2 and S(-2) in porewaters of marine and freshwater sediments. *Environ. Sci. Technol.* 29, 751–761.

Bruchert, V., Jorgensen, B. B., Neumann, K., Riechmann, D., Schlosser, M., and Schulz, H. (2003). Regulation of bacterial sulfate reduction and hydrogen sulfide fluxes in the central Namibian coastal upwelling zone. *Geochim. Cosmochim. Acta* 67, 4505–4518.

Canfield, D. E., and Raiswell, R. (1999). The evolution of the sulfur cycle. *Am. J. Sci.* 299, 697–723.

Canfield, D. E., Stewart, F. J., Thamdrup, B., De Brabandere, L., Dalsgaard, T., Delong, E. F., Revsbech, N. P., and Ulloa, O. (2010). A cryptic sulfur cycle in oxygen-minimum-zone waters off the Chilean coast. *Science* 330, 1375–1378.

Chan, L. K., Morgan-Kiss, R. M., and Hanson, T. E. (2009). Functional analysis of three sulfide:quinone oxidoreductase homologs in *Chlorobaculum tepidum*. *J. Bacteriol.* 191, 1026–1034.

Childress, J. J., Fisher, C. R., Favuzzi, J. A., Kochevar, R., and Sanders, N. K., Alayse, A. M. (1991). Sulfide-driven autotrophic balance in the bacterial symbiont-containing hydrothermal vent tubeworm, *Riftia pachyptila* Jones. *Biol. Bull.* 180, 135–153.

Clement, B. G., Luther, G. W. III, and Tebo, B. M. (2009). Rapid, oxygen-dependent microbial Mn(II) oxidation kinetics at sub-micromolar oxygen concentrations in the Black sea suboxic zone. *Geochim. Cosmochim. Acta* 73, 1878–1889.

Cline, J. D. (1969). Spectrophotometric determination of hydrogen sulfide in natural waters. *Limnol. Oceanogr.* 14, 454–458.

Cottrell, M. T., and Kirchman, D. L. (2003). Contribution of major bacterial groups to bacterial biomass production (thymidine and leucine

incorporation) in the Delaware estuary. *Limnol. Oceanogr.* 48, 168–178.
Eghbal, M. A., Pennefather, P. S., and O'Brien, P. J. (2004). H2S cytotoxicity mechanism involves reactive oxygen species formation and mitochondrial depolarisation. *Toxicology* 203, 69–76.
Ellis, A. J., and Golding, R. M. (1959). Spectrophotometric determination of the acid dissociation constants of hydrogen sulphide. *J. Chem. Soc.* 127–130. doi:10.1039/JR9590000127
Girguis, P. R., and Childress, J. J. (2006). Metabolite uptake, stoichiometry and chemoautotrophic function of the hydrothermal vent tubeworm *Riftia pachyptila*: responses to environmental variations in substrate concentrations and temperature. *J. Exp. Biol.* 209, 3516–3528.
Girguis, P. R., Childress, J. J., Freytag, J. A., Klose, K. A., and Stuber, R. (2002). Effects of metabolite uptake on proton-equivalent elimination by two species of deep-sea vestimentiferan tubeworm, *Riftia pachyptila* and *Lamellibrachia* cf *luymesi*. *J. Exp. Biol.* 205, 3055–3066.
Girguis, P. R., Lee, R. W., Desauliners, N., Childress, J. J., Pospesel, M., Felbeck, H., and Zal, F. (2000). Fate of nitrate acquired by the tubeworm *Riftia pachyptila*. *Appl. Environ. Microbiol.* 66, 2783–2790.
Henry, M. S., Childress, J. J., and Figueroa, D. (2008). Metabolic rates and thermal tolerances of chemoautotrophic symbioses from Lau Basin hydrothermal vents and their implications for species distributions. *Deep Sea Res. Part 1 Oceanogr. Res. Pap.* 55, 679–695.
Jannasch, H. W., and Wirsen, C. O. (1979). Chemosynthetic primary production at east Pacific sea floor spreading centers. *Bioscience* 29, 592–598.
Jorgensen, B. B. (1994). Sulfate reduction and thiosulfate transformations in a cyanobacterial matduring a diel oxygen cycle. *FEMS Microbiol. Ecol.* 13, 303–312.
Jorgensen, B. B., and Gallardo, V. A. (1999). *Thioploca* spp: filamentous sulfur bacteria with nitrate vacuoles. *FEMS Microbiol. Ecol.* 28, 301–313.
Julian, D., April, K. L., Patel, S., Stein, J. R., and Wohlgemuth, S. E. (2005). Mitochondrial depolarization following hydrogen sulfide exposure in erythrocytes from a sulfide-tolerant marine invertebrate. *J. Exp. Biol.* 208, 4109–4122.
Konovalov, S. K., Luther, G. W., Friederich, G. E., Nuzzio, D. B., Tebo, B. M., Murray, J. W., Oguz, T., Glazer, B. T., Trouwborst, R. E., Clement, B., Murray, K., and Romanov, A. (2003). Lateral injection of oxygen with the Bosporus plume: fingers of oxidizing potential in the Black Sea. *Limnol. Oceanogr.*48, 2369–2376.
Lavik, G., Stührmann, T., Brücher, V., Van der Plas, A., Mohrholz, V., Lam, P., Mußmann, M., Fuchs, B. M., Amann, R., Lass, U., and Kuypers, M. M. M. (2009). Detoxification of suphidic African shelf waters by blooming chemolithotrophs. *Nature* 457, 581–584.
Lin, X. J., Scranton, M. I., Chistoserdov, A. Y., Varela, R., and Taylor, G. T. (2008). Spatiotemporal dynamics of bacterial populations in the anoxic Cariaco Basin. *Limnol. Oceanogr.* 53, 37–51.
Luther, G. W. III. (2010). The role of one and two electron transfer reactions in forming thermodynamically unstable intermediates as barriers in multi-electron redox reactions. *Aquat. Geochem.* 16, 395–420.
Luther, G. W. III, Bono, A., Taillefert, M., and Cary, S. C. (2002). "A continuous flow electrochemical cell for analysis of chemical species and ions at high pressure: laboratory, shipboard and hydrothermal vent results," Chapter 4, in *Environmental Electrochemistry: Analyses of Trace Element Biogeochemistry*, Vol. 811, eds M. Taillefert and T. Rozan (Washington, DC: American Chemical Society Symposium Series), 54–73.
Luther, G. W. III, Glazer, B. T., Ma, S., Trouwborst, R. E., Moore, T. S., Metzger, E., Kraiya, C., Waite, T. J., Druschel, G., Sundby, B., Taillefert, M., Nuzzio, D. B., Shank, T. M., Lewis, B. L., and Brendel, P. J. (2008). Use of voltammetric solid-state (micro)electrodes for studying biogeochemical processes: laboratory measurements to real time measurements with an in situ electrochemical analyzer (ISEA). *Mar. Chem.* 108, 221–235.
Ma, S., Noble, A., Butcher, D., Trouwborst, R. E., and Luther, G. W. III. (2006). Removal of H2S via an iron catalytic cycle and iron sulfide precipitation in the water column of dead end tributaries. *Estuar. Coast. Shelf Sci.* 70, 461–472.
Maloy, J. T. (1985). "Nitrogen chemistry," in *Standard Potentials in Aqueous Solution*, 1st Edn, eds A. J. Bard, R. Parsons, and J. Jordan (New York: M. Dekker), 127–139.
Mentel, M., and Martin, W. (2008). Energy metabolism among eukaryotic anaerobes in light of Proterozoic ocean chemistry. *Philos. Trans. R. Soc. Lond. B Biol. Sci.* 363, 2717–2729.
Mickel, T. J., and Childress, J. J. (1982). Effects of pressure and temperature on the EKG and heart rate of the hydrothermal vent crab *Bythograea thermydron* (Brachyura). *Biol. Bull.* 162, 70–82.
Millero, F. J., Hubinger, S., Fernandez, M., and Garnett, S. (1987). Oxidation of H2S in seawater as a function of temperature, ph, and ionic strength. *Environ. Sci. Technol.* 21, 439–443.
Overmann, J., and van Gemerden, H. (2000). Microbial interactions involving sulfur bacteria: implications for the ecology and evolution of bacterial communities. *FEMS Microbiol. Rev.* 24, 591–599.
Poulton, S. W., Krom, M. D., and Raiswell, R. (2004). A revised scheme for the reactivity of iron(oxyhydr)oxide minerals towards dissolved sulfide. *Geochim. Cosmochim. Acta* 68, 3703–3715.
Reinartz, M., Tschape, J., Bruser, T., Truper, H. G., and Dahl, C. (1998). Sulfide oxidation in the phototrophic sulfur bacterium *Chromatium vinosum*. *Arch. Microbiol.* 17, 59–68.
Rozan, T. F., Theberge, S. M., and Luther, G. W. III. (2000). Quantifying elemental sulfur (S0) bisulfide (HS-) and polysulfides (Sx2-) using a voltammetric method. *Anal. Chim. Acta* 415, 175–184.
Stanbury, D. (1989). "Reduction potentials involving inorganic free radicals in aqueous solution," in *Advances in Inorganic Chemistry*, Vol. 33, ed. A. G Sykes (New York: Academic Press), 69–138.
Stumm, W., and Morgan, J. J. (1996). *Aquatic Chemistry*, 3rd Edn. New York: John Wiley.
Theissen, U., Hoffmeister, M., Grieshaber, M., and Martin, W. (2003). Single eubacterial origin of eukaryotic sulfide : quinone oxidoreductase, a mitochondrial enzyme conserved from the early evolution of eukaryotes during anoxic and sulfidic times. *Mol. Biol. Evol.* 20, 1564–1574.
Trouwborst, R. E., Clement, B. G., Tebo, B. M., Glazer, B. T., and Luther, G. W. III. (2006). Soluble Mn(III) in suboxic zones. *Science* 313, 1955–1957.
Trouwborst, R. E., Johnston, A., Koch, G., Luther, G. W. III, and Pierson, B. K. (2007). Biogeochemistry of Fe(II) oxidation in a photosynthetic microbial mat: implications for precambrian Fe(II) oxidation. *Geochim. Cosmochim. Acta* 71, 4629–4643.
Turchyn, A. V., and Schrag, D. P. (2006). Cenozoic evolution of the sulfur cycle: insight from oxygen isotopes in marine sulfate. *Earth Planet. Sci. Lett.* 241, 763–779.
Vazquez, F. G, Zhang, J., and Millero, F. J. (1989). Effect of metals on the rate of the oxidation of H2S in seawater. *Geophys. Res. Lett.* 16, 1363–1366.
Wahlund, T. M., Woese, C. R., Castenholz, R., and Madigan, M. T. (1991). A thermophilic green sulfur bacterium from New Zealand hot springs, *Chlorobium tepidum* sp. nov. *Arch. Microbiol.* 156, 81–90.
Wakeham, S. G., Amann, R., Freeman, K. H., Hopmans, E. C., Jorgensen, B. B., Putnam, I. F., Schouten, S., Damste, J. S. S., Talbot, H. M., and Woebken, D. (2007). Microbial ecology of the stratified water column of the Black Sea as revealed by a comprehensive biomarker study. *Org. Geochem.* 38, 2070–2097.
Wilmot, D. B., and Vetter, R. D. (1990). The bacterial symbiont from the hydrothermal vent tubeworm *Riftia pachyptila* is a sulfide specialist. *Mar. Biol.* 106, 273–283.
Windoffer, R., and Giere, O. (1997). Symbiosis of the hydrothermal vent gastropod *Ifremeria nautilei* (Provannidae) with endobacteria – structural analyses and ecological considerations. *Biol. Bull.* 193, 381–392.
Yakushev, E., Pakhomova, S., Sørenson, K., and Skei, J. (2009). Importance of the different manganese species in the formation of water column redox zones: observations and modeling. *Mar. Chem.* 117, 59–70.
Yücel, M., Luther, G. W., and Moore, W. S. (2010). Earthquake-induced turbidite deposition as a previously unrecognized sink for hydrogen sulfide in the Black Sea sediments. *Mar. Chem.* 121, 176–186.

Conflict of Interest Statement: The authors declare that the research was conducted in the absence of any commercial or financial relationships that could be construed as a potential conflict of interest.

Received: 16 January 2011; accepted: 22 March 2011; published online: 09 April 2011.
*Citation: Luther GW III, Findlay AJ, MacDonald DJ, Owings SM, Hanson TE, Beinart RA and Girguis PR (2011) Thermodynamics and kinetics of sulfide oxidation by oxygen: a look at inorganically controlled reactions and biologically mediated processes in the environment. Front. Microbio. **2**:62. doi: 10.3389/fmicb.2011.00062*
This article was submitted to Frontiers in Microbial Physiology and Metabolism, a specialty of Frontiers in Microbiology.